THE ROLE OF SKELETAL MUSCLE RYANODINE RECEPTOR TYPE 1 (RYR1) IN UTERINE VASCULAR AND MYOMETRIAL SMOOTH MUSCLE FUNCTION DURING PREGNANCY

Mistry, Arti

Awarding institution:
King's College London

THE ROLE OF SKELETAL MUSCLE RYANODINE RECEPTOR TYPE 1 (RYR1) IN UTERINE VASCULAR AND MYOMETRIAL SMOOTH MUSCLE FUNCTION DURING PREGNANCY

ARTI MAHENDRA MISTRY

A thesis submitted to King's College London for the degree of Doctor of Philosophy

Department of Women and Children's Health

King's College London

July 2023

Table of Contents

Acknowledgements

Presentations and publications arising from this work

1. Mistry A., Saldanha G., Bersselaar L R., Knock G A., Goldberg M F., Vanegas M I., Fernandez-Garcia A M., Treves S., Voermans N C., Tribe R M., Jungbluth H. Obstetric and gynaecological features in females carrying variants in the skeletal muscle ryanodine receptor (*RYR1*) gene: a questionnaire study. *Authorea*. June 20, 2023. DOI: 10.22541/au.168727329.97193223/v1 [Preprint]

2. Mistry A., Saldanha G., Bersselaar L R., Knock G A., Goldberg M F., Vanegas M I., Treves S., Voermans N C., Tribe R M., Jungbluth H. Obstetric and gynaecological features in females carrying mutations in the skeletal muscle ryanodine receptor (*RYR1*) gene: a questionnaire study. World Muscle Society 2023 Congress. [Abstract, poster presentation]

3. Mistry A., G Knock., H Jungbluth., R Tribe. Effects of the skeletal Ryanodine Receptor Type 1 mutation on uterine artery vascular smooth muscle function and fetal growth in pregnant *Ryr1$^{Y522S/+}$* mice. New roles for ion channels and transporters in health and disease. OCO4, Online Symposium, Physiological Society, 2021. [Abstract, oral communication].

4. Mistry A., H Jungbluth., R Tribe. Effects of the skeletal ryanodine receptor type 1 mutation on uterine artery vascular smooth muscle function and fetal growth in pregnant *Ryr1$^{Y522S/+}$* mice. School of Life Course and Population Sciences 2021 PGR Awards and Symposium, KCL. 2021. [Abstract, oral communication].

Abstract

Background. Understanding the basis of myometrial and uterine artery smooth muscle contractility is crucial to understanding complications associated with pregnancy and childbirth. Mutations in ryanodine receptor 1 (*RYR1*) are associated with various phenotypes including malignant hyperthermia susceptibility (MHS), central core disease (CCD) and other congenital myopathies; highlighting the role of RYR1 in skeletal muscle function. Some patients with autosomal dominant *RYR1* mutations have reported abnormal bleeding characterised by severe menorrhagia, post-partum bleeding and gum and postoperative bleeding. Excessive bleeding suggests a role of RYR1 in smooth muscle function, an observation experimentally tested by Lopez et al. (2016) who showed that $Ryr1^{Y522S/+}$ mice had prolonged tail artery bleeding times compared to wild-type controls, an effect reversed by pre-treatment with dantrolene, a pharmacological antagonist of the RYR1 channel. Together these observations imply a contribution of RYR1 to vascular smooth muscle function and, the female reproductive system.

Hypothesis. The presence of a gain-of-function *Ryr1* mutation in pregnancy will lead to enhanced vasorelaxation of vascular smooth muscle cells and altered contractility of myometrium. This will impact on fetal and placental development and influence the length of gestation and parturition. The *Ryr1* Y522S mutation will modify the cellular needs of the reproductive tissues resulting in altered global mRNA expression. The *RYR1*-variant carrying human cohort will demonstrate increased bleeding events, longer bleeding times, increased rate of menorrhagia and a shorter length of pregnancy.

Methods. Utilizing the $Ryr1^{Y522S/+}$ mouse model, the impact of the gain-of-function mutation was investigated in late-stage pregnant mice. The impact of *Ryr1* Y522S on vascular smooth muscle function in pregnant uterine arteries was investigated using wire myography with a

pharmacological approach (calcium modulators and dantrolene). In addition, histological analyses of the pregnant uterine artery tissue explored changes in smooth muscle content and vessel morphology. The impact of the *Ryr1* Y522S mutation on myometrial function was studied using video recordings to determine gestation length, isometric tension recordings of spontaneous myometrial contractions and RNAseq to investigate gene expression changes in the pregnant myometrial tissue. Fetal and placental weight measurements were made on gestation day 18.5. Placental morphology was studied using haematoxylin and eosin stains, and immunofluorescence staining. The abnormal bleeding phenomenon in *RYR1* variant-carrying women was further investigated using an online questionnaire regarding generalised bleeding events, menorrhagia, and pregnancy/obstetric history.

Results. Uterine artery vasodilatory response was reduced in phenylephrine pre-constricted vessels from heterozygous $Ryr1^{Y522S/+}$ (mixed litter) dams (a larger IC50) compared to vessels from wildtype (wildtype litter) dams, a response which was reversed by dantrolene. The contractile response of uterine arteries from heterozygous pregnant animals to phenylephrine was not statistically different to that of the wild-type pregnant uterine artery. Myometrial tissue from pregnant $Ryr1^{Y522S/+}$ animals had a total of six differentially expressed genes (padj<0.3) compared to wild-type pregnant myometrium. Gestation length of $Ryr1^{Y522S/+}$ mouse pregnancies was not statistically different to that of the wild-type mouse. The pregnant $Ryr1^{Y522S/+}$ mouse had fewer fetuses in a litter, lower weight fetuses and heavier placentas, compared to wild-type littermates. The $Ryr1^{Y522S/+}$ mouse placenta had a larger labyrinth, and smaller decidua, compared to the wild-type placenta. The RYR1 protein localised to the junctional zone of the placenta and $Ryr1^{Y522S/+}$ placentas had more intense spongiotrophoblast staining of the junctional zone compared to wildtype.

Assessing bleeding symptoms in women, via a customized online questionnaire, revealed that women with *RYR1*-related disorders had higher bleeding scores and more often had pathological bleeding scores compared to control participants. In addition, *RYR1*-mutated participants more often reported having complications during a pregnancy, shorter pregnancies, planned Caesarean sections and gave birth to lower weight babies, in addition to gastrointestinal symptoms.

Conclusions. Through these studies we have shown that the maternal *Ryr1* Y522S influences uterine artery vasodilation and myometrial contraction, suggesting a physiological role of RYR1 in smooth muscle function, which ultimately results in abnormal bleeding, altered fetal-placental growth and fetal survival. Findings in the animal model were corroborated by the findings from our online questionnaire study exploring a range of symptoms in *RYR1*-mutated females. This work highlights potentially modifiable phenotypes associated with pathogenic *RYR1* variants.

Declaration

I declare that the content of this thesis is my own work and that all contributions and collaborations have been listed and acknowledged. No material presented in thesis has been submitted to any other university or for any other degree.

Copyright

The copyright of this thesis rests with the author and no quotation from it or information derived from it may be published without proper acknowledgement.

Abbreviations

AChR	Acetylcholine receptor
AD	Autosomal dominant
APH	Ante-partum haemorrhage
AR	Autosomal recessive
ASM	Airway smooth muscle
AUB	Abnormal uterine bleeding
BK_{Ca}	Big conductance calcium activated potassium channels
cAMP	Cyclic AMP
CAPs	Contractile associated proteins
CCD	Central core disease
CFTD	Congenital fibre type disproportion
CHF	Congestive heart failure
CICR	Calcium-induced calcium-release
CNM	Centronuclear myopathy
CNS	Central nervous system
DAG	Diacylglycerol
DCM	Diabetic cardiomyopathy
DHPR	Dihydropyridine receptor
DMSO	Dimethylsulfoxide
DN	Dominant negative
DUB	Dysfunctional uterine bleeding
E2	Oestradiol
EC	Endothelial cells
ECC	Excitation-contraction coupling
EDH	Endothelium-dependent hyperpolarisation
ENS	Enteric nervous system
ERK	Extra-cellular regulated kinase
ERM	Exertional rhabdomyolysis
FII	Factor VII
FKBP12	FK 506–binding protein 12
FSH	Follicle-stimulating hormone
GA	Gestational age
HMB	Heavy menstrual bleeding

IP3R	Inositol tri-phosphate receptors
IUGR	Intrauterine growth restriction
JZ	Junctional zone
LH	Luteinizing hormone
L-NAME	N(G)-Nitro-L-arginine methyl ester
MCMDM-1VWD	Molecular and Clinical Markers for the Diagnosis and Management of Type 1 von Willebrand disease
MH	Malignant hyperthermia
MHS	Malignant hyperthermia susceptibility
MLCK	Myosin light kinase
MLCP	Myosin light chain phosphatase
MmD	Multi-minicore Disease
NCX	Na/Ca exchanger
NGS	Next generation sequencing
NO	Nitric oxide
NOS	Nitric oxide synthase
OTR	Oxytocin receptor
P4	Progesterone
PCOS	Poly-cystic ovary syndrome
PDGF	Platelet-derived growth factor
PGF2α	Prostaglandin F2α receptor
PGI$_2$	Prostacyclin or prostaglandin I2
PIGF	Placental growth factor
PIP2	Phosphatidylinositol biphosphate
PKC	Phosphokinase C
PLC	Phospholipase C
PMCA	Plasma membranes Ca^{2+}-atpase
PPH	Post-partum haemorrhage
PSS	Physiological salt solution
P-TGCs	Parietal trophoblast giant cells
PVDF	Polyvinylidene difluoride
Rhok	Rho kinase
RT-qPCR	Reverse transcription quantitative polymerase chain reaction
RYR1	Ryanodine receptor type 1
SAH	Subarachnoid haemorrhage

SERCA	Sarcoplasmic reticulum calcium-ATPase
SMC	Smooth muscle cell
SOCE	Store operated calcium entry
SpA-TGCs	Spiral artery trophoblast giant cells
SR	Sarcoplasmic reticulum
S-TGCs	Sinusoidal trophoblast giant cells
STICs	Spontaneous transient inward currents
STOCs	Spontaneous transient outward currents
STREX	Stress axis regulated exon
SynT	Syncytiotrophoblast
TGCs	Trophoblast giant cells
uNK	Uterine natural killer cells
UVR	Uterine vascular resistance
VEGF	Vascular endothelial growth factor
VGCC	Voltage-gated calcium channel
VICaR	Voltage induced Ca^{2+} release
VSMC	Vascular smooth muscle cell
VWD	Von Willebrand disease
VWF	Von Willebrand factor

Table of Figures

17

19

Table of Tables

1 Chapter 1 Introduction

1.1 General introduction

Variants in the skeletal muscle ryanodine receptor *(RYR1)* gene, encoding the principal skeletal muscle Ca^{2+} release channel, are associated with a very wide and expanding phenotypical spectrum. Autosomal dominant variants in *RYR1* are associated with the congenital myopathy central core disease (CCD) (Fujii *et al.*, 1991; Gillard *et al.*, 1991; Otsu *et al.*, 1991; Brandt *et al.*, 1999; Sambuughin *et al.*, 2001; Monnier *et al.*, 2005), the malignant hyperthermia susceptibility (MHS) trait, a potentially fatal anaesthesia complication in response to volatile anaesthetics and certain muscle relaxants, as well as a number of more recently recognized MHS-associated phenotypes, in particular exertional rhabdomyolysis (ERM) (Dlamini *et al.*, 2013), King-Denborough Syndrome, late-onset axial myopathy (Jungbluth *et al.*, 2009). Autosomal recessive variants in *RYR1* have been associated with a wide range of congenital myopathies, including multi-minicore disease (MmD), centronuclear myopathy (CNM) and congenital fibre type disproportion (CFTD), and some rare cases of central core disease (Jungbluth *et al.*, 2002; Romero *et al.*, 2003). Predominantly a skeletal muscle disease associated gene, there is some evidence to suggest that such *RYR1* variants can also influence other tissue types such as smooth muscle.

In particular, Lopez *et al*. (2016) demonstrated that mouse arterial tissue carrying the malignant hyperthermia susceptibility-associated Y522S variant in *Ryr1,* showed reduced contractility in vascular smooth muscle cells resulting in prolonged tail artery bleeding time compared to wild-type controls. Moreover, this bleeding phenotype was reversed by pre-treatment with the specific RYR1 antagonist dantrolene, indicating that the ryanodine receptor channel has a role in regulating the contraction mechanism of vascular smooth muscle. Complementary to the mouse data, abnormal bleeding phenotypes manifesting as severe menorrhagia, postpartum

bleeding, gum and/or postoperative bleeding have been previously reported in a small number of *RYR1*-mutated females who also had evidence of more generalized smooth muscle involvement, particularly concerning the bladder and bowel (Lopez, 2016). There have been several other isolated reports of an increased bleeding tendency in patients carrying pathogenic *RYR1* variants (Coburger *et al.*, 2017; Brackmann *et al.*, 2018).

It is uncertain if the post-partum haemorrhage observed in *RYR1*-mutated females is a reflection of the primary bleeding abnormality in these patients or reflects additional obstetric and/or gynaecological factors. There is no data reporting how *RYR1* variants may affect uterine vascular and myometrium function in pregnancy, although RyR isoform expression has been detected in these tissue types (Martin, Chapman, *et al.*, 1999; Masters, Neal and Gillespie, 1999; Matsuki *et al.*, 2017; Hu *et al.*, 2020). In addition, a recent report detailing the role of RYR1 channels in trophoblast migration within the human placenta indicates a role for RYR1 in the normal development of the placenta (Zheng *et al.*, 2022).

The emergence of a phenotype that may influence reproduction has led me to consider how *RYR1* variants could impact on reproduction and pregnancy outcomes. I was also keen to further explore the clinical bleeding phenotype in affected women. Specifically, the use of a pregnant $Ryr1^{Y522S/+}$ mouse model allowed for the interrogation of how this autosomal dominant variant could affect uterine and uterine artery function and placentation. In parallel, a questionnaire-based study was conducted to investigate bleeding during menstruation, pregnancy, post-partum, generalised bleeding events, smooth muscle function, and to collect an extensive obstetric history in human *RYR1* patients, to provide additional information on the impact of *RYR1* variants on bleeding and reproductive outcomes.

1.2 Ryanodine receptors

Ryanodine receptors (RyR) are homotetrameric intracellular Ca^{2+} channels which comprise four large (~565-kDa) structural units, located on the sarco/endoplasmic reticulum (S/ER) in almost all cell types. The channel has a large N-terminal, cytosolic domain and smaller transmembrane domain containing the channel pore (Block *et al.*, 1988; Lanner *et al.*, 2010; Zalk and Marks, 2017). RyRs are high conductance non-selective calcium channels (~100 pS for Ca^{2+}) (Imagawa *et al.*, 1987; Hymel *et al.*, 1988).

There are three known isoforms of the ryanodine receptor channel protein, RYR1, RYR2 and RYR3, all encoded by different genes. RYR1 was first identified in skeletal muscle (Marks *et al.*, 1989; Takeshima *et al.*, 1989), RYR2 was first described in cardiac muscle (Nakai *et al.*, 1990; Brillantes *et al.*, 1992) and RYR3 was first found in the brain (Hakamata *et al.*, 1992), although all three isoforms are expressed in various tissues (Lanner, 2010). The isoforms share ~65% homology and are all activated by micromolar and inhibited by millimolar concentrations of Ca^{2+} (Bezprozvanny, Watras and Ehrlich, 1991). The central role of intracellular Ca^{2+} handling is evident in RYR dysfunction and disease presentation, described in detail below.

1.2.1 Ryanodine receptor type 1 (*RYR1*)

The large 15400 base pair (bp) human *RYR1* is located on chromosome 19q13.2 and comprises 106 exons. In mice, the equally large 15358 bp *Ryr1* located on chromosome 7 also contains 106 exons. The SR RYR1 channel proteins are most abundantly expressed in skeletal muscle tissue (MacKenzie *et al.*, 1990) but mRNA transcripts are also detected in various other tissue types including uterus, colon, brain, vagina, cervix and various arteries, demonstrated in

Figure 1 (*GTEx Portal*, accesed on 03 March 2023), alongside functional evidence in some of these tissues.
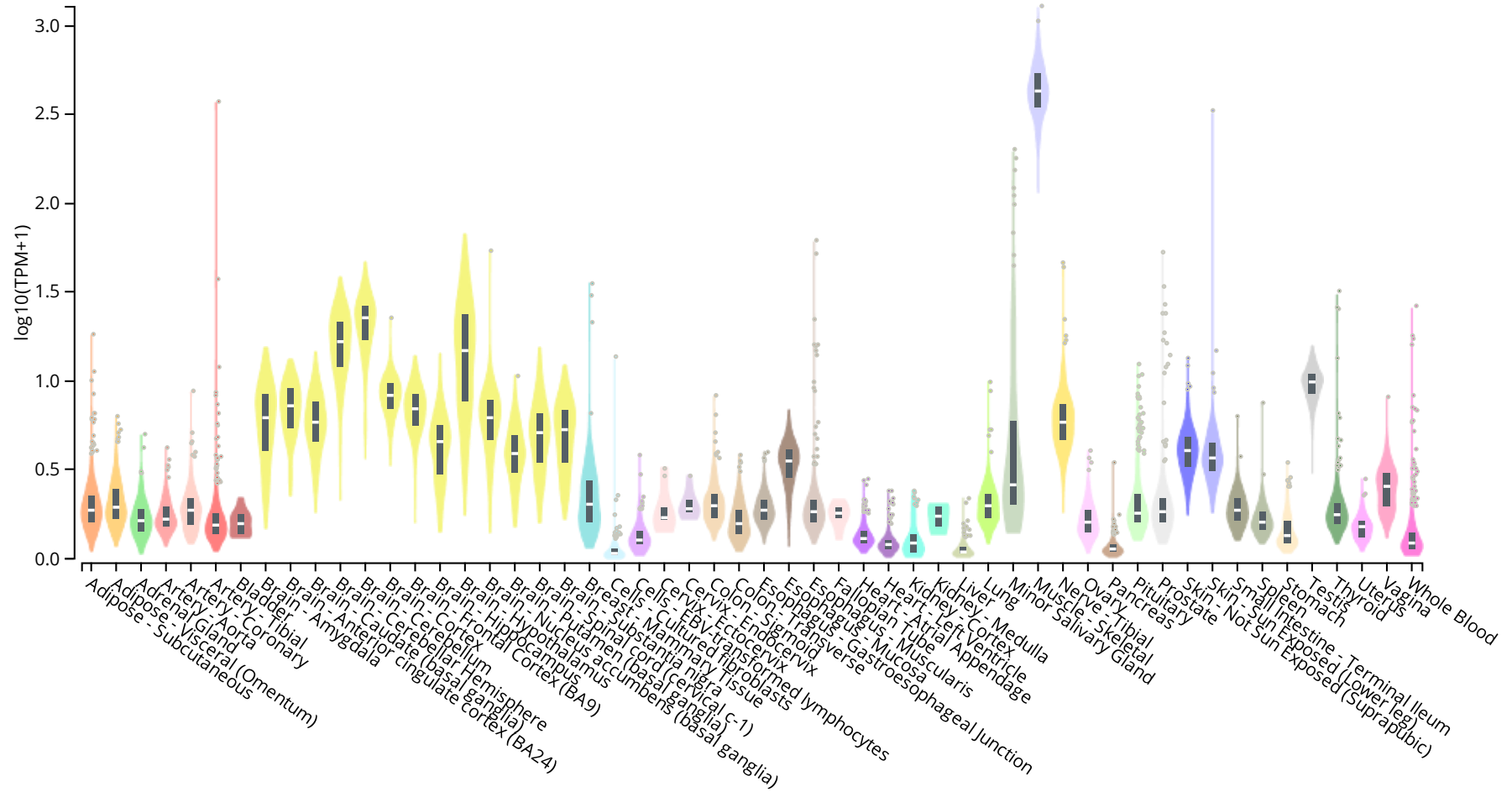
Figure 1. Tissue distribution of human *RYR1* expression in transcripts per million (TPM).

Expression of human *RYR1* transcripts across various tissue types, presented as $_{log}10$(Transcripts Per Million^{+1}). Data Source: GTEx Analysis Release V8, accessed on 03 March 2023 (dbGaP Accession phs000424.v8.p2).

1.2.2 Role of RyR channels in excitation–contraction coupling (ECC)

Muscle contraction in striated muscle begins with the activation of neurotransmitter signals by a neuronal stimulus, which causes depolarisation of the plasma membrane to a more positive value which in turn activates sodium (Na^+) voltage-gated channels resulting in an action potential that propagates along the cell (excitation). The term 'excitation-contraction coupling (ECC)' encompasses the complex pathways that link surface membrane action potentials to shortening of the muscle fibre, in particular the depolarization-dependent response of the dihydropyridine receptors (DHPR) α1 voltage sensor with the release of the Ca^{2+} from the SR, demonstrated in Figure 2. In the skeletal muscle SR, RYR1 bridges the SR and the transverse tubule and is essential for EC coupling (Takeshima *et al.*, 1994; Avila, O'Brien and Dirksen, 2001; Treves *et al.*, 2008; Snoeck *et al.*, 2015). Depolarisation of the T-tubule membrane in response to a muscle action potential induces conformational changes in the voltage sensor DHPR α1S subunit ($Ca_v 1.1$), which in skeletal muscle is mechanically coupled to the ryanodine receptor, and through conformational changes mediates rapid Ca^{2+} release from the SR into the cytosol (Block, 1988; Rfos and Pizarro, 1991; Schneider, 1994; Nakai *et al.*, 1997; Schredelseker *et al.*, 2009; Rebbeck *et al.*, 2014). The opening of DHPRs that are located on sarcotubular profiles (i.e. invaginations of the plasma membrane) releases ions into the intracellular space which also induces opening of SR RYR1 channels and consequent Ca^{2+} release through Ca^{2+} induced Ca^{2+} release (CICR) (Endo, Tanaka and Ogawa, 1970; Ford and Podolsky, 1970; Endo, 2009).

These events are followed by the formation of actin-myosin cross-bridges whereby SR Ca^{2+} release then leads to Ca^{2+} binding to troponin and tropomyosin that block myosin head binding sites on actin, exposing the binding sites and allowing myosin heads to form a cross-bridge with actin filaments, and ultimately skeletal muscle contraction. The process is then terminated

by the reduction of reduced cytosolic Ca^{2+} concentrations predominantly by Ca^{2+} reuptake into the SR through the specialized sarcoendoplasmic reticulum (SR) Ca^{2+} transport ATPase (SERCA) pumps.

It is generally agreed that Ca^{2+} induced Ca^{2+} release (CICR) is also a key physiological mechanism of Ca^{2+} release in cardiac muscle. Depolarization begins in the pacemaker cells in the sinoatrial node spontaneously to produce action potentials. The action potential spreads to the cardiac myocytes where it invades the T-tubules, however unlike skeletal muscle the L-type Ca^{2+} channels are not coupled to RyRs. In cardiomyocytes the influx of Ca^{2+} via the plasma membrane DHPR α1C (CaV1.2) activates Ca^{2+} release through RyRs (predominantly RYR2) via CICR (Fabiato and Fabiato, 1978; Bers and Stiffel, 1993; Adachi-Akahane, Cleemann and Morad, 1996; des Georges *et al.*, 2016).
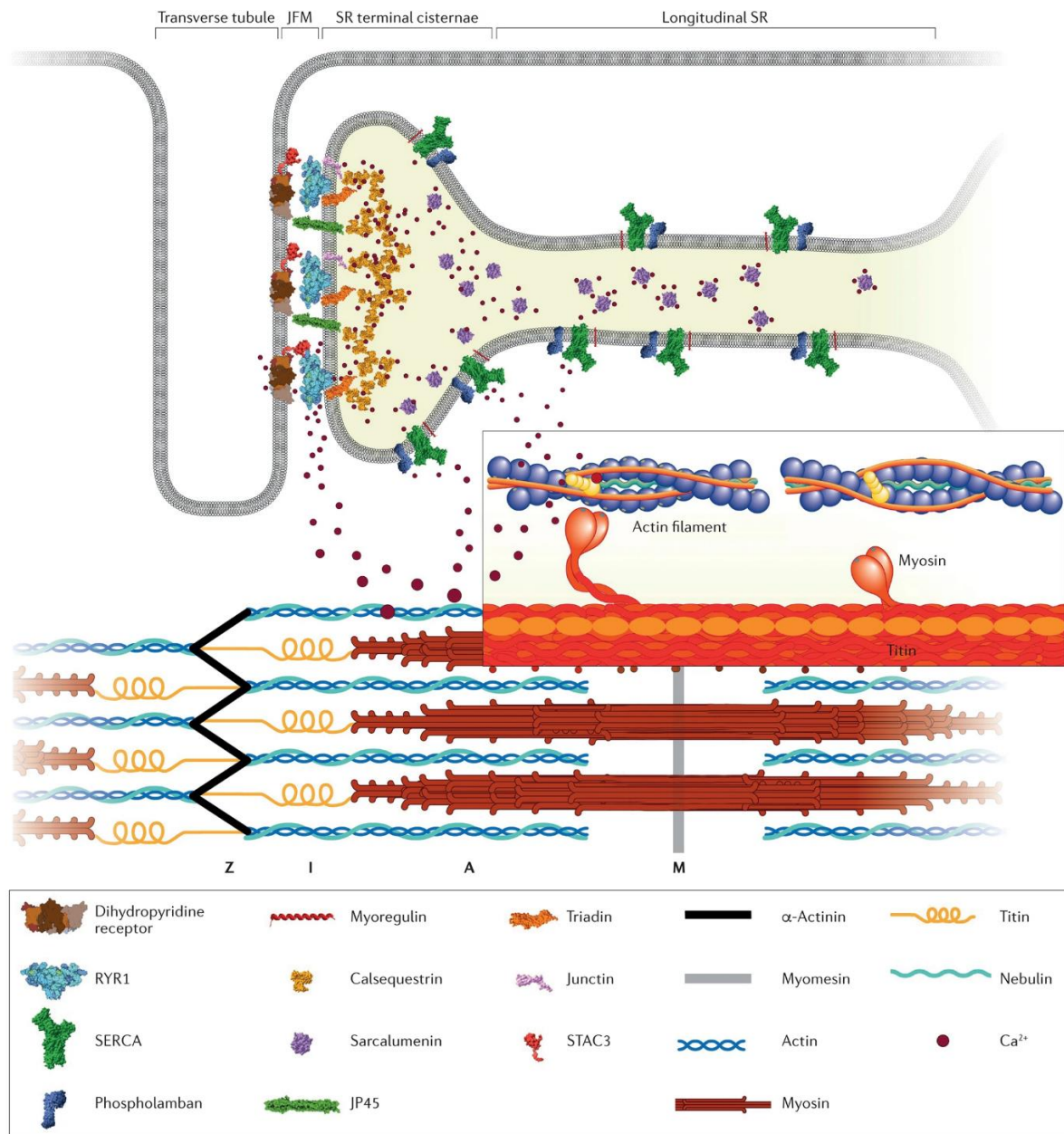
Figure 2. Proteins involved in skeletal muscle excitation contraction coupling.

Diagram illustrating the subcellular localization of the main proteins implicated in skeletal muscle excitation–contraction coupling (ECC) and thin–thick filament interaction and assembly. The transverse tubules are invaginations of the plasma membrane where the dihydropyridine receptor complex is located. This membrane compartment faces the sarcoplasmic reticulum (SR) junctional face membrane (JFM), which contains ryanodine receptor 1 (RYR1) as well as junctional SR protein 1 (JP45) and the structural proteins triadin and aspartyl/asparaginyl β-hydroxylase (junctin). Ca^{2+} release into the cytosol results in sarcomeric shortening through specific interactions between thin and thick filaments, specifically the sliding of actin past myosin filaments. ECC is terminated through SR Ca^{2+} reuptake through sarcoplasmic/endoplasmic reticulum Ca^{2+} ATPase (SERCA) Ca^{2+} pumps. A, A-band; I, I-band; M, M-band; Z, Z-line. Image reproduced courtesy of Christoph Bachmann, Departments of Anaesthesia and Biomedicine, Basel University Hospital, Basel, Switzerland. 3D representations from RSCB PDB (http://www.rcsb.org/pdb/explore.do?structureId=2db6) ; originally published in Jungbluth *et al.*, 2018, permission for reuse obtained on 17/05/2023 as detailed in Appendix 1.

1.3   *RYR*-associated diseases

Dysfunctional RYR1-mediated Ca^{2+} handling has been implicated in the pathogenesis of various inherited conditions. To date, over 300 *RYR1* variants have been identified as pathogenic and associated to disease in the ClinVar database [date accessed 16th March 2023] (Landrum *et al.*, 2020). Variants in *RYR1* have been associated with a range of debilitating and/or life-threatening neuromuscular disorders, ranging from early-onset myopathies with permanent weakness (including central core disease (CCD), multi-minicore disease (MmD), centronuclear myopathy (CNM), and congenital fibre type disproportion, CFTD) to episodic presentations such as exertional rhabdomyolysis/ myalgia (ERM) and malignant hyperthermia (MH) in otherwise healthy individuals.

Recessive variants in *RYR1* have been associated to congenital myopathies, with a wide phenotypic spectrum including MmD, CNM and CFTD and some rare cases of CCD (Jungbluth, 2002; Romero, 2003). Autosomal dominant variants in *RYR1* are associated to CCD, (Fujii, 1991; Gillard, 1991; Otsu, 1991; Brandt, 1999; Sambuughin, 2001; Monnier, 2005), MHS, as well as a number of more recently recognized MHS-associated phenotypes, in particular ERM (Dlamini, 2013), King-Denborough syndrome (KDS), and late-onset axial myopathy (Jungbluth, 2009).

Whilst there are known disorders associated with *RYR2* and *RYR3* mutations, these are relatively rare compared to those of *RYR1*. Although this is not the focus of this thesis, it is worth noting that are specific disorders associated with *RYR2* and *RYR3* variants. Autosomal-dominant variants in *RYR2* have been associated to arrhythmogenic right ventricular dysplasia type 2 (OMIM: 600996), characterized by partial degeneration of the myocardium of the right ventricle, electrical instability and sudden death (Rampazzo *et al.*, 1995; Tiso *et al.*, 2001), and catecholaminergic polymorphic ventricular tachycardia type 1 (OMIM: 604772) characterised

by physical activity or stress-induced polymorphic ventricular tachycardias (Priori *et al.*, 2002; George, Higgs and Lai, 2003).

Variants in *RYR3* have been associated with abnormalities of certain neurons in the central nervous system (Takeshima *et al.*, 1996), altered synaptic plasticity and spatial learning (Balschun *et al.*, 1999), and the regulation of other RyR channels (Jiang *et al.*, 2003). Variants in *RYR3* may be associated, albeit a rare occurrence, to nemaline myopathy (OMIM: 161800) (Nilipour *et al.*, 2018), a form of congenital myopathy characterised by abnormal rod-like structures in muscle fibres and variable clinical presentations primarily involving weakness of proximal muscles with involvement of facial, bulbar and respiratory muscles (Ilkovski *et al.*, 2001). Nilipour and colleagues (2018) found variants of unknown significance in *RYR3* in a patient presenting with characteristics of nemaline myopathy, however functional studies were not performed.

1.3.1 Disease pathophysiology

CCD is closely associated with AD *RYR1* variants, whereas MmD is rather more heterogenous being associated more closely with AR variants. Clinically, CCD is characterised by hip girdle weakness with frequent orthopaedic complications, such as dislocation of the hips and scoliosis, but usually in the absence of significant bulbar and respiratory involvement. The disorder is histopathologically characterised by prominent core areas lacking oxidative enzyme activity that either run through a substantial part of- or the length of the fibre (Romero, 2003; Jungbluth, Sewry and Muntoni, 2011). The clinical MmD phenotype is characterised by a distribution of weakness which may resemble CCD, or a predominantly axial myopathy with external ophthalmoplegia, or pronounced distal weakness and wasting (Jungbluth *et al.*, 2005).

Clinical manifestation of variants in selenoprotein N (*SEPN1*) also manifest as MmD, characterised by severe spinal rigidity, early scoliosis and respiratory impairment (Ferreiro, Quijano-Roy, *et al.*, 2002). It has been suggested that in some families the presentation of CCD from AD *RYR1* variants and MmD from AR *RYR1* variants may represent a clinic-pathologic continuum rather than separate entities (Ferreiro, Monnier, *et al.*, 2002). Dominant variants associated with CCD produce RYR1 channels with reduced Ca^{2+} transporting efficiency, or channels that result in intraluminal SR Ca^{2+} store depletion (Avila, 2001; Ducreux *et al.*, 2004).

CNM is characterised histologically by the presence of prominent central nuclei on muscle biopsies and clinically by features of congenital myopathy, with variable presentation including muscle weakness, hypotonia, external ophthalmoplegia, respiratory failure and occasionally antenatal onset comprising of reduced fetal movements, polyhydramnios and thinning of the ribs (Jungbluth, Wallgren-Pettersson and Laporte, 2008).

Malignant hyperthermia susceptibility is a potentially fatal anaesthesia complication where patients carrying gain-of-function dominant *RYR1* variants adversely react to volatile anaesthetics and certain muscle relaxants, in particular succinylcholine. Administration of volatile anaesthetics lead to the rapid opening of the hypersensitive RYR1 channel and uncontrolled release of Ca^{2+} from the SR, resulting in sustained skeletal muscle contractions (Rosenberg *et al.*, 2007). In response to the elevated Ca^{2+} concentrations, SERCA is activated. Continued activation of SERCA in response to this persistent calcium leak from the SR will consume excessive ATP leading to hypermetabolism and systemic changes such as a drop in available ATP levels, acidosis, tachycardia and an abnormal increase in body temperature (Kuo and Ehrlich, 2015). Dantrolene is a muscle relaxant typically used in the acute treatment of MH patients (Kolb, Horne and Martz, 1982). Dantrolene inhibits abnormal Ca^{2+} release by direct

interaction with RYR1, ameliorating MH crises. Dantrolene exhibits selectivity for RYR1 and possibly RYR3 over RYR2 channels (Fruen, Mickelson and Louis, 1997; Zhao *et al.*, 2001b).

Although MHS presents as a well described phenotype, MHS-associated *RYR1* variants may result in a wider range of disorders with phenotypic heterogeneity. *RYR1*-related King-Denborough syndrome (KDS) is closely associated to MHS and characterised by dysmorphic facial features, short stature, spinal rigidity, scoliosis and various histopathological features (Dowling *et al.*, 2011). MHS-associated variants have also been identified as a cause of exertional myalgia and rhabdomyolysis (ERM), which is clinically recognised in otherwise healthy individuals with variable histopathological findings on muscle biopsy (Dlamini, 2013).

1.3.2 *RYR1*-disorder prevalence

A regionally limited study of a paediatric population from the US, revealed a prevalence of *RYR1*-related congenital myopathies of at least 1 in 90,000 individuals (Amburgey *et al.*, 2011). However, this is likely to be an underestimate of the overall frequency in the general population, due to the age of the study (over 10 years old) predating the more recent advances in next generation sequencing (NGS) techniques in clinical diagnostics, and the focus on a relatively small geographic area. Indeed, other reports have estimated a higher prevalence in certain geographic locations and ethnic populations. For example, a recent study found a higher prevalence of pathogenic *RYR1* variants in the Singaporean population (6 in 4810 individuals) (Foo *et al.*, 2022).

A study from the UK revealed the specific frequency of *RYR1*-related congenital myopathies, suggesting that CCD and MmD are most common, whilst CNM and CFTD are less frequent (Maggi *et al.*, 2013). However, these studies do not consider the prevalence of MH phenotypes

and other MH-associated phenotypes such as exertional myalgia/rhabdomyolysis and late-onset axial myopathy.

The incidence of clinically overt MH events during general anaesthesia is estimated to be 1 in 5000, to 1 in 50,000 - 100,000 individuals (Rosenberg, 2007; Rosero *et al.*, 2009). Yet, the prevalence of MH variants has been estimated to be 1 in 2000–3000 individuals (Bachand *et al.*, 1997; Monnier *et al.*, 2002; Wappler, 2010). The discrepancy between the frequency of MHS *RYR1* genotypes and clinically overt MH events has largely remained unaccounted for, although a recent paper suggests the importance of additional modifier factors, in particular exercise and pyrexia. *RYR1* variants have been associated with 34-86% of reported MH cases (Galli *et al.*, 2006; Ibarra M *et al.*, 2006; Robinson *et al.*, 2006; Gillies *et al.*, 2008, 2015; Broman *et al.*, 2009; Kraeva *et al.*, 2011; Brandom *et al.*, 2013; Miller *et al.*, 2018; Riazi *et al.*, 2022).

1.4   Non-neuromuscular *RYR1*-associated phenotypes

Variants in *RYR1* have been suggested to have a wide phenotypic range, including recently emerging non-neuromuscular phenotypes, including, a neuronal phenotype and selective immune advantages. An CCD-associated *RYR1* variant has been studied in the central nervous system. The study found that the *Ryr1$^{I4895T/WT}$* (IT/$^+$) mouse model exhibits a neuronal phenotype, at least on the cellular level. Specifically, in hypothalamic nerve terminals these mice displayed a lack of voltage-induced Ca^{2+} release (VICaR) from internal Ca^{2+} stores without Ca^{2+} influx, indicating that the mutant RYR1 channels play a role in VICaR, indicating neuronal alteration (De Crescenzo *et al.*, 2012). RYR1 expression has also been confirmed in dendritic cells. A study explored the effect of an MH variant, *Ryr1* Y522S, in a knock-in mouse model on the immune system when treated with an antigenic challenge. They found that MH animals were more efficient at stimulating T cell proliferation, had higher levels of natural IgG1 and IgE antibodies, and were faster and more efficient at mounting a specific immune response in the early phases of immunization (Vukcevic *et al.*, 2013).

1.4.1   Smooth muscle and bleeding *RYR1*-associated phenotypes

RYR1 expression has been confirmed in various smooth muscle tissues and cells including pregnant and non-pregnant myometrium, mouse detrusor muscle (Ji *et al.*, 2004; Nicolas Fritz *et al.*, 2007), rat airway smooth muscle (Du *et al.*, 2006), mouse pulmonary arteries (Li *et al.*, 2009), tail artery and mesenteric arteries (Lopez, 2016). In arterial smooth muscle cells, it is suggested that Ca^{2+} sparks activate spontaneous transient outward currents (STOCs) which are mediated by BK_{Ca} channels in the plasma membrane (Nelson *et al.*, 1995). STOCs produce a K^+ efflux and cause membrane hyperpolarization which reduces Ca^{2+} influx by decreasing the

open-state probability of voltage-dependent Cav1.2 L-type Ca^{2+} channels, which then lowers the global intracellular Ca^{2+} concentration and opposes vasoconstriction.

In mouse detrusor muscle, Fritz *et al* (2007) found that RYR1 localised to the SR, and *Ryr1*^{-/-} mice lost depolarisation-induced Ca^{2+} sparks, demonstrating the importance of RYR1 in depolarization-induced Ca^{2+} sparks. Du *et al* (2006) suggested that in airway smooth muscle (ASM), RYR1 channels and Cav1.1 may be directly coupled as in skeletal muscle, and indicated that KCl-induced depolarisation was partially reversed by administration of 200 μM ryanodine, indicating functional coupling of L-type channels and RyRs in ASM. However the role of ryanodine receptors in phasic smooth muscles such as myometrium and vasculature during pregnancy is less well explored, with only few studies having reported, for example, how RyR channels modulate contractility in human myometrial cultured cells (Martin, 1999; Martin, Hyvelin, *et al.*, 1999).

The phenotypic variability highlighted by the *RYR1*-associated bleeding phenotype has also been identified in other case reports and hence highlighting the vascular involvement of RYR1. Brackmann *et al* (2018) reported a severely affected infant, born at 32 weeks gestation with arthrogryposis multiplex congenita and additional signs of extensive prenatal haemorrhage. Whole exome sequencing revealed pathogenic compound heterozygous MHS-associated *RYR1* variants. Muscle histopathology showed a myopathic pattern with eccentric cores. Interestingly, the patient had prenatal intraventricular haemorrhage resulting in post-haemorrhagic hydrocephalus and epidural haemorrhage affecting the spinal cord (Brackmann, 2018). The CNS bleeding events were considered likely to be at least partially due to the *RYR1* variants identified, as prenatal intraventricular haemorrhage (IVH) is less common with increasing gestational ages and epidural hematomata affecting the brain are uncommon after

atraumatic birth, and particularly rare in the spinal cord (Heyman *et al.*, 2005; Stoll *et al.*, 2010).

Coburger and colleagues reported 10 patients with a history of subarachnoid haemorrhage (SAH) who were systematically screened for *RYR1* variants. Of the four variants found, based on an assessment with standard *in silico* prediction tools, three were predicted as pathogenic with a prevalence of less than 0.0005% in the general population. Although clinical evaluation revealed no differences concerning neurological outcome, presence of vasospasm, ischemic deficits and mean hospital stay between patients with and without *RYR1* variants, the authors concluded that *RYR1* variants may contribute to SAH pathogenesis (Coburger et al., 2017). Furthermore, in a randomised control trial study, dantrolene treatment in patients with vasospasm following aneurysmal SAH demonstrated reduced artery spasm and improved patient recovery. This highlights the role of RyR channels in small vessel constriction and dilation (Sabouri *et al.*, 2017). Further to this, dantrolene combined with nimodipine, resists cerebral artery vasoconstriction in isolated cerebral artery vessels (Salomone *et al.*, 2009) and SAH patients (Muehlschlegel, Rordorf and Sims, 2011).

In 1994, Quane and colleagues first reported the detection of a novel tyrosine to serine variant in a pedigree with MH susceptibility with central cores in muscle biopsies. The pedigree presented with a proband that died during an MH crisis, and several family members diagnosed with MHS. The human substitution variant (rs118192162) originally reported as c.1565A>C (p.Tyr522Ser or Y522S), is found on chromosome 19:38455359 (ENST00000359596.8) (Quane *et al.*, 1994). In mice the same variant c1571A>C (p.Y524S) is found on chromosome 7:28804356 (ENSMUST00000179893.9). Transgenic mice lacking *Ryr1* die perinatally from asphyxia, as a consequence of defective excitation-contraction coupling in the respiratory muscles (Takeshima, 1994). The MH mouse model carrying the knock-in heterozygous *Ryr1*

Y522S variant exhibit typical MH symptoms triggered by isoflurane and heat exposure, as result of increased Ca^{2+} leak from the SR via RyR channels (described further in Chapter 3). The $Ryr1^{Y522S/+}$ mouse model has also been studied in relation to non-neuromuscular phenotypes.

Recently, an abnormal bleeding phenotype in humans has been associated to variants in *RYR1*. Female patients carrying heterozygous or compound heterozygous *RYR1* variants associated with MHS and ERM phenotypes (n=8 of 21 (38%) patients) reported an abnormal bleeding phenotype as determined by a standardized bleeding questionnaire (MCMDM-1VWD). The bleeding abnormality was characterised by severe menorrhagia, postpartum bleeding, gum and/or postoperative bleeding; the same patients may also have evidence of more generalized smooth muscle involvement affecting the bladder and bowel (Lopez, 2016). Lopez and colleagues (2016) demonstrated that the $Ryr1^{Y522S/+}$ mouse had longer tail artery bleeding times compared to wild-type littermates, and more frequent RYR1 associated Ca^{2+} sparks from the SR of $Ryr1^{Y522S/+}$ tail artery smooth muscle cells compared to wild-type cells. This increased bleeding time was suggested to be a result of increased RYR1 channel activity causing increased hyperpolarisation of vascular smooth muscle cells by increased activation of BK_{Ca} channels, thereby decreasing Ca^{2+} influx through the dihydropyridine receptor, leading to smooth muscle relaxation. Interestingly, prolonged bleeding times in Y522S knock-in mice were reversed by pre-treatment with dantrolene, indirectly confirming the adverse impact of the mutant RYR1 channel on vascular smooth muscle contractility. Whilst many of the bleeding symptoms in these *RYR1*-mutated patients could be explained by the adverse impact of dysregulated Ca^{2+} signalling on vascular smooth muscle cell reactivity, post-partum haemorrhage symptoms indicate abnormal myometrial smooth muscle cell contractility as another potential pathogenic mechanism. Further to this, unpublished clinical observations

have highlighted the successful clinical administration of dantrolene in the treatment of menorrhagia in *RYR1*-mutated patients.

1.5 Obstetric bleeding in women with inherited bleeding disorders

Injury to a blood vessel first induces vessel contraction and the initiation of primary haemostasis. Primary haemostasis involves the integration of platelets and von Willebrand factor glycoprotein (VWF). Following injury, collagen, elastin and VWF are exposed which causes platelets to activate and bind to VWF. Activated platelets induce further platelet activation and aggregation which leads to the formation of the haemostatic plug (Orkin *et al.*, 2015). Secondary haemostasis involves coagulation factors, the vessel wall and fibrin. Injury to the endothelial wall of the blood vessel causes the release of tissue factors, which activates Factor VII that forms the activated tissue factor/FVIIa complex which triggers the downstream coagulation pathway and the formation of thrombin. The final step involves the activation of FXIII which crosslinks fibrin to form the fibrin clot. Other coagulation factors such as protein C, S, antithrombin, and plasmin also support the coagulation and balance excessive thrombus formation (Versteeg *et al.*, 2013). Therefore, variants in genes encoding any of these important factors can lead to serious bleeding disorders, with variable degree of presentation.

The most common of these disorders is von Willebrand disease (vWD) which affects 1% of the general population and often remains undiagnosed (Rodeghiero, Castaman and Dini, 1987; Bowman *et al.*, 2010). Von Willebrand disease is an autosomal dominant trait caused by a reduction in plasma VWF (Leebeek and Eikenboom, 2016). The other two most common diseases are haemophilia A (Factor VIII deficiency) and haemophilia B (Factor IX deficiency), both are inherited in an X-linked fashion. Platelet dysfunction disorders are categorised by abnormal platelet aggregation, secretion, coagulant activity or size and number (Sharathkumar and Shapiro, 2008).

VWD is more often diagnosed in women than men, with 7,071 women and 4,081 men diagnosed in the UK however it is estimated that at least 35,000 women are undiagnosed

(*Women with Bleeding Disorders*, date accessed 19th March 2023). Women tend to present with more bleeding symptoms which can be attributed to obstetric haemostatic challenges (Sadler *et al.*, 2000). Women are carriers of the X-linked disorders that predominantly affect males, with the prevalence of haemophilia A affecting 1 in 5000 males and Haemophilia B affecting 1 in 30000 males. Factor X deficiency is a rare disorder that affects 1 in 500,000 individuals (Uprichard and Perry, 2002).

Many individuals with bleeding disorders are diagnosed with the help of a commonly used and validated clinician administered Molecular and Clinical Markers for the Diagnosis and Management of Type 1 (MCMDM-1) VWD bleeding questionnaire. This bleeding assessment tool is used to distinguish whether an individual has a bleeding disorder and which type of VWD (Bowman *et al.*, 2008). Although men and women with bleeding disorders have similar symptoms, women have added complications during menstruation, pregnancy, labour, and delivery, making women disproportionately affected by bleeding disorders (VWD). However, it is estimated that at least 0.017–0.19% of individuals (in the USA), particularly women, have undiagnosed or misdiagnosed VWD or another bleeding disorder (Sidonio, Zia and Fallaize, 2020).

Indeed, coagulopathies and VWD are a leading aetiology of heavy menstrual bleeding (HMB). Studies of women with HMB have shown that between 5% and 24% cases have VWD (Zia *et al.*, 2020). In a systematic review, the incidence of VWD was revealed to be 13% in a cohort of 988 women with HMB (Shankar *et al.*, 2004). However, it is estimated that 50% of HMB cases do not receive a definitive diagnosis (Lee *et al.*, 1984; Oehler and Rees, 2003; Byams, 2007). Post partum haemorrhage (PPH) is also symptom of VWD and other coagulopathies. WF and FVIII levels can rise two- to fivefold by the third trimester in women without VWD. Whereas women with abnormal VWF levels, typically associated with VWD Type 2, do not

maintain increased levels of VWF-FVIII proteins, making them at risk of PPH and often require replacement therapy (Castaman, 2013; Hawke *et al.*, 2016). Of the four T's indicating risk factors of PPH (tone, tissue, trauma and thrombin), 'Thrombin' i.e. coagulation disorders are causative of 1.5% cases of severe PPH (Nyfløt *et al.*, 2017). The reported incidence of PPH is between 5-15% of deliveries (Zwart *et al.*, 2009; Bateman *et al.*, 2010; Tunçalp, Souza and Gülmezoglu, 2013; Dupont *et al.*, 2014), however it is estimated that 11% of vaginal deliveries have undiagnosed PPH (Girault *et al.*, 2018).

1.6 Myometrium in the reproductive cycle, gestation, and parturition

Changes in intracellular calcium regulate the coordinated contraction of smooth muscle cells which plays an important role in myometrial contraction during menstruation and labour (Li *et al.*, 2014; Dodds, Staikopoulos and Beckett, 2015). To understand how variants in *Ryr1* (specifically Y522S), might cause excessive bleeding and abnormal uterine contractions, it is essential to understand how RyR channels normally function in smooth muscle cells of (1) the myometrium during menstruation, gestation, and labour; (2) the uterine vasculature during menstruation, gestation, and post-partum.

1.6.1 Structure of the uterus

The human uterus is pear shaped, with a single triangular shaped cavity located between the fallopian tubes and the cervix. There are three distinct layers of the uterus, the innermost being the endometrium, next to the myometrium and outmost being the perimetrium, see Figure 3A. Of relevance to this thesis, the human myometrium consists of smooth muscle fibres organised into two layers: the inner layer and outer layer which has a higher elastin content although the organisation of fibres is less well defined than in rodents (Baah-Dwomoh *et al.*, 2016).

Female mice have a bicornuate uterus consisting of two lateral horns (cornua) that join to form a single body (corpus), see Figure 3B. Similar to the human uterus, each horn also consists of a smooth muscle layer. The mouse myometrium comprises two distinct smooth muscle layers: an outer layer with longitudinal muscle fibres and a thicker inner layer of circular fibres, which are separated by loose, highly vascular connective tissue, the stratum vasculosum. (Brody and Cunha, 1989; Rendi *et al.*, 2012).
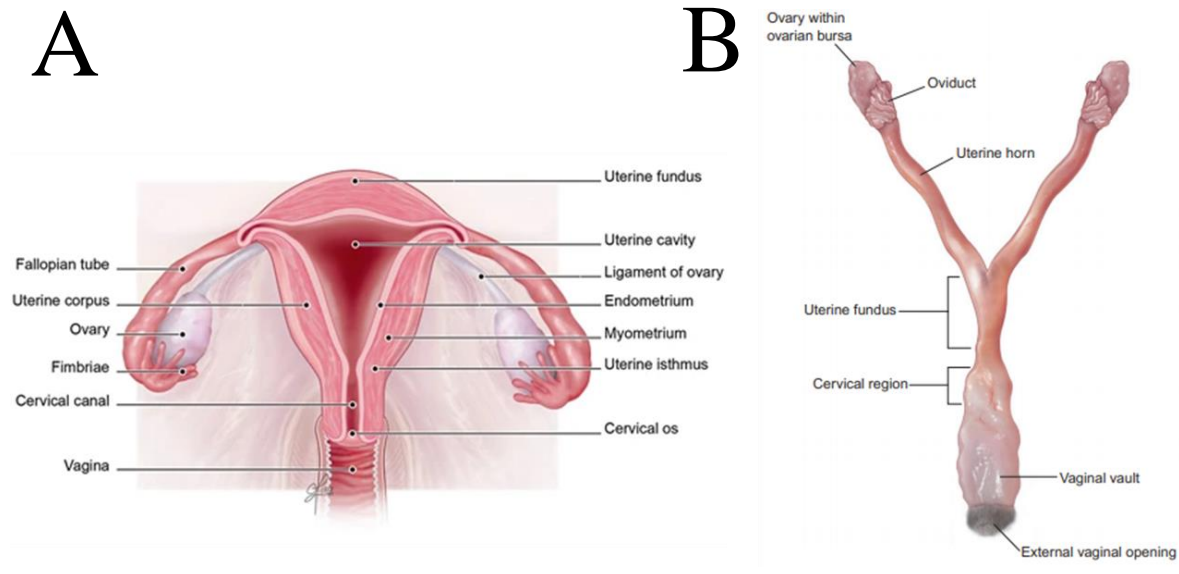
Figure 3. Coronal *ex vivo* sections of the non-pregnant (A) human and (B) mouse reproductive anatomy

(A) A non-pregnant human uterus. From (Ramírez-González *et al.*, 2016). (B) the non-pregnant mouse uterine horns. From (Rendi, 2012), permissions obtained as detailed in Appendices.

1.6.2   The mouse oestrus cycle

The mouse oestrus cycle is 4-6 days in length and is divided into four phases; dioestrus, proestrus, oestrus, and metestrus. The first stage (proestrus) begins when a new batch of eggs reach maturity within ovarian follicles, followed by the ovulation of fully mature oocytes (oestrus). During metestrus, the mature eggs move through the oviducts and into the uterus. At the end of metestrus, the act of successful copulation induces hormonal changes that prepare the uterus for pregnancy. If pregnancy does not occur, the last phase of the cycle, dioestrus, occurs, where unfertilized eggs are eliminated, and new follicles begin to undergo a rapid growth for the next ovulation (Allen, 1922; Ajayi and Akhigbe, 2020).

The propagation speed of contractions in the mouse uterine horns are slower and stronger during oestrus and dioestrus than in proestrus and metestrus. It is presumed that contractions during oestrus serves the functional role of propelling a released ovum toward the uterine horn.

Whereas the erratic contractions during metestrus propagate toward both the oviduct and the uterine body, which is assumed to assist with the implantation of fertilized oocytes in the uterine wall. The short contractile bursts in dioestrus are thought to aid in the movement of unfertilized eggs and endometrial debris along the duct (Dodds, 2015). Thus, RyR channels expressed or even implicated in CICR in the murine non-pregnant myometrial cell, could also play a role in the normal contractility of the non-pregnant mouse myometrium (Taggart and Wray, 1998; McCallum, Greenwood and Tribe, 2009; McCallum *et al.*, 2011).

1.6.3   The human menstrual cycle

The human menstrual cycle is typically 28 days long, however this is highly variable, ranging from 21 to 37 days (Chiazze *et al.*, 1968; Treloar *et al.*, 1970; Long, 1990). The regular menstrual cycle length reflects a woman's general health, with noticeably irregular and long cycles attributed to disruption of the hypothalamic-pituitary-ovarian axis, increasing age, in addition to several other non-communicable diseases ('ACOG Committee Opinion No. 651: Menstruation in girls and adolescents: using the menstrual cycle as a vital sign', 2015; Wang *et al.*, 2020).

The menstrual cycle involves changes in the follicles in the ovary (ovarian cycle), and changes in the endometrial lining of the uterus (uterine cycle), in response to predictable fluctuations of ovarian hormones oestradiol (E2) and progesterone (P4), from the production of luteinizing hormone (LH) and follicle-stimulating hormone (FSH) by the pituitary gland and regulation by the hypothalamus, demonstrated in Figure 4 (Barbieri, 2014). The endometrium undergoes a steroid-induced proliferative stage (regeneration) during the follicular phase, differentiation in the luteal phase and shedding (menstruation). The process of menstruation in the late secretory

phase is the response of the endometrium to progesterone (and oestradiol) withdrawal at regression of the corpus luteum (Jabbour *et al.*, 2006). Progesterone withdrawal results in vasoconstriction, cytokine changes and tissue ischemia (Kelly, King and Crithley, 2001). The endometrium releases prostaglandins that cause contraction of the myometrium and shedding of the endometrium (Henzl *et al.*, 1972). Within two days of the start of menses, oestrogen produced by the growing ovarian follicles stimulates the regeneration of the endometrial epithelium. The oestrogen causes prolonged vasoconstriction enabling the formation of a clot over the endometrial vessels (Edman, 1983; Reed and Carr, 2018).
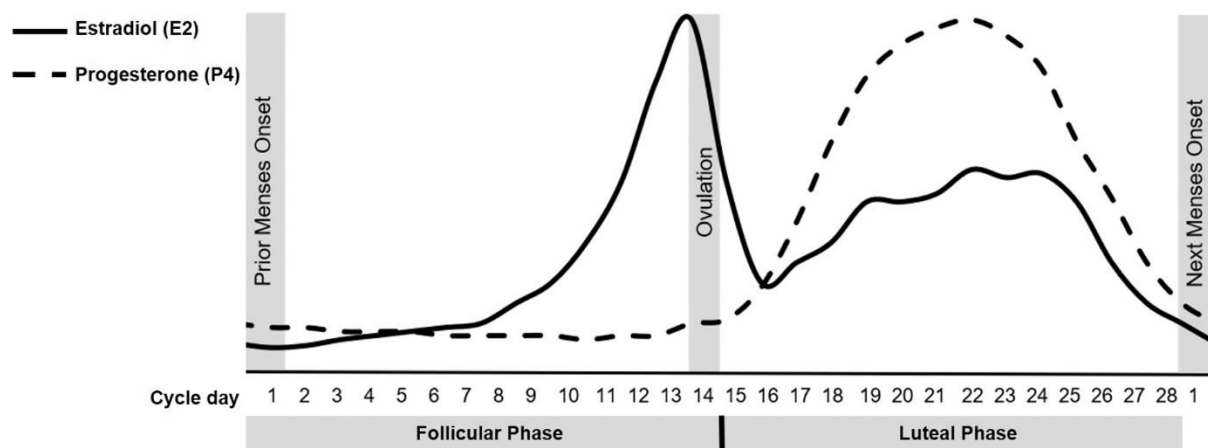
Figure 4. Human menstrual cycle with characteristic fluctuations of the ovarian hormones estradiol (E2) and progesterone (P4) in the follicular and luteal phases, from (Schmalenberger et al., 2021).

The duration of menses is variable, considered to be days 0 to 5 of the menstrual cycle, however menstrual flow can vary from 1 day to 8 days in a healthy female, with the heaviest bleeding reported in the first 2 days of menses (Chiazze, 1968; Treloar, 1970). Menstrual blood is typically arterial, with only 25% being venous. Typical blood loss ranges between slight spotting and 80 mL with an average loss of 30 mL (Hallberg *et al.*, 1966; Sriprasert *et al.*, 2017). The loss of more than 80 mL of blood is considered abnormal and can be attributed to

various factors including coagulation and other bleeding disorders, endometrial thickness, and certain medications (Thiyagarajan, Basit and Jeanmonod, 2022). To ensure the timely cessation of menstrual/endometrial bleeding three events must occur, 1) efficient vasoconstriction of spiral arterioles, 2) an effective haemostasis response, 3) appropriately timed re-epithelialization of the denuded basal endothelium (Maybin and Critchley, 2009; Maybin, Critchley and Jabbour, 2011; Maybin and Critchley, 2015). The failure of any of these responses can lead to aberrant menstrual bleeding.

1.6.4 Myometrial function in menstruation

The smooth muscle of the non-pregnant human uterus exhibits contractile activity during menstruation and can be a cause of dysmenorrhoea. There are 'sustained contractions' during menstruation that are focal and involves sporadic bulging of the myometrium (Togashi, 2007); contractions last for several minutes and often involves the entire layer of myometrium. There is also 'uterine peristalsis' related contractile activity, which initiates rhythmic 'wave-like' contractions that are responsible for the shedding of the sub-endometrial myometrium and helps to transport spermatozoa from the external os of the cervix to the fallopian tubes (Kunz and Leyendecker, 2002). During the early menstrual phase (day -1 to day +2), myometrial contractility is increased (more like labouring tissue with high amplitude, low frequency, and low basal pressure tone) in comparison to the late mentrual phase (day +3 to day +5) (Hauksson, Åkerlund and Melin, 1988; Bulletti *et al.*, 2000, 2004).

1.6.5   Disorders of menstruation

In 2011, the Federation of International Gynaecology and Obstetrics (FIGO) proposed a new classification system for causes of abnormal uterine bleeding, 'PALM-COEIN' (Polyp, Adenomyosis, Leiomyoma, Malignancy and hyperplasia, Coagulopathy, Ovulatory dysfunction, Endometrial, Iatrogenic, and Not yet classified) (Munro *et al.*, 2018; Munro, Critchley and Fraser, 2019). Abnormal uterine bleeding (AUB) (replacing dysfunctional uterine bleeding (DUB), and encompasses various pathologies such as menorrhagia, dysmenorrhoea, irregular, frequent or prolonged periods, oligomenorrhoea and amenorrhoea (Livingstone and Fraser, 2002). Several of these disorders are rooted in disturbances of the hypothalamic-pituitary-ovarian axis, morphological changes within the uterus that are not caused by the endometrium, ovarian failure, disordered regulation of gonadotrophin secretion, and polycystic ovary syndrome (PCOS) (Lemarchand-Béraud *et al.*, 1982; Adams *et al.*, 1985).

The term *heavy menstrual bleeding* (HMB) has been recently favoured over *menorrhagia*, defined by UK NICE as "excessive menstrual blood loss, which interferes with the woman's physical, emotional, social and/or material quality of life" (National Institute for Health and Excellence (UK), 2021). HMB is estimated to affect 18-38% of women of a reproductive age, and may increase in prevalence in women approaching menopause (Santos *et al.*, 2011; Fraser *et al.*, 2015; Samani *et al.*, 2018; Ding *et al.*, 2019; Kocaoz, Cirpan and Degirmencioglu, 2019). Approximately 30,000 women undergo surgical treatment for HMB each year. Almost half of the women that attend their first outpatient gynaecological appointment for HMB, also report problems such as fibroids, endometriosis and/or polyps (Shapley, Jordan and Croft, 2004; The Royal College of Obstetricians and Gynaecologists, 2014). Underlying bleeding disorders such as von Willebrand disease (5-24%) (Rodeghiero, 1987), platelet dysfunction (50%) (Philipp *et al.*, 2003, 2005) and single factor deficiencies (1-4%) (Kadir *et al.*, 1998; Dilley *et al.*, 2001;

Philipp, 2005) account for a large proportion of the women presenting with unexplained menorrhagia. Nevertheless, in a large proportion of women who report HMB (some report as high as 50% of cases) no pathology is determined (Lee, 1984; Oehler, 2003; Borzutzky and Jaffray, 2020).

Studies have suggested that the pathogenesis of menorrhagia lies with abnormal uterine blood flow. For example, lower uterine artery flow resistance (measured as pulsatility index) has been correlated with increased menstrual blood loss (Hurskainen *et al.*, 1999). In addition, the dysregulation of smooth muscle contraction of endometrial vessels (by smoothelin and calponin) could be important in menorrhagia (Shivhare *et al.*, 2014).

1.6.6 Gestation length and labour duration

The normal function of the myometrium is essential during pregnancy, particularly in determining gestation length and duration of labour. The normal length of human gestation is routinely assigned as 280 days after the onset of a woman's last menstrual period, however on average, the time from ovulation to birth has been reported as 268 days (38 weeks, 2 days) (Jukic *et al.*, 2013). Post-term pregnancy is defined as $> 42^{+0}$ weeks of gestation; late term is 41^{+0} to 41^{+6} weeks of gestation; 39^{+0} to 40^{+6} weeks of gestation is considered full-term and 37^{+0} to 38^{+6} weeks of gestation is early-term (*Definition of Term Pregnancy | ACOG*, date accessed 06 March 2023; Spong, 2013). Preterm birth is commonly defined as any birth before 37 weeks of gestation of or fewer than 259 days since the first day of the woman's last menstrual period, and is further subdivided by gestational age (GA) as follows: extremely preterm (< 28 weeks); very preterm (28 to < 32 weeks); moderate or late preterm (32 to < 37 completed weeks of gestation) (Kinney, Lawn and Howson, 2012). Aside from inaccurate dating (Neilson, 2000), increased gestation length is commonly reported in women of an older age, increased BMI in

first trimester, increase cervical length, previous prolonged pregnancies and in women who themselves are products of a prolonged pregnancy (Mogren, Stenlund and Högberg, 1999; Kistka *et al.*, 2007; Denison *et al.*, 2008; Galal *et al.*, 2012; Jukic, 2013; Soysal and Işıkalan, 2020).

In humans the length of labour can vary in response to several factors, including a womans parity (nulliparous women have a longer labour compared to parous women) (Abalos *et al.*, 2018); pelvic shape and size (narrow pelvis may contribute to longer labour); maternal age (labour increase with age) (Chen *et al.*, 2018); BMI (increased labour in those with higher BMI) (Hirshberg, Levine and Srinivas, 2014); fetal position (optimal position will increase speed of labour); myometrial contraction strength and timing; use of labour-inducing drugs (can intensify and speed up labour) (Direkvand-Moghadam *et al.*, 2015); and use of epidural (can reduce duration of labour) (American Society of Anesthesiologists (ASA), no date).

Mouse studies are commonly used to study alterations in gestation length and complications in pregnancy. The length of gestation in the mouse is predominantly genetically determined, varying between 457 to 489 hours (19.04 to 20.4 days), with gestation length being 462.4±21.0 hours (19.3 days) in C57BL/6J, 483±23.3 hours (20.1 days) BALB/cByJ and 486.3±23.2 hours (20.3 days) in 129S1/SvImJ (Murray *et al.*, 2010). The length of mouse gestation has a strong inverse correlation with litter size (larger litters tend to be born earlier) (Rugh, 1968), and increases when the pregnant animal continues to nurse a previous litter (Grüneberg, 1943; Bronson *et al.*, 1967). Similar to humans, in C57BL/6J mice with increasing maternal age the length of gestation and length of labour also increases (Patel *et al.*, 2017).The reported mean length of labour in three month old C57/B6 mice is approximately 1 hour, which increases to approximately 4 hours in 8 month old mice (Patel, 2017). Therefore such well-documented mouse models of pregnancy can be easily manipulated (by transgenic or pharmacological

means) and controlled to enable the precise functional study of alterations in myometrial function that could lead to delayed onset of labour or labour duration.

1.7   Intracellular Ca^{2+} and contractile mechanisms in myometrial smooth muscle cells

Complications of pregnancy and childbirth include pre-eclampsia, preterm labour/birth, premature rupture of membranes, infection, intrauterine growth retardation, prolonged pregnancy (beyond 41 weeks of gestation, see page 53), dysfunctional labour and post-partum haemorrhage (Wray, 2015). Some of these pathologies primarily involve the aberrant contraction/relaxation of the myometrium or the blood flow to the myometrium, therefore understanding the basis of myometrial and uterine artery function is key to understanding the underlying mechanisms in several pregnancy complications.

Uterine smooth muscle is spontaneously active, therefore changes in membrane potential are necessary to initiate contraction, which is dependent on: the generation of an action potential, a transient rise in Ca^{2+}, the presence of contractile machinery and a conductance system between uterine cells (Wray *et al.*, 2003). 'Slow waves' have been reported, when a threshold for action potential activation is reached which then leads to rhythmic contractions. The resting membrane potential is mainly due to the electrochemical gradient largely created by the potassium ions (K^+) concentrated inside the cells and to a lesser extends by calcium, sodium, and chloride ions (Ca^{2+}, Na^+, Cl^-) concentrated extracellularly. During gestation, the myometrial cell maintains a highly negative internal charge, which reduces the likelihood of contraction. This is maintained by the activity of the plasma membrane Na^+/K^+ -ATPase, which expels three Na^+ for every two K^+ that enter the cell and exit of K^+ via a variety of open K^+ channels via the ionic gradient (Smith, 2007). Various factors increase intracellular cyclic AMP (cAMP) which maintain the myocyte in a relaxed state. Increased cAMP activates protein kinase A, which promotes dephosphorylation of myosin light kinase (MLCK) which is required to generate uterine contractions (Smith, 2007; Sanborn, 2016). As term approaches, the resting membrane potential of myometrial cells gradually increases (rising from -70 mV at week 29

to −55 mV at week 40), making the myometrium more excitable (Parkington, Tonta, Brennecke, *et al.*, 1999; Khan *et al.*, 2001; Tribe, 2001; Tribe and Taggart, 2007).

There are two main mechanisms of excitation-contraction coupling: electrochemical coupling and pharmaco-mechanical coupling. In electrochemical coupling, the generation of an action potential in the uterine smooth muscle cell depolarizes the cell membrane and opens the L-type Ca^{2+} channel, the primary ion channel responsible for the Ca^{2+} entry (Shmigol, Eisner and Wray, 1998). The intracellular Ca^{2+} spike in the myometrium is terminated relatively quickly by partial repolarisation by both voltage- (I_{K1}, I_{K2} and $I_{K,A}$) (Knock, Smirnov and Aaronson, 1999; Parkington, Tonta, Davies, *et al.*, 1999) and Ca^{2+}-sensitive (BK_{Ca} [Maxi K] and SK_3) potassium currents (Khan, 2001). The large conductance voltage-gated Ca^{2+}-activated K^+ channel (BK_{Ca}) channels have been proposed to play an important role in buffering contractility of the human myometrium to maintain quiescence during pregnancy, and the shift to a more contractile state during labour (Lorca *et al.*, 2014). It has been suggested that in cultured myometrial cells, the opening of BK_{ca} channels causes a strong repolarising current maintaining myometrial smooth muscle cells at a polarised state, preventing voltage-gated Ca^{2+} entry and contraction (Wakle-Prabagaran *et al.*, 2016), although functional data in rodents and human myometrium taken at term does not always confirm this (Tribe, Moriarty and Poston, 2000; Aaronson *et al.*, 2006). It has been shown that during labour BK_{ca} in the myometrium become more insensitive to Ca^{2+} (Khan *et al.*, 1993, 1997; Khan, 2001).

In pharmaco-mechanical coupling, agonists including oxytocin and prostaglandin F_{2a} drive the increase in intracellular Ca^{2+} by receptor-agonist binding (Shmygol *et al.*, 2006). This causes G-proteins to bind GTP and activate phospholipase C (PLC), which cleaves phosphatidylinositol biphosphate (PIP_2), making inositol triphosphate (IP_3) and diacylglycerol

(DAG). DAG then activates PKC and IP_3 binds to the IP_3 receptor on the sarcoplasmic reticulum, further augmenting uterine contractions, demonstrated in Figure 5.

The central process in generating force from myometrial smooth muscle contraction is the attachment and detachment of cross-bridges between myosin and actin filaments (Word *et al.*, 1993). Myosin light chain is activated by phosphorylation by myosin light chain kinase, which is activated by calmodulin. Calmodulin has four Ca^{2+} binding sites, which when occupied, initiate interactions between calmodulin and MLCK. This is how the Ca^{2+} influx during an action potential is connected to contraction, the process of excitation-contraction coupling (Blanks, Shmygol and Thornton, 2007). For uterine relaxation, myosin light chain phosphatase (MLCP) dephosphorylates the phosphorylated myosin.

Ca^{2+} is stored in the SR of the myometrial cell, as already mentioned in previous sections, and in rat myometrial cells its volume/capacity increases with gestation (Garfield and Somlyo, 1985) and is located close to the periphery (Broderick and Broderick, 1990). Ca^{2+} ions can be released from the SR via two channels 1) IP_3 channels that are activated by IP_3 and 2) RyR channels which are activated by Ca^{2+} (Ca^{2+} induced Ca^{2+} release, CICR). It has been suggested that there is no or little role of Ca^{2+} induced Ca^{2+} release (CICR) in primary human myometrial cells (Holda *et al.*, 1996; Taggart, 1998). However, disturbances in Ca^{2+} release from intracellular stores could impact the normal cytosolic ionic balance within the myometrial cell. The relaxation of myocytes is controlled by the efflux of Ca^{2+} out of the cytosol into the SR and the extracellular space, largely controlled by SERCA channels on the SR membrane and Na/Ca exchanger (NCX) on the plasma membrane.
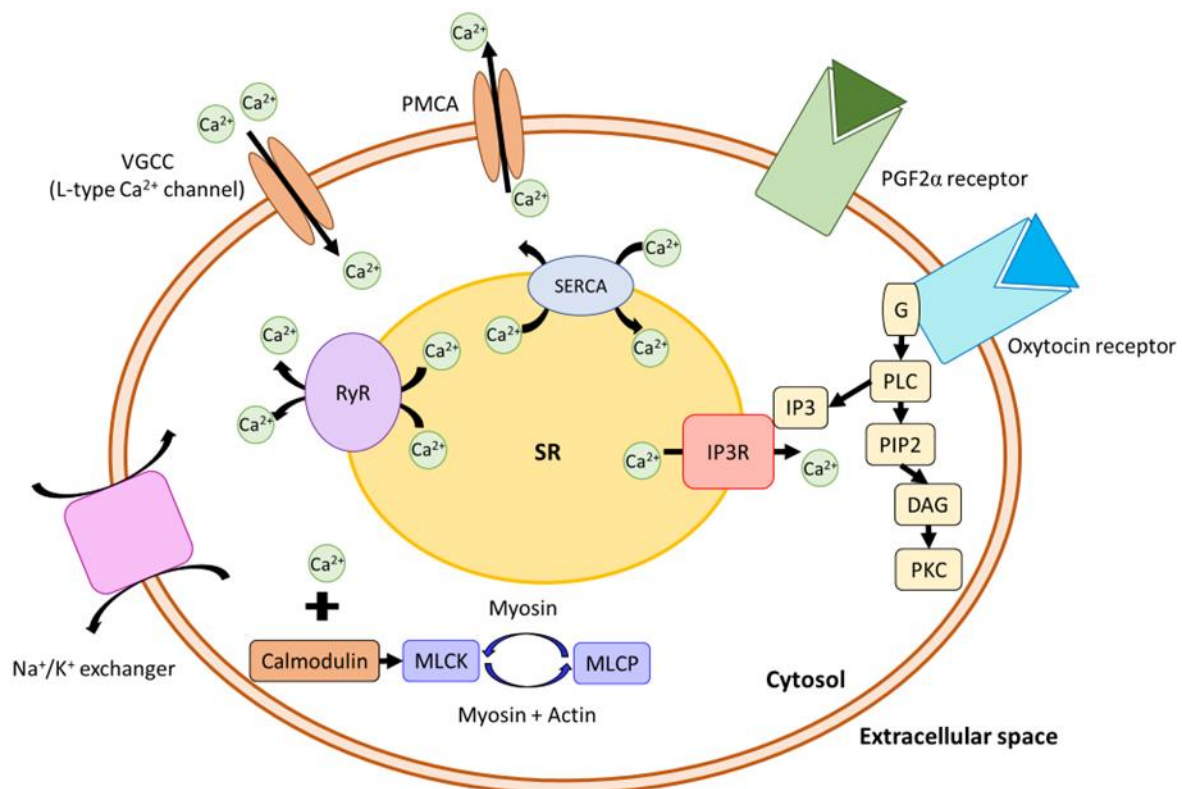
Figure 5. A schematic diagram showing the movement of Ca^{2+} and the initiation of contraction in myometrial smooth muscle cells.

Depolarization of plasma membrane opens the voltage gated Ca^{2+} channel (VGCC, L-type Ca^{2+} channel) resulting in Ca^{2+} influx into the cell. Ca^{2+} binds with calmodulin and activates myosin light chain kinase which then phosphorylates the light chain of myosin. Phosphorylated myosin binds with actin and initiate cross bridge cycling leading to uterine contraction. Relaxation is triggered by dephosphorylation of the light chain of myosin by myosin light chain phosphatase and calcium extrusion outside the cell across the plasma membranes via Ca^{2+}-ATPase and/or sequestration into the SR by SERCA pumps and/or by Na$^+$/ Ca^{2+} exchanger. Oxytocin and other uterine stimulants enhance contraction by binding to their specific receptor on the cell membrane, activating G-proteins to bind GTP and activate PLC. This subsequently cleaves phosphatidylinositol biphosphate and generates inositol triphosphate and diacylglycerol second messengers. IP3 then binds to its receptor at the on the SR and increases [Ca^{2+}]$_i$. VGCC, Voltage-gated Calcium channel (L-type Ca^{2+} channel); MLCK, myosin light chain kinase; MLCP, myosin light chain phosphatase; PMCA, plasma membrane Ca^{2+}-ATPase; SERCA, sarco/endoplasmic reticulum Ca^{2+}-ATPase; PLC, phospholipase C; PIP2, phosphatidylinositol biphosphate; RyR, ryanodine receptor; IP3, inositol triphosphate; PGF2α, Prostaglandin F2α receptor; DAG, diacylglycerol; PKC, phosphokinase C; SR, sarcoplasmic reticulum.

1.7.1 Intracellular mechanisms involved in the onset of labour and during labour

For the most of pregnancy, myometrial contractility is suppressed (quiescent), with only occasional low amplitude, low frequency contractions. During this period, the contractile state of the myometrial smooth muscle is suppressed by the down regulation of contractile associated proteins (CAPs), such as gap junctions proteins, uterotonin receptors, PTGS2, and/or the upregulation of pro-quiescence pathways and changes in Ca^{2+} signalling (Norwitz, Robinson and Challis, 1999; Bernal, 2001; López Bernal, 2003; Smith, 2007; Smith *et al.*, 2007; Kamel, 2010). The uterus undergoes functional changes to having phasic rhythmic contractions towards labour, likely through the activation of CAPs which prime the myometrium to respond to uterotonic agents to develop rhythmic contractions (Mesiano, DeFranco and Muglia, 2015). The primary trigger to spontaneous and agonist induced contractions in the myometrium, is a rise in intracellular Ca^{2+}. RyR channels are considered to be a CAP protein, that is activated by transforming growth factor-beta (TGFbeta), the concentration of which is elevated in the human myometrium before the onset of parturition (Hatthachote *et al.*, 1998), indicating a role of RyR channels in the normal process of myometrial preparation for parturition .

In preparation for parturition, (1) the uterus must be converted from a quiescent structure with dyssynchronous contractions to an organ with active co-ordinated phasic contractions, which requires the formation of gap junctions between myometrial cells, the secretion of neurohypophyseal hormones (vasopressin and oxytocin), and stimulation of prostaglandin synthesis; (2) the cervical connective tissues must shift to a state of dilatation. At the end of pregnancy there is a shift in dominance from progesterone to oestrogen, increased oxytocin receptors, increased prostaglandin synthesis in the uterus, increased myometrial gap junction formation, and increased influx of Ca^{2+} into myocytes (Kota *et al.*, 2013a; Sanborn, 2016).

At the onset of labour, the depolarisation of myocytes occurs when PGF2α and oxytocin bind to the cell surface, as previously described. Increased Ca^{2+} in the cell stimulates the opening of voltage-regulated Ca^{2+}-channels resulting in the rapid influx of Ca^{2+} and subsequently depolarisation (Tribe, 2000). In humans, the mechanism by which labour is initiated is uncertain but it is hypothesised that multiple processes occur in parallel to create 'functional' progesterone withdrawal, as outlined by Mitchell and Taggart (Mitchell and Taggart, 2009). As the pregnancy progresses towards labour, increased expression of prostaglandin receptors and the induction of prostaglandin production appears to stimulate uterine contraction in the rat and human uterus (Hirst *et al.*, 1998; Slater *et al.*, 1999; Fetalvero *et al.*, 2008; Kandola *et al.*, 2014; Kim *et al.*, 2015; Ferreira *et al.*, 2019).

The mechanism of prostaglandin-induced contraction at parturition is not necessary in the mouse uterus, but rather more important for luteolysis and progesterone withdrawal (Sugimoto *et al.*, 1997). In mice, progesterone is produced by the corpus luteum during gestation. At term prostaglandin production destructs the corpus luteum which decreases progesterone levels (Mitchell, 2009). In mice, labour is likely triggered by progesterone withdrawal, as early withdrawal results in preterm labour and supplementation results in prolonged pregnancy (Skarnes and Harper, 1972; Dudley *et al.*, 1996; Herington *et al.*, 2018).

In humans, at the onset of labour a reduction of BK_{Ca} α- and β-subunit expression (possibly hormonally regulated) in pregnant myometrium is observed which is consistent with increased myometrial activity (Song *et al.*, 1999; Gao *et al.*, 2009; Lorca, 2014). It is likely that the short-term loss of BK_{Ca} channel functionality leads to a decrease in its buffering ability, depolarization of myometrial cells, an increase in intracellular Ca^{2+} leading to increased actin-myosin contractility during labour in humans and mice. On the other hand an alternative model

suggests that long term decreases in BK_{Ca} channel activity cause NF-κB-p65 translocation and activation of inflammatory pathways (Li, 2014).

In mice, there is evidence for a splice variant of the BK_{Ca} channel (containing stress axis regulated exon (STREX)) which makes the channels more sensitive to Ca^{2+} and is expressed through pregnancy thus promoting myometrial repolarization (Saito *et al.*, 1997). The variant of BK_{Ca} without STREX is upregulated at term (Benkusky *et al.*, 2000).

1.7.2   Role of RyRs in gestation and labour

The contribution of RYR1 in myometrial contraction and relaxation is not well understood. The inhibitory feedback mechanism shown in the vascular smooth muscle cells (VSMCs), via RYR1 Ca^{2+} interaction with BK_{Ca} is presumed to occur in uterine myocytes since BK_{Ca} channels are present in these rodent and human tissues (Eghbali, Toro and Stefani, 2003; Chanrachakul, Pipkin and Khan, 2004). However, the evidence for Ca^{2+} sparks in myometrium is unclear, and it not known how specific mutations in RyRs may influence myometrial contractility. Using both non-pregnant and term-pregnant rat myometrium, Burdyga and colleagues reported that uterine Ca^{2+} sparks from RyR channels do not occur (Burdyga, Wray and Noble, 2007). However, some studies have demonstrated a role of SR RyRs in myometrial function, although the role of the channels being pro-contractile or pro-relaxant have long been disputed. In isolated myocytes, a small effect of CICR has been shown, and in small intact preparations caffeine either has no effect or causes a reduced force and calcium concentration (Morgan and Gillespie, 1995; Stephen Lynn and Gillespie, 1995; Shmigol, 1998; Taggart, 1998).

However, in myometrial cells, the evidence for the expression of *Ryr1* is conflicting, although there is some data to show RYR1 and its isoforms RYR2 and RYR3 may be involved in intracellular Ca^{2+} fluctuations within cell-cultured myometrium. Few studies using end-point PCR/RT-PCR have shown that mRNA of *RYR* isoforms (*RYR1, RYR2, RYR3*) are expressed in pregnant and non-pregnant human and mouse myometrial tissue (Martin, 1999; Mironneau *et al.*, 2002). Both *RYR2* and *RYR3* isoforms are also expressed in the pregnant human myometrium, with *RYR2* also being expressed in non-pregnant myometrium and confirmed in cultured myometrial cells (Awad *et al.*, 1997). In human myometrium the mRNA expression level of *RYR1* remains consistent throughout pregnancy (in non-pregnant, term labouring and non-labouring) whereas *RYR2* and *RYR3* are downregulated at the end of pregnancy (Martin, 1999). The maintenance of *RYR1* mRNA expression at the end of gestation suggests a role for Ca^{2+} release from intracellular stores in the mechanism of uterine contractility during labour. Previously, it was reported that the expression of *RYR2* increased at the end of human pregnancy as opposed to *RYR1* or *RYR3* (Awad, 1997; Matsuki, 2017), which led the authors to conclude that the RYR2 channels may be involved in the intracellular signalling of human non-labouring myometrial tissue, suggesting it's importance in the preparation of the myometrium for parturition

In pregnant rat myometrium the expression of *Ryr3* is dominant, with reduced *Ryr1* and *Ryr2* (Martin, 1999). There is some evidence that RyR isoforms can modify the functions of other RYR channels. One of the splice variants in *Ryr3* creates a dominant negative (DN) protein which can down regulate RYR2 channels via a dominant negative effect, therefore there is potential that variants in *Ryr1* could potentially have a regulatory effect on the *Ryr2* and *Ryr3* isoforms (Jiang, 2003; Chagovetz *et al.*, 2019). To further confirm *RYR* isoform expression in human and mouse myometrial and uterine vascular tissue, more sensitive methods (RT-qPCR) and protein detection methods (western blotting) must be used.

1.8   Uterine artery and blood supply to the uterus and fetus

The uterine artery provides the main source of blood to the uterus during pregnancy, carrying 11% of total cardiac output in late pregnancy in rodents (Ahokas, Anderson and Lipshitz, 1983). The adaptation of the uterine circulation is complex and involves enhanced vasodilation, vascular remodelling, and adaptation of smooth muscle contraction (Adamova, Ozkan and Khalil, 2010). Each horn of the mouse uterus has an arterial and venous supply from the common iliac vessels (El-Akouri *et al.*, 2002). The uterine arteries run parallel to the uterine horns and branches several times to form arcuate arteries that branch further to form radial arteries supplying the tissues of the uterus, demonstrated in Figure 6. The vessel wall consists of multiple cells including endothelial cells (EC), VSMCs, fibroblasts and pericytes and structural components such as elastin and collagen. Uterine arteries and arterioles are considered resistance arteries due to the small vessel diameter (<500 µm). However, pregnancy is accompanied by significant vascular remodelling and increases in arterial structural diameter resulting in reduced resistance to blood flow (Hilgers *et al.*, 2003; Mandala and Osol, 2011).
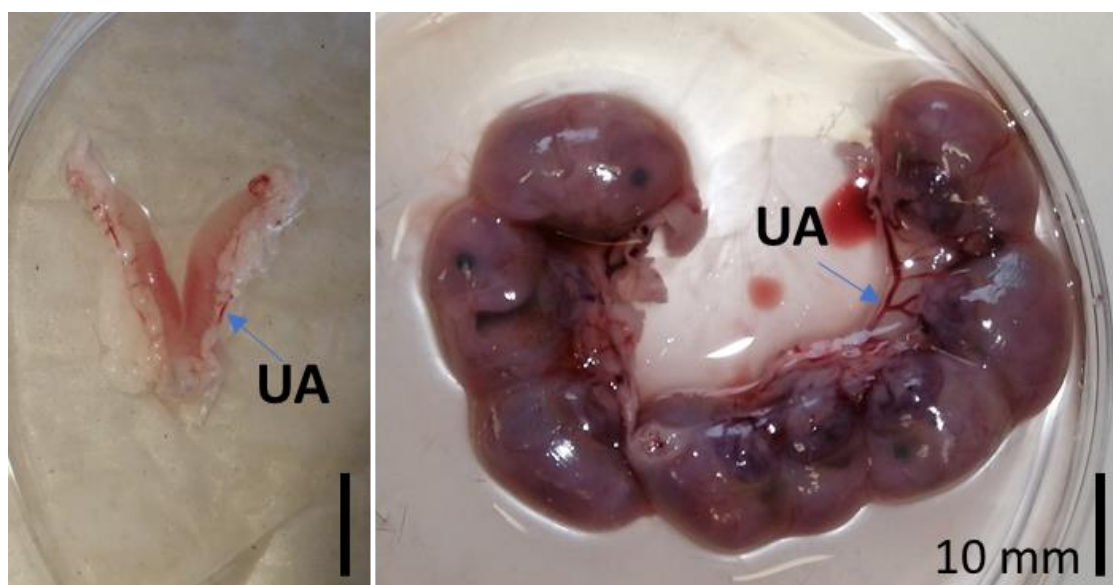
Figure 6. A comparative image of the uterine vasculature in non-pregnant and pregnant mice

Digital images of a non-pregnant uterus with uterine vasculature from a 12-week-old C57/BL6 mouse during oestrus (Left), and a gestation day 18.5 pregnant mouse uterus with attached vasculature and fetuses (Right). UA=Uterine artery. Scale bar=10 mm.

1.8.1 Uterine artery remodelling and adaptation in pregnancy

During pregnancy, arterial remodelling of spiral arteries is essential to the normal progression of pregnancy. The endothelial lining of spiral arteries is replaced by spiral artery trophoblast giant cells (SpA-TGCs) (mice) and extravillous cytotrophoblast cells (humans) cells, resulting in spiral arteries that are extremely dilated and lack smooth muscle (Cross *et al.*, 2002; Harris, 2010). It has been demonstrated that there is cooperation between SpA-TGCs that are required to initiate the process of remodelling, and uterine natural killer cells (uNK) in the regulation of spiral artery remodelling (Hazan *et al.*, 2010; Chakraborty *et al.*, 2011; D. Hu and Cross, 2011; Robson *et al.*, 2012; Rai and Cross, 2014). Therefore, the endometrial vasculature depends on the myometrium to control blood flow to the uterus, which is especially important in controlling blood flow after birth.

Large changes in uteroplacental blood flow are required during gestation and are essential for normal fetal growth. In human pregnancy, the dilated uterine artery diameter is doubled, with similar changes reported in rodents. In mice, during early gestation, uterine artery (by 55.5%) and preplacental radial artery enlarge up to the onset of chorioallantoic placental exchange at ~E9.5, followed by no further increases until a further increase in uterine artery diameter near term (Annibale *et al.*, 1990; Moll, 2003; van der Heijden *et al.*, 2005; Rennie *et al.*, 2016), demonstrated in Figure 6. In human pregnancy, uterine artery diameter increases early in gestation with 70% enlargement of its original diameter by 16 weeks (Dickey and Hower, 1995), and 100% enlargement by 20 weeks (Palmer *et al.*, 1992) and only a further 37% enlargement between 24 weeks and term (Konje *et al.*, 2001).

The growth of the smaller radial vessels precedes that of the larger vessels, suggesting that arterial remodelling may begin in placental and pre-placental vessels, and as gestation continues this progresses proximally to the main uterine artery (Cipolla and Osol, 1994). The

initiation of vascular remodelling is suggested to be influenced by local, rather than systemic factors, as shown in a rodent study where pregnancy was prevented in one uterine horn. At term, the nonpregnant horn was small and showed very little changes in vascular structure, whereas the changes in the pregnant horn were marked. The overall number of fetuses was consistent with 12-14 pups in one horn (twice the normal number per horn) (Forbes and Taku, 1975; Fuller *et al.*, 2009), indicating that local influences such as VEGF/PIGF or PDGF may be responsible.

During the follicular phase of the oestrus cycle in nonpregnant sheep, estrogen (E2):progesterone (P4) ratio is higher and uterine vascular resistance (UVR) is also lower compared to the luteal phase, illustrating the hormonal influence on blood flow. Similarly, during pregnancy there is substantially decreased UVR and increased uterine artery vasodilatation (Sprague *et al.*, 2009), which thought to be the result of estradial 17β and nitric oxide (NO) release linked mechanism and the involvement of the extra-cellular regulated kinase (ERK) pathway (Chen *et al.*, 2004; Sprague, 2009). In healthy pregnancies, uterine blood flow increases 20-50 fold with little change in perfusion pressure (Fuller, Galletti and Takeuchi, 1975; Palmer, 1992), indicating that uterine vascular resistance decreases by the same degree. Early in pregnancy, there is an increase in uterine artery blood flow, due to changes in uterine artery diameter and mean flow velocity, whereas in late pregnancy this rise in blood flow is mainly due to faster mean flow velocity (Palmer, 1992).

1.8.2 Intracellular mechanism of uterine artery vasoconstriction and vasodilation

Vasoconstriction. The contraction of VSMCs of the uterine artery is functionally similar to other VSMCs, i.e., they are dependent on elevation of intracellular Ca^{2+} concentration. However the activation of contraction or the factors that ultimately raise VSMC cytosolic Ca^{2+} concentration, include the myogenic mechanism via activation of stretch-channels, and catecholamines (e.g. norepinephrine and phenylephrine) via adrenergic receptors or anti-diuretic hormones via ADH-receptors (Brozovich *et al.*, 2016).

The main influx of Ca^{2+} into the VSMC cytosol occurs via the voltage-operated L-type Ca^{2+} channels (CaV1.2), and to a lesser extent from the SR via RyR and IP_3R mediated CICR and Rho kinase (Rhok) (Neylon *et al.*, 1995; Sutko and Airey, 1996; Coussin *et al.*, 2000; Löhn *et al.*, 2001; Lopez, 2016), illustrated in Figure 7. These mechanisms allow for the development of contraction within VSMCs to any level of intracellular Ca^{2+}, termed Ca^{2+} sensitization (Somlyo and Somlyo, 2003). Intracellular Ca^{2+} in VSMCs not only determines the contractile state of the cell but also influence the regulation of gene expression of transcription factors which can impact the cell phenotype and vessel reactivity (Cartin, Lounsbury and Nelson, 2000; Kudryavtseva, Aalkjær and Matchkov, 2013).
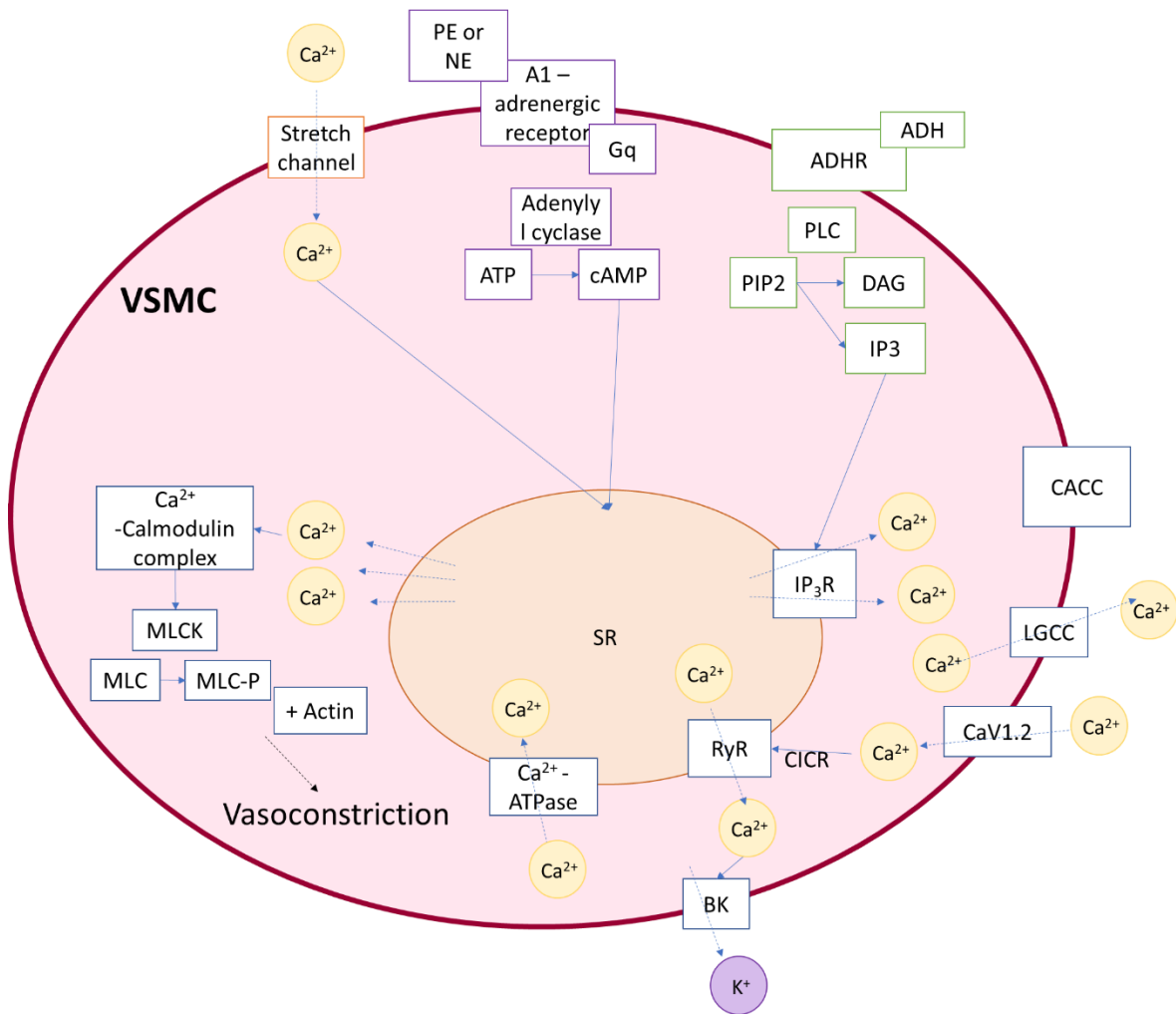
Figure 7. Overview of Ca^{2+} dependent mechanisms regulating vascular smooth muscle cell contraction

Mechanisms of vascular smooth muscle cell (VSMC) contraction and intracellular calcium movement. The main influx of Ca^{2+} into the VSMC cytosol occurs via the voltage-operated L-type Ca^{2+} channels (CaV1.2), and to a lesser extent from the SR via CICR and Rho kinase (not shown). Activation of stretch channels, A1-adrenergic receptors and ADHR induce Ca^{2+} release into the cytosol, enabling the formation of Ca^{2+}-calmodulin complexes which ultimately trigger myosin light chain and actin crossbridge formation. PE, phenylephrine; NE, norepinephrine; ADH, anti-diuretic hormone; PLC, phospholipase C; SR, sarcoplasmic reticulum; LGCC, ligand gated calcium channel; MLCK, myosin light chain kinase; MLC myosin light chain; P, phosphotase; IP$_3$R, inositol tri-phosphate receptor. Image made in Microsoft PowerPoint.

Vasodilation. In vascular smooth muscle cells, regulation of myogenic tone requires the harmononious execution of several contractile and dilatory mechanisms. Relaxation can result from either removal of a contractile stimulus or inhibition of contractility (Freed and Gutterman, 2017). Here I will describe three widely accepted, and arguably most important endothelium dependent vasodilatory mechanisms present in the rodent uterine artery bed (Dalle Lucca, Adeagbo and Alsip, 2000), illustrated in Figure 8, a detailed description of other mechanisms is beyond the scope of this study.

(1) Nitric oxide mediated (second messenger) vasodilation. Numerous stimuli, including acetylcholine, bradykinin, histamine and shear stress can acivate G-protein coupled receptors on the VSMC neighboring endothelial cell membrane which lead to the activation of endthelial nitric oxide synthase (eNOS) that produces NO. Carbachol is an acetylcholine mimetic that stimulates the M3 muscarinic receptors on the uterine artery endothelial cell membrane, that results in IP_3R-mediated release of Ca^{2+} in the cytoplasm (Veerareddy *et al.*, 2002; Stanley *et al.*, 2009). Increased Ca^{2+} ions activate induce NO production, that diffuses into the VSMC and ultimately activates protein kinase G (PKG) (Francis, Busch and Corbin, 2010), which causes VSMC relaxation by 1) negatively regulating membranous and SR Ca^{2+} channels to reduce cytoplasmic Ca^{2+}, 2) positively regulate membrane potassium channels to extrude K^+ ions from the cell and 3) phosphorylating and therefore inactivating MLCK (Mombouli and Vanhoutte, 1999).

(2) *Prostacyclin induced vasodilation*. Increased Ca^{2+} in the endothelial cell also activates phospholipase A_2 (PLA_2), leading to the production of phosphatidylcholine (PC) and arachidonic acid (eicosatetranoic acid) (AA). Cyclo-oxyenase enzymes (COX) convert AA into prostaglandin I_2 (PGI_2), that activates IP receptors on the VSMC membrane, which triggers

downstream signalling and activation of protein kinase A (PKA) which inhibits contraction via phosphorylation of MLCK (Mombouli, 1999; Stanley, 2009; Marshall *et al.*, 2018).

(3) *Endothelium dependent hyperpolarisation-induced vasodilation*. Although this phenomenon is not fully understood, it originates from observations that endothelial cells of small resistance arteries have Ca^{2+} signals (due to shear stress or inflammatory mediators) that are able to hyperpolarise VSMCs (decrease the electrical potential difference across cell membranes i.e. make the membrane more negative) and therefore reduce the activation of VGCCs and, indirectly, the amount of Ca^{2+} ions entering the VSMC (Smiesko and Johnson, 1993; Bevan and Henrion, 1994; Moll, 2003; Gokina, Kuzina and Vance, 2010; Mandala, 2011). There are two widely-accepted mechanisms of EDH beginning in the EC, (1) AA is converted into epoxyeicosatrienoic acid (EET), triggering efflux of K^+ ions from VSMCs, and (2) the contact-mediated pathway, where activation of endothelial intermediate conductance- and small conductance- Ca^{2+} activated potassium channels (IK_{Ca} and SK_{Ca}) induces EC K^+ efflux, and thus K^+ influx from myo-endothelial gap junctions (MEGJ) between EC and VSMCs (Harris *et al.*, 2000; Garland and Dora, 2017). Both of these mechanisms lead to VSMC membrane hyperpolarisation, which inhibits the activation of VGCCs, thus inhibiting the generation of intraceullar Ca^{2+} signals that normally lead to contraction.
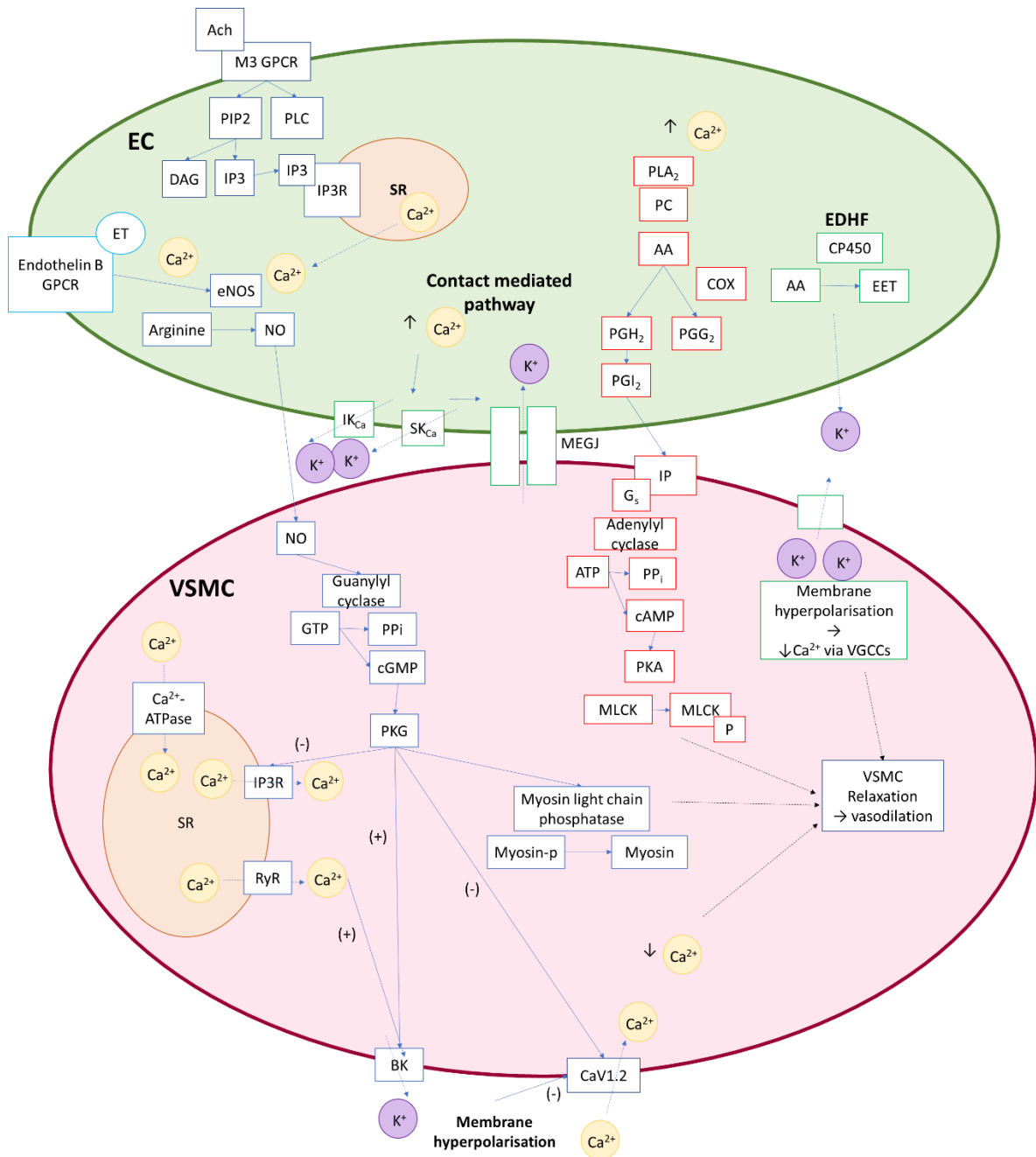
Figure 8. Endothelial dependent mechanisms of vasodilation

Endothelial nitric oxide synthase (eNOS) mediated, contact mediated, prostacyclin mediated, and endothelial derived hyperpolarising (EDH) factor pathways are mechanisms of endothelial dependent vascular smooth muscle cell (VSMC) vasodilation. Endothelial NO production is activated by increases in cytosolic Ca^{2+} by acetylcholine activated M3 endothelial membrane receptors, activation of endothelin receptors. NO localises to the VSMC and triggers PKG activation which reduces cytosolic $[Ca^{2+}]$ leading to vasodilation. As result of increase endothelial Ca^{2+}, prostacyclin are produced which activate IP receptors in the VSMC plasma membrane, resulting in downstream PKA activation and the inhibition of MLCK phosphorylation. EDHF (portrayed as K^+) produced by the endothelial cell causes VSMC hyperpolarisation. GPCR, G-protein coupled receptor; PKG, phosphokinase G; PKA, phosphokinase A; cAMP, cyclic adenosine monophosphate; cGMP, cyclic guanosine monophosphate; RyR, ryanodine receptor channel; SR, sarcoplasmic reticulum; MEGJ, myoendothelial gap junction; ET, endothelin; GTP, guanosine 3′-5′-phosphate; SR, sarcoplasmic reticulum; LGCC, ligand gated calcium channel; MLCK, myosin light chain kinase; MLC myosin light chain; P, phosphatase; IP3R, inositol tri-phosphate receptor.Image made in Microsoft PowerPoint.

1.8.3 RyRs in vasoconstriction and vasodilation

A shift in membrane potential caused by spontaneous transient outward currents (STOCs) at physiological membranes (-30 to -40 mV) is the fundamental regulator of myogenic tone. As described above, in arterial smooth muscle cells, it is suggested that RyR-mediated Ca^{2+} sparks activate STOCs which are mediated by plasma membrane BK_{Ca}, reuslting in K^+ efflux and membrane hyperpolarization. This reduces Ca^{2+} influx by decreasing the open-state probability of voltage-dependent Cav1.2 L-type Ca^{2+} channels, which lowers the global intracellular Ca^{2+} concentration and opposes vasoconstriction (Nelson, 1995; Pérez *et al.*, 1999; Plüger *et al.*, 2000; Yang *et al.*, 2013; Harraz *et al.*, 2014). The RyR Ca^{2+} sparks and BK_{Ca} STOCs are tightly coupled, such that the emergence of a Ca^{2+} spark almost always activates a group of BK_{Ca} channels, and vice versa, inhibition of RyR channels (with ryanodine) suppresses STOCs in VSMCs (Nelson, 1995; Jaggar *et al.*, 2000). Specifically, the β-subunit of the BK_{Ca} channel is critical for the Ca^{2+} sensitivity of the channels, as β-subunit inhibition reduces Ca^{2+} sensitivity, and its presence increases BK_{Ca} channel activity and sensitivity (McCobb *et al.*, 1995; Nimigean and Magleby, 1999; Brenner *et al.*, 2000; Cox and Aldrich, 2000; Amberg *et al.*, 2003; Zhao *et al.*, 2007).

In mouse pregnancy, the BK_{Ca} channel and possibly RYR1 also play an important role in the regulation of uterine artery myogenic tone (X.-Q. Hu *et al.*, 2011; Hu *et al.*, 2017). Rosenfeld and colleagues have shown that blocking BK_{Ca} channels with tetraethylammonium reduces basal uterine flow in pregnant, but not in non-pregnant sheep, indicating that Ca^{2+} spark-STOC coupling is important in regulating uterine blood flow in pregnancy (Rosenfeld *et al.*, 2000; Rosenfeld, Cornfield and Roy, 2001).

Recently, a study has shown that hormone induced pregnancy-like state upregulates RyRs and Ca^{2+} sparks in sheep uterine arteries, which increased STOCs and decreased myogenic tone of

uterine arteries. These STOCs diminished when BK_{Ca} channels and RyRs were inhibited, functionally linking Ca^{2+} sparks and BK_{Ca} channel activity with STOCs (Hu *et al.*, 2019). This indicates that uterine arteries adapt to pregnancy via heightened STOCs and increased Ca^{2+} sparks which ultimately reduces uterine arterial myogenic tone. Therefore the malfunction of RyRs resulting in aberrant Ca^{2+} sparks could impact uterine artery myogenic tone during pregnancy.

Based on our current understanding of intracellular Ca^{2+} movement and signalling in mouse smooth muscle cells of resistance vessels, the gain-of-function RYR1 Y522S channel could alter uterine artery contractility or relaxation based on (i) the cell type it is expressed in (smooth muscle cell or endothelial cell), and (ii) the protein localisation within the cell. Below, I have described four hypothetical scenarios in which the Y522S RYR1 channel could influence uterine artery function.

[1] If the Y522S RYR1 channel is expressed in SMCs, but close to the plasma membrane, the increase in Ca^{2+} could increase activation of plasma membrane BK_{Ca} channels, resulting in a pro-relaxant effect. A hypothesis previously tested and supported by Lopez and colleagues in the tail artery of male $Ryr^{Y522S/+}$ mice and deemed the most likely in this thesis for the reasons outlined above.

[2] If the Y522S RYR1 channel is expressed in SMCs and the channel is deep within the cells, the increase in Ca^{2+} could result in a pro-contractile effect.

[3] If the Y522S RYR1 channel is expressed in endothelial cells, there could be increased activation of small conductance (SK_{Ca}) and intermediate conductance (IK_{Ca}) channels, leading the extrusion of K^+ out of the EC (if EDHF is K^+) and into the SMC, which then activates inwardly rectifying channels and hyperpolarises the cells, resulting in a pro-relaxant effect.

[4] If the Y522S RYR1 channel is expressed in endothelial cells, increased intracellular Ca^{2+} release could trigger endothelin from small intracellular vesicles, resulting in a pro-contractile effect.

1.9 Smooth muscle malfunction and reproductive complications

There are several obstetric disorders associated to dysfunctional SMC contractility or endothelial function, such as pre-eclampsia, ante-partum haemorrhage (APH), and post-partum haemorrhage (PPH). Preeclampsia, or gestational hypertension, is new-onset, persistent hypertension (systolic blood pressure ≥140 mmHg and/or a diastolic blood pressure ≥90 mmHg) in pregnancy which appears most often after 20 weeks gestation and proteinuria. The origins of preeclampsia are associated with failure of trophoblastic invasion of spiral arteries leads to increased vascular resistance of uterine arteries and reduced blood flow (Lin *et al.*, 1995; Phupong *et al.*, 2003; Burton *et al.*, 2019). Antepartum haemorrhage (APH), which complicates 3-5% of pregnancies, is defined as bleeding from the genital tracts occurring from 24^{+0} gestation to prior to the birth of the baby. The causes of APH include placental abruption, placenta praevia, and local causes (for example bleeding from the vulva, vagina or cervix), however often the cause of APH remains unexplained (Royal College of Obstetricians & Gynaecologists (RCOG), 2011).

The WHO report that globally 14 million women experience post-partum haemorrhage (PPH) each year (World Health Organisation (WHO), 2023). Primary PPH is the most common form of obstetric haemorrhage, traditionally defined as the loss of ≥ 500 ml blood from the genital tract within 24 hours of the birth of a baby. PPH can be classified as minor (500 – 1000 ml) or major (> 1000 ml), with the latter being subdivided into moderate (1001 – 2000 ml) and severe (> 2000 ml). Secondary PPH is defined as abnormal or excessive bleeding from the genital tract between 24 hours and 12 weeks post-partum. (Alexander, Thomas and Sanghera, 2002; Mousa *et al.*, 2014). Although women with pre-existing bleeding conditions are at increased risk of PPH, only 1.5 - 3% of those who experience PPH have congenital bleeding disorders (Prendiville W, 1989; James and Jamison, 2007).

The most common risk factor for PPH is uterine atony, followed by retained placenta and cervical/vaginal traumas (*WHO recommendations for the prevention and treatment of postpartum haemorrhage*, no date; Oyelese and Ananth, 2010; Briley *et al.*, 2014; Nyfløt, 2017). Uterine atony is the lack of effective contraction of the uterus in response to oxytocin, and is the most common cause of postpartum haemorrhage being an underlying cause in up to 80% of PPH (Miller and Ansari, 2022). Contraction of the myometrium is required to mechanically compress the SMC-lacking spiral arteries and veins that supply blood to the placental bed, to cause haemostasis, in addition to local haemostatic and coagulation factors.

The failure of the uterine contraction has also been associated with retained placenta or placental fragments. The retained fragment acts as a physical block against uterine contractions, although in most cases uterine atony is the primary reason for placental retention. Placental retention resulting in PPH can also be due to abnormally adherent or invasive placenta causing the placenta to be incapable of separation, a separated placenta being trapped due to the closure of the cervix prior to the delivery of the placenta, or placental hyper perfusion disorders, or infection (Combs, Murphy and Laros, 1991; Kramer *et al.*, 2013; Endler *et al.*, 2014; Urner, Zimmermann and Krafft, 2014; Greenbaum *et al.*, 2017; Perlman and Carusi, 2019). This also highlights the importance of normal placentation in the risk of PPH.

1.10 Placental development and placental vasculature

Considering that RyR channels enable movement of Ca^{2+}, a key signalling molecule in cell growth and proliferation, it is important to understand how RyR channels are involved in the normal development of the placenta to support fetal growth to term. The normal structure, development and implantation of the human placenta differs from the C57/Bl6 mouse placenta but as this thesis is centred on the study of the $Ryr1^{Y522S/+}$ mouse model, the following sections will be focused on mouse placental literature.

1.10.1 A brief description of embryonic placental development

Trophoblast cells and fetal placental vasculature make up the majority of the placenta. The placenta is an organ made of two cell lineages 1) the trophoblast lineage that descends from the trophectoderm which forms the outer layer of the blastocyst, separate to the inner cell mass, and gives rise to placental trophoblast cell types and 2) the extra-embryonic mesoderm, originating from the inner cell mass and epiblast and forming the fetal placental vasculature (Rossant and Cross, 2001).

The first cells to emerge as placental cells form the trophectoderm at the blastocyst stage of development. This outer layer of the blastocyst is set apart from the inner cell mass which goes on to become the embryo proper. The trophectoderm will give rise to all trophoblast cell types in the placenta, except from the fetal endothelial cells of the placental vasculature which arise from the extra-embryonic mesoderm that form the allantois and umbilical cord (Rossant, 2001). The endometrium of the uterus also provides a vital aspect of placental development for the implantation of the blastocyst. The cells of the maternal uterine endometrium undergo decidualization upon blastocyst implantation, this is necessary for embryonic growth and

survival. The decidua goes on to form part of the mature placenta (Ramathal *et al.*, 2010). These tissue contributions are broadly similar in mouse and human placentas, yet the complex composition and interactions of the placenta often makes it difficult to understand where placental malformations originate.

1.10.2 Structure of the mouse placenta

The mature mouse placenta is established around mid-gestation ($\sim$E10.5) and continues to grow in size and complexity up to day 15 and reaches maximum volume by day 18 (Coan, Ferguson-Smith and Burton, 2004). Several studies of placental malformation are strongly focused on the changes in three histologically distinct layers comprising of the labyrinth, junctional zone (JZ) and maternal decidua (illustrated in Figure 9).

Labyrinth

The labyrinth is the largest structure in the placenta and is positioned next to the JZ. The mouse labyrinth contains sinusoids made of syncytiotrophoblast cells that are percolated with maternal blood, across which nutrients and oxygen are transported to the fetal blood circulation (Adamson *et al.*, 2002). There are three continuous cells layers in this exchange barrier; two layers of syncytiotrophoblast (SynT-I and SynT-II) and the extra-embryonic mesoderm-derived fetal endothelial cells (Georgiades, Fergyson-Smith and Burton, 2002). The monolayered sinusoidal trophoblast giant cells (S-TGCs) surround the maternal blood sinusoids, this layer is surrounded by the SynT-I and SynT-II in contact with fetal vessels on the opposite side. The SynT-II cells remain in contact with the fetal endothelial cells. Thus the maternal blood comes into contact with the trophoblast cells rather than the endothelial cells of the vasculature (Watson and Cross, 2005).

The labyrinth layer is the site of placental exchange, in which the maternal blood flow is counter current to the fetal capillary flow. The architecture of the labyrinth provides a large surface area for transport between the maternal and fetal blood supplies, which come into close contact but do not mix (Adamson, 2002). The proper patterning of each cell type ensures the efficient exchange of nutrients and waste between the maternal and fetal blood supplies, which is necessary for proper embryonic growth and viability. Developmental defects in this complicated and intricate structure, including aberrant or underdeveloped vascularisation, branching and dilation can result in impaired placental perfusion and insufficient oxygen and nutrient exchange. Such deficiencies are a frequent cause of developmental failure and growth deficits (Pardi, Marconi and Cetin, 2002; Watson, 2005; Perez-Garcia *et al.*, 2018; Shafiei and Dufort, 2021).

Junctional zone

The junctional zone is situated between the labyrinth and the maternal decidua. The JZ is mostly made up of spongiotrophoblast cells, trophoblast giant cells and glycogen cells, the latter of which invade the decidua from E12.5 and become associated with the maternal blood space. There are two layers that make up the JZ, a layer of trophoblast giant cells (TGC), that directly border the decidua and a spongiotrophoblast layer that contains spongiotrophoblasts and glycogen trophoblast cells. Spongiotrophoblast cells are compact and non-migratory and glycogen trophoblast cells are vacuolated and migrate from the JZ to the decidua (Simmons and Cross, 2005). The spongiotrophoblasts and glycogen cells also surround the central canals that migrate through the labyrinth.

TGCs are known to modify the maternal uterine vasculature, promoting maternal blood flow to the implantation site, and glycogen cells are believed to provide energy and nutrition to the placenta (Simmons, Fortier and Cross, 2007). The junctional zone provides hormones, growth

factors and cytokines for the normal progression of pregnancy that act on both the maternal and fetal physiology (Ain, Canham and Soares, 2003; Soares, 2004). Defects of the JZ cause an altered endocrine environment of the placenta and therefore affect fetal growth due to dysfunctional control of placental growth and structure (Salas *et al.*, 2004; Simmons *et al.*, 2008). JZ defects are considered the leading cause of placental and fetal growth retardations. Such defects can result in systemic effects on both the fetus and mother, for example, alterations in maternal insulin resistance (Fowden and Moore, 2012).

Decidua

The maternal decidua borders the junctional zone. The decidua contains uterine decidual cells, maternal vasculature, immune cells, glycogen trophoblast cells and spiral artery associated trophoblast giant cells (SpA-TGC). The decidual cells are derived from the uterine stromal fibroblast-like cells in the endometrium and are rich in glycogen and lipids. Implantation stimulates stromal cell differentiation and proliferation in response to progesterone. The uterine stromal cells acquire a unique secretory phenotype which facilitate the invasion of trophoblasts and remodelling of the stroma to form the decidua.

After E12.5, the decidua serves as a protective barrier between the developing embryonic tissue and maternal tissue, with high levels of natural killer cells playing an important role in maintaining barrier integrity (Riley, Anson-Cartwright and Cross, 1998; Ma *et al.*, 2001; Escalante-Alcalde *et al.*, 2003). After E16, NK cells decline and the decidua decreases in mass in preparation for birth (Anson-Cartwright *et al.*, 2000). Studies have established that defects in stromal cell decidualisation (or uterine vascular remodelling) at the implantation site leads to a spectrum of pregnancy complications including poor placentation, embryonic rejection or abnormal embryonic development (Woods, Perez-Garcia and Hemberger, 2018).

Bordering the decidua is the metrial gland (metrial cap or metrial triangle), which is a maternal derived placental disc composed of various cells type with a dense bed of winding blood vessels. The metrial gland is formed during the decidualisation process and its function is to aid in the modification of mouse uterine tissue and prepare for placental development during gestation (Elmore *et al.*, 2022).
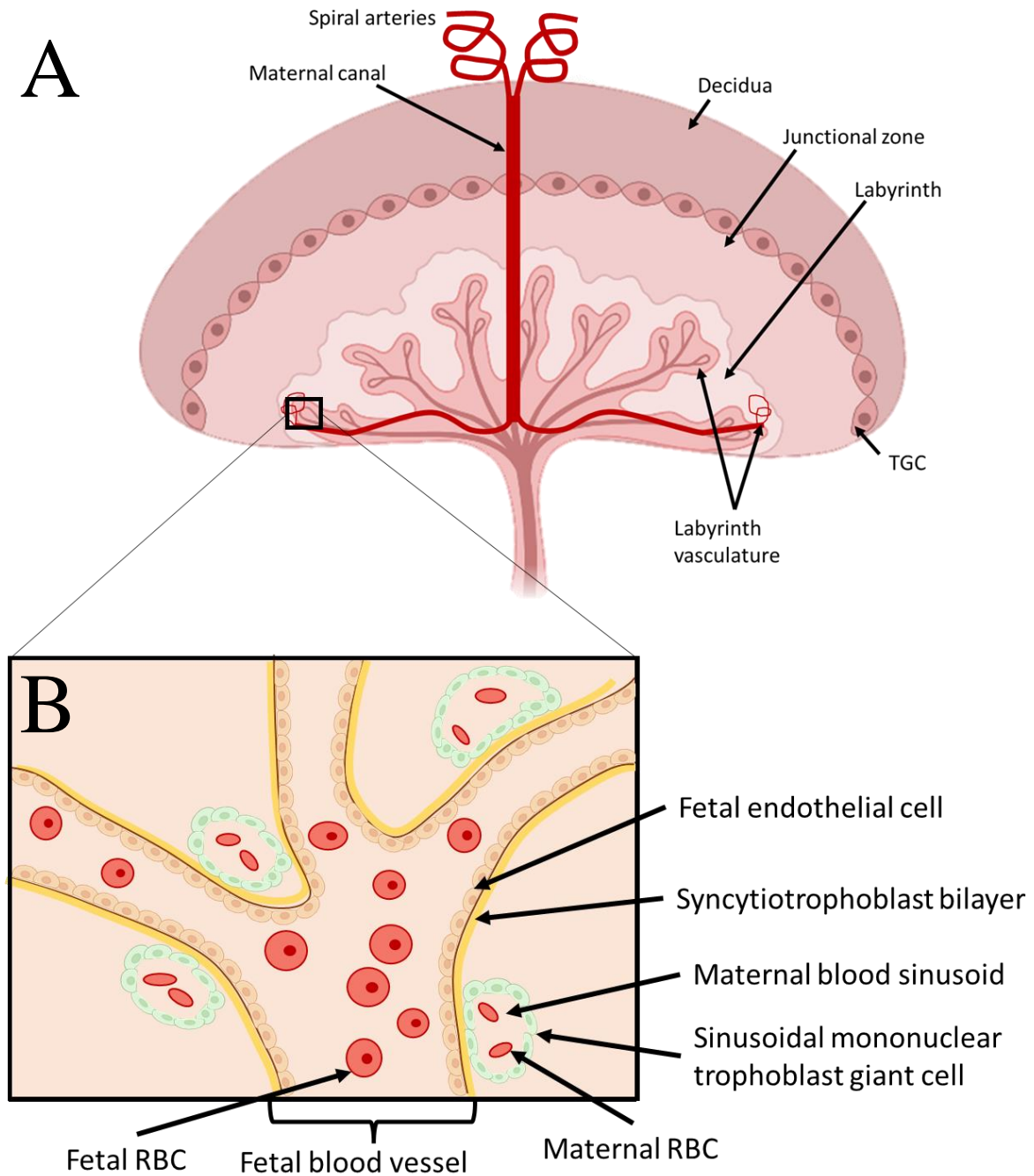
Figure 9. Overview of mouse placental structure around term-gestation.

(A) The three main histologically distinct zones of the placenta are the decidua, junctional zone, and labyrinth. Maternal spiral arteries penetrate the decidua and form the maternal canal which transverses through the junctional zone and labyrinth. **(B)** A close-up view of the interhaemal barrier within the labyrinth. Consists of the fetal side and maternal side. Fetal blood vessels are lined with endothelial cells and the syncytiotrophoblast bilayer (containing cell types I and II), that ate layered against a discontinuous layer of sinusoidal mononuclear trophoblast cells of the maternal sinusoids consisting of maternal red blood cells (description from fetal to maternal side). RBC=red blood cell, TGC=trophoblast giant cell. Imaged created with BioRender.com and Microsoft PowerPoint.

1.10.3 Mouse placental vasculature

Human and rodent placentas are similar in that they are haemochorial in which the fetal blood is surrounded by fetal endothelial cells and maternal blood is surrounded by trophoblast cell types (Wooding and Flint, 1994; Rai, 2014). From E8.0, the embryonic mesoderm gives rise to the fetal vascular compartment (Cross, Simmons and Watson, 2003). The uteroplacental spiral arteries undergo physiological modifications enabling them to cope with an increased blood flow to ensure proper growth of the fetus, such as the SpA-TGC invasion of the lumen of arteries and replacement of the endothelium, causing the progressive disappearance of its normal structure. The uterine blood supply transverses through the myometrium and endometrium and branches into spiral arteries in the decidua that delivers blood to the placenta (Adamson, 2002). The spiral arteries do not branch further into smaller arterioles as in other vascular beds, instead they form straight canals with a large diameter that carry blood from the base of the decidua into small sinusoid spaces, illustrated in Figure 9. After the exchange of nutrients and oxygen in the labyrinth the deoxygenated blood travels out of the complex labyrinth space and converges into channels that transverse the JZ into venous blood spaces. On the venous side, the parietal trophoblast giant cells (P-TGCs) are in direct contact with the decidual endothelial cells (Adamson, 2002; Rai, 2014).

Briefly, in humans, the smaller radial branches of the arcuate arteries travel through the myometrium, progress through the decidua and into the placenta, transforming into spiral arteries (200-500µm diameter) and basal arteries (100-120 µm in diameter) (Brosens, Robertson and Dixon, 1972).

1.10.4 Intracellular Ca^{2+} movement in the developing placenta

Ca^{2+} ions channels are the most widely distributed ion channels in the placenta, although Ca^{2+} movement mainly occurs in the syncytiotrophoblast (Belkacemi *et al.*, 2005; Dörr and Fecher-Trost, 2011). Various voltage-gated L-type Ca^{2+} channels have been identified in the syncytiotrophoblasts (Moreau, Daoud, *et al.*, 2002; Moreau, Hamel, *et al.*, 2002), where they have a role in cell signalling and protein secretion (Belkacemi, 2005). In placental blood vessels, voltage-gated L-type Ca^{2+} channels are involved in regulating fetal-placental vasoconstriction (Jakoubek, Bíbová and Hampl, 2006; Zhao, Pasanen and Rysä, 2023).

RYR1 and *RYR3* mRNA has been detected in human placental cytotrophoblasts and syncytiotrophoblasts (Haché *et al.*, 2011; Zheng, 2022). Recently, RYR1 has been investigated in human placental trophoblast tissues and in BeWo choriocarcinoma cells, a model trophoblast cell-line. Zheng and colleagues (2022) studied the contribution of RyRs in Ca^{2+} signalling and random migration, and the effect of RyR inhibition on reorganization of the F-actin cytoskeleton. The authors found that RYR1 contribute to the reorganization of F-actin filaments in the cytoskeleton induced by angiotensin II, thus demonstrating that RYR1 plays a role in the regulation of trophoblast migration, a key process in placental development (Zheng, 2022).

1.10.5 Disorders of placental formation

The correct development of the placenta plays a pivotal role in determining the aetiology of intrauterine growth restriction (IUGR). In particular, placenta weight has been reported to reflect placental efficiency (Risnes *et al.*, 2009; Eskild and Vatten, 2010; Radan *et al.*, 2022); increased or decreased placenta weight have been associated with adverse fetal outcomes

(Phipps *et al.*, 1993; Khalife *et al.*, 2012). Studies of placental development in mice indicate a molecular basis of pre-eclampsia and early pregnancy termination. Genetically modified mutant mice provide a vital resource for investigating genes that control the differentiation and development of the placental cell lineages, the most important of which is the trophoblast (Cross, 1996; Rossant, 2001). Furthermore, disturbances in Ca^{2+} transport processes are considered to participate in pregnancy-related diseases such as pre-eclampsia and intrauterine growth restriction (Haché, 2011; Woods, 2018).

1.11 Hypothesis and aims of this thesis

Due to the presence of *Ryr1* in several of the reproductive tissues, the impact of the gain-of-function Y522S mutation during pregnancy will be systemic. My working hypothesis is that there will be increased vasorelaxation of vascular smooth muscle cells, impacting on fetal and placental development. Similarly, this will be associated with increased contractility of the uterine myometrium at term, which could impact on the length of gestation and parturition. The *Ryr1* Y522S gain-of-function mutation will modify the cellular needs of the reproductive tissues resulting in altered mRNA expression of *Ryr1* and downstream calcium-handling mechanisms. The *RYR1*-mutated human patient cohort will demonstrate a susceptibility to increased bleeding events, longer bleeding times, increased rate of menorrhagia and a shorter length of pregnancy.

The overarching goal of this study was therefore to determine the impact of the *Ryr1* Y522S gain-of-function mutation on bleeding susceptibility, progression of pregnancy and fetal development. The RyR1 channel modulates calcium movement, therefore several processes can be disrupted during pregnancy as result of channel malfunction. It is therefore unethical and technically difficult to investigate these mechanisms in pregnant women, and as a result, the use of the $Ryr1^{Y522S/+}$ mouse model which closely replicates the previously described human MHS disease phenotype and mild bleeding phenotype is suitable to study the adverse impact of *Ryr1* Y522S on bleeding susceptibility, progression of pregnancy and fetal development.

1.12 Research questions

1. Does *Ryr1* Y522S cause adverse reproductive outcomes?
2. Does *Ryr1* Y522S modify maternal uterine blood flow and fetal development?
3. Does Ryr1 Y522S modify mRNA expression in reproductive tissues?

4. Does the human RYR1 patient cohort demonstrate a susceptibility to bleeding events and adverse reproductive outcomes?

1.13 Objectives

1. To perform a literature review of other predominantly skeletal muscle genes that are also involved in smooth muscle function.

Using the *Ryr1*$^{Y522S/+}$ mouse model:

2. To determine how *Ryr1* Y522S alters pregnant uterine myometrium and uterine blood vessel function *ex vivo.*
3. To determine the impact of *Ryr1* Y522S on fetal and placental development.
4. To determine the effect of *Ryr1* Y522S on gestation length and parturition duration.
5. To investigate the impact of the *Ryr1* Y522S on *Ryr* channels and associated ion channels' mRNA and protein expression in reproductive tissues.

Using a clinical questionnaire:

6. To characterise the impact of human *RYR1* mutations on pregnancy outcomes, fetal development, generalised bleeding events, post-partum haemorrhage and menorrhagia.

2 Chapter 2 Skeletal muscle genes implicated in smooth muscle function: a literature review

Skeletal muscle genes implicated in Ca^{2+} homeostasis and excitation-contraction coupling and their role in organ-specific smooth muscle function – an evolving biological and clinical continuum

Abstract

Skeletal and smooth muscle tissues are both functionally and structurally different, yet they have similarities in Ca^{2+} handling mechanisms and contractile machinery. This review highlights important proteins that are typically involved in skeletal muscle function yet have also been identified to play a role in smooth muscle function including vascular, myometrial, urinary bladder and gastrointestinal smooth muscles. Recent evidence highlights the potential role of skeletal RyR1 in vascular smooth muscle function, as described above. This leads us to consider whether variants in other typically skeletal muscle associated genes could have a wider impact in the body, specifically in the uterus and vascular smooth muscle cells. Malfunction of these proteins could lead to a variety of pregnancy-related problems such as preterm birth, prolonged gestation, and post-partum haemorrhage. The roles of these proteins have been classified into two groups 1) sarcoplasmic reticulum Ca^{2+} release and excitation contraction coupling and 2) thin-thick filament assembly/interaction and myofibrillar force generation. Groups of neuromuscular disorders caused by pathological variants in skeletal muscle associated genes such congenital myopathies often have wide phenotypic heterogeneity with some non-skeletal muscle manifestations. Therefore, it is important to consider a wide variation of clinical symptoms to provide a complete therapeutic approach to patients with such genetic diseases.

Method

This traditional or narrative form of literature review was performed to present a comprehensive background of the literature focused on the topic in the title, highlighting the importance of the research in this thesis. The following search engines or databases were interrogated as part of the literature search PubMed, Google Scholar, ClinVar and Mouse Genome Informatics. The search terms included any combination of the terms; 'smooth muscle', 'gene', 'skeletal', 'uterus', 'vascular' and 'pregnancy'. Publications were included from any year of publication, involving human or animal studies, in English, accessible to King's College London and demonstrated clinical diagnostic or scientific support for the topic. All publications were screened for eligibility first by title, followed by a thorough review of key findings and methodology. The review was first performed between March 2020 – December 2020, the literature was reviewed again in March 2023.

Introduction

Variants in genes encoding proteins involved in cellular Ca^{2+} handling, excitation-contraction coupling and myofibrillar force generation can lead to a wide range of diseases, including congenital myopathies with permanent, often severe weakness, and episodic presentations such as periodic paralysis, exertional rhabdomyolysis and malignant hyperthermia, a potentially fatal anaesthesia complication in otherwise healthy individuals, and, less frequently (in this review), neurological and neurodevelopmental disorders. Although these genetic variants cause predominantly neuromuscular phenotypes, some clinical manifestations suggest a range of other features not only affecting striated but also smooth muscles. For example, as discussed in Chapter 1, patients with MH-associated *RYR1* variants exhibit a bleeding phenotype associated with menorrhagia and post-partum haemorrhage, whose pathophysiology was

recently resolved by Lopez et al. (2016). These findings suggest a role for RyR1 (and, by proxy, other proteins involved in ECC and intramuscular Ca^{2+} homeostasis) in the contraction and/or relaxation of (vascular) smooth muscles in the myometrium and other organs. In the present review I will summarize current knowledge regarding several genes involved in intramuscular Ca^{2+} homeostasis and ECC, and, where applicable, outline the associated clinical phenotypes and findings from relevant animal models. This review will provide the basis for considering genes and proteins previously mainly implicated in neuromuscular disorders with regards to their potential involvement in (vascular) smooth muscle function in various other organs, and potentially associated clinical phenotypes.

Table 1. Described genes involved in neuromuscular/skeletal muscle disorders and evidence for a role in smooth muscle tissues.

Gene	Associated neuromuscular disorder (OMIM)	Evidence for a role in smooth muscle tissues
ACTA1	- Scapulohumeroperoneal (OMIM 616852) - Congenital myopathy with cores (OMIM 161800) - Congenital myopathy with excess of thin myofilaments (OMIM 161800) - Congenital myopathy with fibre-type disproportion 1 (OMIM 255310) - Nemaline myopathy 3 (OMIM 161800).	- Ureteric (Mitchell *et al.*, 2006) - Vascular (Garcia-Angarita *et al.*, 2009) - Gastrointestinal (Ravenscroft *et al.*, 2011; Chou *et al.*, 2013)
CACNA1S	- hypokalemic periodic paralysis type 1 (OMIM 170400) - malignant hyperthermia susceptibility (OMIM 601887) - thyrotoxic periodic paralysis (OMIM 188580)	- Pulmonary (Kil and Kim, 2010) - Myometrium, vascular (Edizadeh *et al.*, 2017; Kumar *et al.*, 2018)
CFL2	- Nemaline myopathy 7 (610687)	- Vascular tissue (Albinsson, Nordström and Hellstrand, 2004; Hellstrand and Albinsson, 2005; Dai *et al.*, 2008; Martín *et al.*, 2008) - Tracheal/airway smooth muscle (Komalavilas *et al.*, 2008; Zhao *et al.*, 2008)
KCNMA1	- Cerebellar atrophy, developmental delay, and seizures (617643) - Liang-Wang syndrome (618729) - Paroxysmal nonkinesigenic dyskinesia, with or without generalized epilepsy (609446)	- Vascular tissue (Yin *et al.*, 2017; Dogan *et al.*, 2019; Zavaritskaya *et al.*, 2020) - Myometrium (Khan, 1993; Zhou *et al.*, 2000; Chanrachakul, 2004)
MTM1	- X-linked Myotubular myopathy (OMIM 310400)	- Vascular (Chaudhari *et al.*, 2011; Koga *et al.*, 2012) - Gastrointestinal (Herman *et al.*, 1999)

ORAI1	- Tubular aggregate myopathy 1 (615883)	- Myometrium (Murtazina *et al.*, 2011) (Sutovska *et al.*, 2015)
RYR1	- Malignant hyperthermia susceptibility (145600) - Central core disease (117000) - King-Denborough syndrome (145600) - Minicore myopathy with external ophthalmoplegia (255320) - Exertional rhabdomyolysis (Dlamini, 2013) - Centronuclear Myopathy (Wilmshurst et al., 2013) - Congenital Fibre Type Disproportion (CFTD) (Clarke *et al.*, 2013)	- Vascular tissue (Nelson, 1995; Lopez, 2016; Coburger, 2017; Brackmann, 2018) - Pulmonary arteries (Li, 2009) - Myometrium (Martin, 1999, 1999) - Airway smooth muscle (Du, 2006) - Detrusor muscle (Ji, 2004; Nicolas Fritz, 2007)
SEPN1	- Muscular dystrophy, rigid spine, 1 (602771) - Congenital myopathy, with fibre-type disproportion (255310) - Multi-minicore Disease (MmD)	- Gastric muscle (Li *et al.*, 2016) - Airway smooth muscle (Ogawa *et al.*, 2013) - Vascular tissue (Kikuchi *et al.*, 2019; Hu *et al.*, 2011) - Myometrium (Zhou *et al.*, 2018; Wang *et al.*, 2019)
STIM1	- Tubular aggregate myopathy 1 (160565) - Stormorken syndrome (185070)	- Vascular tissue, female and male genitourinary muscle (Feldman, Grotegut and Rosenberg, 2017) - Gastrointestinal tissue (Ohta *et al.*, 1995; Petkov and Boev, 1996; Mancarella *et al.*, 2013; Feldman, 2017) - Myometrium (Noble *et al.*, 2009; Chin-Smith *et al.*, 2014; Feldman, 2017)
TNNT1/3	- Nemaline myopathy 5 (605355) - Arthrogryposis, distal, type 2B2 (618435)	- Vascular tissue (Moran *et al.*, 2008)
TPM2	- distal Arthrogryposis (type 1A and type 2B4) (OMIM 108120) - CAP myopathy 2 (OMIM 609285)	- Vascular (Meng et al., 2019, Mroczek et al., 2017)

	- Nemaline myopathy 4 (609285).	
TRPC1	- (modifier of) Duchenne muscular dystrophy (DMD) (Vandebrouck *et al.*, 2002; Gervásio *et al.*, 2008)	- Myometrium (Murtazina, 2011) - Vascular smooth muscle (Shi *et al.*, 2017; Lopez *et al.*, 2020; Miguel A. S. Martín-Aragón Baudel *et al.*, 2020)
TRPC4	-	- Myometrial smooth muscle (Dalrymple *et al.*, 2004; Murtazina *et al.*, 2011) - Vascular smooth muscle (Freichel *et al.*, 2004)
TRPC6	- Focal segmental glomerulosclerosis 2 (OMIM 603965)	- Myometrial smooth muscle (Dalrymple, 2004) - Vascular smooth muscle (Freichel, 2004)
TRPV4	- Brachyolmia type 3 (113500) - Hereditary motor and sensory neuropathy, type IIc / Charcot-Marie-Tooth disease type 2C (CMT2C) (606071) - Neuronopathy, distal hereditary motor, type VIII (600175) - Scapuloperoneal spinal muscular atrophy (18140)	- Myometrium (Singh *et al.*, 2015; Ying *et al.*, 2015; Ducza *et al.*, 2019) - Vascular tissue (Alvarez *et al.*, 2006; Marrelli *et al.*, 2007; Watanabe *et al.*, 2008; Gao and Wang, 2010; Martin *et al.*, 2012; Yang *et al.*, 2012; Filosa, Yao and Rath, 2013) - Urinary bladder (Gevaert *et al.*, 2007)
TTN	- Muscular dystrophy (limb-girdle) 10 (608807) - Myofibrillar myopathy 9 with early respiratory failure (603689) - Salih myopathy (611705) - Tardive tibial muscular dystrophy (600334)	- Female genitourinary system (labour) (Fan *et al.*, 2020)

Genes involved in intracellular Ca^{2+} release and excitation contraction coupling

Transient Receptor Potential Cation Channel 1 (*TRPC1*)

TRPC1 belongs to the transient receptor potential (TRP) superfamily of cation channels that are involved in a variety of processes including receptor- and store-operated Ca^{2+} entry, mineral absorption and cell death, as well as functioning as sensors for pain, heat, cold, sounds, osmotic changes and stretch (Zhang *et al.*, 2009). In skeletal muscle, activated TRPC1 receptors modulate the entry of Ca^{2+} during repeated muscle contractions and help muscles to maintain force during sustained repeated contractions (Zanou *et al.*, 2010; Antigny *et al.*, 2017). TRPC1 channels are suggested to play a role in Duchenne muscular dystrophy (DMD) via a reactive oxygen species (ROS)-Src-TRPC1/caveolin-3 pathway (Vandebrouck, 2002; Gervásio, 2008). Increased TRPC1 expression in diaphragm (the most affected muscle in DMD) in the mdx mouse model of DMD compared with sternomastoid (STN) and limb muscles, may contribute to the different degrees of dystrophic phenotype seen in mdx mice (Matsumura *et al.*, 2011). It has been shown that dystrophin deficiency in mdx mice impacts VSMCs regulation of [Ca^{2+}]$_i$ and [Na$^+$]$_i$. The intracellular Ca^{2+} increase response to mechanical stretch in mdx VSMCs is elevated compared to Wt, which appears to be mediated through TRPC channels (Lopez, 2020).

In vascular smooth muscle, TRPC1 has been implicated in store-operated channels where store-operated STIM1-TRPC1 interactions stimulate Gαq/phospholipase C (PLC) β1/PKCδ activity to induce channel gating upon depletion of Ca^{2+} stores (Shi, 2017; Miguel A. S. Martín-Aragón Baudel, 2020; Bon *et al.*, 2022). Recent data reported by Baudel and colleagues suggest that the TRPC1 PKCδ-PIP2 signalling pathway might be involved in α1-mediated vasoconstriction of mesenteric blood vessels. The researchers found that the α1-adrenoceptor agonist methoxamine significantly increased TRPC1 channel activity and which could be reversed by

δV1-TAT, a PKCδ inhibitor. However, the precise interaction between the PKCδ inhibitor and the physiological α1-agonist-induced response remains unknown (Miguel A.S. Martín-Aragón Baudel *et al.*, 2020).

TRPV4/TRPC1 channels are implicated in the endothelium dependent regulation of vascular tone as a result of Ca^{2+} sensing receptor activation, as evidenced in TRPC1$^{-/-}$ mice (Schmidt *et al.*, 2010; Greenberg *et al.*, 2019). Similarly, overexpression of human TRPC1 is suggested to enhance vasoconstriction of the rat pulmonary artery when intracellular Ca^{2+} stores are depleted (Kunichika *et al.*, 2004; Ng, Airey and Hume, 2010). Trpc1 has also been detected in airway smooth muscle and is suggested to play a role in pressure-mediated airway smooth muscle remodelling (Ong *et al.*, 2003; Li *et al.*, 2019).

Transient Receptor Potential Channel 4 (*TRPC4*) and Transient Receptor Potential Channel 6 (*TRPC6*)

TRPC4 and TRPC6 channels are functional in the sarcolemma of mouse skeletal muscle fibres (Sabourin *et al.*, 2009; Zhang, Soelter and Brinkmeier, 2015). Variants in *TRPC6* are associated to focal segmental glomerulosclerosis 2 (OMIM 603965). Both TRPC4 and TRPC6, as well as TRPC1 and TRPC3 genes and proteins are expressed in human myometrial tissue and cultured human myometrial smooth muscle cells (Dalrymple, 2002). Dalrymple *et al* used mRNA quantification methods to investigate gestational regulation of TrpC proteins in human myometrium, and the potential modulation of TrpC expression by IL–1β, a cytokine implicated in labour. They indicated a potential role for TRPC1 during the end of gestation by observing that Trpc1 mRNA and protein expression were both upregulated in 'term active labour' and 'term not in labour' myometrial tissue. Whereas TrpC3, TrpC4, and TrpC6 are upregulated in 'term active labour' myometrial tissue, indicating a role for myometrial TrpC proteins in labour (Dalrymple, 2004). In human myometrial cells, the simultaneous knockdown of *TRPC1* and *TRPC4* mRNAs induces a decrease in oxytocin-stimulated SR Ca^{2+} entry (Murtazina, 2011),

although this did not affect myometrial ER store refilling in cultured uterine myometrium smooth muscle PHM1-41 cells. Further to this, TRPC4 knock out mice and TRPC6 knock out mice show that they are essential for regulation of vascular tone and regulation of smooth muscle tone in blood vessels and lungs, respectively (Freichel, 2004).

Transient Receptor Potential Cation Channel Subfamily V Member 4 (*TRPV4*)

TRPV4 encodes a non-selective Ca^{2+} permeant cation channel involved in osmotic sensitivity and mechano-sensitivity. Variants in *TRPV4* are associated with neuromuscular disorders and skeletal dysplasias including congenital nonprogressive spinal muscular atrophy, scapuloperoneal spinal muscular atrophy and Charcot-Marie-Tooth disease type IIC phenotype (Evangelista *et al.*, 2015; Sullivan *et al.*, 2015; Jędrzejowska *et al.*, 2019). In murine skeletal muscle the TRPV4 Ca^{2+} channels in the sarcolemma mediates resting Ca^{2+} influx (Pritschow *et al.*, 2011; Zhang, 2015) and may contribute to mechano-sensitivity (Ho *et al.*, 2012).

TRPV4 channels are present in various tissues including lung, vagina, bladder, and oesophagus (GTEx portal). TRPV4 channels are also present in the pregnant and nonpregnant rodent uteri, and their activation by agonists like prostaglandin and antagonists significantly increases and decreases myometrial contractility (Singh, 2015; Ducza, 2019). There is evidence that the blockade of TRPV4 may prolong pregnancy in mouse models of preterm labour (Ying, 2015). TRPV4 channels are also expressed in various vascular smooth muscle cells including rat cerebral arteries (Marrelli, 2007), human and rat extra-alveolar vessels (Alvarez, 2006), rat intra-lobar pulmonary arteries (endothelium denuded) (Martin, 2012; Yang, 2012), rat mesenteric artery (Gao, 2010) and rat and mouse aortic muscle (Watanabe, 2008). Their activation leads to smooth muscle cell hyperpolarization and vasodilatation (Campbell and Fleming, 2010; Filosa, 2013). Bladder muscle strips from a Trpv4 knockout mouse model exhibit abnormal spontaneous contractility, lower frequency of voiding contractions and higher

frequency of non-voiding contractions compared with wild-type mice. This highlights the importance of TRPV4 in non-skeletal muscle urinary bladder physiology (Gevaert, 2007; Everaerts *et al.*, 2010). Thus, variants resulting in the malfunction of the TRPV4 channel may have additional but currently not recognized signs and symptoms beyond skeletal muscle.

Stromal Interaction Molecule 1 (*STIM1*)

Stromal interaction molecule 1 (STIM1) proteins on the S/ER function as Ca^{2+} sensors for the activation of store-operated Ca^{2+} influx channels (SOCs), mediating Ca^{2+} influx in response to depletion of intracellular Ca^{2+} stores. Orai1 and Stim1 are the main components of a Ca^{2+} release- activated Ca^{2+} (CRAC) channel, triggered by a decrease in ER Ca^{2+} concentration which is sensed by Stim1. Decreased ER Ca^{2+} concentration results in a conformational change of the Stim1 protein, resulting in interaction of the Stim1 proteins with Orai1 channels, and opening of Orai1 causing a Ca^{2+} influx into the cell cytoplasm.

Gain-of-function variants in *STIM1* and *ORAI1* have been implicated in tubular aggregate myopathy (TAM1) and Stormorken syndrome, primarily neuromuscular conditions characterised by progressive muscle weakness, cramps, myalgia (Chevessier *et al.*, 2005), and, in the case of the latter, additional multisystem symptoms comprising thrombocytopenia, hyposplenism, ichthyosis, dyslexia, and short stature (Stormorken *et al.*, 2008; Misceo *et al.*, 2014; Endo *et al.*, 2015; Walter *et al.*, 2015; Böhm *et al.*, 2017; Böhm and Laporte, 2018; Garibaldi *et al.*, 2017; Noury *et al.*, 2017). *STIM1* gain-of-function variants cause excessive Ca^{2+} influx (Böhm, 2018); the tubular aggregates derived from sarcoplasmic reticulum and seen in patient muscle biopsies (Salviati *et al.*, 1985) are considered an adaptive mechanism to regulate increased intracellular Ca^{2+} to prevent muscle fibres from hypercontraction and necrosis (Martin, Ceuterick and Van Goethem, 1997; Müller *et al.*, 2001). *STIM1* loss-of-

function variants lead to a phenotype characterised by hypotonia and muscle atrophy of slow twitch fibres.

Although STIM has a strong skeletal muscle-associated disease phenotype, there is evidence for the role of STIM in SOCE in smooth muscle, including vascular, gastrointestinal, and both male and female genitourinary smooth muscle (Feldman, 2017). Smooth muscle specific STIM1 knockout mice (sm-STIM1-KO) have a 30-40% mortality rate and significant thinning of the tunica media (smooth muscle layer of the aorta). Aortic rings harvested from sm-STIM1-KO mice compared to sm-STIM-WT littermates show almost eliminated store-dependent and decreased α1-adrenergic agonist-induced contraction, suggesting that the activation signal muscle contraction may involve STIM1 and SOCE (Mancarella, 2013). STIM1 and ORAI1 are upregulated in spontaneously hypotensive rats; aortic rings revealed increased thapsigargin-induced contraction and basal tone in hypertensive rats compared to wildtype (Giachini *et al.*, 2009). These changes were abolished with STIM1 and ORA1 neutralizing antibody treatment, suggesting a role for STIM1-dependent SOCE and vascular contraction/relaxation, and therefore a potential treatment for spontaneous hypertension.

Sm-STIM1-KO mice also have thinning of the muscularis propria in the stomach and general distention and dilatation of their GI tract, indicating a wider role for STIM in the GI tract (Mancarella, 2013). Ohta et al (1995) found that smooth muscle strips from the ileum of rats exhibited CPA-induced contraction that was resistant to both nifedipine and methoxyverapamil (Ohta, 1995). Further studies in smooth muscle tissue of cat and guinea pig stomach demonstrate CPA-induced tonic contraction that were partially inhibited by nifedipine (Petkov, 1996). Together these findings suggest that STIM1 plays a role in maintaining GI smooth muscle tone.

STIM1-2 and ORAI1-3 mRNA expression has been identified in human pregnant and non-pregnant myometrial tissue (Chin-Smith, 2014) and murine myometrium and fallopian tubes (Feldman, 2017). Noble et al (2009) demonstrated that in late pregnant rat uterus, Ca^{2+} depleted myometrial SR exposed to external Ca^{2+} resulted in Ca^{2+} influx and a profound rise in basal Ca^{2+} concentration and force. Interestingly, this Ca^{2+} influx was mostly due to SOCE, as it was resistant to nifedipine (L-type Calcium channel blocker) but sensitive to the store operated channel inhibitor SKF96365 (Noble, 2009). Feldman et al (2017) reported anecdotal evidence that STIM1 null female mice die during parturition, representative traces of spontaneous contractions that were almost abolished in non-pregnant uterine tissues from STIM1 null mice (Feldman, 2017), implying a role in myometrial contraction.

Orai Ca^{2+} Release-Activated Ca^{2+} Modulator 1 (*ORAI1*)

ORAI1 encodes a plasma membrane Ca^{2+} channel subunit that is activated by the Ca^{2+} sensor STIM1 when Ca^{2+} stores are depleted. In skeletal muscle, ORAI1 is located in the transverse tubule membrane. Gain-of-function variants in *ORAI1* are associated with tubular aggregate myopathy 2 (OMIM 615883), characterised by muscle pain, cramping, weakness or stiffness, exercise-induced muscle fatigue and an abnormal gait (*Tubular aggregate myopathy - Genetics Home Reference - NIH*, no date; Gilchrist, Ambler and Agatiello, 1991; Chevessier, 2005). Dysfunctional STIM1/ORAI1-mediated SOCE also contributes to the pathogenesis of combined immunodeficiency (CID), and Stormorken syndrome, muscular dystrophy (specifically in *mdx* mice), malignant hyperthermia and sarcopenia (Michelucci *et al.*, 2018), with a clinical myopathy the common defining component. Interestingly, activation of Orai1 has an effect on both skeletal muscle and smooth muscle. In skeletal muscle, the Orai1 activator IA65 increases Orai1-mediated Ca^{2+} entry, whilst in vascular smooth muscle, Orai1 activation promotes vascular smooth muscle cell migration, and has been associated with pulmonary hypertension (Beech, 2012; Rode *et al.*, 2018; Azimi *et al.*, 2020).

ORAI1-3 proteins have been implicated in oxytocin-stimulated SR Ca^{2+} entry and cyclopiazonic acid-stimulated signal regulated Ca^{2+} entry in human myometrium. ORAI1 mRNA knockdown slows the rate of ER store replenishment following removing of SERCA inhibition in human myometrial cell, indicating that ORAI may contribute to the regulation of uterine smooth muscle Ca^{2+} dynamics (Murtazina, 2011). Murtazina et al (2011) suggest that the Orai1 (compared to isoforms 2 and 3) is the predominant transcript in cultured pregnant myometrial cells and immortalized cells from pregnant and non-pregnant human myometrium. However, Sutovska et al (2015) reported decreased Orai1 protein expression and activity in human term-pregnant labouring myometrium, although this could be due to differing investigative methods. The frequency of contractions in term pregnant myometrium were supressed by a CRAC channel blocker 3-fluropyridine-4-carboxylic acid (FPCA) and salbutamol reduced the amplitude of contractions in term-pregnant myometrium (Sutovska, 2015).

Selenoprotein 1 (*SEPN1 or SELENON*)

Recessive variants in *SEPN1* have been associated with MmD, congenital muscular dystrophy with rigidity of the spine (RSMD) and Mallory body myopathy; clinically, these conditions are characterised by axial weakness, spinal rigidity, early scoliosis and respiratory impairment (Moghadaszadeh *et al.*, 2001; Jungbluth, 2007). Selenoprotein N has multiple roles, not all of which are fully understood but plays an important role in cell protection against oxidative stress, regulation of redox-related Ca^{2+} homeostasis and satellite cell maintenance. There is some clinical overlap between SEPN1- and *RYR1*-related myopathies as well as a close physical association between the biochemical pathways implicated in these conditions (Jurynec *et al.*, 2008). SELENON absence is associated with increased cell oxidised protein content in myotubes and altered Ca^{2+} homeostasis which may be related to RyR1 dysfunction (Arbogast

et al., 2009). In particular, SELENON regulates ER Ca^{2+} levels by protecting the SERCA2 pump against oxidoreductase ERO1A-mediated oxidative damage (Marino *et al.*, 2014).

There is also evidence that members of the large selenoprotein family may play a role in some smooth muscles. For example, selenium affects rat gastric smooth muscle constriction by regulating Ca^{2+} release, MLCK activation, and MLC phosphorylation through Selenoprotein T (SelT) activation (Li, 2016). Selenoprotein P, another member of the selenoprotein family, suppresses the amplitude of twitch-like contractions of cat bronchiole by acting directly on the bronchiolar smooth muscle (Ogawa, 2013). Interestingly, circulating serum SeP concentrations were significantly higher in patients with pulmonary arterial hypertension compared with controls (Kikuchi, 2019). More specifically, there is evidence for a role of selenoprotein N as a regulator of selenium in uterine smooth muscle contraction in mice (Zhou, 2018). In addition, decreased expression of SelN, SelT, and SelW appear to affect the release of Ca^{2+} in mouse uterine smooth muscle and low plasma selenium have been associated to spontaneous preterm birth (Mistry *et al.*, 2012; Wang, 2019) (Wang et al., 2019). More over in a GWAS study, two loci in *EEFSEC,* an important factor in the production of selonoprotein, were associated with spontaneous preterm deliveries (Bhattacharjee and Maitra, 2021). Together these studies suggest a role for selenoproteins in smooth as well as in striated skeletal muscle function.

Large Conductance Ca^{2+}-Activated Potassium Channel, Subfamily M, Alpha Member 1 / BK_{Ca} Channel (*KCNMA1*)

Variants in *KCNMA1* have been associated to paroxysmal non-kinesigenic dyskinesia, 3 (OMIM: 609446), Liang-Wang syndrome (OMIM 618729), cerebellar atrophy with developmental delay and seizures (OMIM 617643) and idiopathic generalised epilepsy (OMIM 618596). *KCNMA1* encodes the BK_{Ca} channel, expressed in mammalian skeletal and smooth muscles. In skeletal muscle, BK_{Ca} channel opening is triggered by cellular depolarisation, intracellular Ca^{2+} ions and phosphokinase A (PKA) phosphorylation, and prolongs the

hyperpolarisation phase between bursts of action potential, reducing the firing capability and dampening the effect of the accumulation of intracellular Ca^{2+} ions (Latorre *et al.*, 1989; Tricarico, Petruzzi and Conte Camerino, 1997).

The BK_{Ca} channel has been described in various vascular smooth muscle types and play a crucial role in regulation of vascular tone (Dogan, 2019). Pharmacological activation of BK_{Ca} channels (via GoSlo-SR compounds) in rat mesenteric and tail arteries induce vessel relaxation (Zavaritskaya, 2020).

The BK_{Ca} channel is one of the most abundant K^+ channels in the myometrium. There is evidence to suggest that the BK_{Ca} channel is a key regular of myometrial membrane potential and maintenance of uterine quiescence (Khan, 1993; Zhou, 2000; Chanrachakul, 2004). Inhibition of BK_{Ca} channels depolarise myometrial SMCs and increases myometrial contractility in rat and human tissue. Enhancing BK_{Ca} channel opening has a potent relaxant effect on myometrium.

In isolated pregnant sheep uterine artery, Hu et al (2011) demonstrates that BK_{Ca} channel current density is increased, and activation of protein kinase C produces an inhibitory effect on BK_{Ca} channel activity and increased myogenic tone in pregnant uterine arteries. Along with this, steroid hormone treatment of non-pregnant uterine arteries upregulated β1 expression and BK_{Ca} channel activity, indicating a possible role in attenuating myogenic tone of the uterine artery in pregnancy (X.-Q. Hu, 2011).

Ca^{2+} voltage-gated channel subunit alpha1 S (*CACNA1S*)
The *CACNA1S* gene encodes the slowly inactivating L-type voltage-dependent Ca^{2+} channel in skeletal muscle. Variants in this gene have been associated to hypokalemic periodic paralysis type 1 (OMIM 170400), malignant hyperthermia susceptibility (OMIM 601887), thyrotoxic

periodic paralysis (OMIM 188580) and a rare recessive congenital myopathy (with characteristics like recessive *RYR1*-related myopathies) (Schartner *et al.*, 2017). The L-type Ca^{2+} channels play a key role in excitation contraction coupling in skeletal muscle via their interaction with Ryr1, which triggers Ca^{2+} release from the sarcoplasmic reticulum.

Although *CACNA1S* is predominantly expressed in skeletal muscle (108.3 TPM), it is also expressed at low levels in tibial artery (0.403 TPM), colon (0.5 TPM), lung (0.1754 TPM), and uterus (0.02996 TPM) (GTEx Analysis Release V8 (dbGaP Accession phs000424.v8.p2. Date accessed 21-09-2021). Kil and Kim (2010) reported a case of severe respiratory insufficiency in a patient with a *de novo* variant Arg528Gly in *CACNA1S* (Kil, 2010). This respiratory phenotype is unique but it is suggested that its cause is due to skeletal respiratory muscle weakness. It could be plausible that the clinical phenotype was due to changes lung function, specifically airway smooth muscle cells, no further tests were carried out. Unusually there have been two cases of mothers of CACNA1S patients having antepartum symptoms, including pre-term delivery and antepartum haemorrhage (Edizadeh, 2017; Kumar, 2018)

Myotubularin (*MTM1*)
Myotubularin is a lipid phosphatase which depolarises phosphatidylinositol 3-monophosphate (PI3P) and phosphatidylinositol 3,5-bisphosphate (PI(3,5)P2) (Blondeau *et al.*, 2000; Taylor, Maehama and Dixon, 2000; Schaletzky *et al.*, 2003; Tsujita *et al.*, 2004) and importantly it is required for skeletal muscle maintenance (Hnia *et al.*, 2011). Variants in *MTM1* have been associated with X-linked myotubular myopathy (OMIM 310400), characterised by neonatal hypotonia, severe global muscular weakness and respiratory distress. Few patients have been observed to have bleeding-type phenotypes such as bilateral cephalhaematomas and subdural hygromas in twins born following preterm labour (Chaudhari, 2011) and subdural haemorrhage detected in a 6-month year old patient (Koga *et al.*, 2012), all with normal laboratory

investigations. Herman et al (1999) reviewed clinical data of 55 male subjects with variants in *MTM1*, finding four cases reporting gastrointestinal bleeding including gastritis and duodenal perforation (Herman, 1999).

Genes implicated thin-thick filament assembly/interaction and myofibrillar force generation

Cofilin 2 (*CFL2*)

Cofilin 2 is the major component of intranuclear and cytoplasmic actin rods and is required for skeletal muscle maintenance, as it reversibly controls polymerization of G-actin and F-actin depolymerization in a pH-sensitive manner (Gillett *et al.*, 1996). Autosomal recessive variants in *CFL2* are associated with autosomal recessive nemaline myopathy 7 (OMIM: 610687), a very rare form of nemaline myopathy characterised by early onset hypotonia and delayed motor development, slow progressive proximal muscle weakness and nemaline rods and/or minicores, protein aggregates and dystrophic changes on muscle biopsy (Agrawal *et al.*, 2007; Ockeloen *et al.*, 2012).

Cofilin is abundantly expressed in vascular smooth muscle tissues where it has been implicated in the regulation of vascular smooth cell migration (Martín, 2008) and regulation of vascular smooth muscle cell differentiation markers (Albinsson, 2004; Hellstrand, 2005). In canine pulmonary arteries, cofilin phosphorylation stabilizes peripheral actin structures and may contribute to the maximal contraction of pulmonary arteries (Dai, 2008). In an experimental inflammation model (cultured PA SMCs) of hypertension in rat pulmonary artery, cofilin 2 is upregulated indicating a potential role in intensifying the remodelling of actin filaments

contributing to the enhanced invasiveness and growth of SMCs leading to the development of vascular resistance and pulmonary hypertension (Dai *et al.*, 2006).

In tracheal smooth muscle tissues, stimulation via acetylcholine causes dephosphorylation and activation of cofilin, which is inhibited by the expression of dominant-negative cofilin mutant S3E, preventing the increase in actin polymerization (Zhao, 2008). This is consistent with the suggested role of cofilin in regulating availability of G-actin for polymerization in human airway, suggesting a role in regulating actin dynamics in smooth muscle relaxation (Komalavilas, 2008).

Alpha Actin (*ACTA1*)
Alpha-actin is the predominant actin isoform in adult skeletal muscle, forming the thin filamin of the sarcomere which interacts with various proteins to produce contractile force. Variants in *ACTA1* have been associated to various myopathies, including scapulohumeroperoneal (OMIM 616852), congenital myopathy with cores (OMIM 161800), congenital myopathy with excess of thin myofilaments (OMIM 161800), congenital myopathy with fibre-type disproportion 1 (OMIM 255310) and nemaline myopathy 3 (OMIM 161800).

Alpha actin is also ubiquitously expressed in other tissues, albeit in much smaller amounts, specifically, in smooth muscle such as developing mouse ureteric smooth muscle (Mitchell, 2006). Saito *et al* described several non-skeletal phenotypes in a severe congenital myopathy case such as transient supraventricular tachycardia, urinary tract constriction, bone dysplasia and severe failure to thrive (Saito *et al.*, 2011). These symptoms may not be smooth muscle specific, yet they highlight the variety and severity of implications from *ACTA1* variants and therefore indicates the importance of treating wider non-skeletal impact of such variants. Few *ACTA1* variant cases have other non-skeletal phenotypes including gastro-oesophageal reflux

with evidence of aspiration (Ravenscroft, 2011; Chou, 2013) and cerebral haemorrhage (Garcia-Angarita, 2009).

Titin (*TTN*)

Titin (connectin) is the third major filament in the assembly and function of striated muscle where it provides connection at the level of individual microfilaments, contributing to the balance of forces between two halves of the sarcomere (Mayans *et al.*, 1998). The two other major filaments being actin thin filaments and bipolar myosin thick filaments. Variants in *TTN* cause dilated cardiomyopathy and a wide range of neuromuscular disorders, and are also likely to affect ribosome activity, sarcomeric organization and alter cardiac metabolism (Kellermayer, Smith and Granzier, 2019).

The functional role of titin is not exclusive to striated muscle, with some evidence for a potential role in myometrial muscle during labour. Fan et al (2020), identified 322 significantly differential peptides in myometrium tissues between term non-labour and term labour groups. 23 peptides were derived from the precursor protein Titin. Although Titin has not been implicated in myometrial contraction yet, it may play a pivotal role in the onset of labour (Fan, 2020).

Sm-titin, a titin-like protein that could be an alternatively spliced isoform of the *TTN* gene has been identified in chicken gizzard smooth muscle (Kim and Keller, 2002) and various smooth muscle tissues (bovine and porcine aorta, human myometrium, bladder, porcine stomach and carotids)(Labeit *et al.*, 2006). Kim and Keller (2002) demonstrated that sm-titin interacts with smooth muscle myosin (Kim, 2002) and α-actinin (Chi *et al.*, 2005) in vitro. Therefore, it is likely that these interactions with sm-titin play a role in maintaining smooth muscle contractile apparatus and regulating its organisation.

Troponin 1/3 (*TNNT1/3*)

Variants in troponin T (*TNNT1*) are associated to nemaline myopathy 5, Amish type (Johnston *et al.*, 2000; Jin *et al.*, 2003; Wang *et al.*, 2005). The troponin complex consists of three protein subunits: the Ca^{2+}-binding subunit TnC, the inhibitory subunit TnI, and the tropomyosin-binding subunit TnT (Greasers And and Gergely, 1973). These subunits coordinate to convert rising cytosolic Ca^{2+} originating from sarcolemmal electrical activity to myofilament movements with tropomyosin and the actin filament (Tobacman, 1996; Gordon, Homsher and Regnier, 2000; Mondal and Jin, 2016).

Troponin T and troponin I protein translation and localisation unique to the distribution of tropomyosin has been identified in vascular smooth muscle of the aorta, indicating the possible role of the troponin complex also in the contractile machinery of the vascular smooth muscle cell (Moran, 2008). Ju et al (2013) found that Tnnt3 (essential for normal growth and breathing) was not only expressed in mouse skeletal muscle but also smooth muscle cells in the aorta, bladder and bronchus although due to the *Tnnt3*[lacZ/+] mouse model used this evidence was indirect (measurement of β- galactosidase activity), therefore calls for further supporting work (Ju *et al.*, 2013).

Streff *et al* described a 16-month-old female with a homozygous deletion of 19q13.42 encompassing *TNNT1* and *TNNI3* presenting with Amish nemaline myopathy (ANM) with congenital hypotonia and cardiomyopathy and interestingly, recurrent emesis (Streff *et al.*, 2019), indicating potential gastrointestinal muscle misfunction.

Tropomyosin 2 (*TPM2*)

Variants in Tropomyosin 2 have been associated to distal arthrogryposis (type 1A and type 2B4) (OMIM 108120), CAP myopathy 2 (OMIM 609285), nemaline myopathy 4 (609285). *TPM2* encodes beta-tropomyosin and expressed predominantly in slow, type 1 muscle fibres

and to a lesser extent in fast muscle fibres. Tropomyosin, together with actin and troponin form the thin filament that interacts with myosin during muscle contraction. In non-muscle cells the isoform is implicated in stabilizing cytoskeleton actin filaments.

TPM2 is downregulated in atherosclerotic arterial tissues samples compared to non - atherosclerotic arterial tissues samples (Meng, 2019). This signifies potential involvement of TPM2 in the formation and movement of vascular smooth muscle cells. Further to this, Mroczek et al (2017) report of a baby born at 35 weeks' gestation by Caesarean section carrying a splice site variant in TPM2 with intraventricular haemorrhage.

Concluding Remarks

It is evident that several proteins that are involved in skeletal muscle Ca^{2+} regulation, muscle maintenance and the muscle contractile machinery, are also involved in smooth muscle function. Many of the genes highlighted in this review are not only expressed in skeletal muscle tissue, therefore non-skeletal muscle manifestations of disease-causing variants in these genes should not be overlooked, although symptoms may be mild. The studies presented here show that many disease-associated genes are also widely expressed, therefore when studying resultant protein function it is important to consider the impact of variants in both tissues expressing abundance and very little amount of this protein to fully elucidate the their roles.

3 Chapter 3 Materials and methods

3.1 *Ryr1*$^{Y522S/+}$ mouse colony management

To investigate the impact of *RYR1* mutations on smooth muscle function during pregnancy it was imperative that the mouse model selected for this project closely matched the *RYR1*-variant patient phenotype. To date, there are five *Ryr1*[1] mouse strains that display a malignant hyperthermia disease model or increased susceptibility to malignant hyperthermia and three *Ryr1* mouse models of central core disease (Bult *et al.*, 2019). Of these mouse models only the 129S7/SvEvBrd-Hprt$^{b\text{-}m2}$ (Ryr1^{tm1Slh}) strain has previously been investigated for a smooth muscle phenotype (Lopez, 2016). Chelu and colleagues generated the Ryr1^{tm1Slh} mouse model using site-directed mutagenesis; the Tyr522Ser (Y522S) mutation and a *Blp I* restriction site were inserted into a pMGC1 plasmid. The final targeting vector (*Ryr1*^{Y522SNeo}) was electroporated into AB2.2 129Sv/J ES cells. One correctly targeted ES cell carrying the Y522S mutation was inserted into a C57/B6 blastocyst and the resulting chimeras were mated with C57/B6 mice, generating heterozygous *Ryr1*$^{Y522S/+}$ mice (Chelu *et al.*, 2005). The *Ryr1*^{tm1Slh}/*Ryr1*$^+$ mouse model, referred to as *Ryr1*$^{Y522S/+}$, were kindly provided by and generated by the Hamilton group at Baylor College of Medicine, Houston, Texas (Chelu, 2005).

In terms of phenotype, homozygous *Ryr1*$^{Y522S/Y522S}$ mice exhibit skeletal deformations and die between embryonic day 17.5 and postnatal day 1. Heterozygous (Ht) littermates are malignant hyperthermia susceptible, corresponding to the human phenotype associated to this mutation.

---

[1] The nomenclature of genes and protein in this text displayed in accordance with the HUGO Gene Nomenclature Committee (HGNC) guidelines and the NCBI International Protein Nomenclature Guidelines. Briefly, human genes are capitalised and italicised (e.g. *RYR1*), human proteins are capitalised and not italicised (e.g. RYR1), mouse genes are lower case (first letter is uppercase) and italicised (*Ryr1*), mouse proteins are uppercase and not italicised (RYR1).

Heterozygous mice experience whole body contractions and elevated core temperature when exposed to isoflurane or increased heat. Skeletal muscle of $Ryr1^{Y522S/+}$ mice do not exhibit central cores or fibre type changes upon histological examination. Heterozygous mouse skeletal (soleus) muscle tissue exhibits an increased sensitivity to caffeine and an increase in basal tension between 35-36ºC in response to warming. In response to isoflurane concentrations sufficient to induce stage 3 anaesthesia, heterozygous mice show a MH response. Warming to 41ºC for 15 minutes or less can trigger full body contractures in heterozygous mice and apparent rhabdomyolysis as evidenced by increases in serum creatine kinase and potassium levels. A hyperpolarizing shift (to more negative voltages) in the voltage dependence of SR Ca^{2+} release was observed in heterozygous myotubes (Chelu, 2005). There was, however, no specific characterisation relating to uterine function and pregnancy prior to the work presented in this thesis.

3.1.1 Animal housing and husbandry

The usage of animals has been reported in accordance with the ARRIVE guidelines and principles of the 3Rs (replacement, reduction and refinement) (Burch and Russell, 1959; du Sert, Ahluwalia, *et al.*, 2020; du Sert, Hurst, *et al.*, 2020).

The animals used in this study were maintained under controlled conditions in compliance with the Animals (Scientific Procedures) Act (1986). Prior to acceptance to the biological services unit, the transferred animals were quarantined and underwent precautionary veterinary checks. Following which, the animals were housed in individually ventilated cages (IVC, which maintain low ammonia and CO_2 concentrations, to support a low relative humidity, and to reduce spread of infective agents and allergenic contaminants), at 25°C, in 12-hour light and dark cycles and fed a standard chow diet and supplied with water *ad libitum*. Each cage was

supplied with paper nesting material, chippings, and cardboard tubes for enrichment. All regulated procedures, such as the breeding of transgenic animals, were conducted by licenced individuals (Arti Mistry personal license No. I97B46AC2) under the relevant project licence (Professor Gregory A Knock, No. PA607EC40).

3.1.2 Colony management and timed mating

Pregnancy is associated with significant anatomic and physiological remodelling in the cardiovascular system (Rubler, Damani and Pinto, 1977), respiratory system (Baldwin *et al.*, 1977; Hegewald and Crapo, 2011), renal systems (Davison and Dunlop, 1984; Rasmussen and Nielsen, 1988), gastrointestinal system (Parry, Shields and Turnbull, 1970; Cappell and Garcia, 1998), endocrine systems (Glinoer, 1997, 1999) and hematologic and coagulation systems (Pacheco, Costantine and Hankins, 2013). Changes in hormone signals, growth of the fetus and placenta, stretch of the myometrium and vasodilation of the uterine vasculature exhibit the largest fold change at the end of pregnancy (Costantine, 2014). Pregnancy in $Ryr1^{Y522S/+}$ mouse model has not previously been studied, therefore, for this first study it was decided to focus on pregnancy at gestation day 18.5.

Studies have shown that with increases in reproductive age (> 3months) the C57/B6 mouse exhibit longer gestation and labour duration in addition to more frequent and shorter myometrial contractions during pregnancy (Patel, 2017). Bearing this in mind, in the present study all female mice were time-mated strictly between the ages of 8-16 weeks old.

Traditionally, research has suggested that it is mainly maternal genotype, disease and locally acting factors that influence fetal development and disease. However, there is evidence that variation in the fetal genome can also modify pregnancy physiology, to meet increased fetal nutrient demand optimising fetal growth as observed in pregnant mice carrying p57[kip2]-null offspring (Takahashi, Nakayama and Nakayama, 2000; Kanayama *et al.*, 2002; Petry, Ong and

Dunger, 2007). A similar pattern has been observed in human mothers carrying offspring with Beckwith Wiedemann syndrome, and more recently fetal imprinted genes have been investigated in women with gestational hypertension (Wangler *et al.*, 2005; Petry *et al.*, 2016). Thus, in the present study, three pregnant genotype groups were studied: (1) wild-type pregnant mouse with a wild type litter, (2) wild-type pregnant mouse with a litter containing wild-type and *Ryr1$^{Y522S/+}$* fetuses and (3) heterozygous *Ryr1$^{Y522S/+}$* pregnant mouse with a litter containing wild-type and *Ryr1$^{Y522S/+}$* fetuses. Considering cases of increased muscle mass in human *RYR1* variant carriers (Dlamini, 2013), it was intriguing to study any potential impact of mouse fetal Y522S (potentially due to increased fetal demand) on maternal physiology. In addition, since RYR1 may have a functional role in the migration of human placental trophoblasts (Zheng, 2022), this could result in changes in placental growth which may cause upstream changes in maternal vasculature, further supporting the use of the second experimental group.

Female nulligravida C57/B6 heterozygous *Ryr1$^{Y522S/+}$* knock-in mice (Ht(mixed litter)) and female wild-type mice (WT(WT litter)), aged 8 to 14 weeks were time-mated with wild-type males. Wild-type female mice from the same colony were also mated with heterozygous *Ryr1$^{Y522S/+}$* males (WT(mixed litter)). Animal mating was restricted to the hours between 6 pm and 9 am the following day, to obtain an accurate timing of gestation beginning and end. Sighting of a copulatory plug was designated gestation day 0.5.

At gestation day 18.5, females were either video recorded to capture the timing of end of gestation timing or parturition duration measurements or culled using Schedule 1 methods for ex vivo functional studies and molecular studies, as described below. Litter size and resorption numbers were also recorded. Resorbed fetuses were identified as dark /black collection of cells and blood also attached to the uterus, as shown **Figure 10**. Fetuses and placentas were separated and patted dry on a paper towel and weighed.

Figure 10. Representative digital image of a resorption (yellow arrow) in a dissected gestation day 18.5 pregnant mouse uterus

3.2 Monitoring mouse oestrous cycles, vaginal cytology method

The mouse oestrus cycle lasts between four-six days and consists of four over-lapping phases: pro-oestrus, oestrus, metoestrous and dioestrus (Caligioni, 2009; Byers *et al.*, 2012). During proestrus the uterus is hyperaemic and distended with epithelial and leukocyte proliferation in the stroma, in oestrus there is maximum cell proliferation and leukocytes are rare, in metoestrus the uterine wall is no longer distended and the epithelium degenerates and there are many leukocytes and in dioestrus the uterus is collapsed with leukocytes and regeneration (Rendi, 2012).

To determine the stage of the oestrus cycle the 'wet smear' technique/vaginal cytology method was used. Non-pregnant females were then culled during the oestrus stage of the cycle. Prior to animal culling, each female was monitored over two weeks to observe two full cycles. A thin-ended plastic Pasteur pipette was gently inserted into the vaginal opening of a scruffed mouse and sterile water or PBS (approximately 100 µl) was inserted and the vagina was flushed with this fluid approximately 3-5 times, demonstrated in Figure 11. The fluid was placed on a glass microscope slide, covered with a glass coverslip, and inspected under a light microscope. A 20x objective was used to characterise the cell types and the 10x objective was used to
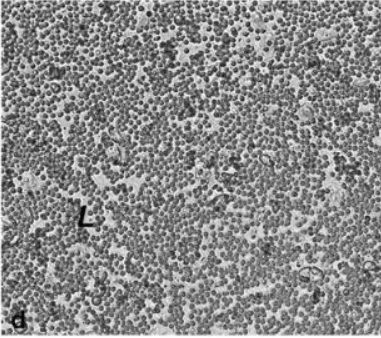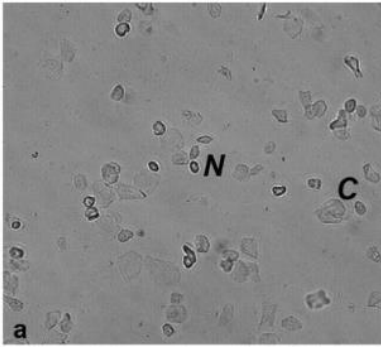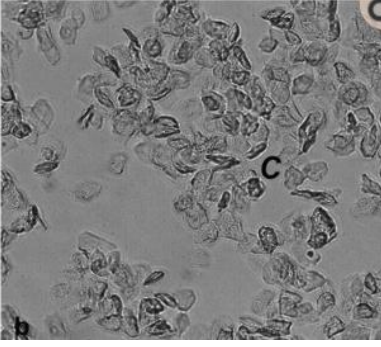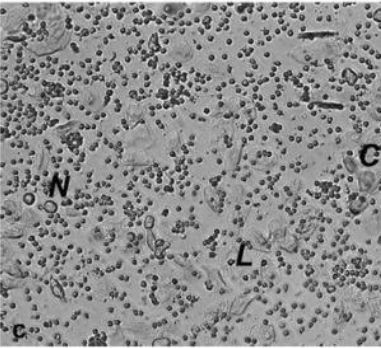
determine the proportion of the three cell types: leukocytes, cornified epithelial cells and nucleated epithelial cells. The ratio of cells was used to determine the stage of the oestrus cycle, see Table 2.

Figure 11. Collection of vaginal fluid secretion in non-pregnant mice.

(A) The correct handling technique to restrain a live mouse with the non-dominant hand of the handler. **(B)** Using the dominant hand, the tip of a fine-tip Pasteur pipette filled with sterile water or PBS is inserted into the vagina of the mouse and the liquid was flushed 3-5 times before collection. Image from (Caligioni, 2009).

Table 2. Stages of the mouse oestrus cycle with descriptions of the vaginal smear cell content and visual appearance of the uterus. Images from (Caligioni, 2009).

Stage	Vaginal Smear	Unstained vaginal secretions	Uterus
Dioestrus	Many leukocytes, and a few nucleated epithelial cells		Small, thin and anaemic
Proestrus	Very few leukocytes and cornified cells, many nucleated epithelial cells		More vascular, increased water content and distended
Oestrus	Lots of large cornified epithelial cells in clusters. Very few, or no nuclei		Vascularised and distended (unless in very late oestrus)
Metestrus	Consists of all three cell types, leukocytes, cornified and nucleated. Mostly leukocytes present, with a few cornified cells		Small pink and vascularised

3.3 Determining gestation length using video camera recordings

Female animals between 8-16 weeks of age were set up in mating pairs as described above. Females were observed for a copulation plug (a hardened white mass in the vaginal opening) to determine successful mating. The time and date was noted, and this was considered as day 0.5 of gestation. Pregnant females were singly housed from gestation day 17.5 in IVC cages with minimal nesting bedding (compared to normal bedding), a large shallow cardboard ring and white pine shavings, to increase visibility. The activity in these cages was recorded until the end of labour on two Gamut 2MP Ultra-low light TVI Pinhole Cameras, which were connected to the Hikvision 8 Channel Hybrid DVR, as demonstrated in Figure 12. The recordings were saved as an MP4 file and viewed on VSPlayer Version 7.4.3. The length of gestation was determined as starting at 0.5 days post-coitum to the sighting of the first pup. Parturition duration was determined as sighting of the first pup to the final pup being birthed.
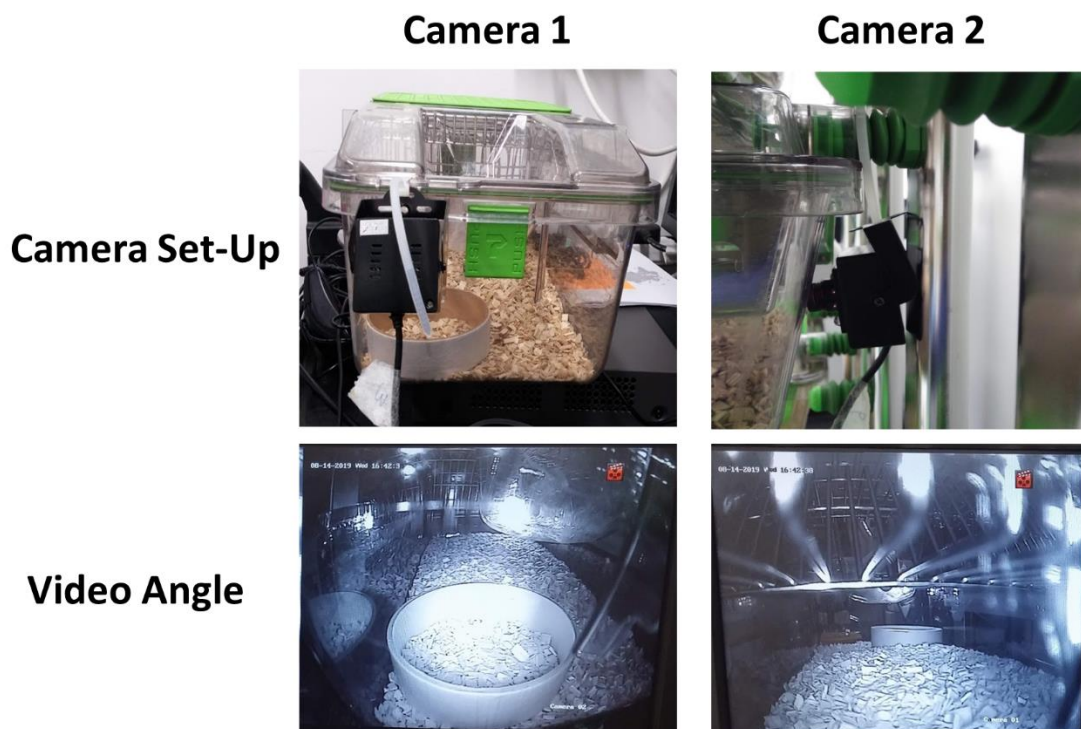
Figure 12. Digital images demonstrating the set of pinhole cameras around a Perspex independently ventilated cage and the field of view inside the cage from each camera.

3.4 Genotyping *Ryr1*^{Y522S/+} and wild-type mice

Ear clippings were collected from mice after 3 weeks of age post-weaning, or tails from culled gestation day 18.5 fetuses and stored at -20⁰C. These ear clipping patterns were also used as a method of identification between individual mice in one cage. The genotyping method originally described by Chelu and colleagues was used to confirm whether an animal was carrying the *Ryr1* Y522S mutation or was a wild-type littermate. Briefly, DNA was extracted and the *Ryr1* region containing the *Blp I* restriction enzyme digestion sites was amplified using the polymerase chain reaction (PCR). PCR amplicons were then digested using *Blp I* and the digestion product was visualised on an agarose gel (Chelu, 2005).

3.4.1 Extraction and purification of total DNA

DNA was extracted from mouse tail or ear clipping samples using the DNeasy Blood and Tissue Kit (QIAGEN, Hilden, Germany). The first step of nucleic acid extraction from tissue is a lysis step. Up 25 mg of tissue was lysed with proteinase K, in a buffer solution at 56⁰C for 3-8 hours. A high concentration of chaotropic salts in the buffer solution destabilizes proteins (including nucleases) and disrupts the association of nucleic acids with water, aiding their transfer to the silica membrane. The serine proteinase, proteinase K digests proteins from the nucleic acid preparation. Following the lysis step, the nucleic acids were separated from the lysate by binding to the silica in the spin column, this is enhanced by the chaotropic salts and the addition of ethanol. After the nucleic acid is bound to the silica membrane, a series of wash steps were carried out to remove impurities such as proteins, polysaccharides and salts. The first wash contains a low concentration of chaotropic salts to remove proteins and the second contains ethanol which is used to remove the residual salts. In this protocol, the second wash step was repeated when the starting sample material was lower to get a higher yield and purity. The final step of the extraction was the elution step where 100 µl of an elution buffer (a more

basic pH than water) was added directly to the membrane of the column and centrifuged to obtain an eluent containing the extracted DNA (Kennedy, 2017).

Mouse tail or ear clipping samples placed in a 1.5 ml microcentrifuge tube with 180 µl Buffer ATL and 20 µl proteinase K, was mixed by using a vortex and incubated at 56°C until completely lysed, in a digital drybath. Tubes were mixed further by vortex intermittently during incubation. Ear clipping samples were lysed for 3 hours and tail samples were lysed overnight. Samples were then mixed using a vortex for 15 seconds before adding 200 µl Buffer AL then mixed again thoroughly. Ethanol (200 µl, 96–100%, Fisher Scientific UK) was added and mixed thoroughly using the vortex. The sample mixture was pipetted into a DNeasy Mini spin column placed in a 2 ml collection tube and centrifuged at ≥6000 x g (8000 rpm) for 1 minute. The flow-through was discarded. The sample was washed with 500 µl Buffer AW1 with centrifugation for 1 min at ≥6000 x g and 500 µl Buffer AW2 and centrifugation for 3 min at 20,000 x g (14,000 rpm). Discarding the flow-through each time. The spin column was transferred to a new 1.5 ml microcentrifuge tube. To elute the DNA, 100 µl Buffer AE was added to the centre of the spin column membrane, incubated for 1 min at room temperature (15–25°C), then centrifuged for 1 min at ≥6000 x g. This final step was repeated to increase the DNA yield. If not being used immediately DNA was stored at -20°C (2-4 days) and -80°C for longer periods of time (more than 7 days).

3.4.2 Quantification of DNA

Spectrophotometry was used to quantify nucleic acids and proteins, using the Nanodrop 2000 spectrophotometer (Thermo Fisher Scientific, Massachusetts, USA). Using the 'Nucleic acid' setting on the Nanodrop programme, the sample pedestal was cleaned with 2 µl PCR-clean

water and calibrated with 2 µl Buffer AE. Each DNA sample (2 µl) was applied to test its quantity, and purity. Typically, a minimum DNA concentration of 20 ng/µl and ratio of 1.8-2.0 at 260:280 and 2.0-2.2 ratio for 260:230 values is considered acceptably pure for use in further amplification steps.

Nucleotides, RNA, ssDNA and dsDNA all absorb at 260 nm and contribute to the absorbance of the sample and therefore it is essential that nucleic acid samples are purified prior to measurement. The 260:280 ratio was used to measure the purity of a DNA or RNA sample.

The five nucleotides (guanine, cytosine, adenine, thymine, uracil) that comprise DNA or RNA exhibit varying 260/280 ratios independently (Thermo Fisher Scientific, no date; Geuther, 1977). The resultant 260:280 ratio is the approximately weighted average of the 4 nucleotides present. When contaminated with proteins, phenols or other contaminants that absorb strongly at or near 280 nm the ratio can appear much lower. The 260:230 ratio is used as a secondary measure of purity. Contaminants such as EDTA, carbohydrates and phenols have absorbance near 230 nm which can drastically reduce the ratio.

The concentration of the nucleic acid sample is determined using a modified version of the Beer-Lambert equation $A = E * b * c$, where A = absorbance, E = extinction coefficient (litre/mol-cm), b=path length (cm) and c = analyte concentration (moles/litre or molarity). The modified equation uses the extinction coefficient with unit's ng/cm/µl to give $c = \frac{A*e}{b}$, where c = nucleic acid concentration in ng/µl.

3.4.3   Amplification of DNA fragment using the polymerase chain reaction (PCR)

The polymerase chain reaction was used to amplify the region of *Ryr1* containing the Y522S mutation and the *BlpI* restriction enzyme site. The components required for a PCR reaction include a buffering solution, magnesium, deoxynucleotides, a forward primer and reverse

primer, nucleotide template, and Taq polymerase. The DreamTaq Green PCR Mastermix 2x (Thermo Fisher Scientific, Massachusetts, USA) contained DNA polymerase, green buffer, dATP, dCTP, dGTP and dTTP, at 0.4 mM each, and 4 mM $MgCl_2$. The following mouse primers were used to amplify the region of site-directed mutagenesis as described in (Chelu, 2005): forward 5'-TCTCCCTGGTCCTGAATTGC-3' and reverse 5'-AGCGTACAGCCACACCATTG-3'(Eurofins Genomics, Ebersberg, Germany). Lyophilised primers were resuspended in nuclease free water to a final concentration of 10 µM before use.

Table 3. Detail of the primers used for the genotyping of the *Ryr1$^{Y522S/+}$* animal model

Primer	Forward 5' TCTCCCTGGTCCTGAATTGC 3'	Reverse 5' AGCGTACAGCCACACCAT TG 3'
Length (bp)	20	20
Weight (g/mol)	6034	6071
T_m (°C)	59.4	59.4
GC content (%)	55	55

The PCR reaction mix was made to test all samples of interest, two positive controls (known wild-type and heterozygous samples), two negative controls (without DNA template) plus an allowance for 10% pipetting error. The following PCR mix was made using the DreamTaq Green PCR Master Mix (2X), in a 2ml PCR-grade Eppendorf tube performed on ice. The reaction mix (40µL) was mixed with the DNA sample (10µL) in each PCR microtube. The DNA was gently mixed by pipetting before adding to the mix to ensure the DNA was evenly distributed in the tube. The PCR tube were quickly but gently spun in a bench top centrifuge before placing in a thermocycler using the following program:

Table 4. Reagent mix used to amplify Ryr1 fragments using PCR

Reagent	Volume (µL)	Reaction concentration
Mastermix	25	1x
Forward primer	2	0.4 µM
Reverse primer	2	0.4 µM
DNA	10	10 pg - 1 µg
Water	11	
Total	**50 per reaction**	

Table 5. Thermocycler heat program used to amplify DNA fragments for animal genotyping

Temperature	Time	
95ºC	2 min	
95ºC	30 s	35 cycles
59ºC	45 s	
72ºC	45 s	
72ºC	5 m	

To determine the annealing temperature of any primers used in this project, the following formulas were used.

For sequences less than 14 nucleotides:

$$Tm= (wA+xT) * 2 + (yG+zC) * 4$$

For sequences longer than 13 nucleotides:

$$Tm= 64.9 +41*(yG+zC-16.4)/(wA+xT+yG+zC)$$

Where w,x,y,z are the number of the bases A,T,G,C in the sequence, respectively.

3.4.4   Enzyme digestion of PCR product

The *BlpI* restriction enzyme digestion sequence was added near the *Ryr1* genetic modification in the *Ryr1*$^{Y522S/+}$ mouse model (Chelu, 2005). *BlpI* is an isoschizomer of Bpu1102I and EspI. The *BlpI* restriction enzyme cut site is GC/TNAGC. The *BlpI* restriction enzyme with the CutSmart Buffer 1X, pH 7.9, containing 50 mM Potassium Acetate, 20 mM Tris-acetate, 10 mM Magnesium Acetate, 100 µg/ml BSA (R0585L, New England Biolabs, Ipswich, Massachusetts, United States) was used to digest the resulting PCR products with the following reaction mixture, which was incubated at 37ºC for 1 hour.

Table 6. Reaction mixture used to perform a *Blp1* enzyme digestion of PCR amplicons

Reagent	Volume (µL)
Enzyme	0.5
Buffer	2.5
Water	2
PCR product	20
Total	**25 per reaction**

3.4.5   Agarose gel electrophoresis

To visualise the size and number of amplified PCR products, the samples were run on a 2%
agarose gel; 2 g of agarose powder (Sigma-Aldrich, UK) was dissolved in 100 ml of 1X Tris-
Borate-EDTA buffer (TBE) (Sigma-Aldrich, UK), melting at approximately 80°C until the
agarose was fully dissolved. The liquid agarose solution was left to acclimatise to a temperature
of 55°C. SYBR safe DNA gel stain (10 µl; Invitrogen, UK) and agarose solution (100 ml) were
added to a horizontal gel tank, stirred to remove bubbles, and set with a comb to allow for the
formation of wells. Once set, the gel was placed in an electrophoresis tank, and covered with
1X TBE; the enzyme digested products (8 µl) were mixed with TriTrack DNA Loading Dye
(1X) (2 µl) (Cat. no. R1161, Thermofisher Scientific, USA) before being loaded into a single
well. Alongside the samples, a 50 base pair ladder (5 µl) (Cat. no. SM0371, GeneRuler,
Thermofisher Scientific) was also loaded for reference amplicon sizes. Samples containing the
heterozygous Y522S mutation were visible as two bands at 800 and 650 base pairs (bp), being
digested at the inserted *BlpI* site, whereas the wild type samples had only one band at 800 base
pairs, due to the lack of a *BlpI* enzyme digestion site, an example is shown in Figure 13.
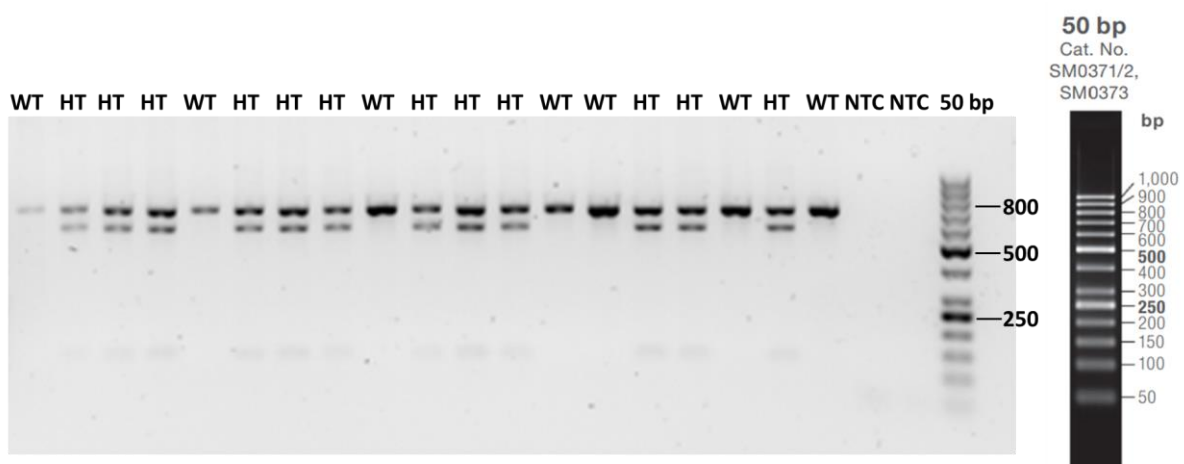
**Figure 13. An example of *BlpI* restriction enzyme digested DNA from wildtype (WT) and heterozygous
Ryr1^{Y522S/+} mutant mice (HT). With a 50 base pair DNA ladder.**

3.5   Non-pregnant and pregnant mouse tissue collection

Non-pregnant animals were confirmed to be at oestrus then humanely killed by cervical dislocation, rising concentration of CO_2 or intraperitoneal injection of pentobarbital in accordance with Schedule 1 of the Home Office UK guidelines (*The Animals (Scientific Procedures) Act 1986 Amendment Regulations 2012*, 2012). The animal was laid supine and covered in 70% ethanol to reduce the risk of contaminating the dissection with hair and other microbes. The skin was pinched with forceps and a lateral incision was made at the midline, the skin was pulled apart to reveal the abdomen. The peritoneum was cut to expose the abdominal cavity and the reproductive organs located in the dorsal region of the body. Using forceps to grasp the ovaries of the non-pregnant animal, the uterine horns were lifted out of the abdominal cavity and cut below the cervix and kept in physiological salt solution (PSS) at 4 ⁰C. Using a sterile scalpel (Ref: 0511, Swann-Morton), sections (≤ 0.5 cm^2) of myometrial, skeletal, cervix, heart, and brain tissue were snap frozen in liquid nitrogen for protein analysis or incubated in RNA*later*™ stabilization solution (Thermofisher Scientific, Massachusetts, United States) at 4°C overnight then stored at -80 °C for RNA extraction later. Myometrial tissue was stored in physiological salt solution (PSS, see Table 9 for recipe) at 4 °C before use for isometric tension recordings.

Pregnant animals were also humanely killed using Schedule 1 methods. The pregnant uterus was removed from the abdominal cavity and immediately placed in ice-cold PSS before further dissection. The uterine artery and all attached connective and adipose tissue were dissected from the uterus and stored in ice-cold PSS for fine dissection for wire myography. The uterine horns were cut along the midline along the placental attachments. The fetuses were carefully removed and immediately culled by placing in ice cold PBS. The amnion and yolk sac covering each fetus was carefully removed and the placenta attached to the fetus was separated, patted

dry on a paper towel, and weighed in a sterile petri dish. The number of fetuses, placentas and resorption sites were recorded. In litters with fetuses of mixed genotypes, from each fetus, a 5 mm tail section and all resorptions were collected and stored at -80 °C for genotyping. Placentas were stabilized in RNAl*ater* reagent or snap-frozen in liquid nitrogen before being stored at -80 °C, and fixed in 4% paraformaldehyde overnight.

3.6 Reverse transcription quantitative real-time PCR (Rt-qPCR)

The reverse transcription quantitative real-time PCR method is based on the detection of an increasingly fluorescent signal with increasing amplification of a nucleic acid fragment. Rt-qPCR is a widely used, efficient and reliable tool that allows for the quantification of nucleic acid fragments such as mRNA transcript expression levels, with small amounts of starting material (Bustin *et al.*, 2009). The resulting fluorescent signal can be quantified using two commonly used methods: relative quantification and absolute quantification. Relative quantification involves standardizing and comparing C_t values between a treatment or disease group and a control group, generating fold changes (Livak and Schmittgen, 2001). Absolute quantification involves the generation of standard curves using samples of known concentration, described further below (Bustin, 2000). Absolute quantification allows for the precise quantification of a gene copy number with greater reliability and was therefore used in this thesis.

Briefly, total RNA was extracted from the tissue and species of interest and transcribed into complementary DNA (cDNA), to control for species and tissue-based transcript variation. Using primers carefully designed to amplify cDNA, the gene of interest (GOI) was amplified using PCR (Bustin and Huggett, 2017). Resulting amplicons were visualised on an agarose gel to check for the expected amplicon size, amplicon bands were then purified and the sequence was verified using Sanger sequencing. Negative controls (replacement of template with water) were used confirm that there was no contamination in the reaction mixture.

Following amplification and confirmation of correct sequence amplification, the concentration of double-stranded cDNA was determined. Using the concentration and known amplicon base pair length the exact copy number was determined, from which serial dilutions were made, this made standards of known concentration which used to generate a standard curve. Following

this, the Rt-qPCR step was performed using SYBR green chemistry. SYBR green is a free-floating fluorescent dye that binds to double-stranded DNA and increases in fluorescence when bound. Consequently, as DNA polymerase and primers duplicate the template strand, increasing numbers of SYBR green molecules bind to double-stranded DNA. The qPCR instrument uses a wavelength of 522 nm to excite the fluorescent molecule at each amplification cycle emitting a fluorescent signal, giving a direct proportion of double stranded cDNA amplicons in the mixture in real-time.

The Minimum Information for Publication of Quantitative Real-Time PCR Experiments, commonly referred to as the MIQE guidelines, were used to develop the protocol below and where possible, the essential and desirable reporting criteria from Table 1 of (Bustin *et al.*, 2009) have been reported in this thesis. Such essential criteria include (but are not limited to) amplicon length, in silico specificity, reaction conditions, thermocycling parameter, PCR efficiency and justification of choice reference genes.

3.6.1   Extraction of total RNA from mouse tissue

The RNeasy Mini kit (QIAGEN, Hilden, Germany) was used to extract RNA from mouse myometrial, placental, uterine artery tissues. Myometrial tissues (<30 mg) stabilised in RNA*later* reagent that were previously stored at -80 °C were disrupted with Buffer RLT and homogenized in the TissueLyser II (QIAGEN, Hilden, Germany). To homogenise the sample, a sterilised 5 mm stainless steel bead was added to each sample and shaken for 2 minutes at 25 Hz. Following centrifugation of the lysate for 3 minutes, the supernatant containing RNA was removed and was used for the subsequent steps; 70% ethanol was added to the supernatant and mixed by pipetting, creating conditions that allow for the binding of RNA to the RNeasy membrane. The sample was then applied to the RNeasy spin-column and centrifuged for 30 seconds at 10,000 g. An on-column DNase digestion was performed using DNase I and buffer

RDD for 15 minutes at room temperature. This was followed by several wash steps using buffers RW1, RPE and then a final elution of the RNA using 30 µl RNase-free water. This step was repeated to obtain a higher concentration of RNA. The eluted RNA was quantified and stored at -80°C. To assess integrity of each RNA sample, the samples were run on a 2% agarose gel, as described in section 3.4.5. Each RNA sample (1-3 µg) was mixed with RNA loading dye (8 µl) before and run at 100 V for approximately 1 hour. Low RNA quality was determined by the appearance of a lower molecular weight smear.

3.6.2   cDNA synthesis

Total RNA (1 µg) was converted to complementary double stranded DNA (cDNA) using the QuantiTect Reverse Transcription Kit (QIAGEN, Hilden, Germany). To calculate the volume required for 1 µg of total RNA the following equation was used:

$$1000 \ (ng)/RNA \ concentration \ (ng/\mu l) = \ volume \ (\mu l) for \ 1\mu g$$

Each reverse transcription reaction was carried out in triplicate for each sample. To remove interfering genomic DNA, 1 µg of total RNA was incubated with a gDNA wipe-out buffer containing DNAse enzyme, at 42⁰C for 2 minutes. Following the gDNA elimination reaction, RNA was incubated with reverse transcriptase, at 42⁰C for 15 minutes to create cDNA, then incubated at 95⁰C for 3 minutes to stop the reaction. The cDNA mixture was diluted to 100 ng template per µl in RNAse-free water and stored at -20⁰C.

3.6.3 Primer design

Where previously published primers were not used, they were designed using mRNA transcripts (RefSeq) and primer designing software Primer3, version 4.1.0 (http://primer3.ut.ee/). The primers were designed to span exon-exon boundaries where possible, to avoid interference by genomic DNA during the amplification stage. The primers were designed to have an annealing temperature in the range of 58 and 62°C, amplicon sizes of <300 bp, <50% GC rich sequences. The specificity of the primers binding to the target transcript were confirmed by ´In-Silico PCR´ (http://genome-euro.ucsc.edu) (Kent *et al.*, 2002). The primer sequences were checked against reference genomes GRCh37/hg19 (human) and GRCm38/mm10 (mouse) for the presence of common SNPs (present in >1% of the population) in the UCSC Browser. Confirmation of primer specificity to produce only one product was determined using melt-curve analysis whereby following a PCR reaction an exponential increase in heat breaks all double stranded products, resulting in peaks at each product made.

3.6.4 Reference gene selection

When selecting a panel of reference genes, it was important to ensure that the genes were from different biological pathways and that their expression was independently regulated. Based on their widely reported stable expression in various published literature the genes *B2M, β-actin, Gapdh* were selected to from a panel of candidate reference genes for downstream absolute quantification (An, et al., 2012). *Desmin* was also selected for its specific known expression in muscle cells (Zhou, et al., 2013; Paulin & Li, 2004).

Table 7. Mouse cDNA primers used in this thesis for the genes *Ryr1, Ryr2, Ryr3-I, Ryr3-II, B2M, β-actin, Gapdh, Ighv2-9, Fcgbp, Ptprm, Igkv17-121, Psg16* and *Nmb* (Eurofins Genomics, Ebersberg, Germany).

Gene (accession number)	Forward Primer (5'-3')	Reverse Primer (5'-3')	Amplicon Size (bp)
Ryr1 (NM_009109.2)	TCACTCACAATGGAAAGCAG	AGCAGAATGACGATAACGAA	298
Ryr2 (NM_023868.2)	CACCAGTACGACACAGGCTT	TCCACCACACAGCCAATCTC	188
Ryr3-I Small (NM_001319156.1)	TGGTGTCATGGCTAAGTTCCA	AGGCAAGGTAGAGAAAGGAGTTG	90
Ryr3-II Large (NM_001319156.1)	TCATGTCGATGGAACTTAGCCT	GCATCTCTGGTGTCATGGTACA	374
B-2-M (NM_009735.3)	TTCAGTATGTTCGGCTTCCC	TGGTGCTTGTCTCACTGACC	103
Gapdh (Nm_008084.3)	TTGATGGCAACAATCTCCAC	CGTCCCGTAGACAAAATGGT	110
Desmin (Nm_010043.2)	TGAGACCATCGCGGCTAAGA	GTGTCGGTATTCCATCATCTCC	136
β-Actin (NM_007393.5)	ATGGAGGGGAATACAGCCC	TTCTTTGCAGCTCCTTCGTT	149
Ighv2-9 (NC_000078.7)	TCCTGGTGCTGTTCCTCTG	TGCTTCCACCACCCCATATT	219
Fcgbp (NM_001122603.1)	GGAGTTCTCCATTGTGCTCG	CTCGGGATGGACATGAGGAT	249
Ptprm (NM_008984.2)	TTCGGTCCAGGAGAGTCAAC	GGCTTGAGTTTGTCTGTGGG	165
Igkv17-121 (NC_000072.7)	TGACCATGTTCTCACTAGCTCT	CCAGGACGAAGAGTATTGCC	235
Psg16 (NM_001310628.1)	AGAATTCAAGTGTGCCAGGC	CATACCGTGGCATTGGATCG	237
Nmb (NM_001291280.1)	CAAGATTCGAGTGCACCCTC	GAGCTTTCTTTCGCAGGAGG	176

The fragments of the gene of interest were amplified using 0.75 µl of each forward and reverse primer listed above (300 nM), 12.5 µl HotStarTaq DNA Polymerase (2.5 units) containing PCR Buffer, 1.5 mM MgCl$_2$ and 200 µM dTNPs, 3.5 µl cDNA template (100 ng/µL) and 7.5 µl RNase free water. The following cycling conditions were used in the G-Storm GS4 thermal cycler (Gene Technologies Ltd, Essex, England).

Table 8. Thermocycler program used to amplify cDNA fragments for qPCR reactions

DNA polymerase Activation	95°C	15 min	
Denaturation	94°C	1 min	
Annealing	50-65°C	1 min	35 cycles
Extension	72°C	2 min	
Final extension	72°C	10 min	

Amplified PCR products were mixed with TriTrack DNA loading dye (1X) (Thermofisher Scientific, Massachusetts, United States) and loaded into a 2% agarose gel made with Tris-Borate-EDTA buffer (1X), which was run in TBE buffer in a horizontal electrophoresis tank at 100 volts for approximately 45 minutes. Once PCR product bands were sufficiently separated the gels were visualised over ultraviolet light, using a UV protective face shield, and each band was cut away using a sterile scalpel. The PCR product (amplicons) in each band was extracted and purified from the gel segments using the QIAQuick Gel Extraction Kit (QIAGEN, Hilden, Germany). Sanger sequencing of the amplicons was outsourced to Eurofins Genomics. Sequence chromatograms were analysed using FinchTV 1.4.0 (http://www.geospiza.com) and Sequencher® version 5.4.6 (http://www.genecodes.com), to confirm amplification of the correct transcript.

3.6.5 Creating standards of known concentrations

The gene copy number in 1 ng of each sample was calculated using the following method:

The average molecular weight of a dNTP is 330 Da, so the molecular weight of double stranded cDNA 2x330 Da=660 Da.

Molecular weight of the gene of interest cDNA product=average dNTP MW in cDNA x total number of bp in amplicon.

e.g.,   660 x 119=78,540 Da

To calculate the number of copies in 1 ng:

Number of molecules in one mole of a given substance=6.02x10^23 (Avogadro's constant), which is equal to the MW in grams.

e.g.,   78,540 g of amplicon=6.02 x 10^{23} amplicon copies

1 ng (10^9) of product=6.02 x 10^{23} / (78,540 x 10^9)

1 ng has 7.66 x 10^9 copies

Using the calculated number of copies in 1 ng, we can then calculate the number of copies in 1 μL using the given concentration from spectrophotometric analysis.

e.g.,   If the given concentration is 14.2 ng/μl

7.66 x 10^9 copies in 1 ng x 14.2 ng/μl=1.09 x 10^{11} copies in 1 μl

Using the known copy number in 1 μl of each sample, standards with known concentrations were made for 10^9 – 10^1 copies, by making serial dilutions from the highest concentration.

e.g.,   To get 10^9 copies in 20 μl

(10000000000 / 1.09 x 10^{11}) x 20=1.83 µl of product will be added to,

20 -1.83=18.17 µl of water

To make subsequent standards, 45 µl of RNase-free water was added to 8 tubes, then 5 µl of 10^9 copies was added to the 10^8 tube and this was repeated for the following tubes to do a serial dilution down to 10^1.

3.6.6   Quantitative reverse transcriptase polymerase chain reaction

Each RT-qPCR reaction contained the following: 0.6 µl forward primer (300 nM), 0.6 µl reverse primer (300 nM), 10 µl SensiFAST SYBR® Hi-ROX Mix 1X (Bioline, London, England), 4.8 µl water and 4 µl of sample cDNA to make up a final reaction volume of 20 µl. The samples with unknown concentrations of cDNA were amplified alongside 8 standards of known concentrations and non-template controls on the RotorGene 600 instrument (Corbett Research, Australia). The following cycling conditions were used: 10 minutes incubation at 95°C, 40 cycles of 15 seconds at 95°C, 30 seconds at 55°C and 50 seconds at 72°C, followed by a final extension at 72°C for 15 seconds.

Melt curve analyses were performed to confirm the presence of one single product, and non-template controls were run to assess contamination. All unknown samples quantification values should fall within the range of the standard curve. Cut off values for efficiency and R^2 were 80% and 0.99 respectively (Bustin *et al.*, 2005). The qPCR products for all genes of interest were Sanger validated and product size was confirmed by gel electrophoresis.
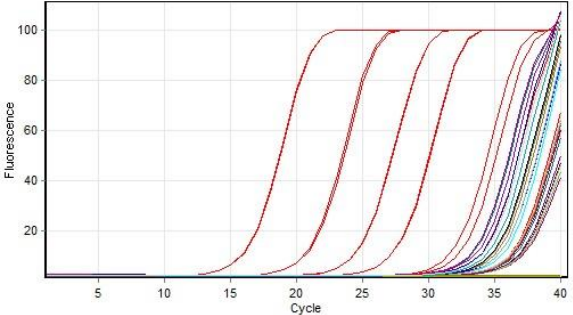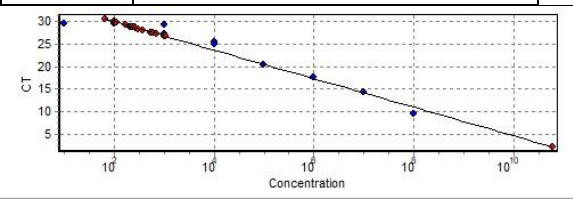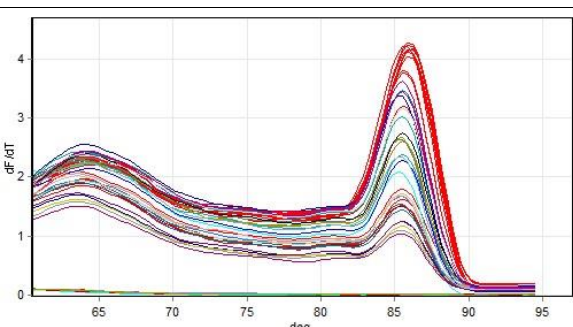
Gene, gene symbol	Ryanodine receptor type 1, *Ryr1*
Sequence ID	NM_009109.2
Product size (bp)	298
Forward primer (5'-3')	TCACTCACAATGGAAAGCAG
Reverse primer (5'-3')	AGCAGAATGACGATAACGAA
Product sequence	**TCACTCACAATGGAAAGCAG**CTGGTGATGACCGTAGGGCTCCTGGCCGTAGTGGTCTACT TGTATACAGTGGTGGCCTTCAACTTCTTCCGCAAATTCTACAACAAGAGCGAAGATGAGG ACGAGCCTGACATGAAGTGTGATGACATGATGACGTGCTACCTGTTCCACATGTATGTGGG CGTCCGGGCCGGTGGAGGGATCGGGGACGAGATCGAGGACCCGGCCGGCGATGAATATG AACTTTACCGGGTCGTCTTCGACATCACCTTTTTCTTC**TTCGTTATCGTCATTCTGCT**
Assay conditions	Activation: 95°C 10 minutes. Denature: 95°C 15 seconds. Annealing: 55 °C 30 seconds. Extension: 72°C 50 seconds.
Melting temperature	84.48°C
Efficiency	1.07557
R^2	0.95636
Raw fluorescence	
Standard curve	
Melt curve	

Figure 14. A representative qPCR validation sheet

3.6.7   QPCR reaction validation

As described in sections 3.6.3 to 3.6.5, various steps were taken to ensure the specificity of primers used in qPCR reactions, such as checking the presence of one amplicon band in an agarose gel and one peak on a melt curve. The validity of the reaction was dependent on various factors including reaction efficiency, the accuracy of the standard curve. These details were collated for all genes of interest and an example is shown in Figure 14.

3.6.8   Data analysis using absolute quantification

Using mean Ct values for each biological sample, the gene of interest copy number was extrapolated from standard curves created from the standards of known concentration, described in section 3.6.5.

To normalise data for genes of interest, a set of reference genes were also run with unknown samples. Quantification data for the genes of interest (gene copy number) were calculated relative to the geometric mean of 3 of the most stable reference genes (Bustin, 2009), this was determined using the GeNorm software (version 3.5) (Vandesompele *et al.*, 2002).GeNorm is a Visual Basic Application (VBA) developed on Microsoft Excel software that provides an automated measure of gene expression stability (M values). The M value is the mean pairwise variation between a particular gene and the other candidate reference genes tested. Using the programme, the worst-scoring reference gene (highest M value) are eliminated, and new M values are calculated for the remaining genes. A normalisation factor is also created relative to the geometric mean of 3 of the most stable reference genes (where M < 1.5, the recommended GeNorm cut off value for stable gene selection) (Vandesompele *et al.*, 2002). The gene of interest copy number in each the sample was divided by its relative normalisation factor to create a normalised copy number value.

3.7 Western blotting

Western blot is often used to separate and identify proteins. The technique is based on the separation of a mixture of proteins by molecular weight through electrophoresis. The size-separated proteins are then transferred to a membrane, which produces a band for each protein. The membrane is then incubated with antibodies, often these are antibodies that are specific to the protein of interest. Unbound antibodies are washed off to reveal only a band specific to the protein of interest when visualised using chemiluminescence.

3.7.1 Protocol optimisation for the detection of high molecular weight proteins

Western blotting methods were optimised to blot high molecular weight proteins such as the RyR1 protein (~560 kDa). Mouse vastus lateralis skeletal muscle was used as a positive sample control due to high RyR1 protein content in the skeletal muscle. α-actin (45 kDa) was selected as a reference protein for its stable expression across several tissue types and its high expression in myometrial tissue, see Figure 15.
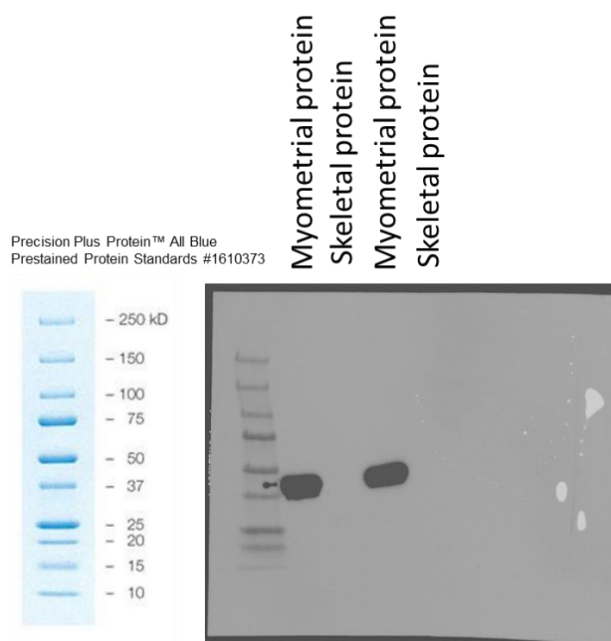
Figure 15. α-actin stained PVDF membrane with myometrial and skeletal protein lysate

Using anti-α-actin antibodies against both mouse wild type pregnant (gestation day 18.5) myometrial and mouse skeletal protein lysate on PVDF membrane

To optimise a standard western blotting protocol for an exceptionally large protein such as RyR1 it was essential to:

1. Ensure the RyR1 protein could unfold sufficiently to migrate through the gel

2. Ensure the RyR1 protein could effectively transfer from the gel to the membrane

Several adjustments to standard western blotting practices were made in series, as discussed briefly below. Pregnant myometrial protein (30 µg) and skeletal protein of wild-type pregnant (gestation day 18.5) animals were separated in a 7.5% gel at 150 V for 4 hours to confirm that proteins above 460 kDa were able to migrate into the gel. This was confirmed using a Coomassie stain (with 10% acetic acid, 30 minutes) which identified if any proteins had been separated into the gel space during electrophoresis, demonstrated in Figure 16.
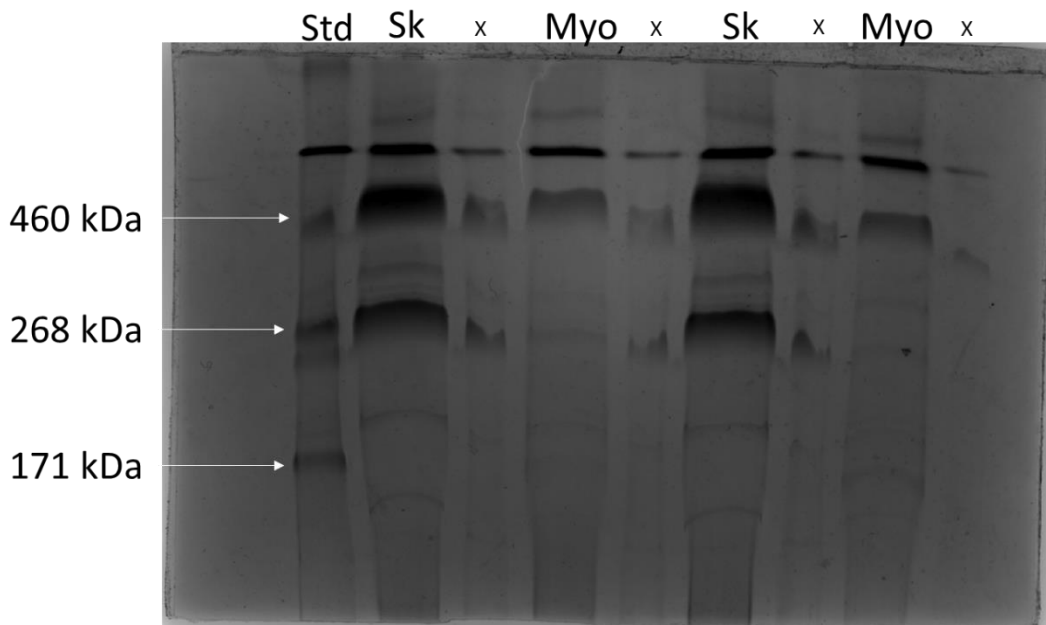
Figure 16. Coomassie blue stain of a myometrial and skeletal proteins separated on a TGX precast gel

Wildtype mouse skeletal (Sk) and pregnant myometrial protein lysate (30 µg) were separated in a TGX precast gel and stained with Coomassie stain (10% acetic acid, 45 minutes). Std, protein standard; X, empty lane.

Initially, 25 µg of protein (myometrial and skeletal) was separated in two 7.5% gels overnight (6pm – 9am). One gel was used to blot proteins on polyvinylidene difluoride (PVDF) membrane using the wet-transfer method, the second gel was used to transfer proteins using the semi-dry turbo blot method. The wet transfer was conducted with transfer buffer with 20% methanol, for 90 minutes, 90V at 4°C. Semi dry transfer was conducted at 1.3A, 25 V for 15 minutes for ryr1 and for 7 minutes for β-actin. The membrane was incubated with the ryr1 primary antibody (1:1000) overnight at 4°C, then incubated with the HRP-conjugated secondary antibody (1:2000) for 90 minutes at RT, on an orbital shaker on a gentle cycle.

Larger proteins did not transfer very well using the wet-transfer method, demonstrated in Figure 17. Moving forward, only the semi-dry transfer method was used. At this point, no RyR1 protein band was identified in wild-type pregnant myometrial protein lysate compared to skeletal protein lysate.
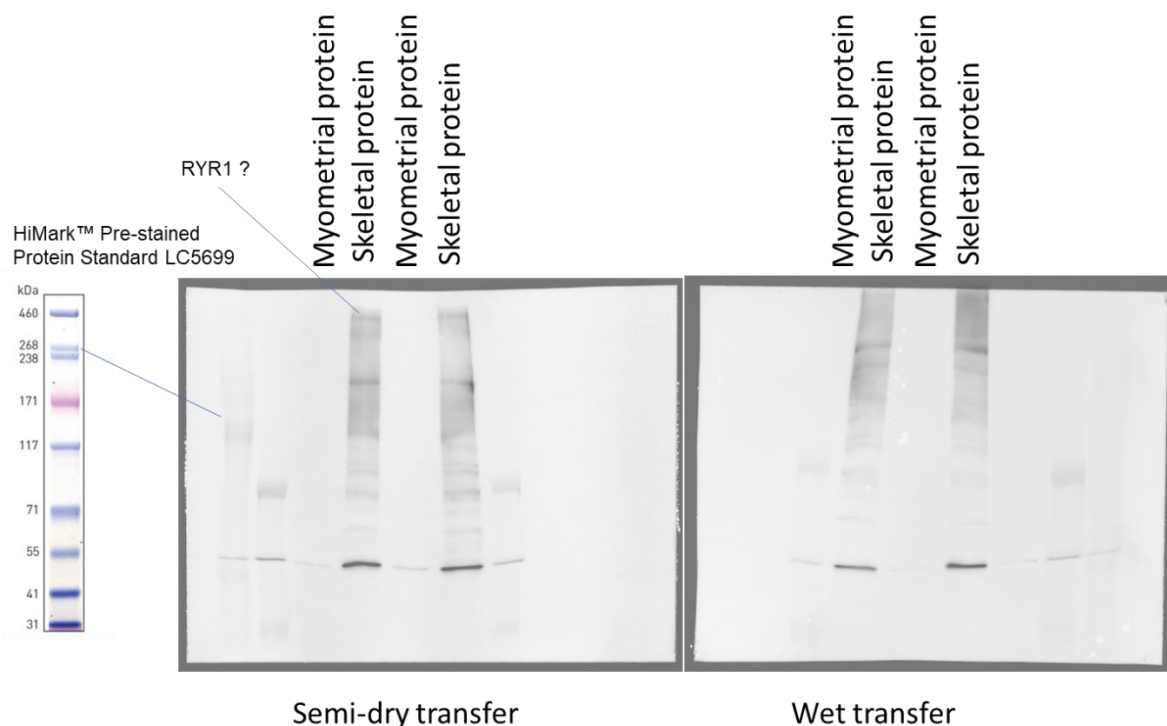
Figure 17. Composite images of RyR1 antibody tagged mouse protein blots obtained using semi-dry transfer and wet transfer methods.

Wild-type pregnant myometrial protein was loaded in increasing amounts (10 µg, 20 µg, 40 µg and 80 µg) to determine the optimum concentration needed to blot RyR1. Proteins were separated by gel electrophoresis at 60 V, overnight (6 pm to 9 am). Protein blotted PVDF membrane was incubated with Ryr1 primary antibody (1:500) overnight, and then with HRP-conjugated secondary antibody (1:2000) at RT for 2 hours.
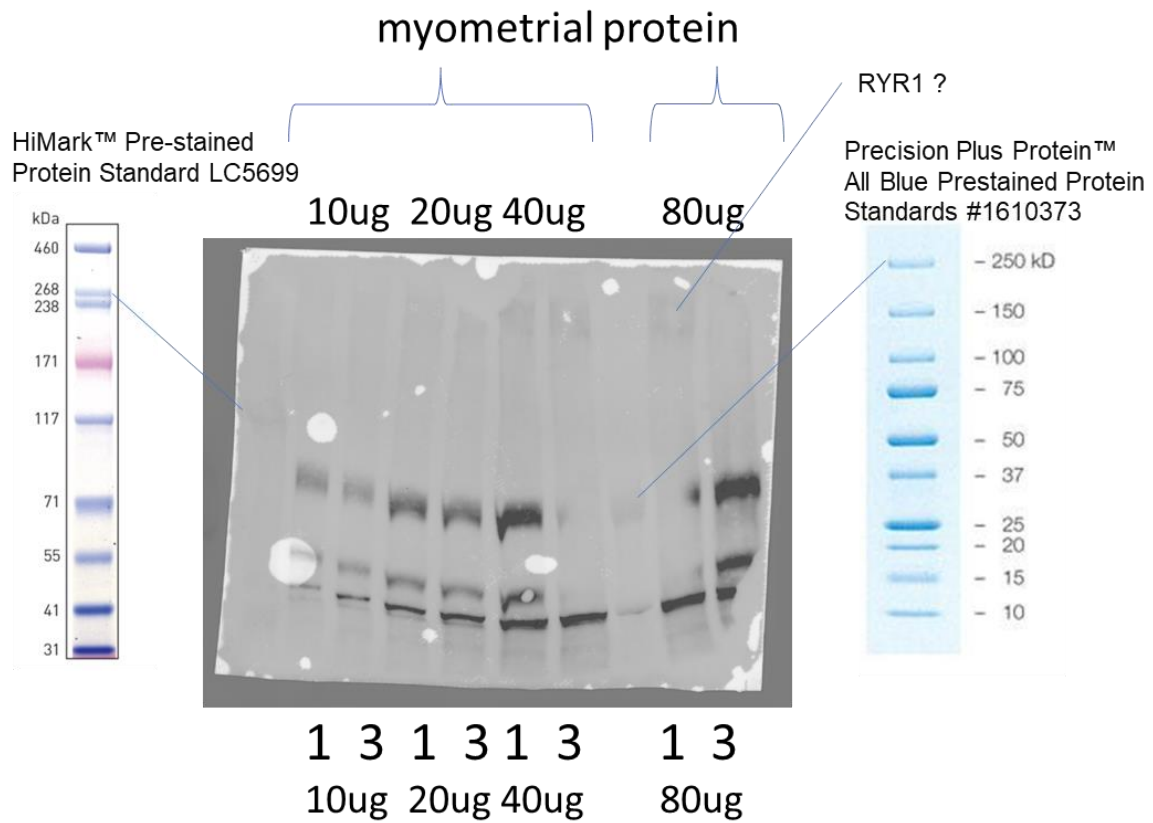
Figure 18. A series of mouse myometrial protein concentrations blotted on PVDF membrane

Finally, pregnant mouse myometrial (3 µg/µL) and skeletal (1 µg/µL) protein lysates were diluted with 4X Laemli buffer and 30% β-ME. Total 90 µg of myometrial protein and 3 µg skeletal protein was loaded in a 4-15% TGX mini gel at 200 V for 2 hours 30 minutes. Semi-dry transfer using Turbo Blot 1.3A, 25 V for 15 minutes, was repeated after cooling the transfer pack for 10 minutes at 4°C. The membrane was incubated with RyR1 primary antibody (1:500) was for 48 hours, and then with secondary HRP-conjugated antibody (1:2000) for 2 hours at RT. After a series of optimisation steps, the skeletal RyR1 protein was successfully blotted onto a membrane.
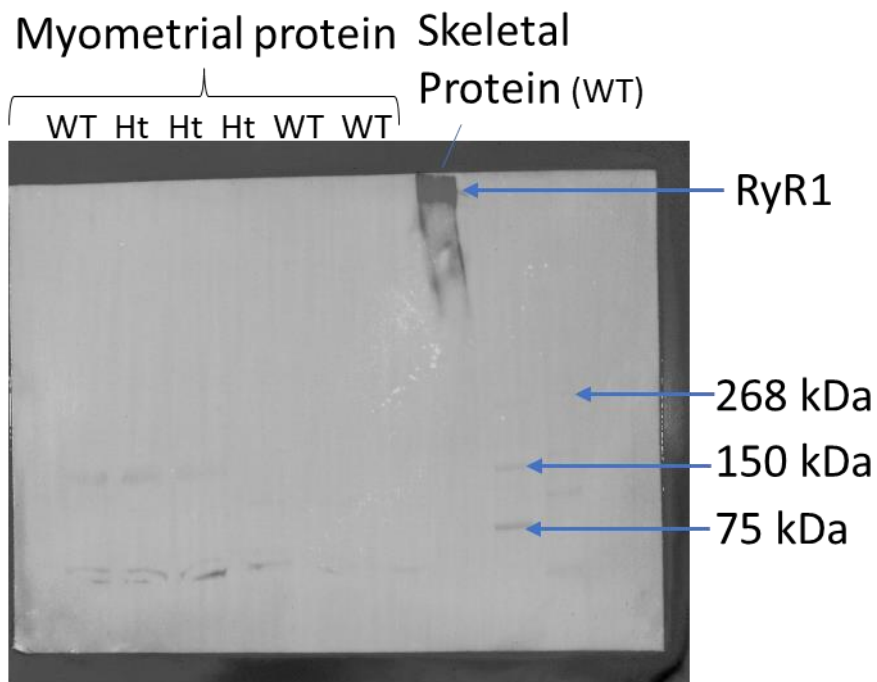
Figure 19. A PVDF membrane blot of pregnant myometrial and skeletal protein lysate stained with anti-RyR1 antibody

A PVDF membrane blot of pregnant myometrial (90 µg) and skeletal (3 µg) protein lysate stained with anti-RyR1 antibody (1:500). After a series of optimization steps, RyR1 protein was detected in skeletal muscle protein lysate but not detected in gestation day 18.5 pregnant myometrial protein lysate. WT, wildtype; Ht, heterozygous Y522S/+.

3.7.2 Extraction of total protein from mouse tissue

Total protein was extracted from mouse myometrial (non-pregnant and pregnant), placental and vastus lateralis skeletal muscle tissues using radio-immunoprecipitation assay (RIPA) buffer, 1 ml:100 mg tissue, (20 mM Tris-HCl (pH 7.5), 150 mM NaCl, 1 mM Na_2EDTA, 1 mM EGTA, 1% NP-40, 1% sodium deoxycholate, 2.5 mM sodium pyrophosphate, 1 mM beta-glycerophosphate, 1 mM Na_3VO_4, 1 µg/ml leupeptin) (9806, Cell Signalling Technology). A protease inhibitor cocktail (5871, Cell Signalling Technology) was diluted in RIPA buffer (1:100) to obtain a 1X working concentration, just prior to use. Pre-cooled round bottomed 2 ml Eppendorf tubes were kept on ice with 200 µl RIPA buffer and 2 x 5 mm stainless steel beads. After weighing, tissues were added to the tube and placed in the Tissuelyser at 25 Hz for 3 minutes. This step was repeated, if necessary, after incubation on ice. The stainless-steel beads were removed, and the remaining buffer was added before mixing by vortex. The samples were centrifuged at 14,000 rpm (approximately 17500 x g) (Eppendorf Centrifuge 5425R, rotor radius 8.4 cm) for 1 minute to remove debris, the supernatant containing protein was aliquoted into clean tubes.

3.7.3 Colorimetric detection and quantitation of total protein

Protein concentration was determined using a Pierce bicinchoninic acid (BCA) protein assay (23225, ThermoFisher). The BCA assay combines the reduction reaction of Cu^{2+} to Cu^{1+} by protein in an alkaline medium with the colorimetric detection of the cuprous cation (Cu^{1+}) by bicinchoninic acid. The first step is based on the biuret reaction, a temperature dependent reaction where peptides containing three or more amino acid residues form a coloured chelate complex with cupric ions in an alkaline environment containing sodium potassium tartrate. The amount of Cu^{2+} reduced is proportional to the amount of protein present in the solution. In the

second step, BCA reacts with the reduced cuprous cation. Two BCA molecules chelate with one cuprous cation resulting in a purple-coloured complex that strongly absorbs light at a wavelength of 562 nm.

Bovine serum albumin (BSA) standards (0.1 – 2.0 mg/ml) were made in ddH$_2$O. Protein samples were diluted 1 in 10 before use in the assay. Protein samples were tested in duplicate according to the manufacturer's instructions including a 30-minute incubation at 37 ˚C. Absorbance values at 562 nm were obtainined using the Biotek Gen5 plate reader (Agilent Technologies, California, United States). A line graph was plotted for standards protein concentration (mg/ml) against average absorbance (nm) to obtain a y = mx + c equation. *e.g. y=0.2983x + 0.0908,* an example of a graph used in this project is provided in Figure 20.
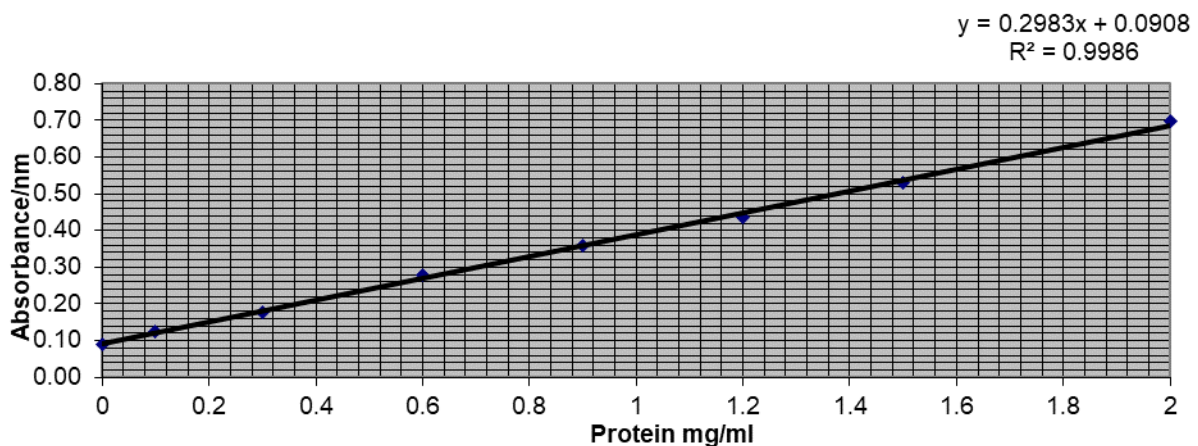
Figure 20. A representative plot used for a BCA assay used to determine protein concentrations.

Absorbance values (nm) for known protein concentrations (mg/ml) were plotted and a from this the y = mx + c and R^2 were obtained.

Using the average protein concetration, the volume of protein needed to load 30 - 80 ug of total protein was calculated. The final gel-loading volume (30 µl) was made up to 20 µl lysis buffer (1X RIPA+ 1X PI), plus 10 µL 3X loading buffer. To denature the proteins the samples were heated in a heat block at 95˚C for 5 minutes then immediately chilled on ice. To reduce freeze-thaw cycles this step was performed in triplicate and stored at -20˚C until needed.

3.7.4 Total protein separation with electrophoresis

Proteins were first separated by molcular weight using gel electrophoresis. Mini-PROTEAN®
TGX™ Precast Gels (4-15%) were placed in Vertical Mini-PROTEAN Tetra Cell tanks
(BioRad) filled with 1X Tris/Glycine/SDS buffer. Protein samples were then carefully pipetted
into the wells, with 10 µL of HiMark™ Pre-stained Protein Standard or Precision Plus
Protein™ All Blue Prestained Protein Standards (#1610373, Bio-Rad). The gel electrophesis
was run at 200 V for 2 hours 45 minutes (for RyR1 560 kDa, until red 171 kDa marker reaches
bottom of tank).

3.7.5 Coomassie blue staining

Coomassie blue staining is used to identify proteins seperated by gel electrophoresis with high
sensitivity, low back background, a large linear ranger and ease of use. On binding to a protein
the negatively changered Coomassie brilliant blue G-250 dye molecule gives an overall
negative charge to the protein, allowing their seperation from the polyacrylamide gel.

The TGX precast gel was stained with Coomassie blue dye (0.1%) dissolved in acetic acid
(10%) and methanol (50%) and water for 30 minutes, then destained twice with acetic acid
(10%) and methanol (50%) and water until clear before imaging.

3.7.6 Semi-dry protein transfer

Proteins were transferred from Mini-PROTEAN® TGX™ Precast Gels to PVDF membranes
using the Trans-Blot Turbo Transfer System (Cat. no. 1704150, Bio-Rad). Extra thick filter
pads were soaked in Trans-Blot Turbo 1x Transfer Buffer (Cat. no. 10026938, Bio-Rad). PVDF

membranes were cut to size and activated in methanol. PVDF is extremely hydrophobic and will not wet in aqueous solution unless activated in methanol. The protein gel was carefully removed for the gel cast, the stacking gel was cut away and the lowermost section of the gel to ensure a smooth gel layer before placing in transfer buffer.

The components were stacked in the Trans-blot Turbo Transfer System cartridge in the order demonstrated in Figure 21. Between each layer, a roller was used to remove excess air bubbles, especially between the PVDF membrane and gel. For Ryr1 protein the following programme was used: 1.3 A, 25 V, 15 minutes, 10 minute incubation at 4 °C and repeat transfer, for all other proteins: 1.3 A, 25 V, 7 minutes.
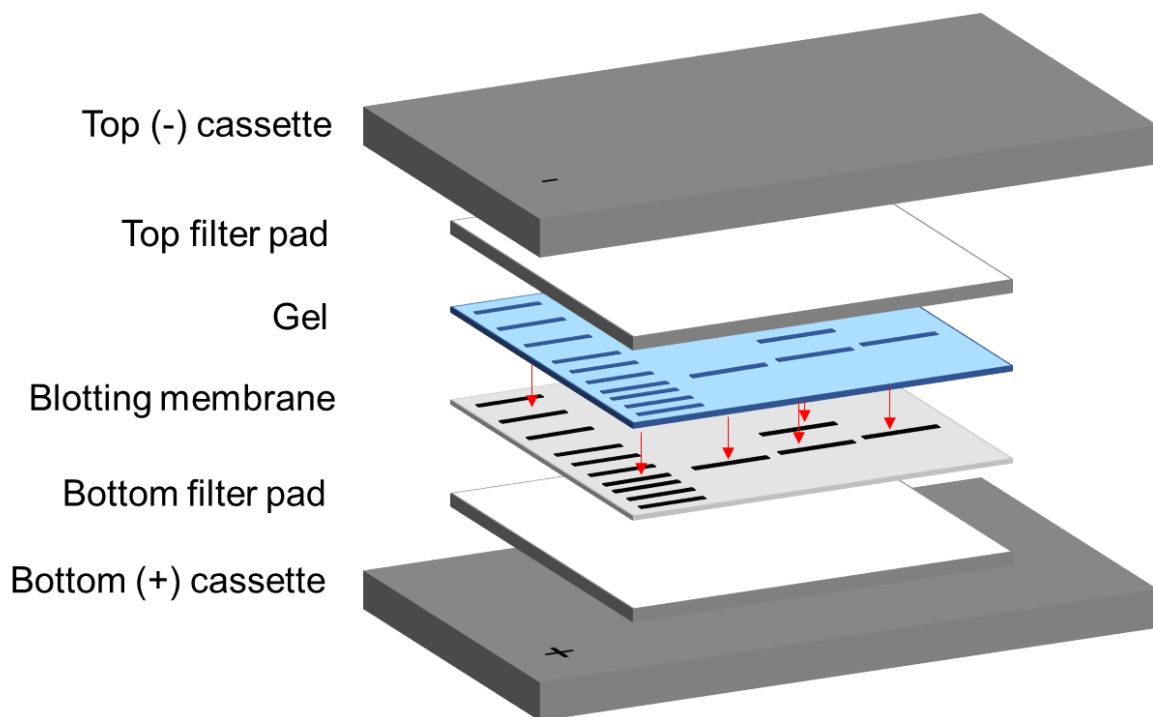
Figure 21. Graphic presentation of the order of a stacking sandwich for a semi-dry protein transfer from a protein gel to a polyvinylidene difluoride (PVDF) membrane.

3.7.7 Membrane blocking

Following successful protein transfer from gel to membrane, the PVDF membrane was incubated at room temperature for 1 hour in 5% skimmed milk, a blocking agent. The milk blocking buffer was diluted in Tris-buffered saline (TBST; 50 mM Tris and 150 mM NaCl, Tween 20, 0.05%, pH 7.6). The blocking agent is used to limit the non-specific binding of primary and secondary antibodies to the membrane (areas without the protein of interest). To ensure uniform blocking of unoccupied binding sites on the membrane, the membrane was placed 'protein side up' and on an orbital shaker on a gentle cycle.

3.7.8 Primary antibody incubation

The antibodies used for primary incubation were selected from published literature; RyR1 (D4E1) Rabbit mAb (#8153, Cell Signalling Technology); β-Actin (13E5) Rabbit mAb (Cat. no. 4970, Cell Signalling Technology). Membranes were incubated in primary antibody 5% milk/TBST solutions (Ryr1 1:500, β-Actin 1:1000) at 4°C overnight, unless otherwise stated.

3.7.9 Secondary antibody incubation

Folllowing primary antibody incubation the membrane was washed with TBST three times for 10 minutes on an orbital shaker at room temperature on a gentle cycle. The secondary antibody anti-rabbit IgG, HRP-linked Antibody (#7074, Cell Signaling Technology) was conjugated with Horseradish Peroxidase (HRP) for chemiluminescent detection. Using a 1:2000 dilution in 5% milk/TBST, the membrane was incubated at room temperature for 90 minutes. Following

secondary antibody incubation the membrane was washed with TBST three times for 10 minutes on an orbital shaker at room temperature.

3.7.10 Chemilumunescent detection

Chemiluminescence occurs when a chemical substrate (luminol) is catalysed by an ezyme (HRP) and produces light as a by-product, which is captured by a digital imaging system (ChemiDoc™ Imaging System, Bio-Rad). Using the Clarity Western ECL Substrate (#1705060S, Bio-Rad) kit, 0.1 ml of solution/cm^2 of membrane was prepared. The membrane was left to incubate in the solution for 5 minutes, before imaging with auto-optimal exposure time for chemiluminescence and colorimetric photos to visualise protein markers.
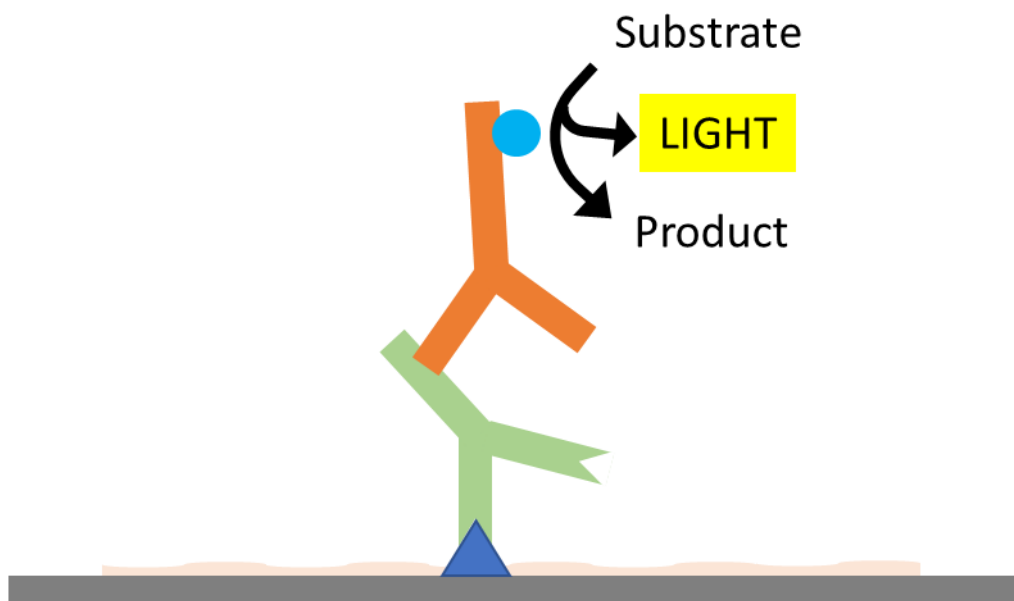
Figure 22. A graphic presenting the mechanism of chemiluminescent detection used to detect protein-bound antibodies on a PVDF membrane.

A detectable signal is generated following the binding of an antibody to the protein of interest. A secondary antibody tagged with an enzyme that converts a substrate into a product, the process of which emits light, the signal is received and quantified by a detection instrument.

3.8   RNA sequencing of *Ryr1$^{Y522S/+}$* mouse myometrium

The central dogma of molecular biology outlines that the flow of information stored as genes in DNA, is transcribed into RNA and translated into proteins (Crick, 1958, 1970). The transcription of a subset of genes into complimentary RNA specifies the cells' identity and determines its biological activities, holding key information on the functional elements of the genome and informs our understanding of diseases. Low-throughput methods of gene expression studies such as northern blots and quantitative polymerase chain reaction (qPCR) are limited to using single transcripts. Over the last two decades methods of studying the transcriptome have evolved (transcriptomics) to provide more high-throughput technologies such as micro-arrays, Sanger sequencing, serial analysis of gene expression (SAGE) and cap analysis gene expression (CAGE). However, these methods are laborious, high-cost and require large amounts of input RNA for very limited uses. High-throughput next-generation sequencing (NGS) methods have revolutionised transcriptomics by sequencing using complementary DNA, termed RNA sequencing.

RNA-sequencing is an NGS-based technique that examines the RNA transcripts produced from DNA, allowing exploration of gene expression. RNA-seq has become a useful tool in many scientific fields, and pregnancy and muscle physiology are no exceptions. Use of RNA-seq in this study was essential to understand how RyR1 Y522S caused gene expression changes globally. This method enables deep profiling of the transcriptome, offering a more detailed and quantitative view of gene expression, splicing events, and allele-specific expression. The benefits of RNA sequencing are extensive, including but not limited to, providing sensitive and accurate measurements of gene expression, ability to capture novel features, generation of both qualitative and quantitative data, ability to study the full transcriptome, and its application to any species (*RNA Sequencing | RNA-Seq methods & workflows*, data accessed 01 March 2023).

3.8.1 Transcriptome sequencing

3.8.1.1 Isolation of RNA

Total RNA was extracted from mouse myometrial tissues processed in RNAlater, as described above in section 3.6.1. The quality of RNA was measured using the Agilent Bioanalyzer (Model 2100, Agilent, Santa Clara, US) which produces an RNA integrity number (RIN) between 1 and 10, 10 having the least degradation. All samples had RIN values >8.5. The RIN is calculated using gel electrophoresis and analysis of the 28s and 18s ribosomal bands' ratio. The area under the curve for each band is calculated as percentage of total area, and a ratio of 28s:18s is calculated. The bioanalyzer instrument uses an algorithm that used the rRNA ratio and the entire electrophoretic trace of the RNA to create the RIN value (Mueller, Lightfoot and Schroeder, 2016).

28s	18s
Area=176.9 % of total area=24.8	Area=99.6 % of total area=13.9
rRNA Ratio (28s/18s)=1.8	
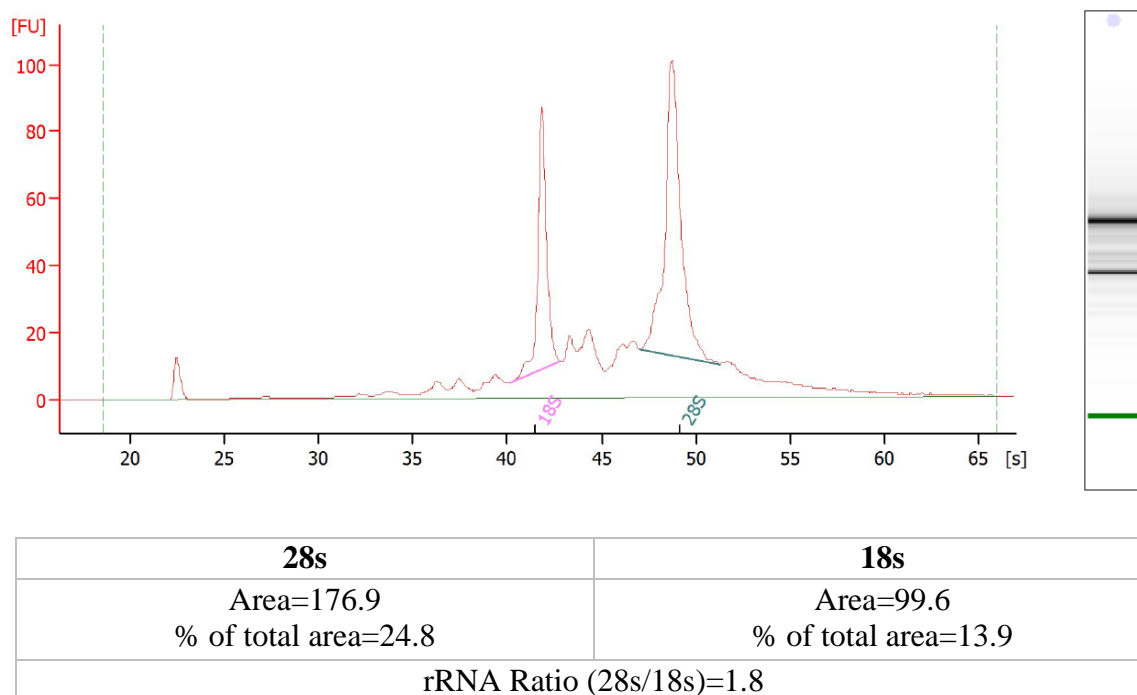
Figure 23. Representative electropherogram summary (above) and representative rRNA ratio calculation (below).

A representative electropherogram summary for a pregnant mouse myometrial sample (above) and an example of a calculation to determine rRNA ratio.

3.8.2 Library preparation and next generation sequencing

RNA sequencing was performed by the King's Collge London genomics centre. Briefly, the NEBNext Ultra II Directional RNA Library Prep Kit for Illumina (New England BioLabs Inc., MA, US) was used for library preparation and the NEBNext Poly(A) mRNA Magnetic Isolation Module was used for rRNA reduction. Library quantification was performed using qPCR, and library pooling. QC sequencing was run on Illumina MiSeq. Subsequent sequencing was performed using the Illumina NovaSeq 6000 sequencing platform at the depth of ~25 million reads pairs (150bp x2) per sample. (Illumina, San Diego, USA).
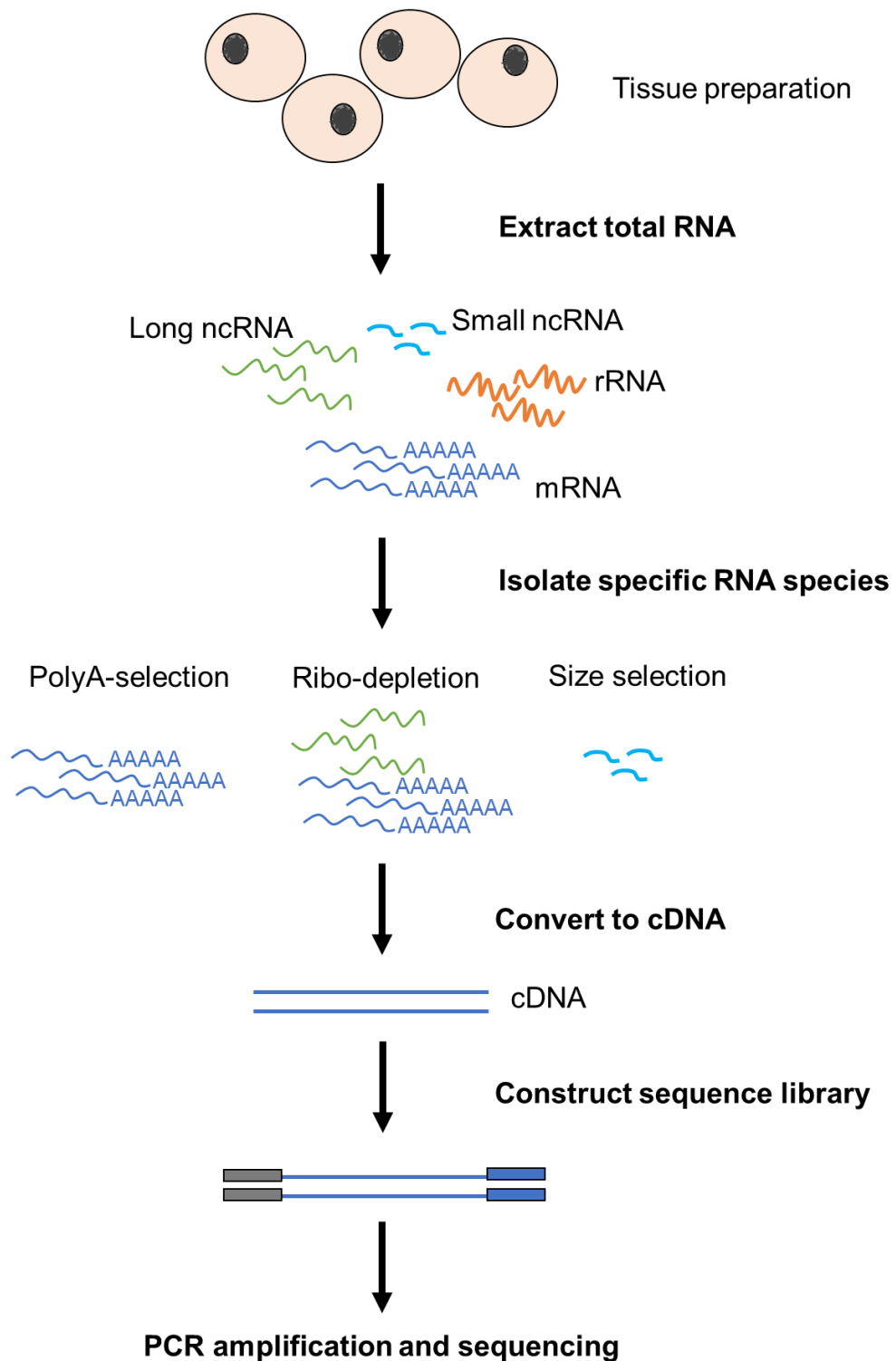
Figure 24. Overview of RNA sequencing workflow

First, total RNA was extracted from the tissue of interest (mouse myometrium). Second, a subset of RNA moleules were isolated using the polyA selection method to enrich for polyadenylated transcripts. Next, the RNA was converted in complementary DNA (cDNA) by reverse transcription and sequencing adapters were ligated to the ends of the cDNA fragments. Follwing this, the fragments are amplified by PCR and the RNA-seq library is now prepared for sequencing.

3.8.3   Transcriptome analysis

As part of a collaboration, Dr Flavia Flaviani and Dr Prasanth Sivakumar have provided analyses of for the transcriptome. Quality control for the raw sequences was performed using FastQC version 0.11.9; subsequently reads where aligned using STAR v2.7.8 on the KCL HPC cluster using reference GRCm39 version 104 (Kings College London, 2022). The index for this was generated with FASTA: Mus_musculus.GRCm39.dna.primary_assembly.fa, and GTF: Mus_musculus.GRCm39.104.gtf, both from Ensembl. Reads were aligned using STAR with default alignment parameters. FASTQ files were converted to Bam files using samtools in R. Integrative Genomics Viewer (IGV) v2.15.x (Robinson *et al.*, 2011, 2017, 2020; Thorvaldsdóttir, Robinson and Mesirov, 2013) was used to confirm the presence of Y522S in heterozygous samples. The counts matrix was generated using featureCounts from subread v2.0.1 using the same GTF as above. Downstream analyses were performed in R version version 4.0.4. Differential abundance analyses were performed using DESeq2 version 1.30.0. Differential expression between genes are estimated using an empirical Bayes model prior to log fold change calculation taking into consideration the dispersion (Love, Huber and Anders, 2014). In this dataset log2 fold changes (FC) were used, and a minimum threshold was set for 1.5.

To further understand the role of differentially expressed genes web-based bioinformatics tools were used to examine gene expression, molecular function, interaction networks and pathway analysis including: Reactome.org (Wu and Haw, 2017; Gillespie *et al.*, 2022), IntAct Molecular Interaction Database v1.0.3 (Orchard *et al.*, 2014), STRING.db v11.5 (Snel *et al.*, 2000; Szklarczyk *et al.*, 2021), Pathway Commons v12 (Rodchenkov *et al.*, 2020; Wong *et al.*, 2021), pantherdb.org v17.0 (Mi and Thomas, 2009; Thomas *et al.*, 2022) and the encodeproject.org (Dunham *et al.*, 2012; Yue *et al.*, 2014; Luo *et al.*, 2020).
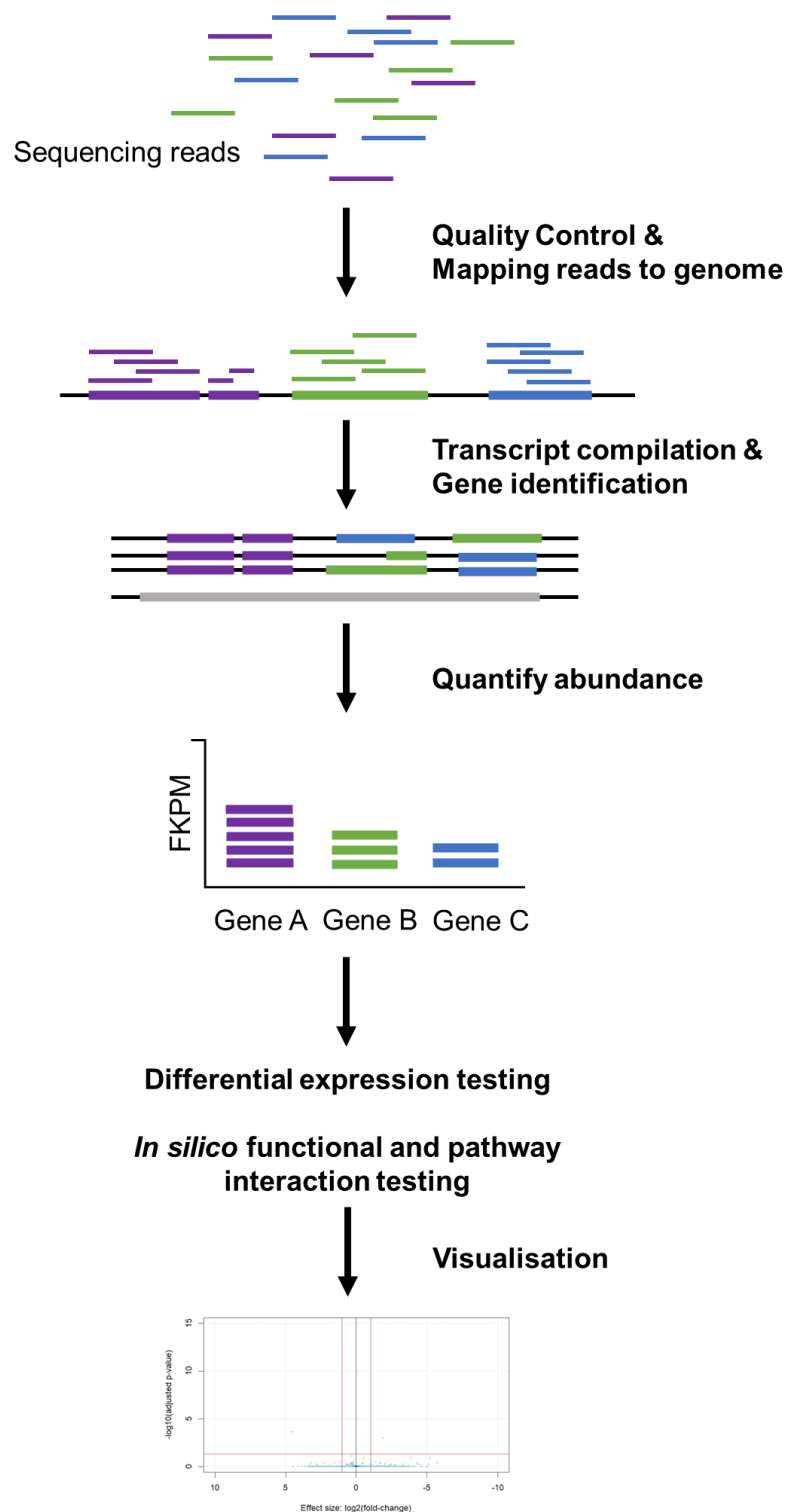
Figure 25. Overview of RNA sequencing data analysis

Following library construction and RNA-sequencing, reads were aligned to a reference genome of the same species of interest (mus Musculus). Second, the reads were assembled into transcripts and invidual genes were identified. Next, the number of reads that align to each exon or full-length transcript were used to estimate the expression levels of each. Donwstream analyses of RNA-seq data between control and Y522S samples included differential gene expression analyses.

3.9 *Ex vivo* isometric contractility measurement using wire myography

Resistance arteries i.e., small arteries with a diameter of less than 500 µm, contribute substantially to the peripheral resistance of blood flow. The ability of these vessels to contract and relax, alters their diameter and therefore resistance to flow, confers ability to regulate the distribution of blood to peripheral organs (Mulvany and Aalkjaer, 1990). Clinically, changes in uterine artery resistance are identified via Doppler waveforms and the calculated resistance or pulsatility indices are used indicatively of alterations in downstream arcuate and radial artery vascular remodelling (Prefumo, Sebire and Thilaganathan, 2004; Cnossen et al., 2008), although these methods do not reliably predict changes in vascular resistance (Aardema et al., 2001) nor localise the site of downstream changes in resistance (Adamson and Langille, 1992; Adamson, 1999).

When it is impossible to study organ physiology and function *in vivo*, it is critical that *ex vivo* studies are conducted on tissues maintained at conditions that mimic normal physiological conditions as closely as possible. Vascular smooth muscles integrate the impact of several factors such as pressure, nervous control, endothelial cell control, vasoactive substances, and hormones. A myograph is a device used to measure the force produced by a muscle during contraction due to these inputs. Commonly used techniques to study *ex vivo* vascular function, are, pin, wire, or pressure myography. Pressure myography involves cannulation of a blood vessel at both ends and setting an intraluminal pressure through the input canula. The intraluminal pressure can be manipulated to study myogenic response, varying flow/shear stress is a crucial regulator of vasocontractility.

The wire myography technique first developed by Mulvany and Halpern, is used to investigate the active and passive properties of small resistance arteries under isometric tension *in vitro* (Mulvany and Halpern, 1977). This is where the internal circumference of the vessel is

controlled and the circumferential wall tension can be measured. In smooth muscle (as with striated muscle) the active isometric tension and resting tension are dependent on length. Wire myography involves mounting a vessel between two fine steel wires and recording the tension generated by the vessel wall. In this scenario the vessel cannot be pressurised and therefore flow/shear stress cannot be studied. Wire myography can be used to study myogenic response and requires pharmacological constriction to generate tension. The ability to study segments of the same artery from the same animal allows differentiation of mechanisms of vascular reactivity. Some experiments (phenylephrine response curve) in pressure myography may produce results with higher sensitivity (Buus, VanBavel and Mulvany, 1994; Falloon *et al.*, 1995), and pressure myography might elicit different endothelial pathways to wire myography (Falloon, 1995). The use of wire myography is ideal for a vascular bed such as the rodent uterine artery that branches regularly in arcuate arteries which may lead to holes in the artery, a problem for pressure myography (Wenceslau *et al.*, 2021). Therefore, wire myography was used in the following study.

Table 9. Kreb's solution (PSS) recipe

Component	Concentration (mM)	Formula Weight	Mass (g) for 1X (1L)
NaCl	119	58.44	6.95
KCl	4.7	74.6	0.35
$MgSO_4 7H_2O$	1.17	246.47	0.28
KH_2PO_4	1.18	136.09	0.16
EDTA	0.025	372.24	0.009
$NaHCO_3$	25	84.01	2.1
$CaCl_2$*	2.5	110.98	0.28g or 2.5ml
D-Glucose	6	180.1	1.08

Table 10. High K^+ modified Kreb's PSS recipe

Component	Concentration (mM)	Formula Weight	Mass (g) for 1X (1L)
NaCl	63.7	58.44	3.723
KCl	60	74.6	4.476
$MgSO_4 7H_2O$	1.17	246.47	0.1408
KH_2PO_4	1.18	136.09	0.160
EDTA	0.025	372.24	0.0093
$NaHCO_3$	25	84.01	2.1
$CaCl_2$*	2.5	110.98	0.28g or 2.5ml
D-Glucose	6	180.1	1.08

* for these studies a 2.5 ml of a 1M $CaCl_2$ stock solution was added to avoid precipitation.

The myograph was heated to 37 ºC and the chamber was supplied with continuous 95%/5% air/oxygen. An acquisition software (Myodaq) was used to record vessel tension (mN). Prior to the preparation of resistance arteries, Kreb's solution (PSS optimised for rodents, 290 mOsm), and a 60 mM K+ Kreb's (PSS) were prepared and stored in a water bath at 37 ºC and gassed with 95%/5% air/oxygen. Ice cold PSS was required for the dissection.

3.9.1 Preparation of uterine artery vessels

Pregnant mice were humanely killed and dissected to remove whole uterus and uterine artery sections, as previously described. Briefly, the uterus with the uterine artery attached was excised from the pregnant mouse. In a sterile petri dish, the uterine artery along with surrounding adipose tissue, was separated from the uterus. This involved cutting through arcuate and radial arteries extending to the uterus as demonstrated in Figure 26. The vessel was placed on a silicone coated petri dish and covered with ice-cold PSS. The vessel was straightened and pinned down, avoiding stretch. Using fine spring scissors and fine forceps the surrounding adipose tissue and connective tissue was carefully removed, without handling the vessel directly. Visual factors were used to distinguish between the uterine artery and vein, the latter being thin-walled and blood filled and the former being muscular and thick walled with little blood. The clean vessel segment was divided into four 2 mm segments and stored in ice-cold PSS until mounting. Some uterine artery sections were stored in RNAlater overnight, then patted dry and stored at -80 °C.
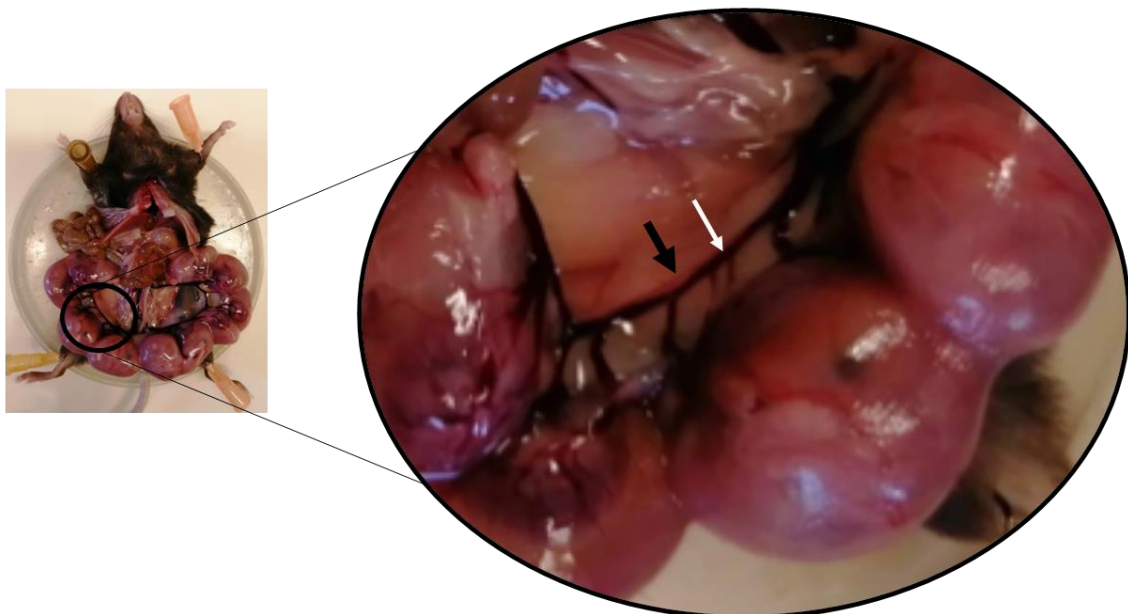
Figure 26. A digital image of a dissection procedure of a pregnant mouse (gestation day 18.5).

The uterus-uterine artery bundle is shown indicating the uterine artery (white arrow) and the uterine vein (black arrow)

3.9.2   Mounting vessels

A four channel myograph was used to simultaneously study multiple vessels in individual organ baths (Danish MyoTechnologies, DMT, Hinnerup, Denmark). Wire myograph baths were washed with distilled water and PSS four times before filling with 5 ml of ice-cold PSS. A wire (5 cm length, 40 µm thickness) was bent half-way and mounted under one screw of the fixed jaw. The vessel segment was gently but swiftly cannulated onto the wire (avoiding damage to the endothelium), and the loose wire end was mounted under the adjacent screw. A second wire was inserted into the lumen alongside the first wire, without disruption to the vessel or entangling with the first wire. The jaws were gently closed to hold the wires in place and the wire ends were mounted under the screws as depicted in Figure 27. The jaws were opened slightly so the wires were not touching and there was no tension on the vessel, and wires were adjusted to the same height. After mounting each vessel, the baths were returned to the base unit, washed with PSS and left to equilibrate for 30 minutes. Throughout the experiments baths were maintained at 37 ⁰C with a continuous supply of 95%/5% air/oxygen. The time between the beginning of gross dissection to the end of the mounting procedure lasted approximately 1.5 to 2 hours.
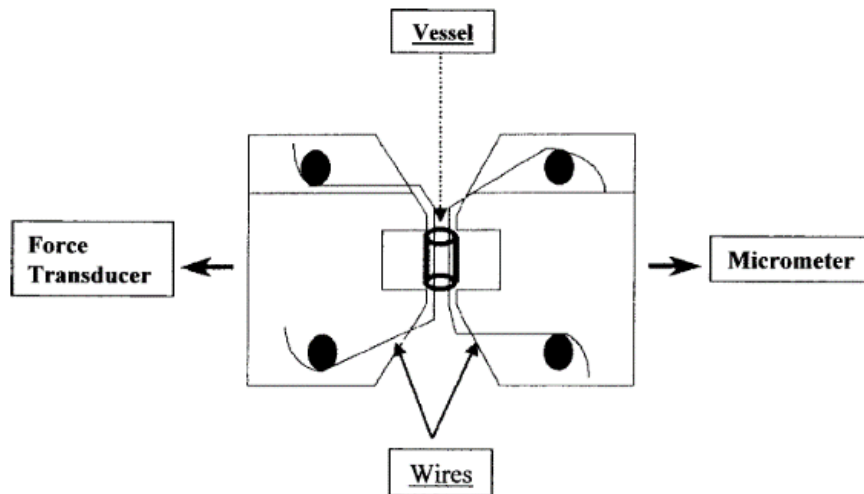
Figure 27. Illustration of a vessel mounted on a wire myograph system

The force transducer is connected to a chart recorder that is connected to a computer, which allows the force across the vessel to be recorded. The vessel segment is immersed in Kreb's physiological salt solution (PSS). The entire myograph including the preparation is kept at 37°C during the experiments. Image originally published in Spiers and Padmanabhan, 2005.

3.9.3   Vessel normalisation

The normalisation procedure is crucial for setting the vessels initial conditions, which may impact the vessels reaction to pharmacological conditions (McPherson, 1992). For the following series of experiments Mulvany and Halpern's method of normalisation was utilised (Mulvany, 1977). This normalisation method determines the internal circumference of a vessel if it was relaxed and under transmural pressure of 100 mmHg or 13.3kPa (IC_{100}), which is widely accepted as the target transmural pressure for adult rodents. Next, the vessel is then set to the sub-optimal 90% tension of the IC_{100} (IC_{90}), where the vessel can develop its maximum active tension; this is calculated from the passive internal circumference/tension relationship of the vessel. Wall tension (T) was calculated by dividing force by twice the vessel length. The internal circumference was calculated using instrument micrometer readings and wire diameter (40 µm), using the following equation, where d is 40 (Danish Myo Technology and AD Instruments, DMT Normalization Guide):

$$IC = 2d \, (\pi + 2) + \, 2 \, x \, gap$$

The increase in pressure was determined using the Laplace equation, assuming that the wall of the artery in thin and the pressure is unaffected by curvature of the wires:

$$P_1 = \frac{wall\ tension}{internal\ circumference \div 2\pi}$$

To begin, after mounting the initial micrometer reading was recorded, then the artery was stretched in small increments over 60 second intervals, each time recording the passive force (F) on the chart recorder and the new micrometer reading. This was repeated approximately 5 times until the pressure exceeds 100 mmHg (13.3 kPa). Using the internal circumference–pressure data an exponential curve was fitted, demonstrated in Figure 28. Where the

exponential curve intersects the isobar determines the IC_{100}. From this the IC_{90} is determined (90% of IC_{100}) and used to calculate the normalised micrometer reading to adjust to set the basal tone. The normalised micrometer setting was calculated using the formula:

$$T\ (mN/mm\ units) = \ Pi\ (mN/mm2\ units) \times IC\ (mm\ units)/\ 2\ \pi$$

The normalised diameter reading was recorded and calculated by dividing the IC_{90} by Pi (π). Following normalisation the vessels were washed with PSS and left to equilibrate for 30 minutes.
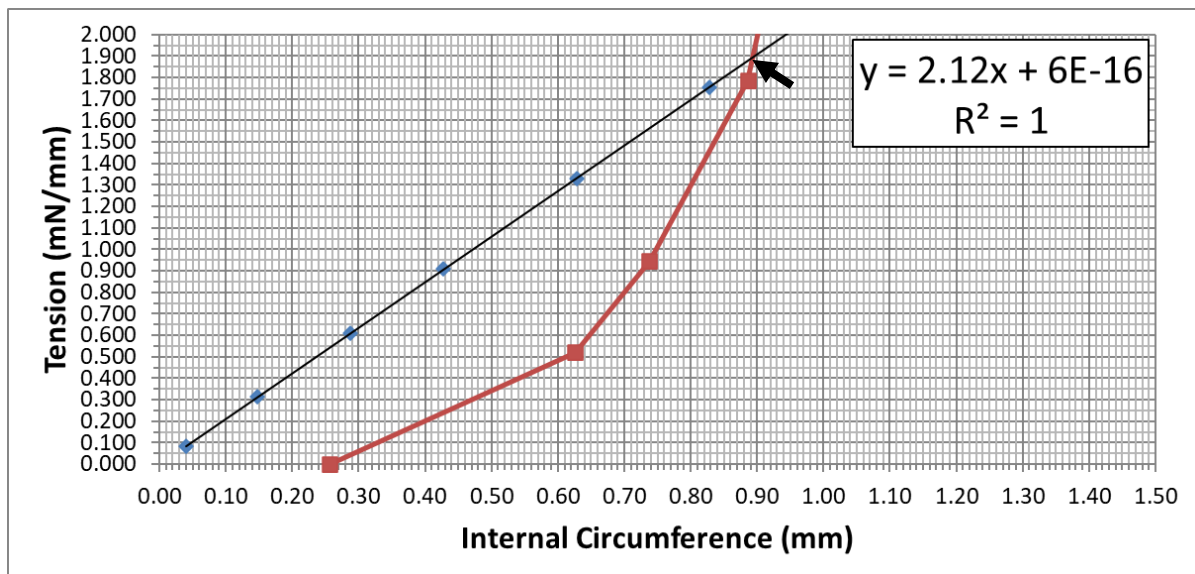
Figure 28. Example passive tension curve generated during the normalisation for systemic arteries with IC_{100} indicated (assuming internal pressure 100 mmHg (13.3 kPa)). Black line is an isobar (*T=(100 mmHg) x (IC/2π)*), red line is passive tension generated during normalisation procedure.

3.9.4 Assessment of tissue viability: 'wake-up protocol'

The viability of a vessel for use in an experiment must be tested to ascertain whether the mounting procedure adversely effected vessel function. Following equilibration, a series of three high K^+ PSS challenges were performed, whereby the bath was emptied and refilled with 5 ml K^+PSS, after three minutes the K^+PSS was washed out with PSS three times to relax the vessel. The peak contraction response to KPSS, demonstrated in Figure 29, was noted for all vessels for every repeat challenge. Following this, the vessels were left to equilibrate for 15 minutes. If a vessel failed to contract to K^+PSS or displayed severe vasomotion, they were excluded from further experimentation. Vasomotion is the periodic, rhythmic oscillation of vascular tone, suggested to be important in the regulation of local blood (Angus and Cocks, 1996; Nilsson and Aalkjaer, 2003; Spiers, 2005). Its unpredictable appearance after stimulation with K^+PSS and extreme difficulty to overcome make it almost impossible to interpret cumulative concentration response curve graphs from vessels with severe vasomotion. Of 289 individual vessels mounted, 19 were not contractile and discarded from further use.
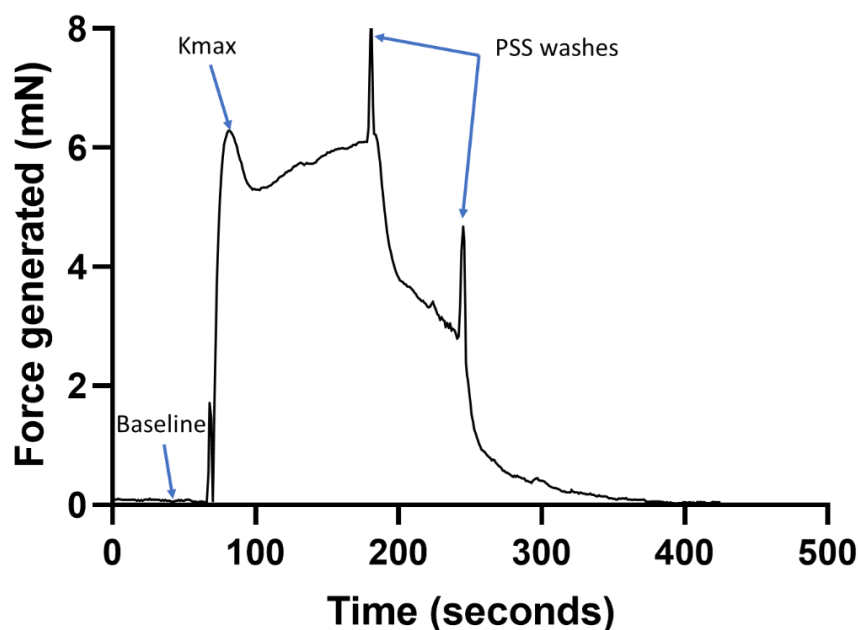
Figure 29. **Representative trace of pregnant mouse uterine artery vessel response to a single high K^+ PSS challenge in a wire myograph system**

3.9.5 Cumulative concentration response curves

A cumulative concentration response curve, also known as a dose-response curve, is used to determine a vessels response to an agonist or antagonist. This usually employs a range of concentrations and is therefore presented logarithmically, with a sigmoidal shape.

In the following experiments, vessels were incubated with dantrolene to determine the impact of RyR channels specifically in the contraction or relaxation of uterine arteries. As mentioned previously, dantrolene is a clinically approved drug for the treatment of malignant hyperthermia, spasticity of voluntary muscle and muscle cramps associated to motor neurone disease and other causes. It is predominantly an antagonist of RyR1 receptors (Zhao *et al.*, 2001a), therefore we expected that the gain-of-function driven by the Y522S mutation, should resemble control responses.

In the uterine artery, phenylephrine (PE) is a potent α1-adrenergic receptor agonist that activates IP_3R to cause intracellular Ca^{2+} release from the SR, which induces tonic contraction in vascular smooth muscle tissue. We know that α-adrenergic activity is significantly increased during gestation, resulting in a threefold shift in the amount of PE required to achieve 50% of maximal contraction (Osol and Cipolla, 1993). Carbochol mimics the effect of acetylcholine on muscarinic and nicotinic receptors, stimulates endothelial NOS, resulting in NO release within the EC, resulting in vasodilation. N(ω)-nitro-L-arginine methyl ester (L-NAME) is an L-arginine analogue commonly used as a nitric oxide synthase inhibitor.

To understand the contractile and relaxant properties of the *Ryr1^{Y522S/+}* pregnant uterine artery, both heterozygous and wild-type litter mates were subjected a vasoconstrictor, phenylephrine (PE), and a vasodilator, carbachol (CCH). Nine doses of PE (1 nM, 3 nM, 10 nM, 30 nM, 100 nM, 300 nM, 1 µM, 3 µM, 10 µM) were cumulatively added to each bath, with a 5-minute

incubation between each dose. The tension at the end of the 5-minute incubation period was recorded. After the final 5-minute incubation, the vessel was washed with PSS 3 times. From the PE dose-response curve, the sub-optimal maximum tension, typically 80% of its maximum tension was determined. The concentration of PE required in the bath to reach 80% tension (EC80) was used to pre-constrict the vessels. Thereafter, when the response plateaued, a well-established range of CCH doses (1 nM, 3 nM, 10 nM, 30 nM, 100 nM, 300 nM, 1 µM, 3 µM, 10 µM) were cumulatively added to each bath, with a 3-minute incubation between each dose (Sigma Aldrich). The tension at the end of the 3-minute incubation period was recorded.

In a clinical setting, dantrolene is administered by rapid intravenous injection (1 – 3 mg/kg for MH), and by mouth (25 – 100 mg) (Ibarra M, 2006; National Institute for Health and Care Excellence (NICE), 2023). To determine if any changes in vessel reaction are due to the Y522S RyR1 channel, vessels were pre-incubated for 30 minutes with dantrolene (30 µM). As a control, vessels from the same animal were pre-incubated for 30 minutes in a vehicle control, dimethyl sulfoxide (DMSO).

To determine the nature of the relaxant properties of the pregnant uterine artery, N(ω)-nitro-L-arginine methyl ester (L-NAME), a nitric oxide synthase inhibitor, was applied to vessels (Sigma Aldrich). Vessels were preincubated with L-NAME (10 µM), 10 minutes before CCH cumulative dose-response experiments.

3.9.6   Data analysis

The peak force generated in response to KPSS was calculated by subtracting baseline tension from high K^+ tension. Vessel response to increasing agonist (PE) concentrations were expressed as a percentage of the maximum high K^+ PSS response for each vessel, or as force

generated (mN). The response to increasing CCH concentrations was calculated as a percentage of the tension generated at the PE IC80. For all cumulative concentration response experiments, a non-linear regression model was used to fit a sigmoidal concentration-response curve. Variables extracted from this model included: maximum, minimum, and EC50 were calculated for each vessel segment (technical repeat), which were then averaged (mean) to create a single value for each animal (biological repeat) at each drug concentration on the curve. Statistical analyses were performed in Microsoft Excel and GraphPad PRISM 8, $p < 0.05$ was considered statistically significant.

3.10 *Ex vivo* tension measurement myometrium

3.10.1 *Ex vivo* isometric tension protocol

After removal of the uterine horns from the lower abdomen of the female animal, uteri were kept in at 4 ºC in PSS, pH 7.4 when gassed with 95% O2 and 5% CO2 mixture. The uterus was cut longitudinally along the midline of each non-pregnant uterine horn and above the placental attachments of pregnant uterine horns. The endometrium was gently scraped away from the flattened uterine strip using a scalpel. The myometrium was cut into small strips approximately 5 x 2 x 2 mm in size and tied at each end with a cotton thread. One end was attached to a metal hook and the other attached to a force transducer, the strip was then lowered into a 10 ml tissue bath chamber containing PSS gassed with 95% O2/5% CO2 mixture at 37.5ºC. The myometrial strips were stretched to approximately 1.5 times the length of the active length (between the knots) at slack, resulting in approximately 3 g of tension (Patel, 2014). The myometrial strips were left to equilibrate for 30 minutes (mouse tissue) or 1-2 hours (human tissue), to allow for spontaneous contractions to resume and to develop a baseline reading. Approximately 20-30 minutes of baseline spontaneous contractions were recorded before any experiments were performed. Following the collection of experimental data, each myometrial strip was challenged with a solution of high potassium PSS (concentrations as for PSS with 63.7 mM NaCl and 60 mN KCl). All data were recorded using Labchart 8 software (ADInstruments Limited, UK). Once tissues were equilibrated, spontaneous contraction were recorded for a minimum of one hour.

3.10.2 Data analysis

Contractile periods were assessed using; mean integral tension (MIT) (the sum of the contraction integrals over duration of the period assessed); contraction force (the mean height of contractions in the period assessed); frequency of contractions (the number of contractions

per second) and duration of contraction (the time in seconds between the start and end of an individual contraction, measured at 50% of the peak amplitude). To confirm that any observed differences in contractile activity were not due bias in dissecting the myometrial strips or their relative weights, measurements were normalised to cross sectional area of strips. Tension recording were taken per one-hundred times per second (100/s).

3.11 Histological investigations

3.11.1 Tissue processing

Paraformaldehyde (PFA) is a commonly used fixation solution for immunohistochemistry and fluorescent protein labelled samples. In a ventilation hood, paraformaldehyde powder was dissolved in 1X PBS at 60˚C with continuous stirring. As PFA powder (Fisher Scientific) does not dissolve instantly, the pH of the mixture was raised by adding 5N NaOH drop by drop until a clear solution formed. The solution was cooled to room temperature and filter to remove small undissolved particles. The pH was adjusted to 6.9 with 1M HCl and 1M NaOH. Freshly made 4% PFA in PBS was stored at -20 °C in 50 ml aliquots.

Whole uterine horns were excised and immediately placed flat in a petri dish, placentas were placed in round bottom Eppendorf microtubes, both were fixed with 4% PFA for 24 hours. Uterine arteries were cleaned of fat and fixed in 4% PFA for 45 minutes. The tissues were then blotted dry on a paper towel and stored in 70% ethanol until the dehydration process. For the following dehydration steps, the tissues were then placed in histology cassettes, uterine arteries were placed between two sponges in the cassette to ensure it remained inside. Using forceps these cassettes were used to move the samples between containers filled with reagents at least 10 times the volume of tissue, as depicted in Figure 30. Histo-Clear (National Diagnostics, Scientific Laboratory Supplies), replaces the previously used toxic xylene, as a clearing agent, used to remove ethanol and make tissue transparent so paraffin can fully envelop the tissue and to remove paraffin from sections so they can be rehydrated.

3.11.2 Tissue embedding

Samples were incubated in melted paraffin wax at 60 °C for 1 hour and then repeated in a fresh beaker of wax for another hour. Placentas were halved longitudinally and placed cut-side down, the enlarged pregnant uterus was cut into 2-3 sections per uterine horn and placed cut-side down, uterine artery was placed to section the lumen. The orientation of the tissue was critical for the purpose of these experiments. Using a modular tissue embedding centre (Leica EG1150 H) the samples were place in the centre of a plastic mould and embedded in paraffin, the cassette base was pressed firmly on top and the whole samples was cooled at 4 °C.
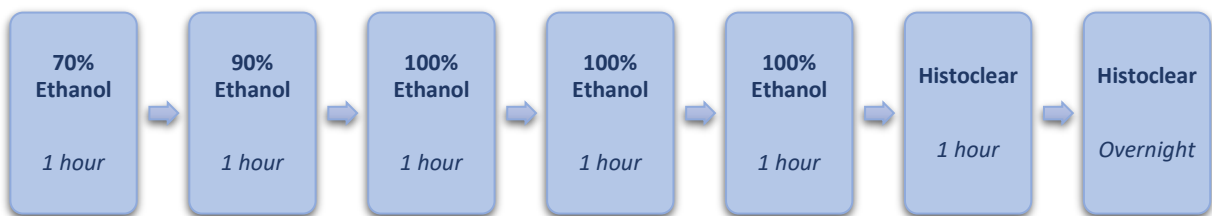
Figure 30. Sequence of incubation steps for the processing of mouse tissue sections before haematoxylin and eosin staining

3.11.3 Tissue sectioning

Paraffin tissue blocks were stored at 4 °C before sectioning into 5 µm thick sections using a semi-automated rotary microtome (Leica RM2245). Wax sections were gently placed in a water bath (40°C), to allow the tissue to spread out evenly before placing on poly-D-lysine coated glass slides (Epredia™ SuperFrost Plus™ Adhesion slides, Fisher Scientific). The slides were incubated at 37°C overnight.

3.11.4 Haematoxylin and eosin staining

To begin the staining process, residual paraffin wax must be removed from tissue sections. Two five-minute incubations in fresh Histoclear, followed by increasing one-minute incubations in decreasing concentrations of ethanol. The tissues were then stained with haematoxylin, with the excess removed using acid alcohol, followed by eosin staining. The specimen was then dehydrated using increasing concentrations of ethanol. The slides were gently wiped dry around the sample and the specimen was mounted onto the slide using DPX mounting medium (Sigma Aldrich) and a glass coverslip was placed on top, avoiding air bubbles over the specimen.

Histoclear	Histoclear	100% Ethanol
5 minutes	*5 minutes*	*1 minute*

90% Ethanol	70% Ethanol	Tap water
1 minute	*1 minute*	*1 minute*

Haemotoxylin	Tap water	Acid Alcohol
3.5 minutes	*1 minute*	*10 seconds*

Eosin	70% Ethanol	90% Ethanol
1.5 minute	*20 seconds*	*30 seconds*

100% Ethanol	Hisotclear	Histoclear
1 minute	*5 minutes*	*5 minutes*

Figure 31. Sequence of incubation stages for haematoxylin and eosin staining of mouse tissue sections.

3.11.5 Imaging and image analysis

Haematoxylin and eosin-stained placenta specimens were imaged using the Eclipse Ti-2 inverted microscope (Nikon Imaging Centre, Kings College London), Nikon DS-Fi2 RGB (for colour), with 10x magnification. To obtain a whole placenta image, 12 x 12 images were stitched together using blending. Exposure time (1 millisecond) and gain were kept consistent across all images to ensure reproducibility and analysis across multiple specimens. Images were analysed using Fiji ImageJ. Specifically, the total area of the whole placenta was 2-dimensionally determined using the lasso tool. Biological sections of the placenta (decidua, labyrinth zone and junctional zone) were outlined, and the area was calculated as a percentage of total placental area.

3.12 Fluorescence immunohistochemistry

The interaction of antibodies and antigens to form large macromolecules provide the basis of key reactions in immunology and in immune defence. Purified antibodies are often used in a laboratory setting to identify proteins in methods such as flow cytometry, western blotting and in immunohistochemistry/immunofluorescence.

The immunofluorescence technique was first described in 1942 and refined in 1950 by Coons and Kaplan (Coons and Kaplan, 1950). Immunofluorescence is a commonly used histological technique that employs antibody specificity to study protein expression and localisation within cells and tissues. It is commonly used with fluorochromes to visualise the location of the antibodies. There are four major IF techniques; direct immunofluorescence, indirect immunofluorescence, indirect immunofluorescence complement-fixation and double immunofluorescence. In this study we used the indirect (double) immunofluorescence technique, where two different antibodies were used to identify target molecules and secondary antibodies that carry the fluorophore recognises and binds to the primary antibody.

Specifically, anti-ryanodine receptor type 1 (anti-RyR1) was used to detect RyR1 localisation in the placenta. The expression of RyR1 is known in the SR of the skeletal muscle cell, and more recently in the vascular smooth muscle of the uterine artery (Hu, 2020; Song *et al.*, 2021), and BeWo cultured trophoblast cells (Zheng, 2022).

Anti-trophoblast specific protein alpha (anti-Tpbpα) is a trophoblast marker to predominantly found in placental junctional zone. Tpbpα is present in ectoplacental cone cells from E7.5 and later in spongiotrophoblasts in the mature placenta. Tpbpα-positive cells are progenitors of several trophoblast subtypes including subtypes of trophoblast giant cells (TGCs) and glycogen

trophoblast cells; these cells are essential for placental function and maternal vasculature remodelling (D. Hu, 2011).

Anti-monocarboxylate transporter 4 (anti-MCT4) was used as a marker of the fetal side of the two cell-layered syncytiotrophoblast used to detect changes in placental labyrinth; MCTs are H^+-coupled, electroneutral, and bi-directional transporters of lactate and other monocarboxylates across the placental barrier (Leichtweiß and Schröder, 1981; Illsley *et al.*, 1986; Garcia *et al.*, 1994). Previous immunohistochemical studies of the mouse placenta have found the polarised localisation of MCT1 on the maternal side and MCT4 on the fetal side of the two cell-layered syncytiotrophoblast; this is the opposite to subcellular localisation in the human placenta. (Nagai *et al.*, 2010).

To detect cellular growth and proliferation antibodies against ki67 were used. It is a protein found on the surface of mitotic chromosomes, and expressed predominantly during late G1, S, G2 and M phases of the cell cycle (Gerdes *et al.*, 1984). Ki67 is required to prevent chromosomes from collapsing into a single mass by forming a steric and electrostatic charge barrier, and binds to supercoiled and AT-rich DNA (MacCallum and Hall, 2000; Cuylen *et al.*, 2016).

3.12.1 Antigen retrieval

To fluorescently stain a specimen the slide is first heated to melt the paraffin wax then incubated in Histoclear to remove residual wax and then a series of decreasing ethanol concentrations for 5 minutes each.

Histoclear	Histoclear	100% Ethanol	90% Ethanol	70% Ethanol	Tap water
5 minutes	5 minutes	1 minute	1 minute	1 minute	1 minute
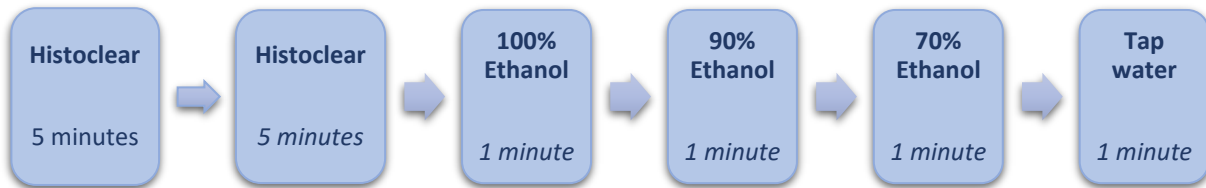
Figure 32. Sequence of incubation steps for the processing of mouse tissue sections before immunostaining

To perform the antigen retrieval, slides were heated in a Na^+ citrate buffer (10 mM Na^+ citrate dihydrate, 0.05% Tween20, pH 6) in a pressure cooker. After allowing the slides to cool in the citric acid buffer, slides were washed in tap water then Tris-buffered saline (TBS) (50 mM tris, 150 mM NaCl, pH 7.4). Using a wax pen the specimen was encircled to incubate specimens individually, without accidental mixing of antibodies. To prevent non-specific binding to epitopes on proteins within tissue sections that show similarities to the antigens of interest, the specimens were blocked with blocking buffer for 1 hour in a humidifying chamber, at room temperature.

3.12.2 Blocking and antibody incubation

Following the blocking step, each specimen was incubated with primary antibodies diluted in blocking buffer (1% bovine serum albumin, 10% normal goat serum (ab7481, Abcam), 0.1% PBST) overnight for approximately 20 hours, at 4°C in a humidifying chamber. A negative

control was tested using block buffer instead of ant primary antibody to show that the signal received is due to the primary antibodies alone and it provides information on the background staining. Rabbit IgG isotype control (Cat no. ab172730, Abcam) and Goat IgG isotype control (Cat no. 02-6202, Thermofisher) were used to ensure that any signal obtained from the antibody of interest was solely due to antibody tagging.

The following day the slides were washed in TBS 3 times for 5 minutes. This is important so that unbound or weakly bound primary antibodies are removed from the sections, so to maximise specificity of staining. The specimen was then incubated in fluorescently tagged secondary antibodies diluted 1:1000 in blocking buffer, at room temperature for 1 hour. The preparation of secondary antibodies and incubation was performed in the dark as secondary antibodies that are fluorescent are light-sensitive and all subsequent steps should avoid light exposure as much as possible. The negative control or isotype control sections were incubated with appropriate secondary antibodies at the same concentrations. Slides were then washed in TBS 3 times for 5 minutes. Specimens were mounted into the slide using DAPI Fluoromount-G® anti-fade mounting medium (Cat no. 0100-20, Cambridge Bioscience) and enclosed with a glass coverslip.

3.12.3 Fluorescence imaging

Fluorescently stained specimens were imaged using the Eclipse Ti-2 inverted microscope (Nikon Imaging Centre, Kings College London), Nikon DS-Qi2 sCMOS (for fluorescence) imaging system, 10x magnification. To image whole placentas 12 x 12 images were stitched together using blending.

3.12.4 Image analysis

Images were analysed using Fiji ImageJ. Macros were used to consistently analyse cell counts using DAPI stain and Ki67-positive cells. Ki67-positive cells were calculated as a percentage of total cells. Using hue thresholds only fluorescent sections of the placenta were selected and the area was analysed. Placenta sections were calculated as a percentage of total area as determined by DAPI coverage.

Table 11. Antibodies used in immunofluorescent staining

Primary Antibody	Dilution	Secondary Antibody	Dilution
Anti-RyR1 (D4E1) Rabbit mAb. Cat no. 8153, Cell Signalling Technology	1:100	Anti-rabbit IgG (H+L), F(ab')2 Fragment (Alexa Fluor® 594 Conjugate) Cat no. 8889, Cell Signalling Technology	1:500
Anti-Ki67 antibody rabbit IgG Cat no. ab15580, Abcam	1:100		
Anti-Monocarboxylate Transporter 4 Antibody polyclonal rabbit IgG Cat no. AB3316P, Merck	1:200		
Anti-Trophoblast specific protein alpha antibody rabbit IgG Cat no. ab104401, Abcam.	1:500		
Recombinant Rabbit IgG, monoclonal [EPR25A] - Isotype Control Cat no. ab172730, Abcam	1:100-1:200		
Anti-VEGF Polyclonal Antibody Goat IgG Cat no. PA5-47021, Thermofisher	10 µg/µL	Donkey Anti-Goat IgG H&L (Alexa Fluor® 488) Cat no. ab150129, Abcam	1:500
Goat IgG Isotype Control Cat no. 02-6202, Thermofisher	1:500		

3.13 Birthweight assessment in *RYR1*-associated MH and ERM human cohorts

As part of an ongoing collaboration with Luuk R. van den Bersselaar, MD and Nicol C. Voermans, MD, PhD, we requested a dataset (provided in Appendix 10), for patients from the MH and ERM cohorts at the national MH Investigation Unit in the Canisius Wilhelmina Hospital, Nijmegen and the neuromuscular outpatient clinic of the Radboud University Medical Centre, Nijmegen. These patients were identified by their treating physicians and their anonymised data was transferred via secure encrypted email to Arti Mistry.

Specifically, birthweight, gestational age, *RYR1* mutation and mutation inheritance (mother or father) data were collected from a cohort of patients with a history of MH susceptibility or ERM, with genetically confirmed *RYR1* variants classified as pathogenic, likely pathogenic or a variant of unknown significance according to the variant curation expert panel recommendations for *RYR1* pathogenicity classifications in MH susceptibility (Johnston *et al.*, 2021).

Using the gestational age and birthweight, birthweight percentile values were calculated using birthweight and gestational age using the "Birth weight assessment calculator" (Nicolaides *et al.*, 2018), (at https://fetalmedicine.org/research/assess/bw, date accessed 05th April 2023). Following this, percentile data were analysed using a linear regression model by Dr Kathryn Dalrymple.

3.14 Assessment of human *RYR1*-related obstetric and bleeding phenotypes

A well-designed and validated questionnaire can yield consistent results when implemented by different researchers over time. Yet there are several caveats to the design of a questionnaire, therefore the use of previously existing, validated questionnaires can be a useful tool to increase questionnaire reliability and minimise time spent on the development of a novel questionnaire (Boynton and Greenhalgh, 2004). The type of question must be considered when designing a questionnaire. Close-ended questions may account for rapid data collection but may not include all possible responses. In addition, Boynton and Greenhalgh (2004) suggest that participants are more likely to select ''yes'' statements, rather than ''no'', therefore it is important to account for this when formulating questions. In addition, the length of the questionnaire impacts participant fatigue and dropout, therefore to is important to avoid unnecessary or irrelevant questions and to choose the most appropriate question formats (Rattray *et al.*, 2007). According to Brace (2018), the absence of an interviewer presents the unique advantage where participants are more likely to respond honestly, however, without an interviewer, misunderstanding and ambiguity cannot be rectified, therefore clear, concise and unambiguous language is imperative (Brace, 2008).

To thoroughly comprehend the impact of *RYR1* mutations on bleeding and obstetric phenotypes in women it was important to gather a larger dataset of bleeding and pregnancy-related symptoms. We developed an online questionnaire to detect abnormal bleeding and uterine abnormalities in the first instance in 'healthy' women of the general population and then in women with *RYR1* mutations. The questionnaire explores the participants typical bleeding events using 'Molecular and Clinical Markers for the Diagnosis and Management of Type 1 (MCMDM-1) VWD'-like questions, other bleeding episodes related to smooth muscle function, determination of period and menstrual cycle abnormalities, issues related to

conception, miscarriage, difficulty during parturition, bleeding during pregnancy or post-partum and offspring birthweight.

This questionnaire was developed as part of an undergraduate Women's Health intercalated BSc project by Georgia Saldanha, with supervisory support from myself and Professor Rachel Tribe.

3.14.1 Study of selected existing questionnaires

A collection of five commonly used questionnaires were considered when developing this customised questionnaire; two are used to recommend further bleeding disorder investigation, three are related to menorrhagia and impact on quality of life.

A high frequency of bleeding symptoms are reported by the general population (Sadler, 2003). To distinguish haemorrhagic symptoms of disease including Type 1 von Willebrand disease the Molecular and Clinical Markers for the Diagnosis and Management of Type 1 von Willebrand disease (**MCMDM-1 VWD**) is regularly used. Rodeghiero et al (2005) and Tosetto et al (2006) first developed the MCMDM-1VWD which has since been thoroughly validated (Rodeghiero *et al.*, 2005; Tosetto *et al.*, 2006). Over 17 pages, this questionnaire comprises detailed questions that were used to score the severity of bleeding symptoms, this usually takes around 40 minutes to administer. Using the MCMDM-1VWD Bowman *et al* (2008) generated a condensed version which uses the original well-recognised scoring system and provides an efficient questionnaire that is still in use today (Bowman, 2008). The MCMDM-VWD1 bleeding questionnaire assesses 12 symptoms; epistaxis, cutaneous, bleeding from minor wounds, oral cavity, gastrointestinal bleeding, tooth extraction, surgery, menorrhagia, postpartum haemorrhage, muscle hematomas, hemarthrosis, central nervous system bleeding.

This questionnaire was a useful tool that we used to evaluate the bleeding phenotype in *RYR1* variant-carrying individuals and to eliminate 'healthy' participants with potential bleeding disorders. An extended section that examined menstruation and menorrhagia was included to evaluate menstruation history.

The **Short form 36 (SF36)** health survey questionnaire is used to determine how much a chronic condition affects an individual's quality of life (QOL) (Jenkinson, Coulter and Wright, 1993). Comprised of 36 questions, it became a popular tool that was validated and reliable within the National Health Service (NHS). In 1996, Jenkinson et al., used the SF36 in patients presenting with menorrhagia and found that several questions were challenging to answer, often due to the cyclic nature of menorrhagia and the ambiguity of the questionnaire (Jenkinson, Peto and Coulter, 1996).

The **menstruation questionnaire** developed by Shaw et al., (1998) provides a more specific method of assessing the impact of heavy menstrual bleeding on components of health, in order of importance, including family life, physical health, psychological health, practical difficulties and social life (Shaw *et al.*, 1998).

The **Menorrhagia-Specific Screening Tool** was designed to help identify cases of unexplained menorrhagia that require further laboratory investigations (Philipp *et al.*, 2008). This questionnaire asks specific questions about the severity of menstrual bleeding, other bleeding episodes, history of anaemia and family history of bleeding symptoms. The tool had a high positive predictive value, however, the specificity of this screening tool was low on its own, and in combination with a pictorial blood assessment chart (PBAC) score or serum ferritin due to high rates of false-positive screens (Philipp *et al.*, 2011). This screening can be administered in 10 minutes and also uses a scoring system.

The current online **NHS heavy periods self-assessment test** comprises 10 simple questions covering the use of sanitary products, leakage, blood clots, change of routine and symptoms of anaemia (National Health Service, 2021). This short self-assessment tool was useful to understand how a participant might interact with a wholly online questionnaire.

After reviewing these questionnaires, the most appropriate questions were selected based on specificity and unambiguity.

3.14.2 Adaptation of MCMDM-1VWD

Typically, the MCMDM-1VWD is administered by a skilled professional. The questionnaire in this study was designed for completion online and by the participant alone, therefore significant changes to the MCMDM-1VWD were necessary. The most important adjustment required was changing the medical terminology to more simplistic language without altering the interpretation of the question, see Appendix 9 for an example. Some questions were removed to shorten the questionnaire and reduce participant fatigue. No questions were removed for the section regarding serious bleeding presentations to enable use of the original scoring method.

The reproducibility of the modified online MCMDM-1VWD questions against the original MCMDM-1VWD questionnaire was tested amongst 5 individuals who completed both the modified online questionnaire and the original questionnaire in an interview format. The results were scored using the original MCMDM-1VWD scoring format. The results from both questionnaires were identical. Only one participant had very little/none bleeding symptoms, producing very low scores. This simple yet useful test confirmed that the modified online

version of the MCMDM-1VWD provided sufficiently similar responses in a population of healthy women.

3.14.3 Confounders

Determining if the bleeding abnormality or pregnancy complication is truly due to the participants *RYR1* mutation was crucial to this study. We included questions to detect and assess possible confounders that might otherwise increase the likelihood of an individual's susceptibility to bleeding abnormalities or pregnancy complications. We have therefore designed questions on medical intervention for conception, experience of miscarriage, polycystic ovary syndrome (PCOS), thyroid hormone imbalance, hyperlipidaemia, and other local uterine pathology.

3.14.4 Ethical considerations

An NIHR-recognised Patient and Public Involvement (PPI) group with experience of miscarriage and related gynaecological issues was consulted and asked to provide feedback on the questionnaire such as question sensitivity, comprehension, structure, and questionnaire length. As a result, the questionnaire was modified to minimise technical language, provide definitions, and shortened where possible. The sensitive topics explored in this questionnaire were approached delicately by first asking if the participant is happy to answer questions regarding the topic and if they responded yes, the following sensitive questions had additional 'prefer not to say', 'don't know', and 'other' answer options.

Upon initial request for ethical approval, the following minor amendments were required:

1. *Section B9: Specify the online platform that will be used to host the questionnaire.*
2. *Section C4: Provide more information about the platforms that will be used to advertise for participants for the second phase of the study.*
3. *Section C6: The Panel is of the view that you are using a gatekeeper. Therefore, you should change your answer accordingly and provide more information about the RYR1 support groups.*
4. *Section H6: Please ensure that your correspondence with the gatekeeper can be made available to the Research Ethics Office upon request.*
5. *Information Sheet:*
   i. *Include a departmental postal address within the contact details provided for your and your academic supervisor.*
   ii. *ii. As this is a student project, the paragraph beginning with 'If this study has harmed you in any way...' should only appear before the College contact details for your academic supervisor. It should be clear that you are to be contacted by those with queries about the study.*

After modifying the application as necessary, ethical approval was granted by the King's

College London BDM Research Ethics Panel (LRS-20/21-22085), correspondence for ethical

approval is include in Appendix 8.

3.14.5 Questionnaire content summary

The contents of the questionnaire sections and subsections are summarised in the table below, and a copy of the questionnaire is included in Appendix 9.

Table 12. Description of contents in questionnaire sections

Section	Content	Description of contents
1	Background	Participants age and ethnic background.
2	Personal medical history	Medical conditions that increase the risk of having a symptom of interest reasons other than an *RYR1* mutation. Includes conditions increasing the risk of abnormal bleeding, changes to menstrual cycle, infertility, and miscarriage. Whether the participant has been diagnosed with an *RYR1* mutation and/ or has ever received the RyR1 antagonist dantrolene. Symptoms often associated with *RYR1* mutation such as myopathies, migraines, bowel problems, and bladder problems.
3	Family history	Family members diagnosed with an inherited bleeding disorder. Participants children have an *RYR1* mutation. This is because a fetus with *RYR1* mutation may significantly influence the bleeding symptoms associated with a pregnancy whether the mother has an *RYR1* mutation or not.
4 – 18	Von-Willebrand's style questions	Modified MCMDM-1VWD questions.

		This includes epistaxis, skin symptoms, bleeding from minor cuts, bleeding from the mouth, and gastrointestinal bleeding.
19	Surgery	Number of operations and whether they had any abnormal bleeding during or following the surgery.

Exposure to general anaesthetic and whether they had a negative reaction including malignant hyperthermia. |
20	Biological sex	Although currently we are only considering females for the study, this question allows for the questionnaire to be dispersed to males in the future. If participants respond that their biological sex is male, then they will skip sections 21 to 23 which are not relevant to males.
21	Periods and menstrual cycle	Long-term history of menstruation and experienced menorrhagia and the severity.
22	Contraception and period	This section addresses whether there has been any change to bleeding and menstrual cramps due to contraception.
23	Obstetric section	This section considers fertility, miscarriage, stillbirth, children, labour and delivery, and any bleeding throughout the duration of the pregnancy.

Women who have never been pregnant are moved on to Section 24.

Birthweights, method of delivery, and the length of each pregnancy and labour. |

		Lastly participants are asked whether they had postpartum haemorrhage, if they did, then whether this was primary or secondary and what management they received. They are then asked whether they had any complications during the pregnancy or birth that might have caused an increased risk of haemorrhage.
24 – 26	Other bleeding episodes	This section mimics the final questions of the MCMDM-1VWD and aims to assess how effectively the questionnaire has considered each aspect of bleeding that an individual might have experienced. If many people respond to this section describing other episodes of abnormal bleeding, the questionnaire does not properly evaluate abnormal bleeding symptoms.

3.14.6 Delivery and question form

It was decided that the questionnaire would be delivered online to expand the participant database and as a precaution during the COVID-19 pandemic. There are several programs that would have been suitable for this questionnaire, including SurveyMonkey and Typeform. It was important that the program enabled multiple question formats, stratifying participants according to responses and immediate viewing and analysis of responses once submitted. Based on these considerations, Microsoft Forms (run by Office 365) was finally selected as the tool to deliver the questionnaire due to its General Data Protection Regulation 2016 (GDPR) compliance, ease of exporting results directly to Microsoft Excel and the instant availability within the already provided Office 365 package through King's College London. The questionnaire was developed and delivered in English but there is scope to translate and validate in other languages to make the questionnaire more widely accessible.

Predominantly closed-ended questions were used for the rapid collection of aggregated data and to decrease the risk of ambiguous responses. An 'other' response option was included in some questions (example question 14), whereby the participant could describe their treatment when all other responses were inappropriate. The use of branching was key to gathering further information based on a specific response to a previous question, similar to a professional changing their questions contingent on how a participant responds during a patient interview.
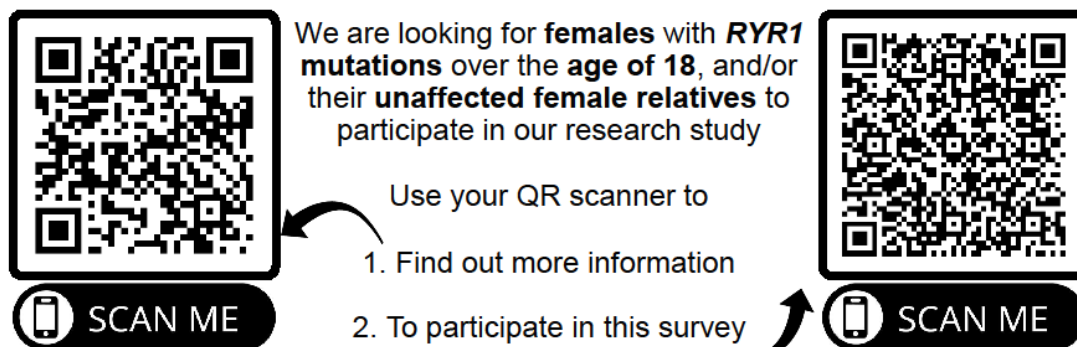
Figure 33. A snapshot of Microsoft forms question branching option.

3.14.7 Participant recruitment

The questionnaire was designed in an online format to overcome limitations of the COVID-19 pandemic and to ensure the maximum possible number of participants were invited to take part. To ensure that all participants could complete a menorrhagia history a minimum age of 18 was required. We invited participants representative of the general healthy population (Phase I) and relatives without a *RYR1* mutation to complete the questionnaire (Phase II) which made up the control group. The *RYR1* group was recruited via the RYR1-Foundation support group (https://www.ryr1.org/), and their treating clinicians, who distributed the invitation (text as per advertising document attached) to participate and questionnaire link via email, advertising on the RYR1-Foundation website, and/or through social media platforms (approved by BDM Research Ethics Panel, Appendix 8). The flyers distributed included hyperlinks or QR codes to the participant information sheet and questionnaire form (see Figure 34, Appendix 6 and Appendix 7).

Figure 34. Participant recruitment flyer with QR codes for a participant information sheet and a questionnaire form

3.14.8 Data analysis

Responses were saved only when the participant fully completed the questionnaire, this eliminated the collection of unfinished questionnaires for subsequent analysis. Where question branching was present, the following questions were analysed as a percentage of total number of respondents of the previous question. Participant responses were downloaded as an Excel file and two separate tables were made for the healthy participants and for the *RYR1*-mutation carrier responses. The responses to every question were tabulated for number of responses for each answer option and calculated as a percentage of total responses. Responses were then displayed as graphs and charts using Microsoft Excel. Bleeding scores were calculated according to a standard MCMDM-1VWD scoring system (Bowman *et al.*, 2022) (see Appendix 5), with an abnormal bleeding score categorized as ≥4.

3.15 Statistical analysis

Graphical and statistical analyses were performed using the Graphpad Prism software (GraphPad version 9, San Diego, CA, USA). All results are presented as mean of biological repeats with standard error of the mean (SEM), unless otherwise stated. All sample sizes are provided as number of subjects (animals or human), and technical repeats (e.g., number of vessels) are provided where necessary. To assess the distribution of data, where $n > 50$, the Kolmogorov-Smirnov test (normality test) was employed. For the statistical analysis of two groups, a two-tailed unpaired t-test was used, and in the circumstances where subjects were matched a paired t-test was utilised. For the statistical analysis of more than two groups a one-way ANOVA (without the assumption of equal variances) was used. Welch's one-way ANOVA was preferred for its consistency and reduction in type 1 error rates, and Brown-Forsythe for average sample sizes < 6 (Tomarken and Serlin, 1986). Dunnett's T3 (when $n < 50$), and Games-Howell (when $n > 50$) multiple comparison tests were used for post-hoc analysis following a one-way ANOVA of parametric data (Lee and Lee, 2018). When data were not normally distributed the Kruskal-Wallis test with the post-hoc Dunn's multiple comparisons test was used. To correct the false discovery rate, the Benjamini-Hochberg method was used. When two categorical variables were present, a two-way ANOVA with Tukey's correction for multiple comparisons was used. Correlation analysis was performed using Pearson's correlation test. Chi square (X^2) tests were used to compare the distribution of categorical data and Fishers exact test was used when more than 20% of cells had frequencies < 5 (Kim, 2017). For all statistical tests, p-values < 0.05 were considered statistically significant.

3.15.1 Power calculations

The sample size of a study should be large enough to give a suitably small standard error. When two groups are compared, a power calculation determines how many subjects are required to have a reasonable (usually 80 to 90%) chance of detecting a biologically important difference.

Power calculations have been carried out for this study based on previously published data exploring the effect of maternal aging on gestational length and parturition duration (Patel, 2014; Patel *et al.*, 2017). A power calculation was used to calculate the numbers of animals required to give a minimum of 80% power to detect a minimum of 50% difference between groups in labour duration at the $p<0.05$ level. For example, to detect a difference (reduction) in labour length by 50% with 80-90% power, a sample size of 17-23 animals is required. Which is based on a 66% increase in labour length as a result in increased maternal age (8 months (n=6) from 3 months (n=8)), after adjustment for litter size.

Based on a study by Marshall *et al.*, (2018) that investigated the impact of relaxin (*Rln*) deficiency on uterine artery dysfunction (constriction response to PE) an estimated sample size of 11 (number of mice) was calculated to give 80% power when detecting a 20% difference in area under the curve (AUC) to cumulative phenylephrine concentrations between vessels from wild-type and heterozygous $Ryr1^{Y522S/+}$ pregnant animals, with a variation coefficient of 15%.

4   Chapter 4 Uterine artery function in the pregnant $Ryr1^{Y522S/+}$ mouse

4.1   Background

This chapter explores the impact of the heterozygous Ryr1 Y522S mutation on uterine artery function during late-stage mouse pregnancy. At the end of pregnancy, resistance to myogenic tone is increased, to maintain adequate blood supply to the fetus. This has been mimicked experimentally in sheep where steroid induced pregnancy-like conditions result in increased Ca^{2+} sparks and STOC frequency in uterine arteries (Hu, 2019). In the uterine artery of near-term pregnant sheep, knockdown of RyR1 channels also decreases Ca^{2+} spark frequency, suppresses STOC frequency and amplitude, and increases pressure-dependent myogenic tone (Song, 2021), indicating an important role of RyR1 channels in the mechanism of vasodilation in the uterine artery.

The proposed mechanism driving the vascular phenotype in the $Ryr1^{Y522S/+}$ mouse is similar, in that increased Ca^{2+} leak from RyR1 Y522S channels leads to increased BK_{Ca} channel activation causing plasma membrane hyperpolarisation which possibly causes inactivation of L-type voltage-dependent Ca^{2+} channels, decreasing intracellular Ca^{2+} and opposing vasoconstriction (Krishnamoorthy *et al.*, 2014; Lopez, 2016). Lopez and colleagues demonstrated the functional impact of the Ryr1 Y522S mutation in a limited number of vascular beds by measuring tail artery bleeding time assays, calcium imaging and spark analysis in conjunction with membrane potential measurements of isolated arterial smooth muscle cells.

To further understand the impact of Ryr1 Y522S within its normal physiological environment and in the context of late-stage pregnancy, here I studied contraction and relaxation mechanisms in the *ex vivo* uterine artery.

4.2 Methods

Studies have shown that mechanical forces due to increased blood flow during a first pregnancy might induce permanently higher conductance of the uterine arcade, making comparison between nulliparous and primi/multi-parous animals unsuitable (Wassel *et al.*, 2005). Therefore, in this study all uterine artery segments were collected from only nulliparous pregnant wildtype (wildtype litter), heterozygous $Ryr1^{Y522S/+}$ (mixed litter) or wildtype (mixed litter) mice aged between 8-16 weeks, on gestation day 18.5.

RT-qPCR was used to determine whether the *Ryr1* Y522S substitution mutation subsequently regulates expression of *Ryr1*. Total RNA was extracted from whole pregnant uterine arteries from wild-type and $Ryr1^{Y522S/+}$ animals and pooled to create a total RNA concentration of >10 ng/µL, the generally accepted minimum concentration of DNA required for a PCR reaction. The normalised *Ryr1* mRNA copy number was determined using primers for *Ryr1* and absolute quantification techniques previously described in Chapter 3.

Uterine artery vessels segments mounted on a wire myograph, were first challenged with to high K^+ PSS to determine vessel viability. After a period of equilibration vessel segments were pre-incubated with 30 µM dantrolene or the vehicle control DMSO for 30 minutes, then contracted with cumulative doses of PE (1 nM - 10 µM) for 5 minutes at each concentration, to obtain individual dose-response curves. Vessel segments were again pre-incubated with dantrolene or DMSO, then contracted to 80% of its respective maximum contractile response to PE until a stable contraction was maintained, then relaxed with cumulative doses of CCH (1 nM - 10 µM), for 3 minutes at each concentration. To distinguish the contribution of the endothelium to the observed responses, in a series of experiments vessels were treated with dantrolene for 30 minutes, plus 10 µM L-NAME for the final 10 minutes, before proceeding to a cumulative dose response to CCH.

Isometric contractility recording data were analysed as described in section 3.9.6. Briefly, the vessel response to PE was expressed as a percentage of the response to KPSS, or as force generated (mN), and the response to increasing CCH concentrations was calculated as a percentage of the tension generated at the PE IC80. The number of samples refers to the number of animals, unless stated otherwise.

Histological methods were used to explore potential morphological changes in the pregnant Ryr1 Y522S uterine artery. Paraffin embedded uterine arteries were sectioned through the lumen and stained with haematoxylin (purple, nuclei) and eosin (pink, cytoplasm). Images of vessel lumens were used to calculate smooth muscle percentage, wall thickness, and lumen diameter.

4.3 Results

4.3.1 *Ryr1* mRNA expression in *Ryr1*$^{Y522S/+}$ pregnant uterine artery

Using RT-qPCR methods, total RNA from pregnant uterine artery segments from all genotype groups revealed *Ryr1* transcripts, implicating the expression of *Ryr1* in pregnant uterine artery. Due to low total RNA concentrations from single uterine artery specimens (3-14 ng/µl), mRNA from vessels of *Ryr1*$^{Y522S/+}$(mixed litter) (n=7), wild-type (mixed litter) (n=6), and wild-type (wild-type litter) (n=11) dams on gestation day 18.5 were pooled to enable successful PCR reaction. The log normalised *Ryr1* copy number was similar in vessels from *Ryr1*$^{Y522S/+}$(mixed litter)=3.547, wild-type (mixed litter)=3.363, and wild-type (wild-type litter)=3.440. Due to the nature of this sampling method, statistical analysis could not be performed.
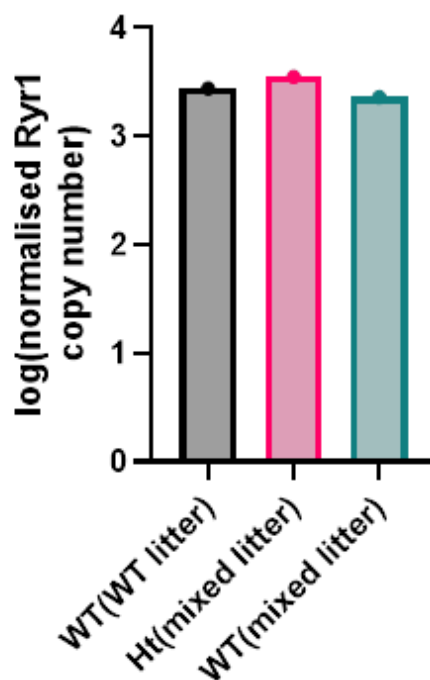
Figure 35. **Normalised *Ryr1* copy number in pregnant uterine artery from *Ryr1*$^{Y522S/+}$(mixed litter), wild-type (mixed litter), and wild-type (wild-type litter) animals on gestation day 18.5.**

Total RNA extracted from pregnant uterine artery vessels from *Ryr1*$^{Y522S/+}$(mixed litter) (n=7), wild-type (mixed litter) (n=6), and wild-type (wild-type litter) (n=11) pregnant animals on gestation day 18.5 were pooled to enable successful PCR reaction and tested for *Ryr1* mRNA expression (primers described in methods). The log(normalised *Ryr1* copy number) was as follows: *Ryr1*$^{Y522S/+}$(mixed litter)=3.547, wild-type (mixed litter) =3.363, and wild-type (wild-type litter)=3.440.

4.3.2 Maximum contractile ability of $Ryr1^{Y522S/+}$ pregnant uterine artery

Force generated in response to high K$^+$PSS challenge (amplitude) was significantly lower in vessels from wildtype (mixed litter) (3.727 ± 0.294 mN, n=85) dams compared to vessels from $Ryr1^{Y522S/+}$(mixed litter) (4.787 ± 0.3732 mN, n=88) and wildtype (wildtype litter) dams (4.659 ± 0.3082 mN, n=97), P=0.0355 (Welch's one-way ANOVA), demonstrated in Figure 37. However, post hoc multiple comparisons testing did not identify a statistical difference between heterozygous (mixed litter) (P=0.9620) and wildtype (mixed litter) (P=0.0763) vessel response compared to wildtype (wildtype litter) (Games-Howell's multiple comparisons test).
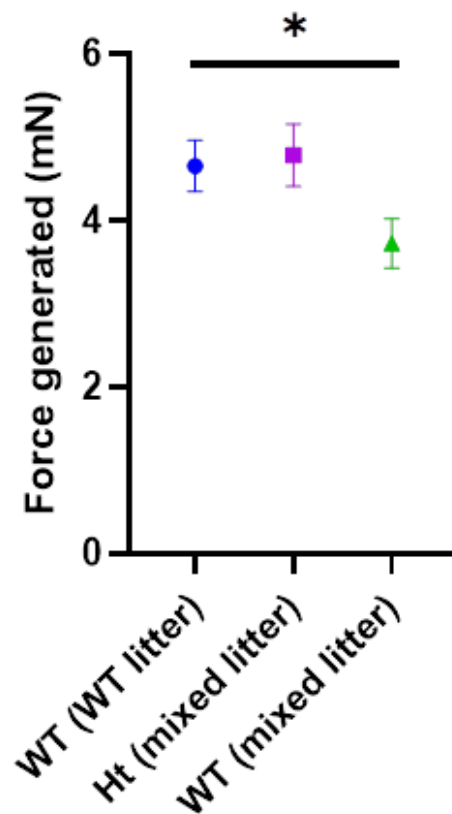
Figure 36. **Maximum contractile responses (mN) to high K$^+$ challenge (60 mM in physiological salt solution, PSS) in uterine artery segments (2mm) from pregnant mice (gestation day 18.5).**

The maximal response to high K$^+$ PSS was statistically reduced in uterine artery vessels from pregnant wildtype (mixed litter) (n=85) compared to heterozygous $Ryr1^{Y522S/+}$(mixed litter) (n=82) and wildtype (wildtype litter) (n=85) animals, P=0.0355 (Welch's ANOVA). No significant differences between specific groups following post hoc comparison testing (Games-Howell). Data presented as mean ± SEM; mN, milli Newtons.
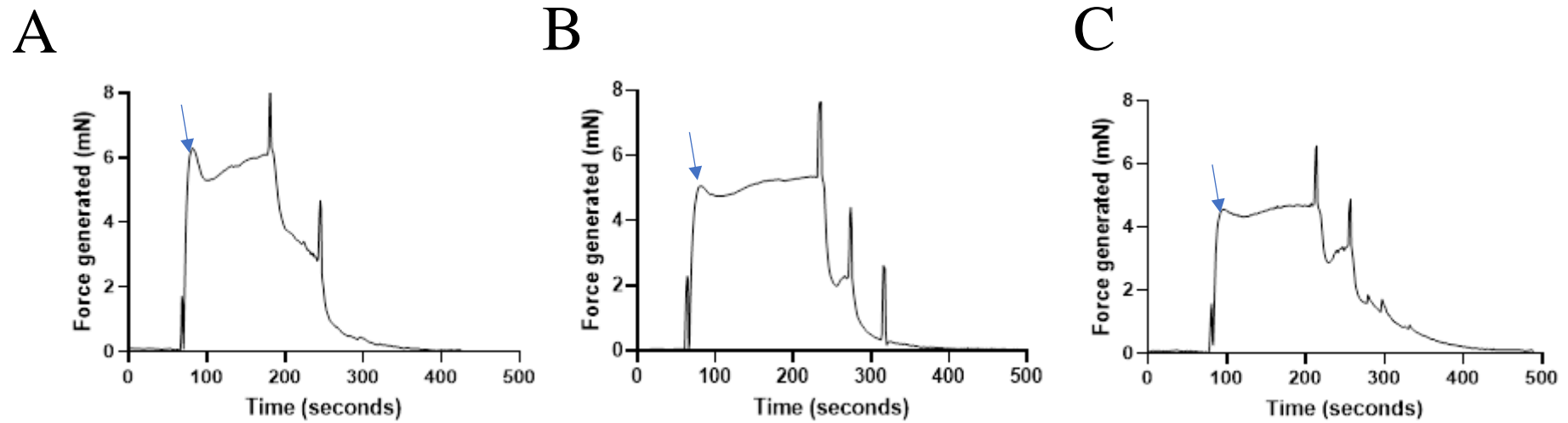
Figure 37. **Representative traces of a gestation day 18.5 pregnant uterine artery response to high K$^+$PSS challenge measured using wire myography**

Vessels from gestation day 18.5 pregnant (A) wildtype (wildtype litter), (B) heterozygous *Ryr*[Y522S/+] (mixed litter), (C) wildtype (mixed litter) animals were challenged with high K$^+$ PSS for three minutes. The peak (arrow) response was noted after three challenges per individual vessel.

4.3.2.1 Normalised Internal Lumen Diameter

When pregnant uterine artery segments were normalised to passive physiological tension (13.3 kPa), the internal lumen diameter of vessels from wild-type(mixed litter) mothers (216.2 ± 3.948 µm, n=23 animals, 78 vessels) were smaller than the internal diameter of vessels from wild-type (wild-type litter) mothers (230.6 ± 3.080 µm, n=28, 104 vessels), P=0.0112, Welch's one-way ANOVA, P=0.0091, Dunnett's T3 multiple comparisons test. Lumen diameter of vessels from heterozygous $Ryr1^{Y522S/+}$ (mixed litter) mothers (220.4 ± 3.530 µm, n=25 animals, 92 vessels) were not statistically different to wildtype(wildtype) vessels, P= 0.0609, Dunnett's T3 multiple comparisons test.
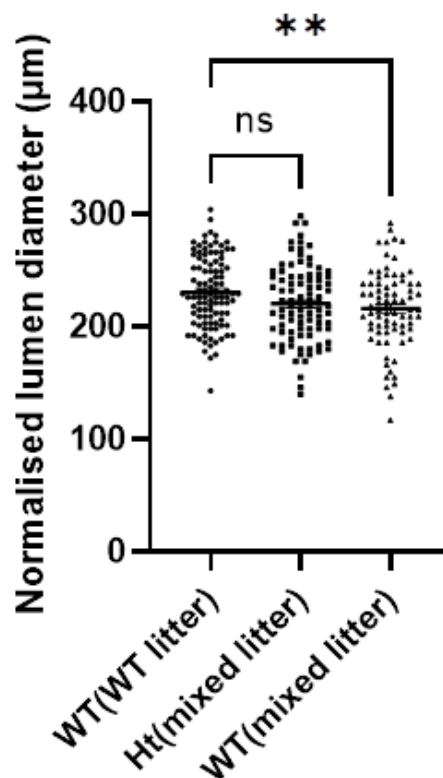
Figure 38. **Internal lumen diameter (µm) of pregnant uterine arteries normalised to passive physiological tension from $Ryr1^{Y522S/+}$ (mixed litter), wild-type (mixed litter), and wild-type (wild-type litter) animals**

The internal lumen diameter was measured after incremental stretches to normalise internal passive physiological tensions with pregnant uterine artery segments from $Ryr1^{Y522S/+}$(mixed litter), wild-type (mixed litter), and wild-type (wild-type litter) animals' mothers, n=25, 23, and 28 animals, respectively. Internal lumen diameter of pregnant uterine arteries from wild-type (mixed litter) were smaller than the diameter of vessels from wild-type wildtype litter) mothers. P=0.0112, one-way ANOVA, P=0.0091, Dunnett's T3 multiple comparisons test. Data presented as mean±SEM.

4.3.2.2 Histological investigations of the pregnant Ryr1$^{Y522S/+}$ uterine artery

There was no reason to suspect a difference in VGCC expression in the *Ryr1*$^{Y522S/+}$ (mixed litter) or wild-type (mixed litter) uterine artery so changes in the internal lumen diameter, wall thickness and vascular smooth muscle content were suspected as cause for difference in the contractile ability of vessels, demonstrated in Figure 39.

The internal lumen diameter measured from cross-sectional images of pregnant uterine arteries from wild-type (mixed litter) mothers (180.9 ± 26.63 µm), heterozygous *Ryr1*$^{Y522S/+}$ (mixed litter) mothers (175.0 ± 21.87 µm) and wild-type (wild-type litter) mothers (203.2 ± 34.13 µm) uterine artery segments were not statistically different, P=0.7654, Brown-Forsythe ANOVA test. N=3 for all groups.

The wall thickness of cross-sections from pregnant uterine artery vessels from *Ryr1*$^{Y522S/+}$ (mixed litter) (17.80 ± 0.8950 µm), wild-type (mixed litter) (18.10 ± 1.087 µm), and wild-type (wild-type litter) (15.94 ± 0.3121 µm) animals were not statistically different. P=0.2480, Brown-Forsythe ANOVA test.

The number of nuclei in the smooth muscle layer of the pregnant uterine artery were counted to reveal that the smooth muscle content was reduced in the lumen of vessels from wild-type (mixed litter) (20.33 ± 6.386), compared to *Ryr1*$^{Y522S/+}$ (mixed litter) (30.67 ± 9.333) and wild-type (wild-type litter) (33.67 ± 6.064) uterine artery segments, however this was not statistically different. P=0.4655, Brown-Forsythe ANOVA test. N=3 for all groups.
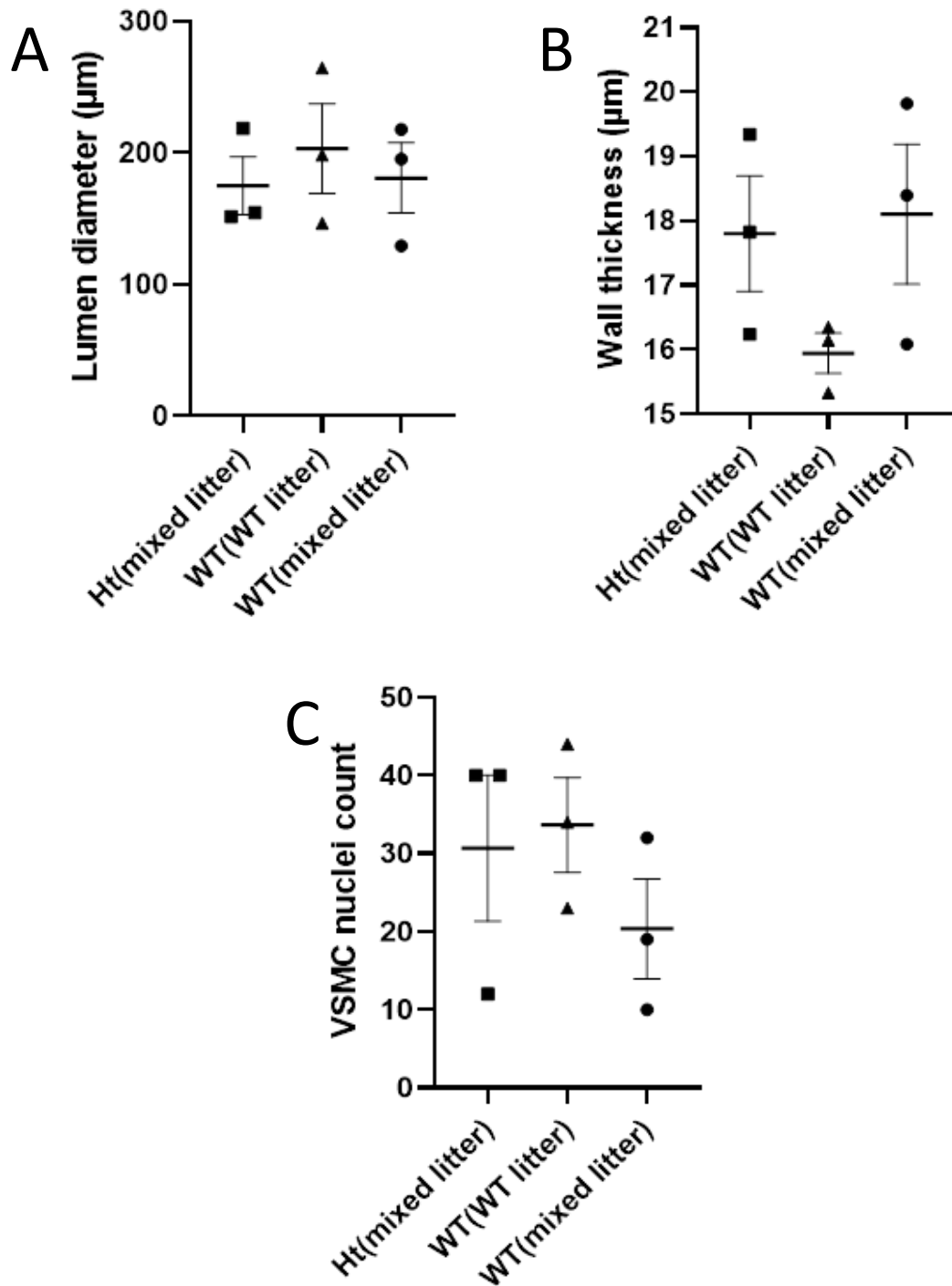
Figure 39. **(A) Internal lumen diameter, (B) luminal wall thickness and (C) vascular smooth muscle cell content of uterine arteries from pregnant gestation day 18.5 *Ryr1$^{Y522S/+}$*(mixed litter), wild-type (mixed litter), and wild-type (wild-type litter) dams**

Cross-sections of pregnant uterine arteries stained with haematoxylin and eosin, were used to measure the (A) internal lumen diameter (µm), (B) luminal wall thickness (µm) and (C) vascular smooth muscle cell content of vessels from *Ryr1$^{Y522S/+}$*(mixed litter), wild-type (mixed litter), and wild-type (wild-type litter) mothers, n=3 for all groups. The luminal diameter, wall thickness and smooth muscle cell nuclei counts of pregnant uterine arteries from all genotype groups were not statistically different. P=0.7654, 0.2480 and 0.4655, respectively. Brown-Forsythe ANOVA tests. Data presented as mean±SEM.

199
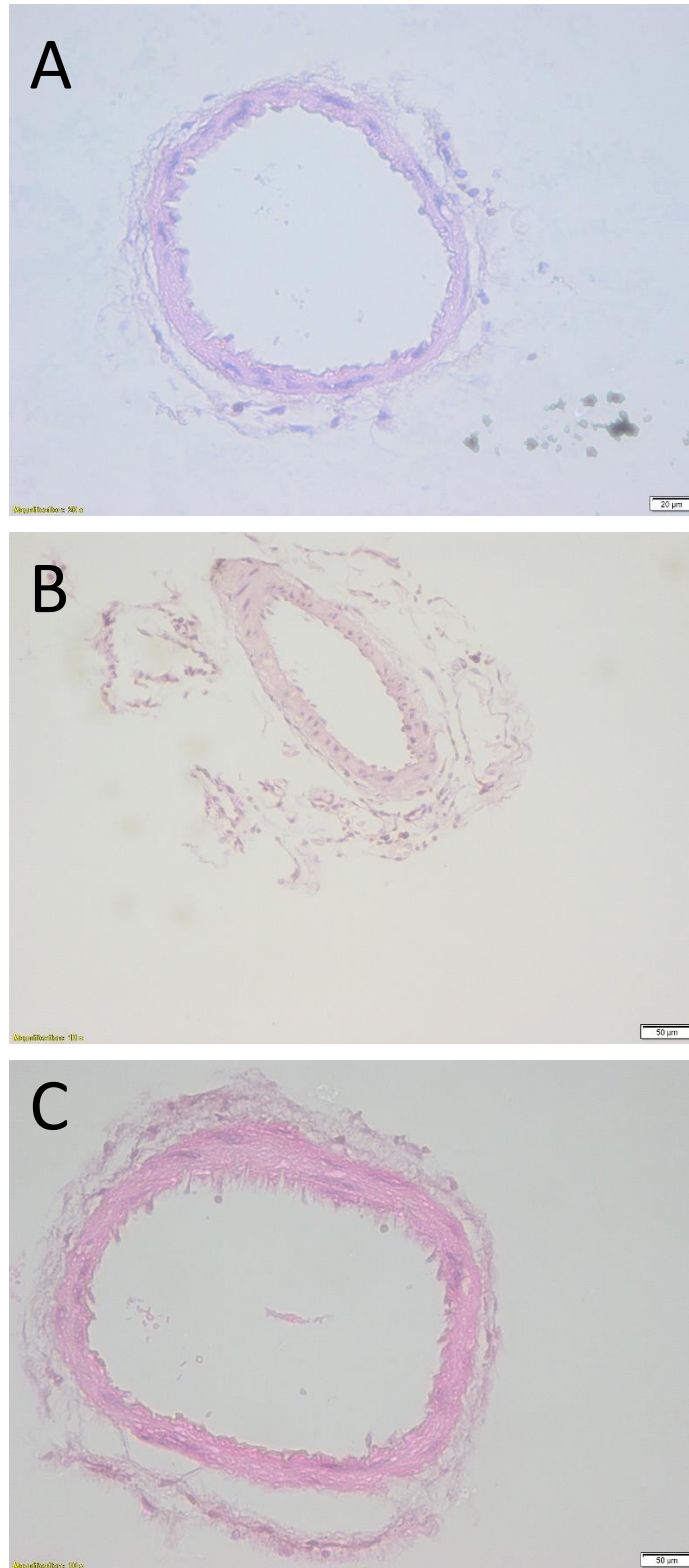
Figure 40. **Representative images of pregnant uterine artery lumen cross-sections from pregnant (A) wild-type (wild-type litter), (B) *Ryr1$^{Y522S/+}$*(mixed litter), and (C) wild-type (mixed litter) dams**

Haematoxylin and eosin-stained formalin-fixed (30 minutes) uterine arteries from gestation day 18.5 pregnant (**A**) wild-type (wild-type litter), (**B**) *Ryr1$^{Y522S/+}$*(mixed litter), and (C) wild-type (mixed litter) dams. Size bar (50 µM) in right hand corner of each image.

4.3.3 Vasoconstriction of the pregnant $Ryr1^{Y522S/+}$ uterine artery

4.3.3.1 Impact of maternal $Ryr1^{Y522S/+}$ genotype on pregnant uterine artery constriction

When adjusting for potential differences in high K^+ PSS responsiveness, comparison of the contractile response of $Ryr1^{Y522S/+}$ (n=20) and wild-type (n=23) gestation day 18.5 pregnant uterine arteries to cumulative concentrations of phenylephrine (PE) did not indicate that there was any statistically significant change in the maximum contraction (P=0.9405) and $logEC_{50}$ (P=0.6005) between heterozygous and wild-type vessels, unpaired t-test, demonstrated in Figure 42 (1A), all mean and SEM values are provided in Table 13.

4.3.3.2 The impact of litter $Ryr1^{Y522S/+}$ genotype on maternal uterine artery constriction

Vessels from wild-type (mixed litter) (n=17) and heterozygous (mixed litter) (n=20) mothers did not contract differently (%Kmax) in response to PE with DMSO pre-treatment in comparison to vessels from wild-type (wild-type litter) (n=23) mothers. There was no statistically significant change in the maximum (P= 0.6549) and $logEC_{50}$ (P=0.9410) between pregnant uterine artery vessels response to cumulative concentrations of phenylephrine (Brown-Forsythe ANOVA test), demonstrated in Figure 42 (1A).

4.3.3.3 Impact of dantrolene on pregnant uterine artery constriction within genotype groups

Following pre-incubation with dantrolene, vessels from heterozygous $Ryr1^{Y522S/+}$ (mixed litter) (n=18) and wild-type (mixed litter) (n=13) mothers did not contract differently in response to cumulative PE (% Kmax) in comparison to vessels from wild-type (wild-type litter) (n=22) mothers. There was no statistically significant change in the maximum (P=0.9008) and $logEC_{50}$ (P=0.9344) between all three vessel responses to PE when pre-treated with dantrolene, one-way ANOVA, demonstrated in Figure 42 (1B).

Vessels from all three pregnant genotype groups were more sensitive to PE constriction when pre-treated with dantrolene compared to vehicle (DMSO) alone, P=0.0211 (two-way ANOVA). As evidenced by a reduced $logEC_{50}$ in vessels from wild-type (mixed litter) (-6.847± 0.1618 to -7.342 ± 0.1337, P=0.0323), $Ryr1^{Y522S/+}$ (-6.873 ± 0.1294 to -7.277 ± 0.1396, P=0.0414) and wild-type (wildtype litter) dams (-6.912 ± 0.1082 to -7.320 ± 0.09408, P=0.0414, (Welch's t-tests). Vessels from heterozygous pregnant animals (-5.55%) had a smaller shift in EC50 compared to both wild-type (wild-type litter) (-6.05%) and wild-type (mixed litter) (-6.74%), demonstrated in Figure 43. The maximum constriction was not statistically different between dantrolene and DMSO treatment in all genotype groups.
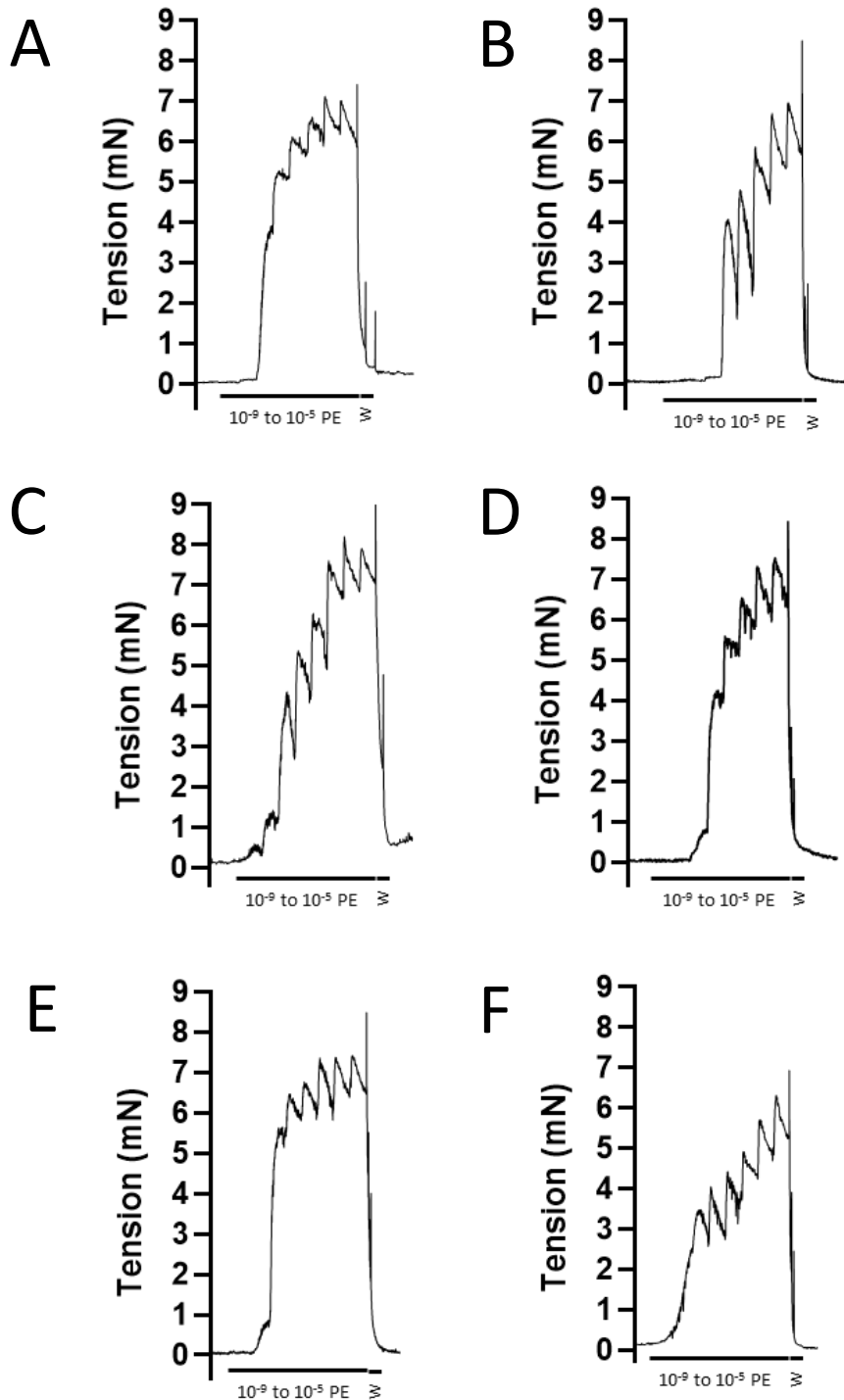
Figure 41. **Representative traces of pregnant uterine artery responses to cumulative concentrations of phenylephrine (PE) with DMSO (A, C and E) and dantrolene (B, D and F) in vessel segments from wild-type (wild-type litter) (A and B), *Ryr1^{Y522S/+}* heterozygous (mixed litter) (B and C) and wild-type(mixed litter) (E and F) mothers**

Representative traces of a pregnant uterine artery vessel segment (2 mm) constriction to cumulative concentrations of phenylephrine (10^{-9} to 10^{-5} M) with DMSO (A, C and E) or Dantrolene (30 µM, 30 minutes, B, D and F). Vessels from wild-type (wild-type litter) (A and B), *Ryr1^{Y522S/+}* heterozygous (mixed litter) (B and C) and wild-type (mixed litter) (E and F) mothers are shown. Treatment with each PE dose for 5 minutes followed by washes (w) with physiological salt solution (PSS).
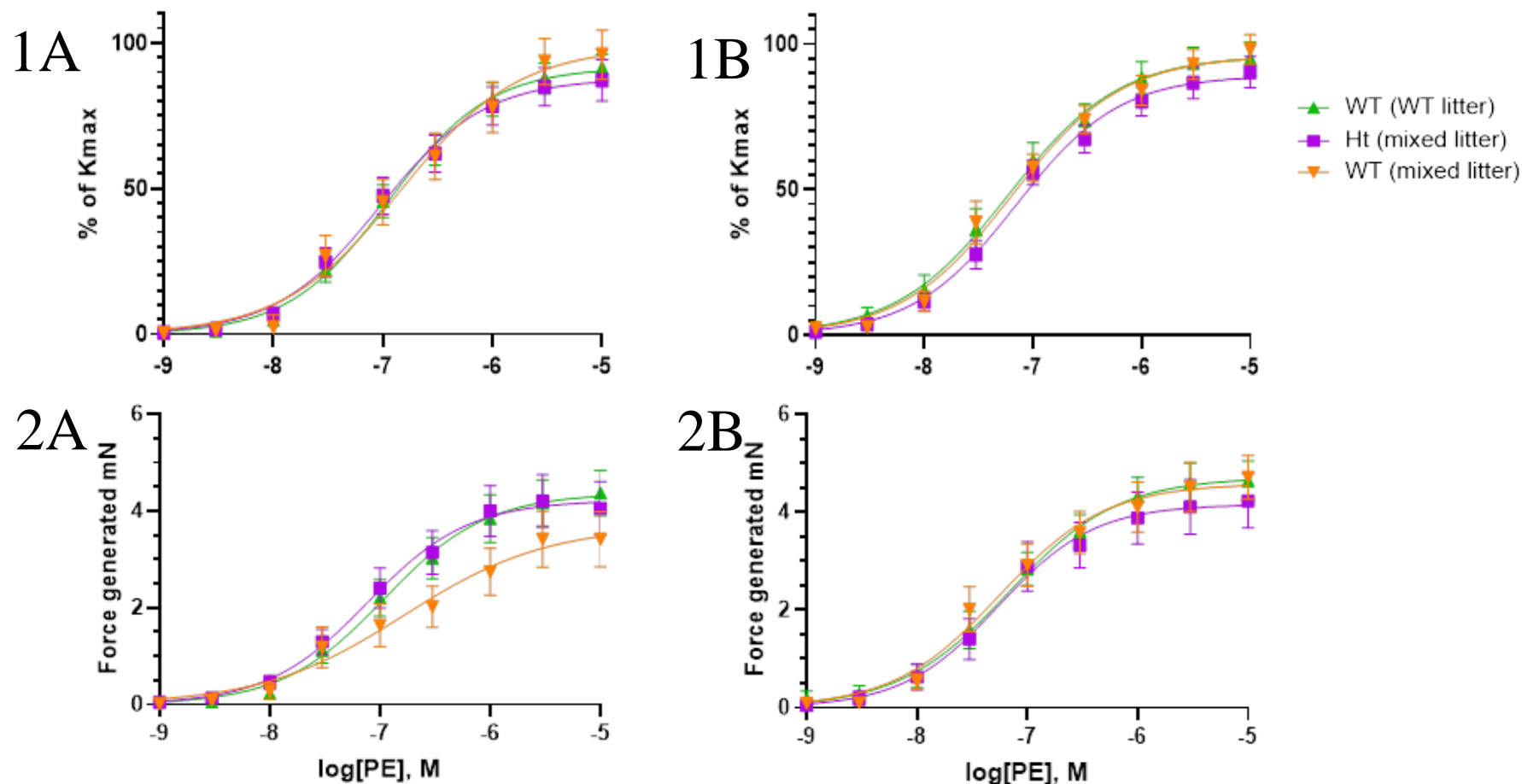
Figure 42. **Concentration-response curves in isolated uterine artery segments from pregnant wild-type (wild-type litter), *Ryr1*[Y522S/+] heterozygous (mixed litter) mothers and wild-type (mixed litter) mothers to cumulative concentrations of phenylephrine, presented as a percentage of Kmax (1A and 1B) and force generated minus baseline (2A and 2B), with vehicle DMSO (1A and 2A), or dantrolene (1B and 2B) pre-treatment.**

Ryr1[Y522S/+] heterozygous (mixed litter) (purple), wild-type (wild-type litter) pregnant (green), wild-type (mixed litter) pregnant (orange) uterine artery vessel segments preincubated with vehicle control (DMSO) (1A and 2A), or dantrolene (30 µM) (1B and 2B) for 30 minutes then contracted with cumulative concentrations of phenylephrine (1 nM - 10 µM). Data shown as a percentage of Kmax per individual vessel (1A and 1B) or as force generated minus baseline (mN) (2A and 2B). N=18 – 23 animals per group.

4.3.3.4 *Comparison of force generated (mN) Vs percentage of Kmax*

As shown in Figure 36, vessels from wildtype (mixed litter) demonstrated a reduced maximum contractile response to high K^+ PSS. This reduced contractile response was also apparent when vessels from wild-type (mixed litter) mothers were contracted with PE. Vessel response is shown as force generated (minus baseline) rather than percentage of maximum response to high K^+ to demonstrate this in Figure 42 (2A and 2B). The curve fit for vessels from wild-type (mixed litter) is shifted to the right compared to the curves fitted for vessels from heterozygous (mixed litter) and wildtype (wildtype litter) pregnant animals with vehicle DMSO pre-treatment (P=0.0085, (two-way ANOVA, not supported by multiple comparisons), which was reversed with dantrolene treatment.
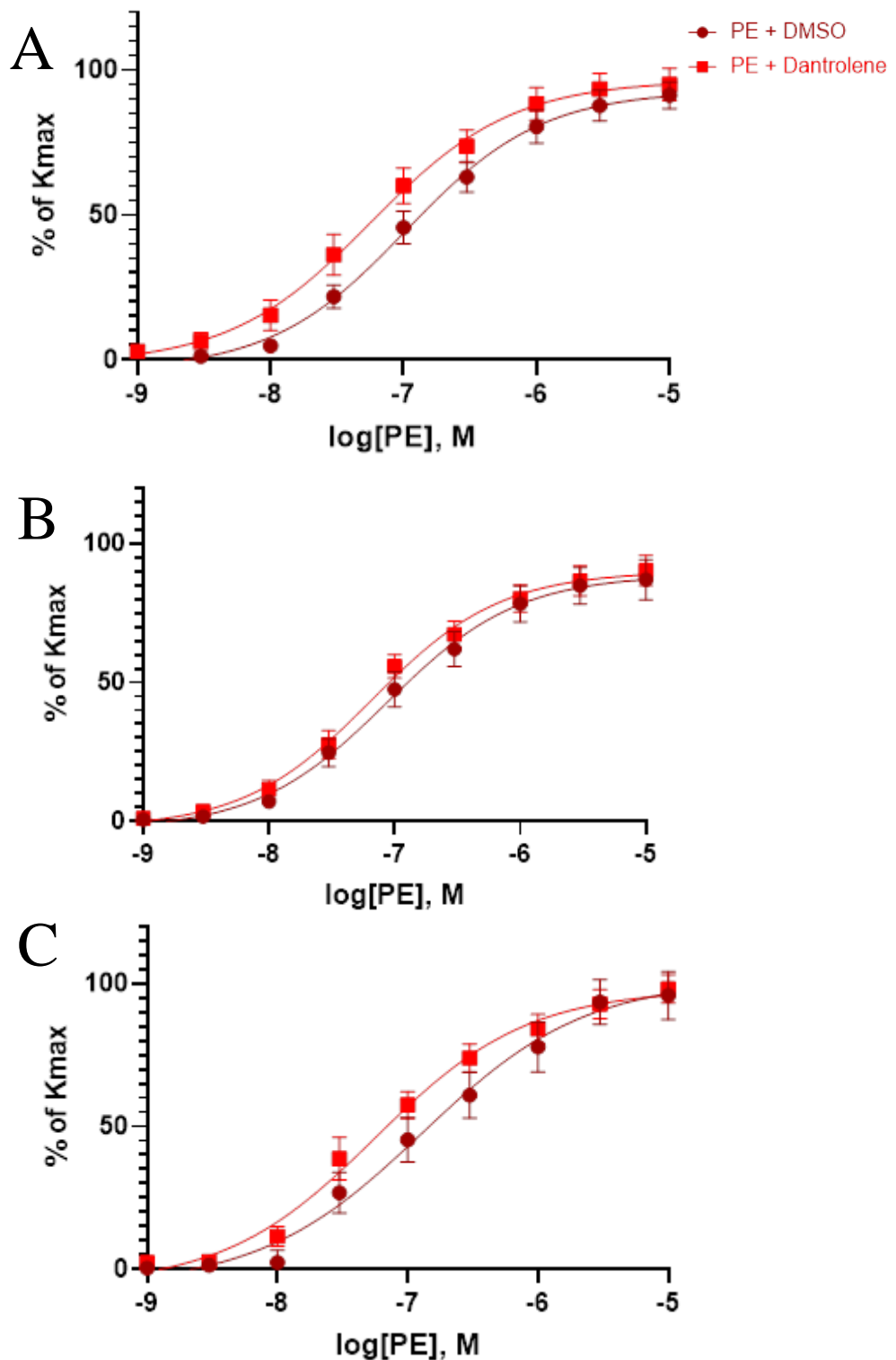
Figure 43. **Concentration response curves to cumulative phenylephrine presented in genotype groups (A) wild-type (wild-type litter), (B) heterozygous (mixed litter), (C) wild-type (mixed litter) with dantrolene/DMSO pre-treatment.**

Pregnant uterine artery segments (2 mm) collected on gestation day 18.5 from (A) Wild-type (wild-type litter), (B) heterozygous $Ryr1^{Y522S/+}$ (mixed litter), (C) wild-type (mixed litter) dams, N=17 – 23 animals. Concentration response curves to cumulative phenylephrine (10^{-9} – 10^{-5}) with 10 µM dantrolene (red) /DMSO (dark red) pre-treatments are shown in individual genotype groups.

206

Table 13. **Variables of interest from phenylephrine cumulative concentration non-linear regression curves.**
Maximum and logEC$_{50}$ obtained from concentration response curves to cumulative phenylephrine (1 nM-10 μM) as a percentage of Kmax contraction. Pregnant uterine artery segments were treated with PE + DMSO or PE+Dantrolene.

		PE		*PE+Dant*	
		Mean	SEM	Mean	SEM
Max.	WT(mixed) N=17, 13	101.625	8.114	95.345	4.469
	Ht(mixed) N= 21, 18	93.983	6.287	92.743	5.508
	WT(WT) N=23, 22	93.420	4.034	95.001	5.377
logEC$_{50}$	WT(mixed) N=17, 13	-6.847	0.162	-7.342	0.134
	Ht(mixed) N= 21, 18	-6.873	0.129	-7.189	0.116
	WT(WT) N=23, 22	-6.912	0.108	-7.320	0.094

4.3.4 Vasodilation of the pregnant $Ryr1^{Y522S/+}$ uterine artery

4.3.4.1 Impact of maternal $Ryr1^{Y522S/+}$ genotype on pregnant uterine artery vascular tone

Comparison of the pregnant uterine artery vessel response to cumulative concentrations of CCh indicated that the $logIC_{50}$ increased in vessels from heterozygous $Ryr1^{Y522S/+}$ mothers (-6.597 $\pm$ 0.1351, n=20) compared to vessels from wild-type (wild-type litter) mothers (-7.275 $\pm$ 0.2922, n=22), P=0.0457. This is seen as a curve shift to the right, presented in Figure 44. There was no statistically significant change in the minimum (P=0.9433) between responses in vessels from heterozygous $Ryr1^{Y522S/+}$ mothers and wild-type (wild-type litter) mothers, Welch's t-test.

Inhibiting RyR1 channels with dantrolene resulted in no statistically significant change in minimum (P=0.6172), and $logIC_{50}$ (P=0.8689), between vessels from heterozygous $Ryr1^{Y522S/+}$ mothers and vessels from wild-type (wild-type litter) mothers, Welch's t-test.

The maximum vasodilatory responses of vessels ('minimum') from $Ryr1^{Y522S/+}$ mothers appeared to be reduced when pre-treated with dantrolene compared to DMSO vehicle treatment alone, although this is not statistically supported, P=0.1656. There was also no statistically significant change in the $logEC_{50}$ (P=0.2510) (Welch's t-test) between treatment with dantrolene (n=17), and DMSO (n=19) of vessels from the $Ryr1^{Y522S/+}$ mother, shown in Figure 44.

The maximum vasodilation of vessels ('minimum') was reduced in vessels from wild-type (wild-type litter) mothers when pre-treated with dantrolene (-10.46±3.859) compared to DMSO treatment (6.697±3.268), P=0.0018 (Welch's t-test). There was no statistically significant change in the $logEC_{50}$ (P=0.3058), between treatment with dantrolene and DMSO.
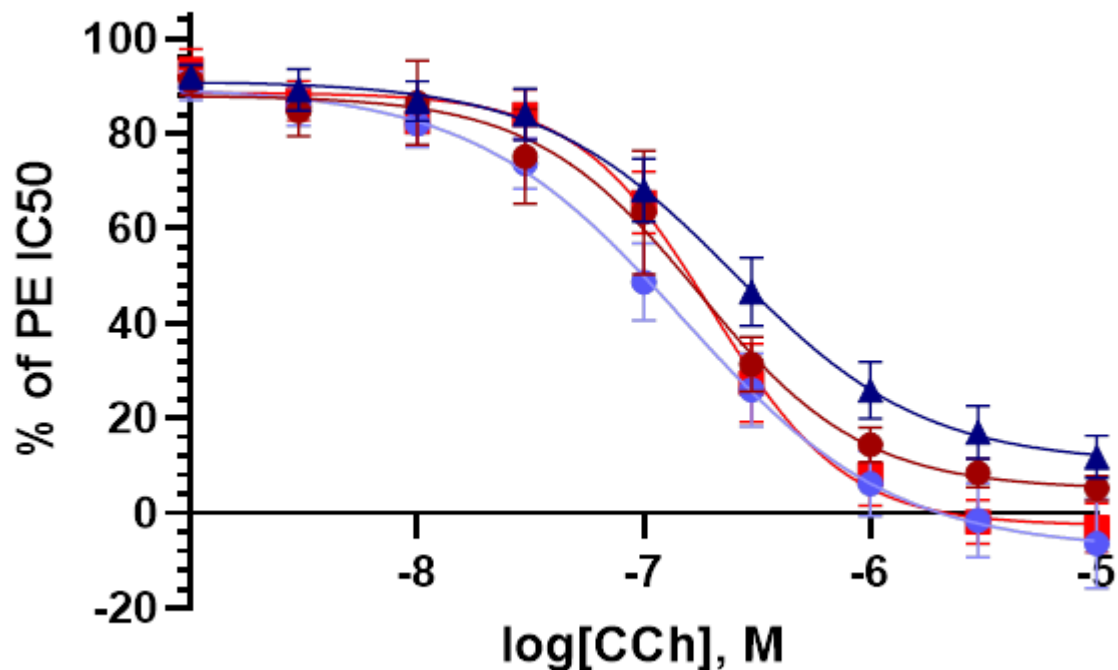
Figure 44. **Concentration response curves in isolated uterine artery segments from pregnant wild-type (wild-type litter) and *Ryr1*^{Y522S/+} heterozygous (mixed litter) mothers to cumulative concentrations of carbachol with dantrolene (30 µM) or vehicle control DMSO treatment**

Uterine artery vessel segments from *Ryr1*$^{Y522S/+}$ heterozygous (mixed litter) (dark blue) and wild-type (wild-type litter) pregnant (dark red), were preincubated with vehicle control (DMSO) for 30 minutes then pre-constricted phenylephrine then vasodilated with cumulative concentrations of carbachol (1nM - 10 µM). *Ryr1*$^{Y522S/+}$ heterozygous (mixed litter) (light blue) and wild-type (wild-type litter) pregnant (light red) uterine artery vessel segments were also preincubated with dantrolene (30 µM) for 30 minutes then pre-constricted phenylephrine then vasodilated with cumulative concentrations of carbachol (1nM - 10 µM). N=18 – 20 animals per group.

4.3.4.2 Impact of litter $Ryr1^{Y522S/+}$ genotype on maternal uterine artery vascular tone

RyR1 channel inhibition did not alter the relaxation response in vessels from wild-type (mixed litter) mothers (n=12) compared to DMSO pre-treatment (n=15). There was no significant change in the minimum (P= 0.8096) and $logEC_{50}$ (P= 0.1585) between treatment with DMSO and dantrolene, shown in Figure 45.

There was no statistically significant change in the minimum (P=0.4766), and $logEC_{50}$ (P=0.0891) between uterine artery vessels from all three genotype groups responses to CCh with dantrolene pre-treatment (Brown-Forsythe ANOVA test).

Vessels from heterozygous $Ryr1^{Y522S/+}$ mothers, wild-type (mixed litter) mothers and wild-type (wild-type litter) mothers did not respond differently to cumulative carbachol with DMSO pre-treatment only. There was no statistically significant change in minimum (P= 0.8101) and $logEC_{50}$ (P=0.3056) between responses to CCh with DMSO pre-treatment in vessels from all three genotype groups (Brown-Forsythe ANOVA test).
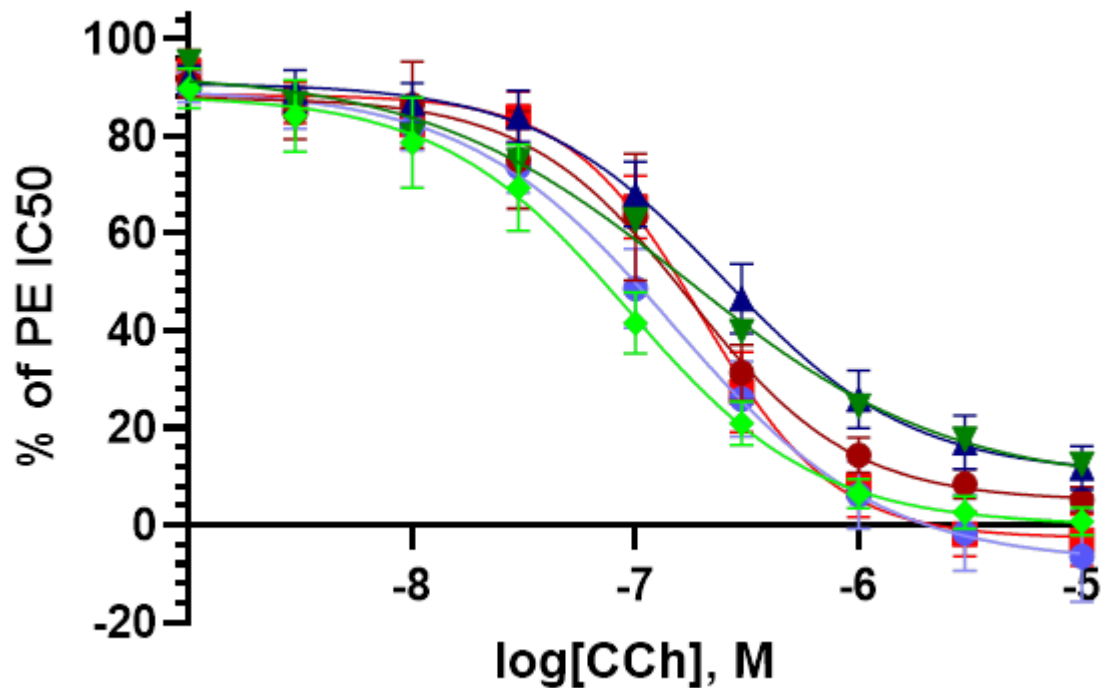
Figure 45. **Concentration response curves in isolated uterine artery segments from pregnant wild-type (wild-type litter), *Ryr1*^{Y522S/+} heterozygous (mixed litter) mothers and wild-type (mixed litter) to cumulative concentrations of carbachol with dantrolene (30 μM) or vehicle control DMSO treatment**

Ryr1$^{Y522S/+}$ heterozygous (mixed litter) (dark blue), wild-type (mixed litter) (dark green) and wild-type (wild-type litter) pregnant (dark red), uterine artery vessel segments preincubated with vehicle control (DMSO) for 30 minutes then pre-constricted phenylephrine then vasodilated with cumulative concentrations of carbachol (1nM - 10 μM). *Ryr1*$^{Y522S/+}$ heterozygous (mixed litter) (light blue), wild-type (wild-type litter) pregnant (light red), wild-type (mixed litter) pregnant (light green) uterine artery vessel segments preincubated with dantrolene (30 μM) for 30 minutes then pre-constricted phenylephrine then vasodilated with cumulative concentrations of carbachol (1nM - 10 μM). N=12 – 20 animals per group.
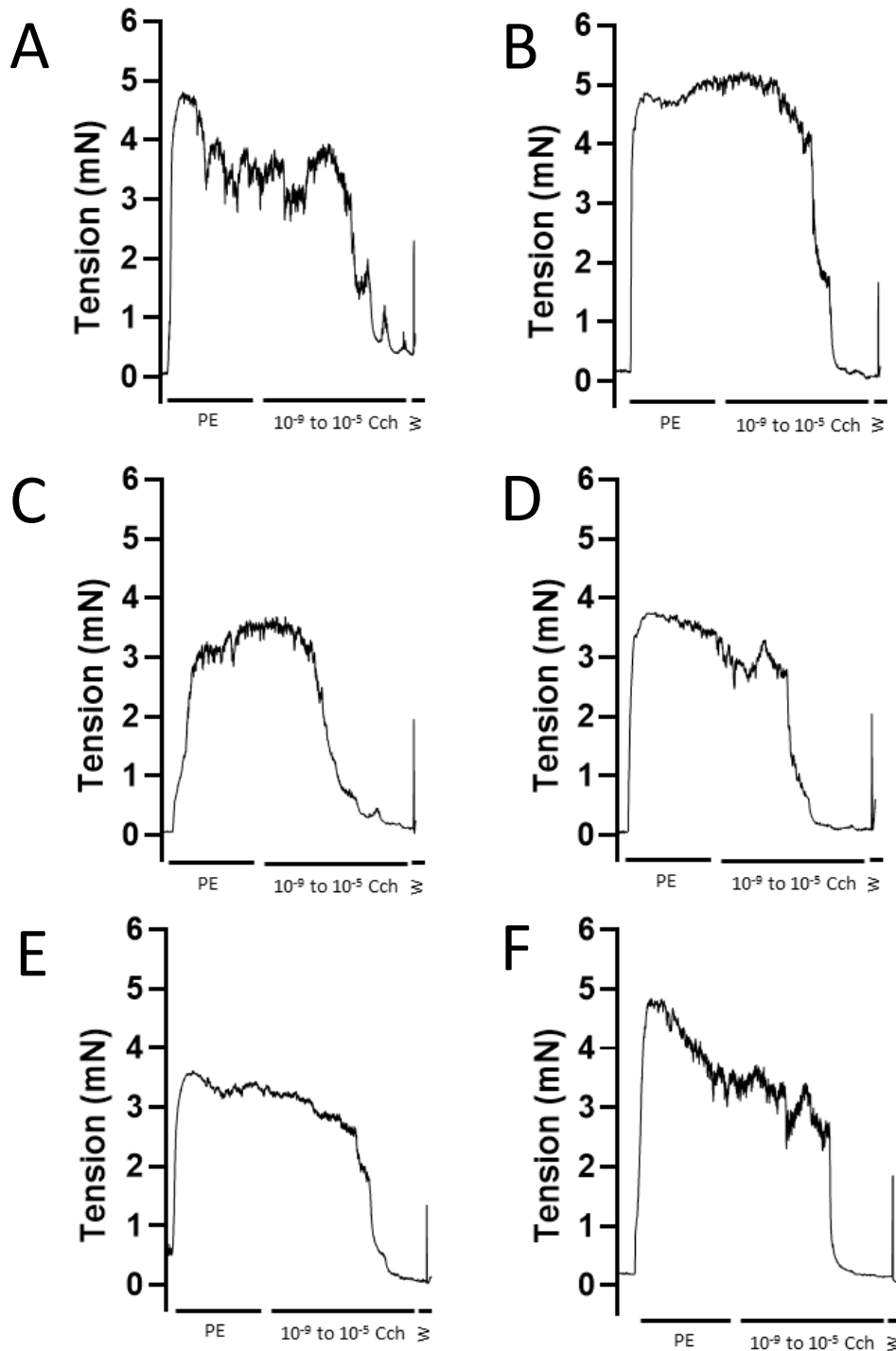
Figure 46. Representative traces of pregnant uterine artery responses to cumulative concentrations of carbachol (CCh) with DMSO (A, C and E) and dantrolene (B, D and F) in vessel segments from wild-type (wild-type litter) (A and B), *Ryr1*^Y522S/+^ heterozygous (mixed litter) (B and C) and wild-type (mixed litter) (E and F) mothers

Representative traces of a pregnant uterine artery vessel segment (2 mm) constriction to cumulative concentrations of carbachol (10^{-9} to 10^{-5} M) with DMSO or Dantrolene (30 µM, 30 minutes). Vessels from wild-type (wild-type litter) (A and B), *Ryr1*^Y522S/+^ heterozygous (mixed litter) (B and C) and wild-type (mixed litter) (E and F) mothers are shown. Treatment with each CCh dose for 5 minutes followed by washes (w) with physiological salt solution (PSS).

4.3.4.3 *Contribution of endothelial nitric oxide on myogenic tone in the Ryr1$^{Y522S/+}$ pregnant uterine artery*

L-NAME was used in *Ryr1*$^{Y522S/+}$ tissues to understand whether any potential changes in relaxation are NOS-based, endothelium hyperpolarisation-based or COX-based. As shown in Figure 47, the data collected from CCh relaxation experiments with NOS inhibition of pregnant uterine artery vessels from *Ryr1*$^{Y522S/+}$ (mixed litter) mothers (n=9), wild-type (mixed litter) mothers (n=10) and wild-type(wild-type) mother (n=12), is extremely varied. Under these conditions, it was difficult to perform a non-linear regression curve fit and obtain reliable data for variables of interest (minimum), therefore limiting the statistical analyses that could be performed.
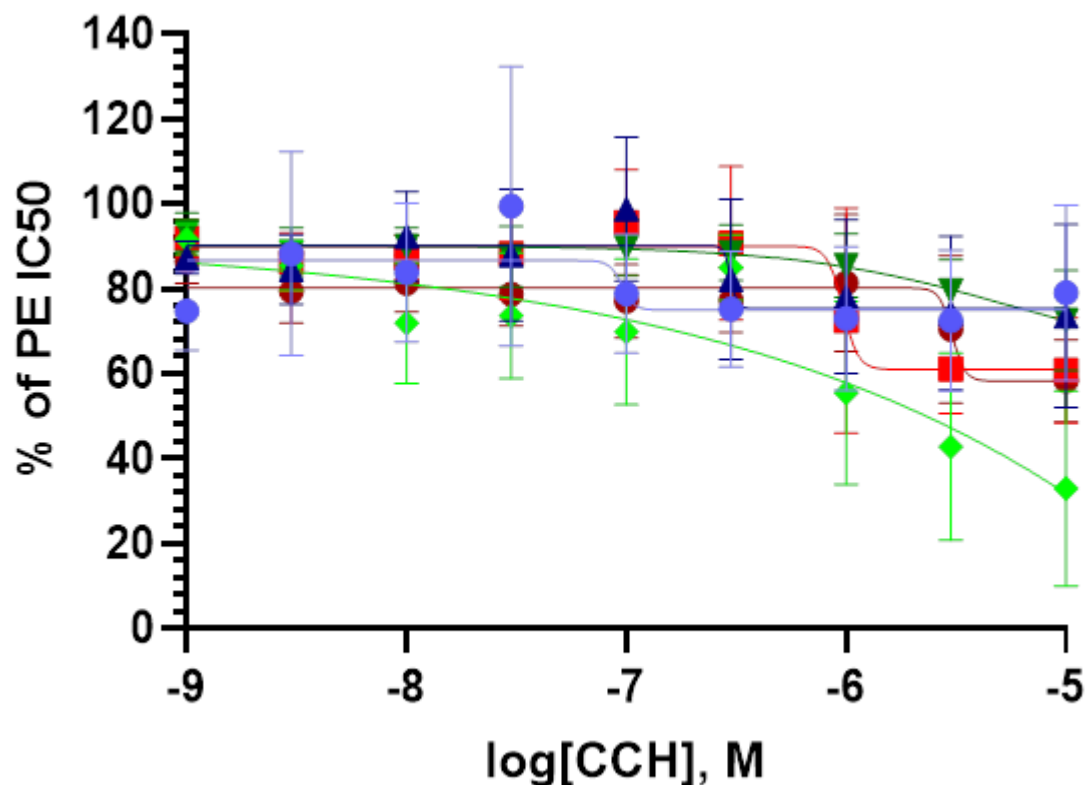
Figure 47. **Concentration response curves in isolated uterine artery segments from pregnant wild-type (wild-type litter), *Ryr1^{Y522S/+}* heterozygous (mixed litter) mothers and wild-type (mixed litter) to cumulative concentrations of carbachol with nitric oxide synthase inhibition (L-NAME) and with dantrolene (30 μM) or vehicle control DMSO pre-treatment**

Nitric oxide synthase inhibition (L-NAME pre-treatment) of uterine artery vessel segments from *Ryr1^{Y522S/+}* heterozygous (mixed litter) (dark blue), wild-type (mixed litter) (dark green) and wild-type (wild-type litter) pregnant (dark red) animals, before preincubation with vehicle control (DMSO) for 30 minutes then pre-constricted with phenylephrine then vasodilated with cumulative concentrations of carbachol (1nM - 10 μM). NOS inhibition of vessels from *Ryr1^{Y522S/+}* heterozygous (mixed litter) (light blue), wild-type (wild-type litter) pregnant (light red), wild-type (mixed litter) pregnant (light green) mothers preincubated with dantrolene (30 μM) for 30 minutes then pre-constricted phenylephrine then vasodilated with cumulative concentrations of carbachol (1nM - 10 μM). N=9 – 12 animals per group.
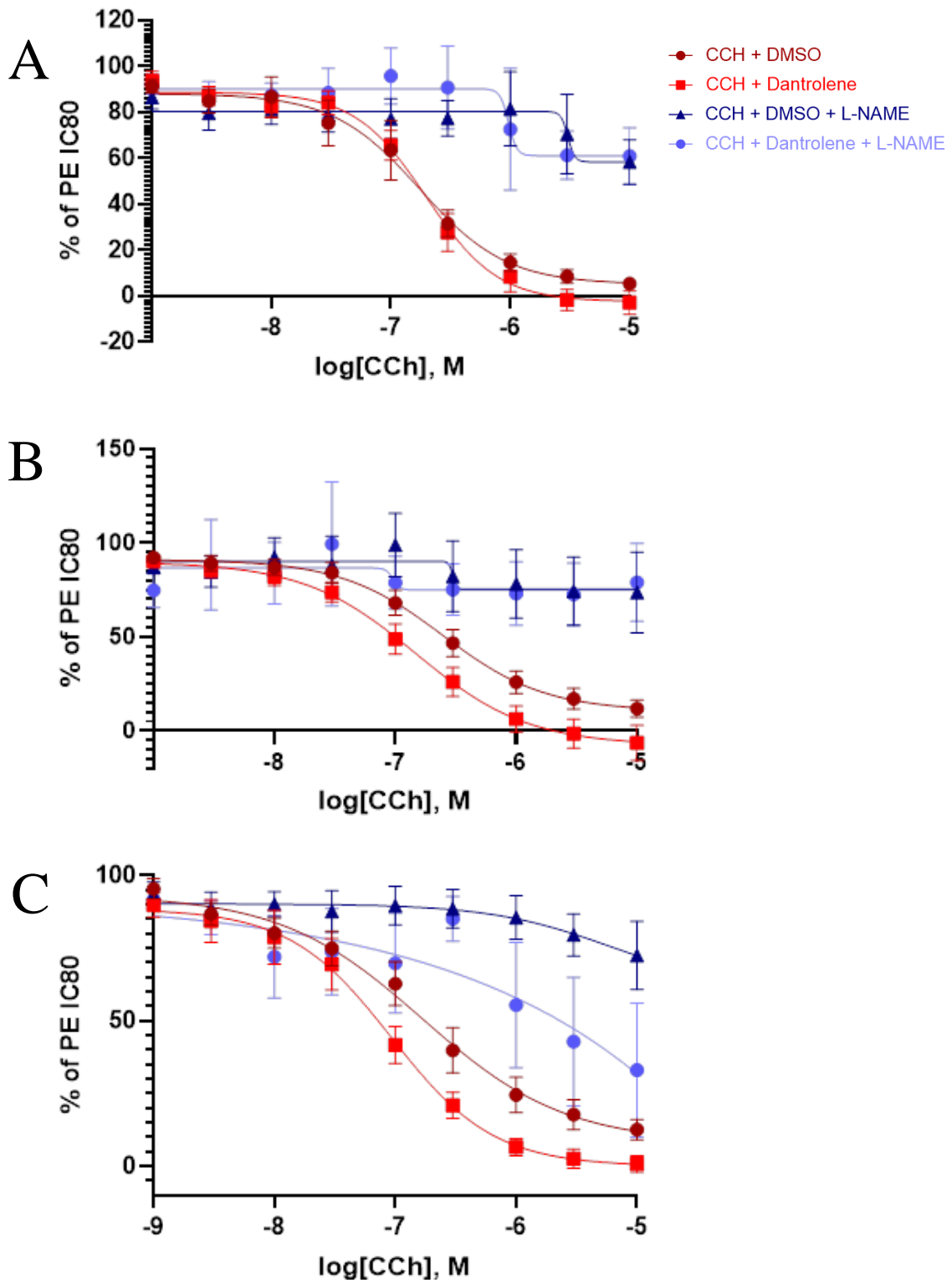
Figure 48. **Concentration response curves to cumulative carbachol in individual genotype groups.**

Response to cumulative concentrations of carbachol (1nM - 10 μM) in vessels from (**A**) Wild-type (wild-type litter), (**B**) heterozygous (mixed litter), (**C**) wild-type (mixed litter) dams with dantrolene (light red or blue)/DMSO (dark red or blue) pre-treatment, with (blue) or without (red) NOS inhibition with L-NAME. N=9 – 22 animals per group.

Table 14. **Variables of interest from carbachol cumulative concentration non-linear regression curves.**

Minimum and $logEC_{50}$ obtained from concentration response curves to cumulative carbachol (1 nM-10 μM), plotted a percentage of relaxation from PE IC80. Pregnant uterine artery segments were treated with CCH + DMSO, CCH+Dantrolene, CCH+DMSO+LNAME, or CCH+ Dantrolene+LNAME.

		CCH		CCH+Dant		CCH+DMSO+LNAME		CCH+Dant+LNAME	
		Mean	SEM	Mean	SEM	Mean	SEM	Mean	SEM
Minimum	WT(mixed)	2.266	5.633	-0.689	2.817	-983.643	1047.00	-14385.088	14282.496
	N=15, 12, 10, 10								
	Ht(mixed)	6.178	5.902	-12.099	11.342	-36923.127	36979.360	27.656	32.735
	N=20, 18, 9, 10								
	WT(WT)	5.728	3.486	-11.341	3.985	-2634.3	2617.696	35.788	11.122
	N=22, 21, 12, 12								
logEC$_{50}$	WT(mixed)	-6.803	0.236	-7.285	0.233	3.021e+128	3.021e+128	-1.362	3.435
	N=15, 12, 10, 10								
	Ht(mixed)	-8.457	1.850	-6.819	0.108	-294310.29	294479.378	-6.225	0.766
	N=20, 18, 9, 10								
	WT(WT)	-6.608	0.413	-6.800	0.117	-6.365	2.847	-11.321	4.142
	N=22, 21, 12, 12								

4.4 Discussion

The aim of this study was to understand whether the *Ryr1* Y522S mutation impacts uterine artery function during pregnancy. This was studied using *ex vivo* isometric tension recordings of late-pregnant uterine artery contractile and relaxation responses to phenylephrine and carbachol, respectively. To further understand the impact of *Ryr1* Y522S on vessel morphology, histological studies were performed, and smooth muscle content, lumen diameter and wall thickness were analysed. Using RT-qPCR, *Ryr1* transcript quantification studies were attempted but were limited by low DNA concentrations.

In this chapter I have demonstrated that there was an inherent difference in the maximal contractile ability of uterine artery segments from pregnant wild-type (mixed litter), heterozygous Ryr$^{Y522S/+}$ (mixed litter) and wild-type (wildtype litter) animals, likely due to changes in smooth muscle mass and lumen diameter in these vessels. There was no difference in inherent PE sensitivity of the vessels between each group, when correcting for high K^{+} response, indicating that the theorised increased Ca^{2+} release through the RyR1 Y522S channel does not limit this response. However, there was some indication that inhibiting RyR1 channels (with dantrolene) made heterozygous vessels less sensitive to PE constriction compared to wild-type vessels (decreased logEC$_{50}$). Pre-constricted vessels from Ryr$^{Y522S/+}$(mixed litter) animals were less sensitive to CCH-based vasodilation which was reversed by RyR1 channel inhibition (increased IC50), this was also observed in vessels from the wildtype (mixed litter) animals, indicating an inhibitory effect of fetal Ryr1 Y522S on maternal vasodilation. Nitric oxide synthase (NOS) inhibition resulted in almost total inhibition of vessel vasodilation, indicating that most of pregnant uterine artery vasodilation is NO-induced.

The remainder of this discussion is structured around each of these findings, followed by a brief consideration of study limitations and proposed future work.

Alterations in contractile amplitude in the wildtype (mixed litter) pregnant uterine artery

Force produced in response to high K^+PSS (amplitude) was reduced in vessels from the wild-type (mixed litter) compared to vessels from both heterozygous (mixed litter) and wild-type (wild-type litter) dams. This suggests that the pregnant uterine artery from the wild-type (mixed litter) animal had a weaker contractile response. To determine whether this difference is true, it is standard practice to adjust for differences in vessel length. i.e., vessel tension (mN/mm), which is the force produced divided by length, however, all vessel segments in this study were cut to 2 mm in length and therefore force was not adjusted for length. This change in maximum contractile ability was evident when vessel response to PE was observed as 'Force (mN) generated' rather than 'percentage of Kmax', where the maximal response to PE was reduced in the wildtype (mixed litter) vessel compared to heterozygous (mixed litter) and wildtype (wildtype litter) vessels.

A difference in Kmax could therefore be due to various factors including an inherent change in smooth muscle contractility i.e., changes at the level of contractile machinery, hypertrophy/hyperplasia, differences in vessel diameter, or altered expression of voltage-gated Ca^{2+} channels. Although VGCCs are a major driving force of intracellular Ca^{2+} flux within the VSMC, it was not considered a factor involved in the differential contractile ability of the vessels in this study due to no known interactions with the RyR1 channel. A change in lumen diameter between vessels was corrected for during the normalisation procedure, described in the methods chapter. I determined that vessels from wild-type (mixed litter) animals, had a smaller lumen diameter when stretched to physiological tension and reduced smooth muscle cell count, although the latter was not statistically supported, most likely due to small sample size. In contrast, the wall thickness of the wildtype (mixed litter) vessels did not follow the same pattern observed in Kmax amplitude and lumen diameter. This indicates a potential fetal

driven mechanism that enhances maternal blood flow to growing fetuses, possibly through further upstream smooth muscle cell remodelling in the uterine artery.

However, the change in contractile amplitude was only observed in the wildtype (mixed litter) vessel, which suggests that the *Ryr1* Y522S mutation in the fetus impacts the contractile response of the maternal uterine artery, in the absence of maternal *Ryr1* Y522S. It is possible that the maternal *Ryr1* Y522S mutation may buffer the fetal signal on maternal uterine vascular tissue. Some similar incidences where fetal genotype induce changes in maternal physiology have been described and are discussed in more detail below. To test the impact of the fetal genotype on maternal vessel physiology, vessels could be tested from heterozygous *Ryr1$^{Y522S/+}$* females crossed with heterozygous *Ryr1$^{Y522S/+}$* males to create a homozygous *Ryr1$^{Y522S/Y522S}$* litter. In this case we would expect to see a more pronounced change in vessel reactivity compared to the Ht(mixed litter) vessel. Ultrasound doppler imaging could be used to investigate potential changes in uterine artery contractility in 'healthy' women carrying fetuses with RYR1 variants.

Changes in the contractile ability of the *Ryr1$^{Y522S/+}$* pregnant uterine artery

There was no change in the constriction of vessels from heterozygous (mixed litter) and wildtype (mixed litter) animals compared to vessels from wild-type (wild-type litter) animals, with vehicle pre-treatment. In sheep uterine artery pregnancy increases RyR1 and Bk$_{Ca}$ α and β1 subunit co-localisation, and the knock-down of RyR1 decreases Ca^{2+} spark frequency, suppresses STOCs frequency and amplitude, and increases pressure-dependent myogenic tone in uterine arteries of pregnant animals (Nagar, Liu and Rosenfeld, 2005; Khan *et al.*, 2010; Song, 2021). In addition, Lopez and colleagues (2016) reported that RyR1 Ca^{2+} spark frequency is increased in *Ryr1$^{Y522S/+}$* tail artery VSMCs. Based on the channel gain-of-function,

and assuming that the RyR1 channel is located close the plasma membrane, I hypothesised that increased RyR1 Ca^{2+} sparks would result in increased Bk_{Ca} activation and therefore increased resistance to vasoconstriction, ultimately causing a pro-relaxant effect. However, the data presented in this chapter suggests that the RyR1 Y522S channel does not cause increased resistance to contraction in the pregnant mouse uterine artery.

On the other hand, blocking RyR1 with dantrolene revealed an underlying pro-relaxant effect of the RyR1 channels in all pregnant mouse uterine arteries (i.e., less PE was required to constrict the vessels when RyR1 channels are blocked). This fits the hypothesis whereby RyR1 channels normally cause a pro-relaxant effect in arterial vessels, and blocking RyR1 channels leads to increased vasoconstriction. Furthermore, vessels from $Ryr1^{Y522S/+}$ (mixed litter) mothers had the smallest decrease (left shift) in $logEC_{50}$ when pre-treated with dantrolene, indicating that heterozygous vessels, were more resistant to vasoconstriction in the presence of dantrolene. This may be due to the inhibition of $RYR1$-Bk_{Ca} channel interaction, inhibiting the pro-relaxant effect and resulting in increased vasoconstriction. The smaller reduction in $logEC_{50}$ in the $Ryr1^{Y522S/+}$ vessel may be a result of increased Ca^{2+} release into the cytosol, whereby dantrolene does not block all RyR1 Y522S activity, leaving some of the RyR- Bk_{Ca} channel interaction, and maintaining some of the opposing vasorelaxation mechanism.

Considering that dantrolene is a selective RyR1 antagonist, the following explanation may be unexpected yet plausible. It is possible that dantrolene does not selectively block RyR1 channels, but may also block RYR3 channels (Zhao, 2001a), that are known to be expressed in uterine arteries (Song, 2021), leaving some RyR1 Y522S channels uninhibited and therefore continue its activation of Bk_{Ca}. It is also possible that there may be other off-target effects of dantrolene such as interaction with functional RyR1 channels vascular endothelial cells, previously demonstrated in human umbilical vein endothelial cells (Chuang *et al.*, 2022).

Impact of *Ryr1^Y522S/+* on pregnant uterine artery vasodilation

A rather unexpected finding of this study, was that pre-constricted vessels from heterozygous *Ryr1^Y522S/+* (mixed litter) dams exhibited a larger IC50 when dilated with Cch (with vehicle pre-treatment), compared to vessels from wildtype (wildtype litter) mothers i.e. more Cch was required to dilate heterozygous vessels to 50% of its maximum vasodilation capacity compared to the concentration for vessels from wildtype(wildtype litter) dams (curve shifted to the right). In addition, blocking RyR1 channels reduced the IC_{50} of the *Ryr1^Y522S/+* vessel to a similar IC_{50} of the vehicle pre-treated vessel from wildtype (wildtype litter) dams. I previously hypothesised that the Ryr1 Y522S channel would create a pro-relaxant effect, whereas this result suggests that myogenic tone is increased in the Y522S vessel, and that blocking RyR1 channels enhances relaxation in these vessels.

To comprehend this apparent increase in myogenic tone, it is important to know how carbachol induces vasodilation in the mouse uterine vascular bed, and the influence of RyR1 on this pathway. As previously described in section 1.8.3, in the perfused uterine vascular bed of pregnant rats, acetylcholine-induced relaxation is mediated by NO, prostanoids and EDH (Dalle Lucca, 2000). Specifically, in endothelium intact vessels, carbachol, an acetylcholine mimetic, is suggested to activate M3 G-protein coupled receptors on the endothelial membrane. Briefly, this triggers IP3R mediated SR Ca^{2+} release which predominantly triggers eNOS production of NO, which travels to VSMCs and induces vasorelaxation through cGMP activation of PKG. Although in this study I did not investigate subcellular localisation of RyR1 channels, it may be that RyR1 are also expressed in the endothelial cells of the pregnant uterine artery, considering that there is evidence for the expression of RyR1 in vascular endothelial cells and rat colonic epithelium (Prinz and Diener, 2008; Chuang, 2022). Therefore, presuming

RyR1 expression in the vascular endothelium, increased Ca^{2+} release via RyR1 Y522S could cause increased NO production and a pro-relaxant effect. This is not what was observed in this experiment, so we must consider how else increased RyR1 Y522S mediated SR Ca^{2+} release may increase myogenic tone. A potential mechanism could be that increased Ca^{2+} release from the SR might instead increase the release of endothelin from cytoplasmic vesicles, resulting increase endothelin-based vasoconstriction of the uterine artery (Hu, Kim and Jeng, 1991; Dechanet *et al.*, 2011; Zhou *et al.*, 2013; Bakrania *et al.*, 2017), however further investigations are required.

Although not statistically significant, in all vessel genotype groups the concentration response curves to cumulative CCh with dantrolene pre-treatment had a reduced minimum value i.e., maximum vasodilation response, compared to vehicle treatment alone. Therefore, it appears that dantrolene enhanced the relaxation response in all vessels. This could also potentially be a side effect of reduced PE pre-constriction rather than dantrolene mediated eNOS release.

Impact of fetal genotype on maternal uterine artery function

In the above experiments, it is evident that vessels from the wild-type (mixed litter) dams responded to PE and CCh in a different manner to vessels from the wild-type (wild-type) dams and in some cases in a manner similar to vessels of the heterozygous *Ryr1*$^{Y522S/+}$ (mixed litter) mother, as shown in Figure 45. This indicates that the fetal Y522S genotype could impact maternal uterine artery function, as opposed to the traditional narrative of maternal genotype and locally acting factors on fetal development and disease. There is some evidence implicating fetal genotypes as influencing factors of maternal physiology during pregnancy. For example, pregnant mice carrying offspring with the p57^{kip2}-null genotype, the mothers displayed symptoms of preeclampsia thought to be result of trophoblastic hyperplasia induced by the

conceptuses without p57Kip2 expression (Takahashi, 2000; Kanayama, 2002; Petry, 2007). Therefore, it is possible that the fetal $Ryr1^{Y522S/+}$ may alter maternal uterine artery constriction and dilatation to fulfil increased fetal nutrient demand, optimising fetal growth.

4.5   Study limitations and future work

In the study above, there were very subtle changes in uterine artery function. This may be a result of studying vessels during pregnancy. It is known that changes in sex-hormone levels impact the vasoconstrictive response to various vasopressors, as reported in male rat mesenteric arteries when treated with 17β-oestradiol have a 4 times weaker response to norepinephrine (Colucci *et al.*, 1982) and in pregnant sheep uterine arteries which have weakened blood flow and uterine vascular resistance in response to α-adrenergic agonists (Magness and Rosenfeld, 1986). Repeating the studies above in non-pregnant $Ryr1^{Y522S/+}$ uterine arteries could provide further information on vessel function without the masking impact of pregnancy-related hormones. Further to this, some pharmacological agents contract peripheral blood vessels more strongly such as metaraminol in uterine arteries, or norepinephrine in mesenteric arteries of pregnant rats (Wang *et al.*, 2021)., Based on my observations, in future studies of $Ryr1^{Y522S/+}$ uterine artery function I recommend the use of an alternative contractile agent with fewer off-target effects such as metaraminol which may provide a larger change in contractile response (through the mechanism of adrenaline receptors stimulation).

In the current study, uterine artery vasodilation was studied using an endothelial-mediated mechanism. This did not directly investigate the role of RyR1 channels in the VSMC and may be avoided in future investigations. Instead, to determine if the RyR1-based vasorelaxation signal is from the SMC or EC, the use of a drug that acts directly on the SMC to cause vasorelaxation in parallel with endothelial vasorelaxant blockers should be considered. Similarly, contraction of the uterine artery vessel could be performed using an agonist with a different mechanism of action, avoiding the activation of the SR IP$_3$R, such as agonists of RyR1 itself, caffeine, and ryanodine. Activation of SR channels, IP$_3$R and RyR, trigger the release of Ca^{2+} from the SR store, this store is then replenished by the SERCA pump. Therefore, it could

be important to control SERCA mediated replenishment of the SR store, using cyclopiazonic acid (CPA) or thapsigargin.

To investigate the wider impact of Ryr1 Y522S on intracellular Ca^{2+} movement within the vascular smooth muscle of uterine arteries, 2-aminoethoxydiphenylborane (2-APB) could be used to block IP_3R channel mediated calcium release from the SR. Possible alterations in RyR1 channel interactions with plasma membrane BK_{Ca} should also be investigated using paxilline (PAX). In addition, it could be beneficial to use endothelium denuded arteries to determine the impact of Y522S on vascular smooth muscle without opposing endothelial based relaxation, and to determine whether changes seen in the vasoconstriction and dilation of $Ryr1^{Y522S/+}$ vessels are due to RyR1 channels function in the endothelium. The residual relaxation after blockade of nitric oxide synthase (NOS) and cyclooxygenase (COX) is attributed to endothelium-derived hyperpolarization (EDH), therefore the use of indomethacin in conjunction with L-NAME should be considered see the impact of RyR1 on EDH only.

Further to this it may be useful to study smaller, lower order resistance vessels such as radial arteries instead of uterine artery, as radial arteries are likely to be responsible for up to 90% of the total resistance of the mouse uterine vascular bed during pregnancy (Rennie, 2016).

It is important to understand the potential real-life implication of the data presented in this study. The administration of dantrolene could be a solution to treating increased/heavy bleeding events *RYR1*-mutated patients. However, it must be noted that dantrolene does not selectively block RyR1 channels only, as described above. Further to this, animal studies show that dantrolene does cross the placenta therefore its use in pregnancy is to be avoided, although teratological studies have proved satisfactory (National Institute for Health and Care Excellence (NICE), 2023). Therefore, in future *ex vivo* studies of the pregnant $Ryr1^{Y522S/+}$ animal the use of alternative drugs that selectively block RyR1 and are safe to use in pregnancy

should be considered, such as oxolinic acid-derivative RyR1-selective inhibitor, 6,7-(methylenedioxy)-1-octyl-4-quinolone-3-carboxylic acid (Compound 1, Cpd1) (Yamazawa *et al.*, 2021), although its safe-use in pregnancy requires much further investigation.

A limitation of this study was the low sample number for RT-qPCR tests and histological studies. Although it was possible to detect *Ryr1* transcripts in pregnant uterine artery vessels from all genotype groups, the volume of mRNA used to study *Ryr1* expression was extremely small and limited the investigation of transcript levels between genotype groups. In addition, the pattern observed in SMC nuclei count dataset correlated with high K^+PSS data, however a limited number of uterine artery sections were available for histological analyses which meant that this study did not reach power to reliably determine statistical significance. Therefore, it is imperative to repeat these tests with a larger sample size.

In addition, to determine the presence of RyR1 protein in pregnant uterine artery smooth muscle and endothelial cells, the use of more precise and sensitive techniques requiring smaller input material could prove useful, such mass spectrometry. Further to this, to determine RyR1 channel localisation in the endothelium and smooth muscle cells of the pregnant uterine artery, it would be extremely useful to perform immunohistochemical studies using RyR1 antibodies and smooth muscle actin.

In the present study, I was unable to confirm the increased Ca^{2+} spark frequency in pregnant *Ryr1*$^{Y522S/+}$ uterine artery smooth muscle cells, that was previously observed by Lopez and colleagues in cultured tail artery VSMCs. It could be extremely useful to investigate *Ryr1*$^{Y522S/+}$ Ca^{2+} spark frequency, amplitude, and localisation in the uterine vascular bed to understand how RyR1 Y522S impacts calcium movement within the uterine VSMC, possibly using patch-clamp techniques or fluorescent intracellular calcium microscopy.

4.6   Conclusions

This study of pregnant $Ryr1^{Y522S/+}$ uterine artery function and morphology has shown that the RyR1 Y522S channel; does not directly impact vessel smooth muscle contractility, but impairs vessel dilation indirectly potentially through endothelial factors, and influences maternal uterine artery function through the fetal $Ryr1^{Y522S/+}$ genotype. It seems that dantrolene may impact wild-type pregnant uterine artery function, informing an important consideration for the clinical administration of dantrolene in pregnant women. Further studies are required to specifically determine the mechanism of altered Ryr1 Y522S channel activity on uterine artery function, in particular live-calcium imaging, to determine how patients with $RYR1$-variants can be clinically supported during abnormal bleeding events.

5 Chapter 5 Myometrial function in the pregnant *Ryr1*^{Y522S/+} mouse

5.1 Background

The described *RYR1*-associated bleeding phenotype was predominantly found in female *RYR1*-mutated patients, suggesting a more intense bleeding abnormality in women characterised by reported heavy menstrual bleeding and post-partum haemorrhage (Lopez, 2016). Which lead us to consider the role of mutant RyR1 channels in the uterus and its vasculature during menstruation and in pregnancy, when changes in the reproductive system are heightened.

As detailed in Chapter 1, uterine activation, to a spontaneous contractile state and sensitivity to endogenous uterotonins during labour is an essential step in the onset of parturition (Kota *et al.*, 2013b). The dysregulation of intracellular Ca^{2+} in the myometrium can often lead to myometrial dysfunction causing untimely contractions leading to preterm delivery, or excessively strong contractions leading to fetal distress/death, or weak contractions/irregular contractions leading to failure to progress during delivery and therefore Caesarean sections (Wray, 2007; Aguilar and Mitchell, 2010).

Although varying levels of *RYR1, RYR2* and *RYR3* mRNA and protein expression have been reported in both human and rodent myometrial cells (S Lynn *et al.*, 1995; Martin, 1999; Dabertrand *et al.*, 2006; Matsuki, 2017), the study of RyR1 calcium channel behaviour in the aberrant function of the uterus has seldom been studied. Some reports have implicated RyR-mediated CICR in the regulation of uterine contractility in labour, (Tribe, 2000; Wray, 2003; Wray, Burdyga and Noble, 2005), and other have argued that RYR3 is the predominant isoform in the uterus and plays an essential role at the end of pregnancy (Mironneau, 2002; Jiang, 2003; Dabertrand *et al.*, 2007). The current data on RyR channel behaviour in the uterus is conflicting, leading to some reports completely disregarding the role of RYR1 in the uterus.

Therefore, the primary objectives of this study were to determine the impact of the mouse *Ryr1* Y522S gain-of-function mutation on (1) myometrial function by measuring gestation length and parturition duration, (2) myometrial contractility using *ex vivo* isometric measurements, (3) myometrial gene expression using next generation RNA sequencing.

5.2 Methods

To understand how the *Ryr1* Y522S mutation impacts the normal function of the myometrium during pregnancy, the gestation length of $Ryr1^{Y522S/+}$ mouse was studied alongside molecular investigations of pregnant myometrial tissue. Some limited (due to the impact of COVID) *ex vivo* measurements of non-pregnant Y522S myometrial contractility were also conducted. Detailed description of methods can be found in Chapter 3.

Briefly, on gestation day 17.5, time-mated pregnant females were singly housed in IVC cages connected to video recording cameras to determine the end of gestation. To investigate contractility of the $Ryr1^{Y522S/+}$ uterus compared to wild-type uterine tissue, spontaneous contractions of the nonpregnant myometrium during oestrus, and pregnant gestation 18.5 myometrium were studied *ex vivo* in heated (37.5°C) and oxygenated (95% O_2 / 5% CO_2) organ baths. The expression *Ryr1, Ryr2,* and *Ryr3* mRNA in Y522S myometrial tissue was studied using RT-qPCR methods, using primers outlined in section 3.6.3. Western blotting methods were optimised to detect high molecular weight proteins such as the RYR1 protein (~560 kDa). Following this, the pregnant mouse uterus was stained with RYR1 antibodies to detect RYR1 protein location in the uterus. Changes in gene expression in the myometrium of pregnant $Ryr1^{Y522S/+}$ animals were explored using high-throughput sequencing methods. The DESeq2 package was used to perform differential expression analyses, and online web-based tools were used to understand differential gene expression location, molecular function, common pathway involvement and protein interactions. Differential gene expression was validated using RT-qPCR, gene copy number was expressed relative to the geometric mean of the most stable reference genes determined by GeNorm software (Vandesompele, 2002).

5.3 Results

5.3.1 Altered gestation and labour length in the $Ryr1^{Y522S/+}$ mouse

Using video camera recordings, gestation length was successfully determined in wild-type (wild-type litter) (n=10), heterozygous $Ryr1^{Y522S/+}$ (mixed litter) (n=9), and wild-type (mixed litter) (n=10) dams. Direct observation and video camera recording of both wild-type and heterozygous pregnant mice revealed that both groups exhibited common behavioural signs prior to and during labour, including whole body shaking, stretching by standing on hind legs, grooming of the vaginal opening and surrounding area and lordosis-like movement. Representative still-frames that illustrate these common labour behaviours are displayed in Figure 49. There were no differences in the behaviours observed between heterozygous and wild-type females. A consequence of IVC housing was that the video cameras used in this study had poor visibility of the mouse contained within the Perspex cages, leading to an inability to always determine the exact time of birth of the first and last pups, hence parturition duration could not be successfully determined.
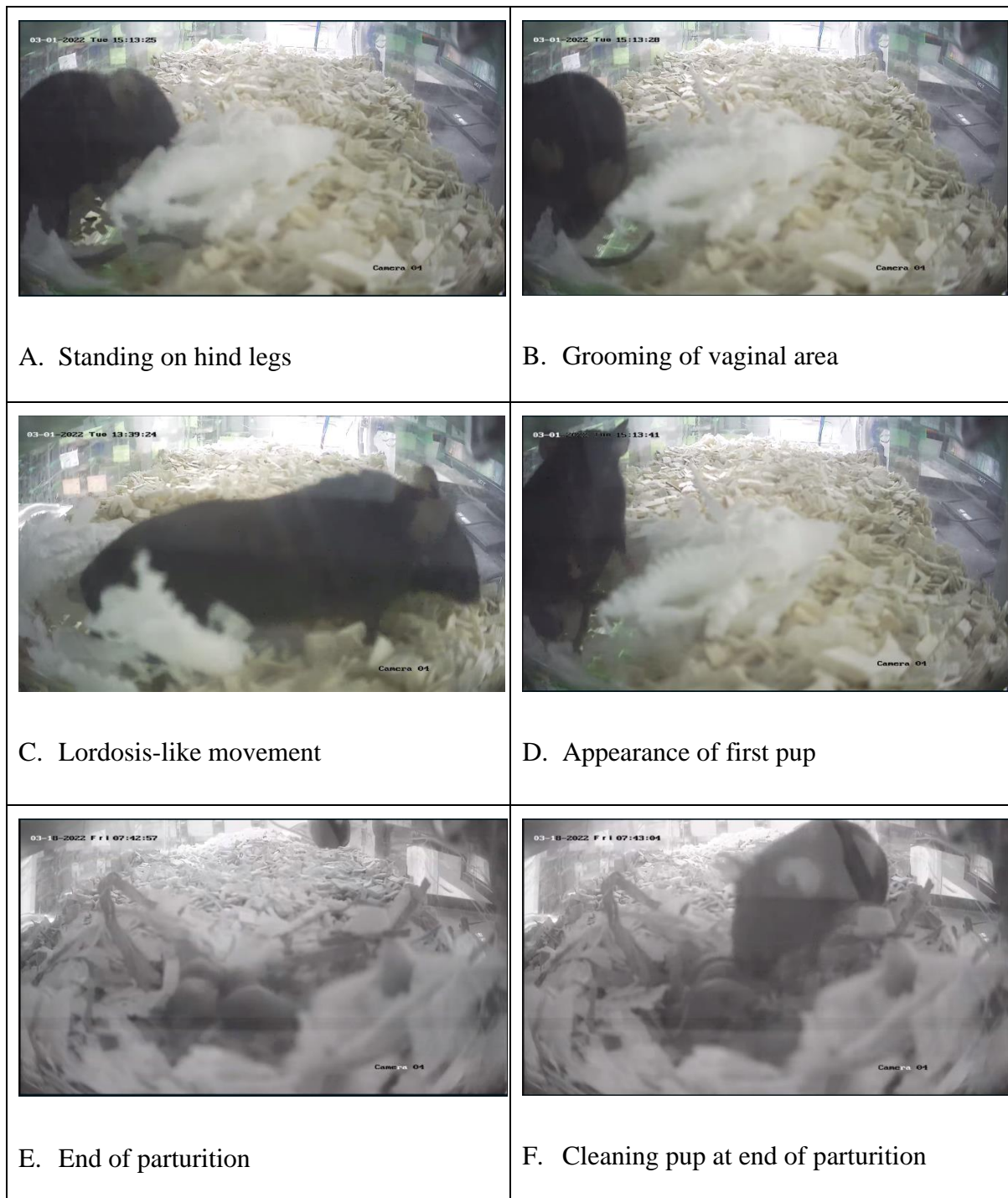
Figure 49. Representative still-frames from video recording data showing common behaviours displayed before and during labour,

A. Standing on hind legs, B. Grooming of vaginal area, C. lordosis-like movement, D. Appearance of first pup, E. End of parturition, F. Cleaning pup at end of parturition. Wild-type (wild-type litter) (n=10), heterozygous *Ryr1*^*Y522S/+*^ (mixed litter) (n=9), and wild-type (mixed litter) (n=10) dams.

The length of gestation was not statistically different between heterozygous (mixed litter) (19.16±0.2025 days), wild-type (mixed litter) (19.15±0.3116 days), and wild-type (wild-type litter) dams (19.00±0.1240 days), P=0.8452, Brown-Forsythe ANOVA test. Data presented as mean days ± SEM.
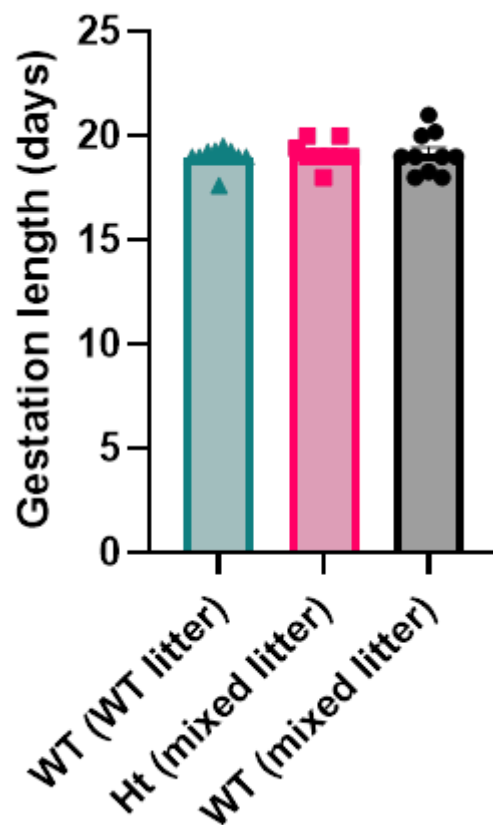
Figure 50. Gestation length in the *Ryr1*$^{Y522S/+}$ mouse model compared to wild-type mice with a wild-type litter or a mixed (wild-type and heterozygous) litter.

Nulliparous wild-type and heterozygous *Ryr1*$^{Y522S/+}$ females aged between 8-16 weeks of age were time-mated with wild-type males or heterozygous *Ryr1*$^{Y522S/+}$ males, sighting of a copulatory plug was determined as 0.5 dpc. On gestation day 17, pregnant females were singly housed with minimal bedding with two video recording cameras to view end of gestation. The length of gestation started at 0.5 days post-coitum to the sighting of the first pup. The length of gestation was not statistically different between heterozygous (mixed litter) (n=9), wild-type (mixed litter) (n=10), and wild-type (wild-type litter) dams (n=10), P=0.8452, Brown-Forsythe ANOVA test. Data presented as mean ± SEM.

5.3.2 Altered spontaneous myometrial contractility in the *Ryr1*^{Y522S/+} mouse

Changes in intracellular Ca^{2+} concentration is crucial to the normal function of contractile cells. Therefore, I used mouse myometrial tissue in *ex vivo* experiments to understand the impact of the gain-of-function Y522S RYR1 calcium channel, in both non-pregnant and pregnant animals. It was unfortunate that the experiments presented below were heavily impacted by the COVID-19 pandemic, therefore data are from a limited number of samples and is considered as preliminary data only to inform future experiments.

Spontaneous myometrial contractions were studied in i) non-pregnant wild-type (10 tissue strips from 5 animals), and heterozygous *Ryr1*^{Y522S/+} (7 tissue strips from 4 animals) animals; and ii) pregnant wild-type (wild-type litter) (6 tissue strips from 1 animal), heterozygous *Ryr1*^{Y522S/+} (mixed litter) (6 tissue strips from 1 animal), and wild-type (mixed litter) animals (6 tissue strips from 1 animal).

5.3.2.1 *Non-pregnant myometrium*

The frequency of myometrial contractions was greater in non-pregnant heterozygous *Ryr1*^{Y522S/+} myometrial tissue (0.05123 ± 0.00389 Hz) compared to wild-type tissue (0.03046 ± 0.00488 Hz), P=0.0046. The duration of myometrial contractions was conversely decreased in non-pregnant heterozygous tissue (22.91 ± 1.416 s) compared to wild-type tissue (45.71 ± 5.106 s), P=0.0014 (Welch's t-test), demonstrated in Figure 51. The mean integral tension (MIT) and amplitude of spontaneous myometrial contractions was not statistically different between non-pregnant wild-type and heterozygous animals.
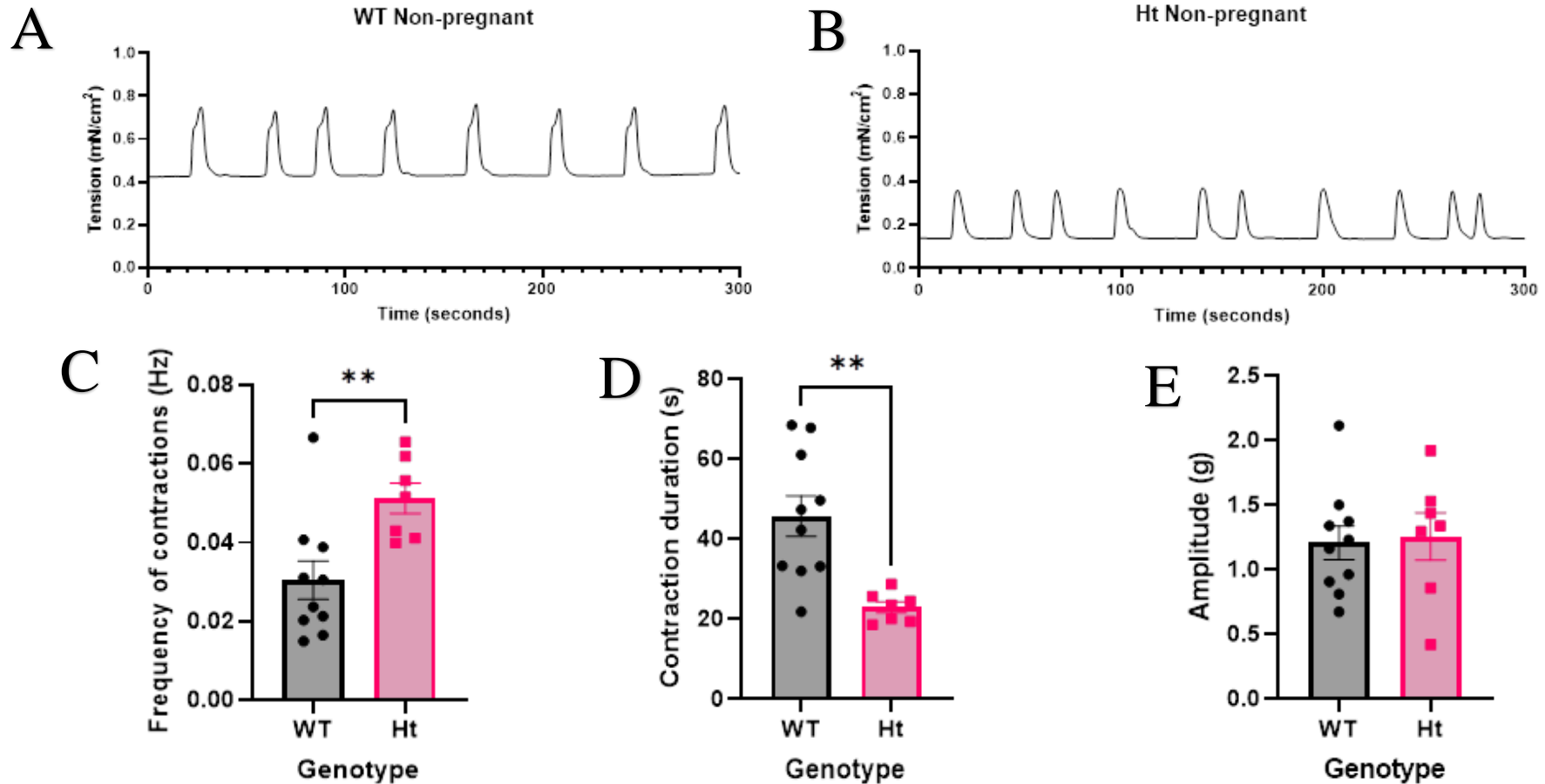
Figure 51. Alterations in spontaneous myometrial contractions in non-pregnant *Ryr1^{Y522S/+}* animals

Representative traces showing spontaneous myometrial contractions from nonpregnant (**A**) wild-type and (**B**) heterozygous *Ryr1^{Y522S/+}*, over five minutes. Note that differences resting tone in A and B are coincidental. (**C**) Spontaneous myometrial contractility frequency (Hz) was significantly increased in heterozygous animals (4 animals, 7 tissue strips) animals compared to wildtype (5 animals, 10 tissue strips), P=0.0046. (**D**) Spontaneous myometrial contractility duration (seconds) was significantly increased in heterozygous animals versus wild-type controls, P=0.0014. (**E**) Contraction amplitude (g) was not statistically different between heterozygous animals versus wild-type controls, P=0.8325. All data expressed as mean ± SEM.

Total RNA was extracted from wild-type (n=4) and heterozygous (n=6) non-pregnant endometrium denuded myometrial tissue from female mice aged 8-16 weeks old. Expression of *Ryr1* (P=0.6004) and *Ryr2* (P=0.9778) mRNA was not significantly different between wild-type (*Ryr1* 3.876±0.1754, *Ryr2* 2.802±0.4361) and heterozygous (*Ryr1* 3.750±0.1460, *Ryr2* 2.786±0.3495) non-pregnant myometrial tissue samples, Welch's t-test. The expression of the *Ryr3* isoform was below the level of detection by this technique.
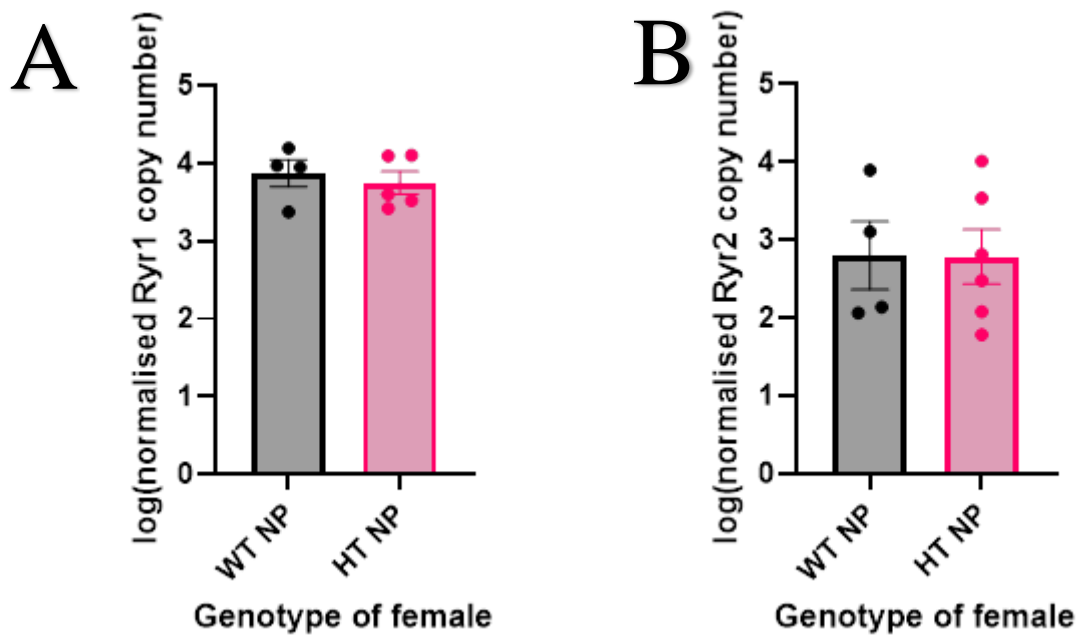
Figure 52. *Ryr1* and *Ryr2* mRNA expression in the *Ryr1*$^{Y522S/+}$ non-pregnant myometrium

Total myometrial mRNA was extracted from myometrial tissue from wild-type (n=4) and heterozygous (n=6) non-pregnant female mice aged 8-16 weeks old. Primers listed in Chapter 3 Materials and methods were used to amplify *Ryr1, Ryr2* and *Ryr3* fragments. The expression of (**A**) *Ryr1* and (**B**) *Ryr2* mRNA was not statistically different between wild-type and heterozygous non-pregnant myometrium, (Welch's t-test). Ryr3 isoforms were not detected by PCR amplification.

Given the low sample number, I was unable to statistically analyse the contraction duration, frequency, and amplitude spontaneous contractions in the pregnant myometrium. Representative traces are shown for n=6 tissue strips from 1 animal.

Contractions in the myometrium from wild-type (wild-type litter) pregnant animals appear to be less frequent and last longer compared to contraction in myometrium from pregnant heterozygous (mixed litter) and wild-type (mixed litter) animals, although this is not yet statistically supported. The myometrial contractions from wild-type (mixed litter) animals appeared to of lower amplitude compared to myometrial contractions from wild-type (wild-type litter) and heterozygous (mixed litter) animals.
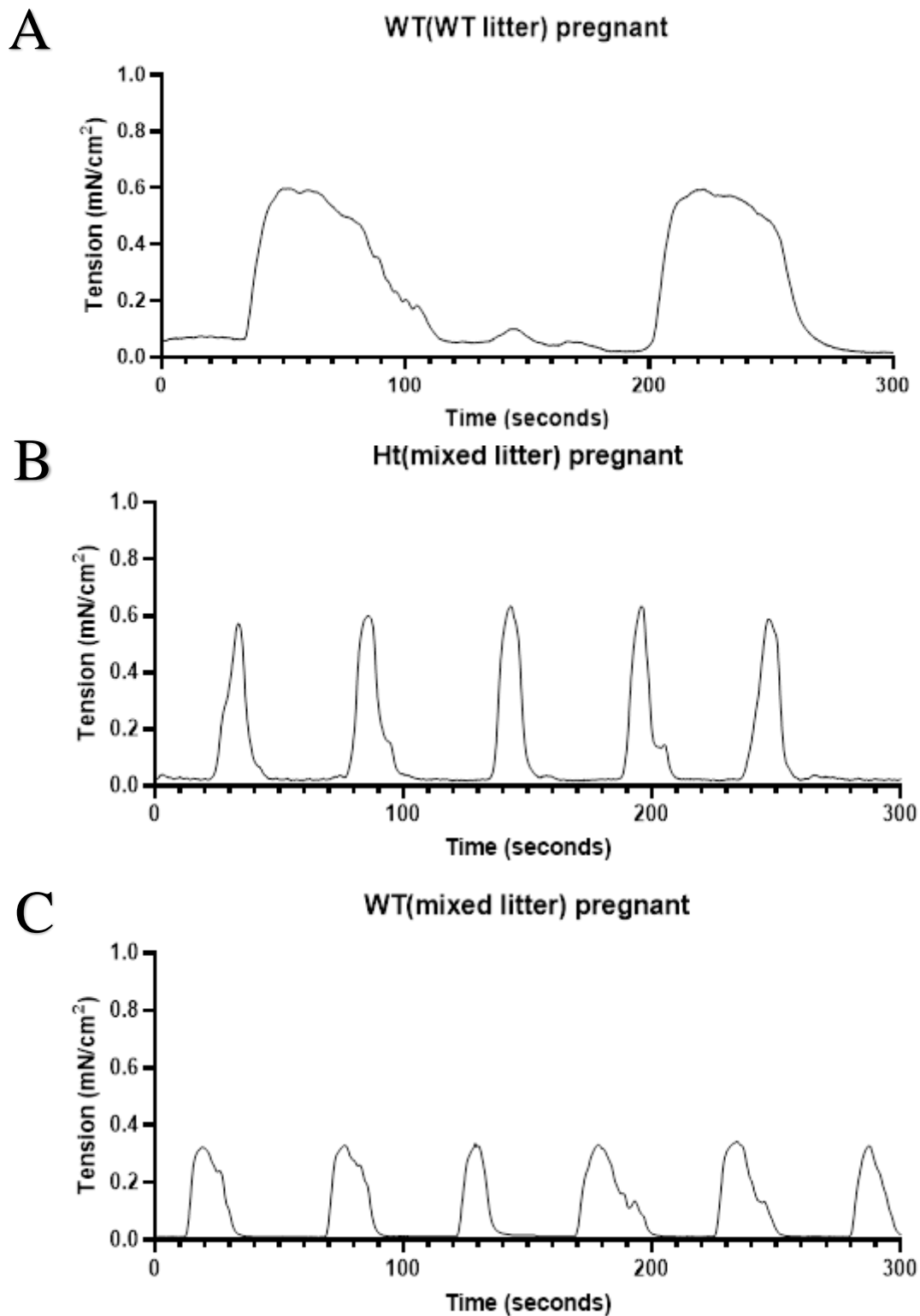
Figure 53. Representative traces of gestation day 18.5 pregnant myometrial spontaneous contractions over five minutes

(**A**) Representative trace of spontaneous contractions in pregnant wild-type mouse myometrial tissue with wild-type fetuses. (**B**) Representative trace of spontaneous contractions in pregnant heterozygous mouse myometrial tissue with mixed genotype fetuses. (**C**) Representative trace of spontaneous contractions in pregnant wild-type mouse myometrial tissue with mixed genotype fetuses.

5.3.2.4 *Ryr isoform expression in the Ryr1$^{Y522S/+}$ in pregnant myometrium*

Expression of *Ryr1* mRNA was elevated in pregnant myometrial tissue from wild-type (mixed litter) dams (tissue from n=6 animals) and heterozygous (mixed litter) dams (n=6 animals) compared to myometrial tissue from wild-type (wild-type litter) dams (n=11 animals), P=0.0216 (Brown-Forsythe one-way ANOVA), P=0.0179, 0.0404 (Dunnett's multiple comparisons test).

Initially, two isoforms of *Ryr3* were detected in pregnant wild-type mouse myometrium using the primers; 5'-AGGTGATCAACAAGTATGGA-3' and 5'-CAACAGATGAGCAGCAAAGA-3'. Sequencing of both bands determined that both amplicons originated from mouse *Ryr3* mRNA. Using the primers described in section 3.6.3, the larger (374 bp) and smaller (90 bp) amplicons (Figure 54), were Sanger sequenced to determine that the larger fragment was indeed an mRNA isoform of *Ryr3* with the inclusion of intron 96-97 (337 base pairs), aligned to ENS00000208290.2, demonstrated in Figure 55.

Acknowledging the presence of two *Ryr3* mRNA isoforms in the pregnant myometrium, these were treated as two separate 'genes of interest' in following RT-qPCR tests and their expression was studied individually (as *Ryr3*-long and *Ryr3*-short). The expression of *Ryr2*, *Ryr3*-short variant and *Ryr3*-long variant in the pregnant myometrium were not statistically different between all genotype groups.
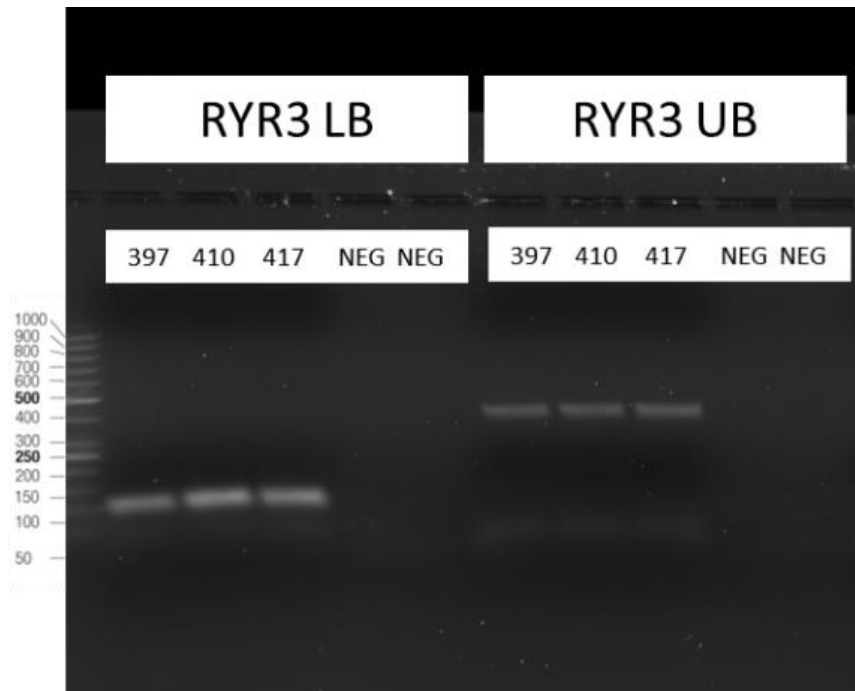
Figure 54. Agarose gel of two *Ryr3* isoforms represented as two amplicon bands at 90bp (Lower Band, LB) and 374 bp (Upper Band, UB) in pregnant wild-type myometrial cDNA

Two isoforms were detected in *Ryr3* cDNA in wild-type pregnant mouse myometrium, represented by two bands at 90bp (Lower Band, LB) and 374 bp (Upper Band, UB) on an agarose gel using SYBR-safe stain. '397', '410' and '417' are sample ID's for wild-type pregnant mice with a wild-type litter (gestation day 18.5); 'NEG' are negative control samples without a cDNA template. GeneRuler 50bp DNA Ladder used (left).
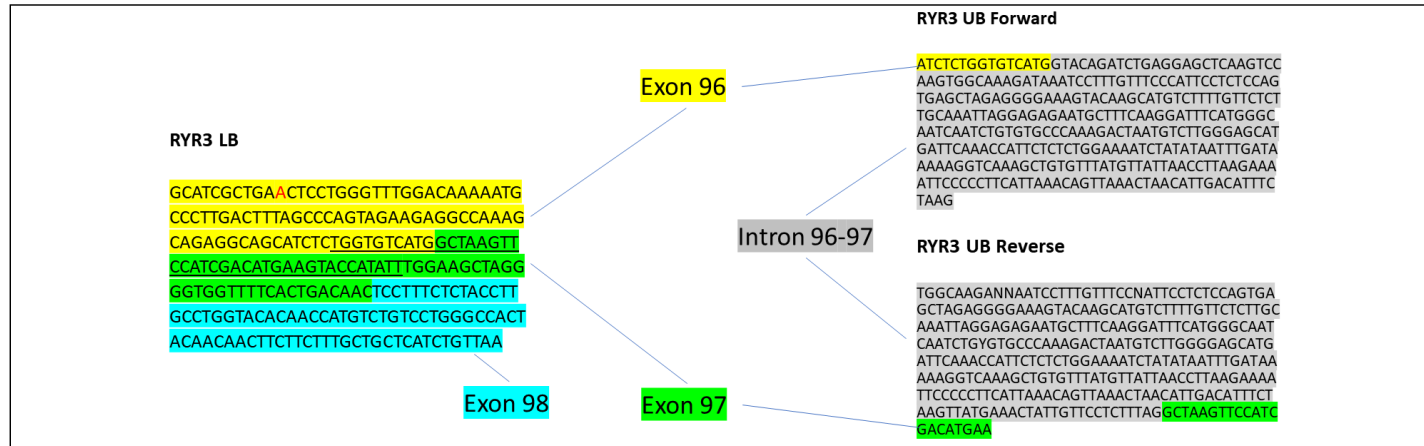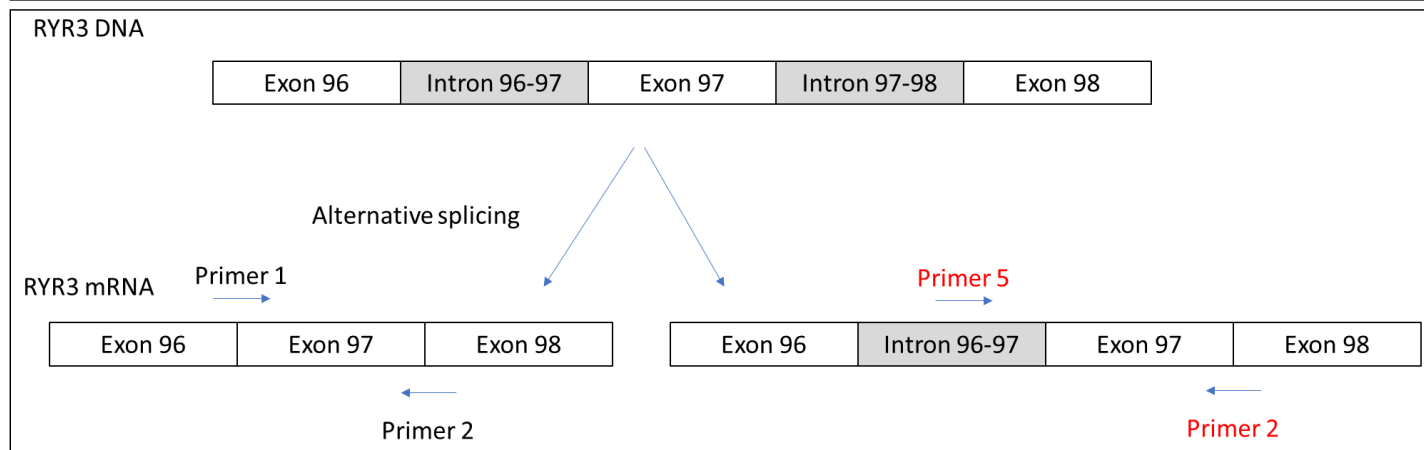
Figure 55. (A) Sanger sequencing of short *Ryr3* isoform and long *Ryr3* isoform. (B) A visual schematic depicting an alternative splicing event in Mus musculus *Ryr3* from wild-type myometrium during pregnancy

(**A**) mRNA sequences of short *Ryr3* isoform and long *Ryr3* isoform. Sanger sequencing of surrounding exons 96 and 97 and the included intron 96-97. (**B**) A schematic figure to visualise the inclusion of Intron 96-97 (337 base pairs) in Mus musculus *Ryr3* from wild-type myometrium during pregnancy (gestation day 18.5). The diagram shows that Intron 96-97 is transcribed from *Ryr3* DNA in an alternative *Ryr3* isoform. Primer 1 and primer 2, placed on exon-exon junctions were used to amplify the short *Ryr3* mRNA isoform (90bp). Primer 5, placed within the intron 96-97 was used with primer 2 to amplify the longer *Ryr3* mRNA isoform (374bp). Exons are aligned to ENS00000208290.2 (Ensembl [date accessed 18th January 2022]).

241
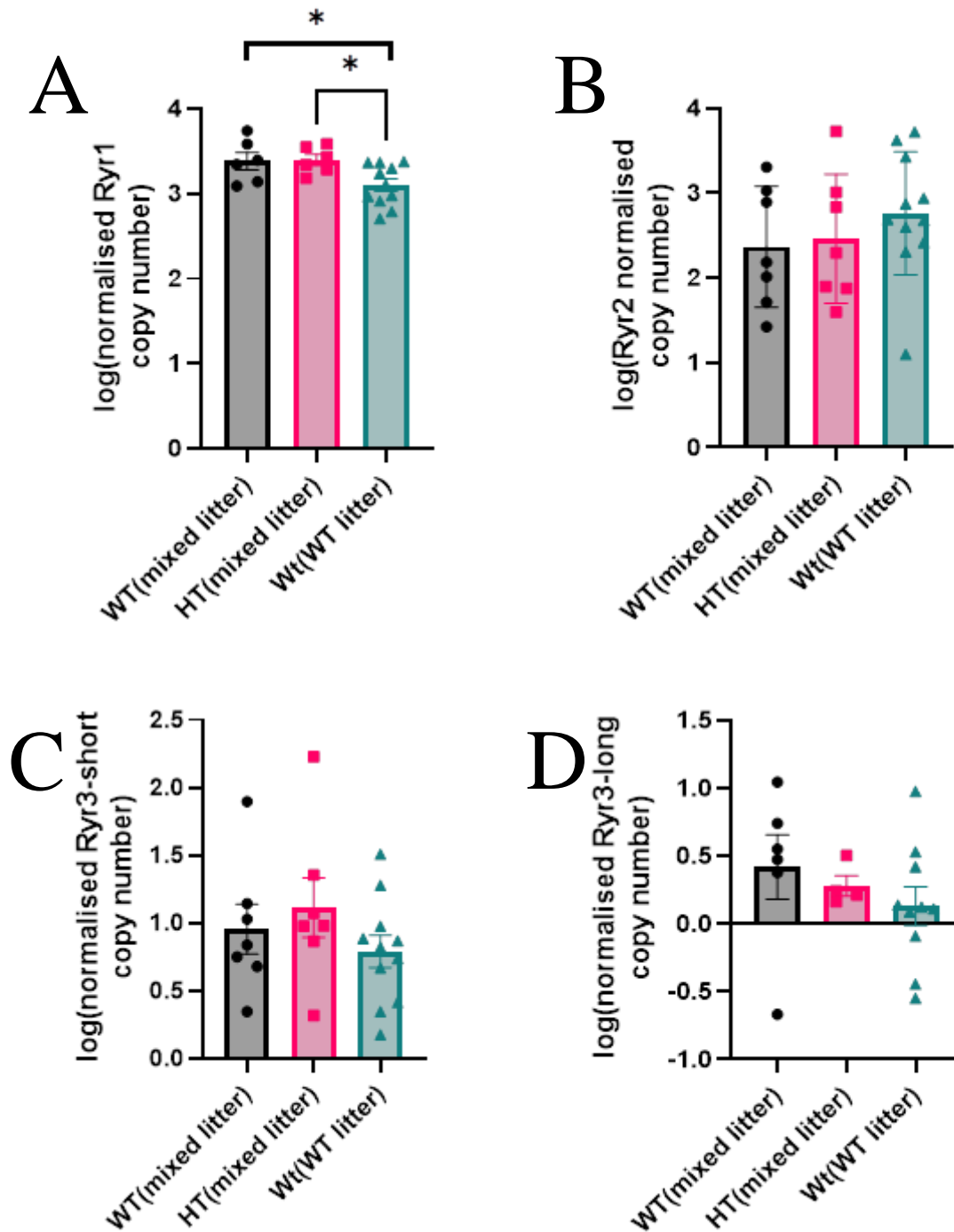
Figure 56. *Ryr* **isoform expression in the** *Ryr1*$^{Y522S/+}$ **in pregnant mouse myometrium**

Total RNA was extracted from myometrial tissue from gestation day 18.5 pregnant wild-type (wild-type litter) (n=11 animals), heterozygous (mixed litter) (n=6 animals) and wild-type (mixed litter) (n=6 animals). Primers listed in Chapter 3 were used to amplify *Ryr1*, *Ryr2* and *Ryr3* (short and long) fragments. The mRNA expression of *Ryr1* was increased in the pregnant myometrium from heterozygous (mixed litter) and wild-type (mixed litter) compared to myometrium from wild-type (wild-type litter), P=0.0216 (Brown-Forsythe one-way ANOVA). Expression of *Ryr2, Ryr3*-short and *Ryr3*-long mRNA was not statistically different in pregnant myometrial tissue between wild-type (wild-type litter), heterozygous (mixed litter) and wild-type (mixed litter) animals.

5.3.2.5   Detection of RYR1 protein in pregnant $Ryr1^{Y522S/+}$ myometrial tissue

Western blotting methods were optimised to blot high molecular weight proteins such as the RYR1 protein (~560 kDa). After a series of optimisation steps (see section 3.7.1), the skeletal RYR1 protein was successfully blotted onto a membrane. However the myometrial RYR1 protein was still undetectable in both pregnant wild-type (n=3), and $Ryr1^{Y522S/+}$ (n=3) myometrial tissue, likely due to overall low RYR1 protein concentration in the mouse myometrial tissue, previously demonstrated in Figure 19.

5.3.3   Histological investigations of the *Ryr1*$^{Y522S/+}$ myometrium

As an alternative to Western blot, the presence of RYR1 channels in the smooth muscle cells of the uterine myometrium was validated using immunohistochemistry techniques instead. Gestation day 18.5 wild-type mouse uterus (n=3) displayed positive RYR1 staining when incubated with anti-RYR1 (Figure 57A). The RYR1-positive staining was localised to the myometrium and endometrium of the uterus, as demonstrated by positive control alpha smooth muscle actin staining in (Figure 57B). Magnified smooth muscle cells stained with anti-RYR1 can be seen in Figure 57C. A negative control without primary RYR1 antibody staining was used to demonstrate the antibody-specific fluorescence in uterine tissue (Figure 57D).
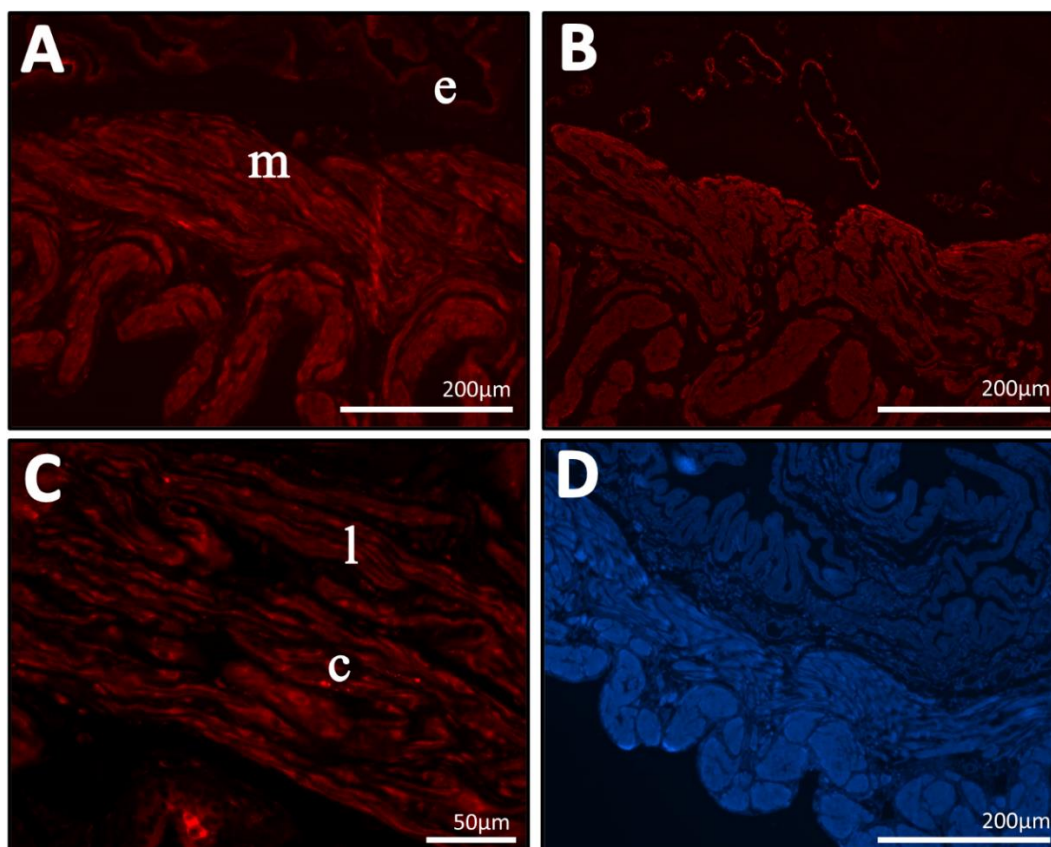
Figure 57. Anti-RYR1 stained gestation day 18.5 pregnant wild-type uterus cross-sections.

Gestation day 18.5 pregnant wild-type uterus cross-sections (N=3) stained with primary: (A) anti-RYR1 (1:50), 10X magnification, (B) anti α-smooth muscle actin (1:150) positive gestation day 18.5 mouse uterus, 10X magnification, (C) anti-RYR1 (1:200) positive gestation day 18.5 mouse uterus, 20X magnification (D) Negative control (no primary antibody) with DAPI nuclei stain, 10X magnification. e = endometrium, m = myometrium, l = longitudinal myometrium, c = circular myometrium.

5.3.4 The molecular profile of the pregnant $Ryr1^{Y522S/+}$ mouse myometrium

5.3.4.1 Exploration of the RNA library

Alterations in intracellular Ca^{2+} signals, such that might be anticipated with an *RYR1* mutation, have potential to influence gene and protein expression and functional end points such as contractility. To this end, tissue RNAseq was used to explore whether myometrium from pregnant wildtype versus $Ryr1^{Y522S/+}$ heterozygous dams demonstrated differential gene expression profiles. Total myometrial RNA from n=7 wild-type (wildtype litter) and n=6 $Ryr1^{Y522S/+}$ heterozygous (mixed litter) gestation day 18.5 pregnant females successfully passed quality checks prior to RNA-sequencing.

Total number of reads for each sample ranged between 21,434,123 and 66,573,460 reads, base yield ranged between 6,430- 19,972 Mbases, and % Bases >= 30 (the sum of the populations in bins with a quality value of 30 or greater divided by the total non-N base calls) were above 94% for all samples. The number of reads per sample were lower for two samples (samples 8 and 9) and higher for sample 13. To better understand the quality of the RNA-seq output, the total number of reads per sample and percentage of null counts per sample were examined and visualised in Figure 59. Distribution of the counts in all samples were visualised using a boxplot shown in Figure 60. The genes with counts of less than five across samples were removed. This cut-off was considered stringent based on the size of the smallest variable of interest – 1 (6-1=5).
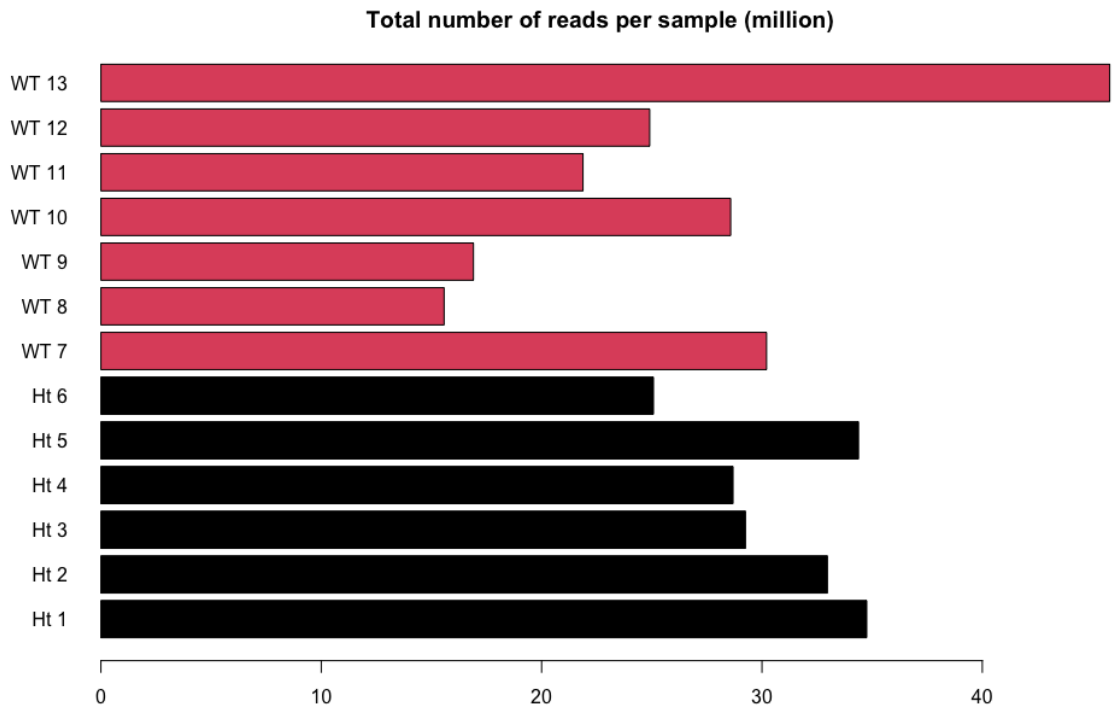
Figure 58. Barplot of library sizes as total number of reads (per million counts) in each pregnant mouse myometrial RNA sample. WT, wildtype (red); Ht, heterozygous (black).
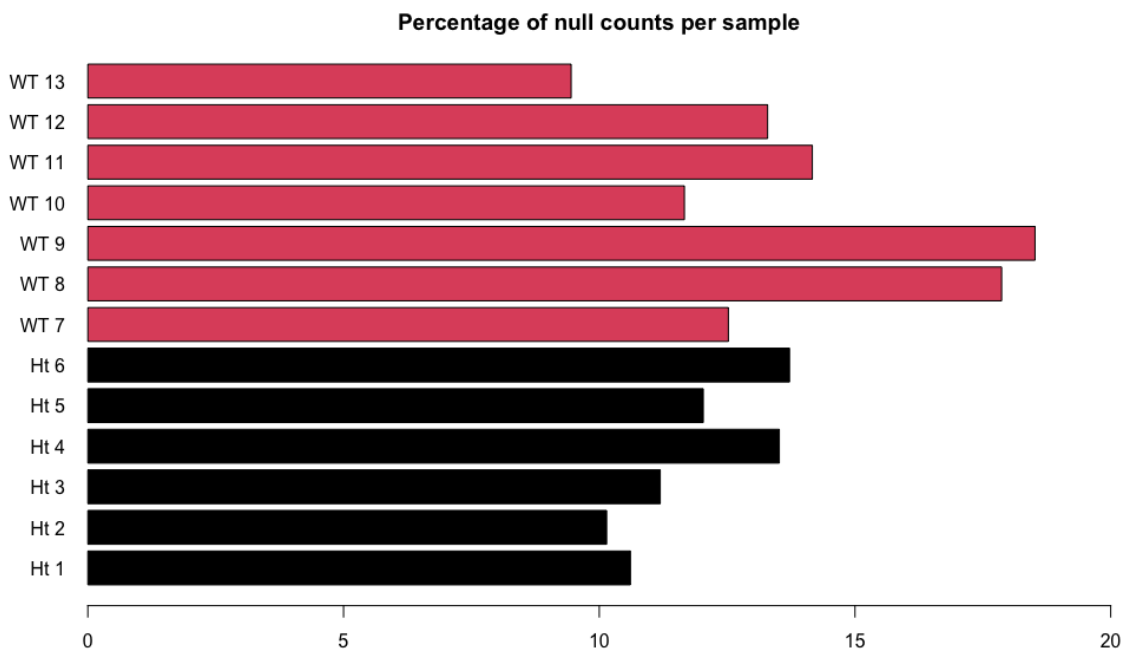
Figure 59. Barplot of percentage of null counts #per million counts) in each pregnant mouse myometrial sample. WT, wildtype (red); Ht, heterozygous (black).

246
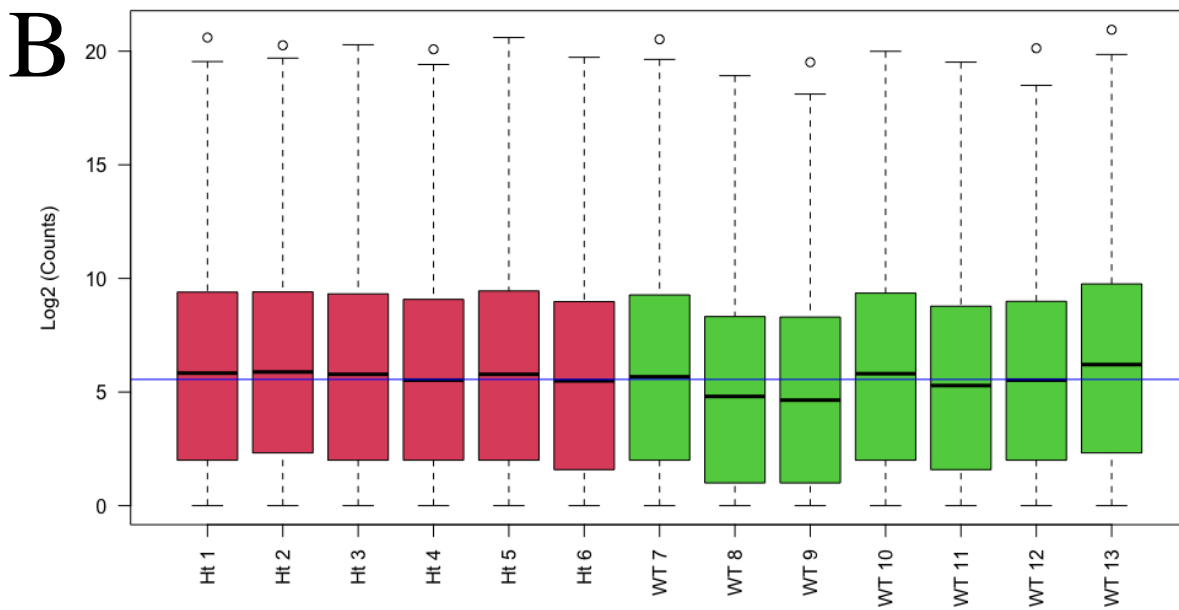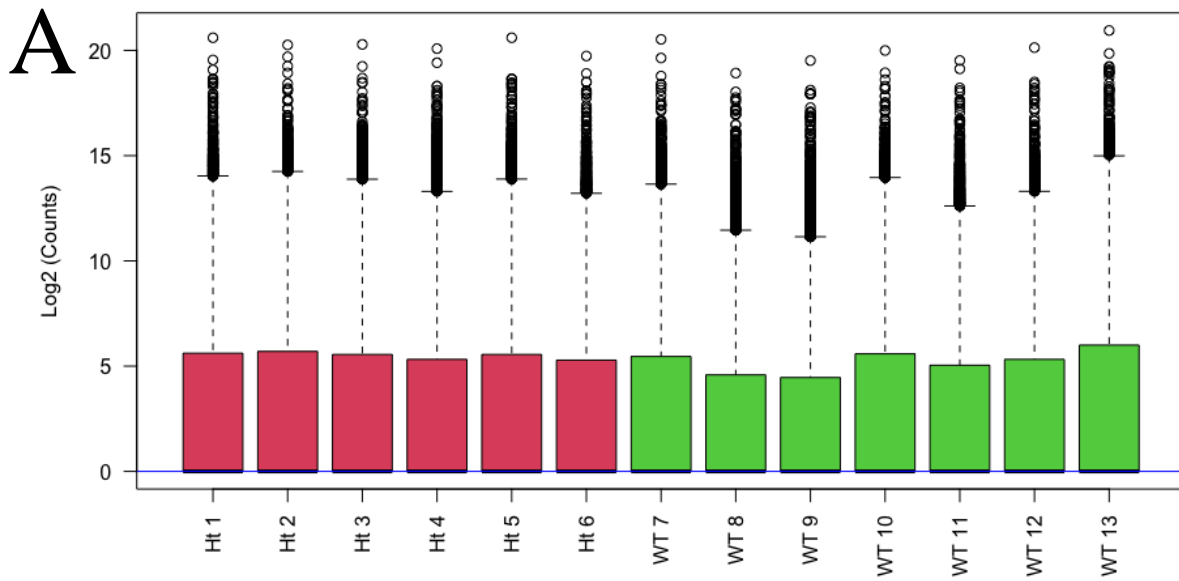
Figure 60. Distribution of counts generated with STAR and FeatureCounts for genes in wild-type (green) and heterozygous (red) pregnant mouse myometrial RNA samples (A) prior to and (B) after normalisation.

Bar plots showing count distribution generated with STAR (alignment tool) and FeatureCounts (count extraction) for genes in wild-type (green) and heterozygous (red) pregnant mouse myometrial RNA samples (**A**) prior to and (**B**) after normalisation using cut off value of 5. Samples 1-6 were heterozygous (Ht, red) and samples 7-13 were wildtype (WT, green).

To investigate the similarity between the samples, a heatmap and a PCA plot was first plotted using the distance matrix. Investigations of gene expression profiles revealed that the wild-type and heterozygous gestation day 18.5 pregnant myometrial samples did not differentially cluster, likely due to a small sample size, as shown in the heatmap and PCA plot in Figure 61.
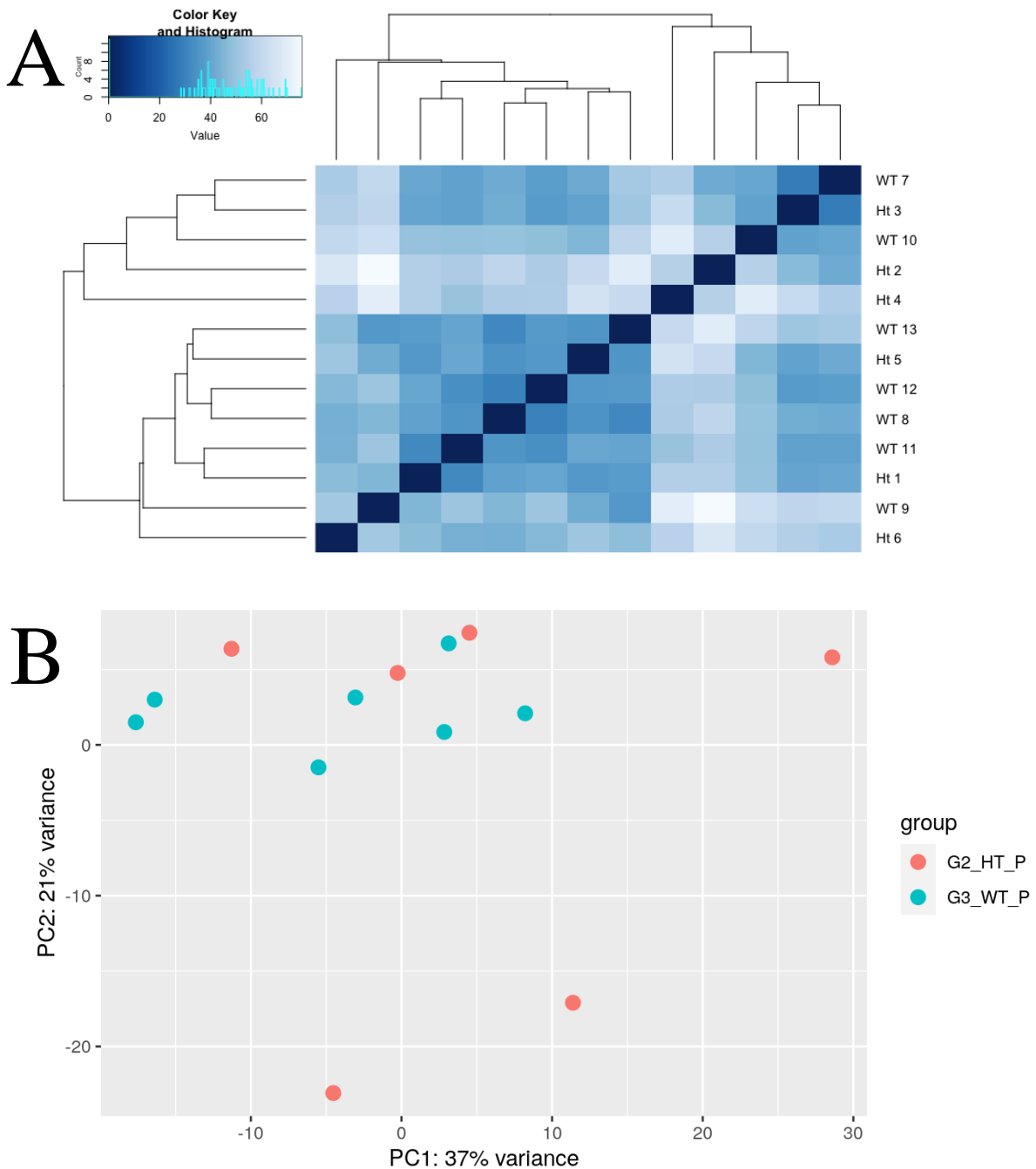
Figure 61. Similarity between individual pregnant myometrial gene expression profiles from wildtype (samples 7 to 13, green) and heterozygous gestation day 18.5 pregnant dams (samples 1 to 6, orange).

(**A**) A heatmap using the distance matrix to demonstrate the similarity between the samples (**B**) A PCA plot showing the similarity of wild-type (WT, green) and heterozygous (Ht, orange) samples.

5.3.4.2 *Differential gene expression*

Differential expression analysis was used to compare gene expression values across all wild-type and heterozygous samples. As shown in Figure 62, only two genes reached the p-adjusted >0.05 significance threshold, with decreased mRNA expression of *Ighv2-9*, ENSMUSG00000096638 (log2 FC=-4.58887, padj=0.000273) and increased *Fcgbp*, ENSMUSG00000047730 (log2 FC=1.921279, p. adj=0.001201) in heterozygous pregnant myometrial tissues compared to wild-type tissue. Using a p-value adjusted to 0.3; *Ighv2-9*, *Ptprm*, *Igkv17-121* had negative fold change indicating that the gene could be reduced in heterozygous samples compared to wild-type, and *Fcgbp*, *Psg16*, *Nmb* had positive fold changes, allowing us to propose that the expression of these genes could be increased in heterozygous samples compared to wild-type.
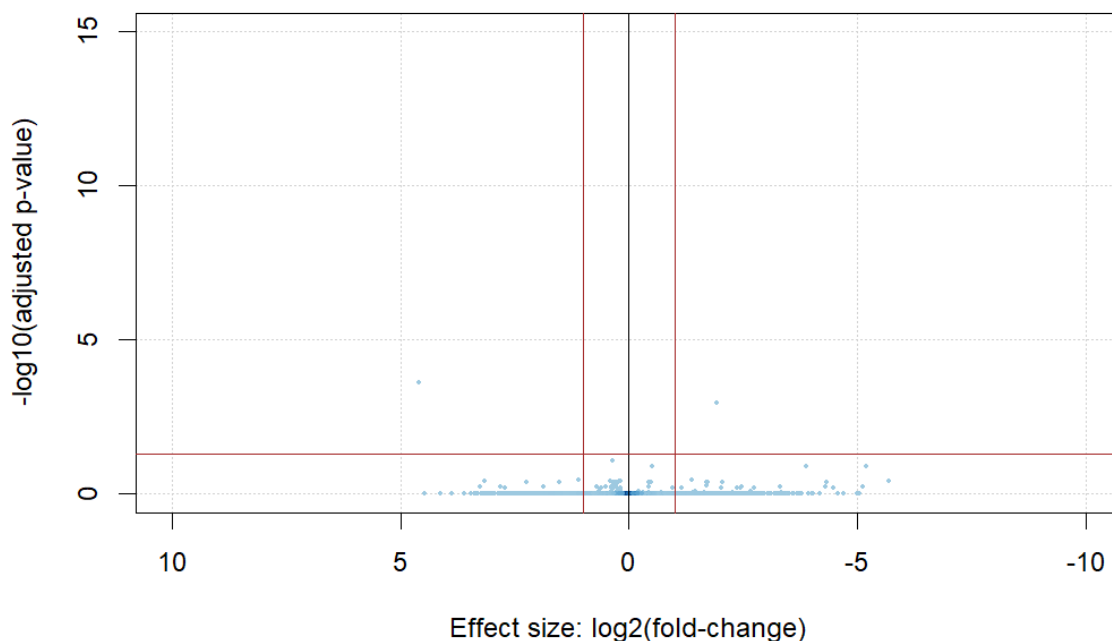
Figure 62. Volcano plot comparing differentially expressed genes between gestation day 18.5 wild-type and *Ryr1*$^{Y522S/+}$ pregnant myometrial total RNA

Total RNA from wild-type (n=7) and *Ryr1*$^{Y522S/+}$ (n=6) gestation day 18.5 pregnant myometrial tissue were used to create libraries for high-throughput RNA sequencing. Effect size (log2(fold-change)) was plotted against -log10(adjusted p-value), demonstrating two genes with padj<0.05; *Ighv2-9* (ENSMUSG00000096638) and *Fcgbp* (ENSMUSG00000047730) are respectively significantly decreased [right] and increased [left] in the comparison of heterozygous vs wildtype myometrial gene expression.

STRING mapped gene	Annotation	baseMean	log2 Fold Change	lfcSE	Stat	Pvalue	padj
ENSMUSG00000096638	*Ighv2-9*	16.06135	-4.58887	0.801039	-5.72864	1.01E-08	0.000273
ENSMUSG00000047730	*Fcgbp*	3716.552	1.921279	0.359263	5.347833	8.90E-08	0.001201
ENSMUSG00000033278	*Ptprm*	375.9892	-0.36014	0.080992	-4.44661	8.72E-06	0.078435
ENSMUSG00000076514	*Igkv17-121*	50.45888	-3.16617	0.756403	-4.18582	2.84E-05	0.109488
ENSMUSG00000066760	*Psg16*	108.7426	5.188528	1.23435	4.203449	2.63E-05	0.109488
ENSMUSG00000025723	*Nmb*	232.0276	0.502654	0.119889	4.192665	2.76E-05	0.109488

Table 15. Differentially expressed genes in total RNA from gestation day 18.5 pregnant heterozygous *Ryr1$^{Y522S/+}$* mouse myometrium

STRING mapped differentially expressed genes with p-adjusted values below 0.3 from RNA-sequencing data. Total RNA extracted from gestation day 18.5 *RyR1$^{Y522S/+}$* mouse myometrium, compared to wild-type tissues. BaseMean represents the mean of the normalised counts for all samples, lfcSE: log fold change standard error, Stat: Wald Statistic, Padj: Benjamini – Hockemberg adjusted p-values.* p-adj < 0.05.

RT-qPCR was used to molecularly validate the change in expression of the differentially expressed genes; *Ighv2-9*, *Ptprm*, *Igkv17-121*, *Fcgbp*, *Psg16*, and *Nmb,* in gestation day 18.5 pregnant *Ryr1*$^{Y522S/+}$ myometrial tissue (n=6) compared to wild-type (n=7) myometrial tissue. Mean copy number was normalised to the most stably expressed reference gene in the pregnant mouse myometrium from an array of reference genes (*β2-M, β-actin, Gapdh and Desmin*) and presented as log(mean copy number) ± SEM.

There were no statistically significant changes in the expression of the genes *Ighv2-9*, *Fcgbp*, *Ptprm*, *Igkv17-121*, *Psg16*, and *Nmb* between wild-type and *Ryr1*$^{Y522S/+}$. P values=0.6371, 0.9777, 0.2080, 0.0998, 0.0703, 0.1081, respectively (Student's unpaired t-tests). However, it was apparent that the direction of change in gene expression from wildtype to heterozygous was replicated in RT-qPCR studies to the direction of change identified by RNA-seq methods, although this was not statistically significant.

Table 16. Differentially expressed genes as determined by RNA sequencing and Rt-qPCR validation.

Differentially Expressed Genes	RNAseq log2FoldChange	RNAseq direction of change	RT-qPCR direction of change
Fcgbp	1.921	+	+
Ighv2-9	-4.589	-	-
Igkv17-121	-3.166	-	-
Ptprm	-0.360	-	-
Psg16	5.189	+	+
Nmb	0.503	+	+
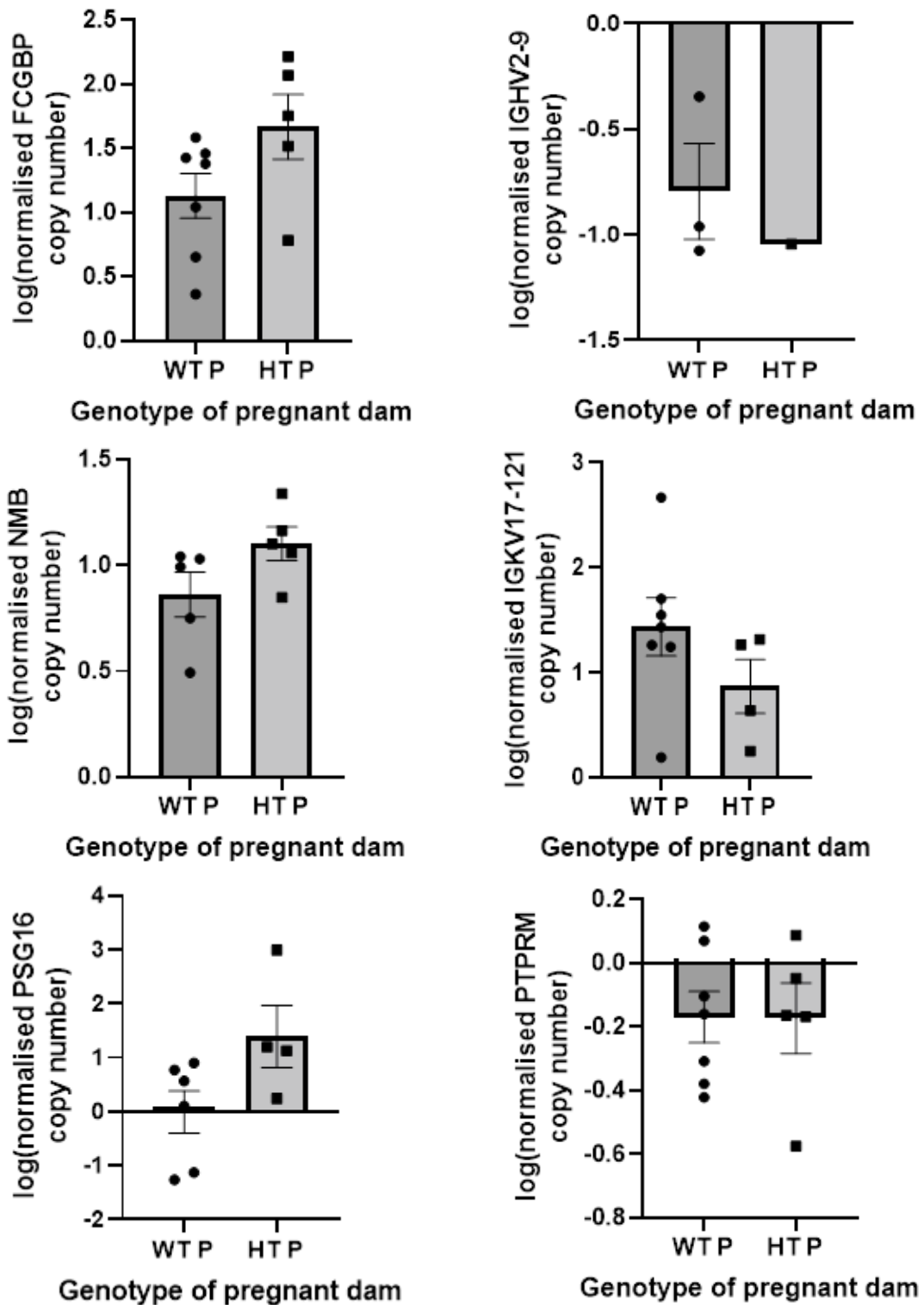
Figure 63. Expression differentially expressed genes *Fcgbp, Ighv2-9, Igkv17-121, Ptprm, Psg16* and *Nmb* in pregnant heterozygous *Ryr1^{Y522S/+}* myometrium compared to wildtype pregnant myometrium

RT-qPCR was used to determine log(mean copy number) ± SEM of genes *Fcgbp, Ighv2-9, Igkv17-121, Ptprm, Psg16* and *Nmb* in total RNA from pregnant *Ryr1^{Y522S/+}* (HT P, n=6) versus wild-type (WT P, n=7) myometrium. Copy number values were normalised to stably expressed reference genes in pregnant myometrium. All statistical comparisons across all groups were non-significant, P>0.05.

5.3.4.4 Gene list interpretation using web-based tools

Following differential expression analyses, a range of bioinformatic tools were used to interpret the differentially expressed gene list between pregnant heterozygous vs wildtype myometrium. The various tools were used to analyse gene tissue expression, protein functions and common pathways of the six differentially expressed gene with padj<0.3. All tools were accessed in January 2023.

PANTHER was used to understand the molecular functions and biological processes of the DEGs with padj<0.3. The report concluded that the most common molecular function associated with these genes were binding (GO:0005488), followed by catalytic activity (GO:00033824) and molecular function regulators (GO:0098772). The most common biological processes that the genes are involved in are cellular process (GO:0009987) and immune system process (GO:0002376).
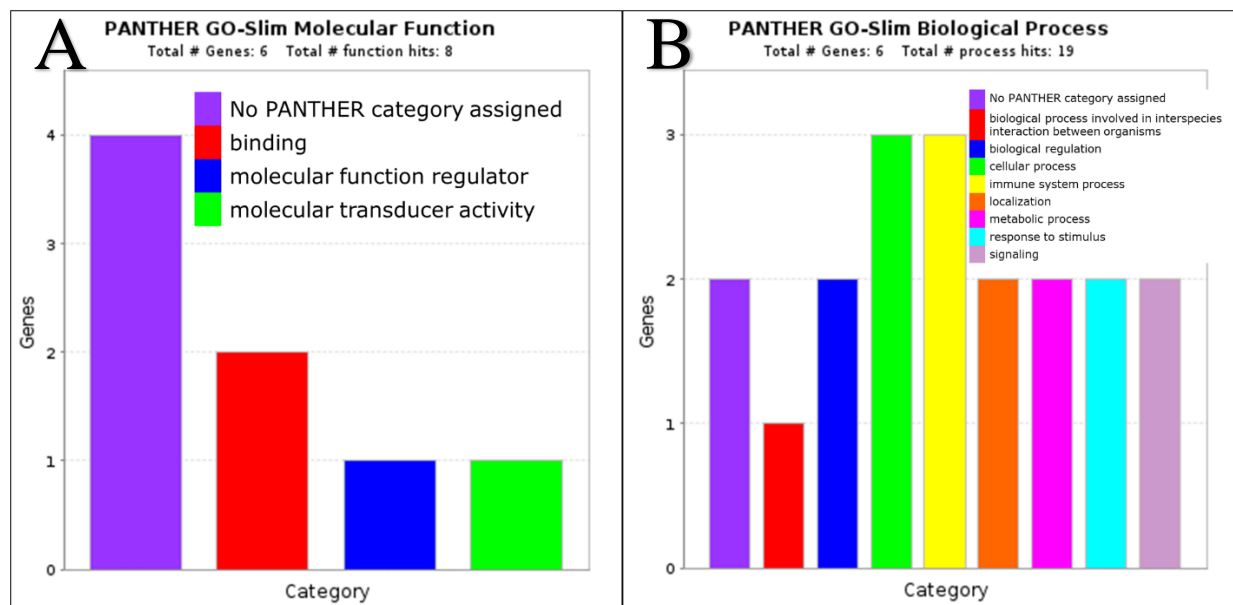
Figure 64. Summary report of molecular functions and biological processes of differentially expressed genes (padj<0.3) using PANTHER.db.

Online web-based bioinformatics tool PANTHER.db was used to investigate the molecular functions (**Chart A**) and biological processes (**Chart B**) of the differentially expressed gene list (padj<0.3).

Reactome was used to determine overrepresentation analysis of the six DEGs, and the tool generated seven key pathways. These pathways were predominantly involved signal transduction, specifically, "peptide ligand-binding receptors, G alpha (q) signalling events, Class A/1 (Rhodopsin-like receptors), GPCR ligand binding, GPCR downstream signalling, and signalling by GPCR".

The six DEGs with the lowest padj (<0.3) were entered into the *IntAct* network. The physical interaction network revealed a network centred around *Ptprm*, connected to genes *Ctnnb1, Cdh1, Itga3* and *Ptprn*.
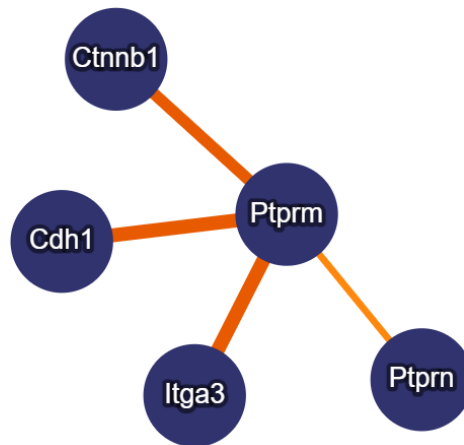
Figure 65. Pathway output from IntAct database using differentially expressed genes' list with padj <0.5.

(Six differentially expressed genes (padj<0.3) were entered in the IntAct database. A network centred around Ptprm was revealed, including genes Ctnnb1, Cdh1, Itga3 and Ptprn.

The mouse ENCODE database was used to understand the tissue expression of the DEG's (padj<0.3), *Fcgbp, Ptrprm, Psg16* and *Nmb*. [Date accessed 14/01/2023].

Fcgbp, Fc fragment of IgG binding protein

Ptprm, protein tyrosine phosphatase, receptor type, M

255
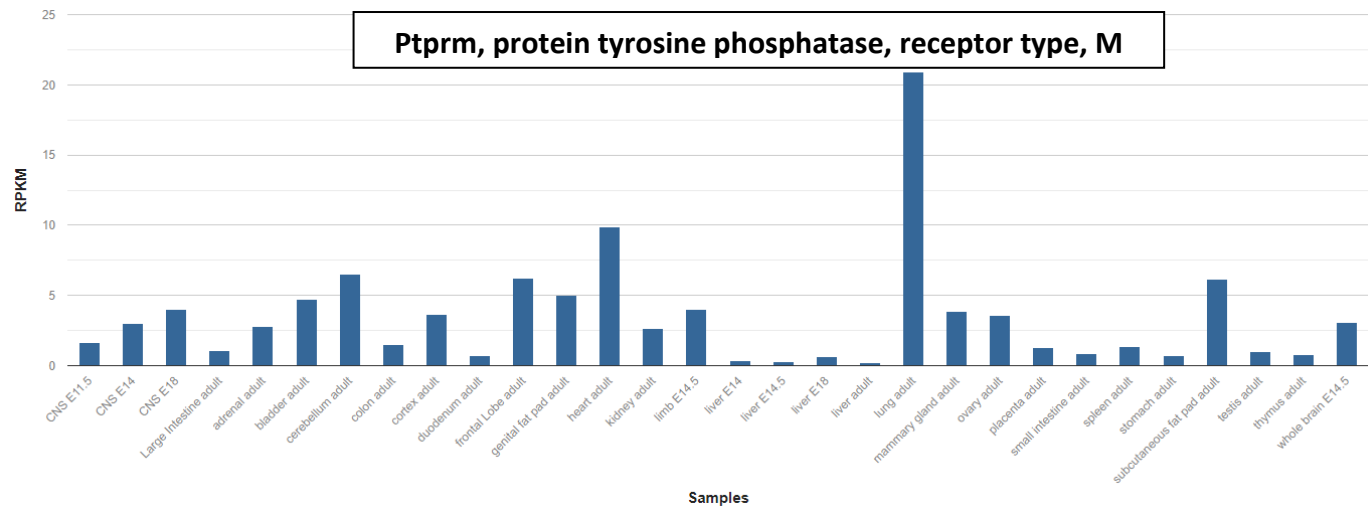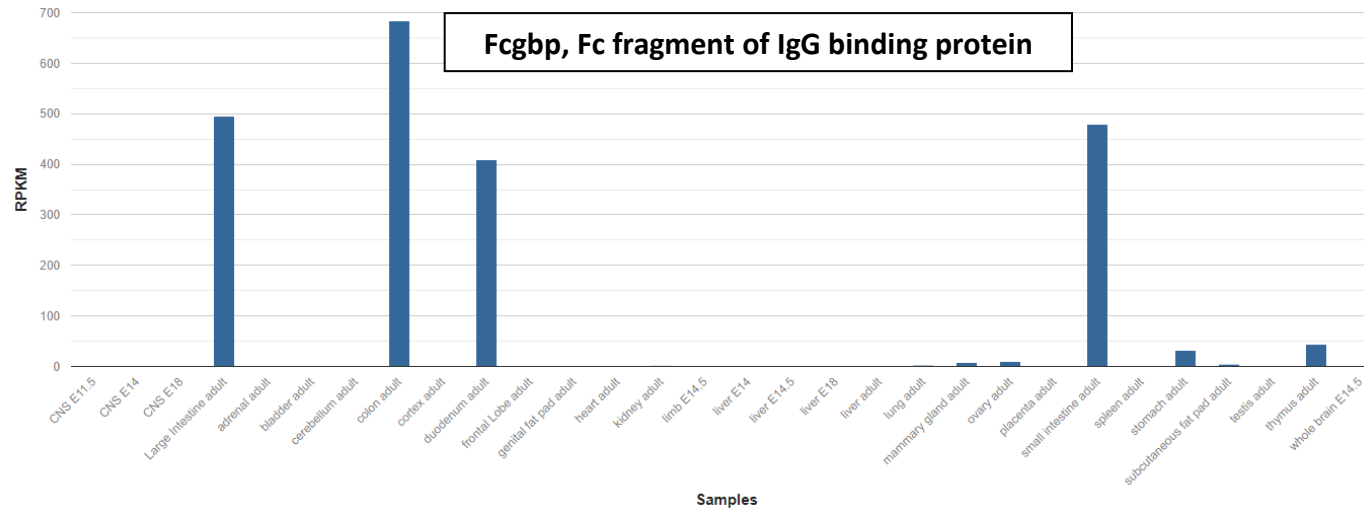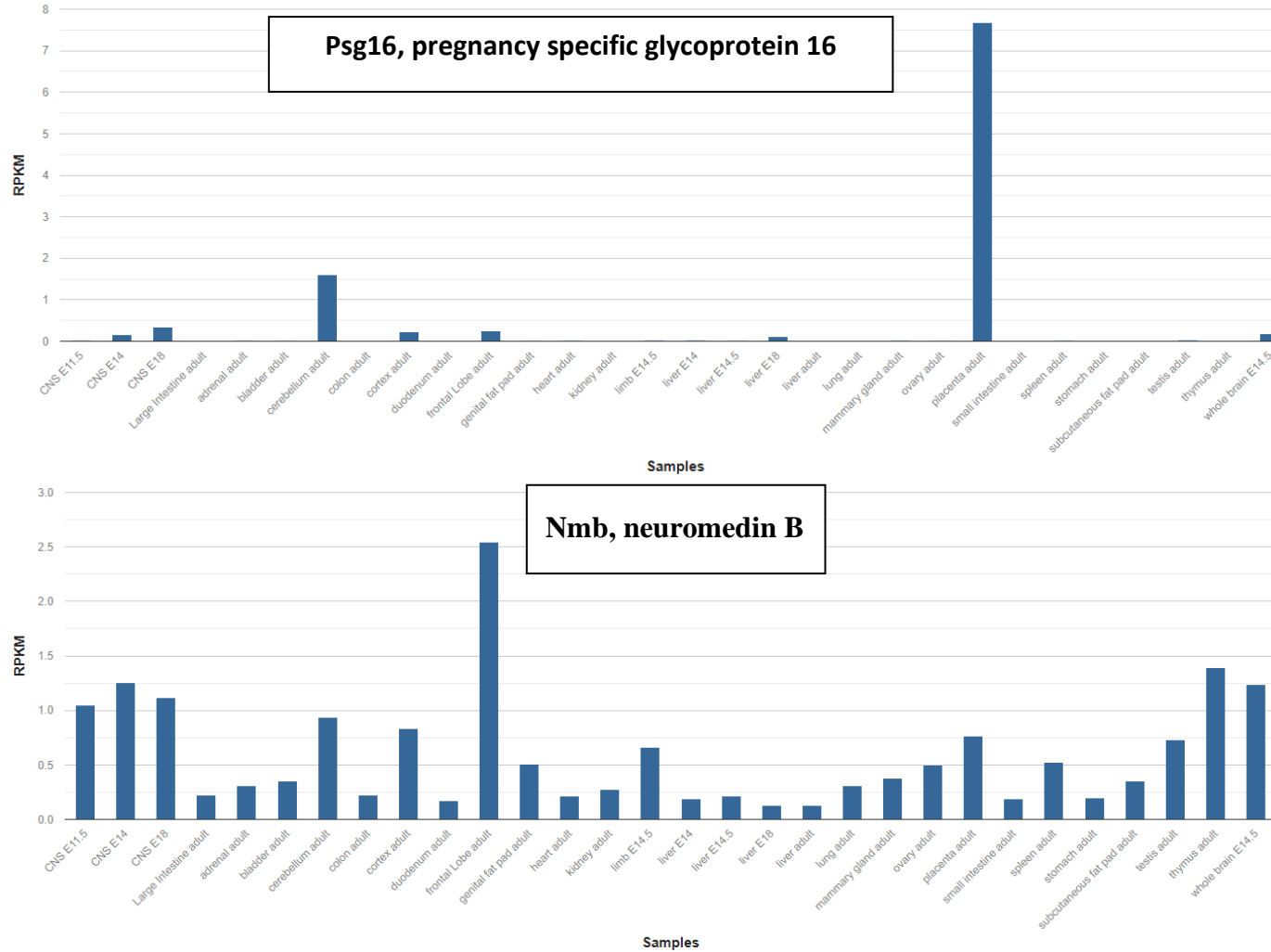
Figure 66. Gene expression profiles of differentially expressed genes from the mouse ENCODE Project.

RNA profiling data sets generated by the Mouse ENCODE project for *Fcgbp, Ptrprm, Psg16* and *Nmb*. [Date accessed 14/01/2023].

5.4 Discussion

This chapter explored the hypothesis that a recognised *Ryr1* mutation, associated with skeletal muscle dysfunction in MH, would also present with a uterine smooth muscle phenotype. Using the established $Ryr1^{Y522S/+}$ pregnant mouse model, I examined how myometrium, the smooth muscle rich tissue of the uterus, might be affected. This work was heavily impacted by the COVID-19 pandemic, so unfortunately more detailed, functional studies could not be undertaken. Studies of gestation length revealed no change in the length of gestation between $Ryr1^{Y522S/+}$ and wild-type animals, indicating that the timing of labour was unchanged in the *Ryr1*-mutated animal. However, initial experiments indicated that spontaneous myometrial contractions (measured *ex vivo*) in the non-pregnant heterozygous mouse were significantly different to that of the wildtype mouse; contractions were more frequent and of shorter duration. Molecular studies were performed to determine whether these differences were due to changes in gene expression as a result of the RYR1 Y522S channel gain-of function and its proposed impact on intracellular Ca^{2+} release. *Ryr1* mRNA was upregulated in gestation day 18.5 pregnant heterozygous $Ryr1^{Y522S/+}$ myometrium compared to wildtype myometrium, and RYR1 protein expression was confirmed in uterine myometrium and endometrium using fluorescent immunohistochemistry. High-throughput NGS RNA-sequencing was performed which identified a limited number of interesting candidate genes that were differentially expressed in pregnant Y522S myometrium. Further work would be needed to determine how these changes might induce any observed functional effects. The remainder of this discussion is structured around each of these findings, following by a brief consideration of study limitations and proposed future work.

Gestation length in $Ryr1^{Y522S/+}$ mice

The length of gestation in the time-mated heterozygous *Ryr1* Y522S mouse (19.15 days or 460 hours) was similar to that of the wild-type mouse and the reported average gestation length (463 hours) of the C57Bl/6J mouse (Murray, 2010), indicating that timing of the initiation of labour was unchanged in heterozygous *Ryr1* Y522S animals. Although some studies of pregnant myometrial tissue have suggested that uterine Ca^{2+} sparks from RyR channels do not occur, as described in (Burdyga, 2007), there is some evidence for the role RyR channel Ca^{2+} sparks in the regulation of myometrial cell contractility. Specifically, the process of ryanodine activated Ca^{2+} release has been confirmed in cultured human non-pregnant and (labouring and pre-labour) term-pregnant myometrial cells (Morgan, 1995; Martin, 1999), and cultured pregnant rat myometrial cells demonstrate sensitivity to ryanodine and caffeine resulting in intracellular Ca^{2+} fluctuation (Martin, 1999). Previous studies have indeed shown that caffeine, an activator of RyR does not contract, but relaxes the pregnant rat myometrium (Savineau and Mironneau, 1990). However findings in this study suggests that that initiation of labour is more heavily dependent on factors independent of a rise in intracellular Ca^{2+}, such as progesterone withdrawal and changes in BK_{Ca} channel expression (Skarnes, 1972; Dudley, 1996; Benkusky, 2000).

However, it must be noted that the window for mating was relatively long (18 hours) and this reduced the sensitivity of gestation length measurements. Ideally, shorter windows for mating would be useful – either 3 or 6 hours. This is challenging as it takes longer to obtain pregnant mice, and often requires out of hours working or reversal of the light/dark cycle in the rooms housing the mice. Whilst both options are now possible, during the COVID pandemic working restrictions did not allow for this.

Similarly, although I was unable to examine myometrial contractions from the end of gestation *ex vivo*, the more frequent contractions with shorter duration observed in non-pregnant tissue, if the pattern is retained, would be less likely to be effective during the end of gestation, which is likely to limit the propulsive force of any given contraction of the uterus. It had been anticipated that this could have been assessed by determining labour length through video recording as our group have done previously, but since then the biological services unit has implemented the use of IVC cages that have reduced visibility. It is possible that the use of more sensitive cameras combined with a reduction in bedding material could improve this approach in the future.

Ryr1$^{Y522S/+}$ non-pregnant spontaneous myometrial contractions

There are differences in mouse myometrial contractility during oestrus compared to proestrus and metestrus, with the propagation speed of mouse uterine contractions being slower and stronger in oestrus (Dodds, 2015). In the present experiment the non-pregnant uterus was collected from mice in oestrus only, to control for changes in uterine contractility through the oestrus cycle. In *ex vivo* experiments, non-pregnant heterozygous *Ryr1$^{Y522S/+}$* myometrial contractions were more frequent and shorter (in duration) compared to wild-type myometrial contractions. The faster termination of contraction is suggestive that there is upregulation of the mechanisms that control membrane potential and/or Ca^{2+} removal. Myometrial contractions in non-pregnant women are normally high amplitude, low frequency, and low in basal pressure tone (Bulletti, 2000, 2004), and are necessary for efficient haemostasis and control of bleeding from the SMC-lacking spiral arteries that transverse through the uterus (Shivhare, 2014). Should these findings translate to human myometrium, such less efficient myometrial contractions could impact on myometrial

contractions, thus impacting on menstruation for women with *RYR1* variants and in part explain the high incidence of menorrhagia in *RYR1*-mutated patients previously reported by Lopez and colleagues (Lopez, 2016).

Ryr1 expression in *Ryr1*$^{Y522S/+}$ uterus

In the present study *Ryr1* and *Ryr2* mRNA expression was confirmed in the non-pregnant myometrium, although expression levels were not altered between *Ryr1*$^{Y522S/+}$ and wildtype tissues. Others have previously detected low *Ryr1* mRNA expression in non-pregnant mouse myometrium and although *Ryr3* appears to be the predominantly expressed murine isoform, *Ryr3* is still considered to have no role in Ca^{2+} release in myometrial cells (Mironneau, 2002).

I observed increased expression of *Ryr1* mRNA in the *Ryr1*$^{Y522S/+}$ heterozygous (mixed litter) and wildtype (mixed litter) pregnant myometrium compared to wildtype (wildtype litter) gestation day 18.5 pregnant myometrium. Using fluorescent immunohistochemical techniques, I have also confirmed the expression of RYR1 protein in the wild-type pregnant mouse localised to the myometrium and endometrium but was unable to compare myometrium from *Ryr1*$^{Y522S/+}$ mothers. Others have reported that the expression of *Ryr1* and *Ryr2* is also low in the pregnant mouse myometrium, and that *Ryr3* is downregulated at the end of mouse pregnancy, and even dominant-negative variant of *Ryr3* which causes the downregulation of full-length *Ryr3* toward term of pregnancy has been reported (Dabertrand, 2007; Matsuki, 2017).

To the best of my knowledge, this is the only report of increased *Ryr1* mRNA expression in tissues from the *Ryr1*$^{Y522S/+}$ mouse model (Durham *et al.*, 2008; Lopez, 2016). However a study has

previously reported increased expression of *RYR1* in human failing cardiomyocytes (Münch *et al.*, 2001). Other *Ryr* isoform gain-of-function mutations have no impact on *Ryr* mRNA expression in cultured human myotubes and myoblasts and human induced pluripotent stem cells differentiated into cardiomyocytes (Conte *et al.*, 2021; Hopton *et al.*, 2022). It is therefore somewhat unexpected that in the present study, *Ryr1* expression was higher in the pregnant mouse myometrium from *Ryr1^{Y522S/+}* mothers compared to wildtype, suggestive of upregulation, rather than a negative feedback response to enhanced Ca^{2+} release. Interestingly, increased *Ryr1* mRNA expression was also detected in pregnant myometrium of wildtype mothers with a mixed genotype (wild type and Y522S) litter, indicating that increased maternal myometrial *Ryr1* expression during may be in part due to the *Ryr1* Y522S fetal genotype, possibly resulting in increased fetal demand. As previously described in section 4.4, increasing evidence shows that during pregnancy, fetal genetics can influence maternal physiology (blood pressure, gestational diabetes, metabolism, and preeclampsia), which is ultimately driven by changes in maternal gene expression and protein translation (Petry, 2007, 2016; Traglia *et al.*, 2017, 2018).

It is important to note that RYR1 staining was also evident in the endometrium of the pregnant wild-type uterus. The endometrium consists of epithelial, endothelial, stromal and leukocyte cell populations (Deane *et al.*, 2016). The expression of RYR1 has not previously been confirmed in the uterine endometrium but its expression has been determined in colonic endothelium and vascular endothelium (Prinz, 2008; Chuang, 2022). This raises the possibility that increased Ca^{2+} release from RYR1 Y522S channels could cause functional effects in the endometrial tissue.

Ryr2 and *Ryr3* expression

Comparison of absolute copy number expression of all three *Ryr* mRNA isoforms in pregnant mouse myometrium (g.d. 18.5), suggests that *Ryr1* and *Ryr2* are more abundant than *Ryr3* in both wild-type and *Ryr1$^{Y522S/+}$* tissues. This conflicts with older previous reports of *Ryr* isoform expression in the pregnant rat myometrium (gestation day 19) measured using less sensitive and semi quantitative RT-PCR. For example, Martin *et al*., reported that *Ryr3* was most abundantly expressed compared to *Ryr1* and *Ryr2* (Martin, 1999).

In the present study, mRNA expression levels of *Ryr2*, *Ryr3*-short isoform and *Ryr3*-long isoform (inclusion of intron 96-97) were unchanged between the *Ryr1$^{Y522S/+}$* and wild-type pregnant myometrium. To date, up to 8 different *Ryr3* transcripts have been identified [NCBI gene, date accessed: 26/01/2023] (Sayers *et al.*, 2022), with some evidence to support the differential function of the alternatively spliced variants.

The genetic sequence of the long *Ryr3* isoform identified in this study does not appear to be the same as previously reported alternatively spliced *Ryr3* isoforms in various mouse tissues, including non-pregnant myometrium (Miyatake *et al.*, 1996; Mironneau, 2002). Although the function of these *Ryr3* isoforms were not studied presently, previous reports have found that a dominant negative splice variant of *Ryr3*, specifically lacking 29 amino acid residues corresponding to exon 97, does not have a channel function but instead negatively regulates *Ryr2* and full-length *Ryr3* at term pregnancy in mice (Jiang, 2003; Dabertrand, 2006, 2007), however others have disputed its necessity in parturition (Matsuki, 2017). Thus, the *Ryr1* Y522S channel does not impact the expression of either *Ryr2* or *Ryr3* isoforms at the end of pregnancy, but a novel *Ryr3* isoform may

have been uncovered and could be investigated for its functional impact on the mouse myometrium.

Differential gene expression in pregnant *Ryr1$^{Y522S/+}$* myometrium

The data presented above are suggestive that the function of the non-pregnant *Ryr1$^{Y522S/+}$* myometrium may be altered, thus RNA-seq was undertaken to assess the potential impact of the *Ryr1* Y522S gain-of-function mutation on global gene expression in late pregnant myometrium. However, PCA analysis failed to show any clear-cut clustering of the wild-type and heterozygous samples. This was an early indication that there was minimal impact of the gain-of-function mutation on myometrial gene expression. Differential expression analyses showed statistically increased *Fcgbp,* and decreased *Ighv2-9,* expression in the pregnant heterozygous *Ryr1$^{Y522S/+}$* myometrium compared to wild-type. Further, ranking of differentially expressed genes, albeit including those that did not quite reach statistical significance, suggested that *Psg16*, and *Nmb* mRNA expression increased and *Ptprm* and *Igkv17-121* decreased in pregnant heterozygous *Ryr1$^{Y522S/+}$* myometrium compared to wild type.

Fcgbp encodes the Fc fragment of IgG binding protein, located in the extracellular matrix and expressed in genitourinary system, gut, immune system; and integumental system, specifically amniotic fluid, cerebrospinal fluid, and urine and saliva (Harada *et al.*, 1997; Zhao *et al.*, 2018; Liu *et al.*, 2019). The production of human FCGBP has been described in the placenta, intestinal epithelial cells, and thyroid tissue (Harada, 1997; O'Donovan *et al.*, 2002). The human FCGBP protein shares significant similarity with von Willebrand factor (VWF) and mucin-2 (MUC2), and

263

also colocalizes with MUC2 in colon large mucin granules of goblet cells (Harada, 1997). Although the complete biological function of Fcgbp is unknown, it is considered to provide immunological protection to the intestinal tissue and facilitates the interaction between intestinal mucus and potentially harmful stimuli, ultimately protecting the mucosal surface (Kobayashi, Blaser and Brown, 1989; Kobayashi *et al.*, 1991). Furthermore, Fcgbp (or FcγBP) has been shown to be one of the most abundant proteins in the amniotic fluid, present in the second trimester of uncomplicated pregnancies (Liu, 2019). The presence of intra-amniotic infections has been associated with elevated FCGBP concentrations in pregnancies with preterm premature rupture of the membranes (PPROM) and pre-term labour with intact membranes (PTL), whereas elevated FCGBP in cervical fluid is associated with PPROM only (Stranik *et al.*, 2021). Although there are no previous reports of *Fcgbp* expression in myometrial tissue, the elevated expression of *Fcgbp* mRNA in the myometrium of the *Ryr1$^{Y522S/+}$* mouse indicates a potentially increased immunological profile in the Y522S pregnant myometrium.

The expression of *Ighv2-9* mRNA was reduced in heterozygous *Ryr1$^{Y522S/+}$* pregnant myometrium. *Ighv2-9* encodes the immunoglobulin heavy variable 2-9, a protein predicted to enable antigen binding activity and immunoglobulin receptor binding activity. The Ighv2-9 protein is localised to the external side of the plasma membrane, and is predicted to be involved in the activation of the immune response and phagocytosis [NCBI gene, date accessed: 26/01/2023],(Sayers, 2022). The expression of *Ighv2-9* is very high in the mouse uterus, only second to the highest expression level in the spleen, as confirmed by RNA-Seq (Bgee.org, [data accessed 20/01/2023]). Functional studies of Ighv2-9 on the uterus have not yet been conducted, but its high expression in the unaffected mouse uterus and its role in the immune response indicate an important role in the normal function of the uterus during pregnancy. The downregulation of *Ighv2-9* in *Ryr1$^{Y522S/+}$*

pregnant myometrium indicates an effect of RYR1 channel calcium release in the regulation of the immune response at term pregnancy. In addition, the mRNA expression of *Igkv17-121* was numerically lower in *Ryr1*$^{Y522S/+}$ pregnant myometrial tissue, albeit not statistically significant. *Igkv17-121* encodes the immunoglobulin kappa variable 17-121, a protein located in the extracellular space of cells expressed ubiquitously in mouse tissues. The protein is also involved in the immune response to stimuli, further supporting the role of RYR1 Y522S Ca^{2+} release in the regulation of the immune response.

Pregnant heterozygous *Ryr1*$^{Y522S/+}$ myometrial tissue also displayed increased expression of *Psg16* (although not statistically supported), which encodes pregnancy specific beta-1-glycoprotein 16, a cell surface protein likely to be involved in phagocytosis. Its expression has been reported in the mouse placenta, brain, lung, and spleen. PSGs are produced by the placenta of rodents and secreted into the blood stream, and are among the most abundant fetal proteins, reaching concentrations of 200-400 μg/ml in the serum of pregnant women at term (Lin, Halbert and Spellacy, 1974). Seventeen different murine *Psg* genes (Psg16-32) have been identified, with different levels of expression at different points during pregnancy (McLellan *et al.*, 2005), and 11 members of the PSG family (PSG1–11) have been identified in humans (Thompson *et al.*, 1990). Murine PSGs are reported to be involved in placentation (Ha *et al.*, 2010; Lisboa *et al.*, 2010) and to modulate interactions between the fetus and maternal immune system (Bebo and Dveksler, 2005). Through protein-protein interactions, Psg16 has been related to reduced fertilization rate and early embryo development in a chronic unpredictable stress mouse model (Zhao *et al.*, 2021). The expression and function of Psg16 has been well studied in the rodent placenta, with some PSGs reported to play a role in placental vascularisation (Wu *et al.*, 2008), however its role in the normal function of the myometrium is unknown. Whilst there are no reported specific interactions between Psg16

and RYR1, the increased expression of *Psg16* in the *Ryr1*$^{Y522S/+}$ pregnant myometrium indicates abnormal placentation or decidualisation in the *Ryr1*$^{Y522S/+}$ animal, mediated via Ca^{2+} signalling and/or immunological mechanisms.

A study investigating the *Ryr1*$^{Y522S/+}$ mouse model, reported that the heterozygous *Ryr1* Y522S mutation may offer a subtle immune advantage compared to their wild-type counterparts. RYR1 expression has been confirmed in human and murine B-lymphocytes and dendritic cells, an important observation considering dendritic cells are the most potent antigen presenting cells connecting the innate and adaptive immune systems (Sei, Gallagher and Basile, 1999; Girard *et al.*, 2001; O'Connell, Klyachko and Ahern, 2002; Bracci *et al.*, 2007; Uemura *et al.*, 2007). Vukcevic and colleagues, found that *Ryr1*$^{Y522S/+}$ mice possess dendritic cells with a more mature phenotype, that they were also more potent at stimulating T-cells and serum concentrations of natural IgG1 and IgE were elevated. Furthermore, when challenged with primary antigens *Ryr1*$^{Y522S/+}$ mice produced higher levels of antigen-specific IgG (Vukcevic, 2013). In the present study, the findings of RNA-seq in pregnant *Ryr1*$^{Y522S/+}$ myometrial tissue also indicate a potentially altered immunological profile in the *Ryr1*$^{Y522S/+}$ mouse. This is particularly relevant in pregnancy where the initiation of labour and pregnancy loss are thought to have an immunological component.

In the *Ryr1*$^{Y522S/+}$ pregnant myometrium *Nmb* mRNA expression was increased compared to wildtype, although not statistically different. The neuromedin B protein is a precursor that is cleaved to produce a biologically active neuropeptide that plays a role in reproduction, satiety, thermoregulation, stress, and other behavioural responses. Nmb expression in the human myometrium increases with the advancement of gestation and is upregulated during labour

(spontaneous and oxytocin-induced) (Zhang *et al.*, 2007). In mouse myometrium *Nmbr* mRNA and Nmbr protein expression peak at parturition and decrease sharply after delivery (Zhang *et al.*, 2011). In primary human myometrial cells, Nmb activates nuclear factor kappa B (NF-κB) transcription factor p65 (p65) and activator protein 1 (AP-1) (factors associated with labour onset), which in turn, induce expression of interleukin 6 (IL-6) and type 2 cyclo-oxygenase enzyme (COX-2) (Zhu *et al.*, 2019; Chen *et al.*, 2020). In addition, maternal exposure to Nmb protein has been shown to shorten the gestational age of pups in mice (Zhang, 2011). Furthermore, Nmb/Nmbr interaction in pregnant mouse myometrial primary cells influences uterine activity via the regulation of intracellular [Ca2$^+$] (Zhang *et al.*, 2012). All of the above indicate that NMB and its receptor are important to induce the onset of labour and could be of interest to explore further in *Ryr1$^{Y522S/+}$* myometrium.

The expression of protein-tyrosine phosphatase type M (*Ptprm*) mRNA was reduced in *Ryr1$^{Y522S/+}$* pregnant mouse myometrium. *Ptprm* is typically expressed in the adherens junctions, lamellipodium and perinuclear region of cytoplasm of structures of the alimentary system, brain, cardiovascular system, and genitourinary system. There is currently no research on the role of Ptprm in the female reproductive system, however the role of Ptprm has been implicated with B lymphoma Mo-MLV insertion region 1 (BMI1) in the maintenance of spermatogonia proliferation (Zhang *et al.*, 2021). To understand the interaction networks of the DEGs in the pregnant *Ryr1$^{Y522S/+}$* myometrium, in particular the impact of reduced *Ptprm*, the web-based *IntAct* tool was utilised. The results revealed an interaction network of Ptprm with the genes *Ctnnb1, Cdh1, Itga3* and *Ptprn*, that are known to produce proteins involved in the maintenance of fertility (*Ptprn*) (Kubosaki *et al.*, 2006; Sokanovic *et al.*, 2023), conceptus implantation and trophoblast invasion (*Cdh1, Itga3*) (Paria *et al.*, 1999), recurrent spontaneous abortion (*Itga3*) (Liang *et al.*, 2019; Wang

267

et al., 2022), and uterine decidualisation and degradation (*Ctnnb1*) (Herington *et al.*, 2007) processes during pregnancy. If with further study, downregulation of *Ptprm* mRNA (and protein) in the *Ryr1$^{Y522S/+}$* pregnant mouse can be demonstrated it could indicate that increased Ca^{2+} release from RYR1 Y522S channels could impact murine fertility, and the proper implantation of the conceptus to the uterus, a concept aligned to investigations presented in Chapter 6.

After generating differential gene expression profiles for heterozygous and wildtype animals, I used *in silico* tools to analyse protein function and common pathways of differentially expressed genes (padj<0.3). Common molecular functions associated with the differentially expressed genes included binding, catalytic activity, and molecular function regulators (most to least common). The common pathways identified predominantly involved signal transduction. These results broadly highlight the important functions of the proteins encoded by *Fcgbp, Ighv2-9, Psg16*, *Nmb, Ptprm* and *Igkv17-121* in normal cellular function. To better understand the impact of RYR1 Y522S channels on their protein functions, further functional studies in the *Ryr1$^{Y522S/+}$* animal are necessary.

5.5 Study limitations and future work

Some limitations of the work presented here have been highlighted above, but the overarching limitation of this study rests with the technique used to determine the end of gestation and labour length of the $Ryr1^{Y522S/+}$ mouse. Due to strict restrictions in animal housing the video cameras were placed outside of Perspex individually vented cages, during 12-hour light-dark cycles. Together, this greatly limited the visual capacity of the cameras, the resolution of the picture and video recording angle (due to metal frames around cages). As a result, many of the recorded births that occurred during the dark cycles could not be included in this dataset. In addition, the parturition duration of the $Ryr1^{Y522S/+}$ could not be observed, a measurement that could have provided critical information on the contractile behaviour of the $Ryr1$-mutated myometrium during labour. To determine parturition duration and to better visualise the end of gestation in the $Ryr1^{Y522S/+}$ model, the study of end of gestation using video cameras could be repeated. For a low-cost method, it would be sufficient to use an open-top old-style cage to house pregnant dams, if biological service unit restrictions allow. This method can generate an unobstructed, higher resolution image and therefore a more accurate measurement of the end of gestation and the capture of parturition duration. If an individually ventilated cage must be used to house the pregnant dam, it would be wise to use a cage-camera set up such as those commonly used in behavioural studies (Singh *et al.*, 2019; Grieco *et al.*, 2021).

To study *ex vivo* function, myometrium was collected from both non-pregnant and pregnant animals, the latter of which were time-mated. Due to the COVID-19 pandemic and associated mandatory lockdowns, many pregnant tissues were not collected for experimentation. Following on from this period this thesis was refocused towards the investigation of uterine artery functions

in the pregnant $Ryr1^{Y522S/+}$ animal, as described in the **Error! Reference source not found.** and section 8.

Ex vivo myometrial contractility experiments should be repeated with concentration-response tests with dantrolene pre-incubation. Although a study has shown that dantrolene has no effect on the spontaneous contractility of human uterine smooth muscle (Shin *et al.*, 1995), it could be beneficial to use dantrolene to determine if the impact of *Ryr1* Y522S can be reversed in the mouse myometrium. Such experiments in addition to molecular experiments could provide valuable insight into determining whether the changes observed in this study are due to RYR1 over-activation and to ultimately uncover the role of RYR1 channels in the myometrium.

In this chapter I have shown that *Ryr1* mRNA expression is elevated in the $Ryr1^{Y522S/+}$ pregnant mouse myometrium, following which I confirmed the presence of RyR1 protein in the uterine myometrium and endometrium. The use of mass spectrophotometry could be an ideal technique to validate the presence of- and precisely quantify the RyR1 protein in mouse myometrial protein tissue lysate. This method will overcome the difficulties in extracting and blotting a high molecular weight protein such as RyR1 and can detect extremely low volumes of the protein as suspected in the myometrial tissue. In particular, mass spectrophotometry could prove useful to quantify RYR3 protein which was undetectable at the RNA level in non-pregnant myometrium.

When performing RNA-seq analysis, the adjusted p-value was kept below 0.3 as there were few genes that met the typical p<0.05 cut-off, this was likely due to a limited number of samples. Few samples were available for RNA-sequencing, limiting the variety of continuously differentially expressed genes that could be observed from this dataset. Another consideration is that the small number of differentially expressed genes could also be a result of the study model used. The use

of a heterozygous knock-in animal model; a substitution mutation carried only in one allele of a gene, reduces the effect of the malfunctioning (gain-of-function) gene as it may be diluted by the normally functioning protein consequently making the isolation of differences in gene expression challenging. Therefore, genes of interest were selected irrespective of the adjusted p-value, although the value was kept to a minimum. Due to the utilisation of the high p-values, I used multiple bioinformatic tools to validate the results from RNA-seq tests, in addition to RT-qPCR. These tools were used to identify genes with potentially the most significant role in myometrial function in the $Ryr1^{Y522S/+}$ model, such as $Ptprm,$ streamlining the selection of genes for future analyses such as western blotting or immunohistochemical analyses, or functional immunological testing. Following high-throughput RNA sequencing, RT-qPCR was used to validate changes in gene expression. Six genes of interest were selected for their low adjusted p-values and availability of mRNA sequences. The number of genes studied was also subject to limitations, such as the maximum number of samples loaded per run, the cost of experimental reagents and machinery.

Finally, in future experiments myometrial spontaneous contractility tests and histological tests should be repeated with a larger sample size. Moreover, additional genes might have been identified if a larger sample size was used in the RNA-seq analysis.

5.6 Conclusions

The heterozygous *Ryr1* Y522S mutation induces an abnormal myometrial contractile pattern in the non-pregnant uterus, and potentially an altered immunological state in the *Ryr1*$^{Y522S/+}$ pregnant mouse uterus. Further studies are required to determine whether *Ryr1* Y522S might impact parturition duration and to further elucidate the mechanism of impact in myometrial contractility.

6 Chapter 6 Fetal and placental development in the *Ryr1*^{*Y522S/+*} mouse

6.1 Background

The ability of a fetus to develop until full-term of pregnancy provides a plethora of advantages to the health of the offspring. By day 18.5 of gestation, C57Bl/6J fetuses reach a weight of approximately 1 g, increasing in weight almost twice from gestation day 15.5, whereas placental growth slows in late gestation (Kulandavelu *et al.*, 2006). This pattern is similar in the developing human fetus, where during the last stage of pregnancy, fetal weight almost doubles (Cunningham *et al.*, 1989), whereas the weight of the placenta does not increase significantly (Furuya *et al.*, 2008). The mature mouse placenta is established around mid-gestation (~E10.5) and continues to grow in size and complexity up to day 15, reaching maximum volume by day 18 (Coan, 2004). The mouse placenta is organised into three histologically distinct layers: the labyrinth, the junctional zone (JZ), and the maternal decidua (Woods, 2018), as discussed in detail in section 1.10.2 and Figure 9.

As previously described in Chapter 1, the architecture of the placental labyrinth provides a large surface area for transport between the counter current flowing maternal and fetal blood supplies, which come into close contact but do not mix. Defects and deficiencies in this complicated and intricate structure are a frequent cause of developmental failure and growth deficits (Watson, 2005; Perez-Garcia, 2018). The junctional zone provides hormones, growth factors and cytokines for the normal progression of pregnancy, that act on both the maternal and fetal physiology (Ain, 2003; Soares, 2004), defects in which result in an altered endocrine environment of the placenta, thus dysfunctional control of placental growth/structure and fetal growth (Salas, 2004; Simmons, 2008). In particular, placenta weight has been reported to reflect placental efficiency (Risnes,

2009; Eskild, 2010; Radan, 2022); and increased or decreased placenta weight have been associated with adverse fetal outcomes such as intrauterine growth restriction (IUGR) (Phipps, 1993; Khalife, 2012).

In addition to previously reported longer tail artery bleeding times in $Ryr1^{Y522S/+}$ mice (Lopez, 2016), data presented in Chapter 4, indicated altered $Ryr1^{Y522S/+}$ and wildtype (mixed litter) pregnant uterine artery relaxation. Therefore, I hypothesised that increased uterine artery blood flow will enhance fetoplacental growth in $Ryr1^{Y522S/+}$ pregnant dams as increases in fetal or placental weight. In this chapter, I found interesting changes in fetal and placental weight at gestation day 18.5, this prompted further histological investigations of placentas of the $Ryr1^{Y522S/+}$ dam. Studies have demonstrated the presence of *RYR1* and *RYR2* mRNA in human trophoblast tissues and the BeWo (trophoblast) cell line (Haché, 2011; Zheng, 2022), however the presence of ryanodine receptor proteins in mouse placental tissues is yet to be determined, thus, I also investigated RYR1 localisation in placenta of the $Ryr1^{Y522S/+}$ dam.

Full descriptions of methods are included in Chapter 3. To investigate the impact of *Ryr1* Y522S on fetal and placental development, it was important to identify the greatest possible change in development, which could be observed towards the end of pregnancy where fetal growth vastly increases. On gestation day 18.5 pregnant female mice and fetuses were culled using Schedule 1 methods, and litter size (fully developed fetuses present in both uterine horns), resorbed fetuses (blood-filled bundles of tissue attached to the uterus), fetal and placental weight were recorded. Only before weighing, fetuses were separated from their individual placentas to record matched fetus-placenta weights. In litters consisting of mixed fetal genotypes, fetuses were genotyped as previously described in section 3.4.

Histological methods were used to investigate morphological changes and to quantify differences in size of placental functional areas. Paraffin-embedded placenta sections were stained in haematoxylin and eosin, or immunofluorescent-tagged antibodies, as previously described. Briefly, an RYR1-specific antibody was used to identify whether RYR1 channels proteins are present in the placenta, and second to determine if there are any localisation or expression differences (fluorescence intensity) between placenta genotypes. An anti-Mct4 antibody was used to fluorescently tag the fetal side of the two cell-layered syncytiotrophoblast, anti-Tpbpα, a trophoblast marker for the placental junctional zone and anti-ki67 antibody, a protein found on the surface of mitotic chromosomes, was used to detect changes in cellular growth and proliferation. Nuclei were stained with DAPI, this was used to calculate % Ki67 cells of total placental cells.

To obtain whole placenta images, 12 x 12 digital images (10x magnification) were stitched together via blending using an inverted widefield microscope. Measurements of the placental

labyrinth, junctional zone and decidua were made from digitized images of midline placenta sections stained with haematoxylin and eosin using the polygon selection tool and area measure tool in Fiji ImageJ. This was used to calculate the ratio of the labyrinth area to junctional zone area. The Lb:Jz ratio is a validated measure that is used to indicate the composition of the placenta (De Clercq *et al.*, 2019). Macros were created to analyse fluorescence intensity in Fiji ImageJ, see Appendix 3 for macro parameters. Statistical tests used were one way ANOVA and students t-test, unless stated otherwise.

6.3   Results

6.3.1   Impact of maternal $Ryr1^{Y522S/+}$ on fetal and placental weights

At gestation day 18.5, fetuses from $Ryr1^{Y522S/+}$ heterozygous dams were lighter (0.8909 ± 0.03088g, n=106 fetuses from 15 litters) than fetuses from wildtype (wildtype litter) dams (0.9931 ± 0.01643g, n=134 fetuses from 16 litters), P= 0.0473 (Kruskal-Wallis test), wildtype (wildtype litter) vs. heterozygous (mixed litter) P=0.0405 (Dunnett's T3 multiple comparisons test), demonstrated in Figure 67. The weight of fetuses from wildtype (mixed litter) dams (0.9469 ± 0.02832g, n=103 fetuses, 16 litters) were not statistically different compared to fetuses from wild-type (wild-type litter) dams, P=0.8210 (Dunn's multiple comparisons test).
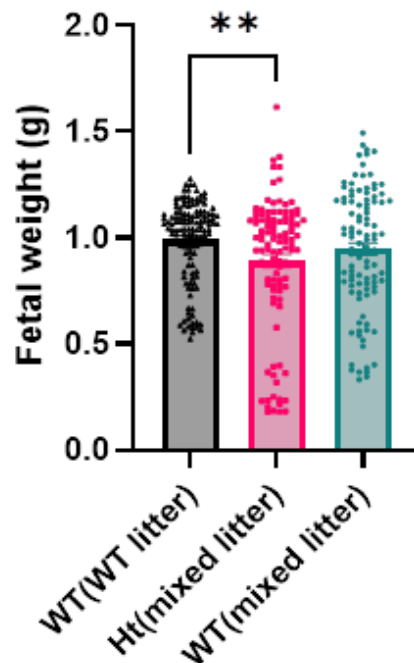
Figure 67. **Weight of fetuses on gestation day 18.5 from $Ryr1^{Y522S/+}$ heterozygous (mixed litter), wild-type(wild-type litter) and wild-type (mixed litter) dams**

On gestation day 18.5 fetuses from $Ryr1^{Y522S/+}$ heterozygous (mixed litter) were lighter in weight (n=106 fetuses, 15 litters) than fetuses from wildtype (wildtype litter) (n=134 fetuses, 16 litters) P=0.0473 (Kruskal-Wallis test) P=0.0405 (Dunn's multiple comparisons test). Fetus weights from wildtype (mixed litter) dams (n=103 fetuses, 16 litters), were not statistically different to fetus weights from heterozygous (mixed litter) or wild-type(wild-type) dams. Data presented as mean ± SEM.

At gestation day 18.5, placentas from $Ryr1^{Y522S/+}$ heterozygous (mixed litter) dams were heavier (0.1012 ± 0.0022 g, n=99 placentas, 13 litters) than placentas from wildtype (wildtype litter) dams (0.0930 ± 0.0013 g, n=134 placentas, 16 litters) P=0.0462 (Kruskal-Wallis test), P=0.0419 (Dunn's multiple comparisons test), demonstrated in Figure 68. Placental weight from wildtype (mixed litter) dams (0.0960 ± 0.0015 g, n=96 placentas, 15 litters) were not statistically different from wildtype (wildtype litter) dams' placental weights, P= 0.5471 (Dunn's multiple comparisons).
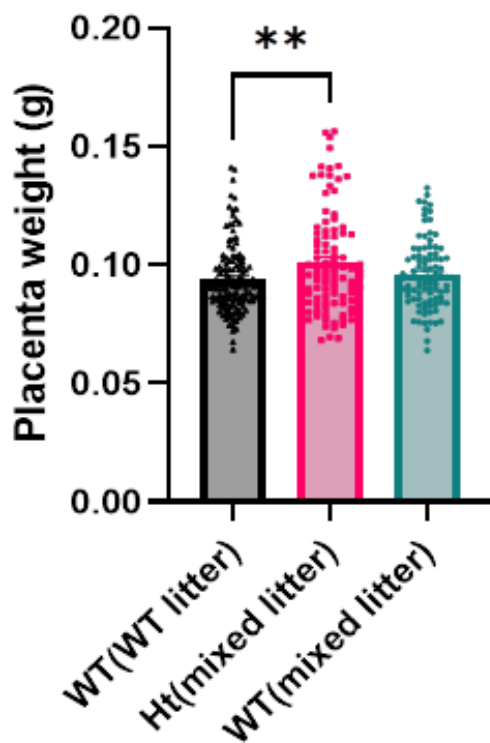
Figure 68. **Weight of placentas on gestation day 18.5 from $Ryr1^{Y522S/+}$ heterozygous (mixed litter), wild-type(wild-type litter) and wild-type (mixed litter) dams**

On gestation day 18.5 placentas from $Ryr1^{Y522S/+}$ heterozygous (mixed litter) (n=99 placentas, 13 litters) were lighter in weight than placentas from wildtype (wildtype litter) (n=134 placentas, 16 litters), P=0.0462 (Kruskal-Wallis test), P=0.0419 (Dunn's multiple comparisons test). Placenta weight from wildtype (mixed litter) dams (n=96 placentas, 15 litters), were not statistically different compared to placentas from wildtype (wildtype litter) dams, P= 0.5471 (Dunn's multiple comparisons test). Data presented as mean ± SEM.

6.3.1.1 Impact of Ryr1^{Y522S/+} on fetal:placental weight ratios

The mean of individual fetal weights divided by corresponding placenta weights are shown as fetal:placental (f:p) ratios in Figure 69. As expected, the f:p ratios for heterozygous (mixed litter) and were lower (9.36 ± 0.4195, n=99 pairs from 14 litters) compared to wildtype (wildtype litter) (10.88 ± 0.2445, n=134 from 16 litters) dams, P=0.0139 (Kruskal-Wallis test), P=0.0132 (Dunn's multiple comparisons test). F:P of wildtype (mixed litter) dams (9.897 ± 0.3541, n=111 pairs from 15 litters) were not statistically different to that of wildtype(wildtype), P=0.0609 (Dunn's multiple comparisons test).
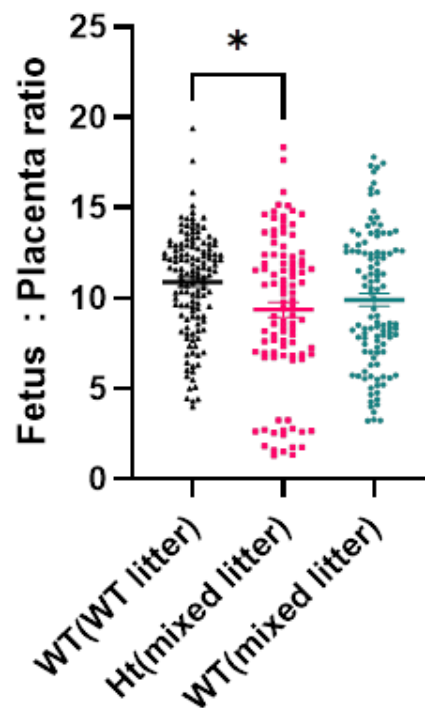
Figure 69. **Gestation day 18.5 fetal : Placental ratios of fetal/placenta pairs from *Ryr1*^{Y522S/+} heterozygous (mixed litter), wild-type(wild-type litter) (n=134, 16 litters) and wild-type (mixed litter) dams**

Fetus:placenta weight ratios of individual fetus-placenta pairs from *Ryr1*^{Y522S/+} heterozygous (mixed litter) (n=99 pairs, 14 litters) were reduced compared to f:p of wild-type(wild-type litter) (n=134, 16 litters) dams. P=0.0139 (Kruskal-Wallis test), P=0.0132 (Dunn's multiple comparisons test). There was no statistical difference in F:P in wild-type (mixed litter) (n=111 pairs, 15 litters) dams compared to wildtype (wildtype litter), P=0.0609. Data presented as mean ± SEM.

6.3.1.2 *Impact of fetal genotype on fetal-placental weights*

The weight of both fetuses and placentas were not impacted by mixed (wild-type or heterozygous) fetal genotype litters from either wild-type or heterozygous mothers, as demonstrated in Figure 70. Specifically, a wildtype or heterozygous fetal genotype did not statistically impact the weight of the respective fetus or placenta in wild-type (mixed litter) and heterozygous mothers (mixed litter) litters, $P>0.05$ (two-way ANOVAs). Similarly, f:p ratios of wild-type or heterozygous fetus/placenta pairs were not statistically different in wildtype (mixed litter) or heterozygous (mixed litter) dams, $P>0.05$ (two-way ANOVA), demonstrated in Figure 70. Wild-type (n=57) and heterozygous (n=44) fetuses and placentas from wildtype (mixed litter) dams (n=13 litters). Wild-type (n=28) and heterozygous (n=23) fetuses and placentas from heterozygous (mixed litter) dams (n=10 litters).
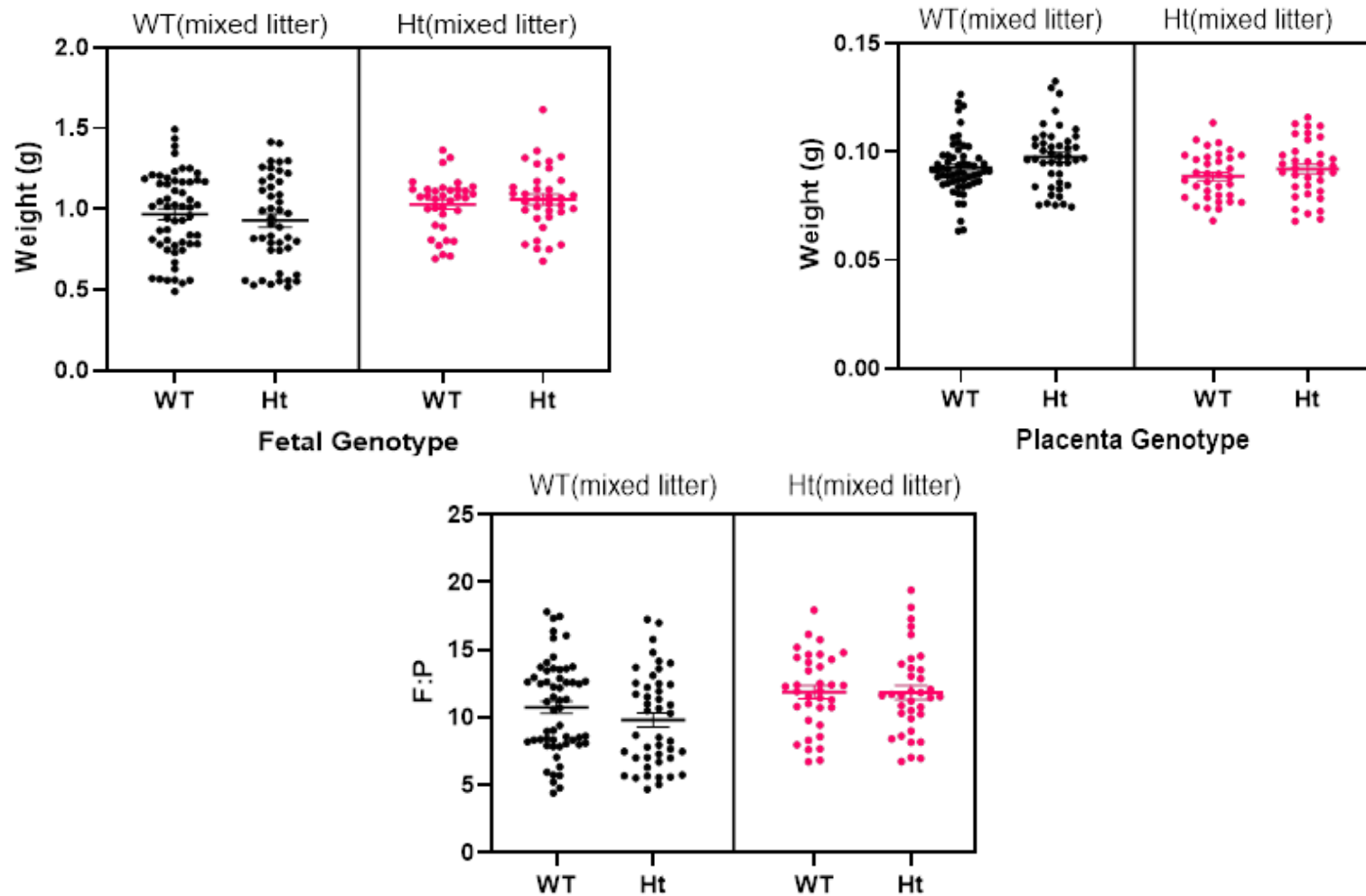
Figure 70. **Weights and fetal/placental ratios of wild-type and heterozygous fetuses and placentas from wildtype (mixed litter) and heterozygous $Ryr1^{Y522S/+}$ (mixed litter) pregnant dams on gestation day 18.5**

The weight (gram) of wild-type (n=57) and heterozygous (n=44) fetuses and placentas from wild-type (mixed litter) dams (n=13 litters), and wild-type (n=28) and heterozygous (n=23) fetuses and placentas from Ht(mixed litter) dams (n=10 litters) are presented. The genotype of fetus did not impact the weight of fetus or placentas in either wildtype of heterozygous mothers, P > 0.05 (two-way ANOVAs). Data presented as mean ± SEM.

6.3.2 Impact of *Ryr1*$^{Y522S/+}$ on litter size

At gestation day 18.5, heterozygous (mixed litter) dams had fewer fetuses in a litter (7.364 ± 0.3054, n=22) compared to wild-type (wild-type litter) dams (8.481 ± 0.2225, n=27), P=0.0248 (Kruskal-Wallis), heterozygous (mixed litter) Vs wild-type (wild-type litter) P=0.0148 (Dunn's multiple comparisons test). Wild-type (mixed litter) litter size (8.000 ± 0.4918, n=18) was not significantly different from wild-type (wild-type litter) litter size, (P= 0.9481, Dunn's multiple comparisons test).
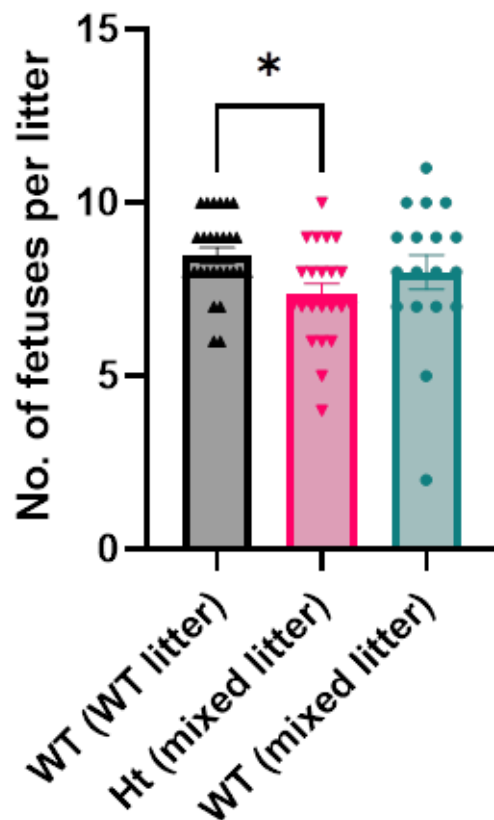
Figure 71. **Number of fetuses in a litter grouped by maternal genotype and litter genotype.**

Litter size from wild-type (wild-type litter) n=27, heterozygous (mixed litter) n=22, wild-type (mixed litter) n=18, gestation day 18.5 pregnant dams. Heterozygous (mixed litter) dams had fewer fetuses in a litter compared to wild-type (wild-type litter) mothers, P=0.0248 (Kruskal-Wallis), P=0.0148 (Dunn's multiple comparisons test). Wild-type (mixed litter) litter size was not significantly different from wild-type (wild-type litter) litter size. Data presented as mean ± SEM.

Fetal genotypes of litters from both wild-type (mixed litter) mothers and heterozygous (mixed litter) mothers are presented in Figure 72, as a percentage of total litter size, to control for differences in litter size between dams. Wildtype (mixed litter) dams (n=17) were equally likely to have wildtype fetuses (54.5 ± 2.753) and heterozygous *Ryr1$^{Y522S/+}$* fetuses (44.43 ± 2.955), P=0.0944, demonstrated in Figure 72A. Similarly, heterozygous (mixed litter) mothers (n=14) were equally likely to have wildtype (46.56 ± 6.799) and heterozygous *Ryr1$^{Y522S/+}$* (53.44 ± 6.799) fetuses P=0.6215 (paired t-tests), demonstrated in Figure 72B.
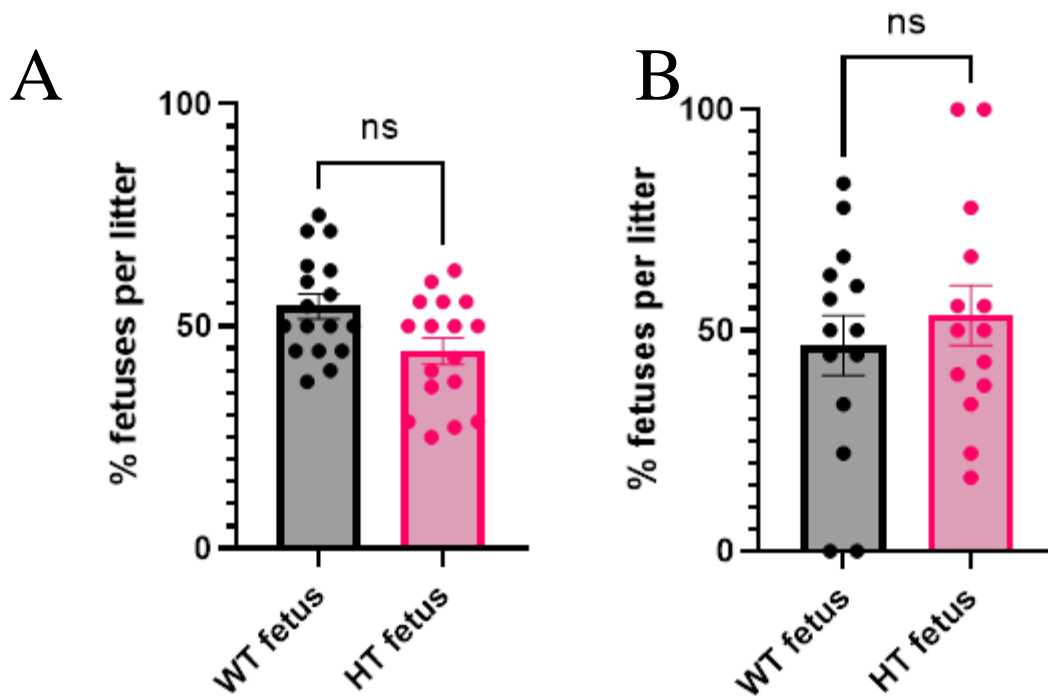
Figure 72. **Fetal genotypes present in (A) wild-type (mixed litter) and (B) heterozygous *Ryr1$^{Y522S/+}$* (mixed litter) pregnant dams on gestation day 18.5.**

Gestation day 18.5 fetuses from (A) wildtype (mixed litter) n=17 and (B) Heterozygous dams n=14, were genotyped to study differences in fetal genotype survival. Wild-type (mixed litter) dams, and heterozygous dams were equally likely to give birth to both wild-type and heterozygous *Ryr1$^{Y522S/+}$* fetuses, P=0.0944, P=0.6215 respectively (paired t-tests). Data presented as mean ± SEM.

6.3.2.2 Impact of Ryr1^{Y522S/+} on fetal resorptions

Of the total number of litters observed, the number of litters with a single or more resorptions were not statistically different between heterozygous (mixed litter) n=8 or 36.36% of total litters, wild-type (wild-type litter) n=9 or 33.33% of total litters and wild-type (mixed litter) n=7 or 38.88% of total litters, P=0.4938 (Welch's one-way ANOVA). The median resorption values are heterozygous (mixed litter)=2, wild-type (wild-type litter)=1 and wild-type (mixed litter)=1, demonstrated in Figure 73, plotted as the median, 25% percentile and 75% percentile. However, the median value of resorbed fetuses in litters from heterozygous dams were twice that of both wild-type dams with wild-type or mixed litters.
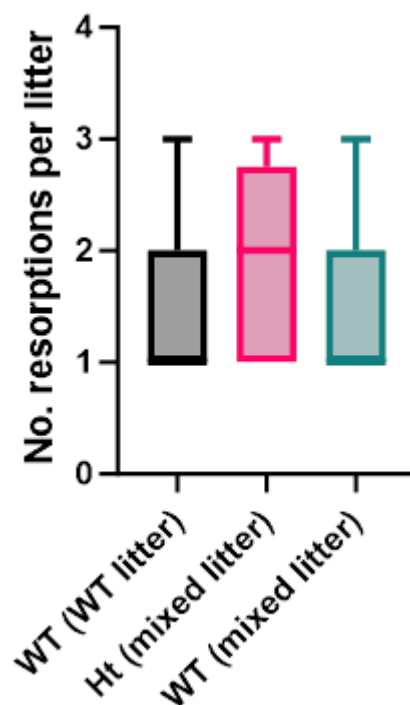
Figure 73. **Number of resorptions observed in a litter grouped by maternal genotype and litter genotype.**

At gestation day 18.5 the number of resorption sites were not statistically different between litters from wild-type (mixed litter) (n=7, 38.88% of total litters), heterozygous (mixed litter) (n=8, 36.36% of total litters), and wild-type (wild-type litter) (n=9, 36.36% of total litters), P=0.4938 (one-way ANOVA). Data presented as median, 25% percentile and 75% percentile and range.

6.3.2.3   Resorption genotypes

The distribution of genotypes associated with fetal resorptions collected at gestation day 18.5 from wild-type (mixed litter) and heterozygous (mixed litter) pregnant dams are shown in Figure 74. Wild-type (mixed litter) dams (n=12 litters) had more wild-type resorptions (1.750 ± 0.5522) than heterozygous resorptions (0.2500 ± 0.1306), P=0.0373. Heterozygous (mixed litter) dams (n=7 litters) had more heterozygous resorptions (1.286 ± 0.1844) than wild-type resorptions (0.1429 ± 0.1429), P=0.0002, Paired t-tests.
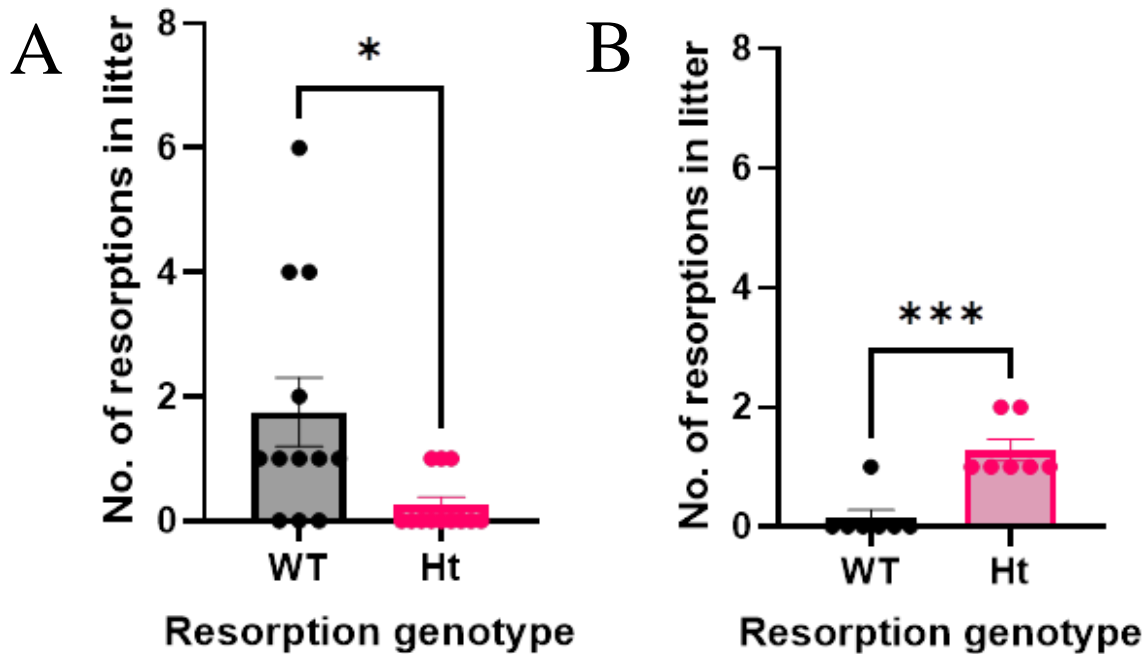
Figure 74. **Genotype of resorptions in litters from (A) wildtype (mixed litter) and (B) *Ryr1*$^{Y522S/+}$ heterozygous (mixed litter) dams on gestation day 18.5**

Total number of litters with resorptions were wild-type (mixed litter) dams n=12, heterozygous (mixed litter) dams n=7. Resorptions were either WT=wild-type, or Ht=heterozygous for the *Ryr1* Y522S mutation. (**A**) Wild-type mothers were more likely to have wild-type resorptions, P= 0.0373. (**B**) Heterozygous mothers were more likely to have heterozygous resorptions, P= 0.0002. Paired t-tests. Data presented as mean ± SEM.

6.3.3 Histological investigations of the *Ryr1*^{*Y522S/+*} placenta

To further investigate the cause of heavier placentas in the heterozygous (mixed litter) dams demonstrated in Figure 68, placental morphology and functional zones were examined using haematoxylin and eosin staining, and placenta genotypes were inferred from fetal tail genotypes, representative images are included in Figure 75.
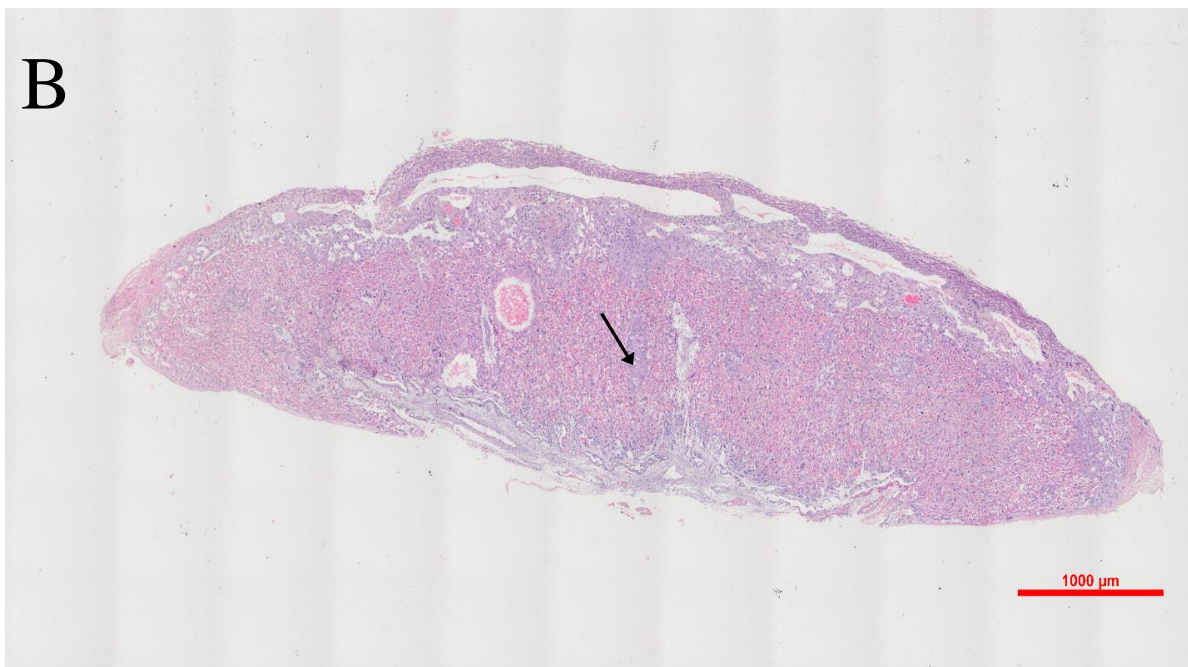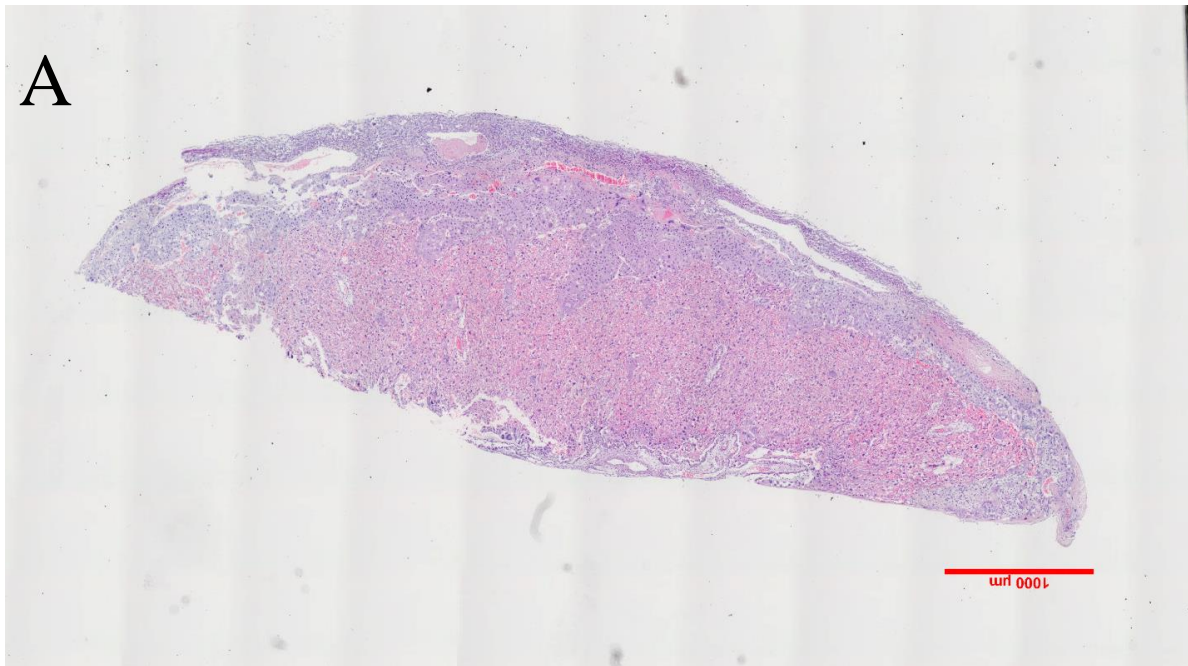
Figure 75. **Representative images of (A) wild-type and (B) heterozygous _Ryr1_^{Y522S/+} placenta midline sections in haematoxylin and eosin stain.**

Placental tissues collected from heterozygous _Ryr1_$^{Y522S/+}$ (mixed litter) pregnant dams on gestation day 18.5 (n=27 sections, 9 placentas). Heterozygous placentas (**B**) appear to have more junctional zone invaginations into the labyrinth (black arrow) compared to wild-type placentas (**A**).

287

6.3.3.1 Morphological Observations in the Ryr1^{Y522S/+} placenta

6.3.3.1 Morphological Observations in the Ryr1$^{Y522S/+}$ placenta

Observations of heterozygous placenta cross-sections revealed an increased number of JZ invaginations into the labyrinth, which was anticipated for larger sized placentas, and is demonstrated by a black arrow on Figure 75.

Using placenta sections with chorionic plates in view at 20x magnification, dense labyrinth areas were examined, to reveal that the labyrinth of heterozygous placentas appeared less densely packed, more air-filled and avascular, with apparent increased stromal cells compared to the blood-filled highly vascularised wild-type labyrinth network, as shown in Figure 76. Statistical analyses of this observation would require further histological tests such as an endo-mucin stain, discussed at the end of this chapter.
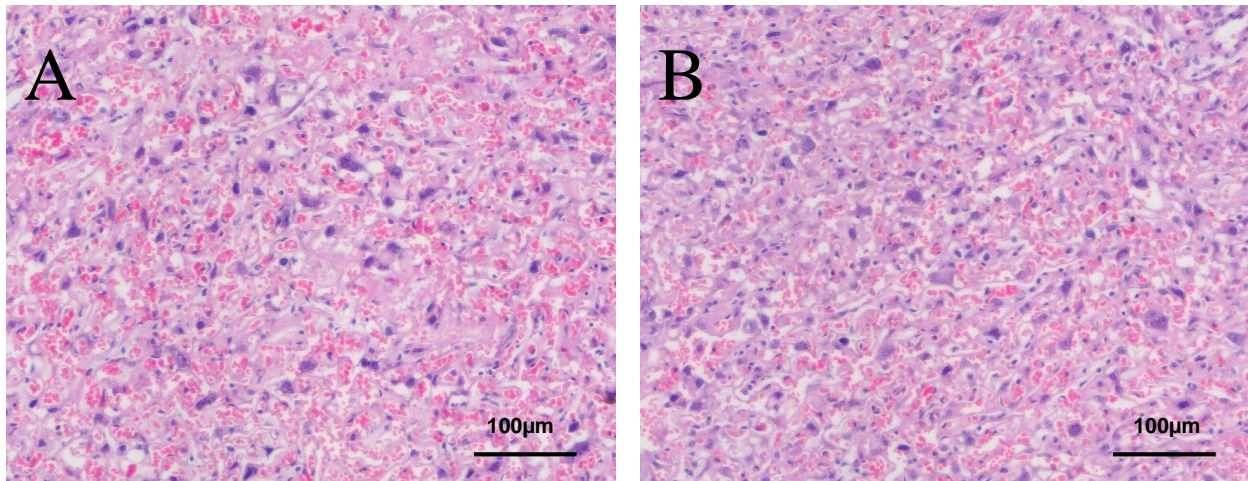
Figure 76. **Representative images of (A) wild-type and (B) heterozygous *Ryr1$^{Y522S/+}$* placenta labyrinth**

Representative images of placental labyrinth from wild-type and heterozygous *Ryr1$^{Y522S/+}$* placentas from heterozygous *Ryr1$^{Y522S/+}$* (mixed litter) pregnant dams at gestation day 18.5. Images show a blood-filled highly vascularised network of labyrinth in wild-type placenta tissue, and a less vascularised heterozygous labyrinth with increased stromal cells (n=27 sections from 9 wild-type placentas, n=27 sections from 9 heterozygous placentas).

The area of each functional section is presented as a percentage of the whole placenta area ± SEM in Figure 77. The labyrinth zone was not statistically different in $Ryr1^{Y522S/+}$ placentas (55.15 ± 1.913 nm^2, n=27 sections from 9 placentas) compared to wild-type placentas (52.46 ± 1.25 nm^2, n=27 sections from 9 placentas), P=0.2599 (Unpaired t-test with Welch's correction). The decidual area was also similar in the $Ryr1^{Y522S/+}$ placentas (10.85 ± 0.7319 nm^2) compared to wild-type placentas (12.54 ± 0.5449 nm^2), P=0.0841. The junctional zone of $Ryr1^{Y522S/+}$ placentas (23.73 ± 1.641 nm^2) were not statistically different to wild-type placentas (25.54 ± 1.593 nm^2), P= 0.4406. The labyrinth zone:junctional zone ratio (LZ:JZ), a measure that is used to indicate the composition of the placenta appeared to be increased in heterozygous placentas (2.452 ± 0.2489) compared to wild-type placentas (2.156 ± 0.2111), but this change was not statistically significant, P=0.3768 (unpaired t-test), data not shown.
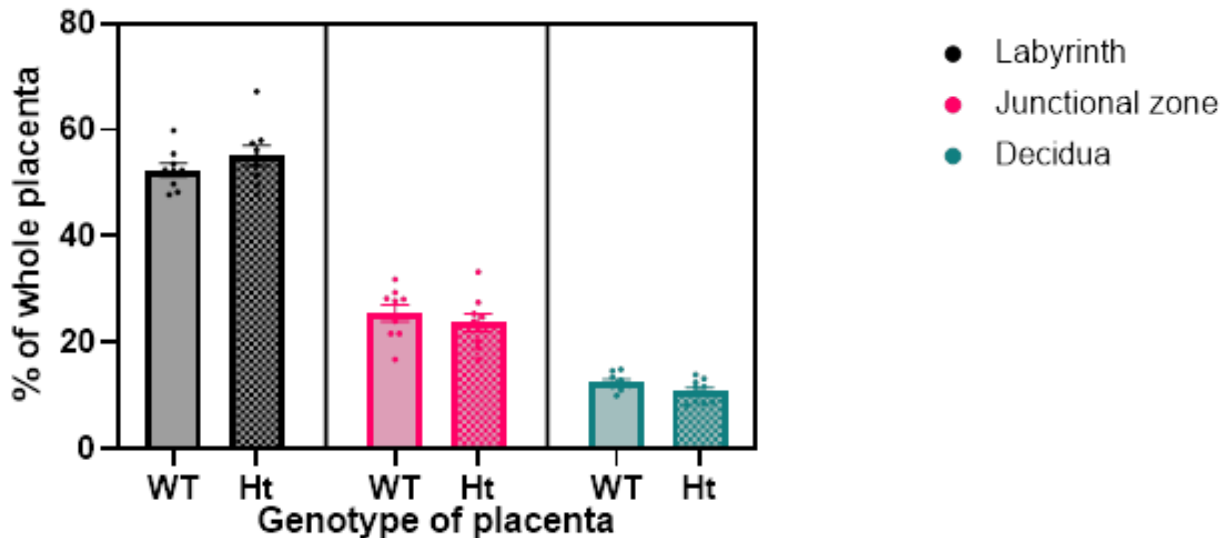
Figure 77. **Area comparison of placental labyrinth zone, junctional zone, and decidua in wild-type and heterozygous gestation day 18.5 placentas presented as percentage of total placenta area**

Placental labyrinth zone (black), junctional zone (pink), and decidua (green) area as a percentage of total placenta area in wild-type and heterozygous $Ryr1^{Y522S/+}$ placentas from gestation day 18.5 heterozygous $Ryr1^{Y522S/+}$ (mixed litter) dams. The labyrinth zone, junctional zone, and decidua areas in heterozygous placentas were not statistically different to wild-type placentas, P = 0.2599, 0.4406, 0.0841 respectively. (unpaired t-tests with Welch's correction). N=27 individual sections (triplicates) from 9 heterozygous placentas and 9 wild-type placentas. Data presented as mean ± SEM.

Correlation analyses of heterozygous placentas revealed that the percentage of labyrinth area decreased, and percentage of decidua area increased with increasing placental weight, P=0.0117 and 0.0162 respectively (Pearson correlation), detailed in Table 17. In wild-type placentas there were no statistically significant correlations in term of labyrinth, junctional zone and decidua area versus placental weight.

Table 17. **Pearson correlation coefficients for placental weight versus mean labyrinth, junctional zone and decidua areas. *P<0.05.**

	Placenta weight vs.	Pearson r coefficient	95% confidence interval	R squared	P value (two-tailed)
Wildtype (n=9)	Mean Labyrinth area	-0.3165	-0.8103 to 0.4401	0.1002	0.4067
	Mean Junctional area	0.4295	-0.3283 to 0.8509	0.1845	0.2486
	Mean Decidua area	-0.5738	-0.8963 to 0.1460	0.3292	0.1062
***Ryr1*$^{Y522S/+}$ (n=9)**	Mean Labyrinth area	-0.7876	-0.9532 to -0.2588	0.6203	*0.0117
	Mean Junctional area	0.5697	-0.1519 to 0.8951	0.3246	0.1093
	Mean Decidua area	0.7657	0.2066 to 0.9478	0.5863	*0.0162

Using a linear regression model, slopes were fitted for total placental weight versus labyrinth, junctional zone and decidua areas and compared between heterozygous (n=9) and wildtype placentas (n=9), demonstrated in Figure 78. The decidua area increased with increasing weight of heterozygous placentas (positive slope), whereas the decidua area decreased with increasing weight of wild-type placentas, P=0043. The correlation (slope) of labyrinth area and JZ area with placenta weight were not significantly different between wild-type and heterozygous placentas, P= 0.1973 and 0.9595. The labyrinth area of heterozygous placentas was generally increased in comparison to wildtype placenta, as previously demonstrated in Figure 77.
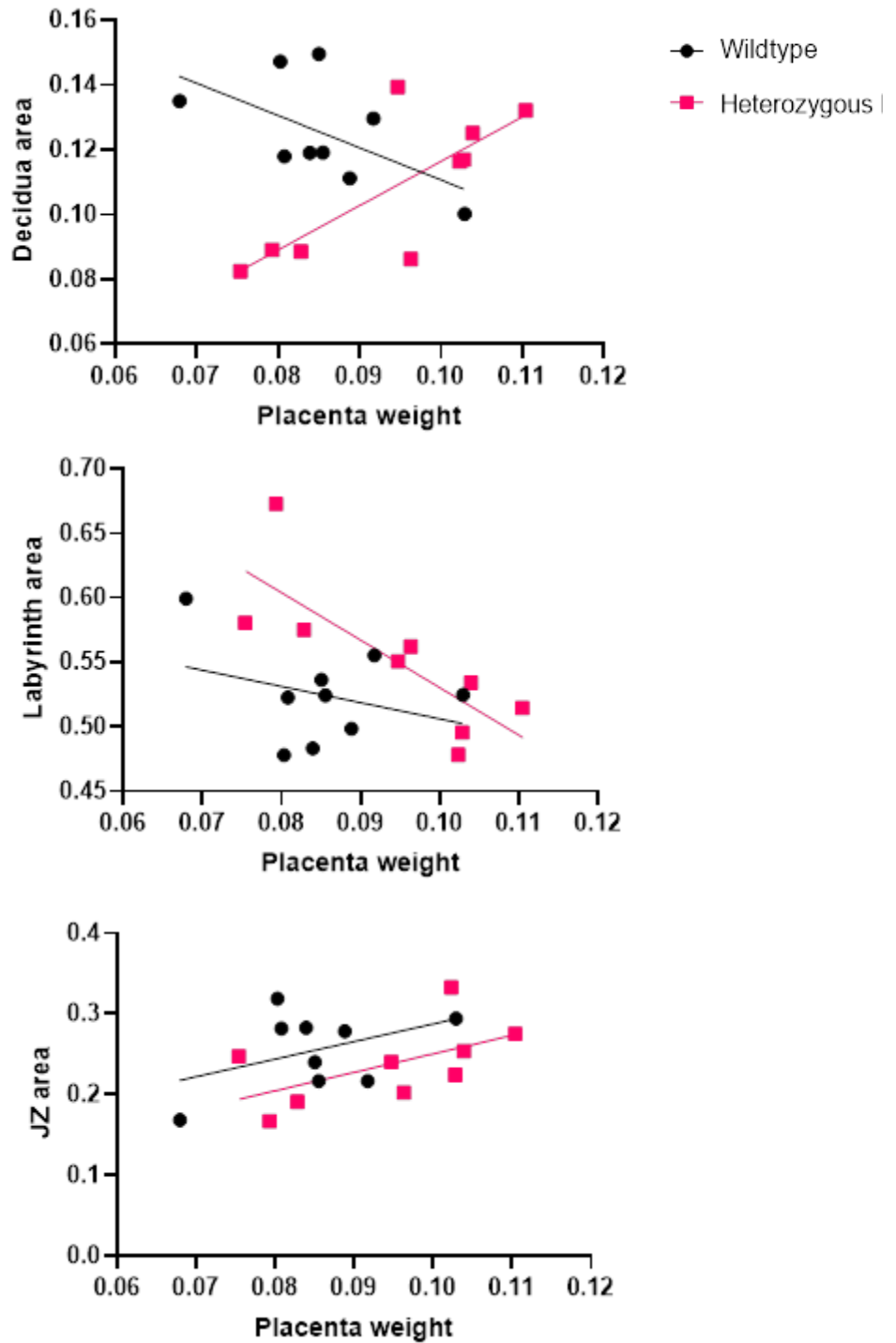
Figure 78. **Linear regression slopes comparing heterozygous (pink) and wildtype (black) placental weight versus placental section areas (labyrinth, junctional zone and decidua) as a percentage of total placenta area.**

Decidua area increases with increasing heterozygous placenta weight, compared to reduced decidua area with increasing wildtype placenta weight, P=0043. The slope of labyrinth and decidua versus placenta weight were not statistically different between heterozygous and wildtype placentas, n=9 for both.

6.3.4 Fluorescent immunohistology of the *Ryr1^{Y522S/+}* placenta

6.3.4.1 RYR1 localisation and expression

As described above, wild-type and heterozygous placentas from *Ryr1^{Y522S/+}* heterozygous dams were stained with various antibodies to study changes in functional placenta sections. RYR1 protein expression was detected in the junctional zone, as confirmed by trophoblast marker Tpbpα, demonstrated in Figure 79 to Figure 82. The mean RYR1 fluorescence intensity of the whole placenta area was not statistically different between heterozygous placenta sections (20.52±0.8651, n=49 sections, 10 heterozygous placentas) and wild-type placenta sections, (20.52±0.9935, n=40 sections, 10 wild-type placentas), P=0.9959 (unpaired two-tailed t-test), indicating that there was no change in RYR1 expressing cell population between wild-type and Y522S heterozygous placenta midline sections.
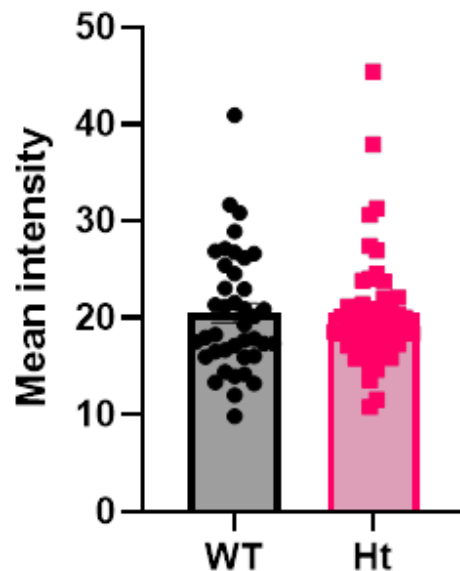
Figure 79. **Mean anti-RYR1 fluorescence intensity in wild-type and heterozygous placentas from heterozygous (mixed litter) mothers on gestation ay 18.5**

Mean fluorescence intensity in anti-RYR1 stained heterozygous placenta sections was not statistically different compared to wild-type placenta midline sections from 10 wild-type placentas (40 sections), and 10 Y522S heterozygous placentas (49 sections). P=0.9959, unpaired two-tailed t-test. Data presented as mean ± SEM.
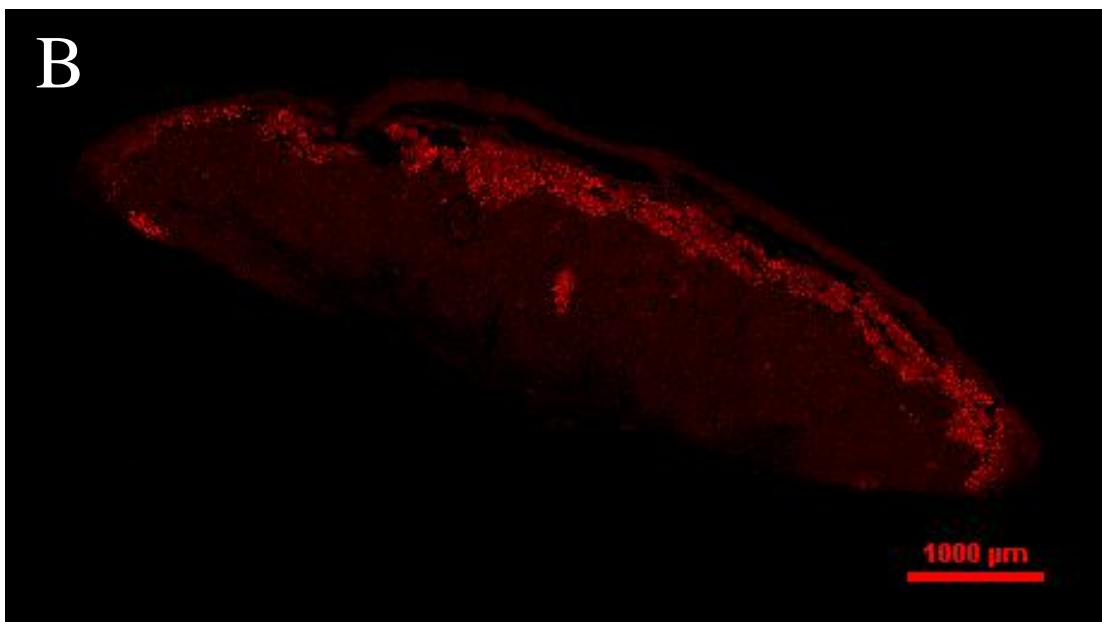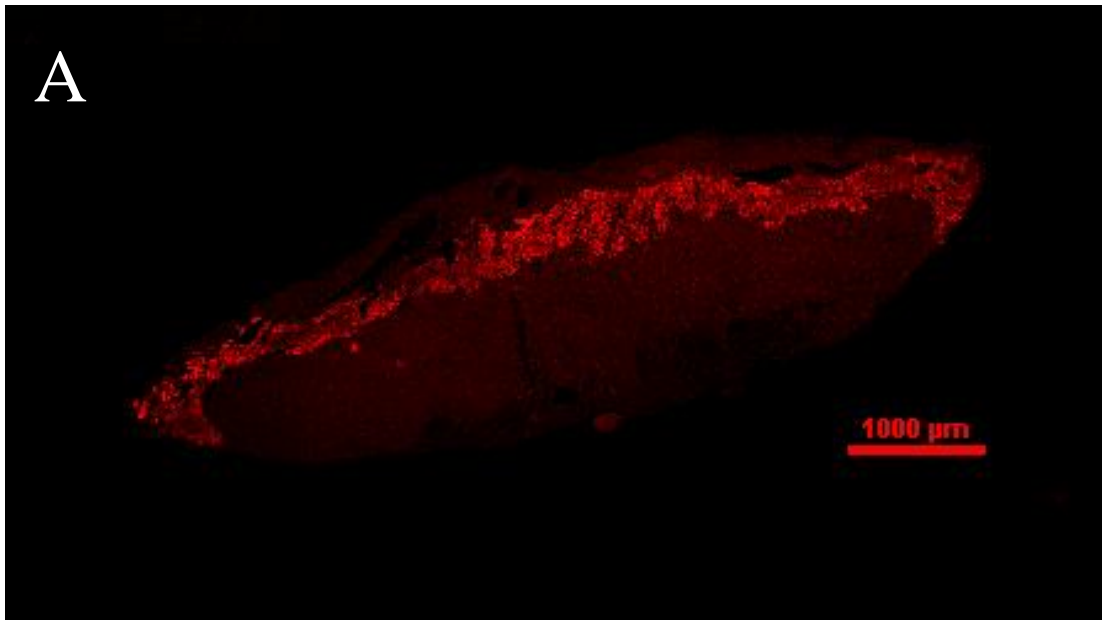
Figure 80. **Representative images of RYR1-positive immunofluorescent stained (A) wild-type and (B) heterozygous gestation day 18.5 placentas.**

(**A**) Wild-type (n=40 sections, 10 wild-type placentas) (**B**) and heterozygous (n=49 sections, 10 heterozygous placentas) midline placental cross-sections collected from pregnant heterozygous (mixed litter) dams on gestation day 18.5. Anti-RYR1 (1 in 100) stain. Cy3 200ms exposure time, 11 x 11 fields, 15% overlap stitched by blending, 10X magnification. Scale bar=1000 µm.

6.3.4.2 Junctional zone development

The JZ largely consists of several types of trophoblasts including glycogen cells, parietal giant cells, and spongiotrophoblast cells after E12.5 (Georgiades *et al.*, 2001; Coan, Ferguson-Smith and Burton, 2005; Coan *et al.*, 2006; Fowden, 2012; Sarkar *et al.*, 2014; Woods, 2018). The spongiotrophoblast-tagging tpbpα-antibody revealed a higher mean fluorescence intensity in heterozygous placenta sections (28.86 ± 1.218, n=49 sections, 10 heterozygous placentas), compared to wild-type placenta sections, (24.80 ± 1.422, n=43 sections, 10 wild-type placentas), P=0.0320, unpaired two-tailed t-test.
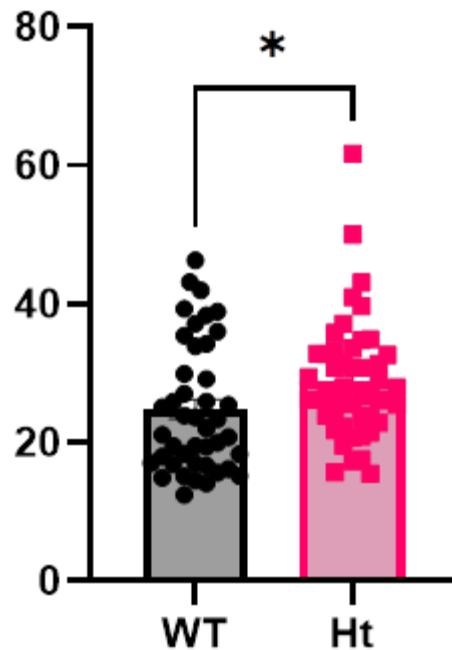
Figure 81. **Mean anti-Tpbpα fluorescence intensity in wild-type and heterozygous from heterozygous (mixed litter) mothers on gestation ay 18.5**

Mean fluorescence intensity in anti-Tpbpα stained heterozygous placenta midline sections was higher compared to wild-type placenta midline sections from 10 wild-type placentas (43 sections), and 10 Y522S heterozygous placentas (49 sections). P=0.0320, unpaired two-tailed t-test. Data presented as mean ± SEM.
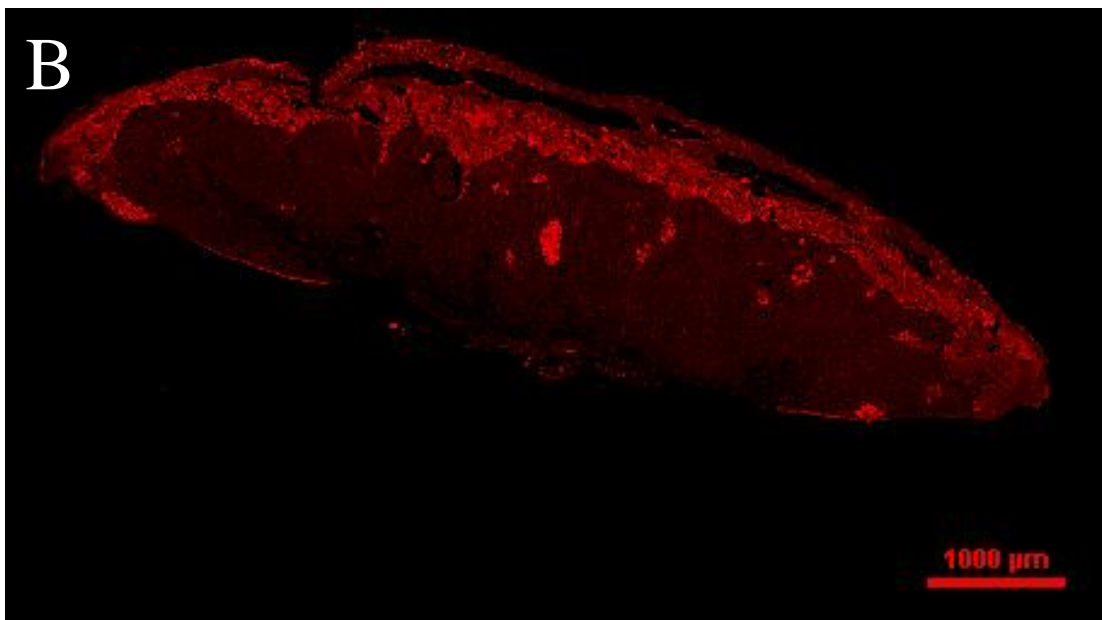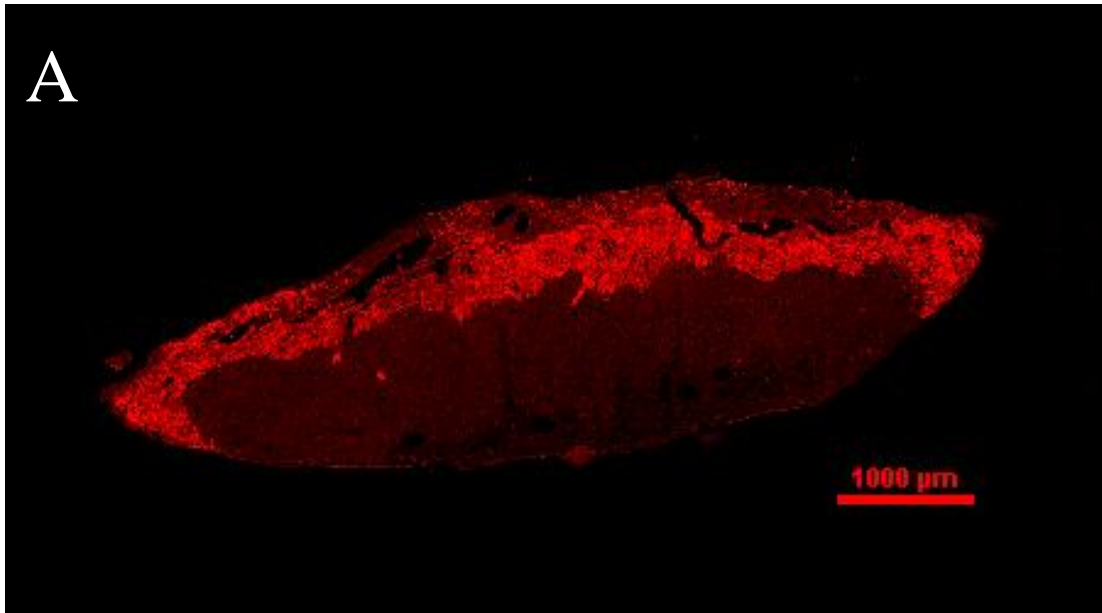
Figure 82. **Representative images of Tpbα-positive immunofluorescent stained (A) wild-type and (B) heterozygous gestation day 18.5 placentas.**

(**A**) Wild-type (n=43 sections, 10 wild-type placentas) (**B**) and heterozygous (n=49 sections, 10 heterozygous placentas) placental cross-sections collected from pregnant heterozygous (mixed litter) dams on gestation day 18.5. Anti-tpbpα (1 in 500) stain. Cy3 200ms exposure time, 11 x 11 fields, 15% overlap stitched by blending, 10X magnification. Scale bar=1000 μm.

6.3.4.3 Development of labyrinth

Mean fluorescent intensity of anti-Mct4, a marker of the fetal side of the two cell-layered syncytiotrophoblast, was not statistically different between heterozygous placenta sections (16.02 ± 0.9450, n=38 sections from 8 heterozygous placentas), and wild-type placenta sections (14.82 ± 0.8950, n=37 sections from 10 wild-type placentas), P=0.3623, unpaired two-tailed t-test.
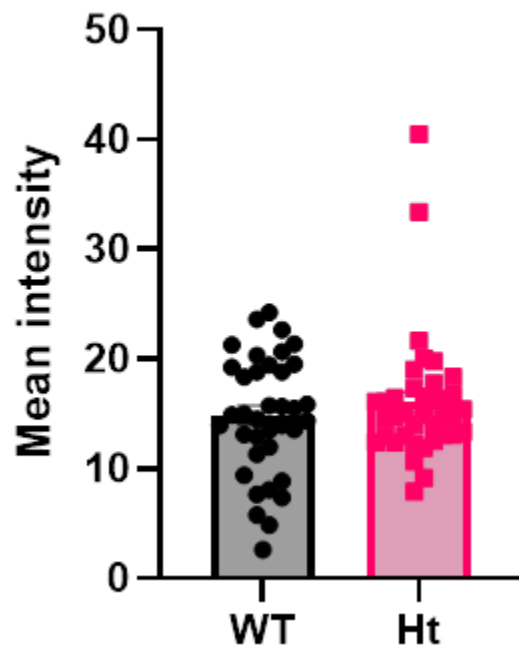
Figure 83. **Mean anti-Mct4 fluorescence intensity in wild-type and heterozygous from heterozygous (mixed litter) mothers on gestation day 18.5.**

Mean fluorescence intensity in anti-mct4 stained heterozygous placenta midline sections was not statistically different compared to wild-type placenta midline sections from wild-type (37 sections, 10 wild-type placentas), and heterozygous placentas (38 sections, 8 heterozygous placentas). P=0.3623, unpaired two-tailed t-test. Data presented as mean ± SEM.
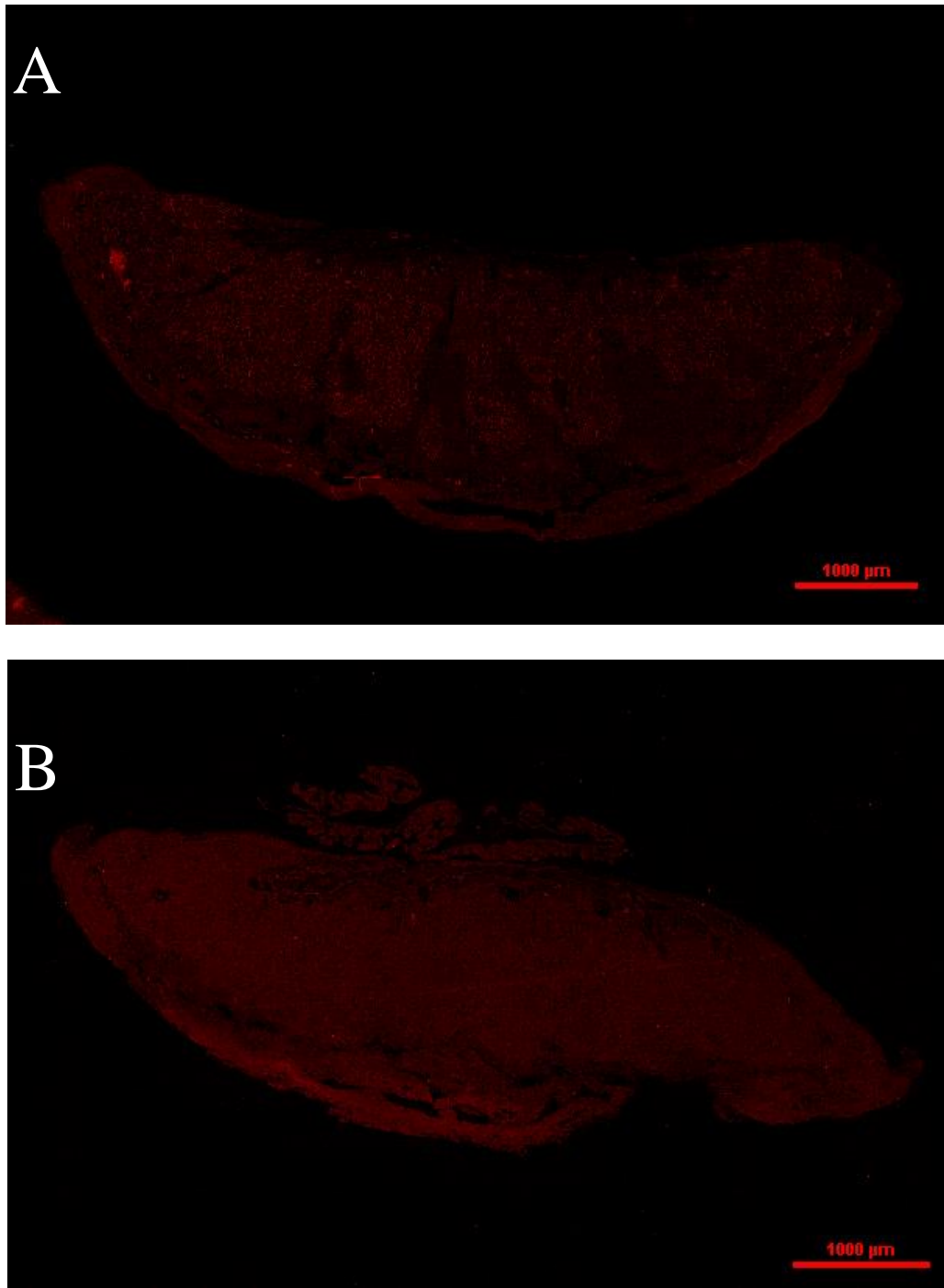
Figure 84. **Representative images of Mct4 immunofluorescent stained wild-type and heterozygous gestation day 18.5 placentas.**

(**A**) Wild-type (n=37 sections from 10 placentas) and (**B**) heterozygous (n=38 sections from 8 placentas) placental cross-sections collected from pregnant heterozygous dams on gestation day 18.5. Anti-Mct4 (1 in 200) stain. Cy3 200ms exposure time, 11 x 11 fields, 15% overlap stitched by blending, 10X magnification. Scale bar=1000 µm.

297

6.3.4.4 Cellular growth and proliferation

An antibody against proliferation marker Ki-67, was used to detect cellular division and proliferation. The mean anti-ki67 fluorescence intensity was not significantly different between heterozygous placenta sections 18.01 ± 0.6793 (n=44 sections, 9 heterozygous placentas), and wild-type placenta sections, 18.32 ± 0.9646 (n=40 sections, 10 wild-type placentas), P=0.7916, unpaired two-tailed t-test.

Ki67-positive cells as a percentage of total placental cells determined by DAPI-positive cell count, were not statistically different between heterozygous ($2.045 \pm 0.1760\%$, n=43 sections, 9 placentas) and wild-type ($2.985 \pm 0.4797\%$, n=20 sections, 4 placentas) placenta, P=0.0781. (Welch's two-tailed t-test).
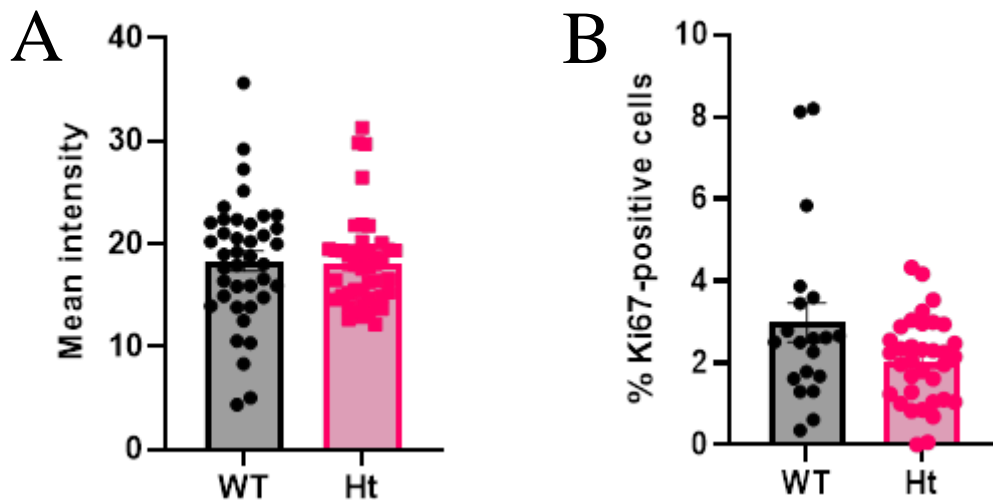
Figure 85. **(A) Mean anti-Ki67 fluorescence intensity and (B) percentage of ki67-positive cells in wild-type and heterozygous from heterozygous (mixed litter) mothers on gestation day 18.5.**

(**A**) Mean fluorescence intensity in anti-ki67 stained heterozygous placenta midline sections was not significantly different compared to wild-type placenta midline sections from 10 wild-type placentas (40 sections), and 9 Y522S heterozygous placentas (44 sections). P=0.7916, unpaired two-tailed t-test. (**B**) The percentage of Ki-67 positive cells of total DAPI stained cells were not statistically different between heterozygous (n=43 sections, 9 placentas) and wild-type (n=20 sections, 4 placentas) placentas, P=0.0781 (two-tailed t-test). Data presented as mean ± SEM.
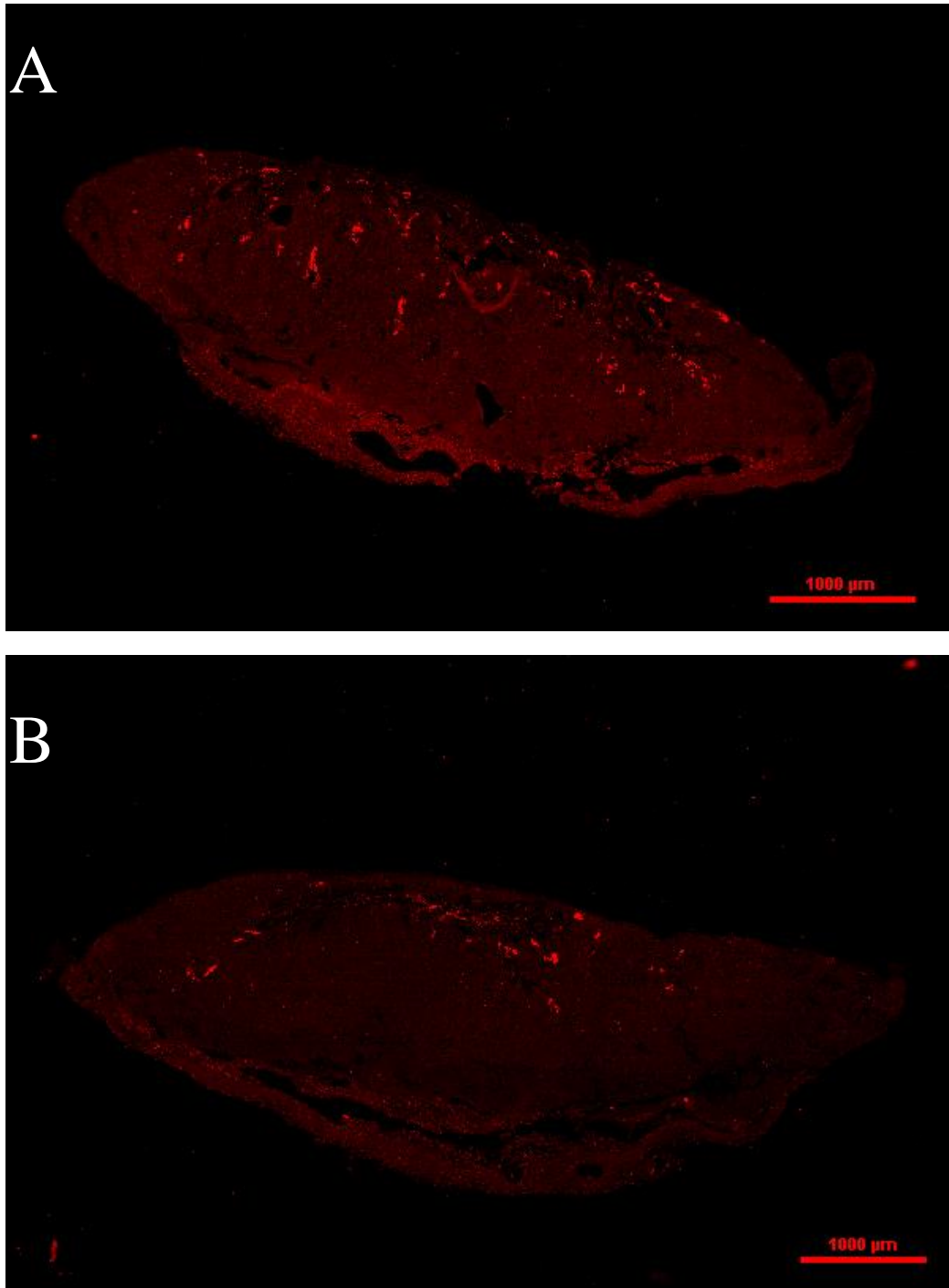
Figure 86. **Representative images of Ki67-positive immunofluorescent stained wild-type and heterozygous gestation day 18.5 placentas.**

(**A**) Wild-type (n=40 sections, 10 placentas) (**B**) and heterozygous (n=44 sections, 9 placentas) placental cross-sections collected from pregnant heterozygous (mixed litter) dams on gestation day 18.5. Anti-ki67 (1 in 100) stain. Cy3 200ms exposure time, 11 x 11 fields, 15% overlap stitched by blending, 10X magnification. Scale bar=1000 µm.
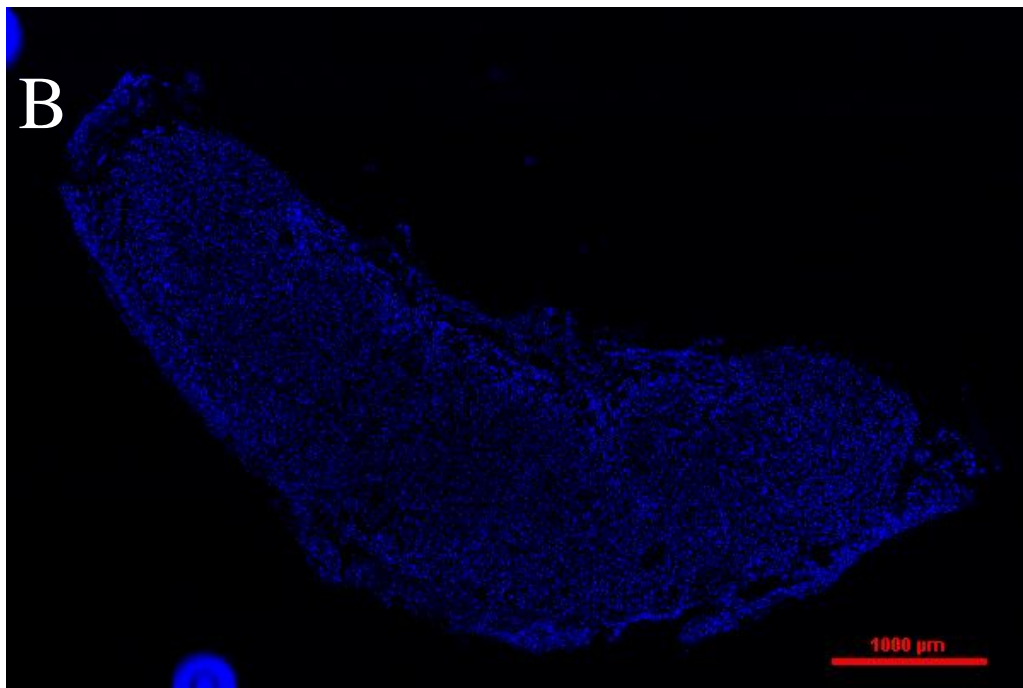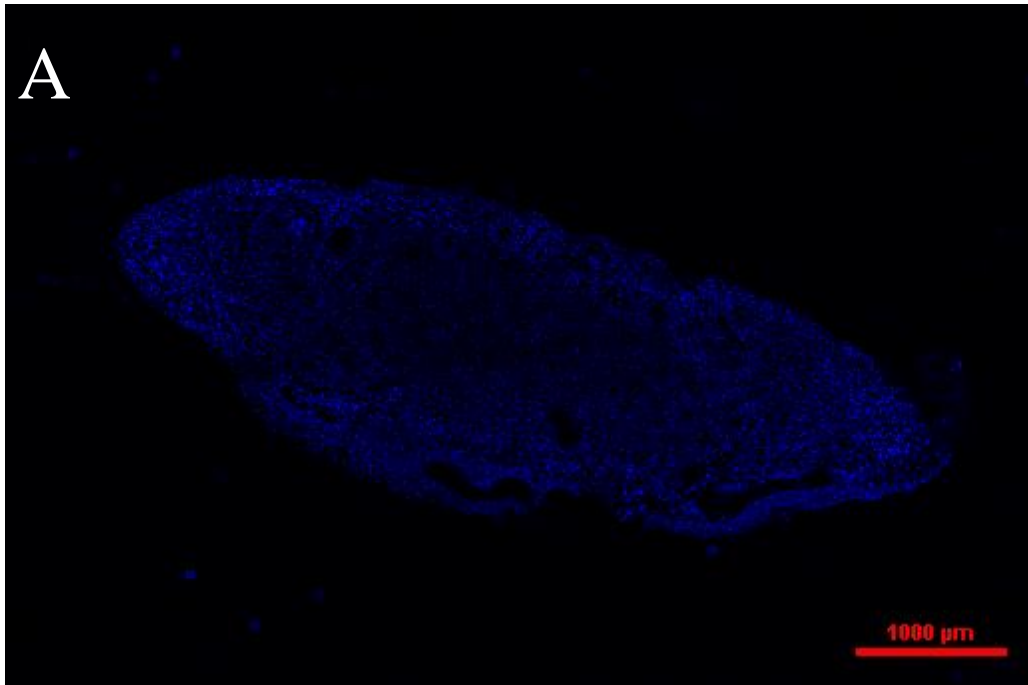
Figure 87. **Representative images of DAPI-positive immunofluorescent stained (A) wild-type and (B) heterozygous gestation day 18.5 placentas.**

(**A**) Wild-type (**B**) and heterozygous placental cross-sections collected from pregnant heterozygous (mixed litter) dams on gestation day 18.5. DAPI stain. DAPI 20ms exposure time, 11 x 11 fields, 15% overlap stitched by blending, 10X magnification. Scale bar=1000 µm.
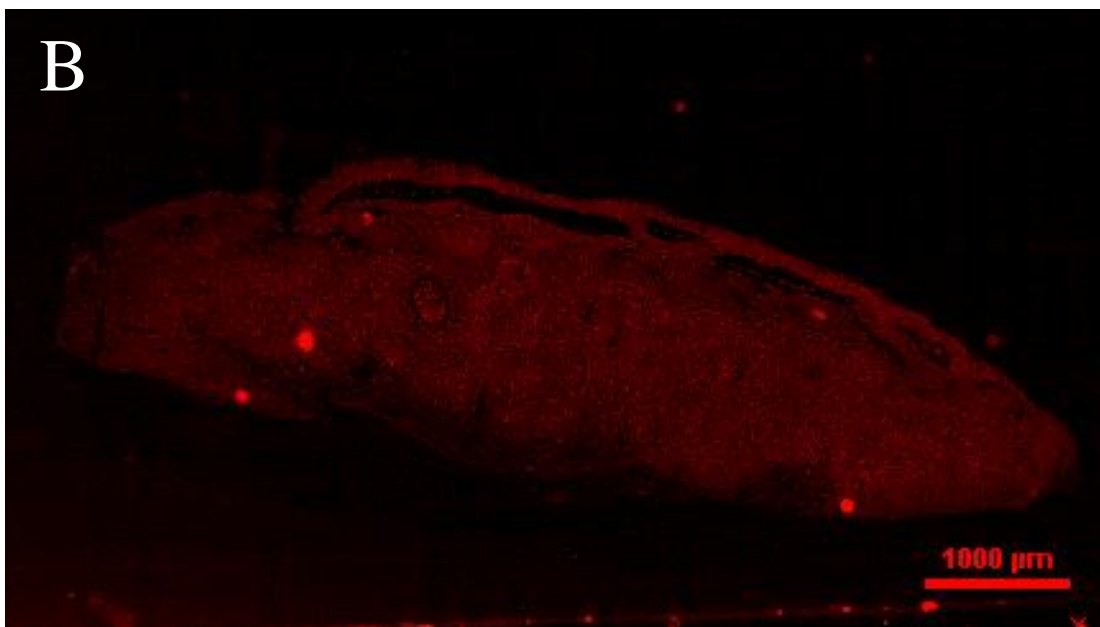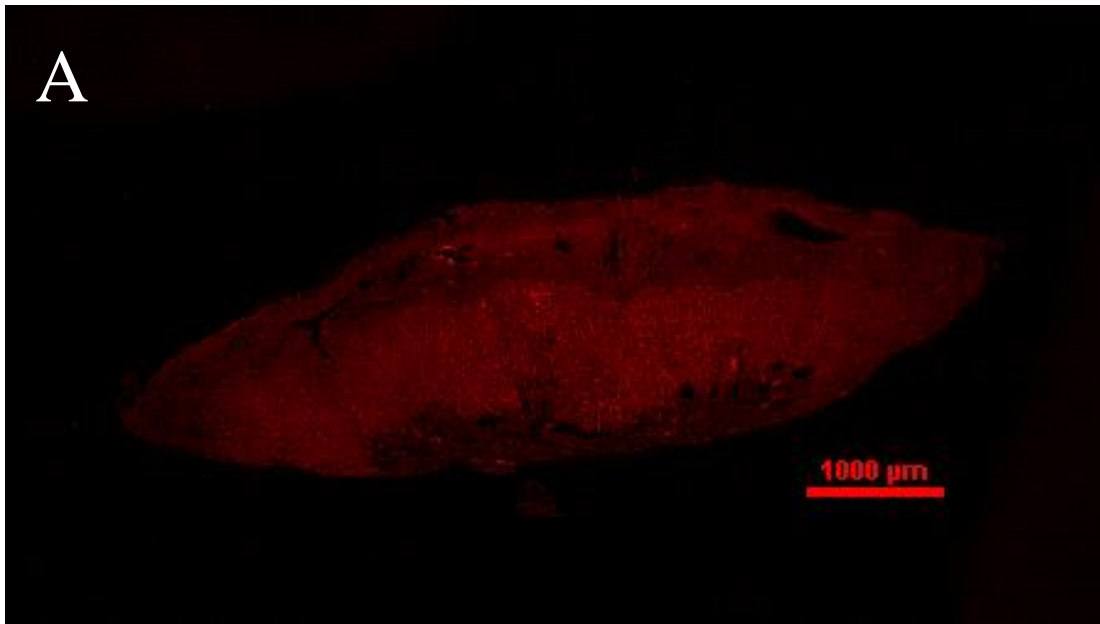
Figure 88. **Representative images of Rabbit isotype control immunofluorescent stained (A) wild-type and (B) heterozygous gestation day 18.5 placentas.**

(**A**) Wild-type (**B**) and heterozygous placental cross-sections collected from pregnant heterozygous (mixed litter) dams on gestation day 18.5. Anti-rabbit isotype (1 in 200) stain. Cy3 200ms exposure time, 11 x 11 fields, 15% overlap stitched by blending, 10X magnification. Scale bar=1000 μm.

6.3.5 Altered mRNA expression in the $Ryr1^{Y522S/+}$ placenta

Ryr1, *Ryr2* and *Ryr3* mRNA copy number were investigated in total RNA from whole wild-type (n=9) and heterozygous (n=9) placentas from gestation day 18.5 heterozygous (mixed litter) dams using RT-qPCR methods previously described in section 3.6.3. *Ryr1* mRNA copy number expression was not statistically different between heterozygous (1.166 ± 0.03134) and wild-type (1.133 ± 0.07536) placentas, P=0.6879. *Ryr2* mRNA expression was also not statistically different between heterozygous (0.6840 ± 0.07339) and wild-type (0.5874 ± 0.08482) placentas, P=0.4021 (unpaired t-tests), demonstrated in Figure 89. *Ryr3* mRNA was undetectable upon agarose gel analysis. Data presented as log(mean $\pm$ SEM).
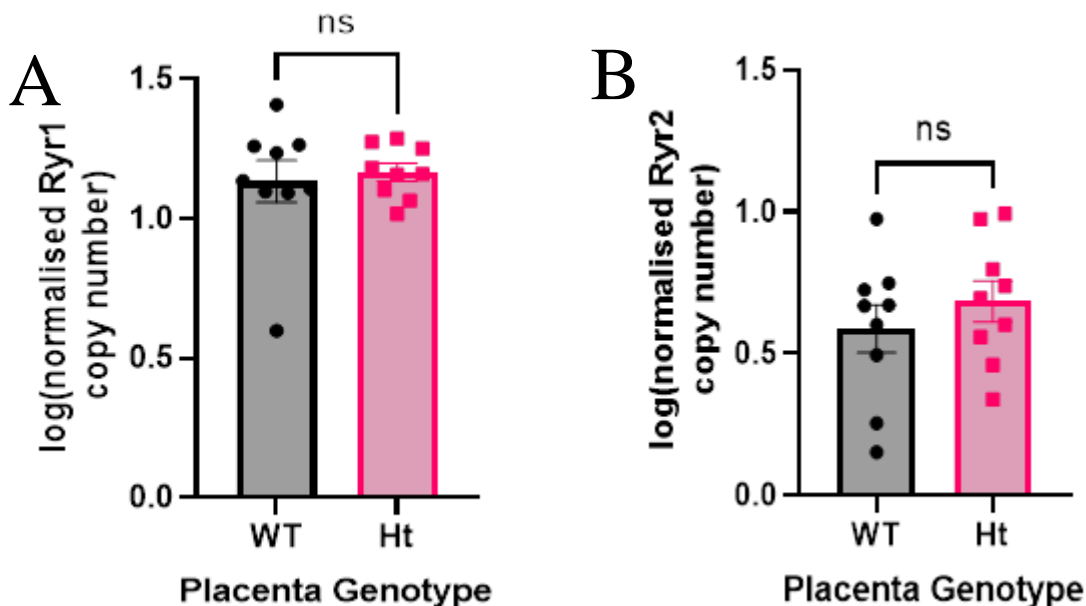
Figure 89. **(A)** *Ryr1* and **(B)** *Ryr2* mean copy number in wild-type and heterozygous $Ryr1^{Y522S/+}$ placentas from gestattion day 18.5 heterozygous (mixed litter) pregnant dams.

(**A**) *Ryr1* and (**B**) *Ryr2* copy number in total RNA from wild-type (n=9) and heterozygous (n=9) placentas from gestation day 18.5 heterozygous (mixed litter) pregnant dams were normalised to the expression of a stable reference gene. The expression of *Ryr1* and *Ryr2* mRNA were not statistically significant between wild-type and heterozygous placentas, P=0.6879 and P=0.4021, respectively (unpaired t-tests). Data presented as log(mean $\pm$ SEM).

6.3.6 RYR1 protein detection in placentas

Whole gestation day 18.5 placenta protein lysate (90 µg) from n=9 heterozygous $Ryr1^{Y522S/+}$ and 9 wild-type placentas from heterozygous $RyR1^{Y522S/+}$ (mixed litter) dams, was separated by gel electrophoresis, blotted on PVDF membrane, and with anti-RYR1 (1:500) and secondary anti-Rabbit HRP (1:2000) as described previously in section 3.7. The RYR1 protein concentration could not be determined in the mouse placenta due to the absence of signal at the expected 580kDa band size, as demonstrated by positive control skeletal tissue protein lysate in Figure 90.
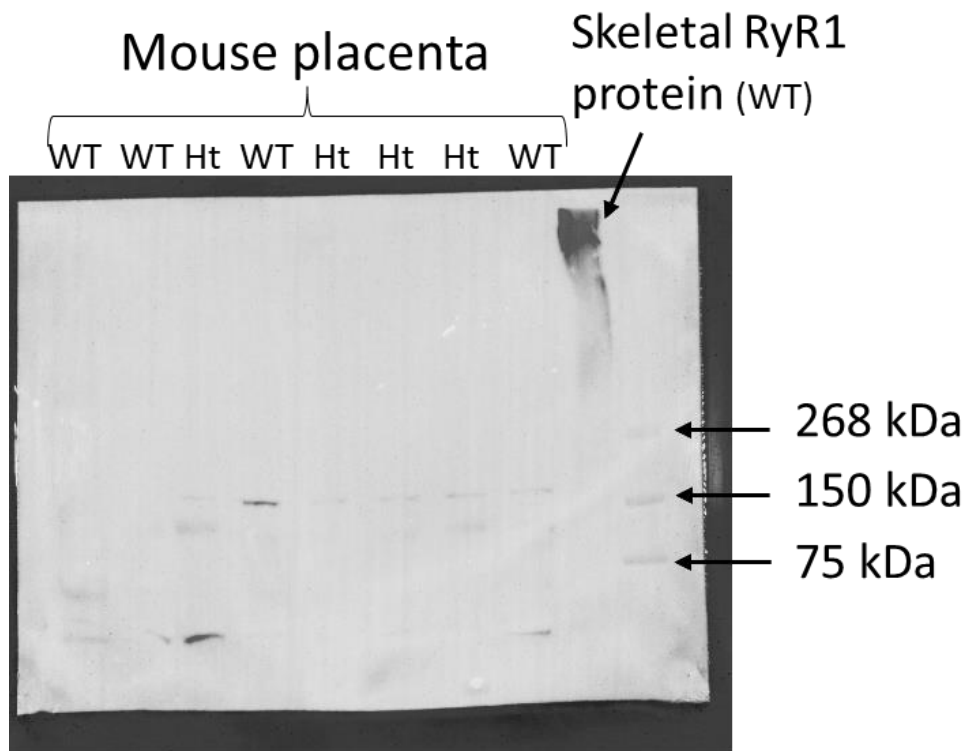
Figure 90. **A representative polyvinylidene fluoride (PVDF) blot of wild-type and heterozygous $Ryr1^{Y522S/+}$ placentas from heterozygous $Ryr1^{Y522S/+}$ (mixed litter) dams with primary RYR1 antibody**

A representative PVDF blot of mouse wild-type (n=9) and heterozygous $Ryr1^{Y522S/+}$ (n=9) placentas from gestation day 18.5 heterozygous $Ryr1^{Y522S/+}$ (mixed litter) dams with primary antibody anti-RYR1 (1:500) and secondary HRP conjugated antibody (1:2000). Placental protein lysate (90µg) diluted in 4X Laemli and 30% β-Mercaptoethanol was separated in a 4-15% TGX mini gel then blotted using the semi-dry transfer method using the Turbo blot system. Skeletal protein lysate was used as a positive control (3µg). Mouse placental RYR1 protein was not detectable.

6.3.7 Differentially expressed genes in the *Ryr1*$^{Y522S/+}$ placenta

The mRNA expression of six differentially expressed genes in gestation day 18.5 pregnant heterozygous *Ryr1*$^{Y522S/+}$ myometrial tissue, *Fcgbp*, *Ptprm*, *Psg16*, *Nmb*, *Igkv17-121*, and *Ighv2-9*, were also investigated in whole wildtype (n=9) and heterozygous (n=9) placentas from heterozygous (mixed litter) dams.

Fcgbp mRNA expression was elevated in heterozygous placentas (1.819 ± 0.0429) compared to wild-type placentas (1.590 ± 0.05477), P=0.0047 (unpaired t-test). Data presented as log(mean copy number ± SEM). *Ptprm*, *Psg16*, *Nmb* and *Igkv17-121*, mRNA expression was not statistically different between heterozygous and wild-type placentas, P>0.05, (unpaired t-tests). *Ighv2-9* mRNA was undetectable upon agarose gel analysis. The direction of changes in *Fcgbp*, *Psg16* and *Nmb* mRNA copy number expression between heterozygous and wild-type placenta tissues mirror the direction of change revealed by RNA sequencing of myometrial tissue, detailed in Table 18.

Table 18. **The direction of mRNA copy number changes in heterozygous *Ryr1*$^{Y522S/+}$ placentas compared to wild-type placental tissues for genes *Fcgbp*, *Ptprm*, *Psg16*, *Nmb*, and *Igkv17-121,* determined by RT-qPCR**

Differentially expressed genes	RNAseq log2FoldChange	RNAseq direction of change	RT-qPCR direction of change
FCGBP	1.92	+	+
PSG16	5.19	+	+
NMB	0.50	+	+
IGKV17-121	-3.17	-	+
PTPRM	-0.36	-	+
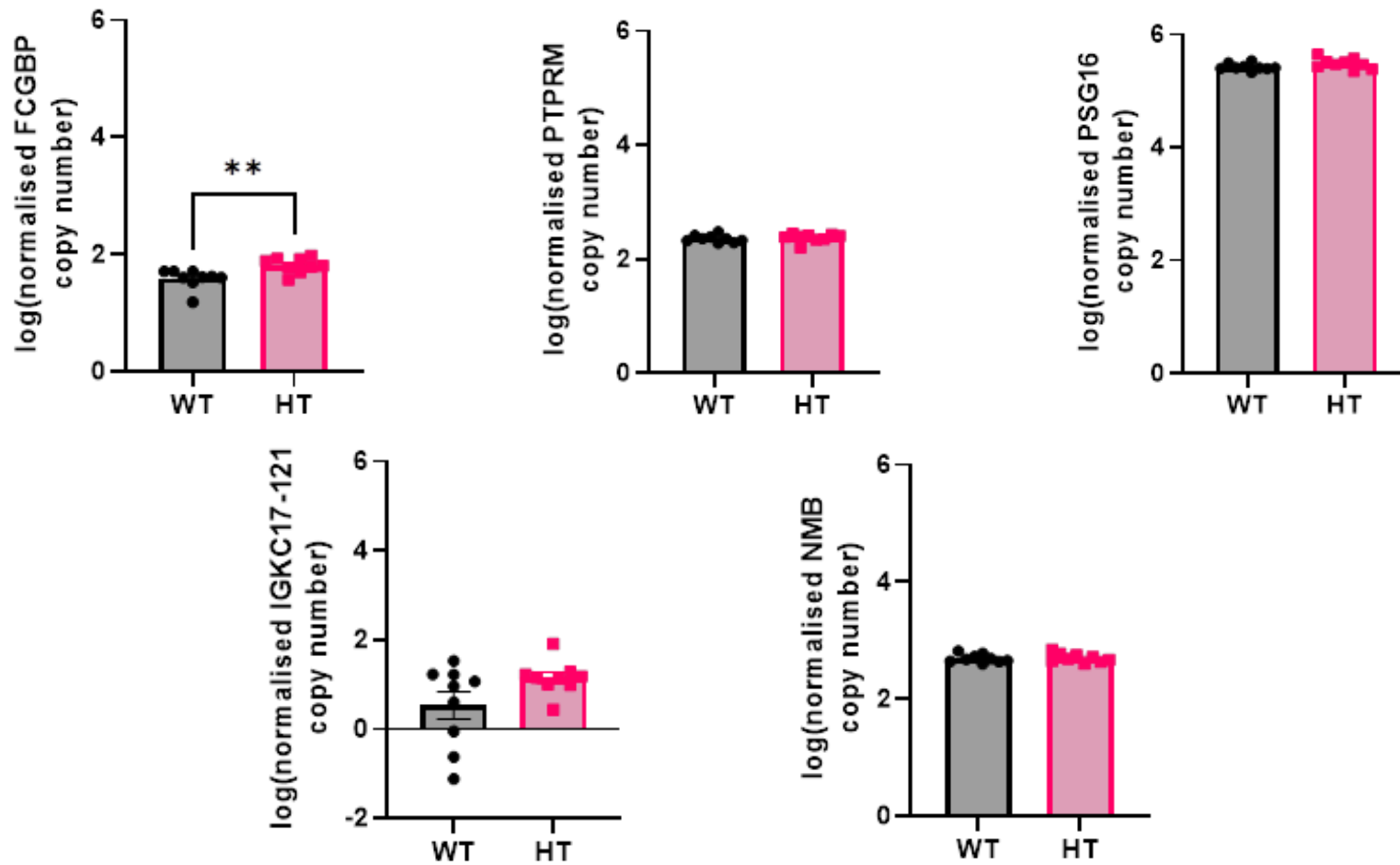
Figure 91. **Mean copy number of differentially expressed genes previously discovered in the heterozygous myometrium by RNA sequencing, investigated in wild-type (WT) and heterozygous *Ryr1^{Y522S/+}* (HT) placentas from gestation day 18.5 heterozygous *Ryr1^{Y522S/+}* (mixed litter) dams.**

Fcgbp, Ptprm, Psg16, Nmb and *Igkv17-121* mRNA copy number in total placental RNA from gestation day 18.5 wildtype (WT, n=9) and heterozygous (HT, n=9) placentas. The mRNA expression *Fcgbp* was increased heterozygous placentas compared to wild-type placentas, P=0.0047. The expression of *Ptprm, Psg16, Nmb,* and *Igkv17-121* mRNA were not statistically different between heterozygous and wild-type placentas, P>0.05 (unpaired t-test). Data presented as log(mean ± SEM).

305

6.4   Discussion

The aim of this study was to determine if the maternal and fetal *Ryr1* Y522S mutation impacts fetal and placental development. In summary, I found that at gestation day 18.5 pregnant heterozygous (mixed litter) dams had poorer placental efficiency as indicated by lower weight fetuses, heavier placentas, and lower f:p, compared to wildtype (wildtype litter) dams. This is unlikely to be due to changes in litter size as heterozygous mothers had fewer fetuses in a litter, which would not typically result in lower weight fetuses (Cowley *et al.*, 1989). Such differences are likely due to the maternal *Ryr1*$^{Y522S/+}$ genotype as it appeared that the fetal genotype did not effect the weight of the respective fetus or placenta within heterozygous (mixed litter) dams and wildtype (mixed litter) dams. Although there was no statistical difference in the number of resorptions present in the litter of the heterozygous dams compared to wildtype dams with wildtype or a mixed litter, the heterozygous (mixed litter) dams tended to have an increased number of heterozygous resorptions compared to wildtype resorptions, indicating poor survival of *Ryr1*$^{Y522S/+}$ fetuses. However, this was not supported by the proportion of heterozygous to wild-type fetus genotypes present in a gestation day 18.5 litter.

Histological investigations of placentas from heterozygous *Ryr1*$^{Y522S/+}$ (mixed litter) dams revealed no change in the distinct placenta zones between heterozygous *Ryr1*$^{Y522S/+}$ placentas and wildtype placentas from the same heterozygous maternal genotype. Closer inspection of the heterozygous labyrinth revealed an apparent less densely packed labyrinth and an increased number of blood-filled vessels on cross-sections compared to wildtype placentas, although this was observational rather than statistically analysed. Immunofluorescent imaging confirmed the presence of RYR1 protein in the placental junctional zone. Although there was not a statistical difference in RYR1 protein content or localisation between heterozygous and wild-type placentas, there was an increased trophoblast-specific (anti-tpbpα) stain in the heterozygous

placenta, indicating increased endocrine function, potentially due to increased Ca^{2+} release into the $Ryr1^{Y522S/+}$ trophoblast cell cytoplasm. Differentially expressed genes in the pregnant $Ryr1^{Y522S/+}$ myometrium, *Fcgbp, Psg16,* and *Nmb* also increased in mRNA copy number in heterozygous $Ryr1^{Y522S/+}$ placentas, albeit not all were statistically different, but provides critical information on the potential downstream effect of RYR1 overactivation.

The wildtype (mixed litter) dam was used to better understand the impact of maternal or fetal $Ryr1^{Y522S/+}$. These animals were more likely to have wildtype resorptions, however the remainder of fetal and placental outcomes in this model of pregnancy remained closer to the outcomes of wildtype (wildtype litter) dams than heterozygous (mixed litter) dams, indicating little or no impact of the fetal genotype in fetal outcomes presently studied. It's possible that increased wildtype resorptions in wildtype (mixed litter) dams and increased heterozygous resorptions in heterozygous (mixed litter) litters may be due to technical errors in the processing of tissue for genotyping (i.e., tissue contamination). Such resorptions ranged from small, underdeveloped masses of fetal tissue surrounded by large blood clots, therefore remnants of maternal tissue and thus DNA could have influenced genotyping data for these resorptions. Altogether, this indicates that differences seen in the litters of the heterozygous $Ryr1^{Y522S/+}$ dams was likely due to the presence of the maternal not fetal *Ryr1* Y522S.

The remainder of this discussion is structured around each of these findings, followed by a brief consideration of study limitations and proposed future work.

Ryr1 Y522S and fetal-placental growth

The data presented in this chapter demonstrate that _Ryr1_ Y522S is associated with enhanced placental growth and fetal growth restriction. Others have reported that on embryonic day 19 the f:p ratio in C57BL/6J mice is typically ~11-14 (Coan _et al._, 2008), making f:p ratios in heterozygous(mixed litter) (f:p 9.36) and wildtype (mixed litter) dams (f:p 9.897) lower than the average at this gestational age. A larger placenta in the _Ryr1_ mutated animal could also indicate potential for larger placentas in the human _RYR1_-mutated individual. Interestingly, increased placenta weight (>1100g) has previously been associated with increased prevalence and severity of post-partum-haemorrhage (Eskild and Vatten, 2011). In light of this, a future research direction could involve the collection of human placental weights from medical registries such as NHS records along with corresponding DNA samples to check for _RYR1_ mutations using a whole genome sequencing or microarray approach.

The apparent increased number of large blood-filled vessels in placenta cross-sections and junctional zone invaginations in the placenta are likely due to enlarged placental size. A large placenta is indicative of low placental efficiency (Coan, 2008), which could explain why corresponding fetuses are lighter in weight. Furthermore, one could speculate that offspring of the _Ryr1_$^{Y522S/+}$ animal, and by extension, children of patients with _RYR1_-mutations, might be predisposed to cardiovascular and other diseases. In humans, low fetus:placenta weight ratio is associated with gestational diabetes (Lao, Lee and Wong, 1997), hyperemesis gravidarum (Vandraas _et al._, 2013), neonatal morbidity (Salavati _et al._, 2018); and in the offspring risk of cardiovascular disease and blood pressure in adulthood (Godfrey, 2002; Risnes, 2009; Matsumoto _et al._, 2020). This should be investigated in the offspring of the _Ryr1_$^{Y522S/+}$ mouse model and _RYR1_-mutated patients using measurements of validated biomarkers or medical histories for cardiovascular diseases.

Fetal survival in the *Ryr1*$^{Y522S/+}$ mouse model

The maternal *Ryr1* Y522S mutation could also negatively impact fetal survival, as evidenced by reduced litter size and potentially increased resorptions. Although the authors that generated the *Ryr1*$^{Y522S/+}$ mouse model did not report findings of reduced litter size (Chelu, 2005). Other authors have found that *Ryr1*$^{Y522S/+}$ mouse skeletal muscle fibres have increased reactive oxygen species (ROS) production via the mitochondria which is normally associated with contractile activity (Canato *et al.*, 2019). If there is also increased ROS in the pregnant *Ryr1*$^{Y522S/+}$ myometrium, this could provide an explanation for reduced litter size, considering that altered ROS can impact gestation. For example, altered ROS production has been reported to be; critical for gestation and modulating fetal development (Hiramoto, Yamate and Sato, 2017), associated with infertility in women (Lim and Luderer, 2011; Li *et al.*, 2012; Tilly and Sinclair, 2013), metabolic disturbances in developing embryos in C57BL/6 mice (Guo *et al.*, 2021) and developing follicle depletion (Sobinoff *et al.*, 2013). Considering the expression of *Ryr1* expression in the murine myometrium, uterine artery, and placenta (as discussed in previous chapters), it would be interesting to understand any potential impact of oxidative stress as a result of increased Ca^{2+} extrusion from the SR by RYR1 Y522S channels, within reproductive tissues and to determine if this impacts on fetal survival in utero or oocyte toxicity in pregnant *Ryr1*$^{Y522S/+}$ animals.

In addition, apparent increased expression of *Nmb* detected in the *Ryr1*$^{Y522S/+}$ placenta (although not statistically increased), could indicate failure of conceptus attachment to the uterine lining as another explanation for small litter size in the heterozygous *Ryr1*$^{Y522S/+}$ animal. As previously discussed in Chapter 5, in the pregnant pig endometrium increased *Nmb* expression has been suggested to play a role in failure of conceptus attachment to the uterine surface and induction of endometrial responses that disrupt the establishment of a viable pregnancy (Ross

et al., 2007). Thus, if it is proven that *Nmb* expression is increased in *Ryr1* Y522S endometrium, this could lead to the failure of conceptus attachment which may result in reduced litter size in pregnant *Ryr1*$^{Y522S/+}$ dams.

The gain-of-function *Ryr1* Y522S mutation, might also induce fetal loss via immunological mechanisms. Increased activation of the dendritic Y522S RYR1 channel has been suggested to play a role in the early stages of infection, providing a rapid immune response, and facilitating the presentation of antigens to T cells by dendritic cells before their full maturation*,* inducing an immune advantage in mouse carriers (Vukcevic *et al.*, 2008; Vukcevic, 2013). This is important considering that the activation of dendritic cells has also been suggested to play a role in the initiation of fetal loss in mice (Negishi et al., 2018). This indicates the potential for an immunological mechanism of fetal loss in the pregnant *Ryr1*$^{Y522S/+}$ animal, however more research is needed to support this theory.

Placental morphology in the *Ryr1* Y522S litter

In the present study, using immunofluorescent techniques I found that RYR1 protein is predominantly localised to the placental junctional zone, and RYR1 protein concentration does not differ between heterozygous *Ryr1* Y522S and wild-type placentas from the *Ryr1*$^{Y522S/+}$ pregnant animal, however RYR1 protein was undetectable in whole placental lysate using Western blotting methods. Likewise, mRNA expression of *Ryr1* and *Ryr2* was also unchanged in the *Ryr1*$^{Y522S/+}$ placenta compared to the wild-type placenta. This indicates that the gain-of-function *Ryr1* Y522S mutation does not impact the transcription or translation of *Ryr* isoforms in the placenta. Only a limited number of studies have investigated RYR1 in the mouse placenta but a recent study suggests that RYR1 protein plays a role in the regulation of human trophoblast migration, a key process in placental development (Zheng, 2022).

Heterozygous *Ryr1* Y522S placentas also exhibited more intense staining of spongiotrophoblasts with anti-Tpbpα. The junctional zone is the least understood compartment of the mouse placenta. It is endocrine in function and primarily responsible for hormone secretion, production of growth factors and cytokines, that are important for the normal progression of pregnancy (Ain, 2003; Soares, 2004; Watson, 2005). The Tpbpα cell-lineage is critical for placental function and maternal spiral artery remodelling. Specifically, ablation of Tpbpα-positive cells reduces the number of cells that associate maternal blood spaces, spiral artery TGCs and canal TGCs, and glycogen trophoblast cells, which correlates with decreased maternal spiral artery diameters (D. Hu, 2011). Therefore, increased Tpbpα-postive cell fluorescence in the Y522S placenta is indicative of increased trophoblast cell association with maternal blood spaces, and therefore increased spiral artery diameter and increased blood flow to the placenta.

RYR1 and RYR3 proteins have previously been detected in cytotrophoblasts and syncytiotrophoblasts of human first trimester and term placental villi (Haché, 2011; Zheng, 2022). These authors reported that trophoblasts contain a collection of proteins similar to those cell types possessing highly developed Ca^{2+} signal transduction systems, such as skeletal muscle, and that RyRs contribute to reorganization of the F-actin cytoskeleton in response to angiotensin II. Therefore, RYR1 channel based Ca^{2+} signalling and their accessory proteins (triadin and calsequestrin) may be involved in migration of trophoblast cells, a process that plays a key role in development of the placenta (Zheng, 2022). Calcium homeostasis and transport through the placental syncytiotrophoblast as a result of altered expression of calcium transport proteins, including decreased RYR1 expression, is associated with preeclamptic pregnancies, and appears to be affected by lack of ATP and excess oxidative stress (Haché, 2011). The findings from this study, further supports a role for RYR1 in normal placentation and maternal vascular remodelling in the placenta.

Ryr1 Y522S and placental labyrinth development

From the literature it is known that the labyrinth zone volume increases during the second half of pregnancy, and it is the main exchange point for nutrient transfer in the mouse placenta during late gestation (Coan, 2004). The labyrinth is structured with maternal cells grouped in blood sinuses of the spongiotrophoblasts, and fetal cells are organised in rings surrounding the blood sinuses (Vernochet, Caucheteux and Kanellopoulos-Langevin, 2007)..

Another interesting observation in the heterozygous *Ryr1* Y522S placenta includes an apparent underdeveloped labyrinth for gestation day 18.5, characterised by a less densely packed labyrinth with increased stromal cells and an increased avascular appearance. Although this

was not systematically analysed, this observation should be further investigated by staining fetal vascular endothelial cells, using an endomucin (EMCN) stain. Nevertheless, at gestation day 18.5, the mouse placenta should be substantially filled with fetal endothelium and therefore blood cells, whereas the younger placenta the labyrinth is less compact as the networks continues to develop (Coan, 2005). Therefore, it may be that the heterozygous *Ryr1* Y522S fetal blood vessels fail to or less efficiently invade the placental labyrinth, limiting labyrinth development.

Placental expression of differentially expressed genes

The differences in *Ptprm, Psg16, Nmb* and *Igkv17-121* mRNA expression were not statistically significant between $Ryr1^{Y522S/+}$ and wild-type placentas, however the elevated mRNA expression of *Fcgbp, Psg16,* and *Nmb,* matches the direction of mRNA expression change identified in $Ryr1^{Y522S/+}$ pregnant mouse myometrium. *This* implicates the gain-of-function *Ryr1* Y522S mutation in the upregulation of these genes, not only in the myometrium but also in the $Ryr1^{Y522S/+}$ placenta of the $Ryr1^{Y522S/+}$ pregnant animal.

Fcgbp mRNA expression was elevated in the heterozygous placenta (as it is in the pregnant heterozygous myometrium). As mentioned in Chapter 5, the Fcgbp protein forms a structural part of the intestinal mucosa (Johansson, Thomsson and Hansson, 2009), and has been suggested to play an important role in immune protection and inflammation in the intestines (Harada, 1997). Fcgbp is also expressed in human placenta (Harada, 1997), however, it is unclear what part of the placenta is the source of Fcgbp. In a cohort of women with preterm prelabour rupture of membranes (PPROM) and preterm labour with intact membranes (PTL), intra-amniotic infection was associated with elevated Fcgbp concentrations in amniotic fluid,

and in cervical fluid (only in PPROM) (Stranik, 2021). The role of Fcgbp in the placenta remains unclear, but its upregulation via increased Ca^{2+} signalling through RYR1 channels indicates an activated immune response in the $Ryr1^{Y522S/+}$ placenta.

The mRNA expression of *Psg16* was increased in the $Ryr1^{Y522S/+}$ placenta compared to wild-type placentas. As previously described, PSGs are the most abundant fetal proteins in the maternal bloodstream in late pregnancy and may play a role in placentation and vascularisation of the placenta (Lisboa *et al.*, 2011). Murine PSGs (protein and mRNA) have previously been detected in trophoblast giant cells, and spongiotrophoblasts as early as embryonic day 6.5 (McLellan, 2005). The expression of *PSG16* has previously been determined in human placental trophoblast cells, however further functional studies have not been performed (Yang Chou and Zilberstein, 1990). Human PSG1 (Ha, 2010; Lisboa, 2011) and murine PSG23 (Wu, 2008) induce endothelial tube formation and the secretion of proangiogenic factors transforming-growth factor beta 1 (TGF-β1) and vascular endothelial growth factor A (VEGF-A). TGF-β1 itself is known for its functions in immunoregulation, but during pregnancy it has been suggested to play a role in implantation, trophoblast differentiation and in the activation and resolution phases of angiogenesis (Tamada *et al.*, 1990; Irving and Lala, 1995). Furthermore, certain Psgs may be associated to maternal vasculature, a study reports that Psg proteins predominantly associated with endothelial cells lining maternal vascular channels in the decidua, rather than with maternal immune cell markers (Wynne et al., 2006). Therefore, *Ryr1* Y522S could impact placental implantation and vascularisation through interactions or regulation of Psg16 and related Psg proteins. The detection of increased Psg16 may be heightened due to possibly increased maternal vasculature in the $Ryr1^{Y522S/+}$ placenta of the $Ryr1^{Y522S/+}$ pregnant animal.

6.5 Study limitations and future work

The impact of *Ryr1^{Y522S/+}* on fetal weight should also be examined with regards to the influence of fetal sex. Sex-specific differences in offspring have repeatedly been reported in studies of developmental origins of health and disease (Tarrade *et al.*, 2015; Eriksson *et al.*, 2018; Sato *et al.*, 2019; Tekola-Ayele *et al.*, 2019). Fetal sex has been known to determine minor but significant differences in fetal weight. Specifically, male fetuses tend to be larger than females between gestation day 11.5 to 17.5 (Ishikawa *et al.*, 2006). This sex-specific different was not investigated in this study but should be investigated using stored fetal DNA to fully understand the impact of *Ryr1^{Y522S/+}* on fetal/placental weight.

In this study, paraformaldehyde fixed placenta cross-sections were stained with haematoxylin and eosin to investigate placental structure. Formalin acts by diffusing through tissue and binding to amino groups, producing a network of cross-linked proteins and nucleic acids, causing cell shrinkage and distortion (Hsu *et al.*, 2007). These cellular changes can have a global impact on whole tissue specimens, causing shrinkage in varying amounts (2.7-20%) (Boonstra *et al.*, 1983; Siu, Cheung and Wong, 1986; Johnson *et al.*, 1997; Watanabe *et al.*, 2004; Palaia *et al.*, 2011). Therefore, there may have been significant shrinkage in the placenta tissues used in this study, which could have impacted the accuracy and precision of downstream analyses.

Furthermore, it was apparent that whole placentas were too large to be imaged using a standard light microscope, instead, I utilized a widefield microscope which enabled stitching of several fields using a blending method, constricted to 15%. This method of joining via blending is known to have limited accuracy, thus further influencing the accuracy of downstream analyses. In addition, the chosen method of two-dimensional placental section analysis was constrained due to human error and inaccuracy in identification of boundaries between junctional zone,

labyrinth, and decidua areas. Other studies have reported successfully utilizing a combination of resin-embedding (to reduce shrinkage and improve resolution to better identify boundaries and cell types), and stereology, (to generate three-dimensional quantities, such as, volumes and surface area from two-dimensional sections) to quantitatively describe mouse placentas (Coan, 2004). It could be beneficial to utilise the above-mentioned methods in future studies of the $Ryr1^{Y522S/+}$ placenta sectional areas.

As previously mentioned, to further study development of the labyrinth, an endo-mucin stain for fetal blood vessel membrane should be considered. This may help to determine precisely how the fetal placental vasculature might be altered in the labyrinth of heterozygous $Ryr1^{Y522S/+}$ placentas. Further to this, placentas of wildtype (wil-type litter) and wild-type (mixed litter) pregnant dams should also be histologically studied in comparison with placentas from heterozygous (mixed litter) dams, to determine whether maternal $Ryr1^{Y522S/+}$, fetal $Ryr1^{Y522S/+}$ or a combination of both mutation carriers may impact fetal and placental growth.

In addition, studies have shown that multiple abnormalities in placental development not only appear at the end of gestation but also appear in early pregnancy (gestation day 5-8), in addition to alterations in embryo implantation and decidualization (Yang *et al.*, 2021). Therefore, to investigate alterations in intrauterine development in the $Ryr1^{Y522S/+}$ mouse model, it may prove beneficial to study fetal and placental development through various stages of pregnancy.

6.6 Conclusions

It is apparent that maternal $Ryr1^{Y522S/+}$ results in reduced fetal survival, restricted fetal development and irregular placental development, specifically underdeveloped labyrinth zones and overactive junctional zones leading to reduced placental efficiency which may be exacerbated in the $Ryr1^{Y522S/+}$ fetus. Looking at this data together I conclude that the mouse *Ryr1* Y522S mutation disrupts Ca^{2+} homeostasis which could lead to altered trophoblast cell movement, cellular oxidative stress, and expression of immune response genes which leads to fetal loss, enhanced placental and restricted fetal growth.

7 Chapter 7 Assessment of an abnormal bleeding and obstetric history in carriers of *RYR1* variants

7.1 Background

Mutations in *RYR1* have been associated with a wide-spectrum of neuromuscular disorders, ranging from early-onset congenital myopathies to malignant hyperthermia susceptibility (MHS) and related disorders. The prevalence of pathological *RYR1* mutations in the population is expected to be present in at least 1 in 2000 individuals (Monnier, 2002).

Whilst the expression of *RYR1* has been reported in various human and murine tissues, the non-neuromuscular phenotypes associated with *RYR1* are rarely reported or recognised. Such phenotypes are potentially due to the altered function of vascular smooth muscles, the immune system, and the central nervous system, as outlined in Chapter 1. Previously, a small cohort of *RYR1*-mutated patients have been reported to have a mild bleeding abnormality, with symptoms related to menorrhagia, post-partum haemorrhage and gum-bleeding in human patients, which aligns mechanistically with the observation that the heterozygous knock-in $Ryr1^{Y522S/+}$ mouse model of MH, display prolonged tail artery bleeding times that were reversed by dantrolene pre-treatment (Lopez, 2016).

Typically, 5-24% of the female population present with menorrhagia (Shankar, 2004). Whilst known bleeding disorders, platelet-dysfunction, ovulatory-dysfunction may account for a percentage of women with heavy menses or menorrhagia, of the 5% that seek medical treatment annually (Rees, 1987; Kadir, 1998; Dilley, 2001; Philipp, 2003, 2005; Borzutzky, 2020; Vannuccini *et al.*, 2022), approximately 50% are left with unexplained menorrhagia because of the failure to identify a definite pathology (Lee, 1984; Oehler, 2003).

To date, very little data has been collected on the non-neuromuscular phenotypes associated with *RYR1* mutations. In addition, the apparent increased bleeding tendency in female *RYR1*-muated patients and the lack of clinical diagnoses for large percentage of women seeking treatment for heavy menstrual bleeding (HMB) calls for systematically gathered information on the non-neuromuscular bleeding and reproductive outcomes in a larger cohort of females carrying pathogenic *RYR1* variants.

7.2 Methods

A questionnaire to systematically detect changes in generalised bleeding tendency, menstruation, fertility, pregnancy complications and offspring birthweight in women with pathogenic *RYR1* variants was developed. Specifically, this bleeding questionnaire explores typical bleeding events such as epistaxis, bruising, and post-operative bleeding (minus muscle hematomas, hemarthrosis, central nervous system bleeding symptoms) using questions from the validated MCMDM-1VWD questionnaire (Bowman, 2008), see Appendix 4. The questions were expanded to investigate other smooth muscle layered organs such as the GI tract and cerebral blood vessels. Questions based on the NHS heavy bleeding tool were used to determine heavy menstrual bleeding. There were additional questions to collect an extensive obstetric history (i.e., menstrual cycle length/abnormalities, fertility, recurrence of miscarriage, complications during gestation/parturition, antenatal or post-partum bleeding and offspring birthweight).

This 15-minute questionnaire was designed in an online format to overcome limitations of the COVID-19 pandemic and to ensure the maximum possible number of participants were invited to take part. Few restrictions were placed on the recruitment of participants, however, to ensure all participants could complete a menstrual cycle history a minimum age of 18 was required.

Data was analysed as described in section 3.14.8, briefly, bleeding scores were calculated according to a standard MCMDM-1VWD scoring system (Bowman, 2022) (see Appendix 5), with an abnormal bleeding score categorized as ≥4, and Fishers exact or Chi square tests were used to determine statistical significance.

Ethical approval for this study was granted by the King's College London BDM research ethics panel (reference number: LRS-20/21-22085), see Appendix 8 for notice of ethical approval. A

detailed description of questionnaire development, evaluation and ethical considerations is provided in section 3.14. See Appendix 6 and Appendix 7 for patient information sheets and Appendix 9 for an example of the full questionnaire form.

7.3 Results

7.3.1 Cohort summary

In total, 66 *RYR1* variant carriers and, 88 control participants completed the online questionnaire. Of the number of total participants, 154 were female and 1 was male (as the questionnaire was intended for females only, this participant's data was not included in analysis). The age range was 20-67 years in the *RYR1*-mutated group (median=39.00,), compared to 19-68 years in the control group (median=32.50), demonstrated in Figure 92A. Thus, the age of participants in the *RYR1*-mutated group was skewed to an older population compared to control participants. Age of participants from *RYR1*-mutated group were normally distributed P > 0.1, whereas age of participants in control group were not normally distributed P=0.003 (Kolmogorov-Smirnov test), demonstrated in Figure 92B.

The ethnicity of *RYR1*-mutated participants was distributed as 89.39% White (n=59), 4.55% Black (n=3), 4.55% Mixed/multiple ethnic groups (n=3), 1.52% Ashkenazi (n=1), demonstrated in Figure 93B, with further categorisation, see Appendix 9. The ethnicity of control participants was distributed as 77.27% White (n=68), 1.14% Black (n=1), 4.55% Mixed/multiple ethnic groups (n=4), 15.91% Asian (n=14), 1.14% Iranian (n=1), demonstrated in Figure 93A.

Of the 66 participants in the *RYR1*-mutated group, 53% (n=35) carried autosomal dominant (AD) *RYR1* variants and 19.7% (n=13) carried autosomal-recessive (AR) *RYR1* variants; the remaining 27.3% of participants did not answer the question regarding inheritance.

A total of 65 *RYR1*-mutated participants described their *RYR1*-related phenotypes, listed in Table 19, note that some participants were diagnosed with multiple disorders. The autosomal dominant *RYR1* variant carrying participants were mostly diagnosed with the following

phenotypes: MH (n=12, 26.09%), CCD (n=13, 28.26%), (exertional) rhabdomyolysis (n=4, 8.70%) and (exertional) heat illness (n=3, 6.52%). Few patients had diagnoses for congenital myopathy (without specific muscle biopsy findings) (n=2, 4.35%) and MmD and periodic paralyses (n=1, 2.17% each). The participants with autosomal recessive *RYR1* variants were diagnosed with CNM, MH and CCD equally (n=3, 21.43% each), and rarely, with congenital fibre type disproportion (CFTD), (exertional) heat illness, and periodic paralyses (n=1 or 7.14% each).

Potentially confounding medical factors

Inherited bleeding disorders were not common among either of the two groups, with two *RYR1*-mutated participants with Factor V Leiden, one participant with Factor X deficiency and one participant with Factor II (Prothrombin K) deficiency (6% of *RYR1* mutation carriers). From the control group, one participant had acquired thrombophilia and one had Factor V Leiden deficiency. Other potentially confounding medical conditions that could increase risk of abnormal bleeding, changes to menstrual cycle, infertility and miscarriage were also rare in both groups. Polycystic ovary syndrome (PCOS) and hypothyroidism was reported most often in both groups (*RYR1*-mutated n=6 or 9.09% for both conditions; control n=5 or 5.68% for PCOS and n=6 (6.82%) for hypothyroidism).

A

B
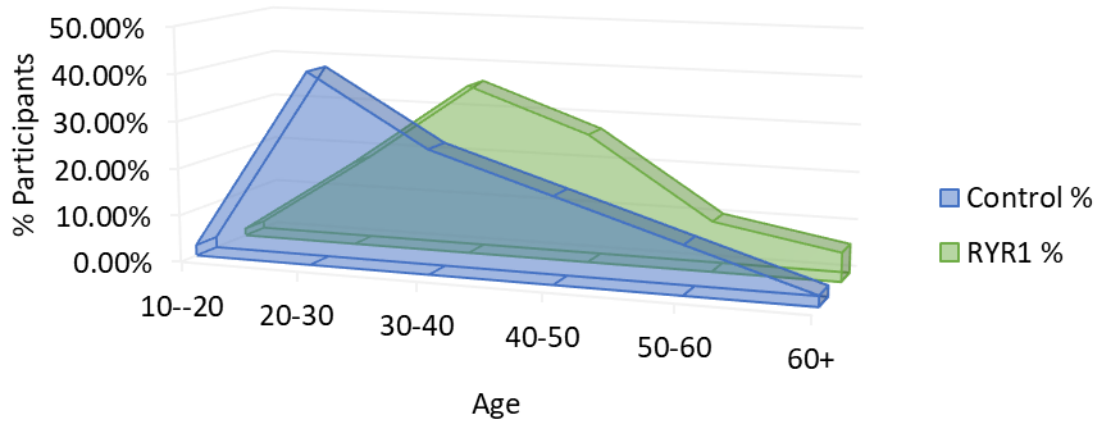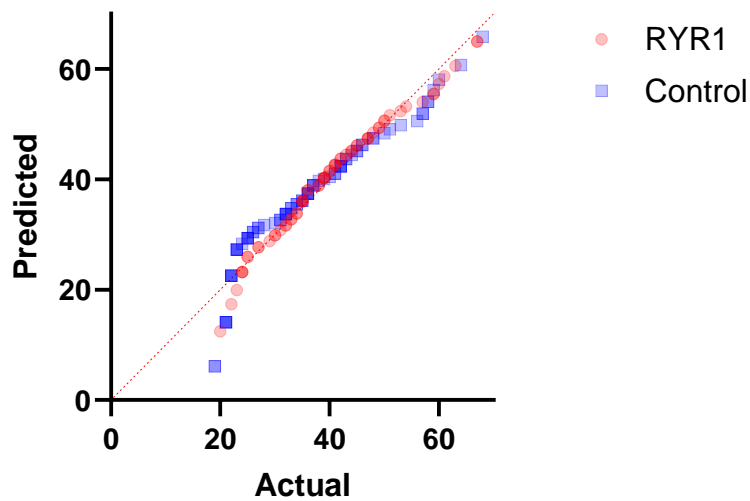
Figure 92. The distribution of age in the control and *RYR1*-mutated groups, presented as a percentage of total number of participants in respective groups.

(**A**) The age of participants in control group (blue) and *RYR1*-mutated group (green) displayed as a three-dimensional area chart. Ages are grouped by increments of 10 years starting from 10 to 60 + years of age (**B**) QQ plot displaying distribution of control and *RYR1*-mutated group participant ages. Age of participants from *RYR1*-mutated group were normally distributed P > 0.1, whereas the age of participants in control group were not normally distributed P=0.003 (Kolmogorov-Smirnov test).
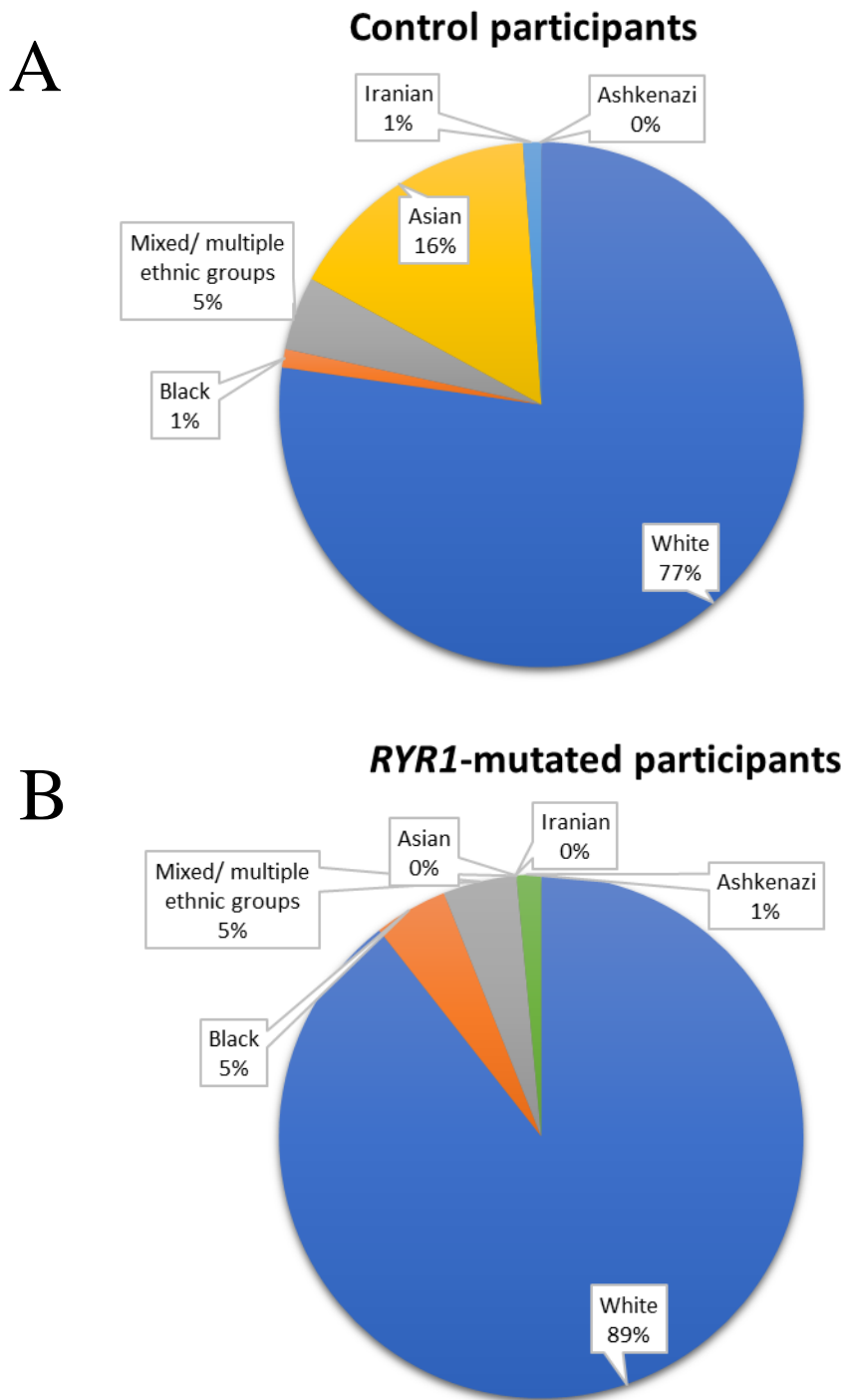
Figure 93. Ethnicity distribution of control (A) and *RYR1*-mutated (B) participants

Ethnicity of participants is demonstrated as a percentage of total participants within the control (n=88) or *RYR1*-mutated group (n=66). Both pie charts show that the majority of participants in both groups identified as white (77%, 89%). The ethnicities of the remaining participants in the control groups were Asian (16%), mixed/multiple ethnicities (5%), black (1%) and Iranian (1%), and in the RYR1-mutated group, mixed/multiple ethnicities (5%), black (5%) and ashkenazi (1%).

Table 19. *RYR1*-assoicated disorders diagnosed in dominant and recessive *RYR1*-variant carriers.

	RYR1-mutated		*AR mutation*		*AD mutation*	
	N	**%**	**N**	**%**	**N**	**%**
Centronuclear myopathy (CNM)	3	3.66%	3	21.43%	0	0.00%
Malignant hyperthermia (MH)	22	26.83%	3	21.43%	12	26.09%
Congenital fibre type disproportion (CFTD)	1	1.22%	1	7.14%	0	0.00%
Central core disease (CCD)	22	26.83%	3	21.43%	13	28.26%
Multi-minicore disease (MmD)	2	2.44%	0	0.00%	1	2.17%
Congenital myopathy (without muscle biopsy findings)	3	3.66%	0	0.00%	2	4.35%
King-Denborough syndrome (KDS)	0	0.00%	0	0.00%	0	0.00%
(Exertional) rhabdomyolysis	4	4.88%	0	0.00%	4	8.70%
(Exertional) heat illness (heatstroke)	4	4.88%	1	7.14%	3	6.52%
Periodic paralyses	3	3.66%	1	7.14%	1	2.17%
Awaiting biopsy results	1	1.22%	0	0.00%	0	0.00%
None of the above	17	20.73%	2	14.29%	10	21.74%
Total	**82**		**14**		**46**	

7.3.2 Modified MCMDM-1VWD bleeding questionnaire

RYR1-mutated participants were more likely to have more severe cases of, epistaxis, bruising, bleeding episodes after a minor cut, bleeding after tooth removal, bleeding after surgery, menorrhagia, and post-partum bleeding. Participants in the *RYR1*-mutated group had higher bleeding scores (4.16 ± 0.4553) than the control group (1.28 ± 0.1898), P<0.0001 (Welch's two-tailed t-test), demonstrated in Figure 94. Of 66 participants in the *RYR1*-mutated group 32 participants (48.48%) had pathological bleeding scores (≥4), compared to 11 of 88 participants (12.50%) of the control group with pathological bleeding scores, P<0.0001 (Fisher's exact test).
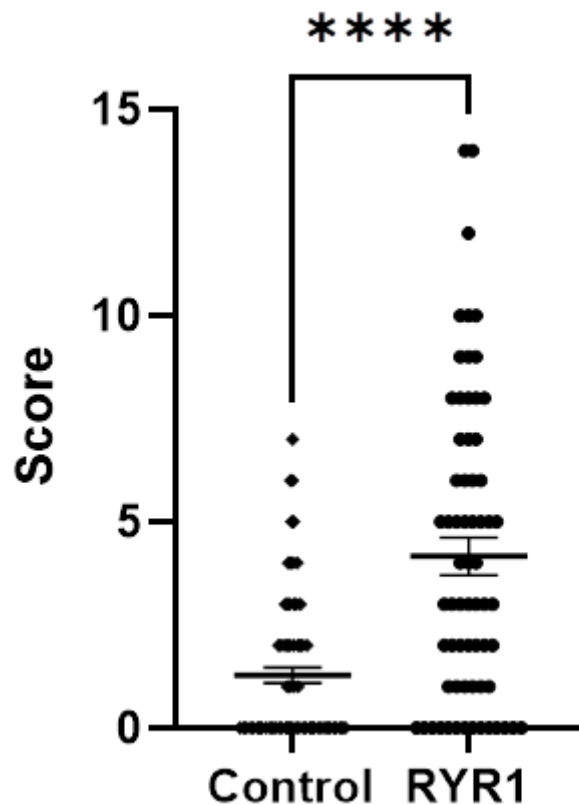
Figure 94. Bleeding scores obtained from modified MCMDM-1VWD questions in control and *RYR1*-mutated participants as a group.

Bleeding scores in response to the modified MCMDM-1VWD questions were significantly higher from *RYR1*-mutated participants (n=66) compared to bleeding scores from control participants (n=88), P<0.0001 (Welch's two-tailed t-test). Presented as individual scores and mean scores ± SEM.

7.3.3 Gynaecological symptoms associated to *RYR1* variants

7.3.3.1 Menstruation and menstrual cycle

The *RYR1*-mutated group had increased menstrual flow compared to the control group. In response to the heavy periods assessment questions, *RYR1*-mutated participants were more likely to select 'Often, or most periods' for the following items during menstruation: avoid travelling (*RYR1*-mutated 29.23%, control 13.64%), [X^2 (1, N=65,88, df=1)=4.315, P=0.0378], change of sanitary product overnight (*RYR1*-mutated 42.19%, control 20.45%), [X^2 (N=64,88, df=1)=4.85, P=0.0276], demonstrated in Figure 94. The *RYR1*-mutated group also reported the following outcomes more often during menstruation, although the increase was not statistically significant: passing clots larger than 10p coin (*RYR1*-mutated 32.81%, control 21.84%), change of routine (*RYR1*-mutated 36.92%, control 27.27%), change of sanitary product every 2 hours (*RYR1*-mutated 50%, control 37.50%), use of two types of protection (*RYR1*-mutated 40%, control 26.44%), experiencing period cramps (*RYR1*-mutated 78.46%, control 65.91%), P>0.05. The *RYR1*-mutated group (6.56%) did not report bleeding between periods more often than the control group (8.86%).

The *RYR1*-mutated group were more likely to have had treatment for heavy periods (n=26, 42.628%) than the control group (n=21, 26.58%), P=0.0499 (Fisher exact test). After hormonal contraception (*RYR1*-mutated n=11 or 42.31%, control n=15 or 62.50%), the most common treatment to control heavy periods was a hysterectomy (*RYR1*-mutated n=8, 30.77%, control n=0), demonstrated in Figure 96.

Menstrual cycle length and length of periods did not differ between the *RYR1*-mutated and control group, X^2 P=0.6853, 0.4031, respectively, demonstrated in Figure 97. It appeared that collectively the *RYR1*-mutated group (n=10, 15.63%) report longer periods (> 8 days) compared to the control group (n=6, 6.9%), however this was not statistically significant.
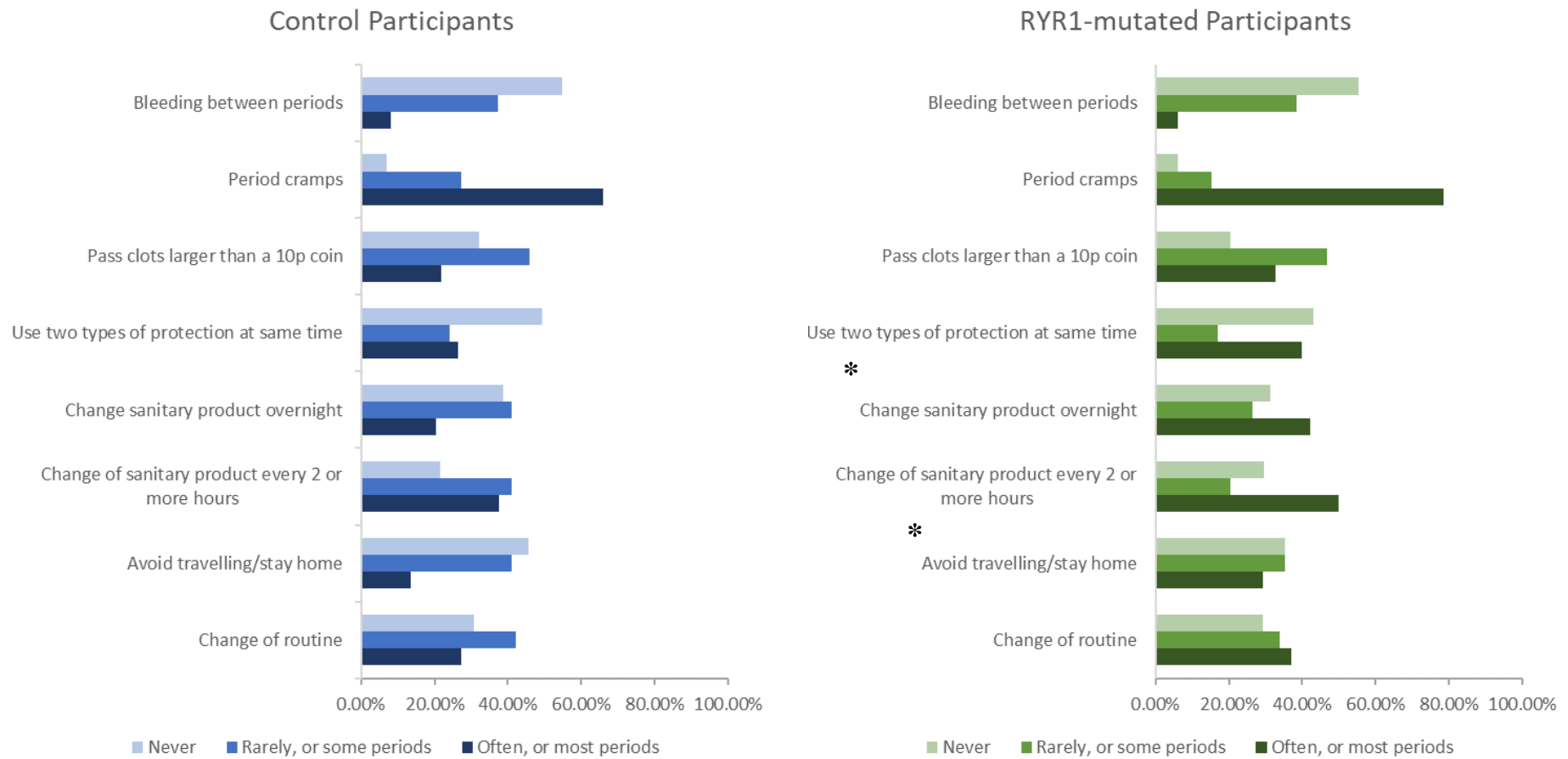
Figure 95. Responses to heavy menstruation assessment questions from control (blue, n=88) and *RYR1*-mutated (green, n=66) participants.

Participants selected how often each action was performed during menstruation with the following options to determine severity: 'often, or most periods', 'rarely, some periods' and 'never'. *RYR1*-mutated participants were more likely to indicate changes in behaviour during menstruation categorised by increased avoidance of travelling P=0.0378, and changing sanitary products overnight P=0.0276 (Chi square tests). * P<0.05.

329
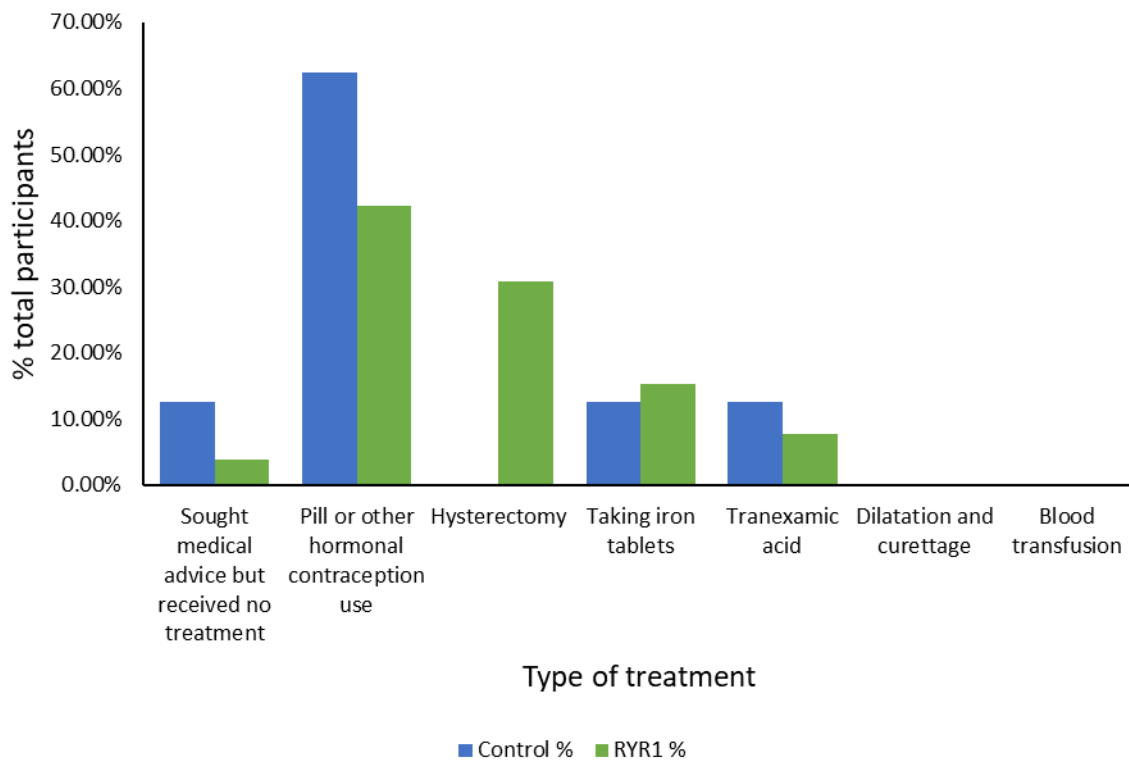
Figure 96. Types of treatment received for heavy periods in *RYR1*-mutated (green, n=66) and control (blue, n=88) participants

Type of treatments administered for heavy menstrual bleeding, presented as a percentage of total *RYR1*-mutated (green) (n=66) and control (blue) participants (n=88). In the *RYR1*-mutated group, hormonal contraception was the most common treatment (*RYR1* 42.31%, control 62.50%), followed by a hysterectomy (*RYR1*- mutated 30.77%, control n=0).
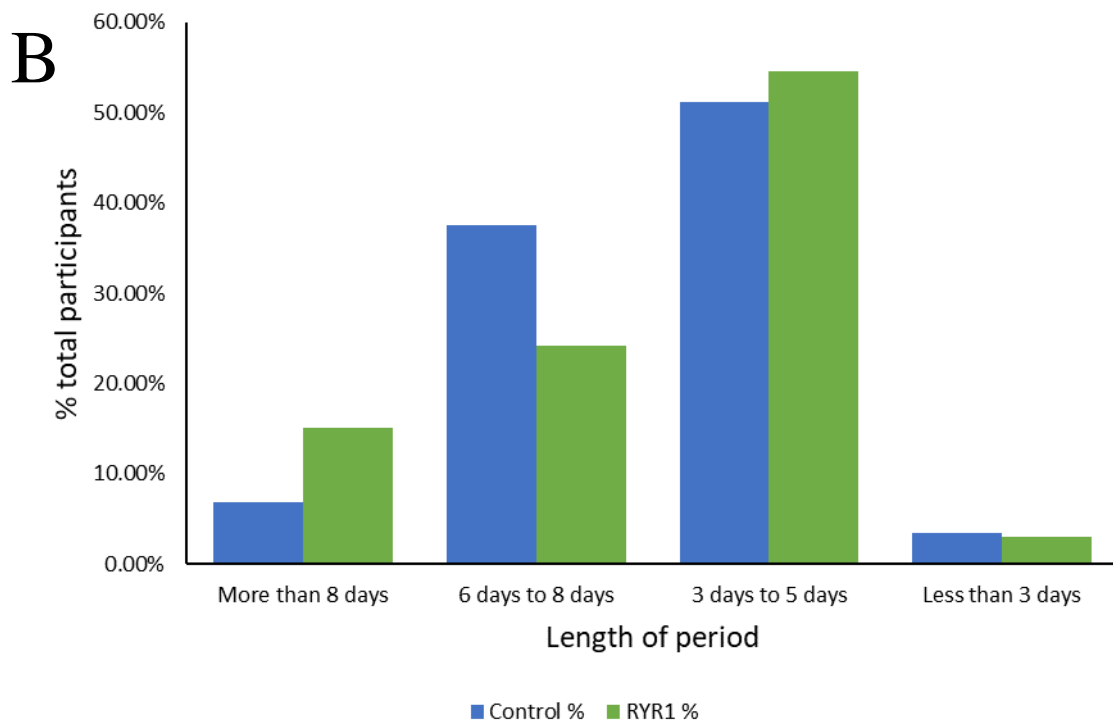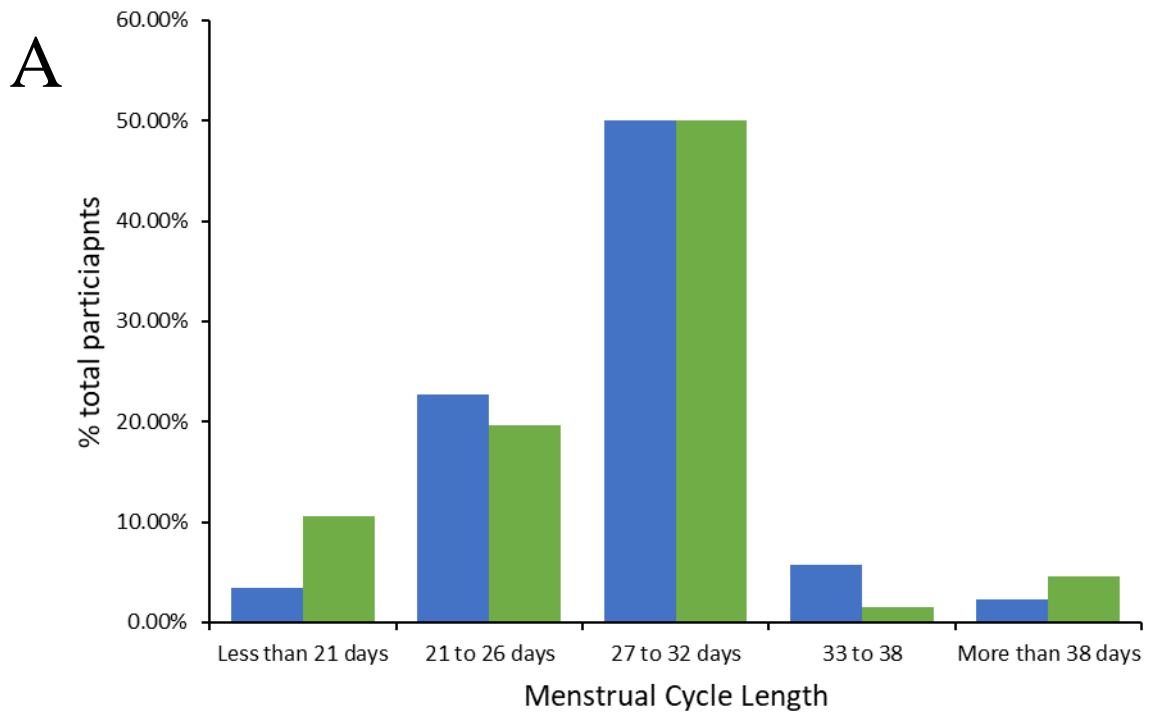
Figure 97. (A) Menstrual cycle length and (B) length of period (days) in *RYR1*-mutated (green, n=66) and control (blue, n=88) participants.

Both (**A**) menstrual cycle lengths and (**B**) length of periods were not statistically different between *RYR1*-mutated (n=66) and control participants (n=88).

7.3.3.2   Contraception and menstrual changes

Twelve participants in the *RYR1*-mutated group (18.46%) and thirty-five participants in the control group (39.77%), reported being on long term contraception. *RYR1*-mutated participants did not report statistically significant changes to menstrual bleeds or periods cramps (dysmenorrhea) after using long-term contraception compared to control participants, demonstrated in Figure 98.
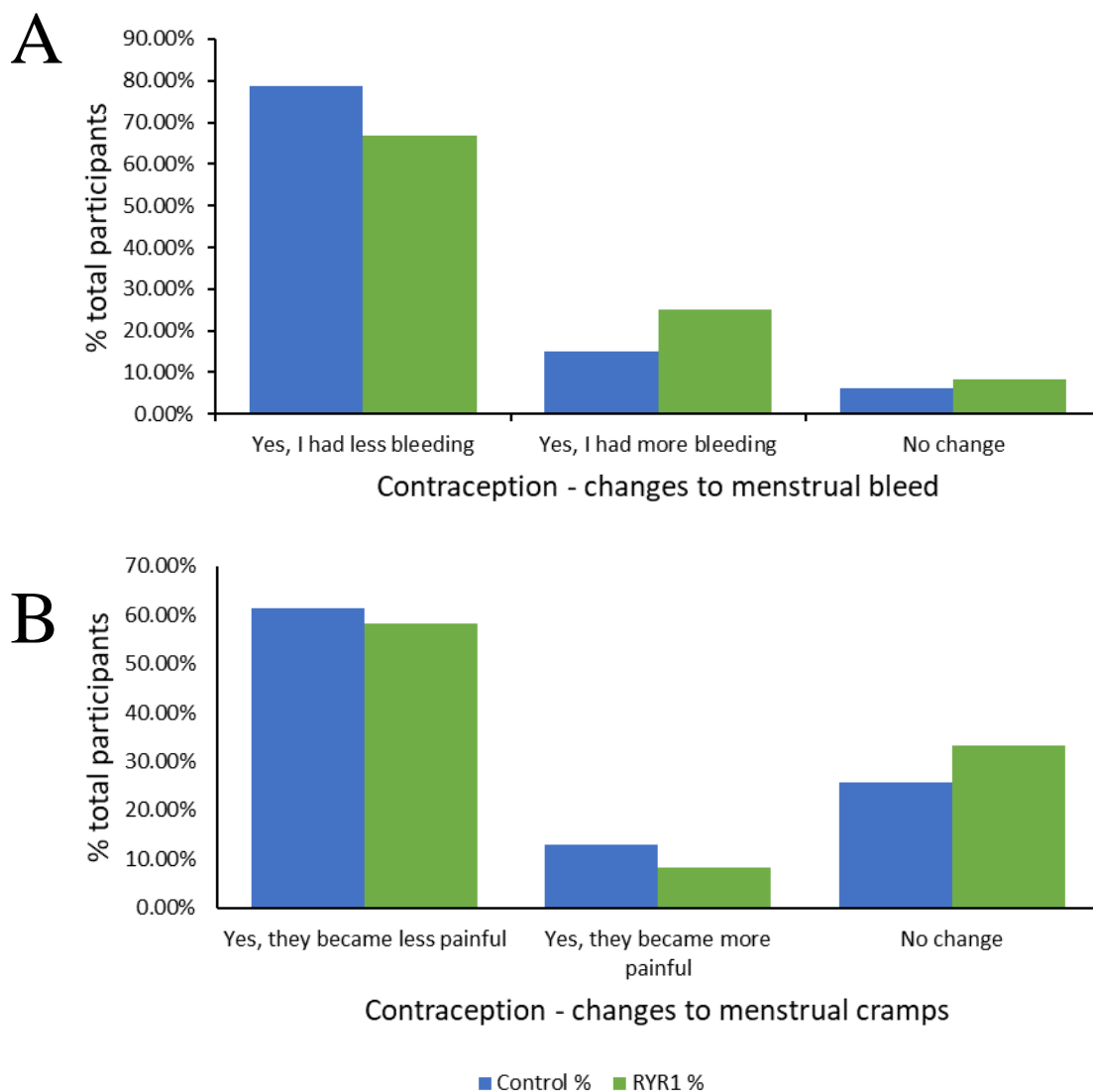
Figure 98. Changes to menstrual bleed and menstrual cramp pain after using long-term contraception in *RYR1*-mutated (n=12) and control participants (n=35).

RYR1-mutated participants (n=12) did not report statistically significant changes to menstrual bleeds or periods cramps (dysmenorrhea) after using long-term contraception in comparison to control participants (n=35). Data presented as percentage of total participants on long-term contraception.

7.3.3.3 Conception and miscarriages

Forty-nine participants (74.24%) in the *RYR1*-mutated group and forty-six participants (52.27%) in the control group reported having been pregnant. There was no statistical difference in likelihood of *RYR1*-mutated or control participants requiring support from doctors to conceive, P=0.0601 (Chi square test). For assisted conception, more *RYR1*-mutated participants reported being on Clomid medication (for ovarian malfunction) (n=4, 6.12%) than control participants (n=0), demonstrated in Figure 99. Miscarriages (multiple and single) before 13 weeks (P=0.8440) or between 14-24 weeks (P=0.3633), 3 or more consecutive miscarriages (P=0.6285) and bleeding after miscarriage (P=0.2448) were not statistically different between the *RYR1*-mutated and the control group.
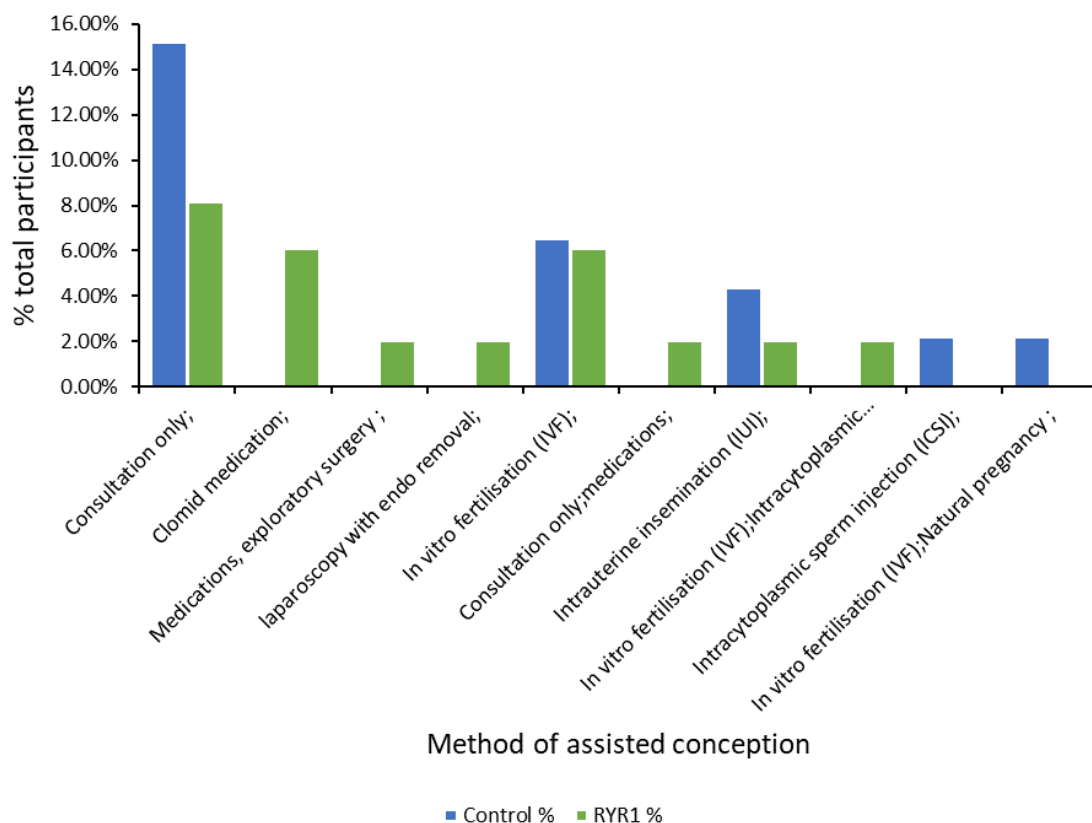
Figure 99. Interventions received to support conception in participants from *RYR1*-mutated (n=49) and control (n=46) groups.

The requirement for assisted conception was not statistically different between *RYR1*-muated (n=49) and control participants (n=46). Data presented as a percentage of total participants with previous pregnancies.

7.3.4 Obstetric history of *RYR1* variant carriers

Upon studying the first pregnancy of nulliparous women alone, there was no difference in method of delivery P= 0.3652, length of gestation P= 0.3013, labour length P= 0.3197, unusually heavy bleeding post-partum P= 0.166, complications during pregnancy P= 0.4772 (Fisher's exact test).

7.3.4.1 *Birthweight*

In the *RYR1*-mutated group, 41 participants previously had children (100 total pregnancies), compared to 34 participants in the control group (68 total pregnancies). The birthweight of offspring from *RYR1*-mutated participants was lower (2.26-3.18 kg) than offspring from mothers in the control group that were more likely to be heavier (3.2-4.54 kg), [X^2 (N=100 and 68, df=1)=5.910, P=0.0151], demonstrated in Figure 99. The birthweights of the first-born babies of *RYR1* mutated women were lower compared to babies from control women, P<0.0001 (Fisher's exact test). No such difference was observed in later pregnancies.

In a *separate* cohort of MH patients from the MH Investigation Unit in the Canisius Wilhelmina Hospital and the neuromuscular outpatient clinic of the Radboud University Medical Centre (Nijmegen, The Netherlands), *RYR1*-mutated patients (n=27) reported lower offspring birthweights than non-mutated family members (n=7), -457.18 g (-857.20, -57.16), P= 0.026, presented as adjusted* B-coef and 95%CI when adjusted for gestational age and sex. This is demonstrated with decreased z-scores and birthweight percentiles in the *RYR1*-mutated group in Table 20. Interestingly, a lower birthweight did not correlate with inheritance of the *RYR1* variant from the mother compared to inheritance from the father, as observed in the *Ryr1*$^{Y522S/+}$ mouse model in Chapter 6.
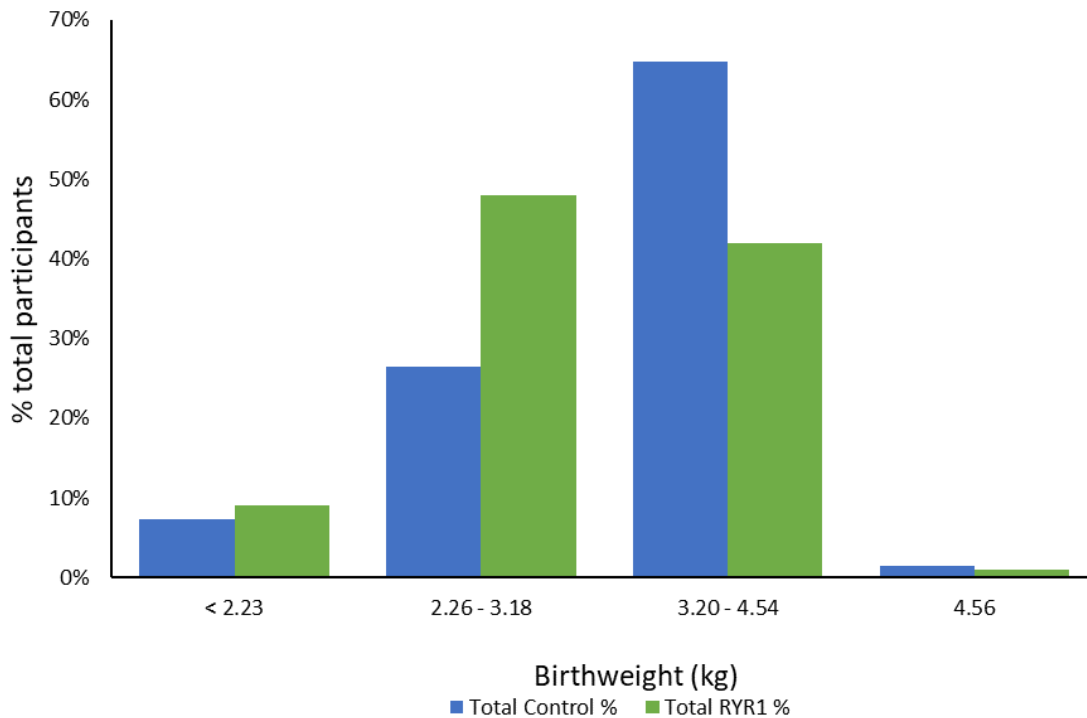
Figure 100. Birthweight of offspring from *RYR1*-mutated and control participants.

RYR1-mutated participants (n=100 total live births) were more likely to have lighter weight babies (between 2.26-3.18 kg) than participants in the control group that more often gave birth to heavier babies (between 3.2-4.54 kg) (n=68 total live births), P=0.0151, Chi square test.

Table 20. Offspring birthweight, z-score, and percentiles in a cohort of malignant hyperthermia susceptible *RYR1*-mutated patients in Nijmegen, The Netherlands.

*adjusted model for gestational age (days) and sex. β This model excludes one person where it is unknown if the gene belonged to the mother or the father. Analysis performed using linear regression.

		Unadjusted B-coef (95%CI)	p-value	Adjusted* B-coef (95%CI)	p-value
Mutation (n=27) vs no mutation (n=7)	Birthweight (g)	-311.9 (-737.90, 114.02)	0.146	-457.18 (-857.20, -57.16)	0.026
	z-score	-2.04 (-3.48, -0.60)	0.007	-1.45 (-2.64, -0.20)	0.024
	percentile	-30.7 (-54.82, -6.57)	0.014	-28.8 (-54.72, -2.87)	0.031
Mutated mother (n=6) vs mutated father (n=20) β	Birthweight (g)	-97.28 (-587.28, 392.71)	0.686	-77.38 (-495.20, 340.44)	0.705
	z-score	-0.08 (-0.98, 0.82)	0.860	-0.12 (-1.07, 0.83)	0.799
	percentile	-3.93 (-31.36, 23.49)	0.770	-5.20 (-33.95, 23.54)	0.711

7.3.4.2 *Gestation length and pregnancy complications*

The length of the pregnancy was reduced in *RYR1*-mutated participants, with more participants reporting gestation length under 37 weeks (n=32, 31.68%), compared to the control cohort (n=11, 15.71%), [X^2 (N=101 and 70, df=1)=5.789, P=0.0161], demonstrated in Figure 101.

More *RYR1*-mutated participants (n=31, 47%) reported complications during pregnancy or birth than control participants (n=16, 18.2%), P=0.0002 (Fisher's exact test). *RYR1*-mutated participants were more likely to have placenta praevia (P=0.0140), and preeclampsia (P=0.0073), than control participants, demonstrated in Figure 102.
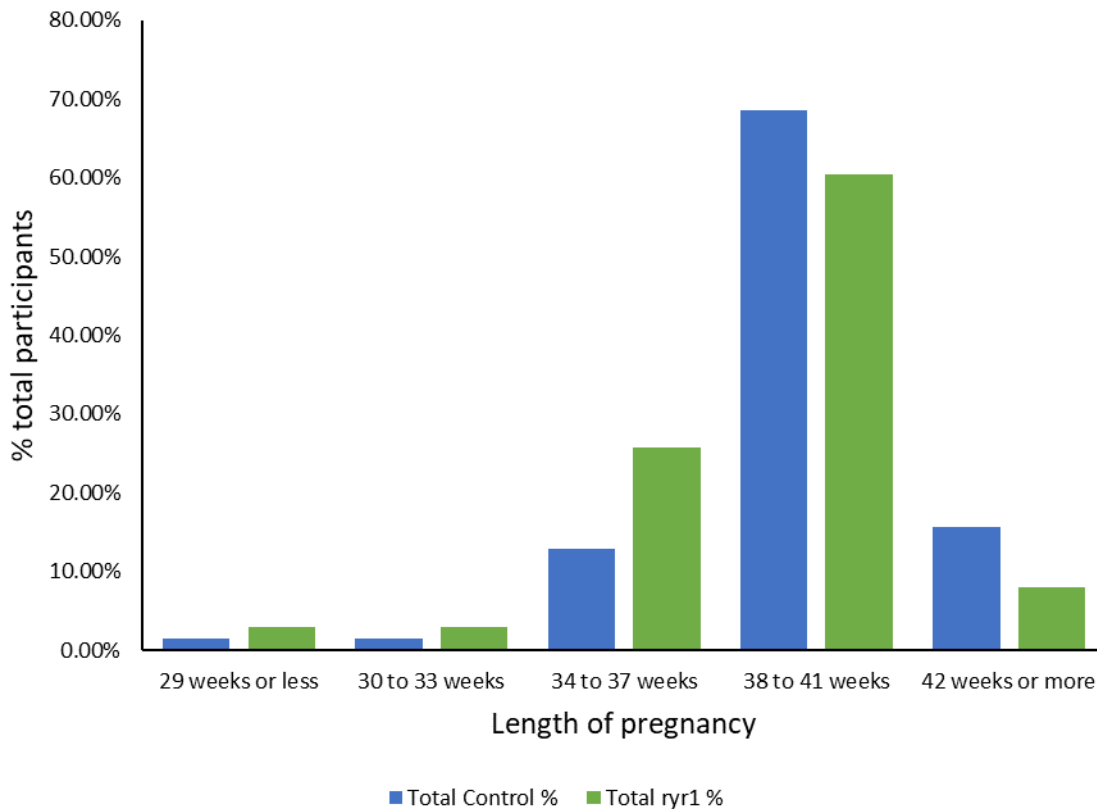
Figure 101. Length of pregnancy in *RYR1*-mutated and control participants.

Length of the pregnancy was shorter (37 weeks or less) for *RYR1*-mutated participants (n=32, 31.68%), compared to the control cohort (n=11, 15.71%), P=0.0161, Chi square test.
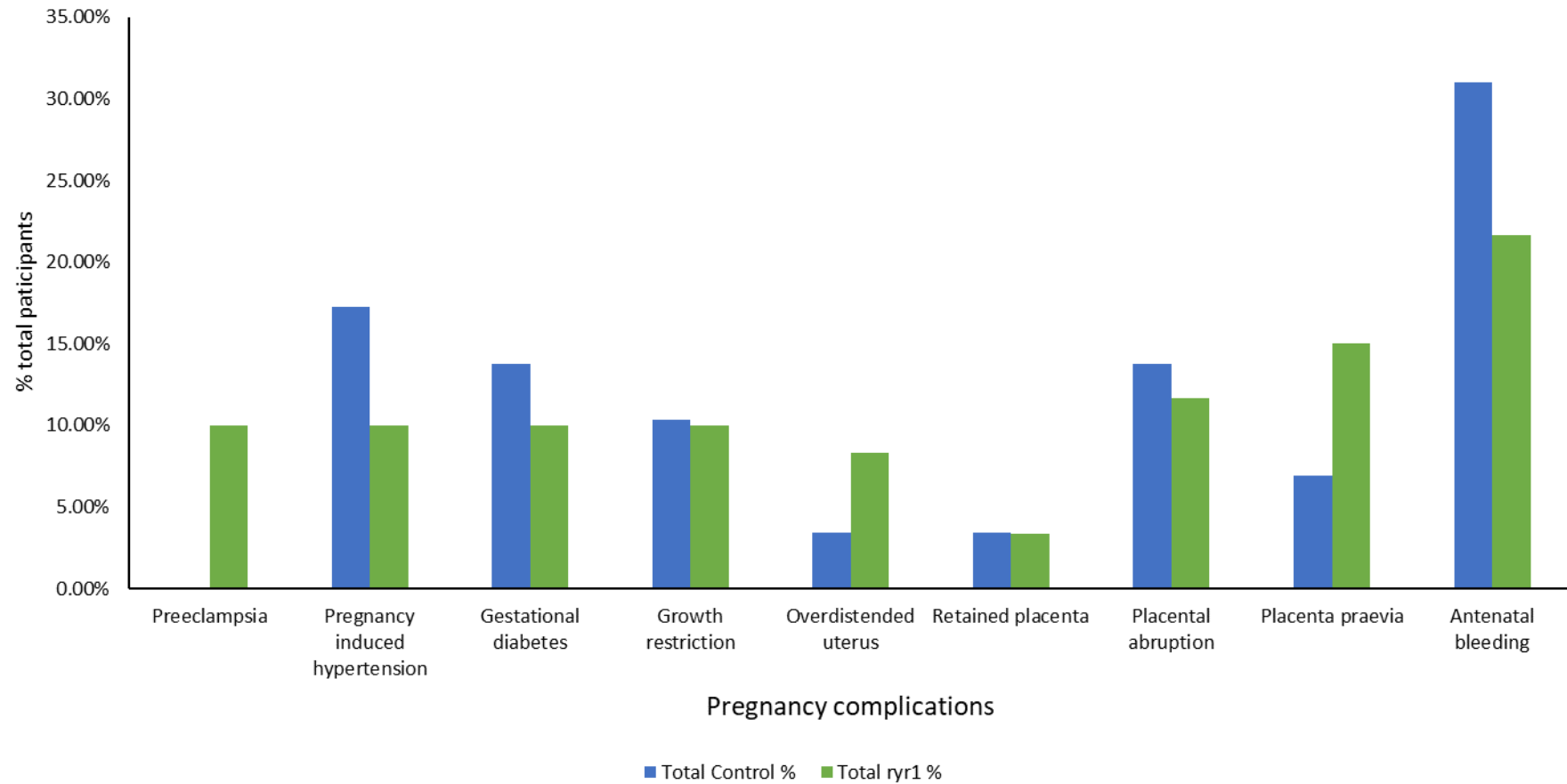
Figure 102. Complications reported during pregnancy or delivery in *RYR1*-mutated and control group participants.

RYR1-mutated participants (n=31, 47%) more often reported complications during pregnancy or birth than control participants (n=16, 18.2%) (p=0.0002, Fisher's exact test). *RYR1*-mutated participants were more likely to have placenta praevia (p=0.0140), and preeclampsia (p=0.0073) than control participants.

337

7.3.4.3 Labour and Delivery

The *RYR1*-mutated participants (n=20, 19.80%) were more likely to have a planned Caesarean section than the control group (n=6, 8.82%), [X^2 (N=101 and 68, df=1)=8.851, P=0.0313], demonstrated in Figure 103. The length of labour was not statistically different in the *RYR1*-mutated group compared to the control group, P=0.3583, demonstrated in Figure 103.

7.3.4.4 Post-partum haemorrhage

A larger proportion of *RYR1*-mutated participants (n=8, 18.18%) reported unusually heavy bleeding post-partum compared to control participants (n=2, 5.71%), although this change was not statistically significant P=0.1717 (Fishers exact test). Of the *RYR1*-mutated participants that reported PPH, 3 participants had primary bleeding (heavy bleeding in the first 24 hours following delivery), 2 participants (25%) had secondary bleeding (heavy bleeding between 24 hours and up to 2 weeks following delivery) and 1 had both. The two control participants with PPH reported only primary bleeding post-partum. Reported blood loss volume in *RYR1*-mutated participants were 500 ml - 950 ml in 2 individuals, and ≥1000 ml (1000 ml, 1704 ml, 3500 ml) in 3, whereas the 2 control participants with PPH reported blood loss volume of <1000ml (800 ml and 900 ml).
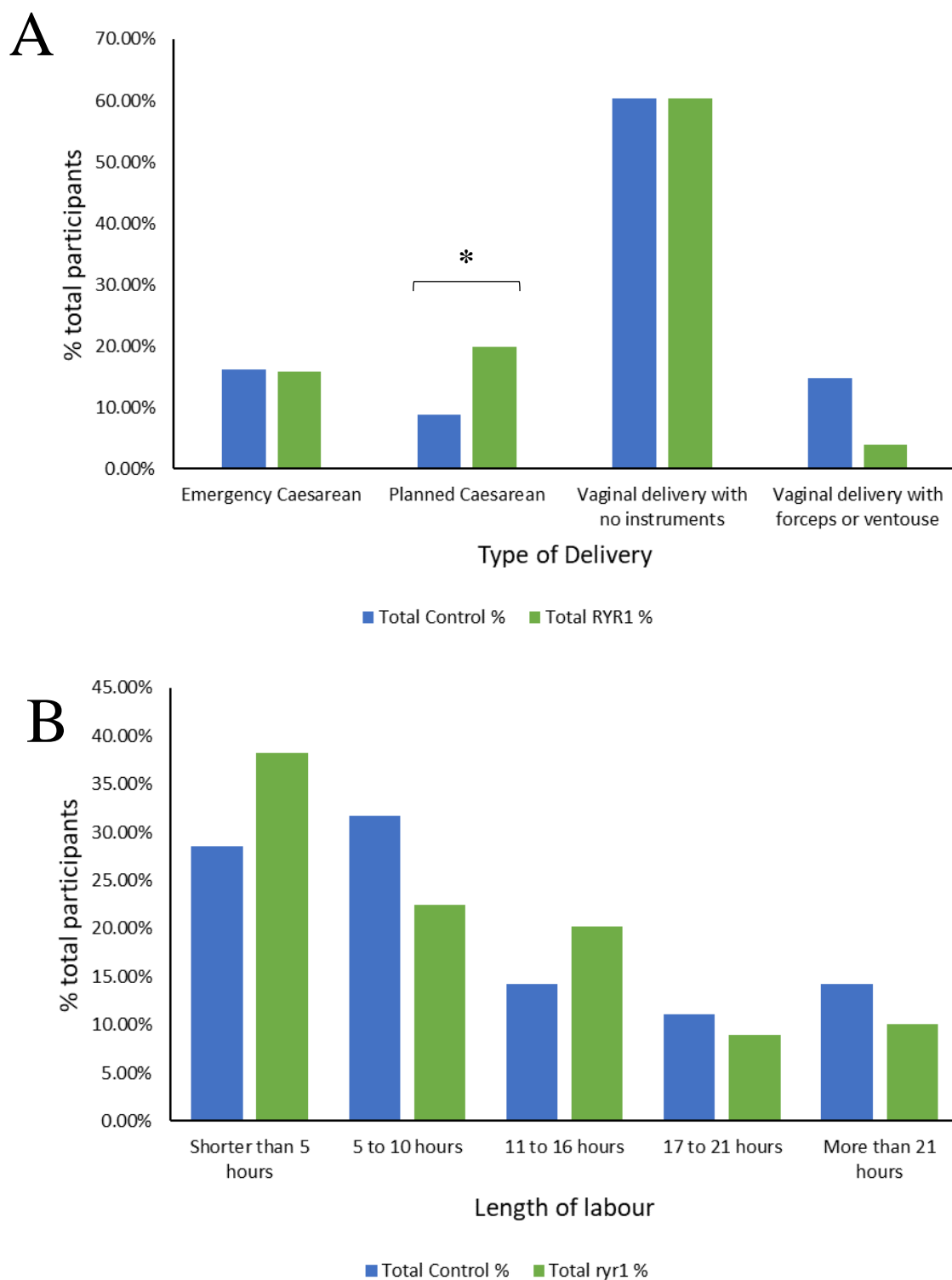
Figure 103. (A) Type of delivery and (B) length of labour in *RYR1*-mutated and control participants.

(**A**) *RYR1*-mutated participants were more likely to have a planned Caesarean section than the control group, P=0.0313, Chi square test. (**B**) Length of labour was not statistically different between control and *RYR1*-mutated participants.

7.3.5   Other bleeding episodes

As part of the questionnaire, all participants were given an opportunity to report any other bleeding episodes that were not covered in the main body of the questionnaire, displayed in Table 21 and Table 22.

The control group reported individual accounts of "bleeding after menopause", "bleeding after insertion of Mirena coil for four hours, with clots", "cervical vaginal bleeding" and "bleeding during pregnancy, twice" (n=4 reports). Follow-up treatments included taking iron tablets (n=1) and further investigations to establish a cause (n=1).

The *RYR1*-mutated participants appeared to report more serious bleeding episodes (n=6 reports), as evidenced by the need for more intensive treatments. For example, there were individual accounts of "antenatal bleeding for both pregnancies", "heavy menstrual bleeding for more than 11 days", "an incident of bleeding heavily in between periods… was extremely heavy and continuous for about 8 hours before stopping", "placenta previa with [a first child] and it abrupted causing a lot of bleeding", "a period for three months…", "bleeding after my hysterectomy also needed transfusion". The follow-up treatments involved blood transfusion (n=2), medication to stop bleeding (n=1), birth control and iron supplement (n=1).

Table 21. Patient descriptions of other bleeding events

Patient description of bleeding	RYR1 N	Healthy N
Antenatal bleeding - both pregnancies	1	0
Allergies, chronic migraines, anxiety, had severe pre-eclampsia that progressed into HELLP syndrome	1	0
Heavy menstrual bleeding for more than 11 days	1	0
One incident of bleeding heavily in between periods. It was like a period but was extremely heavy and continuous for about 8 hours before stopping. There was no chance that I was pregnant at that time, otherwise I might have suspected a miscarriage. I have no idea what caused it, and it has never happened again.	1	0
Placenta previa with my first pregnancy and it abrupted causing a lot of bleeding and an emergency in the hospital.	1	0
One occasion where I had a period for three months, stopped with birth control pills	1	0
Bleeding after my hysterectomy also needed transfusion	1	0
Bleeding after menopause	0	1
after insertion of Mirena coil - clots ++ lasting 4 hours	0	1
Cervical/vaginal bleeding	0	1
Bleeding during pregnancy (twice)	0	1
Total	**7**	**4**

Table 22. Participant reports of treatment for other bleeding episodes

Treatment for bleeding	RYR1 N	Healthy N
Blood transfusion	2	0
Medication to stop bleeding	1	0
Birth control and iron	1	0
Investigations, ultrasound, and biopsy to establish cause	0	1
Iron tablets	0	1
Total	**4**	**2**

7.3.6   Medical history related to other smooth muscle symptoms

More *RYR1*-mutated participants reported bowel or bladder symptoms (n=32, 48.48%) than the control group (n=18, 20.45%) [X^2 (N=65,87, df =1)=13.73, P=0.0002], demonstrated in Figure 104. Of total reports of bowel/bladder problems, the most common symptoms in the *RYR1*-mutated group were constipation (n=14, 31.82%), diarrhoea (n=12, 27.27%), and urinary incontinence (n=7, 15.91%), compared to the control group (n=8, 42.11%; n=2, 10.53%; n=3, 15.79%, respectively), however the difference was not statistically significant (see Table 23).

There were no other statistically different changes in medical history related to the function of other smooth muscle-lined organs. However*, RYR1*-mutated participants appeared to be more likely to have severe migraines (n=24, 36.36%, P=0.0732), anaemia (n=27, 43.55%, P=0.1218), and hypotension or hypertension that required medical attention or medication (n=13, 20.63% and n=11, 17.46%, respectively, P >0.999, Fisher exact tests) than control participants (Severe migraines n=20, 22.73%; anaemia n=27, 30.68%, hypo-and hypertension n=7, 8.33%), the latter was concurrent with more intensive blood pressure treatment.
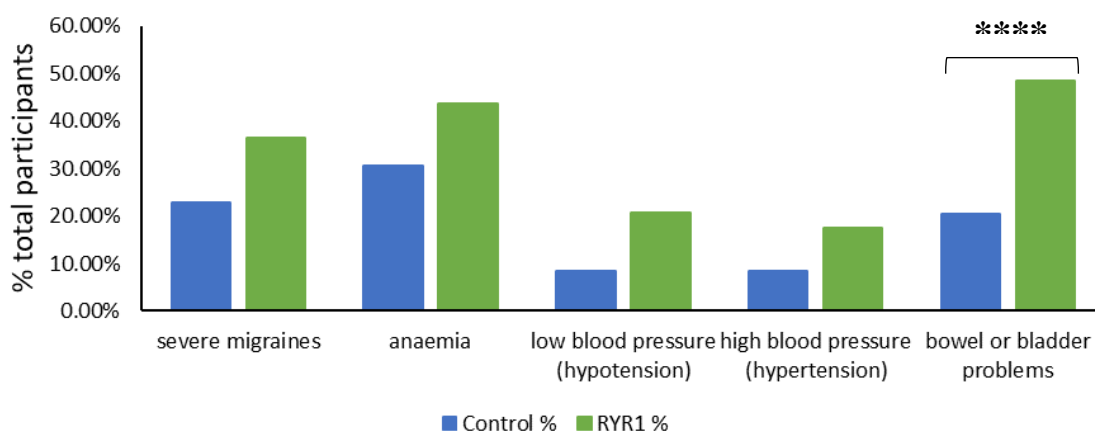
Figure 104. Medical conditions concerning smooth muscle-lined organs in *RYR1*-mutated (green) and control (blue) group participants.

The percentage of participants in the *RYR1*-mutated (n=66, green) and control (n=88, blue) groups with a previous medical history of migraines, anaemia, hypo- or hypertension, bowel and bladder problems are shown. Bowel or bladder problems were more likely to be reported by *RYR1*-mutated patients compared to control participants, P=0.0002 (Chi square tests). There were no statistically different changes in the incidence of the remaining medical conditions between *RYR1*-mutated and control participants.

Table 23. Type of bowel and bladder problems in *RYR1*-mutated and control participants.

	RYR1		Control	
	Count	**%**	**Count**	**%**
Constipation	14	31.82%	8	42.11%
Diarrhoea	12	27.27%	2	10.53%
Bowel inflammation	3	6.82%	3	15.79%
Vesicourethral reflux	0	0.00%	0	0.00%
Urinary incontinence	7	15.91%	3	15.79%
Irritable bowel syndrome (IBS)	4	9.09%	1	5.26%
Dual ureter on one kidney, frequent UTI/kidney stones	1	2.27%	0	0.00%
Bilateral Kidney Reflux	1	2.27%	0	0.00%
Paralytic Ileus (morphine induced)	1	2.27%	0	0.00%
"Surgery for rectocele and enterocele"	1	2.27%	0	0.00%
"Post-partum following tear in childbirth. Required surgical repair"	0	0.00%	1	5.26%
"Frequent UTI s and a consequent kidney inflammation"	0	0.00%	1	5.26%
Total	**44**		**19**	

7.3.7 Genotype-phenotype correlations

Variants in *RYR1* cause disease via different pathophysiological mechanisms and therefore manifest as clinically different phenotypes, such that CNM is predominantly associated with AR mutations and MH and CCD with AD inheritance. Consequently, I examined genotype specific traits among the population of *RYR1*-mutated patients. The following comparisons are reported as a percentage of total participants responses with either AR (n=13) or AD (n=35) *RYR1* variants. Specific *RYR1* mutational information was available from 3 participants with AR inheritance and 10 with AD inheritance, shown in Table 24 and Table 25, along with *RYR1*-related phenotypes.

Table 24. Phenotypes in participants with recessive *RYR1* mutations

Autosomal recessive *RYR1* mutations	Phenotypes
c.325>T (p.Arg109Trp); c.1453A>G (p.Met485Val); c.8140_8141delTA (p.Tyr2714Cysfs*8)	Central Core Disease
p.Ty4631Cys; p.Arg4564Gln	Central Core Disease
c.1250T>C (p.Leu417Pro); c.1250T>C (p.Leu417Pro)	None of the above; MH after the genetic analysis, but never had an episode
-	Centronuclear Myopathy
-	Congenital Fibre Type Disproportion
-	Malignant hyperthermia
-	Centronuclear Myopathy
-	Centronuclear Myopathy; Atypical periodic paralysis
-	(Exertional) heat illness (sometimes also called heatstroke); Periodic paralyses; MH risk
-	Malignant hyperthermia
-	Central Core Disease; Malignant hyperthermia

Table 25. Phenotypes in participants with dominant _RYR1_ mutations.

Autosomal dominant _RYR1_ mutation	Phenotypes
c.6814 C>T	None of the above
c.13912G>A (p.Gly4638Ser)	Central Core Disease
c.1267_1276dup10 (p.Gly426GlufsX82)	-
c.6617C>T	Malignant hyperthermia
c.6617CT (p.Thr2206Met)	Malignant hyperthermia; Congenital myopathy (without specific muscle biopsy findings) ;(Exertional) rhabdomyolysis
p.Phe4808Asn	Central Core Disease
c.14918T>C (p.P4973L)	Malignant hyperthermia
c.6797-1G>A	None of the above
c.14693T>C (p.Ile4898Thr)	Central Core Disease
c.7025A>G (p.Asn2342Ser)	Periodic paralyses; Malignant hyperthermia
-	Malignant hyperthermia
-	Malignant hyperthermia
-	None of the above
-	Malignant hyperthermia;(Exertional) rhabdomyolysis ;(Exertional) heat illness (heatstroke)
-	Central Core Disease
-	Central Core Disease; Malignant hyperthermia
-	Central Core Disease; Malignant hyperthermia
-	Central Core Disease
-	(Exertional) heat illness (heatstroke); Congenital myopathy (without specific muscle biopsy findings)
-	Central Core Disease
-	Central Core Disease; Malignant hyperthermia

-	(Exertional) rhabdomyolysis ;(Exertional) heat illness (heatstroke)
-	Central Core Disease
-	Malignant hyperthermia
-	(Exertional) rhabdomyolysis; Central Core Disease
-	Malignant hyperthermia
-	Central Core Disease
-	Multi-minicore Disease
-	Central Core Disease

7.3.7.1 MCMDM-1VWD Bleeding Questionnaire

Individuals with dominant *RYR1* variants appeared to have higher bleeding scores (4.057 ± 0.5724, n= 35) compared to those with recessive *RYR1* variants (3.385 ± 0.8882, n=13), although this was not statistically supported P=0.5309 (Welch's two-tailed t-test), demonstrated in Figure 105. More AD variant carriers (n=17, 48.57%) had a pathogenic bleeding score (>4) compared to AR variant carriers (n=5, 38.46%), however, this was also not statistically different, P=0.7456 (Fisher's exact test).
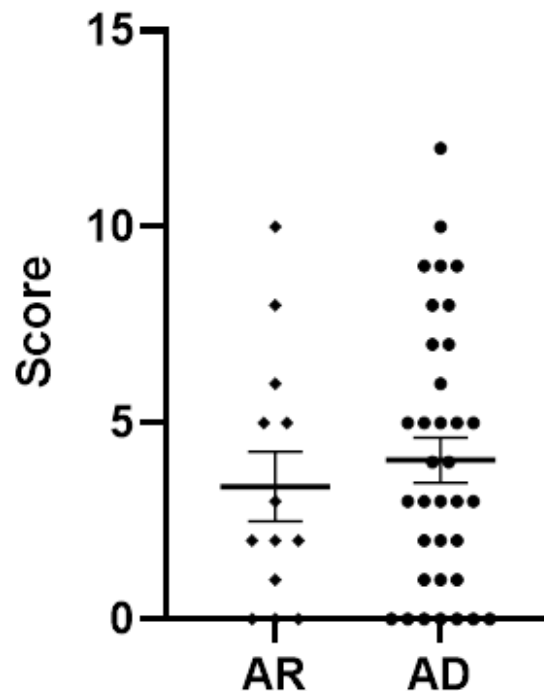
Figure 105. Bleeding scores obtained from modified MCMDM-1VWD questions in *RYR1*-mutated participants subdivided by autosomal recessive (AR) or autosomal dominant (AD) inheritance.

Bleeding scores were not statistically different between participants with autosomal recessive (AR) (n=13) and autosomal dominant (AD) *RYR1* variants (n=35), P=0.5309 (Welch's two-tailed t-test). Presented as individual scores and mean ± SEM.

7.3.7.2 Periods and Menstrual Cycle

Individuals with AD *RYR1*-variants were more likely to experience bleeding between periods than individuals with AR *RYR1*-variants, [X^2 (df=1, N=13,32)=4.202, P=0.0404], demonstrated in Figure 106A.

7.3.7.3 Obstetric History

Participants with AD *RYR1*-mutations were more likely to give birth to babies with a lower birthweight (< 3.18kg) compared to AR *RYR1*-mutated participants that were more likely to report birthweights between 3.20 and 4.54kg, P=0.0335 (Chi square test), demonstrated in Figure 106B.

There were no other statistically significant changes in actions during menstruation or changes in menstrual cramp pain, post-partum bleeding events, treatment required to conceive, frequency of miscarriage and bleeding thereafter between recessive and dominant *RYR1*-mutated participants. Similarly, reports of anaemia, hypotension, hypertension, migraines, or GI problems were not statistically different between participants with AD and AR *RYR1*-mutated participants.
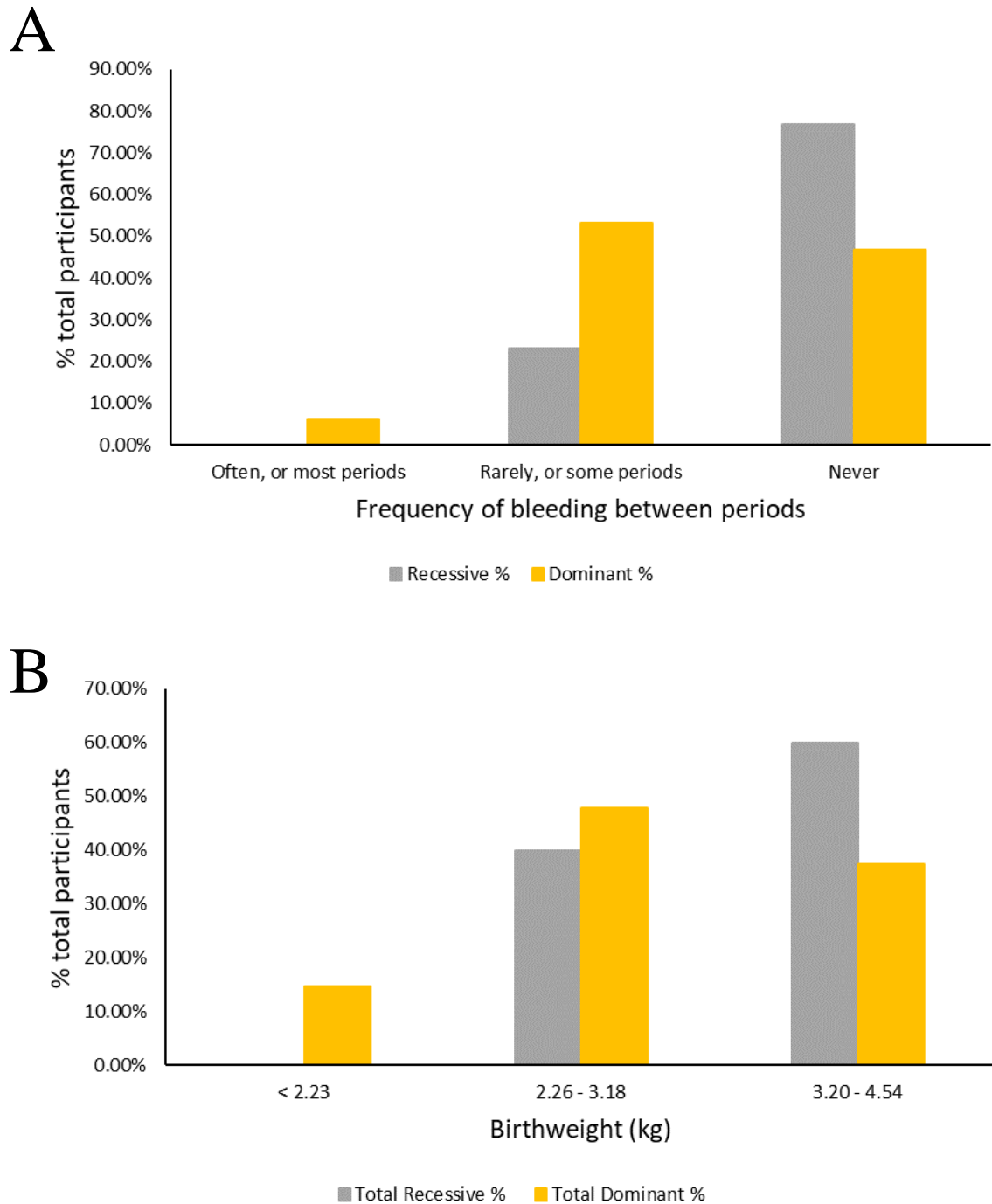
Figure 106. (A) Changes in menstrual bleeding and (B) birthweight of offspring in dominant and recessive *RYR1*-mutated participants

(**A**) Participants with autosomal dominant *RYR1* mutations (n=32) were more likely to report bleeding between periods compared to autosomal recessive mutated patients (n=13), P=0.0404. (**B**) The weight of offspring from AD *RYR1*-mutated patients (n=48 live births) was lower in comparison to offspring from carriers of AR variants that gave birth to heavier offspring (n=20 live births), P=0.0335 (Chi square tests).

7.4 Discussion

In summary, this study demonstrates that individuals with pathogenic *RYR1* variants have a range of bleeding, gynaecological and obstetric manifestations. These symptoms manifest as abnormal bleeding as evidenced by pathological bleeding scores, heavy menstrual bleeding, increased complications during pregnancies, Caesarean sections, shorter pregnancies, and offspring with lower birth weight. Individuals with AD inherited *RYR1* variants were more likely to have bleeding between periods and give birth to babies with a lower birthweight compared to those with AR mutations. The findings from this study corroborate and expand preliminary findings reported by Lopez and colleagues (2016) in a much smaller cohort.

As described in Chapter 2, there are several other predominantly skeletal muscle associated genes that have also been implicated in the normal function of various smooth muscle types, therefore it is unsurprising that *RYR1* mutations may also manifest as non-skeletal muscle symptoms. The findings from this study correspond with the clinical features previously reported by Lopez and colleagues in a smaller cohort of patients with mainly dominant *RYR1* mutations. Furthermore, this study highlights other previously unrecognized aspects of the *RYR1*-related bleeding phenotype, further expanding the phenotypic range of *RYR1*-related disorders.

The remainder of this discussion is structured around each of these findings, followed by a brief consideration of study limitations and proposed future work.

Bleeding Scores

Using modified and validated questions from the MCMDM-1VWD bleeding questionnaire, this study demonstrates that participants with pathogenic *RYR1*-variants display higher bleeding scores and an increased percentage of pathological scores compared to control participants, corroborating the increased bleeding tendency in *RYR1*-variant carrying women. Lopez and colleagues utilized the MCMDM-1VWD in a small cohort of patients with clinically diagnosed MH, ERM, congenital myopathy (CCD or MmD), associated mainly with dominant heterozygous *RYR1* missense mutations. The authors reported that 8 of 21 patients had pathological bleeding scores (≥4), compared to zero control patients. The bleeding symptoms that were common in *RYR1*-mutation carriers were characterised by severe menorrhagia, post-partum bleeding, epistaxis and easy bruising in males (Lopez, 2016). In light of this, in the present study I used a more extensive, focussed questionnaire to investigate other aspects of the *RYR1*-related phenotype, including abnormal bleeding in relation to menstruation, contraception, conception, gestation, and delivery, the results of which are discussed in detail below.

In the present study, *RYR1*-mutated patients presented with more severe menstrual bleeding requiring medical intervention, shorter pregnancies, and increased bowel or bladder problems. Further to this, *RYR1*-mutated participants were also more likely to report complications during pregnancy including increased reports of Caesarean sections although it must noted that women diagnosed with *RYR1* mutations or multiparous women may already be candidates for C-sections.

Menorrhagia/Heavy menstrual bleeding

During menstruation *RYR1*-mutated participants were more likely to experience symptoms indicative of heavy bleeding, and to seek medical treatment to control heavy bleeding. For the *RYR1*-mutated group, the most common treatment following hormonal contraception was a hysterectomy, a treatment that was not reported by any control participant, indicating the severity of menstrual bleeding in *RYR1* variant carriers. Whilst ovulatory dysfunction, platelet-dysfunction and single factor deficiencies may account for approximately 50% of menorrhagia cases, a large proportion of women (almost 50%) are left with unexplained menorrhagia (Lee, 1984; Oehler, 2003). Over half of all hysterectomies (52%) are performed for reasons that can be confirmed by pathological examination e.g., endometrial hyperplasia, cervical intraepithelial neoplasia, and leiomyomas, however the remaining 48% cases are performed for reasons that cannot be confirmed by pathology. The most frequent of these diagnoses being menstrual bleeding disorders (21%), being the single leading cause of hysterectomies behind only leiomyomas with pathology (30%), followed by pelvic relaxation (11%), or pelvic pain (10%) (Lee, 1984).

Increased vascularisation or poor vasoconstriction has been suggested as an underlying cause of menorrhagia or heavy menses (Abberton *et al.*, 1999; Hurskainen, 1999). In the *Ryr1*$^{Y522S/+}$ mouse model, tail artery bleeding times are prolonged compared to that of wild-type littermates, and in *Ryr1*$^{Y522S/+}$ vascular smooth muscle cells RYR1 channel mediated calcium sparks from the SR are more frequent compared to wild-type VSMCs (Lopez, 2016). Both findings in the animal model were reversed with dantrolene pre-treatment, indicating a role of the mutated RYR1 channel in increased inhibition of vasoconstriction, via previously described mechanisms (Krishnamoorthy, 2014; Lopez, 2016). Heavy menstrual bleeding as reported by

RYR1-mutated participants in our study, together with previous data presented in Chapter 4, of RYR1 involvement in VSMC function suggest that increased vascularisation and blood flow to the uterus via the uterine artery could indeed exacerbate menstrual bleeding in *RYR1*-mutated individuals. More *ex vivo* studies, including investigations of the spatial organisation of RYR1 channels in uterine artery vascular smooth muscle cells of non-pregnant *Ryr1$^{Y522S/+}$* animals should be performed to confirm this.

Furthermore, there is some emerging evidence for the role of myometrial smooth muscle in menorrhagia. The direction of uterine contraction is dependent on the phase of the menstrual cycle. Antegrade direction of contraction (fundus to cervix) is believed to assist the shedding of the endometrium during menstruation, whereas retrograde direction of contraction (cervix to fundus) is assumed to facilitate transportation of sperm into the uterus (Arrowsmith *et al.*, 2012). During menstruation, contractions are thought to be of low frequency and high amplitude (Aguilar, 2010). Recent studies have also found reduced uterine mobility in women with menorrhagia (Ting and Burke, 2019). Considering there is recognized SMC involvement in the mouse model of *RYR1*-assoicated MH, a myometrial SMC contribution to the observed menorrhagia phenotype is plausible and warrants further investigation of uterine contractility in *RYR1* patients using transvaginal ultrasound measurements.

Post-partum haemorrhage

In this study, although not statistically significant, there was a history of more severe and more frequent post-partum bleeding among *RYR1*-mutated participants (18.18%) compared to control participants (5.71%). In the *RYR1*-mutated cohort, the reported blood loss volumes (>1000 ml) by 3 participants, are clinically categorized as major-severe PPH, compared to only

two cases of minor PPH reported in the control and *RYR1*-mutated cohorts, as defined by the Royal College of Obstetricians and Gynaecologists' (Anderson and Etches, 2017). In the general population, spontaneous PPH is estimated to have a prevalence of 0.3-5.1% (Al-Zirqi *et al.*, 2008; Calvert *et al.*, 2012; Kramer, 2013; Nyfløt, 2017; Liu *et al.*, 2021). This indicates an increased prevalence of severe PPH among the *RYR1*-mutated cohort in comparison to the control group that was representative of the general population.

Furthermore, studies have revealed that the prevalence of some *RYR1* mutations is increased in the African-Caribbean population (1 in 800 to 1 in 1000) (Altshuler *et al.*, 2012). Interestingly, researchers have also found that women of black African ethnicity are at higher risk of severe PPH, severe morbidity and mortality associated with PPH (Calvert, 2012; Briley, 2014; Gyamfi-Bannerman *et al.*, 2018; Jardine *et al.*, 2022). Therefore, it is compelling to suggest that increased prevalence of *RYR1* mutations may be responsible for the proportional increase of PPH in Black women. This should prompt further studies and clinical genetic testing in this population.

Complications during pregnancy

In the present study, *RYR1*-mutated participants were more likely to report having medical complications during pregnancy, specifically, preeclampsia, and placenta praevia. The precise pathophysiology of these manifestations in the *RYR1*-mutated females is currently unclear, but there are some potential plausible mechanisms that may provide some explanation.

The mechanism by which gestational hypoxia affects uterine vascular adaption, which is believed to be a major cause of increased risk of pregnancy complications, including

preeclampsia and fetal intrauterine growth restriction, may be relevant in the pathophysiology of preeclampsia in *RYR1*-mutated patients (Ducsay *et al.*, 2018; Tong and Giussani, 2019). In cases of gestational hypoxia, vascular Ca^{2+} sparks and STOCs coupling are suppressed, leading to increased uterine vascular tone via reversible enhanced endoplasmic reticulum (ER)/oxidative stress (Hu, 2020). Enhanced oxidative stress is prominent with *RYR1* variants, in particular MH-associated $RyR1^{Y522S/+}$ myotubes display a temperature dependent increase in both reactive oxygen species (ROS) and reactive nitrogen species (RNS) production (Durham, 2008). This indicates that *RYR1*-patients may be predisposed to preeclampsia via an RYR1-oxidative stress related pathway.

Placenta praevia is typically described as placental location in the lower uterine segment with partial or complete covering of the endocervical os. Placenta praevia is the leading cause of post-partum haemorrhage, and when combined with abnormal placenta implantation in the uterine wall, may lead to severe postpartum haemorrhage, which requires emergent hysterectomy (Lee *et al.*, 2017). Approximately 3% of women with placenta praevia are also diagnosed with placenta accreta, where excessive invasion of trophoblasts in the placenta leads to abnormal adherence to the decidua and myometrium (Silver *et al.*, 2006; American College of Obstetricians and Gynecologists (ACOG) *et al.*, 2018; Jauniaux *et al.*, 2019). In this case the trophoblast is significantly exposed to the myometrium and its vasculature, leading to excessive vascular remodelling and more invasive vascular connections (Jauniaux and Jurkovic, 2012; Sundheimer and Pisarska, 2017). Recently, RYR1 channel activity has been implicated in the regulation of trophoblast migration in the BeWo cell model (Zheng, 2022). Thus, implicating RYR1 channels as an important factor in the altered placentation of *RYR1*-mutated women and further describing a mechanism by which *RYR1*-mutated patients may be at risk of PPH.

Birthweights and gestation length

Another interesting finding from this study was that *RYR1*-mutated participants gave birth to offspring with reduced birthweight compared to control participants, in both the questionnaire study and in the separate cohort of MH patients adjusted for gestational age and sex. This finding is consistent with the discovery of lower weight fetuses at gestation day 18.5 from *Ryr1*$^{Y522S/+}$ animals in Chapter 6, supporting the notion that *RYR1* mutations could lead to restricted fetal development. It is possible that the smaller offspring birthweight among *RYR1*-mutated participants could be a direct result of shorter pregnancies, limiting fetal growth in the final weeks of gestation however this factor was controlled in the MH patient cohort and in the mouse model. Nevertheless, fetal development in the pregnant *RYR1*-mutated patient may need additional clinical monitoring, considering that low birthweight has been associated with increased risk of cardiovascular disease and Type 2 diabetes in adult life (Barker, 1990, 1999; Phipps, 1993).

Placental weight is also a potential indicator of fetal outcomes. In section 6.3.1 I demonstrated that decreased fetal weight corresponded with increased placental weight from litters of the pregnant heterozygous *Ryr1* Y522S animal compared to their wild-type littermates. Regrettably, human *RYR1*-associated placental weight was not investigated in this questionnaire study, due to difficulties obtaining placental weight retrospectively, in addition to being unaware of the mouse fetoplacental weight ratio at the time of questionnaire design and implementation. In future investigations of pregnant *RYR1*-mutated patients, it could be beneficial to collect placental weights and to examine placental vascular resistance during the final trimester to better understand how mutations in *RYR1* might impact placental growth and vascularisation.

In conjunction, a shorter gestation length (<37 weeks) in *RYR1*-mutated participants may reflect RYR1 involvement in myometrial cell function, however the role of RYR1 in short gestation or preterm labour has not been extensively established. As previously discussed, *RYR1* mRNA and protein have been identified in human myometrium, with some evidence to support its role in both myometrial cell contraction and relaxation but less so at the end of gestation (Martin, 1999; Mironneau, 2002; Matsuki, 2017). Increased oxidative stress has been previously associated with both spontaneous and non-spontaneous preterm birth (Duhig, Chappell and Shennan, 2016; Rosen *et al.*, 2019). Thus, *RYR1* gain-of-function channels that enhance oxidative stress in myotubes may also contribute to the early onset of labour. In future clinical investigations of pregnant *RYR1*-mutated patients it could be useful to measure a biomarker of oxidative stress such as the urinary 8-iso-PGF2α metabolite to determine risk for preterm delivery (Rosen, 2019). Although in this thesis, video recording data of gestation length in the pregnant *Ryr1*$^{Y522S/+}$ animal did not correlate this decrease in gestation length, the decreased litter size in *Ryr1*$^{Y522S/+}$ dams provide some indication of the pathological involvement of *RYR1* mutations in myometrial malfunction which could lead to a shorter gestation in female *RYR1*-mutated patients.

Other smooth muscle symptoms

RYR1-mutated patients were more likely to report gastrointestinal (bowel and bladder) symptoms, with symptoms including constipation, diarrhoea and urinary incontinence, potential indicators of dysfunctional colonic and urinary bladder smooth muscle function. Reduced colonic smooth muscle cell function, along with defects in smooth muscle innervation (via the interstitial cells of Cajal and the Auerbach's plexus (Sanders, 1996)) contribute to

reduced peristalsis and GI transit (Gabella, 1972; Wedel *et al.*, 2006; Bharucha, 2007; Yang *et al.*, 2019). Human *RYR1* expression in colonic smooth muscle (*GTEx Portal*, data accessed 07 January 2023), and colonic epithelium (Prinz, 2008), is downregulated in Hirschsprung's disease (O' Donnell, Nakamura and Puri, 2019). RyR and its regulatory protein FK506-binding protein (FKBP12) have been suggested to play a role in intracellular Ca^{2+} release in guinea pig colonic myocytes (Flynn *et al.*, 2001; MacMillan *et al.*, 2008). This suggests an important role of RYR1 channels in GI tract and bladder function, and mutations which may form the basis of clinical manifestations such as constipation, diarrhoea, and urinary incontinence.

Genotype: phenotype correlations

AR *RYR1*-variants typically manifest as MmD, CNM and CFTD, whereas AD *RYR1* variants are more often associated with MHS, ERM and CCD. AD *RYR1* variants are typically gain-of-function resulting in a "hypersensitive" RYR1 channel and in some cases cause loss of channel function, whereas AR *RYR1* genotypes often lead to reduced RYR1 protein expression, and sometimes include loss-of-function channels (Tong, McCarthy and MacLennan, 1999; Dirksen and Avila, 2002). Individuals with AD mutations were more likely to have bleeding between menstrual cycle bleeds and offspring with lower birthweight compared to participants with AR mutations. In addition, although not statistically proven, more AD participants had pathological bleeding scores and were more likely to be treated for anaemia. In line with previous preliminary findings, this study emphasizes that AD *RYR1* gain-of-function variants are more frequently associated with excessive bleeding and other gynaecological and obstetric complications (Lopez, 2016).

MH mutation prevalence

According to the European Malignant Hyperthermia Group (https://emhg.org/genetics/, accessed on 27 February 2023), there are currently 66 *RYR1* mutations that are 'pathogenic' or 'likely pathogenic' for MH (Weiss *et al.*, 2004; Eltit *et al.*, 2012). Studies have estimated the prevalence of *RYR1* MH-associated mutations to be 1 in 2000–3000 individuals (Bachand, 1997; Monnier, 2002; Wappler, 2010; Miller, 2018). Therefore, it is likely that there may be between 40000-100000 MH susceptible individuals in the UK alone, most of them otherwise asymptomatic. Furthermore, it is suspected that many MH cases have not come to medical attention, and the frequency of MH mutations may be estimated to be as high as 1 in 400 individuals (Gonsalves *et al.*, 2013). Therefore, the findings of this study may be relevant in a much larger portion of the population than originally suspected. Although this study focussed on female health, the results may be relevant in males, albeit as less severe bleeding symptoms. It is possible that there are far more male and female individuals with an undiscovered bleeding phenotype, and many more women at risk of obstetric complications as outlined in this study.

Moreover, dantrolene has been shown to improve bleeding symptoms in women presenting with heavy menstrual bleeding (unpublished clinical observation), providing a potential pre-approved and well-tolerated clinical treatment for these individuals. However, the intravenous use of dantrolene in pregnancy is recommended only if "potential benefit outweighs risk" by NICE, and oral use should be avoided even though teratological studies in animals have been satisfactory, as the drug crosses into the placenta (https://bnf.nice.org.uk/drugs/dantrolene-sodium/). *In vitro* studies of guinea pig uterus have found that dantrolene reversibly increases spontaneous contraction frequency, and reversibly reduces contractile responses to oxytocin in a dose dependent manner (Conte-Camerino *et al.*, 1983). A previous study found that low-dose dantrolene administered to mothers during Caesarean sections has low risk to the mother,

however neonates are considered to be at risk of 'floppy child syndrome' (Shime *et al.*, 1988). Therefore, dantrolene could prove to be a useful treatment for bleeding symptoms outside of pregnancy, particularly for heavy menstrual bleeding.

7.5 Study limitations and future work

Age and medical conditions

The age of control participants was generally lower than the age of the *RYR1*-mutated participants. This was also evident in the disparity between the number of control participants and *RYR1*-mutated participants currently experiencing menstrual bleeds, menopause, use of contraception and likelihood of having been pregnant. In medical research it is also important to remember that the older population is more likely to have confounding medical conditions such as cardiovascular, immunological, and degenerative diseases. In terms of reproductive health, advanced maternal age is associated with increased likelihood of Caesarean section delivery, endometriosis, infertility/reduced fertility, pregnancy loss, fetal anomalies, stillbirth, and obstetric complications (illnesses such as pre-eclampsia, hypertension and gestational diabetes) (Kirz, Dorchester and Freeman, 1985; Gordon *et al.*, 1991; Bianco *et al.*, 1996; Cnattingius, Cnattingius and Notzon, 1998; Main, Main and Moore, 2000; Smith *et al.*, 2008; Schoen and Rosen, 2009; Sauer, 2015). An increased possibility of medical conditions in the *RYR1*-mutated group could skew the results from this questionnaire and limit the ability to compare between both cohorts, although there was no such increase in reported medical conditions in the *RYR1*-mutated group compared to controls. In addition, an older population may be more likely to be subjected to recall bias, where information may be remembered less accurately compared to a younger cohort. We should also consider that *RYR1*-mutated participants are likely to be in contact with a physician regularly as result of their muscular diagnosis and therefore more likely select the 'consulted a doctor' option about symptoms and have received some treatment, potentially creating a bias towards the perceived severity of a condition in the *RYR1*-mutated group.

Ethnicity and participant recruitment

There was a lack of representation of individuals with black ethnicity in both control and *RYR1*-mutated groups and an over-representation of Indian-Asian ethnicity in the control group. A disparity in ethnic groups across both cohorts, could manifest as differences in confounding medical conditions, limiting the comparability of results between both groups, and limiting representativity of the general population. For example, PCOS and hypothyroidism were most common in both *RYR1*-mutated and control groups (7.58% and 4.55% respectively, in both groups). In the general population the prevalence of PCOS ranges from 6% to 46.8% (Deswal *et al.*, 2020), with the higher prevalence of 46.8% reported in the Indian population (Nidhi *et al.*, 2011). Similarly, prevalence of hypothyroidism is increased in India (11%), compared with the UK (2%) and the USA (4.6%) (Bagcchi, 2014). This may pose an overrepresentation of some disease conditions in the 'healthy' cohort that might otherwise be abnormally increased in the *RYR1*-mutated population.

Recruitment method

It has become common practice to use social media platforms to recruit participants for scientific or clinical studies. For example, the well-known 'Born in Bradford' study, used Facebook and Twitter as a platform to recruit prospective participants and to inform the public of their research (https://borninbradford.nhs.uk/). This method of recruitment can be an excellent way to reach a large, diverse, and representative samples of the general population. In the present study, I used social media platforms (Facebook and Twitter) and the internal King's College London circular participant recruitment email to recruit several participants in a limited amount of time. Recruiting using personal social media accounts could have

potentially skewed the background (age and ethnicity) of recruited control participants in this study.

Questionnaire design

The specifically designed modified version of the MCMDM-1VWD questionnaire employed in this study did not survey 3 symptoms (muscle hematomas, hemarthrosis, central nervous system bleeding) that are included the original MCMDM-1VWD bleeding questionnaire. The present study focused on determining smooth muscle related symptoms, whereas the 3 symptoms described above were not relevant to the purpose of this study, and may thus indeed underestimate the bleeding severity in *RYR1*-mutated patients. Furthermore, extensive follow-up questions and robust statistical tests ensured the informative examination of bleeding related to menstruation, gestation and delivery, and further complications during pregnancy and delivery.

Of 66 *RYR1*-mutated participants, approximately 20% of participants did not provide a response for the question their diagnosed *RYR1*-related disorder. This highlights an oversight during question development, where the question should have provided an open-ended 'other' option, which would have allowed participants to describe any *RYR1*-related diagnosed disorder.

In this study the questionnaire determined *current* experiences of abnormal bleeding and severity. However, the questionnaire did not collect reports on whether the bleeding improved after treatment (other than after use of contraception). It could be useful to know if the treatment improves bleeding symptoms, and if the bleeding did not improve this would provide insight

into whether RYR1 was the cause of bleeding and whether administration of dantrolene could potentially be used as a treatment.

A potential design issue for the study was that question phrasing or spelling, and questionnaire layout was altered between Phase I (control) and Phase II (*RYR1*-mutated), resulting in problematic downstream data analysis. For example, the participants 'country of residence' was only requested in Phase II and not Phase I causing inconsistency between the two groups. This highlights the importance of using consistent materials throughout a study. In addition, open-ended questions were used to allow participants to elaborate upon their responses, thus allowing us to gather detailed information regarding a bleeding symptom, however, the answers were often difficult to interpret when not explained thoroughly.

7.6   Conclusions

This study clearly demonstrates that pathogenic *RYR1* mutations are associated with prolonged bleeding, obstetric, gynaecological and bowel and bladder symptoms, thus further widening the pool of *RYR1* associated non-neuromuscular phenotypes. *RYR1*-mutated patients are likely to have a bleeding disorder that manifests as heavy menstrual bleeding, post-partum haemorrhage, preterm birth, and low birthweight in addition to GI tract smooth muscle dysfunction. Thus altered RYR1 function may be a potentially modifiable cause of currently unresolved cases of menorrhagia and post-partum haemorrhage and this should be further explored with a clinical trial of dantrolene.

8   Chapter 8 General discussion and future work

In this thesis, the impact of *RYR1* mutations on myometrial and uterine vascular smooth muscle function have been studied in pregnancy and in relation to other gynaecological disorders, in an MH mouse model and in human *RYR1*-variant carriers. This chapter provides a general discussion of the main findings, as well general methodological strengths and weaknesses, and future research considerations.

Using a wide range of methodologies, I aimed to determine how *Ryr1* Y522S alters pregnant uterine myometrium and uterine blood vessel function *ex vivo,* and how this might impact on gestation length, parturition duration and fetal and placental development. I also investigated the impact of *Ryr1* Y522S on other *Ryr* isoform mRNA and protein expression in mouse reproductive tissues, including the myometrium, uterine artery, and placenta. To understand how *RYR1* variants impact bleeding during menstruation, pregnancy, and post-partum in addition to fetal growth and other obstetric complications, I developed and implemented a focused online questionnaire. These aims were based on my overarching hypothesis that the impact of the gain-of-function Y522S mutation during pregnancy will be systemic, leading to increased vasorelaxation of vascular smooth muscle cells, increased contractility of the uterine myometrium in labour and modified cellular needs of reproductive tissues.

Using isometric tension measurements of pregnant uterine artery contractile and dilatory responses, I confirmed that the $Ryr1^{Y522S/+}$ mouse model displays altered vasodilatory properties during pregnancy, albeit not in the manner that was hypothesised. The suppression of $Ryr1^{Y522S/+}$ uterine artery vasodilation was rather unexpected, as previous experiments by Lopez and colleagues demonstrated that the smooth muscle cells of the $Ryr1^{Y522S/+}$ tail artery promoted vasodilation. To determine how uterine arteries with the gain-of-function RYR1 Y522S channel results in an increased inhibition of uterine artery vasodilation, protein

subcellular localisation studies in the vascular smooth muscle and endothelium should be performed in the uterine vascular bed, but also in several vascular beds under normal pregnancy and non-pregnant conditions. Further to this, real-time calcium imaging of RYR1 Ca^{2+} sparks in uterine artery vascular smooth muscle cells could provide critical insight into the channel function, as determined in the tail VSMCs by Lopez and colleagues (2016).

In wire myography preparations, treating separate arterial segments from the same animal as independent measurements may appear to help with RRR in a single study; but in the long run such research is underpowered and potentially misleading. Thus, myography experiments in this thesis were described with the number of animals as individual samples (n of biological repeats), opposed to individual arterial segments that were used as technical repeats (2 – 4 segments per animal). Ultimately, this makes the study more strongly powered but inevitably resulted in the excessive use of animals.

Investigations of the $Ryr1^{Y522S/+}$ mouse pregnancy revealed no change in the length of gestation compared to wild-type animals, indicating that the timing of labour was unchanged in the $Ryr1$-mutated animal. It is important to note that the mechanisms by which labour is initiated in the uterus are different between mice and humans. In mice, progesterone withdrawal is thought to be the dominant factor that triggers the initiation of labour, whereas in humans, short-term loss of BK_{Ca} channel functionality and cervical ripening are the key contributary factors. Thus, as with several biological models of human disorders, the mouse model of pregnancy is not completely representative of human pregnancy, specifically the initiation and timing of labour. To overcome this limitation, it could be beneficial to study the arguably more physiologically similar guinea pig model of pregnancy (Mitchell, 2009).

Initial experiments indicated that spontaneous non-pregnant myometrial contractions (measured *ex vivo*) from the heterozygous $Ryr1^{Y522S/+}$ mouse were significantly different to that

of the wildtype mouse; contractions were more frequent and of shorter duration. These findings may be relevant in the non-pregnant menstruating *RYR1*-mutated female, as changes in non-pregnant uterine contractions could influence menstrual flow and may contribute to the heavy menstrual bleeding reported by *RYR1*-mutated patients. To further demonstrate alterations in pregnant or non-pregnant myometrial activity, the investigation of myometrial tissue contractility from *RYR1*-variant carriers undergoing Caesarean sections or hysterectomies could be performed. Previous unpublished clinical observations have demonstrated the effectiveness of dantrolene, a pre-approved drug in the UK and many other countries, in reducing heavy menstrual bleeding in MH *RYR1* variant carriers, yet further clinical investigations should be performed.

RNA sequencing of the pregnant $Ryr1^{Y522S/+}$ myometrium, and follow-up investigations in the placenta, has revealed some interesting potential RYR1-interaction pathways that warrant further investigation. In particular, there is strong indication for RYR1 involvement in the immune system. It is therefore plausible that current research by the Treves group at the University Hospital Basel, Basel, Switzerland, reports the impact of gain-of-function *RYR1* variants on the altered function of dendritic cells, ultimately enhancing the immune response. Considering the heavier placentas of the $Ryr1^{Y522S/+}$ dam, it could also be beneficial to study the impact of *RYR1* variants on Hofbauer (HB) cells that are fetal macrophages of the human placenta. Although, the *in vitro* culture of HB cells does not entirely recapitulate the complexity of the villous stromal microenvironment, so experimental procedures should be adapted accordingly (Hunt and Pollard, 1992).

It should be noted that bulk RNA sequencing is insightful at the gene level, however itself lacks translatability at a functional level in tissues of interest. Thus, single cell RNA-sequencing or spatial transcriptomics should be considered for more detailed understanding of changes within

tissue cell types and proteomic studies should be considered to obtain dynamic and functional insights into the impact of the *Ryr1* Y522S in reproductive tissues on a protein level.

In this thesis, I have uncovered some interesting alterations in fetal development associated with maternal *RYR1* variants; including reduced individual fetal weights in the litter of *Ryr1*$^{Y522S/+}$ (mixed litter) dams, and lower birthweight of offspring in women carrying MH or CCD associated *RYR1* mutations. To further complement these findings, it may be beneficial to also investigate both birthweight, gestation length and parturition duration in the established MH Piétrain pig model. This reduction in offspring birthweight was compensated with increased placental weight in the *Ryr1*$^{Y522S/+}$ (mixed litter) dam. This change is an important clinical consideration as larger placentas have repeatedly been associated with increase prevalence and severity of PPH (Eskild, 2011). A future research direction could involve the collection of placental weights (from hospital records) and cases of PPH in combination with patient DNA to identify potential *RYR1* variants i.e., through a long-term follow-up study via MH patient clinics or by interrogating existing databases such as the 1000 Genomes Project and hospital records.

The shorter gestation length (<37 weeks) in *RYR1*-mutated females may reflect the role of the RYR1 channel in myometrial cell contractility, however this has not yet been supported by *ex vivo* studies in the *Ryr1*-mutated mouse myometrium. Unfortunately, due to COVID-19 restrictions, the *ex vivo* study of spontaneous contractions of the pregnant *Ryr1*$^{Y522S/+}$ myometrium were limited, and considering the promising preliminary findings in this thesis, this research should be prioritised going forward. More biological repeats are required, and experiments should be expanded to investigate the impact of RYR1 inhibitors on myometrial contractility in the pregnant Y522S mouse model. Nevertheless, this finding also warrants further investigation of preterm labour in *RYR1*-mutated patients through pre-existing medical

databases, and the investigation of oxidative stress biomarkers in pregnant *RYR1*-mutated human myometrium which may be a useful approach to determine risk for preterm delivery in future studies (Duhig, 2016; Rosen, 2019).

I hypothesised that the RYR1 human patient cohort will demonstrate a susceptibility to increased bleeding events, longer bleeding times, increased rate of menorrhagia and a shorter length of pregnancy. The findings of this thesis indeed support the above-mentioned hypothesis, and does so using a much larger cohort of participants than previous reports (Lopez, 2016). Thus, highlighting the necessity of a clinical trial investigating the impact of dantrolene, in the treatment of women with heavy menstrual or post-partum bleeding. Not only did the questionnaire study corroborate reports of HMB, PPH, and reduced offspring birthweight, this study highlights previously unrecognised aspects of *RYR1*-related smooth muscle dysfunction, specifically involving the GI tract, further expanding the phenotypic spectrum of *RYR1*-related disorders. This warrants further investigation but was beyond the scope of this study.

Other limitations still to be addressed, are relatively low sample numbers for some experiments, and a focus on gene expression rather than protein. Protein validation could be achieved using mass spectrometry, and subcellular localisation and protein functionality imaging studies, which would contribute greatly to the understanding of *RYR1*-mutations in pregnancy and obstetric complications.

9   Conclusion

In summary, this thesis has established that variants in the ryanodine receptor gene (*RYR1)* alter intracellular calcium signalling within vascular and myometrial smooth muscle cells and placental tissues. Altered calcium levels in these cells lead to altered pregnant uterine artery vasodilation and non-pregnant myometrial contractility, that may contribute to abnormal bleeding events during menstruation, pregnancy, and post-partum, and restricted fetal development, which may be further exacerbated by abnormal placental development. This thesis has also uncovered the contribution of RYR1 in the function of other smooth muscle lined organs, expanding the phenotypic spectrum of *RYR1*-related disorders. Overall, this work has provided several observations and raised a number of interesting questions that need to be explored in the future.

10 References

Aardema, M. W., Oosterhof, H., Timmer, A., Van Rooy, I. and Aarnoudse, J. G. (2001) 'Uterine artery Doppler flow and uteroplacental vascular pathology in normal pregnancies and pregnancies complicated by pre-eclampsia and small for gestational age fetuses', *Placenta*. W.B. Saunders Ltd, 22(5), pp. 405–411. doi: 10.1053/plac.2001.0676.

Aaronson, P. I., Sarwar, U., Gin, S., Rockenbauch, U., Connolly, M., Tillet, A., Watson, S., Liu, B. and Tribe, R. M. (2006) 'A role for voltage-gated, but not Ca 2+-activated, K + channels in regulating spontaneous contractile activity in myometrium from virgin and pregnant rats', *British Journal of Pharmacology*, 147(7), pp. 815–824. doi: 10.1038/sj.bjp.0706644.

Abalos, E., Oladapo, O. T., Chamillard, M., Díaz, V., Pasquale, J., Bonet, M., Souza, J. P. and Gülmezoglu, A. M. (2018) 'Duration of spontaneous labour in "low-risk" women with "normal" perinatal outcomes: A systematic review', *European Journal of Obstetrics and Gynecology and Reproductive Biology*. Elsevier Ireland Ltd, 223, pp. 123–132. doi: 10.1016/j.ejogrb.2018.02.026.

Abberton, K. M., Taylor, N. H., Healy, D. L. and Rogers, P. A. W. (1999) 'Vascular smooth muscle cell proliferation in arterioles of the human endometrium', *Human Reproduction*. Oxford Academic, 14(4), pp. 1072–1079. doi: 10.1093/HUMREP/14.4.1072.

'ACOG Committee Opinion No. 651: Menstruation in girls and adolescents: using the menstrual cycle as a vital sign' (2015) *Obstetrics and Gynecology*, 126(6), pp. e143–e146. doi: 10.1097/AOG.0000000000001215.

Adachi-Akahane, S., Cleemann, L. and Morad, M. (1996) 'Cross-signaling between L-type Ca2+ channels and ryanodine receptors in rat ventricular myocytes', *Journal of General Physiology*, 108(5). doi: 10.1085/jgp.108.5.435.

Adamova, Z., Ozkan, S. and Khalil, R. (2010) 'Vascular and Cellular Calcium in Normal and Hypertensive Pregnancy', *Current Clinical Pharmacology*, 4(3). doi: 10.2174/157488409789375320.

Adams, J., Polson, D. W., Abdulwahid, N., Morris, D. V., Franks, S., Mason, H. D., Tucker, M., Price, J. and Jacobs, H. S. (1985) 'Multifollicular ovaries: clinical and endocrine features and response to pulsatile gonadotropin releasing hormone', *The Lancet*. Elsevier, 326(8469–8470), pp. 1375–1379. doi: 10.1016/S0140-6736(85)92552-8.

Adamson, S. L. (1999) 'Arterial pressure, vascular input impedance, and resistance as determinants of pulsatile blood flow in the umbilical artery', in *European Journal of Obstetrics and Gynecology and Reproductive Biology*. Elsevier Ireland Ltd, pp. 119–125. doi: 10.1016/S0301-2115(98)00320-0.

Adamson, S. L. and Langille, B. L. (1992) 'Factors determining aortic and umbilical blood flow pulsatility in fetal sheep', *Ultrasound in Medicine and Biology*, 18(3), pp. 255–266. doi: 10.1016/0301-5629(92)90095-R.

Adamson, S. L., Lu, Y., Whiteley, K. J., Holmyard, D., Hemberger, M., Pfarrer, C. and Cross,

J. C. (2002) 'Interactions between trophoblast cells and the maternal and fetal circulation in the mouse placenta', *Developmental Biology*. Academic Press, 250(2), pp. 358–373. doi: 10.1006/DBIO.2002.0773.

Agrawal, P. B., Greenleaf, R. S., Tomczak, K. K., Lehtokari, V. L., Wallgren-Pettersson, C., Wallefeld, W., Laing, N. G., Darras, B. T., Maciver, S. K., Dormitzer, P. R. and Beggs, A. H. (2007) 'Nemaline myopathy with minicores caused by mutation of the CFL2 gene encoding the skeletal muscle actin-binding protein, cofilin-2', *American Journal of Human Genetics*. University of Chicago Press, 80(1), pp. 162–167. doi: 10.1086/510402.

Aguilar, H. N. and Mitchell, B. F. (2010) 'Physiological pathways and molecular mechanisms regulating uterine contractility', *Human Reproduction Update*. Oxford Academic, 16(6), pp. 725–744. doi: 10.1093/humupd/dmq016.

Ahokas, R. A., Anderson, G. D. and Lipshitz, J. (1983) 'Cardiac output and uteroplacental blood flow in diet-restricted and diet-repleted pregnant rats', *American Journal of Obstetrics and Gynecology*, 146(1). doi: 10.1016/0002-9378(83)90918-3.

Ain, R., Canham, L. N. and Soares, M. J. (2003) 'Gestation stage-dependent intrauterine trophoblast cell invasion in the rat and mouse: novel endocrine phenotype and regulation', *Developmental Biology*. Academic Press, 260(1), pp. 176–190. doi: 10.1016/S0012-1606(03)00210-0.

Ajayi, A. F. and Akhigbe, R. E. (2020) 'Staging of the estrous cycle and induction of estrus in experimental rodents: an update', *Fertility Research and Practice 2020 6:1*. BioMed Central, 6(1), pp. 1–15. doi: 10.1186/S40738-020-00074-3.

Al-Zirqi, I., Vangen, S., Forsen, L. and Stray-Pedersen, B. (2008) 'Prevalence and risk factors of severe obstetric haemorrhage', *BJOG: An International Journal of Obstetrics & Gynaecology*. John Wiley & Sons, Ltd, 115(10), pp. 1265–1272. doi: 10.1111/J.1471-0528.2008.01859.X.

Albinsson, S., Nordström, I. and Hellstrand, P. (2004) 'Stretch of the vascular wall induces smooth muscle differentiation by promoting actin polymerization', *Journal of Biological Chemistry*, 279(33), pp. 34849–34855. doi: 10.1074/jbc.M403370200.

Alexander, J., Thomas, P. W. and Sanghera, J. (2002) 'Treatments for secondary postpartum haemorrhage', *The Cochrane database of systematic reviews*. Cochrane Database Syst Rev, (1). doi: 10.1002/14651858.CD002867.

Allen, E. (1922) 'The oestrous cycle in the mouse', *American Journal of Anatomy*. John Wiley & Sons, Ltd, 30(3), pp. 297–371. doi: 10.1002/AJA.1000300303.

Altshuler, D. M., Durbin, R. M., Abecasis, G. R., Bentley, D. R., Chakravarti, A., Clark, A. G., Donnelly, P., Eichler, E. E., Flicek, P., Gabriel, S. B., *et al.* (2012) 'An integrated map of genetic variation from 1,092 human genomes', *Nature*, 491(7422). doi: 10.1038/nature11632.

Alvarez, D. F., King, J. A., Weber, D., Addison, E., Liedtke, W. and Townsley, M. I. (2006) 'Transient receptor potential vanilloid 4-mediated disruption of the alveolar septal barrier: A novel mechanism of acute lung injury', *Circulation Research*, 99(9), pp. 988–995. doi:

10.1161/01.RES.0000247065.11756.19.

Amberg, G. C., Bonev, A. D., Rossow, C. F., Nelson, M. T. and Santana, L. F. (2003) 'Modulation of the molecular composition of large conductance, Ca 2+ activated K+ channels in vascular smooth muscle during hypertension', *Journal of Clinical Investigation*, 112(5). doi: 10.1172/JCI200318684.

Amburgey, K., McNamara, N., Bennett, L. R., McCormick, M. E., Acsadi, G. and Dowling, J. J. (2011) 'Prevalence of congenital myopathies in a representative pediatric united states population', *Annals of neurology*, 70(4), pp. 662–665. doi: 10.1002/ANA.22510.

American College of Obstetricians and Gynecologists (ACOG), Society for Maternal–Fetal Medicine, Cahill, A. G., Beigi, R., Heine, R. P., Silver, R. M. and Wax, J. R. (2018) *Placenta Accreta Spectrum, Obstetric Care Consensus (7)*. Available at: https://www.acog.org/clinical/clinical-guidance/obstetric-care-consensus/articles/2018/12/placenta-accreta-spectrum (Accessed: 17 April 2023).

American Society of Anesthesiologists (ASA) (no date) *Epidural - Benefits & Side Effects of Anesthesia During Labor, Made for This Moment*. Available at: https://www.asahq.org/madeforthismoment/pain-management/techniques/epidural/ (Accessed: 8 March 2023).

Anderson, J. M. and Etches, D. (2017) 'Prevention and management of postpartum haemorrhage', *BJOG: An International Journal of Obstetrics & Gynaecology*, 124(5), pp. e106–e149. doi: 10.1111/1471-0528.14178.

Angus, J. A. and Cocks, T. M. (1996) 'Pharmacology of human isolated large and small coronary arteries', *The Pharmacology of Vascular Smooth Muscle*. Oxford University Press. doi: 10.1093/ACPROF:OSO/9780192623874.003.0012.

Animals (Scientific Procedures) Act 1986 (c.14) (1986).

Annibale, D. J., Rosenfeld, C. R., Stull, J. T. and Kamm, K. E. (1990) 'Protein content and myosin light chain phosphorylation in uterine arteries during pregnancy', *American Journal of Physiology - Cell Physiology*, 259(3 28-3). doi: 10.1152/ajpcell.1990.259.3.c484.

Anson-Cartwright, L., Dawson, K., Holmyard, D., Fisher, S. J., Lazzarini, R. A. and Cross, J. C. (2000) 'The glial cells missing-1 protein is essential for branching morphogenesis in the chorioallantoic placenta', *Nature Genetics*, 25(3). doi: 10.1038/77076.

Antigny, F., Sabourin, J., Saüc, S., Bernheim, L., Koenig, S. and Frieden, M. (2017) 'TRPC1 and TRPC4 channels functionally interact with STIM1L to promote myogenesis and maintain fast repetitive Ca2 + release in human myotubes', *Biochimica et Biophysica Acta - Molecular Cell Research*, 1864(5), pp. 806–813.

Arbogast, S., Beuvin, M., Fraysse, B., Zhou, H., Muntoni, F. and Ferreiro, A. (2009) 'Oxidative stress in SEPN1-related myopathy: From pathophysiology to treatment', *Annals of Neurology*. John Wiley & Sons, Ltd, 65(6), pp. 677–686. doi: 10.1002/ana.21644.

Arrowsmith, S., Robinson, H., Noble, K. and Wray, S. (2012) 'What do we know about what

happens to myometrial function as women age?', *Journal of Muscle Research and Cell Motility*. Springer, 33(3–4), pp. 209–217. doi: 10.1007/S10974-012-9300-2/FIGURES/3.

Avila, G., O'Brien, J. J. and Dirksen, R. T. (2001) 'Excitation - Contraction uncoupling by a human central core disease mutation in the ryanodine receptor', *Proceedings of the National Academy of Sciences of the United States of America*. National Academy of Sciences, 98(7), pp. 4215–4220. doi: 10.1073/pnas.071048198.

Awad, S. S., Lamb, H. K., Morgan, J. M., Dunlop, W. and Gillespie, J. I. (1997) 'Differential expression of ryanodine receptor RyR2 mRNA in the non-pregnant and pregnant human myometrium', *Biochemical Journal*. Portland Press Ltd, 322(3), pp. 777–783. doi: 10.1042/bj3220777.

Azimi, I., Stevenson, R. J., Zhang, X., Meizoso-Huesca, A., Xin, P., Johnson, M., Flanagan, J. U., Chalmers, S. B., Yoast, R. E., Kapure, J. S., *et al.* (2020) 'A new selective pharmacological enhancer of the orai1 ca2+ channel reveals roles for orai1 in smooth and skeletal muscle functions', *ACS Pharmacology and Translational Science*. American Chemical Society, 3(1), pp. 135–147. doi: 10.1021/acsptsci.9b00081.

Baah-Dwomoh, A., McGuire, J., Tan, T. and De Vita, R. (2016) 'Mechanical properties of female reproductive organs and supporting connective tissues: a review of the current state of knowledge', *Applied Mechanics Reviews*. doi: 10.1115/1.4034442.

Bachand, M., Vachon, N., Boisvert, M., Mayer, F. M. and Chartrand, D. (1997) 'Clinical reassessment of malignant hyperthermia in Abitibi-Témiscamingue', *Canadian journal of anaesthesia = Journal canadien d'anesthesie*, 44(7), pp. 696–701. doi: 10.1007/BF03013380.

Bagcchi, S. (2014) 'Hypothyroidism in India: More to be done', *The Lancet Diabetes and Endocrinology*. doi: 10.1016/S2213-8587(14)70208-6.

Bakrania, B., Duncan, J., Warrington, J. P. and Granger, J. P. (2017) 'The endothelin type a receptor as a potential therapeutic target in preeclampsia', *International Journal of Molecular Sciences*. doi: 10.3390/ijms18030522.

Baldwin, G. R., Moorthi, D. S., Whelton, J. A. and MacDonnell, K. F. (1977) 'New lung functions and pregnancy', *American Journal of Obstetrics and Gynecology*, 127(3). doi: 10.1016/0002-9378(77)90460-4.

Balschun, D., Wolfer, D. P., Bertocchini, F., Barone, V., Conti, A., Zuschratter, W., Missiaen, L., Lipp, H. P., Frey, J. U. and Sorrentino, V. (1999) 'Deletion of the ryanodine receptor type 3 (RyR3) impairs forms of synaptic plasticity and spatial learning', *EMBO Journal*, 18(19). doi: 10.1093/emboj/18.19.5264.

Barbieri, R. L. (2014) 'The endocrinology of the menstrual cycle', *Methods in Molecular Biology*. Humana Press Inc., 1154, pp. 169–180. doi: 10.1007/978-1-4939-0659-8_7/COVER.

Barker, D. J. P. (1990) 'The fetal and infant origins of adult disease.', *BMJ : British Medical Journal*. BMJ Publishing Group, 301(6761), p. 1111. doi: 10.1136/BMJ.301.6761.1111.

Barker, D. J. P. (1999) 'Fetal origins of cardiovascular disease.', *Annals of medicine*. Royal

Society of Medicine Press Ltd, 31(sup1), pp. 3–6. doi: 10.1080/07853890.1999.11904392.

Bateman, B. T., Berman, M. F., Riley, L. E. and Leffert, L. R. (2010) 'The epidemiology of postpartum hemorrhage in a large, nationwide sample of deliveries', *Anesthesia and Analgesia*. Lippincott Williams and Wilkins, 110(5), pp. 1368–1373. doi: 10.1213/ANE.0b013e3181d74898.

Baudel, Miguel A. S. Martín-Aragón, Shi, J., Large, W. A. and Albert, A. P. (2020) 'Insights into activation mechanisms of store-operated trpc1 channels in vascular smooth muscle', *Cells*. MDPI AG, 9(1), p. 179. doi: 10.3390/cells9010179.

Baudel, Miguel A.S. Martín-Aragón, Shi, J., Large, W. A. and Albert, A. P. (2020) 'Obligatory role for PKCδ in PIP2-mediated activation of store-operated TRPC1 channels in vascular smooth muscle cells', *Journal of Physiology*. Blackwell Publishing Ltd, 598(18), pp. 3911–3925. doi: 10.1113/JP279947.

Bebo, B. F. and Dveksler, G. S. (2005) 'Evidence that pregnancy specific glycoproteins regulate T-Cell function and inflammatory autoimmune disease during pregnancy', *Current drug targets. Inflammation and allergy*, 4(2), pp. 231–237. doi: 10.2174/1568010053586255.

Beech, D. J. (2012) 'Orai1 calcium channels in the vasculature', *Pflugers Archiv European Journal of Physiology*. doi: 10.1007/s00424-012-1090-2.

Belkacemi, L., Bédard, I., Simoneau, L. and Lafond, J. (2005) 'Calcium channels, transporters and exchangers in placenta: A review', *Cell Calcium*. doi: 10.1016/j.ceca.2004.06.010.

Benkusky, N. A., Fergus, D. J., Zucchero, T. M. and England, S. K. (2000) 'Regulation of the Ca2+-sensitive domains of the maxi-K channel in the mouse myometrium during gestation', *The Journal of biological chemistry*, 275(36), pp. 27712–27719. doi: 10.1074/JBC.M000974200.

Bernal, A. L. (2001) 'Overview of current research in parturition', *Experimental Physiology*, 86(2). doi: 10.1113/eph8602178.

Bers, D. M. and Stiffel, V. M. (1993) 'Ratio of ryanodine to dihydropyridine receptors in cardiac and skeletal muscle and implications for E-C coupling', *American Journal of Physiology - Cell Physiology*, 264(6 33-6). doi: 10.1152/ajpcell.1993.264.6.c1587.

Bevan, J. A. and Henrion, D. (1994) 'Pharmacological implications of the flow-dependence of vascular smooth muscle tone', *Annual Review of Pharmacology and Toxicology*. doi: 10.1146/annurev.pa.34.040194.001133.

Bezprozvanny, I., Watras, J. and Ehrlich, B. E. (1991) 'Bell-shaped calcium-response curves of lns(l,4,5)P3- and calcium-gated channels from endoplasmic reticulum of cerebellum', *Nature*, 351(6329). doi: 10.1038/351751a0.

Bharucha, A. E. (2007) 'Constipation', *Best Practice & Research Clinical Gastroenterology*. Baillière Tindall, 21(4), pp. 709–731. doi: 10.1016/J.BPG.2007.07.001.

Bhattacharjee, E. and Maitra, A. (2021) 'Spontaneous preterm birth: the underpinnings in the

maternal and fetal genomes', *npj Genomic Medicine*. doi: 10.1038/s41525-021-00209-5.

Bianco, A., Stone, J., Lynch, L., Lapinski, R., Berkowitz, G. and Berkowitz, R. L. (1996) 'Pregnancy outcome at age 40 and older', *Obstetrics and Gynecology*, 87(6). doi: 10.1016/0029-7844(96)00045-2.

Blanks, A. M., Shmygol, A. and Thornton, S. (2007) 'Myometrial function in prematurity', *Best Practice & Research Clinical Obstetrics & Gynaecology*. Baillière Tindall, 21(5), pp. 807–819. doi: 10.1016/J.BPOBGYN.2007.03.003.

Block, B. A., Imagawa, T., Campbell, K. P. and Franzini-Armstrong, C. (1988) 'Structural evidence for direct interaction between the molecular components of the transverse tubule/sarcoplasmic reticulum junction in skeletal muscle.', *Journal of Cell Biology*. The Rockefeller University Press, 107(6), pp. 2587–2600. doi: 10.1083/JCB.107.6.2587.

Blondeau, F., Laporte, J., Bodin, S., Superti-Furga, G., Payrastre, B. and Mandel, J. (2000) 'Myotubularin, a phosphatase deficient in myotubular myopathy, acts on phosphatidylinositol 3-kinase and phosphatidylinositol 3-phosphate pathway', *Human molecular genetics*, 9(15), pp. 2223–2229. doi: 10.1093/OXFORDJOURNALS.HMG.A018913.

Böhm, J., Bulla, M., Urquhart, J. E., Malfatti, E., Williams, S. G., O'Sullivan, J., Szlauer, A., Koch, C., Baranello, G., Mora, M., *et al.* (2017) 'ORAI1 mutations with distinct channel gating defects in tubular aggregate myopathy', *Human Mutation*. John Wiley and Sons Inc., 38(4), pp. 426–438. doi: 10.1002/humu.23172.

Böhm, J. and Laporte, J. (2018) 'Tubular aggregate myopathy and Stormorken syndrome', *Medecine/Sciences*. Editions EDK, 34, pp. 26–31. doi: 10.1051/medsci/201834s208.

Bon, R. S., Wright, D. J., Beech, D. J. and Sukumar, P. (2022) 'Pharmacology of TRPC channels and its potential in cardiovascular and metabolic medicine', *Annual review of pharmacology and toxicology*. doi: 10.1146/annurev-pharmtox-030121-122314.

Boonstra, H., Oosterhuis, J. W., Oosterhuis, A. M. and Fleuren, G. J. (1983) 'Cervical tissue shrinkage by formaldehyde fixation, paraffin wax embedding, section cutting and mounting', *Virchows Archiv. A, Pathological anatomy and histopathology*. Virchows Arch A Pathol Anat Histopathol, 402(2), pp. 195–201. doi: 10.1007/BF00695061.

Borzutzky, C. and Jaffray, J. (2020) 'Diagnosis and management of heavy menstrual bleeding and bleeding disorders in adolescents', *JAMA Pediatrics*. American Medical Association, 174(2), pp. 186–194. doi: 10.1001/JAMAPEDIATRICS.2019.5040.

Bowman, M., Hopman, W. M., Rapson, D., Lillicrap, D. and James, P. (2010) 'The prevalence of symptomatic von Willebrand disease in primary care practice', *Journal of Thrombosis and Haemostasis*. doi: 10.1111/j.1538-7836.2009.03661.x.

Bowman, M., Mundell, G., Grabell, J., Hopman, W. M., Rapson, D., Lillicrap, D. and James, P. (2008) 'Generation and validation of the condensed MCMDM-1VWD bleeding questionnaire for Von Willebrand disease', *Journal of Thrombosis and Haemostasis*. John Wiley & Sons, Ltd, 6(12), pp. 2062–2066. doi: 10.1111/J.1538-7836.2008.03182.X.

Bowman, M., Mundell, G., Grabell, J., Hopman, W., Rapson, D., Lillicrap, D. and James, P. (2022) *Condensed MCMDM-1 VWD*, *Condensed Molecular and Clinical Markers for the Diagnosis and Management of Type 1 (MCMDM-1) VWD Bleeding Questionnaire*. Available at: https://elearning.wfh.org/resource/condensed-mcmdm-1-vwd/#:~:text=Scale%3A 3 categories are scored,total score%3A –3 to 45 (Accessed: 2 December 2022).

Boynton, P. M. and Greenhalgh, T. (2004) 'Selecting, designing, and developing your questionnaire', *BMJ*. British Medical Journal Publishing Group, 328(7451), pp. 1312–1315. doi: 10.1136/BMJ.328.7451.1312.

Bracci, L., Vukcevic, M., Spagnoli, G., Ducreux, S., Zorzato, F. and Treves, S. (2007) 'Ca2+ signaling through ryanodine receptor 1 enhances maturation and activation of human dendritic cells', *Journal of cell science*. J Cell Sci, 120(Pt 13), pp. 2232–2240. doi: 10.1242/JCS.007203.

Brace, I. (2008) 'Questionnaire design : how to plan, structure and write survey material for effective market research'. Kogan Page, p. 305. Available at: https://books.google.com/books/about/Questionnaire_Design.html?id=0r8xOI5rBZoC (Accessed: 11 July 2022).

Brackmann, F., Türk, M., Gratzki, N., Rompel, O., Jungbluth, H., Schröder, R. and Trollmann, R. (2018) 'Compound heterozygous RYR1 mutations in a preterm with arthrogryposis multiplex congenita and prenatal CNS bleeding', *Neuromuscular Disorders*. Elsevier Ltd, 28(1), pp. 54–58. doi: 10.1016/j.nmd.2017.09.009.

Brandom, B. W., Bina, S., Wong, C. A., Wallace, T., Visoiu, M., Isackson, P. J., Vladutiu, G. D., Sambuughin, N. and Muldoon, S. M. (2013) 'Ryanodine receptor type 1 gene variants in the malignant hyperthermia-susceptible population of the United States', *Anesthesia and Analgesia*, 116(5). doi: 10.1213/ANE.0b013e31828a71ff.

Brandt, A., Schleithoff, L., Jurkat-Rott, K., Klingler, W., Baur, C. and Lehmann-Horn, F. (1999) 'Screening of the ryanodine receptor gene in 105 malignant hyperthermia families: Novel mutations and concordance with the in vitro contracture test', *Human Molecular Genetics*. doi: 10.1093/hmg/8.11.2055.

Brenner, R., Peréz, G. J., Bonev, A. D., Eckman, D. M., Kosek, J. C., Wiler, S. W., Patterson, A. J., Nelson, M. T. and Aldrich, R. W. (2000) 'Vasoregulation by the beta1 subunit of the calcium-activated potassium channel', *Nature*. Nature, 407(6806), pp. 870–876. doi: 10.1038/35038011.

Briley, A., Seed, P. T., Tydeman, G., Ballard, H., Waterstone, M., Sandall, J., Poston, L., Tribe, R. M. and Bewley, S. (2014) 'Reporting errors, incidence and risk factors for postpartum haemorrhage and progression to severe PPH: a prospective observational study', *BJOG: An International Journal of Obstetrics & Gynaecology*. John Wiley & Sons, Ltd, 121(7), pp. 876–888. doi: 10.1111/1471-0528.12588.

Brillantes, A. M., Allen, P., Takahashi, T., Izumo, S. and Marks, A. R. (1992) 'Differences in cardiac calcium release channel (ryanodine receptor) expression in myocardium from patients with end-stage heart failure caused by ischemic versus dilated cardiomyopathy', *Circulation Research*, 71(1). doi: 10.1161/01.RES.71.1.18.

Broderick, R. and Broderick, K. A. (1990) 'Ultrastructure and Calcium Stores in the Myometrium', in *Uterine Function*. doi: 10.1007/978-1-4613-0575-0_1.

Brody, J. R. and Cunha, G. R. (1989) 'Histologic, morphometric, and immunocytochemical analysis of myometrial development in rats and mice: I. Normal development', *American Journal of Anatomy*, 186(1), pp. 1–20. doi: 10.1002/aja.1001860102.

Broman, M., Gehrig, A., Islander, G., Bodelsson, M., Ranklev-Twetman, E., Rüffert, H. and Müller, C. R. (2009) 'Mutation screening of the RYR1-cDNA from peripheral B-lymphocytes in 15 Swedish malignant hyperthermia index cases', *British journal of anaesthesia*. Br J Anaesth, 102(5), pp. 642–649. doi: 10.1093/BJA/AEP061.

Bronson, F. H., Dagg, C. P., Snell, G. D. and Heston, W. E. (1967) 'Reproduction', in Green, E. L. (ed.) *Biology of the Laboratory Mouse*. doi: 10.1093/oxfordjournals.jhered.a107528.

Brosens, I. A., Robertson, W. B. and Dixon, H. G. (1972) 'The role of the spiral arteries in the pathogenesis of preeclampsia', *Obstetrics and Gynecology annual*, 1(April), pp. 177–191.

Brozovich, F. V., Nicholson, C. J., Degen, C. V., Gao, Y. Z., Aggarwal, M. and Morgan, K. G. (2016) 'Mechanisms of vascular smooth muscle contraction and the basis for pharmacologic treatment of smooth muscle disorders', *Pharmacological Reviews*. American Society for Pharmacology and Experimental Therapy, pp. 476–532. doi: 10.1124/pr.115.010652.

Bulletti, C., De Ziegler, D., Polli, V., Diotallevi, L., Del Ferro, E. and Flamigni, C. (2000) 'Uterine contractility during the menstrual cycle', *Human Reproduction*. Oxford Academic, 15(suppl_1), pp. 81–89. doi: 10.1093/HUMREP/15.SUPPL_1.81.

Bulletti, C., De Ziegler, D., Setti, P. L., Cicinelli, E., Polli, V. and Flamigni, C. (2004) 'The Patterns of Uterine Contractility in Normal Menstruating Women: From Physiology to Pathology', *Annals of the New York Academy of Sciences*. John Wiley & Sons, Ltd, 1034(1), pp. 64–83. doi: 10.1196/ANNALS.1335.007.

Bult, C. J., Blake, J. A., Smith, C. L., Kadin, J. A., Richardson, J. E., Anagnostopoulos, A., Asabor, R., Baldarelli, R. M., Beal, J. S., Bello, S. M., *et al.* (2019) 'Mouse Genome Database (MGD) 2019', *Nucleic Acids Research*. Oxford Academic, 47(D1), pp. D801–D806. doi: 10.1093/NAR/GKY1056.

Burch, R. and Russell, W. (1959) *The Principles of Humane Experimental Technique by W.M.S. Russell and R.L. Burch*, *John Hopkins Bloomberg School of Public Health*.

Burdyga, T., Wray, S. and Noble, K. (2007) 'In Situ calcium signaling: No calcium sparks detected in rat myometrium', in *Annals of the New York Academy of Sciences*. John Wiley & Sons, Ltd (10.1111), pp. 85–96. doi: 10.1196/annals.1389.002.

Burton, G. J., Redman, C. W., Roberts, J. M. and Moffett, A. (2019) 'Pre-eclampsia: pathophysiology and clinical implications', *The BMJ*. doi: 10.1136/bmj.l2381.

Bustin, S. A. (2000) *Absolute quantification of mRNA using real-time reverse transcription polymerase chain reaction assays*, *Journal of Molecular Endocrinology*. Available at: http://www.endocrinology.org (Accessed: 21 February 2019).

Bustin, S. A., Benes, V., Garson, J. A., Hellemans, J., Huggett, J., Kubista, M., Mueller, R., Nolan, T., Pfaffl, M. W., Shipley, G. L., Vandesompele, J. and Wittwer, C. T. (2009) 'The MIQE Guidelines: Minimum Information for Publication of Quantitative Real-Time PCR Experiments'. doi: 10.1373/clinchem.2008.112797.

Bustin, S. A., Benes, V., Nolan, T. and Pfaffl, M. W. (2005) 'Quantitative real-time RT-PCR - A perspective', *Journal of Molecular Endocrinology*. doi: 10.1677/jme.1.01755.

Bustin, S. and Huggett, J. (2017) 'qPCR primer design revisited.', *Biomolecular detection and quantification*. Elsevier, 14, pp. 19–28. doi: 10.1016/j.bdq.2017.11.001.

Buus, N. H., VanBavel, E. and Mulvany, M. J. (1994) 'Differences in sensitivity of rat mesenteric small arteries to agonists when studied as ring preparations or as cannulated preparations', *British Journal of Pharmacology*. John Wiley & Sons, Ltd, 112(2), pp. 579–587. doi: 10.1111/J.1476-5381.1994.TB13114.X.

Byams, V. R. (2007) 'Women with Bleeding Disorders', *Journal of Women's Health*. Mary Ann Liebert, Inc. 2 Madison Avenue Larchmont, NY 10538 USA , 16(9), pp. 1249–1251. doi: 10.1089/JWH.2007.CDC11.

Byers, S. L., Wiles, M. V., Dunn, S. L. and Taft, R. A. (2012) 'Mouse Estrous Cycle Identification Tool and Images', *PLoS ONE*. Edited by S. R. Singh, 7(4), p. e35538. doi: 10.1371/journal.pone.0035538.

Caligioni, C. S. (2009) 'Assessing reproductive status/stages in mice.', *Current protocols in neuroscience*. Hoboken, NJ, USA: NIH Public Access, Appendix 4(1), p. Appendix 4I. doi: 10.1002/0471142301.nsa04is48.

Calvert, C., Thomas, S. L., Ronsmans, C., Wagner, K. S., Adler, A. J. and Filippi, V. (2012) 'Identifying regional variation in the prevalence of postpartum haemorrhage: a systematic review and meta-analysis', *PloS one*. PLoS One, 7(7). doi: 10.1371/JOURNAL.PONE.0041114.

Campbell, W. B. and Fleming, I. (2010) 'Epoxyeicosatrienoic acids and endothelium-dependent responses', *Pflugers Archiv European Journal of Physiology*. NIH Public Access, pp. 881–895. doi: 10.1007/s00424-010-0804-6.

Canato, M., Capitanio, P., Cancellara, L., Leanza, L., Raffaello, A., Reane, D. V., Marcucci, L., Michelucci, A., Protasi, F. and Reggiani, C. (2019) 'Excessive accumulation of Ca2 + in mitochondria of Y522S-RYR1 knock-in mice: a link between leak from the sarcoplasmic reticulum and altered redox state', *Frontiers in Physiology*, 10. doi: 10.3389/fphys.2019.01142.

Cappell, M. S. and Garcia, A. (1998) 'Gastric and duodenal ulcers during pregnancy', *Gastroenterology Clinics of North America*, 27(1). doi: 10.1016/S0889-8553(05)70352-6.

Cartin, L., Lounsbury, K. M. and Nelson, M. T. (2000) 'Coupling of Ca2+ to CREB Activation and Gene Expression in Intact Cerebral Arteries From Mouse', *Circulation Research*. Lippincott Williams & Wilkins, 86(7), pp. 760–767. doi: 10.1161/01.RES.86.7.760.

Castaman, G. (2013) 'Changes of von willebrand factor during pregnancy in women with and without von willebrand disease', *Mediterranean Journal of Hematology and Infectious Diseases*. doi: 10.4084/mjhid.2013.052.

Chagovetz, A. A., Klatt Shaw, D., Ritchie, E., Hoshijima, K. and Grunwald, D. J. (2019) 'Interactions among ryanodine receptor isotypes contribute to muscle fiber type development and function', *Disease models & mechanisms*. NLM (Medline), 13(2). doi: 10.1242/dmm.038844.

Chakraborty, D., Karim Rumi, M. A., Konno, T. and Soares, M. J. (2011) 'Natural killer cells direct hemochorial placentation by regulating hypoxia-inducible factor dependent trophoblast lineage decisions', *Proceedings of the National Academy of Sciences of the United States of America*. National Academy of Sciences, 108(39), pp. 16295–16300. doi: 10.1073/PNAS.1109478108/SUPPL_FILE/PNAS.201109478SI.PDF.

Chanrachakul, B., Pipkin, F. B. and Khan, R. N. (2004) 'Contribution of coupling between human myometrial β2- adrenoreceptor and the BKCa channel to uterine quiescence', *American Journal of Physiology - Cell Physiology*, 287(6 56-6). doi: 10.1152/ajpcell.00236.2004.

Chaudhari, T., Todd, D. A., Kent, A. L., Dopita, B., Hallam, L., Freckmann, M.-L. and Johnston, H. M. (2011) 'Bilateral subdural hygromas and cephalhaematomas in male twins with severe myotubular myopathy caused by a Novel c.431delT (p.Leu144fs) mutation in MTM1 gene', *Journal of Paediatrics and Child Health*. John Wiley & Sons, Ltd, 47(1–2), pp. 64–65. doi: 10.1111/J.1440-1754.2010.01737.X.

Chelu, M. G., Goonasekera, S. A., Durham, W. J., Tang, W., Lueck, J. D., Riehl, J., Pessah, I. N., Zhang, P., Bhattacharjee, M. B., Dirksen, R. T. and Hamilton, S. L. (2005) 'Heat-and anesthesia-induced malignant hyperthermia in an RyR1 knock-in mouse', *The FASEB Journal*. doi: 10.1096/fj.05-4497fje.

Chen, D. B., Bird, I. M., Zheng, J. and Magness, R. R. (2004) 'Membrane estrogen receptor-dependent extracellular signal-regulated kinase pathway mediates acute activation of endothelial nitric oxide synthase by estrogen in uterine artery endothelial cells', *Endocrinology*, 145(1), pp. 113–125. doi: 10.1210/en.2003-0547.

Chen, H., Cao, L., Cao, W., Wang, H., Zhu, C. and Zhou, R. (2018) 'Factors affecting labor duration in Chinese pregnant women', *Medicine (United States)*. Lippincott Williams and Wilkins, 97(52). doi: 10.1097/MD.0000000000013901.

Chen, J., Shi, Y., Huang, J., Luo, J. and Zhang, W. (2020) 'Neuromedin B receptor mediates neuromedin B-induced COX-2 and IL-6 expression in human primary myometrial cells', *Journal of Investigative Medicine*. BMJ Publishing Group, 68(6), p. 1171. doi: 10.1136/JIM-2020-001412.

Chevessier, F., Bauché-Godard, S., Leroy, J.-P. P., Koenig, J., Paturneau-Jouas, M., Eymard, B., Hantaï, D. and Verdière-Sahuqué, M. (2005) 'The origin of tubular aggregates in human myopathies', *Journal of Pathology*. John Wiley and Sons Ltd, 207(3), pp. 313–323. doi: 10.1002/path.1832.

Chi, R. J., Olenych, S. G., Kim, K. and Keller, T. C. S. (2005) 'Smooth muscle α-actinin

interaction with smitin', *International Journal of Biochemistry and Cell Biology*. Elsevier Ltd, 37(7), pp. 1470–1482. doi: 10.1016/j.biocel.2005.02.014.

Chiazze, L., Brayer, F. T., Macisco, J. J., Parker, M. P. and Duffy, B. J. (1968) 'The length and variability of the human menstrual cycle', *JAMA*. American Medical Association, 203(6), pp. 377–380. doi: 10.1001/JAMA.1968.03140060001001.

Chin-Smith, E. C., Slater, D. M., Johnson, M. R. and Tribe, R. M. (2014) 'STIM and Orai isoform expression in pregnant human myometrium: A potential role in calcium signaling during pregnancy', *Frontiers in Physiology*, p. 169. doi: 10.3389/fphys.2014.00169.

Chou, P. C., Liang, W. C., Nonaka, I., Mitsuhashi, S., Nishino, I. and Jong, Y. J. (2013) 'Intranuclear rods myopathy with autonomic dysfunction', *Brain and Development*. Elsevier, 35(7), pp. 686–689. doi: 10.1016/J.BRAINDEV.2012.09.011.

Chuang, C. M., Chen, C. Y., Yen, P. S., Wu, C. H., Shiao, L. R., Wong, K. L., Chan, P. and Leung, Y. M. (2022) 'Propofol causes sustained Ca2+ elevation in endothelial cells by stimulating ryanodine receptor and suppressing plasmalemmal Ca2+ pump', *Journal of Cardiovascular Pharmacology*. Lippincott Williams and Wilkins, 79(5), pp. 749–757. doi: 10.1097/FJC.0000000000001246.

Cipolla, M. and Osol, G. (1994) 'Hypertrophic and hyperplastic effects of pregnancy on the rat uterine arterial wall', *American Journal of Obstetrics and Gynecology*, 171(3), pp. 805–811. doi: 10.1016/0002-9378(94)90102-3.

Clarke, N. F., Amburgey, K., Teener, J., Camelo-Piragua, S., Kesari, A., Punetha, J., Waddell, L. B., Davis, M., Laing, N. G., Monnier, N., North, K. N., Hoffman, E. P. and Dowling, J. J. (2013) 'A novel mutation expands the genetic and clinical spectrum of MYH7-related myopathies', *Neuromuscular disorders : NMD*. NIH Public Access, 23(5), p. 432. doi: 10.1016/J.NMD.2013.02.009.

De Clercq, K., Persoons, E., Napso, T., Luyten, C., Parac-Vogt, T. N., Sferruzzi-Perri, A. N., Kerckhofs, G. and Vriens, J. (2019) 'High-resolution contrast-enhanced microCT reveals the true three-dimensional morphology of the murine placenta', *Proceedings of the National Academy of Sciences of the United States of America*. National Academy of Sciences, 116(28), pp. 13927–13936. doi: 10.1073/PNAS.1902688116/VIDEO-5.

Cnattingius, R., Cnattingius, S. and Notzon, F. C. (1998) 'Obstacles to reducing cesarean rates in a low-cesarean setting: The effect of maternal age, height, and weight', *Obstetrics and Gynecology*, 92(4). doi: 10.1016/s0029-7844(98)00244-0.

Cnossen, J. S., Morris, R. K., Ter Riet, G., Mol, B. W. J., Van Der Post, J. A. M., Coomarasamy, A., Zwinderman, A. H., Robson, S. C., Bindels, P. J. E., Kleijnen, J. and Khan, K. S. (2008) 'Use of uterine artery Doppler ultrasonography to predict pre-eclampsia and intrauterine growth restriction: A systematic review and bivariable meta-analysis', *CMAJ*. CMAJ, 178(6), pp. 701–711. doi: 10.1503/cmaj.070430.

Coan, P. M., Angiolini, E., Sandovici, I., Burton, G. J., Constância, M. and Fowden, A. L. (2008) 'Adaptations in placental nutrient transfer capacity to meet fetal growth demands depend on placental size in mice', *Journal of Physiology*, 586(18). doi:

10.1113/jphysiol.2008.156133.

Coan, P. M., Conroy, N., Burton, G. J. and Ferguson-Smith, A. C. (2006) 'Origin and characteristics of glycogen cells in the developing murine placenta', *Developmental Dynamics*. John Wiley & Sons, Ltd, 235(12), pp. 3280–3294. doi: 10.1002/DVDY.20981.

Coan, P. M., Ferguson-Smith, A. C. and Burton, G. J. (2004) 'Developmental Dynamics of the Definitive Mouse Placenta Assessed by Stereology', *Biology of Reproduction*. Oxford Academic, 70(6), pp. 1806–1813. doi: 10.1095/BIOLREPROD.103.024166.

Coan, P. M., Ferguson-Smith, A. C. and Burton, G. J. (2005) 'Ultrastructural changes in the interhaemal membrane and junctional zone of the murine chorioallantoic placenta across gestation', *Journal of Anatomy*. Wiley-Blackwell, 207(6), p. 783. doi: 10.1111/J.1469-7580.2005.00488.X.

Coburger, J., Kapapa, T., Wirtz, C. R., Jurkat-Rott, K. and Klingler, W. (2017) 'High prevalence of rare ryanodine receptor type 1 variants in patients suffering from aneurysmatic subarachnoid hemorrhage: A pilot study', *Journal of Clinical Neuroscience*. Churchill Livingstone, 45, pp. 209–213. doi: 10.1016/j.jocn.2017.06.029.

Colucci, W. S., Gimbrone, M. A., McLaughlin, M. K., Halpern, W. and Alexander, R. W. (1982) 'Increased vascular catecholamine sensitivity and α-adrenergic receptor affinity in female and estrogen-treated male rats', *Circulation Research*, 50(6). doi: 10.1161/01.RES.50.6.805.

Combs, C. A., Murphy, E. L. and Laros, R. K. (1991) 'Factors associated with hemorrhage in cesarean deliveries', *Obstetrics and Gynecology*, 77(1), pp. 77–82.

Conte-Camerino, D., Lograno, M. D., Siro-Brigiani, G. and Megna, G. (1983) 'Dantrolene sodium: Stimulatory and depressant effects on the contractility of guinea-pig uterus in vitro', *European Journal of Pharmacology*. Elsevier, 92(3–4), pp. 291–294. doi: 10.1016/0014-2999(83)90301-1.

Conte, E., Pannunzio, A., Imbrici, P., Camerino, G. M., Maggi, L., Mora, M., Gibertini, S., Cappellari, O., De Luca, A., Coluccia, M. and Liantonio, A. (2021) 'Gain-of-function STIM1 L96V mutation causes myogenesis alteration in muscle cells from a patient affected by tubular aggregate myopathy', *Frontiers in Cell and Developmental Biology*. Frontiers Media S.A., 9, p. 635063. doi: 10.3389/FCELL.2021.635063/FULL.

Coons, A. H. and Kaplan, M. H. (1950) 'Localization of antigen in tissue cells; improvements in a method for the detection of antigen by means of fluorescent antibody.', *The Journal of Experimental Medicine*, 91(1). doi: 10.1084/jem.91.1.1.

Costantine, M. M. (2014) 'Physiologic and pharmacokinetic changes in pregnancy', *Frontiers in Pharmacology*. Frontiers Media SA, 5 APR, p. 65. doi: 10.3389/FPHAR.2014.00065/BIBTEX.

Coussin, F., Macrez, N., Morel, J. L. and Mironneau, J. (2000) 'Requirement of ryanodine receptor subtypes 1 and 2 for Ca2+-induced Ca2+ release in vascular myocytes', *Journal of Biological Chemistry*. J Biol Chem, 275(13), pp. 9596–9603. doi: 10.1074/jbc.275.13.9596.

Cowley, D. E., Pomp, D., Atchley, W. R., Eisen, E. J. and Hawkins-Brown, D. (1989) 'The impact of maternal uterine genotype on postnatal growth and adult body size in mice', *Genetics*, 122(1). doi: 10.1093/genetics/122.1.193.

Cox, D. H. and Aldrich, R. W. (2000) 'Role of the β1 subunit in large-conductance Ca2+-activated K+ channel gating energetics: Mechanisms of enhanced Ca2+ sensitivity', *Journal of General Physiology*, 116(3), pp. 411–432. doi: 10.1085/jgp.116.3.411.

De Crescenzo, V., Fogarty, K. E., Lefkowitz, J. J., Bellve, K. D., Zvaritch, E., MacLennan, D. H. and Walsh, J. V. (2012) 'Type 1 ryanodine receptor knock-in mutation causing central core disease of skeletal muscle also displays a neuronal phenotype', *Proceedings of the National Academy of Sciences of the United States of America*. National Academy of Sciences, 109(2), pp. 610–615. doi: 10.1073/pnas.1115111108.

Crick, F. (1970) 'Central dogma of molecular biology', *Nature*. Nature, 227(5258), pp. 561–563. doi: 10.1038/227561A0.

Crick, F. H. (1958) 'On protein synthesis', *Symposia of the Society for Experimental Biology*. Symp Soc Exp Biol, 12, pp. 138–163. Available at: https://pubmed.ncbi.nlm.nih.gov/13580867/ (Accessed: 21 January 2023).

Cross, J. C. (1996) 'Trophoblast function in normal and preeclamptic pregnancy', *Fetal and Maternal Medicine Review*. Cambridge University Press, pp. 57–66. doi: 10.1017/s0965539500001492.

Cross, J. C., Hemberger, M., Lu, Y., Nozaki, T., Whiteley, K., Masutani, M. and Adamson, S. L. (2002) 'Trophoblast functions, angiogenesis and remodeling of the maternal vasculature in the placenta', *Molecular and Cellular Endocrinology*. Elsevier, 187(1–2), pp. 207–212. doi: 10.1016/S0303-7207(01)00703-1.

Cross, J. C., Simmons, D. G. and Watson, E. D. (2003) 'Chorioallantoic morphogenesis and formation of the placental villous tree', *Annals of the New York Academy of Sciences*. John Wiley & Sons, Ltd, 995(1), pp. 84–93. doi: 10.1111/J.1749-6632.2003.TB03212.X.

Cunningham, F. G., Leveno, K. J., Bloom, S. L., Dashe, J. S., Hoffman, B. L., Casey, B. M. and Spong, C. Y. (1989) 'The morphological and functional development of the fetus', in *Williams Obstetrics*. 18th edn. Prentice-Hall International Inc, pp. 87–128. Available at: https://accessmedicine.mhmedical.com/book.aspx?bookID=1918 (Accessed: 5 January 2021).

Cuylen, S., Blaukopf, C., Politi, A. Z., Muller-Reichert, T., Neumann, B., Poser, I., Ellenberg, J., Hyman, A. A. and Gerlich, D. W. (2016) 'Ki-67 acts as a biological surfactant to disperse mitotic chromosomes', *Nature*, 535(7611). doi: 10.1038/nature18610.

Dabertrand, F., Fritz, N., Mironneau, J., Macrez, N. and Morel, J. L. (2007) 'Role of RYR3 splice variants in calcium signaling in mouse nonpregnant and pregnant myometrium', *American Journal of Physiology - Cell Physiology*. American Physiological Society, 293(3), pp. 848–854. doi: 10.1152/AJPCELL.00069.2007/ASSET/IMAGES/LARGE/ZH00090753510006.JPEG.

Dabertrand, F., Morel, J. L., Sorrentino, V., Mironneau, J., Mironneau, C. and Macrez, N.

(2006) 'Modulation of calcium signalling by dominant negative splice variant of ryanodine receptor subtype 3 in native smooth muscle cells', *Cell Calcium*. Churchill Livingstone, 40(1), pp. 11–21. doi: 10.1016/J.CECA.2006.03.008.

Dai, Y.-P., Bongalon, S., Mutafova-Yambolieva, V. N. and Yamboliev, I. A. (2008) 'Distinct effects of contraction agonists on the phosphorylation state of cofilin in pulmonary artery smooth muscle', *Advances in Pharmacological Sciences*. Hindawi Limited, 2008, pp. 1–9. doi: 10.1155/2008/362741.

Dai, Y. P., Bongalon, S., Tian, H., Parks, S. D., Mutafova-Yambolieva, V. N. and Yamboliev, I. A. (2006) 'Upregulation of profilin, cofilin-2 and LIMK2 in cultured pulmonary artery smooth muscle cells and in pulmonary arteries of monocrotaline-treated rats', *Vascular Pharmacology*. Vascul Pharmacol, 44(5), pp. 275–282. doi: 10.1016/j.vph.2005.11.008.

Dalle Lucca, J. J., Adeagbo, A. S. O. and Alsip, N. L. (2000) 'Oestrous cycle and pregnancy alter the reactivity of the rat uterine vasculature', *Human Reproduction*, 15(12). doi: 10.1093/humrep/15.12.2496.

Dalrymple, A. (2002) 'Molecular identification and localization of Trp homologues, putative calcium channels, in pregnant human uterus', *Molecular Human Reproduction*. Oxford University Press, 8(10), pp. 946–951. doi: 10.1093/molehr/8.10.946.

Dalrymple, A., Slater, D. M., Poston, L. and Tribe, R. M. (2004) 'Physiological induction of transient receptor potential canonical proteins, calcium entry channels, in human myometrium: Influence of pregnancy, labor, and interleukin-1β', *Journal of Clinical Endocrinology and Metabolism*. J Clin Endocrinol Metab, 89(3), pp. 1291–1300. doi: 10.1210/jc.2003-031428.

Danish Myo Technology and AD Instruments (no date) 'DMT Normalization Guide'.

Davison, J. M. and Dunlop, W. (1984) 'Changes in renal hemodynamics and tubular function induced by normal human pregnancy', *Seminars in Nephrology*, 4(3).

Deane, J. A., Rue Ong, Y., Cain, J. E., Jayasekara, W. S. N., Tiwari, A., Carlone, D. L., NeilWatkins, D., Breault, D. T. and Gargett, C. E. (2016) 'The mouse endometrium contains epithelial, endothelial and leucocyte populations expressing the stem cell marker telomerase reverse transcriptase', *Molecular Human Reproduction*. Oxford University Press, 22(4), p. 272. doi: 10.1093/MOLEHR/GAV076.

Dechanet, C., Fort, A., Barbero-Camps, E., Dechaud, H., Richard, S. and Virsolvy, A. (2011) 'Endothelin-dependent vasoconstriction in human uterine artery: Application to Preeclampsia', *PLoS ONE*, 6(1). doi: 10.1371/journal.pone.0016540.

Definition of Term Pregnancy | ACOG (no date). Available at: https://www.acog.org/clinical/clinical-guidance/committee-opinion/articles/2013/11/definition-of-term-pregnancy (Accessed: 6 March 2023).

Denison, F. C., Price, J., Graham, C., Wild, S. and Liston, W. A. (2008) 'Maternal obesity, length of gestation, risk of postdates pregnancy and spontaneous onset of labour at term', *Bjog*. Wiley-Blackwell, 115(6), p. 720. doi: 10.1111/J.1471-0528.2008.01694.X.

Deswal, R., Narwal, V., Dang, A. and Pundir, C. S. (2020) 'The prevalence of polycystic ovary syndrome: A brief systematic review', *Journal of Human Reproductive Sciences*. doi: 10.4103/jhrs.JHRS_95_18.

Dickey, R. P. and Hower, J. F. (1995) 'Pregnancy: Ultrasonographic features of uterine blood flow during the first 16 weeks of pregnancy', *Human Reproduction*. Oxford University Press, 10(9), pp. 2448–2452. doi: 10.1093/oxfordjournals.humrep.a136317.

Dilley, A., Drews, C., Miller, C., Lally, C., Austin, H., Ramaswamy, D., Lurye, D. and Evatt, B. (2001) 'von Willebrand disease and other inherited bleeding disorders in women with diagnosed menorrhagia', *Obstetrics and Gynecology*, 97(4), pp. 630–636. doi: 10.1016/S0029-7844(00)01224-2.

Ding, C., Wang, J., Cao, Y., Pan, Y., Lu, X., Wang, W., Zhuo, L., Tian, Q. and Zhan, S. (2019) 'Heavy menstrual bleeding among women aged 18-50 years living in Beijing, China: prevalence, risk factors, and impact on daily life', *BMC Women's Health*, 19(1). doi: 10.1186/S12905-019-0726-1.

Direkvand-Moghadam, A., Delpisheh, A., Rezaeian, M. and Khosravi, A. (2015) 'Factors Affecting the Labor : A Review Article', *Biomedical and Pharmacology Journal*. Oriental Scientific Publishing Company, 6(2), pp. 161–167. doi: 10.13005/BPJ/399.

Dirksen, R. T. and Avila, G. (2002) 'Altered ryanodine receptor function in central core disease: Leaky or uncoupled Ca2+ release channels?', *Trends in Cardiovascular Medicine*. doi: 10.1016/S1050-1738(02)00163-9.

Dlamini, N., Voermans, N. C., Lillis, S., Stewart, K., Kamsteeg, E.-J., Drost, G., Quinlivan, R., Snoeck, M., Norwood, F., Radunovic, A., *et al.* (2013) 'Mutations in RYR1 are a common cause of exertional myalgia and rhabdomyolysis', *Neuromuscular Disorders*. Elsevier, 23(7), pp. 540–548. doi: 10.1016/J.NMD.2013.03.008.

Dodds, K. N., Staikopoulos, V. and Beckett, E. A. H. (2015) 'Uterine contractility in the nonpregnant mouse: changes during the estrous cycle and effects of chloride channel blockade', *Biology of Reproduction*. Narnia, 92(6). doi: 10.1095/biolreprod.115.129809.

Dogan, M. F., Yildiz, O., Arslan, S. O. and Ulusoy, K. G. (2019) 'Potassium channels in vascular smooth muscle: a pathophysiological and pharmacological perspective', *Fundamental & Clinical Pharmacology*. Blackwell Publishing Ltd, 33(5), pp. 504–523. doi: 10.1111/fcp.12461.

Dörr, J. and Fecher-Trost, C. (2011) 'TRP channels in female reproductive organs and placenta', in *Advances in Experimental Medicine and Biology*. doi: 10.1007/978-94-007-0265-3_47.

Dowling, J. J., Lillis, S., Amburgey, K., Zhou, H., Al-Sarraj, S., Buk, S. J. A., Wraige, E., Chow, G., Abbs, S., Leber, S., *et al.* (2011) 'King-Denborough syndrome with and without mutations in the skeletal muscle ryanodine receptor (RYR1) gene', *Neuromuscular Disorders*, 21(6). doi: 10.1016/j.nmd.2011.03.006.

Du, W., McMahon, T. J., Zhang, Z. S., Stiber, J. A., Meissner, G. and Eu, J. P. (2006)

'Excitation-contraction coupling in airway smooth muscle', *Journal of Biological Chemistry*. J Biol Chem, 281(40), pp. 30143–30151. doi: 10.1074/jbc.M606541200.

Ducreux, S., Zorzato, F., Müller, C., Sewry, C., Muntoni, F., Quinlivan, R., Restagno, G., Girard, T. and Treves, S. (2004) 'Effect of ryanodine receptor mutations on interleukin-6 release and intracellular calcium homeostasis in human myotubes from malignant hyperthermia-susceptible individuals and patients affected by central core disease', *Journal of Biological Chemistry*. American Society for Biochemistry and Molecular Biology Inc., 279(42), pp. 43838–43846. doi: 10.1074/jbc.M403612200.

Ducsay, C. A., Goyal, R., Pearce, W. J., Wilson, S., Hu, X. Q. and Zhang, L. (2018) 'Gestational hypoxia and developmental plasticity', *Physiological Reviews*. doi: 10.1152/physrev.00043.2017.

Ducza, E., Csányi, A., Szőke, É., Pohóczky, K., Hajagos-Tóth, J., Kothencz, A., Tiszai, Z. and Gáspár, R. (2019) 'Significance of transient receptor potential vanilloid 4 and aquaporin 5 co-expression in the rat uterus at term', *Heliyon*. Elsevier Ltd, 5(10). doi: 10.1016/j.heliyon.2019.e02697.

Dudley, D. J., Branch, D. W., Edwin, S. S. and Mitchell, M. D. (1996) 'Induction of preterm birth in mice by RU486', *Biology of Reproduction*, 55(5), pp. 992–995. doi: 10.1095/BIOLREPROD55.5.992.

Duhig, K., Chappell, L. C. and Shennan, A. H. (2016) 'Oxidative stress in pregnancy and reproduction', *Obstetric Medicine*. SAGE Publications, 9(3), p. 113. doi: 10.1177/1753495X16648495.

Dunham, I., Kundaje, A., Aldred, S. F., Collins, P. J., Davis, C. A., Doyle, F., Epstein, C. B., Frietze, S., Harrow, J., Kaul, R., *et al.* (2012) 'An integrated encyclopedia of DNA elements in the human genome', *Nature*, 489(7414). doi: 10.1038/NATURE11247.

Dupont, C., Rudigoz, R.-C., Cortet, M., Touzet, S., Colin, C., Rabilloud, M., Lansac, J., Harvey, T., Tessier, V., Chauleur, C., Pennehouat, G., Morin, X., Bouvier-Colle, M.-H. and Deneux-Tharaux, C. (2014) 'Frequency, causes and risk factors of postpartum haemorrhage: A population-based study in 106 French maternity units', *Journal de Gynecologie Obstetrique et Biologie de la Reproduction*, 43(3). doi: 10.1016/j.jgyn.2013.05.003.

Durham, W. J., Aracena-Parks, P., Long, C., Rossi, A. E., Goonasekera, S. A., Boncompagni, S., Galvan, D. L., Gilman, C. P., Baker, M. R., Shirokova, N., Protasi, F., Dirksen, R. and Hamilton, S. L. (2008) 'RyR1 S-nitrosylation underlies environmental heat stroke and sudden death in Y522S RyR1 knockin mice', *Cell*. doi: 10.1016/j.cell.2008.02.042.

Edizadeh, M., Vazehan, R., Javadi, F., Dehdahsi, S., Fadaee, M., Zonooz, M. F., Parsimehr, E., Ahangari, F., Abolhassani, A., Kalhor, Z., *et al.* (2017) 'De novo mutation in CACNA1S gene in a 20-year-old man diagnosed with metabolic myopathy', *Archives of Iranian Medicine*. Academy of Medical Sciences of I.R. Iran, 20(9), pp. 617–620. doi: 0172009/AIM.0010.

Edman, C. D. (1983) 'The Effects of Steroids on the Endometrium', *Seminars in Reproductive Endocrinology*. Copyright © 1983 by Thieme Medical Publishers, Inc., 1(03), pp. 179–187. doi: 10.1055/S-2008-1067953.

Eghbali, M., Toro, L. and Stefani, E. (2003) 'Diminished surface clustering and increased perinuclear accumulation of large conductance Ca2+-activated K+ channel in mouse myometrium with pregnancy', *Journal of Biological Chemistry*, 278(46). doi: 10.1074/jbc.M306564200.

El-Akouri, R. R., Kurlberg, G., Dindelegan, G., Mölne, J., Wallin, A., Brännström, M., Molne, J., Brannstrom, M. and Wallin, A. (2002) 'Heterotopic uterine transplantation by vascular anastomosis in the mouse', *Journal of Endocrinology*, 174(2), pp. 157–166. doi: 10.1677/joe.0.1740157.

Elmore, S. A., Cochran, R. Z., Bolon, B., Lubeck, B., Mahler, B., Sabio, D. and Ward, J. M. (2022) 'Histology atlas of the developing mouse placenta', *Toxicologic pathology*. NIH Public Access, 50(1), p. 60. doi: 10.1177/01926233211042270.

Eltit, J. M., Bannister, R. A., Moua, O., Altamirano, F., Hopkins, P. M., Pessah, I. N., Molinski, T. F., López, J. R., Beam, K. G. and Allen, P. D. (2012) 'Malignant hyperthermia susceptibility arising from altered resting coupling between the skeletal muscle L-type Ca2+ channel and the type 1 ryanodine receptor', *Proceedings of the National Academy of Sciences of the United States of America*, 109(20), pp. 7923–7928. doi: 10.1073/PNAS.1119207109/-/DCSUPPLEMENTAL/PNAS.201119207SI.PDF.

Endler, M., Saltvedt, S., Cnattingius, S., Stephansson, O. and Wikström, A. K. (2014) 'Retained placenta is associated with pre-eclampsia, stillbirth, giving birth to a small-for-gestational-age infant, and spontaneous preterm birth: a national register-based study', *BJOG : an international journal of obstetrics and gynaecology*. BJOG, 121(12), pp. 1462–1470. doi: 10.1111/1471-0528.12752.

Endo, M. (2009) 'Calcium-induced calcium release in skeletal muscle', *Physiological Reviews*. Physiol Rev, pp. 1153–1176. doi: 10.1152/physrev.00040.2008.

Endo, M., Tanaka, M. and Ogawa, Y. (1970) 'Calcium induced release of calcium from the sarcoplasmic reticulum of skinned skeletal muscle fibres', *Nature*. Nature Publishing Group, 228(5266), pp. 34–36. doi: 10.1038/228034a0.

Endo, Y., Noguchi, S., Hara, Y., Hayashi, Y. K., Motomura, K., Miyatake, S., Murakami, N., Tanaka, S., Yamashita, S., Kizu, R., *et al.* (2015) 'Dominant mutations in ORAI1 cause tubular aggregate myopathy with hypocalcemia via constitutive activation of store-operated Ca2+ channels', *Human Molecular Genetics*, 24(3), pp. 637–648. doi: 10.1093/hmg/ddu477.

Eriksson, J. G., Salonen, M. K., Kajantie, E. and Osmond, C. (2018) 'Prenatal growth and ckd in older adults: longitudinal findings from the Helsinki birth cohort study, 1924-1944', *American Journal of Kidney Diseases*. W.B. Saunders, 71(1), pp. 20–26. doi: 10.1053/J.AJKD.2017.06.030.

Escalante-Alcalde, D., Hernandez, L., Le Stunff, H., Maeda, R., Lee, H. S., Gang-Cheng, J. R., Sciorra, V. A., Daar, I., Spiegel, S., Morris, A. J. and Stewart, C. L. (2003) 'The lipid phosphatase LPP3 regulates extra-embryonic vasculogenesis and axis patterning', *Development*, 130(19). doi: 10.1242/dev.00635.

Eskild, A. and Vatten, L. J. (2010) 'Do pregnancies with pre-eclampsia have smaller placentas?

A population study of 317 688 pregnancies with and without growth restriction in the offspring', *BJOG: An International Journal of Obstetrics & Gynaecology*. John Wiley & Sons, Ltd, 117(12), pp. 1521–1526. doi: 10.1111/J.1471-0528.2010.02701.X.

Eskild, A. and Vatten, L. J. (2011) 'Placental weight and excess postpartum haemorrhage: a population study of 308 717 pregnancies', *BJOG: An International Journal of Obstetrics & Gynaecology*. John Wiley & Sons, Ltd, 118(9), pp. 1120–1125. doi: 10.1111/J.1471-0528.2011.02954.X.

Evangelista, T., Bansagi, B., Pyle, A., Griffin, H., Douroudis, K., Polvikoski, T., Antoniadi, T., Bushby, K., Straub, V., Chinnery, P. F., Lochmüller, H. and Horvath, R. (2015) 'Phenotypic variability of TRPV4 related neuropathies', *Neuromuscular Disorders*. Elsevier Ltd, 25(6), pp. 516–521. doi: 10.1016/j.nmd.2015.03.007.

Everaerts, W., Zhen, X., Ghosh, D., Vriens, J., Gevaert, T., Gilbert, J. P., Hayward, N. J., McNamara, C. R., Xue, F., Moran, M. M., *et al.* (2010) 'Inhibition of the cation channel TRPV4 improves bladder function in mice and rats with cyclophosphamide-induced cystitis', *Proceedings of the National Academy of Sciences of the United States of America*. National Academy of Sciences, 107(44), pp. 19084–19089. doi: 10.1073/pnas.1005333107.

Fabiato, A. and Fabiato, F. (1978) 'Calcium-induced release of calcium from the sarcoplasmic reticulum of skinned cells from adult human, dog, cat, rabbit, rat, and frog hearts and from fetal and new-born rat ventricles', *Annals of the New York Academy of Sciences*, 307(1). doi: 10.1111/j.1749-6632.1978.tb41979.x.

Falloon, B. J., Stephens, N., Tulip, J. R. and Heagerty, A. M. (1995) 'Comparison of small artery sensitivity and morphology in pressurized and wire-mounted preparations', *https://doi.org/10.1152/ajpheart.1995.268.2.H670*. American Physiological Society, 268(2 37-2). doi: 10.1152/AJPHEART.1995.268.2.H670.

Fan, Q., Chen, F., Zhang, W., Du, E., Zhao, N., Huang, S., Guo, W., Yan, X., Chen, M. and Wei, J. (2021) 'Maternal magnolol supplementation alters placental morphology, promotes placental angiogenesis during mid-gestation and improves offspring growth in a pregnant mouse model', *Reproductive Biology*, 21(4). doi: 10.1016/j.repbio.2021.100567.

Fan, Y., Hou, W., Xing, Y., Zhang, L., Zhou, C., Gui, J., Xu, P., Wang, A., Fan, X., Zeng, X., Feng, S. and Li, P. (2020) 'Peptidomics analysis of myometrium tissues in term labor compared with term nonlabor', *Journal of Cellular Biochemistry*. Wiley-Liss Inc., 121(2), pp. 1890–1900. doi: 10.1002/jcb.29424.

Feldman, C. H., Grotegut, C. A. and Rosenberg, P. B. (2017) 'The role of STIM1 and SOCE in smooth muscle contractility', *Cell Calcium*. Elsevier Ltd, pp. 60–65. doi: 10.1016/j.ceca.2017.02.007.

Ferreira, J. J., Butler, A., Stewart, R., Gonzalez-Cota, A. L., Lybaert, P., Amazu, C., Reinl, E. L., Wakle-Prabagaran, M., Salkoff, L., England, S. K. and Santi, C. M. (2019) 'Oxytocin can regulate myometrial smooth muscle excitability by inhibiting the Na + -activated K + channel, Slo2.1', *Journal of Physiology*. Blackwell Publishing Ltd, 597(1), pp. 137–149. doi: 10.1113/JP276806.

Ferreiro, A., Monnier, N., Romero, N. B., Leroy, J. P., Bönnemann, C., Haenggeli, C. A., Straub, V., Voss, W. D., Nivoche, Y., Jungbluth, H., *et al.* (2002) 'A recessive form of central core disease, transiently presenting as multi-minicore disease, is associated with a homozygous mutation in the ryanodine receptor type 1 gene', *Annals of Neurology*, 51(6). doi: 10.1002/ana.10231.

Ferreiro, A., Quijano-Roy, S., Pichereau, C., Moghadaszadeh, B., Goemans, N., Bönnemann, G., Jungbluth, H., Straub, V., Villanova, M., Leroy, J. P., *et al.* (2002) 'Mutations of the selenoprotein N gene, which is implicated in rigid spine muscular dystrophy, cause the classical phenotype of multiminicore disease: Reassessing the nosology of early-onset myopathies', *American Journal of Human Genetics*, 71(4). doi: 10.1086/342719.

Fetalvero, K. M., Zhang, P., Shyu, M., Young, B. T., Hwa, J., Young, R. C. and Martin, K. A. (2008) 'Prostacyclin primes pregnant human myometrium for an enhanced contractile response in parturition', *Journal of Clinical Investigation*, 118(12). doi: 10.1172/JCI33800.

Filosa, J. A., Yao, X. and Rath, G. (2013) 'TRPV4 and the regulation of vascular tone', *Journal of Cardiovascular Pharmacology*. NIH Public Access, 61(2), pp. 113–119. doi: 10.1097/FJC.0b013e318279ba42.

Flynn, E. R. M., Bradley, K. N., Muir, T. C. and McCarron, J. G. (2001) 'Functionally separate intracellular Ca2+ stores in smooth muscle', *Journal of Biological Chemistry*, 276(39). doi: 10.1074/jbc.M104308200.

Foo, C. T. Y., To, Y. H., Irwanto, A., Ng, A. Y. J., Yan, B., Chew, S. T. H., Liu, J. and Ti, L. K. (2022) 'Variant landscape of the RYR1 gene based on whole genome sequencing of the Singaporean population', *Scientific Reports*. Nature Publishing Group, 12(1), p. 5429. doi: 10.1038/S41598-022-09310-W.

Forbes, T. R. and Taku, E. (1975) 'Vein size in intact and hysterectomized mice during the estrous cycle and pregnancy', *The Anatomical Record*, 182(1), pp. 61–65. doi: 10.1002/ar.1091820107.

Ford, L. E. and Podolsky, R. J. (1970) 'Regenerative calcium release within muscle cells', *Science*. American Association for the Advancement of Science, 167(3914), pp. 58–59. doi: 10.1126/science.167.3914.58.

Fowden, A. L. and Moore, T. (2012) 'Maternal-fetal resource allocation: Co-operation and conflict', *Placenta*. W.B. Saunders, 33(SUPPL. 2), pp. e11–e15. doi: 10.1016/J.PLACENTA.2012.05.002.

Francis, S. H., Busch, J. L. and Corbin, J. D. (2010) 'cGMP-dependent protein kinases and cGMP phosphodiesterases in nitric oxide and cGMP action', *Pharmacological Reviews*. doi: 10.1124/pr.110.002907.

Fraser, I. S., Mansour, D., Breymann, C., Hoffman, C., Mezzacasa, A. and Petraglia, F. (2015) 'Prevalence of heavy menstrual bleeding and experiences of affected women in a European patient survey', *International Federation of Gynaecology and Obstetrics*, 128(3), pp. 196–200. doi: 10.1016/J.IJGO.2014.09.027.

Freed, J. K. and Gutterman, D. D. (2017) 'Communication is key: mechanisms of intercellular signaling in vasodilation', *Journal of Cardiovascular Pharmacology*. doi: 10.1097/FJC.0000000000000463.

Freichel, M., Vennekens, R., Olausson, J., Hoffmann, M., Müller, C., Stolz, S., Scheunemann, J., Weißgerber, P. and Flockerzi, V. (2004) 'Functional role of TRPC proteins in vivo: lessons from TRPC-deficient mouse models', *Biochemical and Biophysical Research Communications*. Academic Press, 322(4), pp. 1352–1358. doi: 10.1016/J.BBRC.2004.08.041.

Fritz, N., Morel, J.-L., Jeyakumar, L. H., Fleischer, S., Allen, P. D., Mironneau, J. and Macrez, N. (2007) 'RyR1-specific requirement for depolarization-induced Ca2+ sparks in urinary bladder smooth muscle', *Journal of Cell Science*. doi: 10.1242/jcs.009415.

Fritz, Nicolas, Morel, J. L., Jeyakumar, L. H., Fleischer, S., Allen, P. D., Mironneau, J. and Macrez, N. (2007) 'RyR1-specific requirement for depolarization-induced Ca2+ sparks in urinary bladder smooth muscle', *Journal of Cell Science*. J Cell Sci, 120(21), pp. 3784–3791. doi: 10.1242/jcs.009415.

Fruen, B. R., Mickelson, J. R. and Louis, C. F. (1997) 'Dantrolene inhibition of sarcoplasmic reticulum Ca2+release by direct and specific action at skeletal muscle ryanodine receptors', *Journal of Biological Chemistry*. doi: 10.1074/jbc.272.43.26965.

Fujii, J., Otsu, K., Zorzato, F., De Leon, S., Khanna, V. K., Weiler, J. E., O'Brien, P. J. and Maclennan, D. H. (1991) 'Identification of a mutation in porcine ryanodine receptor associated with malignant hyperthermia', *Science*. doi: 10.1126/science.1862346.

Fuller, E. O., Galletti, P. M. and Takeuchi, T. (1975) 'Major and collateral components of blood flow to pregnant sheep uterus', *American Journal of Physiology*. American Physiological Society, 229(2), pp. 279–285. doi: 10.1152/ajplegacy.1975.229.2.279.

Fuller, R., Barron, C., Mandala, M., Gokina, N. and Osol, G. (2009) 'Predominance of local over systemic factors in uterine arterial remodeling during pregnancy', *Reproductive Sciences*, 16(5), pp. 489–500. doi: 10.1177/1933719108329816.

Furuya, M., Ishida, J., Aoki, I. and Fukamizu, A. (2008) *Pathophysiology of placentation abnormalities in pregnancy-induced hypertension*, *Vascular Health and Risk Management*.

Gabella, G. (1972) 'Fine structure of the myenteric plexus in the guinea-pig ileum.', *Journal of Anatomy*. Wiley-Blackwell, 111(Pt 1), p. 69. Available at: https://www.ncbi.nlm.nih.gov/pmc/articles/PMC1271115/ (Accessed: 22 February 2023).

Galal, M., Symonds, I., Murray, H., Petraglia, F. and Smith, R. (2012) 'Postterm pregnancy', *Facts, Views & Vision in ObGyn*. Vlaamse Vereniging voor Obstetrie en Gynaecologie, 4(3), p. 175. Available at: /pmc/articles/PMC3991404/ (Accessed: 6 March 2023).

Galli, L., Orrico, A., Lorenzini, S., Censini, S., Falciani, M., Covacci, A., Tegazzin, V. and Sorrentino, V. (2006) 'Frequency and localization of mutations in the 106 exons of the RYR1 gene in 50 individuals with malignant hyperthermia', *Human Mutation*, 27(8). doi: 10.1002/humu.9442.

Gao, F. and Wang, D. H. (2010) 'Hypotension induced by activation of the transient receptor potential vanilloid 4 channels: Role of Ca2+-activated K+ channels and sensory nerves', *Journal of Hypertension*. Lippincott Williams and Wilkins, 28(1), pp. 102–110. doi: 10.1097/HJH.0b013e328332b865.

Gao, L., Cong, B., Zhang, L. and Ni, X. (2009) 'Expression of the calcium-activated potassium channel in upper and lower segment human myometrium during pregnancy and parturition', *Reproductive Biology and Endocrinology*, 7, p. 27. doi: 10.1186/1477-7827-7-27.

Garcia-Angarita, N., Kirschner, J., Heiliger, M., Thirion, C., Walter, M. C., Schnittfeld-Acarlioglu, S., Albrecht, M., Müller, K., Wieczorek, D., Lochmüller, H. and Krause, S. (2009) 'Severe nemaline myopathy associated with consecutive mutations E74D and H75Y on a single ACTA1 allele', *Neuromuscular Disorders*. Elsevier, 19(7), pp. 481–484. doi: 10.1016/J.NMD.2009.05.001.

Garcia, C. K., Goldstein, J. L., Pathak, R. K., Anderson, R. G. W. and Brown, M. S. (1994) 'Molecular characterization of a membrane transporter for lactate, pyruvate, and other monocarboxylates: Implications for the Cori cycle', *Cell*, 76(5). doi: 10.1016/0092-8674(94)90361-1.

Garfield, R. E. and Somlyo, A. P. (1985) 'Structure of Smooth Muscle', in *Calcium and Contractility*. doi: 10.1007/978-1-4612-5172-9_1.

Garibaldi, M., Fattori, F., Riva, B., Labasse, C., Brochier, G., Ottaviani, P., Sacconi, S., Vizzaccaro, E., Laschena, F., Romero, N. B., Genazzani, A., Bertini, E. and Antonini, G. (2017) 'A novel gain-of-function mutation in ORAI1 causes late-onset tubular aggregate myopathy and congenital miosis', *Clinical Genetics*. Blackwell Publishing Ltd, 91(5), pp. 780–786. doi: 10.1111/cge.12888.

Garland, C. J. and Dora, K. A. (2017) 'EDH: endothelium-dependent hyperpolarization and microvascular signalling', *Acta physiologica (Oxford, England)*. Acta Physiol (Oxf), 219(1), pp. 152–161. doi: 10.1111/APHA.12649.

George, C. H., Higgs, G. V. and Lai, F. A. (2003) 'Ryanodine receptor mutations associated with stress-induced ventricular tachycardia mediate increased calcium release in stimulated cardiomyocytes', *Circulation Research*, 93(6), pp. 531–540. doi: 10.1161/01.RES.0000091335.07574.86.

des Georges, A., Clarke, O. B., Zalk, R., Yuan, Q., Condon, K. J., Grassucci, R. A., Hendrickson, W. A., Marks, A. R. and Frank, J. (2016) 'Structural basis for gating and activation of RyR1', *Cell*, 167(1). doi: 10.1016/j.cell.2016.08.075.

Georgiades, P., Fergyson-Smith, A. C. and Burton, G. J. (2002) 'Comparative developmental anatomy of the murine and human definitive placentae', *Placenta*. W.B. Saunders, 23(1), pp. 3–19. doi: 10.1053/PLAC.2001.0738.

Georgiades, P., Watkins, M., Burton, G. J. and Ferguson-Smith, A. C. (2001) 'Roles for genomic imprinting and the zygotic genome inplacental development', *Proceedings of the National Academy of Sciences of the United States of America*. National Academy of Sciences, 98(8), p. 4522. doi: 10.1073/PNAS.081540898.

Gerdes, J., Lemke, H., Baisch, H., Wacker, H. H., Schwab, U. and Stein, H. (1984) 'Cell cycle analysis of a cell proliferation-associated human nuclear antigen defined by the monoclonal antibody Ki-67.', *Journal of immunology (Baltimore, Md. : 1950)*, 133(4).

Gervásio, O. L., Whitehead, N. R., Yeung, E. W., Phillips, W. D. and Allen, D. G. (2008) 'TRPC1 binds to caveolin-3 and is regulated by Src kinase - Role in Duchenne muscular dystrophy', *Journal of Cell Science*. The Company of Biologists Ltd, 121(13), pp. 2246–2255. doi: 10.1242/jcs.032003.

Geuther, R. (1977) 'A. L. LEHNINGER, Biochemistry. The Molecular Basis of Cell Structure and Function (2nd Edition). 1104 S., zahlr. Abb., zahlr. Tab. New York 1975. Worth Publ. Inc. $ 17.50', *Zeitschrift für allgemeine Mikrobiologie*. John Wiley & Sons, Ltd, 17(1), pp. 86–87. doi: 10.1002/JOBM.19770170116.

Gevaert, T., Vriens, J., Segal, A., Everaerts, W., Roskams, T., Talavera, K., Owsianik, G., Liedtke, W., Daelemans, D., Dewachter, I., Van Leuven, F., Voets, T., De Ridder, D. and Nilius, B. (2007) 'Deletion of the transient receptor potential cation channel TRPV4 impairs murine bladder voiding', *Journal of Clinical Investigation*. American Society for Clinical Investigation, 117(11), pp. 3453–3462. doi: 10.1172/JCI31766.

Giachini, F. R. C., Chiao, C. W., Carneiro, F. S., Lima, V. V., Carneiro, Z. N., Dorrance, A. M., Tostes, R. C. and Webb, R. C. (2009) 'Increased activation of stromal interaction molecule-1/Orai-1 in aorta from hypertensive rats: a novel insight into vascular dysfunction.', *Hypertension*. Lippincott Williams & Wilkins, 53(2), pp. 409–416. doi: 10.1161/HYPERTENSIONAHA.108.124404.

Gilchrist, J. M., Ambler, M. and Agatiello, P. (1991) 'Steroid-responsive tubular aggregate myopathy', *Muscle & Nerve*. Muscle Nerve, 14(3), pp. 233–236. doi: 10.1002/mus.880140306.

Gillard, E. F., Otsu, K., Fujii, J., Khanna, V. K., de Leon, S., Derdemezi, J., Britt, B. A., Duff, C. L., Worton, R. G. and MacLennan, D. H. (1991) 'A substitution of cysteine for arginine 614 in the ryanodine receptor is potentially causative of human malignant hyperthermia', *Genomics*. doi: 10.1016/0888-7543(91)90084-R.

Gillespie, M., Jassal, B., Stephan, R., Milacic, M., Rothfels, K., Senff-Ribeiro, A., Griss, J., Sevilla, C., Matthews, L., Gong, C., *et al.* (2022) 'The reactome pathway knowledgebase 2022', *Nucleic Acids Research*, 50(D1). doi: 10.1093/nar/gkab1028.

Gillett, G. T., Fox, M. F., Rowe, P. S. N., Casimer, C. M. and Povey, S. (1996) 'Mapping of human non-muscle type cofilin (CFL1) to chromosome 11q13 and muscle-type cofilin (CFL2) to chromosome 14', *Annals of Human Genetics*. Blackwell Publishing Ltd, 60(3), pp. 201–211. doi: 10.1111/j.1469-1809.1996.tb00423.x.

Gillies, R. L., Bjorksten, A. R., Davis, M. and Du Sart, D. (2008) 'Identification of genetic mutations in Australian malignant hyperthermia families using sequencing of RYR1 hot-spots', *Anaesthesia and Intensive Care*, 36(3). doi: 10.1177/0310057x0803600311.

Gillies, R. L., Bjorksten, A. R., Du Sart, D. and Hockey, B. M. (2015) 'Analysis of the entire ryanodine receptor type 1 and alpha 1 subunit of the dihydropyridine receptor (CACNA1S) coding regions for variants associated with malignant hyperthermia in Australian families',

Anaesthesia and Intensive Care, 43(2). doi: 10.1177/0310057x1504300204.

Girard, T., Cavagna, D., Padovan, E., Spagnoli, G., Urwyler, A., Zorzato, F. and Treves, S. (2001) 'B-lymphocytes from malignant hyperthermia-susceptible patients have an increased sensitivity to skeletal muscle ryanodine receptor activators', *The Journal of biological chemistry*. J Biol Chem, 276(51), pp. 48077–48082. doi: 10.1074/JBC.M107134200.

Girault, A., Deneux-Tharaux, C., Sentilhes, L., Maillard, F. and Goffinet, F. (2018) 'Undiagnosed abnormal postpartum blood loss: Incidence and risk factors', *PLoS ONE*. PLOS, 13(1). doi: 10.1371/JOURNAL.PONE.0190845.

Glinoer, D. (1997) 'The regulation of thyroid function in pregnancy: pathways of endocrine adaptation from physiology to pathology', *Endocrine Reviews*, 18(3). doi: 10.1210/er.18.3.404.

Glinoer, D. (1999) 'What happens to the normal thyroid during pregnancy?', in *Thyroid*. doi: 10.1089/thy.1999.9.631.

Godfrey, K. M. (2002) 'The role of the placenta in fetal programming - A review', *Placenta*. W.B. Saunders Ltd, 23(SUPPL. 1). doi: 10.1053/plac.2002.0773.

Gokina, N. I., Kuzina, O. Y. and Vance, A. M. (2010) 'Augmented EDHF signaling in rat uteroplacental vasculature during late pregnancy', *American Journal of Physiology - Heart and Circulatory Physiology*, 299(5), pp. 1642–1652. doi: 10.1152/AJPHEART.00227.2010/ASSET/IMAGES/LARGE/ZH40111095800008.JPEG.

Gonsalves, S. G., Ng, D., Johnston, J. J., Teer, J. K., S Tenson, P. D., Cooper, D. N., Mullikin, J. C. and Biesecker, L. G. (2013) 'Using exome data to identify malignant hyperthermia susceptibility mutations', *Anesthesiology*. NIH Public Access, 119(5), p. 1043. doi: 10.1097/ALN.0B013E3182A8A8E7.

Gordon, A. M., Homsher, E. and Regnier, M. (2000) 'Regulation of contraction in striated muscle', *Physiological Reviews*. American Physiological Society, pp. 853–924. doi: 10.1152/physrev.2000.80.2.853.

Gordon, D., Milberg, J., Daling, J. and Hickok, D. (1991) 'Advanced maternal age as a risk factor for cesarean delivery', *Obstetrics and Gynecology*, 77(4). doi: 10.2307/1966546.

Greasers And, M. L. and Gergely, J. (1973) *Purification and Properties of the Components from Troponin**, *The Journal of Biological Chemistry*. Available at: http://www.jbc.org/ (Accessed: 19 October 2020).

Greenbaum, S., Wainstock, T., Dukler, D., Leron, E. and Erez, O. (2017) 'Underlying mechanisms of retained placenta: Evidence from a population based cohort study', *European Journal of Obstetrics, Gynecology, and Reproductive Biology*, 216, pp. 12–17. doi: 10.1016/J.EJOGRB.2017.06.035.

Greenberg, H. Z. E., Carlton-Carew, S. R. E., Zargaran, A. K., Jahan, K. S., Birnbaumer, L. and Albert, A. P. (2019) 'Heteromeric TRPV4/TRPC1 channels mediate calcium-sensing receptor-induced relaxations and nitric oxide production in mesenteric arteries: comparative study using wild-type and TRPC1−/- mice', *Channels*. Taylor and Francis Inc., 13(1), pp. 410–

423. doi: 10.1080/19336950.2019.1673131.

Grieco, F., Bernstein, B. J., Biemans, B., Bikovski, L., Burnett, C. J., Cushman, J. D., van Dam, E. A., Fry, S. A., Richmond-Hacham, B., Homberg, J. R., *et al.* (2021) 'Measuring behavior in the home cage: Study design, applications, challenges, and perspectives', *Frontiers in Behavioral Neuroscience*, 15, p. 219. doi: 10.3389/FNBEH.2021.735387/BIBTEX.

Grüneberg, H. (1943) *The genetics of the mouse*. England: The University Press, Cambridge. Available at: https://www.worldcat.org/title/769921 (Accessed: 7 March 2023).

GTEx Portal (no date). Available at: https://gtexportal.org/home/gene/RYR1 (Accessed: 5 September 2020).

Guo, Y., Cao, Z., Jiao, X., Bai, D., Zhang, Y., Hua, J., Liu, W. and Teng, X. (2021) 'Pre-pregnancy exposure to fine particulate matter (PM2.5) increases reactive oxygen species production in oocytes and decrease litter size and weight in mice', *Environmental Pollution*, 268. doi: 10.1016/j.envpol.2020.115858.

Gyamfi-Bannerman, C., Srinivas, S. K., Wright, J. D., Goffman, D., Siddiq, Z., D'Alton, M. E. and Friedman, A. M. (2018) 'Postpartum hemorrhage outcomes and race', *American Journal of Obstetrics and Gynecology*. Mosby Inc., 219(2), pp. 185.e1-185.e10. doi: 10.1016/j.ajog.2018.04.052.

Ha, C. T., Wu, J. A., Irmak, S., Lisboa, F. A., Dizon, A. M., Warren, J. W., Ergun, S. and Dveksler, G. S. (2010) 'Human Pregnancy Specific Beta-1-Glycoprotein 1 (PSG1) has a potential role in placental vascular morphogenesis', *Biology of Reproduction*. Oxford University Press, 83(1), p. 27. doi: 10.1095/BIOLREPROD.109.082412.

Haché, S., Takser, L., Lebellego, F., Weiler, H., Leduc, L., Forest, J. C., Giguère, Y., Masse, A., Barbeau, B. and Lafond, J. (2011) 'Alteration of calcium homeostasis in primary preeclamptic syncytiotrophoblasts: Effect on calcium exchange in placenta', *Journal of Cellular and Molecular Medicine*, 15(3). doi: 10.1111/j.1582-4934.2010.01039.x.

Hakamata, Y., Nakai, J., Takeshima, H. and Imoto, K. (1992) 'Primary structure and distribution of a novel ryanodine receptor/calcium release channel from rabbit brain', *FEBS Letters*, 312(2–3). doi: 10.1016/0014-5793(92)80941-9.

Hallberg, L., Hôgdahl, A. -M, Nilsson, L. and Rybo, G. (1966) 'Menstrual blood loss--a population study. Variation at different ages and attempts to define normality', *Acta Obstetricia et Gynecologica Scandinavica*, 45(3), pp. 320–351. doi: 10.3109/00016346609158455.

Harada, N., Iijima, S., Kobayashi, K., Yoshida, T., Brown, W. R., Hibi, T., Oshima, A. and Morikawa, M. (1997) 'Human IgGFc binding protein (FcγBP) in colonic epithelial cells exhibits mucin-like structure', *Journal of Biological Chemistry*, 272(24). doi: 10.1074/jbc.272.24.15232.

Harraz, O. F., Abd El-Rahman, R. R., Bigdely-Shamloo, K., Wilson, S. M., Brett, S. E., Romero, M., Gonzales, A. L., Earley, S., Vigmond, E. J., Nygren, A., *et al.* (2014) 'Cav3.2 channels and the induction of negative feedback in cerebral arteries', *Circulation Research*. Lippincott Williams and Wilkins, 115(7), pp. 650–661. doi:

10.1161/CIRCRESAHA.114.304056.

Harris, D., Martin, P. E. M., Evans, W. H., Kendall, D. A., Griffith, T. M. and Randall, M. D. (2000) 'Role of gap junctions in endothelium-derived hyperpolarizing factor responses and mechanisms of K(+)-relaxation', *European Journal of Pharmacology*, 402(1–2), pp. 119–128. doi: 10.1016/S0014-2999(00)00512-4.

Harris, L. K. (2010) 'Review: Trophoblast-Vascular Cell Interactions in Early Pregnancy: How to Remodel a Vessel', *Placenta*. W.B. Saunders, 31(SUPPL.), pp. S93–S98. doi: 10.1016/J.PLACENTA.2009.12.012.

Hatthachote, P., Morgan, J., Dunlop, W., Europe-Finner, G. N. and Gillespie, J. I. (1998) 'Gestational Changes in the Levels of Transforming Growth Factor-β1 (TGFβ1) and TGFβ Receptor Types I and II in the Human Myometrium1', *The Journal of Clinical Endocrinology & Metabolism*, 83(8). doi: 10.1210/jcem.83.8.4992.

Hauksson, A., Åkerlund, M. and Melin, P. (1988) 'Uterine blood flow and myometrial activity at menstruation, and the action of vasopressin and a synthetic antagonist', *BJOG: An International Journal of Obstetrics & Gynaecology*, 95(9), pp. 898–904. doi: 10.1111/J.1471-0528.1988.TB06577.X.

Hawke, L., Grabell, J., Sim, W., Thibeault, L., Muir, E., Hopman, W., Smith, G. and James, P. (2016) 'Obstetric bleeding among women with inherited bleeding disorders: a retrospective study', *Haemophilia*. John Wiley & Sons, Ltd, 22(6), pp. 906–911. doi: 10.1111/HAE.13067.

Hazan, A. D., Smith, S. D., Jones, R. L., Whittle, W., Lye, S. J. and Dunk, C. E. (2010) 'Vascular-leukocyte interactions: Mechanisms of human decidual spiral artery remodeling in vitro', *American Journal of Pathology*. Elsevier Inc., 177(2), pp. 1017–1030. doi: 10.2353/AJPATH.2010.091105.

Hegewald, M. J. and Crapo, R. O. (2011) 'Respiratory Physiology in Pregnancy', *Clinics in Chest Medicine*. doi: 10.1016/j.ccm.2010.11.001.

van der Heijden, O. W. H., Essers, Y. P. G., Fazzi, G., Peeters, L. L. H., De Mey, J. G. R. and van Eys, G. J. J. M. (2005) 'Uterine artery remodeling and reproductive performance are impaired in endothelial nitric oxide synthase-deficient mice', *Biology of Reproduction*. Oxford University Press (OUP), 72(5), pp. 1161–1168. doi: 10.1095/biolreprod.104.033985.

Hellstrand, P. and Albinsson, S. (2005) 'Stretch-dependent growth and differentiation in vascular smooth muscle: Role of the actin cytoskeleton', *Canadian Journal of Physiology and Pharmacology*, pp. 869–875. doi: 10.1139/y05-061.

Henzl, M. R., Smith, R. E., Boost, G. and Tyler, E. T. (1972) 'Lysosomal Concept of Menstrual Bleeding in Humans', *The Journal of Clinical Endocrinology & Metabolism*. Oxford Academic, 34(5), pp. 860–875. doi: 10.1210/JCEM-34-5-860.

Herington, J. L., Bi, J. J., Martin, J. D. and Bany, B. M. (2007) 'β-Catenin (CTNNB1) in the mouse uterus during decidualization and the potential role of two pathways in regulating its degradation', *Journal of Histochemistry and Cytochemistry*. SAGE PublicationsSage CA: Los Angeles, CA, 55(9), pp. 963–974. doi:

10.1369/JHC.7A7199.2007/ASSET/IMAGES/LARGE/10.1369_JHC.7A7199.2007-FIG2.JPEG.

Herington, J. L., O'Brien, C., Robuck, M. F., Lei, W., Brown, N., Slaughter, J. C., Paria, B. C., Mahadevan-Jansen, A. and Reese, J. (2018) 'Prostaglandin-Endoperoxide synthase 1 mediates the timing of parturition in mice despite unhindered uterine contractility', *Endocrinology*, 159(1). doi: 10.1210/en.2017-00647.

Herman, G. E., Finegold, M., Zhao, W., De Gouyon, B. and Metzenberg, A. (1999) 'Medical complications in long-term survivors with X-linked myotubular myopathy', *The Journal of Pediatrics*. Mosby, 134(2), pp. 206–214. doi: 10.1016/S0022-3476(99)70417-8.

Heyman, R., Heckly, A., Magagi, J., Pladys, P. and Hamlat, A. (2005) 'Intracranial Epidural Hematoma in Newborn Infants: Clinical Study of 15 Cases', *Neurosurgery*, 57(5), pp. 924–929. doi: 10.1227/01.NEU.0000180026.73246.bf.

Hilgers, R. H. P., Bergaya, S., Schiffers, P. M. H., Meneton, P., Boulanger, C. M., Henrion, D., Lévy, B. I. and De Mey, J. G. R. (2003) 'Uterine artery structural and functional changes during pregnancy in tissue kallikrein–deficient mice', *Arteriosclerosis, Thrombosis, and Vascular Biology*. Lippincott Williams & Wilkins, 23(10), pp. 1826–1832. doi: 10.1161/01.ATV.0000090672.07568.60.

Hiramoto, K., Yamate, Y. and Sato, E. F. (2017) 'Gp91phox NADPH oxidase modulates litter size by regulating mucin1 in the uterus of mice', *Systems Biology in Reproductive Medicine*, 63(2). doi: 10.1080/19396368.2017.1282063.

Hirshberg, A., Levine, L. D. and Srinivas, S. (2014) 'Labor length among overweight and obese women undergoing induction of labor', *Journal of Maternal-Fetal and Neonatal Medicine*. Taylor & Francis, 27(17), pp. 1771–1775. doi: 10.3109/14767058.2013.879705.

Hirst, J. J., Mijovic, J. E., Zakar, T. and Olson, D. M. (1998) 'Prostaglandin endoperoxide H synthase-1 and -2 mRNA levels and enzyme activity in human decidua at term labor', *Journal of the Society for Gynecologic Investigation*, 5(1), pp. 13–20. doi: 10.1016/S1071-5576(97)00101-9.

Hnia, K., Tronchère, H., Tomczak, K. K., Amoasii, L., Schultz, P., Beggs, A. H., Payrastre, B., Mandel, J. L., Jocelyn Laporte, Hnia, K., *et al.* (2011) 'Myotubularin controls desmin intermediate filament architecture and mitochondrial dynamics in human and mouse skeletal muscle', *Journal of Clinical Investigation*, 121(1), pp. 70–85. doi: 10.1172/JCI44021.

Ho, T. C., Horn, N. A., Huynh, T., Kelava, L. and Lansman, J. B. (2012) 'Evidence TRPV4 contributes to mechanosensitive ion channels in mouse skeletal muscle fibers', *Channels*. Taylor and Francis Inc., 6(4). doi: 10.4161/chan.20719.

Holda, J. R., Oberti, C., Perez-Reyes, E. and Blatter, L. A. (1996) 'Characterization of an oxytocin induced rise in [Ca2+](i) in single human myometrium smooth muscle cells', *Cell Calcium*. doi: 10.1016/S0143-4160(96)90049-4.

Hopton, C., Tijsen, A. J., Maizels, L., Arbel, G., Gepstein, A., Bates, N., Brown, B., Huber, I., Kimber, S. J., Newman, W. G., Venetucci, L. and Gepstein, L. (2022) 'Characterization of the

mechanism by which a nonsense variant in RYR2 leads to disordered calcium handling', *Physiological Reports*. Wiley-Blackwell, 10(8), p. 15265. doi: 10.14814/PHY2.15265.

Hsu, P. K., Huang, H. C., Hsieh, C. C., Hsu, H. S., Wu, Y. C., Huang, M. H. and Hsu, W. H. (2007) 'Effect of formalin fixation on tumor size determination in stage I non-small cell lung cancer', *The Annals of Thoracic Surgery*, 84(6), pp. 1825–1829. doi: 10.1016/J.ATHORACSUR.2007.07.016.

Hu, D. and Cross, J. C. (2011) 'Ablation of Tpbpa-positive trophoblast precursors leads to defects in maternal spiral artery remodeling in the mouse placenta', *Developmental Biology*. Academic Press, 358(1), pp. 231–239. doi: 10.1016/J.YDBIO.2011.07.036.

Hu, S., Kim, H. S. and Jeng, A. Y. (1991) 'Dual action of endothelin-1 on the Ca2+-activated K+ channel in smooth muscle cells of porcine coronary artery', *European Journal of Pharmacology*, 194(1). doi: 10.1016/0014-2999(91)90120-F.

Hu, X.-Q., Dasgupta, C., Chen, M., Xiao, D., Huang, X., Han, L., Yang, S., Xu, Z. and Zhang, L. (2017) 'Pregnancy Reprograms Large-Conductance Ca^{2+}-Activated K$^+$ Channel in Uterine ArteriesNovelty and Significance', *Hypertension*, 69(6).

Hu, X.-Q. Q., Song, R., Romero, M., Dasgupta, C., Huang, X., Holguin, M. A., Williams, V. S., Xiao, D., Wilson, S. M. and Zhang, L. (2019) 'Pregnancy increases Ca2+ sparks/spontaneous transient outward currents and reduces uterine arterial myogenic tone', *Hypertension*. Lippincott Williams and Wilkins, 73(3), pp. 691–702. doi: 10.1161/HYPERTENSIONAHA.118.12484.

Hu, X.-Q., Song, R., Romero, M., Dasgupta, C., Min, J., Hatcher, D., Xiao, D., Blood, A., Wilson, S. M., Zhang, L., *et al.* (2020) 'Gestational hypoxia inhibits pregnancy-induced upregulation of ca 2+ sparks and spontaneous transient outward currents in uterine arteries via heightened endoplasmic reticulum/oxidative stress', *Hypertension*, 76(3), pp. 930–942. doi: 10.1161/HYPERTENSIONAHA.120.15235.

Hu, X.-Q., Xiao, D., Zhu, R., Huang, X., Yang, S., Wilson, S. and Zhang, L. (2011) 'Pregnancy upregulates large-conductance Ca 2+-activated K + channel activity and attenuates myogenic tone in uterine arteries', *Hypertension*. NIH Public Access, 58(6), pp. 1132–1139. doi: 10.1161/HYPERTENSIONAHA.111.179952.

Hunt, J. S. and Pollard, J. W. (1992) 'Macrophages in the uterus and placenta', in *Current Topics in Microbiology and Immunology*. Springer, pp. 39–63. doi: 10.1007/978-3-642-77377-8_2/COVER.

Hurskainen, R., Teperi, J., Paavonen, J. and Cacciatore, B. (1999) 'Menorrhagia and uterine artery blood flow', *Human Reproduction*. Oxford Academic, 14(1), pp. 186–189. doi: 10.1093/HUMREP/14.1.186.

Hymel, L., Inui, M., Fleischer, S. and Schindler, H. (1988) 'Purified ryanodine receptor of skeletal muscle sarcoplasmic reticulum forms Ca2+-activated oligomeric Ca2+ channels in planar bilayers.', *Proceedings of the National Academy of Sciences*, 85(2), pp. 441–445. doi: 10.1073/PNAS.85.2.441.

Ibarra M, C. A., Wu, S., Murayama, K., Minami, N., Ichihara, Y., Kikuchi, H., Noguchi, S., Hayashi, Y. K., Ochiai, R. and Nishino, I. (2006) 'Malignant hyperthermia in Japan: Mutation screening of the entire ryanodine receptor type 1 gene coding region by direct sequencing', *Anesthesiology*, 104(6). doi: 10.1097/00000542-200606000-00008.

Ilkovski, B., Cooper, S. T., Nowak, K., Ryan, M. M., Yang, N., Schnell, C., Durling, H. J., Roddick, L. G., Wilkinson, I., Kornberg, A. J., *et al.* (2001) 'Nemaline myopathy caused by mutations in the muscle α-skeletal-actin gene', *American Journal of Human Genetics*, 68(6), pp. 1333–1343. doi: 10.1086/320605.

Illsley, N. P., Wootton, R., Penfold, P., Hall, S. and Duffy, S. (1986) 'Lactate transfer across the perfused human placenta', *Placenta*, 7(3). doi: 10.1016/S0143-4004(86)80159-X.

Imagawa, T., Smith, J. S., Coronado, R. and Campbell, K. P. (1987) 'Purified ryanodine receptor from skeletal muscle sarcoplasmic reticulum is the Ca2+-permeable pore of the calcium release channel.', *Journal of Biological Chemistry*. Elsevier, 262(34), pp. 16636–16643. doi: 10.1016/S0021-9258(18)49303-9.

Irving, J. A. and Lala, P. K. (1995) 'Functional role of cell surface integrins on human trophoblast cell migration: Regulation by TGF-β, IGF-II, and IGFBP-1', *Experimental Cell Research*, 217(2), pp. 419–427. doi: 10.1006/excr.1995.1105.

Ishikawa, H., Seki, R., Yokonishi, S., Yamauchi, T. and Yokoyama, K. (2006) 'Relationship between fetal weight, placental growth and litter size in mice from mid- to late-gestation', *Reproductive Toxicology*. Pergamon, 21(3), pp. 267–270. doi: 10.1016/J.REPROTOX.2005.08.002.

Jabbour, H. N., Kelly, R. W., Fraser, H. M. and Critchley, H. O. D. (2006) 'Endocrine Regulation of Menstruation', *Endocrine Reviews*. Oxford Academic, 27(1), pp. 17–46. doi: 10.1210/ER.2004-0021.

Jaggar, J. H., Porter, V. A., Lederer, W. J. and Nelson, M. T. (2000) 'Calcium sparks in smooth muscle.', *American Journal of Physiology - Cell physiology*. doi: 10.1152/ajpcell.2000.278.2.C235.

Jakoubek, V., Bíbová, J. and Hampl, V. (2006) 'Voltage-gated calcium channels mediate hypoxic vasoconstriction in the human placenta', *Placenta*, 27(9–10). doi: 10.1016/j.placenta.2005.10.006.

James, A. H. and Jamison, M. G. (2007) 'Bleeding events and other complications during pregnancy and childbirth in women with von Willebrand disease', *Journal of Thrombosis and Haemostasis*. Elsevier, 5(6), pp. 1165–1169. doi: 10.1111/J.1538-7836.2007.02563.X.

Jardine, J., Gurol-Urganci, I., Harris, T., Hawdon, J., Pasupathy, D., van der Meulen, J. and Walker, K. (2022) 'Risk of postpartum haemorrhage is associated with ethnicity: A cohort study of 981 801 births in England', *BJOG : an international journal of obstetrics and gynaecology*. BJOG, 129(8), pp. 1269–1277. doi: 10.1111/1471-0528.17051.

Jauniaux, E. and Jurkovic, D. (2012) 'Placenta accreta: pathogenesis of a 20th century iatrogenic uterine disease', *Placenta*, 33(4), pp. 244–251. doi:

10.1016/J.PLACENTA.2011.11.010.

Jauniaux, E. R. M., Alfirevic, Z., Bhide, A. G., Belfort, M. A., Burton, G. J., Collins, S. L., Dornan, S., Jurkovic, D., Kayem, G., Kingdom, J., Silver, R. and Sentilhes, L. (2019) 'Placenta Praevia and Placenta Accreta: Diagnosis and Management', *BJOG: An International Journal of Obstetrics & Gynaecology*. John Wiley & Sons, Ltd, 126(1), pp. e1–e48. doi: 10.1111/1471-0528.15306.

Jędrzejowska, M., Dębek, E., Kowalczyk, B., Halat, P., Kostera-Pruszczyk, A., Ciara, E., Jezela-Stanek, A., Rydzanicz, M., Gasperowicz, P. and Gos, M. (2019) 'The remarkable phenotypic variability of the p.Arg269HiS variant in the TRPV4 gene', *Muscle and Nerve*. John Wiley and Sons Inc., 59(1), pp. 129–133. doi: 10.1002/mus.26346.

Jenkinson, C., Coulter, A. and Wright, L. (1993) 'Short form 36 (SF36) health survey questionnaire: normative data for adults of working age.', *BMJ : British Medical Journal*. BMJ Publishing Group, 306(6890), p. 1437. doi: 10.1136/BMJ.306.6890.1437.

Jenkinson, C., Peto, V. and Coulter, A. (1996) 'Making sense of ambiguity: evaluation in internal reliability and face validity of the SF 36 questionnaire in women presenting with menorrhagia.', *Quality in Health Care*. BMJ Publishing Group, 5(1), p. 9. doi: 10.1136/QSHC.5.1.9.

Ji, G., Feldman, M. E., Greene, K. S., Sorrentino, V., Xin, H. B. and Kotlikoff, M. I. (2004) 'RYR2 proteins contribute to the formation of Ca2+ sparks in smooth muscle', *Journal of General Physiology*. The Rockefeller University Press, 123(4), pp. 377–386. doi: 10.1085/jgp.200308999.

Jiang, D., Xiao, B., Li, X. and Chen, S. R. W. W. (2003) 'Smooth muscle tissues express a major dominant negative splice variant of the type 3 Ca2+ release channel (ryanodine receptor)', *Journal of Biological Chemistry*. American Society for Biochemistry and Molecular Biology, 278(7), pp. 4763–9. doi: 10.1074/jbc.M210410200.

Jin, J. P., Brotto, M. A., Hossain, M. M., Huang, Q. Q., Brotto, L. S., Nosek, T. M., Morton, D. H. and Crawford, T. O. (2003) 'Truncation by Glu180 nonsense mutation results in complete loss of slow skeletal muscle troponin T in a lethal nemaline myopathy', *Journal of Biological Chemistry*. American Society for Biochemistry and Molecular Biology, 278(28), pp. 26159–26165. doi: 10.1074/jbc.M303469200.

Johansson, M. E. V, Thomsson, K. A. and Hansson, G. C. (2009) 'Proteomic analyses of the two mucus layers of the colon barrier reveal that their main component, the muc2 mucin, is strongly bound to the fcgbp protein', *Journal of Proteome Research*, 8(7), pp. 3549–3557. doi: 10.1021/pr9002504.

Johnson, R. E., Sigman, J. D., Funk, G. F., Robinson, R. A. and Hoffman, H. T. (1997) 'Quantification of surgical margin shrinkage in the oral cavity', *Head and Neck*, 19(4). doi: 10.1002/(sici)1097-0347(199707)19:4<281::aid-hed6>3.0.co;2-x.

Johnston, J. J., Dirksen, R. T., Girard, T., Gonsalves, S. G., Hopkins, P. M., Riazi, S., Saddic, L. A., Sambuughin, N., Saxena, R., Stowell, K., Weber, J., Rosenberg, H. and Biesecker, L. G. (2021) 'Variant curation expert panel recommendations for RYR1 pathogenicity classifications

in malignant hyperthermia susceptibility', *Genetics in Medicine*. Springer Nature, 23(7), pp. 1288–1295. doi: 10.1038/s41436-021-01125-w.

Johnston, J. J., Kelley, R. I., Crawford, T. O., Morton, D. H., Agarwala, R., Koch, T., Schäffer, A. A., Francomano, C. A. and Biesecker, L. G. (2000) 'A novel nemaline myopathy in the Amish caused by a mutation in troponin T1', *American Journal of Human Genetics*. Elsevier, 67(4), pp. 814–821. doi: 10.1086/303089.

Ju, Y., Li, J., Xie, C., Ritchlin, C. T., Xing, L., Hilton, M. J. and Schwarz, E. M. (2013) 'Troponin T3 expression in skeletal and smooth muscle is required for growth and postnatal survival: Characterization of Tnnt3tm2a(KOMP)Wtsi mice', *Genesis*. NIH Public Access, 51(9), pp. 667–675. doi: 10.1002/dvg.22407.

Jukic, A. M., Baird, D. D., Weinberg, C. R., Mcconnaughey, D. R. and Wilcox, A. J. (2013) 'Length of human pregnancy and contributors to its natural variation', *Human Reproduction (Oxford, England)*. Oxford University Press, 28(10), p. 2848. doi: 10.1093/HUMREP/DET297.

Jungbluth, H. (2007) 'Multi-minicore Disease.', *Orphanet journal of rare diseases*. BioMed Central, 2, p. 31. doi: 10.1186/1750-1172-2-31.

Jungbluth, H., Lillis, S., Zhou, H., Abbs, S., Sewry, C., Swash, M. and Muntoni, F. (2009) 'Late-onset axial myopathy with cores due to a novel heterozygous dominant mutation in the skeletal muscle ryanodine receptor (RYR1) gene', *Neuromuscular Disorders*. doi: 10.1016/j.nmd.2009.02.005.

Jungbluth, H., Müller, C. R., Halliger-Keller, B., Brockington, M., Brown, S. C., Feng, L., Chattopadhyay, A., Mercuri, E., Manzur, A. Y., Ferreiro, A., *et al.* (2002) 'Autosomal recessive inheritance of RYR1 mutations in a congenital myopathy with cores', *Neurology*. Lippincott Williams and Wilkins, 59(2), pp. 284–287. doi: 10.1212/WNL.59.2.284.

Jungbluth, H., Sewry, C. A. and Muntoni, F. (2011) 'Core myopathies', *Seminars in pediatric neurology*. Semin Pediatr Neurol, 18(4), pp. 239–249. doi: 10.1016/J.SPEN.2011.10.005.

Jungbluth, H., Treves, S., Zorzato, F., Sarkozy, A., Ochala, J., Sewry, C., Phadke, R., Gautel, M. and Muntoni, F. (2018) 'Congenital myopathies: Disorders of excitation-contraction coupling and muscle contraction', *Nature Reviews Neurology*. Nature Publishing Group, pp. 151–167. doi: 10.1038/nrneurol.2017.191.

Jungbluth, H., Wallgren-Pettersson, C. and Laporte, J. (2008) 'Centronuclear (myotubular) myopathy', *Orphanet Journal of Rare Diseases*, 3(1). doi: 10.1186/1750-1172-3-26.

Jungbluth, H., Zhou, H., Hartley, L., Halliger-Keller, B., Messina, S., Longman, C., Brockington, M., Robb, S. A., Straub, V., Voit, T., *et al.* (2005) 'Minicore myopathy with ophthalmoplegia caused by mutations in the ryanodine receptor type 1 gene', *Neurology*, 65(12), pp. 1930–1935. doi: 10.1212/01.wnl.0000188870.37076.f2.

Jurynec, M. J., Xia, R., Mackrill, J. J., Gunther, D., Crawford, T., Flanigan, K. M., Abramson, J. J., Howard, M. T. and Grunwald, D. J. (2008) 'Selenoprotein N is required for ryanodine receptor calcium release channel activity in human and zebrafish muscle', *Proceedings of the*

National Academy of Sciences of the United States of America, 105(34), pp. 12485–12490. doi: 10.1073/pnas.0806015105.

Kadir, R. A., Economides, D. L., Sabin, C. A., Owens, D. and Lee, C. A. (1998) 'Frequency of inherited bleeding disorders in women with menorrhagia', *Lancet*, 351(9101). doi: 10.1016/S0140-6736(97)08248-2.

Kamel, R. M. (2010) 'The onset of human parturition', *Archives of Gynecology and Obstetrics*, 281(6), pp. 975–982. doi: 10.1007/s00404-010-1365-9.

Kanayama, N., Takahashi, K., Matsuura, T., Sugimura, M., Kobayashi, T., Moniwa, N., Tomita, M. and Nakayama, K. (2002) 'Deficiency in p57Kip2 expression induces preeclampsia-like symptoms in mice', *Molecular Human Reproduction*. Oxford Academic, 8(12), pp. 1129–1135. doi: 10.1093/MOLEHR/8.12.1129.

Kandola, M. K., Sykes, L., Lee, Y. S., Johnson, M. R., Hanyaloglu, A. C. and Bennett, P. R. (2014) 'EP2 receptor activates dual g protein signaling pathways that mediate contrasting proinflammatory and relaxatory responses in term pregnant human myometrium', *Endocrinology*, 155(2). doi: 10.1210/en.2013-1761.

Kellermayer, D., Smith, J. E. and Granzier, H. (2019) 'Titin mutations and muscle disease', *Pflugers Archiv European Journal of Physiology*. Springer Verlag. doi: 10.1007/s00424-019-02272-5.

Kelly, R. W., King, A. E. and Crithley, H. O. D. (2001) 'Cytokine control in human endometrium', *Reproduction (Cambridge, England)*. Reproduction, 121(1), pp. 3–19. doi: 10.1530/REP.0.1210003.

Kennedy, S. (2017) *How DNA extraction kits work in the lab*, *BiteSizeBio, New England Biolabs*. Available at: https://bitesizebio.com/13516/how-dna-extraction-rna-miniprep-kits-work/ (Accessed: 23 January 2020).

Kent, J. W., Sugnet, C. W., Furey, T. S., Roskin, K. M., Pringle, T. H., Zahler, A. M. and Haussler, D. (2002) 'The human genome browser at UCSC', *Genome Research*, 12(6), pp. 996–1006. doi: 10.1101/gr.229102. Article published online before print in May 2002.

Khalife, N., Glover, V., Hartikainen, A. L., Taanila, A., Ebeling, H., Järvelin, M. R. and Rodriguez, A. (2012) 'Placental size is associated with mental health in children and adolescents', *PLOS ONE*. Public Library of Science, 7(7), p. e40534. doi: 10.1371/JOURNAL.PONE.0040534.

Khan, L. H., Rosenfeld, C. R., Liu, X. T. and Magness, R. R. (2010) 'Regulation of the cGMP-cPKG pathway and large-conductance Ca 3+-activated K+ channels in uterine arteries during the ovine ovarian cycle', *American Journal of Physiology - Endocrinology and Metabolism*, 298(2). doi: 10.1152/ajpendo.00375.2009.

Khan, R. N., Matharoo-Ball, B., Arulkumaran, S. and Ashford, M. L. J. J. (2001) 'Potassium channels in the human myometrium', *Experimental Physiology*, 86(2), pp. 255–264. doi: 10.1113/eph8602181.

Khan, R. N., Smith, S. K., Morrison, J. J. and Ashford, M. L. J. (1993) 'Properties of large-conductance K+ channels in human myometrium during pregnancy and labour', *Proceedings of the Royal Society: Biological Sciences*. Royal Society, 251(1330), pp. 9–15. doi: 10.1098/rspb.1993.0002.

Khan, R. N., Smith, S. K., Morrison, J. J. and Ashford, M. L. J. (1997) 'Ca2+ dependence and pharmacology of large-conductance K+ channels in nonlabor and labor human uterine myocytes', *The American Journal of Physiology*, 273(5). doi: 10.1152/AJPCELL.1997.273.5.C1721.

Kikuchi, N., Satoh, K., Satoh, T., Yaoita, N., Siddique, M. A. H., Omura, J., Kurosawa, R., Nogi, M., Sunamura, S., Miyata, S., Misu, H., Saito, Y. and Shimokawa, H. (2019) 'Diagnostic and prognostic significance of serum levels of SeP (Selenoprotein P) in patients with pulmonary hypertension', *Arteriosclerosis, Thrombosis, and Vascular Biology*. Lippincott Williams and Wilkins, 39(12), pp. 2553–2562. doi: 10.1161/ATVBAHA.119.313267.

Kil, T. H. and Kim, J. B. (2010) 'Severe respiratory phenotype caused by a de novo Arg528Gly mutation in the CACNA1S gene in a patient with hypokalemic periodic paralysis', *European Journal of Paediatric Neurology*. W.B. Saunders, 14(3), pp. 278–281. doi: 10.1016/J.EJPN.2009.08.004.

Kim, H.-Y. (2017) 'Statistical notes for clinical researchers: Chi-squared test and Fisher's exact test', *Restorative Dentistry & Endodontics*, 42(2). doi: 10.5395/rde.2017.42.2.152.

Kim, K. and Keller, T. C. S. (2002) 'Smitin, a novel smooth muscle titin-like protein, interacts with myosin filaments in vivo and in vitro', *Journal of Cell Biology*. The Rockefeller University Press, 156(1), pp. 101–111. doi: 10.1083/jcb.200107037.

Kim, S. H., MacIntyre, D. A., Firmino Da Silva, M., Blanks, A. M., Lee, Y. S., Thornton, S., Bennett, P. R. and Terzidou, V. (2015) 'Oxytocin activates NF-κB-mediated inflammatory pathways in human gestational tissues', *Molecular and cellular endocrinology*. Mol Cell Endocrinol, 403, pp. 64–77. doi: 10.1016/J.MCE.2014.11.008.

Kings College London, K. (2022) 'King's Computational Research, Engineering and Technology Environment (CREATE)'. Available at: https://doi.org/10.18742/rnvf-m076.

Kinney, M., Lawn, J. and Howson, C. (2012) *March of Dimes, PMNCH, Save the Children, WHO. Born Too Soon: The Global Action Report on Preterm Birth*, *World Health Organization*. World Health Organization, Geneva.

Kirz, D. S., Dorchester, W. and Freeman, R. K. (1985) 'Advanced maternal age: The mature gravida', *American Journal of Obstetrics and Gynecology*, 152(1). doi: 10.1016/S0002-9378(85)80166-6.

Kistka, Z. A. F., Palomar, L., Boslaugh, S. E., DeBaun, M. R., DeFranco, E. A. and Muglia, L. J. (2007) 'Risk for postterm delivery after previous postterm delivery', *American Journal of Obstetrics & Gynecology*, 196(3), pp. 241.e1-241.e6. doi: 10.1016/J.AJOG.2006.10.873.

Knock, G. A., Smirnov, S. V. and Aaronson, P. I. (1999) 'Voltage-gated K+ currents in freshly isolated myocytes of the pregnant human myometrium', *Journal of Physiology*. doi:

10.1111/j.1469-7793.1999.0769p.x.

Kobayashi, K., Blaser, M. J. and Brown, W. R. (1989) 'Identification of a unique IgG Fc binding site in human intestinal epithelium', *Journal of immunology (Baltimore, Md. : 1950)*, 143(8), pp. 2567–74. Available at: https://pubmed.ncbi.nlm.nih.gov/2529312/ (Accessed: 21 January 2023).

Kobayashi, K., Hamada, Y., Blaser, M. J. and Brown, W. R. (1991) 'The molecular configuration and ultrastructural locations of an IgG Fc binding site in human colonic epithelium', *Journal of immunology (Baltimore, Md. : 1950)*. J Immunol, 146(1), pp. 68–74. Available at: https://pubmed.ncbi.nlm.nih.gov/1984453/ (Accessed: 21 January 2023).

Kocaoz, S., Cirpan, R. and Degirmencioglu, A. Z. (2019) 'The prevalence and impacts heavy menstrual bleeding on anemia, fatigue and quality of life in women of reproductive age', *Pakistan journal of medical sciences*. Pak J Med Sci, 35(2), pp. 365–370. doi: 10.12669/PJMS.35.2.644.

Koga, H., Miyako, K., Suga, N., Hidaka, T. and Takahashi, N. (2012) 'Predisposition to Subdural Hemorrhage in X-Linked Myotubular Myopathy', *Pediatric Neurology*. Elsevier, 46(5), pp. 332–334. doi: 10.1016/J.PEDIATRNEUROL.2012.02.026.

Kolb, M. E., Horne, M. L. and Martz, R. (1982) 'Dantrolene in human malignant hyperthermia.', *Anesthesiology*, 56(4), pp. 254–262. doi: 10.1097/00000542-198204000-00005.

Komalavilas, P., Penn, R. B., Flynn, C. R., Thresher, J., Lopes, L. B., Furnish, E. J., Guo, M., Pallero, M. A., Murphy-Ullrich, J. E. and Brophy, C. M. (2008) 'The small heat shock-related protein, HSP20, is a cAMP-dependent protein kinase substrate that is involved in airway smooth muscle relaxation', *American Journal of Physiology - Lung Cellular and Molecular Physiology*. NIH Public Access, 294(1), p. L69. doi: 10.1152/ajplung.00235.2007.

Konje, J. C., Kaufmann, P., Bell, S. C. and Taylor, D. J. (2001) 'A longitudinal study of quantitative uterine blood flow with the use of color power angiography in appropriate for gestational age pregnancies', *American Journal of Obstetrics and Gynecology*. Mosby Inc., 185(3), pp. 608–613. doi: 10.1067/mob.2001.117187.

Kota, Sunil K., Gayatri, K., Jammula, S., Kota, Siva K., Krishna, S. V. S., Meher, L. K. and Modi, K. D. (2013a) 'Endocrinology of parturition', *Indian Journal of Endocrinology and Metabolism*. Wolters Kluwer -- Medknow Publications, 17(1), p. 50. doi: 10.4103/2230-8210.107841.

Kota, Sunil K., Gayatri, K., Jammula, S., Kota, Siva K., Krishna, S. V. S., Meher, L. K. and Modi, K. D. (2013b) 'Endocrinology of parturition', *Indian Journal of Endocrinology and Metabolism*. Wolters Kluwer -- Medknow Publications, 17(1), p. 50. doi: 10.4103/2230-8210.107841.

Kraeva, N., Riazi, S., Loke, J., Frodis, W., Crossan, M. Lou, Nolan, K., Kraev, A. and MacLennan, D. H. (2011) 'Ryanodine receptor type 1 gene mutations found in the Canadian malignant hyperthermia population', *Canadian Journal of Anesthesia*, 58(6). doi: 10.1007/s12630-011-9494-6.

Kramer, M. S., Berg, C., Abenhaim, H., Dahhou, M., Rouleau, J., Mehrabadi, A. and Joseph, K. S. (2013) 'Incidence, risk factors, and temporal trends in severe postpartum hemorrhage', *American Journal of Obstetrics and Gynecology*. Mosby Inc., 209(5), pp. 449.e1-449.e7. doi: 10.1016/j.ajog.2013.07.007.

Krishnamoorthy, G., Sonkusare, S. K., Heppner, T. J. and Nelson, M. T. (2014) 'Opposing roles of smooth muscle BK channels and ryanodine receptors in the regulation of nerve-evoked constriction of mesenteric resistance arteries', *American Journal of Physiology - Heart and Circulatory Physiology*, 306(7). doi: 10.1152/ajpheart.00866.2013.

Kubosaki, A., Nakamura, S., Clark, A., Morris, J. F. and Notkins, A. L. (2006) 'Disruption of the transmembrane dense core vesicle proteins IA-2 and IA-2β causes female infertility', *Endocrinology*, 147(2). doi: 10.1210/en.2005-0638.

Kudryavtseva, O., Aalkjær, C. and Matchkov, V. V. (2013) 'Vascular smooth muscle cell phenotype is defined by Ca2+-dependent transcription factors', *The FEBS Journal*. John Wiley & Sons, Ltd, 280(21), pp. 5488–5499. doi: 10.1111/FEBS.12414.

Kulandavelu, S., Qu, D., Sunn, N., Mu, J., Rennie, M. Y., Whiteley, K. J., Walls, J. R., Bock, N. A., Sun, J. C. H., Covelli, A., Sled, J. G. and Adamson, S. L. (2006) 'Embryonic and neonatal phenotyping of genetically engineered mice'. ILAR J, 47(2), pp. 103–117. Available at: https://pubmed.ncbi.nlm.nih.gov/16547367/ (Accessed: 21 November 2022).

Kumar, S., Offiong, E. E., Sangita, S. and Hussain, N. (2018) 'Phenotypical variation with same genetic mutation in familial hypokalemic periodic paralysis', *Journal of Pediatric Neurosciences*. Wolters Kluwer -- Medknow Publications, 13(2), p. 218. doi: 10.4103/JPN.JPN_44_17.

Kunichika, N., Yu, Y., Remillard, C. V., Platoshyn, O., Zhang, S. and Yuan, J. X. J. (2004) 'Overexpression of TRPC1 enhances pulmonary vasoconstriction induced by capacitative Ca2+ entry', *American Journal of Physiology - Lung Cellular and Molecular Physiology*, 287(5 31-5). doi: 10.1152/ajplung.00452.2003.

Kunz, G. and Leyendecker, G. (2002) 'Uterine peristaltic activity during the menstrual cycle: characterization, regulation, function and dysfunction.', *Reproductive biomedicine online*, 4 Suppl 3, pp. 5–9. Available at: http://www.ncbi.nlm.nih.gov/pubmed/12470555 (Accessed: 28 February 2019).

Kuo, I. Y. and Ehrlich, B. E. (2015) 'Signaling in muscle contraction', *Cold Spring Harbor Perspectives in Biology*. doi: 10.1101/cshperspect.a006023.

Labeit, S., Lahmers, S., Burkart, C., Fong, C., McNabb, M., Witt, S., Witt, C., Labeit, D. and Granzier, H. (2006) 'Expression of distinct classes of titin isoforms in striated and smooth muscles by alternative splicing, and their conserved interaction with filamins', *Journal of Molecular Biology*. Academic Press, 362(4), pp. 664–681. doi: 10.1016/j.jmb.2006.07.077.

Landrum, M. J., Chitipiralla, S., Brown, G. R., Chen, C., Gu, B., Hart, J., Hoffman, D., Jang, W., Kaur, K., Liu, C., *et al.* (2020) 'ClinVar: improvements to accessing data', *Nucleic acids research*. Nucleic Acids Res, 48(D1), pp. D835–D844. doi: 10.1093/NAR/GKZ972.

Lanner, J. T., Georgiou, D. K., Joshi, A. D. and Hamilton, S. L. (2010) 'Ryanodine receptors: structure, expression, molecular details, and function in calcium release.', *Cold Spring Harbor perspectives in biology*. Cold Spring Harbor Laboratory Press. doi: 10.1101/cshperspect.a003996.

Lao, T. T., Lee, C. P. and Wong, W. M. (1997) 'Placental weight to birthweight ratio is increased in mild gestational glucose intolerance', *Placenta*. W.B. Saunders, 18(2–3), pp. 227–230. doi: 10.1016/S0143-4004(97)90097-7.

Latorre, R., Oberhauser, A., Labarca, P. and Alvarez, O. (1989) 'Varieties of calcium-activated potassium channels', *Annual Review of Physiology*, pp. 385–399. doi: 10.1146/annurev.ph.51.030189.002125.

Lee, H. J., Lee, Y. J., Ahn, E. H., Kim, H. C., Jung, S. H., Chang, S. W. and Lee, J. Y. (2017) 'Risk factors for massive postpartum bleeding in pregnancies in which incomplete placenta previa are located on the posterior uterine wall', *Obstetrics & Gynecology Science*, 60(6), pp. 520–526. doi: 10.5468/OGS.2017.60.6.520.

Lee, N. C., Dicker, R. C., Rubin, G. L. and Ory, H. W. (1984) 'Confirmation of the preoperative diagnoses for hysterectomy', *American Journal of Obstetrics and Gynecology*, 150(3), pp. 283–287. doi: 10.1016/S0002-9378(84)90366-1.

Lee, S. and Lee, D. K. (2018) 'What is the proper way to apply the multiple comparison test?', *Korean Journal of Anesthesiology*, 71(5). doi: 10.4097/kja.d.18.00242.

Leebeek, F. W. G. and Eikenboom, J. C. J. (2016) 'Von Willebrand's Disease', *The New England journal of medicine*. Edited by D. L. Longo. N Engl J Med, 375(21), pp. 2067–2080. doi: 10.1056/NEJMRA1601561.

Leichtweiß, H. P. and Schröder, H. (1981) 'l-Lactate and d-lactate carriers on the fetal and the maternal side of the trophoblast in the isolated guinea pig placenta', *Pflügers Archiv European Journal of Physiology*, 390(1). doi: 10.1007/BF00582716.

Lemarchand-Béraud, T., Zufferey, M. M., Reymond, M. and Rey, I. (1982) 'Maturation of the hypothalamo-pituitary-ovarian axis in adolescent girls', *The Journal of clinical endocrinology and metabolism*. J Clin Endocrinol Metab, 54(2), pp. 241–246. doi: 10.1210/JCEM-54-2-241.

Li, J. ping, Zhou, J. xuan, Wang, Q., Gu, G. qin, Yang, S. jin, Li, C. ye, Qiu, C. wei, Deng, G. zhen and Guo, M. yao (2016) 'Se enhances MLCK activation by regulating Selenoprotein T (SelT) in the gastric smooth muscle of rats', *Biological Trace Element Research*. Humana Press Inc., 173(1), pp. 116–125. doi: 10.1007/s12011-016-0620-8.

Li, N., He, Y., Yang, G., Yu, Q. and Li, M. (2019) 'Role of TRPC1 channels in pressure-mediated activation of airway remodeling', *Respiratory Research*. BioMed Central Ltd., 20(1). doi: 10.1186/s12931-019-1050-x.

Li, Q., Geng, X. D., Zheng, W., Tang, J., Xu, B. and Shi, Q. H. (2012) 'Current understanding of ovarian aging', *Science China Life Sciences*. doi: 10.1007/s11427-012-4352-5.

Li, X. Q., Zheng, Y. M., Rathore, R., Ma, J., Takeshima, H. and Wang, Y. X. (2009) 'Genetic

evidence for functional role of ryanodine receptor 1 in pulmonary artery smooth muscle cells', *Pflugers Archiv European Journal of Physiology*. Springer, 457(4), pp. 771–783. doi: 10.1007/s00424-008-0556-8.

Li, Y., Lorca, R. A., Ma, X., Rhodes, A. and England, S. K. (2014) 'BK channels regulate myometrial contraction by modulating nuclear translocation of NF-κB', *Endocrinology*. Endocrine Society, 155(8), pp. 3112–3122. doi: 10.1210/en.2014-1152.

Liang, X., Jin, Y., Wang, H., Meng, X., Tan, Z., Huang, T. and Fan, S. (2019) 'Transgelin 2 is required for embryo implantation by promoting actin polymerization', *The FASEB Journal*. John Wiley & Sons, Ltd, 33(4), pp. 5667–5675. doi: 10.1096/FJ.201802158RRR.

Lim, J. and Luderer, U. (2011) 'Oxidative damage increases and antioxidant gene expression decreases with aging in the mouse ovary', *Biology of Reproduction*, 84(4). doi: 10.1095/biolreprod.110.088583.

Lin, S., Shimizu, I., Suehara, N., Nakayama, M. and Aono, T. (1995) 'Uterine artery Doppler velocimetry in relation to trophoblast migration into the myometrium of the placental bed', *Obstetrics and Gynecology*, 85(5 Pt 1), pp. 760–765. doi: 10.1016/0029-7844(95)00020-R.

Lin, T. M., Halbert, S. P. and Spellacy, W. N. (1974) 'Measurement of pregnancy-associated plasma proteins during human gestation', *The Journal of Clinical Investigation*, 54(3), pp. 576–582. doi: 10.1172/JCI107794.

Lisboa, F. A., Warren, J., Sulkowski, G., Aparicio, M., David, G., Zudaire, E. and Dveksler, G. S. (2011) 'Pregnancy-specific Glycoprotein 1 Induces Endothelial Tubulogenesis through Interaction with Cell Surface Proteoglycans', *The Journal of Biological Chemistry*. American Society for Biochemistry and Molecular Biology, 286(9), p. 7577. doi: 10.1074/JBC.M110.161810.

Lisboa, F. A., Warren, J., Sulkowski, G., Aparicio, M., Guido, D., Zudaire, E. and Dveksler, G. S. (2010) 'Pregnancy-specific Glycoprotein 1 Induces Endothelial Tubulogenesis through Interaction with Cell Surface Proteoglycans', *The Journal of Biological Chemistry*. American Society for Biochemistry and Molecular Biology, 286(9), p. 7577. doi: 10.1074/jbc.M110.161810.

Liu, C. ning, Yu, F. bing, Xu, Y. zhe, Li, J. sheng, Guan, Z. hong, Sun, M. na, Liu, C. an, He, F. and Chen, D. jin (2021) 'Prevalence and risk factors of severe postpartum hemorrhage: a retrospective cohort study', *BMC Pregnancy and Childbirth*. BioMed Central, 21(1). doi: 10.1186/S12884-021-03818-1.

Liu, X., Song, Y., Guo, Z., Sun, W. and Liu, J. (2019) 'A comprehensive profile and inter-individual variations analysis of the human normal amniotic fluid proteome', *Journal of Proteomics*, 192, pp. 1–9. doi: 10.1016/J.JPROT.2018.04.023.

Livak, K. J. and Schmittgen, T. D. (2001) 'Analysis of relative gene expression data using real-time quantitative PCR and the 2-ΔΔCT method', *Methods*. Academic Press Inc., 25(4), pp. 402–408. doi: 10.1006/meth.2001.1262.

Livingstone, M. and Fraser, I. S. (2002) 'Mechanisms of abnormal uterine bleeding', *Human*

Reproduction Update. Oxford Academic, 8(1), pp. 60–67. doi: 10.1093/HUMUPD/8.1.60.

Löhn, M., Jessner, W., Fürstenau, M., Wellner, M., Sorrentino, V., Haller, H., Luft, F. C., Gollasch, M., Löhn, M., Jessner, W., *et al.* (2001) 'Regulation of calcium sparks and spontaneous transient outward currents by RyR3 in arterial vascular smooth muscle cells', *Circulation Research*. Lippincott Williams & Wilkins, 89(11), pp. 1051–1057. doi: 10.1161/hh2301.100250.

Long, W. N. (1990) 'Abnormal Vaginal Bleeding', in Walker HK, Hall WD, and Hurst JW (eds) *Clinical Methods: The History, Physical, and Laboratory Examinations*. 3rd edn. Boston: Butterworths. Available at: https://www.ncbi.nlm.nih.gov/books/NBK282/ (Accessed: 7 March 2023).

López Bernal, A. (2003) 'Mechanisms of labour - Biochemical aspects', in *BJOG: An International Journal of Obstetrics and Gynaecology*. doi: 10.1016/S1470-0328(03)00023-5.

Lopez, J. R., Uryash, A., Faury, G., Estève, E. and Adams, J. A. (2020) 'Contribution of Trpc channels to intracellular Ca2 + dyshomeostasis in smooth muscle from mdx mice', *Frontiers in Physiology*. Frontiers Media S.A., 11. doi: 10.3389/fphys.2020.00126.

Lopez, R. J., Byrne, S., Vukcevic, M., Sekulic-Jablanovic, M., Xu, L., Brink, M., Alamelu, J., Voermans, N., Snoeck, M., Clement, E., *et al.* (2016) 'An RYR1 mutation associated with malignant hyperthermia is also associated with bleeding abnormalities', *Science Signaling*. doi: 10.1126/scisignal.aad9813.

Lorca, R. A., Prabagaran, M., England, S. K. and Khan, R. N. (2014) 'Functional insights into modulation of BKCa channel activity to alter myometrial contractility', *Frontiers in Physiology*. doi: 10.3389/fphys.2014.00289.

Love, M. I., Huber, W. and Anders, S. (2014) 'Moderated estimation of fold change and dispersion for RNA-seq data with DESeq2', *Genome Biology*. BioMed Central Ltd., 15(12), pp. 1–21. doi: 10.1186/S13059-014-0550-8/FIGURES/9.

Luo, Y., Hitz, B. C., Gabdank, I., Hilton, J. A., Kagda, M. S., Lam, B., Myers, Z., Sud, P., Jou, J., Lin, K., *et al.* (2020) 'New developments on the Encyclopedia of DNA Elements (ENCODE) data portal', 48(D1). doi: 10.1093/NAR/GKZ1062.

Lynn, Stephen and Gillespie, J. I. (1995) 'Basic properties of a novel ryanodine-sensitive, caffeine-insensitive calcium-induced calcium release mechanism in permeabilised human vascular smooth muscle cells', *FEBS Letters*, 367(1), pp. 23–27. doi: 10.1016/0014-5793(95)00499-Y.

Lynn, S, Morgan, J. M., Lamb, H. K., Meissner, G. and Gillespie, J. I. (1995) 'Isolation and partial cloning of ryanodine-sensitive Ca2+ release channel protein isoforms from human myometrial smooth muscle.', *FEBS letters*, 372(1), pp. 6–12. Available at: http://www.ncbi.nlm.nih.gov/pubmed/7556644 (Accessed: 15 February 2019).

Ma, G. T., Soloveva, V., Tzeng, S. J., Lowe, L. A., Pfendler, K. C., Iannaccone, P. M., Kuehn, M. R. and Linzer, D. I. H. (2001) 'Nodal regulates trophoblast differentiation and placental development', *Developmental Biology*, 236(1). doi: 10.1006/dbio.2001.0334.

MacCallum, D. E. and Hall, P. A. (2000) 'The biochemical characterization of the DNA binding activity of pKi67', *Journal of Pathology*, 191(3). doi: 10.1002/1096-9896(2000)9999:9999<::AID-PATH628>3.0.CO;2-J.

MacKenzie, A. E., Korneluk, R. G., Zorzato, F., Fujii, J., Phillips, M., Iles, D., Wieringa, B., Leblond, S., Bailly, J., Willard, H. F., Duff, C., Worton, R. G. and MacLennan, D. H. (1990) 'The human ryanodine receptor gene: Its mapping to 19q13.1, placement in a chromosome 19 linkage group, and exclusion as the gene causing myotonic dystrophy', *American Journal of Human Genetics*, 46(6), pp. 1082–1089.

MacMillan, D., Currie, S., McCarron, J. G., D, M., S, C. and JG, M. (2008) 'FK506-binding protein (FKBP12) regulates ryanodine receptor-evoked Ca2+ release in colonic but not aortic smooth muscle', *Cell Calcium*, 43(6), pp. 539–549. doi: 10.1016/J.CECA.2007.09.002.

Maggi, L., Scoto, M., Cirak, S., Robb, S. A., Klein, A., Lillis, S., Cullup, T., Feng, L., Manzur, A. Y., Sewry, C. A., Abbs, S., Jungbluth, H. and Muntoni, F. (2013) 'Congenital myopathies – Clinical features and frequency of individual subtypes diagnosed over a 5-year period in the United Kingdom', *Neuromuscular Disorders*. Elsevier, 23(3), pp. 195–205. doi: 10.1016/J.NMD.2013.01.004.

Magness, R. R. and Rosenfeld, C. R. (1986) 'Systemic and uterine responses to α-adrenergic stimulation in pregnant and nonpregnant ewes', *American Journal of Obstetrics and Gynecology*, 155(4). doi: 10.1016/S0002-9378(86)80047-3.

Main, D. M., Main, E. K. and Moore, D. H. (2000) 'The relationship between maternal age and uterine dysfunction: A continuous effect throughout reproductive life', *American Journal of Obstetrics and Gynecology*, 182(6). doi: 10.1067/mob.2000.106249.

Mancarella, S., Potireddy, S., Wang, Y., Gao, H., Gandhirajan, R. K., Autieri, M., Scalia, R., Cheng, Z., Wang, H., Madesh, M., Houser, S. R. and Gill, D. L. (2013) 'Targeted STIM deletion impairs calcium homeostasis, NFAT activation, and growth of smooth muscle', *The FASEB Journal*. John Wiley & Sons, Ltd, 27(3), pp. 893–906. doi: 10.1096/fj.12-215293.

Mandala, M. and Osol, G. (2011) 'Physiological Remodelling of the Maternal Uterine Circulation during Pregnancy', *Basic & Clinical Pharmacology & Toxicology*. John Wiley & Sons, Ltd, 110(1), pp. 12–18. doi: 10.1111/j.1742-7843.2011.00793.x.

Marino, M., Stoilova, T., Giorgi, C., Bachi, A., Cattaneo, A., Auricchio, A., Pinton, P. and Zito, E. (2014) 'SEPN1, an endoplasmic reticulum-localized selenoprotein linked to skeletal muscle pathology, counteracts hyperoxidation by means of redox-regulating SERCA2 pump activity', *Human Molecular Genetics*. Oxford University Press, 24(7), pp. 1843–1855. doi: 10.1093/hmg/ddu602.

Marks, A. R., Tempst, P., Hwang, K. S., Taubman, M. B., Inui, M., Chadwick, C., Fleischer, S. and Nadal-Ginard, B. (1989) 'Molecular cloning and characterization of the rynanodine receptor/junctional channel complex cDNA from skeletal muscle sarcoplasmic reticulum', *Proceedings of the National Academy of Sciences of the United States of America*, 86(22). doi: 10.1073/pnas.86.22.8683.

Marrelli, S. P., O'Neil, R. G., Brown, R. C. and Bryan, R. M. (2007) 'PLA2 and TRPV4

channels regulate endothelial calcium in cerebral arteries', *American Journal of Physiology - Heart and Circulatory Physiology*, 292(3). doi: 10.1152/ajpheart.01006.2006.

Marshall, S. A., Senadheera, S. N., Jelinic, M., O'Sullivan, K., Parry, L. J. and Tare, M. (2018) 'Relaxin deficiency leads to uterine artery dysfunction during pregnancy in mice', *Frontiers in Physiology*. Frontiers Media S.A., 9(MAR). doi: 10.3389/fphys.2018.00255.

Martín, A. S., Lee, M. Y., Williams, H. C., Mizuno, K., Lassègue, B. and Griendling, K. K. (2008) 'Dual regulation of cofilin activity by LIM kinase and slingshot-1L phosphatase controls platelet-derived growth factor-induced migration of human aortic smooth muscle cells', *Circulation Research*. Lippincott Williams & Wilkins, 102(4), pp. 432–438. doi: 10.1161/CIRCRESAHA.107.158923.

Martin, C., Chapman, K. E., Thornton, S. and Ashley, R. H. (1999) 'Changes in the expression of myometrial ryanodine receptor mRNAs during human pregnancy', *Biochimica et Biophysica Acta - Molecular Cell Research*. Elsevier, 1451(2–3), pp. 343–352. doi: 10.1016/S0167-4889(99)00104-4.

Martin, C., Hyvelin, J. M., Chapman, K. E., Marthan, R., Ashley, R. H. and Savineau, J. P. (1999) 'Pregnant rat myometrial cells show heterogeneous ryanodine- and caffeine-sensitive calcium stores', *American Journal of Physiology - Cell Physiology*. American Physiological Society, 277(2), pp. 243–252. doi: 10.1152/AJPCELL.1999.277.2.C243/ASSET/IMAGES/LARGE/ACEL00803006X.JPEG.

Martin, E., Dahan, D., Cardouat, G., Gillibert-Duplantier, J., Marthan, R., Savineau, J. P. and Ducret, T. (2012) 'Involvement of TRPV1 and TRPV4 channels in migration of rat pulmonary arterial smooth muscle cells', *Pflugers Archiv European Journal of Physiology*. Pflugers Arch, 464(3), pp. 261–272. doi: 10.1007/s00424-012-1136-5.

Martin, J. J., Ceuterick, C. and Van Goethem, G. (1997) 'On a dominantly inherited myopathy with tubular aggregates', *Neuromuscular Disorders*. Elsevier, 7(8), pp. 512–520. doi: 10.1016/S0960-8966(97)00119-3.

Masters, J. G., Neal, D. E. and Gillespie, J. I. (1999) 'The contribution of intracellular Ca2+ release to contraction in human bladder smooth muscle', *British Journal of Pharmacology*. doi: 10.1038/sj.bjp.0702640.

Matsuki, K., Takemoto, M., Suzuki, Y., Yamamura, H., Ohya, S., Takeshima, H. and Imaizumi, Y. (2017) 'Ryanodine receptor type 3 does not contribute to contractions in the mouse myometrium regardless of pregnancy', *Pflugers Archiv European Journal of Physiology*. Springer Berlin Heidelberg, 469(2), pp. 313–326. doi: 10.1007/s00424-016-1900-z.

Matsumoto, M., Tsuchiya, K. J., Yaguchi, C., Horikoshi, Y., Furuta-Isomura, N., Oda, T., Kohmura-Kobayashi, Y., Tamura, N., Uchida, T. and Itoh, H. (2020) 'The fetal/placental weight ratio is associated with the incidence of atopic dermatitis in female infants during the first 14 months: The Hamamatsu Birth Cohort for Mothers and Children (HBC Study)', *International Journal of Women's Dermatology*, 6(3), pp. 176–181. doi: 10.1016/J.IJWD.2020.02.009.

Matsumura, C. Y., Taniguti, A. P. T., Pertille, A., Neto, H. S. and Marques, M. J. (2011) 'Stretch-activated calcium channel protein TRPC1 is correlated with the different degrees of the dystrophic phenotype in mdx mice', *American Journal of Physiology - Cell Physiology*, 301(6). doi: 10.1152/ajpcell.00056.2011.

Mayans, O., Van Der Ven, P. F. M., Wilm, M., Mues, A., Young, P., Fürst, D. O., Wilmanns, M. and Gautel, M. (1998) 'Structural basis for activation of the titin kinase domain during myofibrillogenesis', *Nature*. Nature, 395(6705), pp. 863–869. doi: 10.1038/27603.

Maybin, J. A. and Critchley, H. O. D. (2015) 'Menstrual physiology: Implications for endometrial pathology and beyond', *Human Reproduction Update*, 21(6). doi: 10.1093/humupd/dmv038.

Maybin, J. A., Critchley, H. O. D. and Jabbour, H. N. (2011) 'Inflammatory pathways in endometrial disorders', *Molecular and Cellular Endocrinology*. doi: 10.1016/j.mce.2010.08.006.

Maybin, J. and Critchley, H. (2009) 'Repair and regeneration of the human endometrium', *Expert Review of Obstetrics and Gynecology*. doi: 10.1586/eog.09.6.

McCallum, L. A., Greenwood, I. A. and Tribe, R. M. (2009) 'Expression and function of Kv7 channels in murine myometrium throughout oestrous cycle', *Pflugers Archiv European Journal of Physiology*. Springer, 457(5), pp. 1111–1120. doi: 10.1007/s00424-008-0567-5.

McCallum, L. A., Patel, R., Weidmann, H., Kadri, A., Greenwood, I. A. and Tribe., R. M. (2011) 'Functional effect of a novel BKCa channel opener (NS11021) on non-pregnant and pregnant mouse myometrium', *Reproductive Sciences*.

McCobb, D. P., Fowler, N. L., Featherstone, T., Lingle, C. J., Saito, M., Krause, J. E. and Salkoff, L. (1995) 'A human calcium-activated potassium channel gene expressed in vascular smooth muscle', *The American Journal of Physiology*, 269(3 Pt 2). doi: 10.1152/AJPHEART.1995.269.3.H767.

McLellan, A. S., Fischer, B., Dveksler, G., Hori, T., Wynne, F., Ball, M., Okumura, K., Moore, T. and Zimmermann, W. (2005) 'Structure and evolution of the mouse pregnancy-specific glycoprotein (Psg) gene locus', *BMC Genomics*. BioMed Central, 6, p. 4. doi: 10.1186/1471-2164-6-4.

McPherson, G. A. (1992) 'Assessing vascular reactivity of arteries in the small vessel myograph', *Clinical and Experimental Pharmacology and Physiology*. John Wiley & Sons, Ltd, 19(12), pp. 815–825. doi: 10.1111/J.1440-1681.1992.TB00420.X.

Meng, L.-B., Shan, M.-J., Qiu, Y., Qi, R., Yu, Z.-M., Guo, P., Di, C.-Y. and Gong, T. (2019) 'TPM2 as a potential predictive biomarker for atherosclerosis', *Aging (Albany NY)*. Impact Journals, LLC, 11(17), p. 6960. doi: 10.18632/AGING.102231.

Mesiano, S., DeFranco, E. and Muglia, L. J. (2015) 'Parturition', in *Knobil and Neill's Physiology of Reproduction: Two-Volume Set*. doi: 10.1016/B978-0-12-397175-3.00042-9.

Mi, H. and Thomas, P. (2009) 'PANTHER Pathway: an ontology-based pathway database

coupled with dataanalysis tools', *Methods in molecular biology (Clifton, N.J.)*. NIH Public Access, 563, p. 123. doi: 10.1007/978-1-60761-175-2_7.

Michelucci, A., García-Castañeda, M., Boncompagni, S. and Dirksen, R. T. (2018) 'Role of STIM1/ORAI1-mediated store-operated Ca2+ entry in skeletal muscle physiology and disease', *Cell Calcium*. Elsevier Ltd, pp. 101–115. doi: 10.1016/j.ceca.2018.10.004.

Miller, D. M., Daly, C., Aboelsaod, E. M., Gardner, L., Hobson, S. J., Riasat, K., Shepherd, S., Robinson, R. L., Bilmen, J. G., Gupta, P. K., Shaw, M. A. and Hopkins, P. M. (2018) 'Genetic epidemiology of malignant hyperthermia in the UK', *BJA: British Journal of Anaesthesia*. Elsevier, 121(4), p. 944. doi: 10.1016/J.BJA.2018.06.028.

Miller, H. E. and Ansari, J. R. (2022) 'Uterine atony', *Current Opinion in Obstetrics and Gynecology*. Lippincott Williams and Wilkins, 34(2), pp. 82–89. doi: 10.1097/GCO.0000000000000776.

Mironneau, J., Macrez, N., Morel, J. L., Sorrentino, V. and Mironneau, C. (2002) 'Identification and function of ryanodine receptor subtype 3 in non-pregnant mouse myometrial cells', *The Journal of Physiology*. Wiley-Blackwell, 538(Pt 3), p. 707. doi: 10.1113/JPHYSIOL.2001.013046.

Misceo, D., Holmgren, A., Louch, W. E., Holme, P. A., Mizobuchi, M., Morales, R. J., De Paula, A. M., Stray-Pedersen, A., Lyle, R., Dalhus, B., Christensen, G., Stormorken, H., Tjønnfjord, G. E. and Frengen, E. (2014) 'A Dominant STIM1 Mutation Causes Stormorken Syndrome', *Human Mutation*. Wiley-Liss Inc., 35(5), pp. 556–564. doi: 10.1002/humu.22544.

Mistry, H. D., Broughton Pipkin, F., Redman, C. W. G. and Poston, L. (2012) 'Selenium in reproductive health', *American Journal of Obstetrics and Gynecology*. doi: 10.1016/j.ajog.2011.07.034.

Mitchell, B. F. and Taggart, M. J. (2009) 'Are animal models relevant to key aspects of human parturition?', *American Journal of Physiology. Regulatory, Integrative and Comparative Physiology*, 297(3). doi: 10.1152/AJPREGU.00153.2009.

Mitchell, E., Taylor, D., Woods, K., Davis, M., Nelson, A., Teasdale, R., Grimmond, S., Little, M., Bertram, J. and Caruana, G. (2006) 'Differential gene expression in the developing mouse ureter', *Gene Expression Patterns*, 6(5), pp. 519–538. doi: 10.1016/J.MODGEP.2005.10.008.

Miyatake, R., Furukawa, A., Matsushita, M., Iwahashi, K., Nakamura, K., Ichikawa, Y. and Suwaki, H. (1996) 'Tissue-specific alternative splicing of mouse brain type ryanodine receptor/calcium release channel mRNA', *FEBS Letters*. Elsevier B.V., 395(2–3), pp. 123–126. doi: 10.1016/0014-5793(96)01022-8.

Moghadaszadeh, B., Petit, N., Jaillard, C., Brockington, M., Roy, S. Q., Merlini, L., Romero, N., Estournet, B., Desguerre, I., Chaigne, D., Muntoni, F., Topaloglu, H. and Guicheney, P. (2001) 'Mutations in SEPN1 cause congenital muscular dystrophy with spinal rigidity and restrictive respiratory syndrome', *Nature Genetics*. Presse Dienstleistungsgesellschaft mbH und Co. KG, 29(1), pp. 17–18. doi: 10.1038/ng713.

Mogren, I., Stenlund, H. and Högberg, U. (1999) 'Recurrence of prolonged pregnancy',

International Journal of Epidemiology, 28(2), pp. 253–257. doi: 10.1093/IJE/28.2.253.

Moll, W. (2003) 'Structure adaptation and blood flow control in the uterine arterial system after hemochorial placentation.', *European Journal of Obstetrics, Gynecology, and Reproductive Biology*, 110, pp. S19-27. doi: 10.1016/s0301-2115(03)00169-6.

Mombouli, J. V. and Vanhoutte, P. M. (1999) 'Endothelial dysfunction: from physiology to therapy', *Journal of Molecular and Cellular Cardiology*, 31(1), pp. 61–74. doi: 10.1006/JMCC.1998.0844.

Mondal, A. and Jin, J. P. (2016) 'Protein structure-function relationship at work: Learning from myopathy mutations of the slow skeletal muscle isoform of troponin T', *Frontiers in Physiology*. Frontiers Research Foundation, p. 449. doi: 10.3389/fphys.2016.00449.

Monnier, N., Kozak-Ribbens, G., Krivosic-Horber, R., Nivoche, Y., Qi, D., Kraev, N., Loke, J., Sharma, P., Tegazzin, V., Figarella-Branger, D., *et al.* (2005) 'Correlations between genotype and pharmacological, histological, functional, and clinical phenotypes in malignant hyperthermia susceptibility', *Human Mutation*. doi: 10.1002/humu.20231.

Monnier, N., Krivosic-Horber, R., Payen, J. F., Kozak-Ribbens, G., Nivoche, Y., Adnet, P., Reyford, H. and Lunardi, J. (2002) 'Presence of two different genetic traits in malignant hyperthermia families: implication for genetic analysis, diagnosis, and incidence of malignant hyperthermia susceptibility', *Anesthesiology*, 97(5), pp. 1067–1074. doi: 10.1097/00000542-200211000-00007.

Moran, C. M., Garriock, R. J., Miller, M. K., Heimark, R. L., Gregorio, C. C. and Krieg, P. A. (2008) 'Expression of the fast twitch troponin complex, fTnT, fTnI and fTnC, in vascular smooth muscle', *Cell Motility and the Cytoskeleton*. NIH Public Access, 65(8), pp. 652–661. doi: 10.1002/cm.20291.

Moreau, R., Daoud, G., Bernatchez, R., Simoneau, L., Masse, A. and Lafond, J. (2002) 'Calcium uptake and calcium transporter expression by trophoblast cells from human term placenta', *Biochimica et Biophysica Acta - Biomembranes*, 1564(2). doi: 10.1016/S0005-2736(02)00466-2.

Moreau, R., Hamel, A., Daoud, G., Simoneau, L. and Lafond, J. (2002) 'Expression of calcium channels along the differentiation of cultured trophoblast cells from human term placenta', *Biology of Reproduction*, 67(5). doi: 10.1095/biolreprod.102.005397.

Morgan, J. M. and Gillespie, J. I. (1995) 'The modulation and characterisation of the Ca2+-induced Ca2+ release mechanism in cultured human myometrial smooth muscle cells', *FEBS Letters*, 369(2–3), pp. 295–300. doi: 10.1016/0014-5793(95)00771-Z.

Mousa, H. A., Blum, J., Abou El Senoun, G., Shakur, H. and Alfirevic, Z. (2014) 'Treatment for primary postpartum haemorrhage', *The Cochrane database of systematic reviews*. Cochrane Database Syst Rev, 2014(2). doi: 10.1002/14651858.CD003249.PUB3.

Muehlschlegel, S., Rordorf, G. and Sims, J. (2011) 'Effects of a single dose of dantrolene in patients with cerebral vasospasm after subarachnoid hemorrhage: A prospective pilot study', *Stroke*. Lippincott Williams & WilkinsHagerstown, MD, 42(5), pp. 1301–1306. doi:

10.1161/STROKEAHA.110.603159.

Mueller, O., Lightfoot, S. and Schroeder, A. (2016) *RNA Integrity Number (RIN)-Standardization of RNA Quality Control Application*. Available at: https://www.agilent.com/cs/library/applications/5989-1165EN.pdf (Accessed: 18 July 2022).

Müller, H. D., Vielhaber, S., Brunn, A. and Schröder, M. J. (2001) 'Dominantly inherited myopathy with novel tubular aggregates containing 1-21 tubolofilamentous structures', *Acta Neuropathologica*. Springer Verlag, 102(1), pp. 27–35. doi: 10.1007/s004010000342.

Mulvany, M. J. and Aalkjaer, C. (1990) 'Structure and function of small arteries', *Physiological Reviews*, pp. 921–961. doi: 10.1152/physrev.1990.70.4.921.

Mulvany, M. J. and Halpern, W. (1977) 'Contractile Properties of Small Arterial Resistance Vessels in Spontaneously Hypertensive and Normotensive Rats', *Circulation Research*, 41(1), pp. 19–26. doi: 10.1161/01.RES.41.1.19.

Münch, G., Bölck, B., Sugaru, A., Brixius, K., Bloch, W. and Schwinger, R. H. G. (2001) 'Increased expression of isoform 1 of the sarcoplasmic reticulum Ca2+-release channel in failing human heart', *Circulation*. Lippincott Williams & Wilkins, 103(22), pp. 2739–2744. doi: 10.1161/01.CIR.103.22.2739.

Munro, M. G., Critchley, H. O. D. and Fraser, I. S. (2019) 'Corrigendum to "The two FIGO systems for normal and abnormal uterine bleeding symptoms and classification of causes of abnormal uterine bleeding in the reproductive years: 2018 revisions" [Int J Gynecol Obstet 143(2018) 393–408.]', *International Journal of Gynecology & Obstetrics*. John Wiley & Sons, Ltd, 144(2), pp. 237–237. doi: 10.1002/IJGO.12709.

Munro, M. G., Critchley, H. O. D., Fraser, I. S., Haththotuwa, R., Kriplani, A., Bahamondes, L., Füchtner, C., Tonye, R., Archer, D., Abbott, J., *et al.* (2018) 'The two FIGO systems for normal and abnormal uterine bleeding symptoms and classification of causes of abnormal uterine bleeding in the reproductive years: 2018 revisions', *International Journal of Gynecology & Obstetrics*. John Wiley & Sons, Ltd, 143(3), pp. 393–408. doi: 10.1002/IJGO.12666.

Murray, S. A., Morgan, J. L., Kane, C., Sharma, Y., Heffner, C. S., Lake, J. and Donahue, L. R. (2010) 'Mouse gestation length is genetically determined', *PLoS ONE*. PLOS, 5(8). doi: 10.1371/JOURNAL.PONE.0012418.

Murtazina, D. A., Chung, D., Ulloa, A., Bryan, E., Galan, H. L. and Sanborn, B. M. (2011) 'TRPC1, STIM1, and ORAI influence signal-regulated intracellular and endoplasmic reticulum calcium dynamics in human myometrial cells.', *Biology of reproduction*. Oxford University Press, 85(2), pp. 315–26. doi: 10.1095/biolreprod.111.091082.

Nagai, A., Takebe, K., Nio-Kobayashi, J., Takahashi-Iwanaga, H. and Iwanaga, T. (2010) 'Cellular Expression of the Monocarboxylate Transporter (MCT) Family in the Placenta of Mice', *Placenta*. W.B. Saunders, 31(2), pp. 126–133. doi: 10.1016/J.PLACENTA.2009.11.013.

Nagar, D., Liu, X. T. and Rosenfeld, C. R. (2005) 'Estrogen regulates β1-subunit expression

in Ca 2+-activated K+ channels in arteries from reproductive tissues', *American Journal of Physiology - Heart and Circulatory Physiology*, 289(4 58-4). doi: 10.1152/ajpheart.01174.2004.

Nakai, J., Imagawa, T., Hakamata, Y., Shigekawa, M., Takeshima, H. and Numa, S. (1990) 'Primary structure and functional expression from cDN A of the cardiac ryanodine receptor/calcium release channel', *FEBS Letters*, 271(1–2). doi: 10.1016/0014-5793(90)80399-4.

Nakai, J., Ogura, T., Protasi, F., Franzini-Armstrong, C., Allen, P. D. and Beam, K. G. (1997) 'Functional nonequality of the cardiac and skeletal ryanodine receptors', *Proceedings of the National Academy of Sciences of the United States of America*, 94(3). doi: 10.1073/pnas.94.3.1019.

National Health Service (2021) *Overview - Heavy periods*. Available at: https://www.nhs.uk/conditions/heavy-periods/ (Accessed: 12 July 2022).

National Institute for Health and Care Excellence (NICE) (2023) *Dantrolene sodium: BNF, NICE, British National Formulary (BNF)*. Available at: https://bnf.nice.org.uk/drugs/dantrolene-sodium/ (Accessed: 13 February 2023).

National Institute for Health and Excellence (UK) (2021) *Heavy menstrual bleeding: assessment and management*, *Heavy menstrual bleeding (update). NICE guideline No.88*. National Institute for Health and Care Excellence (NICE). Available at: https://www.ncbi.nlm.nih.gov/books/NBK493300/ (Accessed: 8 March 2023).

National Institutes of Health (NIH) Office on Women's Health (OWH) (2018) *Labor and Birth , Maternal Morbidity & Mortality Web Portal*. Available at: https://orwh.od.nih.gov/research/maternal-morbidity-and-mortality/information-for-women/labor-and-birth (Accessed: 8 March 2023).

Negishi, Y., Ichikawa, T., Takeshita, T. and Takahashi, H. (2018) 'Miscarriage induced by adoptive transfer of dendritic cells and invariant natural killer T cells into mice', *European journal of immunology*. Eur J Immunol, 48(6), pp. 937–949. doi: 10.1002/EJI.201747162.

Neilson, J. P. (2000) 'Ultrasound for fetal assessment in early pregnancy', *The Cochrane database of systematic reviews*. Cochrane Database Syst Rev, (2). doi: 10.1002/14651858.CD000182.

Nelson, M. T., Cheng, H., Rubart, M., Santana, L. F., Bonev, A. D., Knot, H. J. and Lederer, W. J. (1995) 'Relaxation of arterial smooth muscle by calcium sparks', *Science*. doi: 10.1126/science.270.5236.633.

Neylon, C. B., Richards, S. M., Larsen, M. A., Agrotis, A. and Bobik, A. (1995) 'Multiple types of ryanodine receptor/Ca2+ release channels are expressed in vascular smooth muscle', *Biochemical and Biophysical Research Communications*, 215(3), pp. 814–821. doi: 10.1006/bbrc.1995.2536.

Ng, L. C., Airey, J. A. and Hume, J. R. (2010) 'The contribution of TRPC1 and STIM1 to capacitative Ca2+ entry in pulmonary artery', in *Advances in Experimental Medicine and*

Biology. Adv Exp Med Biol, pp. 123–135. doi: 10.1007/978-1-60761-500-2_8.

Nicolaides, K. H., Wright, D., Syngelaki, A., Wright, A. and Akolekar, R. (2018) 'Fetal Medicine Foundation fetal and neonatal population weight charts', *Ultrasound in Obstetrics & Gynecology*, 52(1), pp. 44–51. doi: 10.1002/UOG.19073.

Nidhi, R., Padmalatha, V., Nagarathna, R. and Amritanshu, R. (2011) 'Prevalence of Polycystic Ovarian Syndrome in Indian Adolescents', *Journal of Pediatric and Adolescent Gynecology*, 24(4). doi: 10.1016/j.jpag.2011.03.002.

Nilipour, Y., Nafissi, S., Tjust, A. E., Ravenscroft, G., Hossein Nejad Nedai, H., Taylor, R. L., Varasteh, V., Pedrosa Domellöf, F., Zangi, M., Tonekaboni, S. H., *et al.* (2018) 'Ryanodine receptor type 3 (RYR3) as a novel gene associated with a myopathy with nemaline bodies', *European Journal of Neurology*. Blackwell Publishing Ltd, 25(6), pp. 841–847. doi: 10.1111/ene.13607.

Nilsson, H. and Aalkjaer, C. (2003) 'Vasomotion: Mechanisms and Physiological Importance', *Molecular Interventions*. American Society for Pharmacology and Experimental Therapeutics, 3(2), p. 79. doi: 10.1124/MI.3.2.79.

Nimigean, C. M. and Magleby, K. L. (1999) 'The beta subunit increases the Ca2+ sensitivity of large conductance Ca2+-activated potassium channels by retaining the gating in the bursting states', *The Journal of general physiology*. J Gen Physiol, 113(3), pp. 425–439. doi: 10.1085/JGP.113.3.425.

Niu, L., Wang, J., Shen, F., Gao, J., Jiang, M. and Bai, G. (2022) 'Magnolol and honokiol target TRPC4 to regulate extracellular calcium influx and relax intestinal smooth muscle', *Journal of Ethnopharmacology*, 290. doi: 10.1016/j.jep.2022.115105.

Noble, K., Matthew, A., Burdyga, T. and Wray, S. (2009) 'A review of recent insights into the role of the sarcoplasmic reticulum and Ca entry in uterine smooth muscle', *European Journal of Obstetrics & Gynecology and Reproductive Biology*. Elsevier, 144, pp. S11–S19. doi: 10.1016/j.ejogrb.2009.02.010.

Norwitz, E. R., Robinson, J. N. and Challis, J. R. G. (1999) 'The control of labor', *New England Journal of Medicine*. Massachussetts Medical Society, pp. 660–666. doi: 10.1056/NEJM199908263410906.

Noury, J. B., Böhm, J., Peche, G. A., Guyant-Marechal, L., Bedat-Millet, A. L., Chiche, L., Carlier, R. Y., Malfatti, E., Romero, N. B. and Stojkovic, T. (2017) 'Tubular aggregate myopathy with features of Stormorken disease due to a new STIM1 mutation', *Neuromuscular Disorders*. Elsevier Ltd, 27(1), pp. 78–82. doi: 10.1016/j.nmd.2016.10.006.

Nyfløt, L. T., Sandven, I., Stray-Pedersen, B., Pettersen, S., Al-Zirqi, I., Rosenberg, M., Jacobsen, A. F. and Vangen, S. (2017) 'Risk factors for severe postpartum hemorrhage: a case-control study', *BMC pregnancy and childbirth*. BMC Pregnancy Childbirth, 17(1). doi: 10.1186/S12884-016-1217-0.

O' Donnell, A. M., Nakamura, H. and Puri, P. (2019) 'Altered ryanodine receptor gene expression in Hirschsprung's disease', *Pediatric surgery international*. Pediatr Surg Int, 35(9),

pp. 923–927. doi: 10.1007/S00383-019-04504-2.

O'Connell, P. J., Klyachko, V. A. and Ahern, G. P. (2002) 'Identification of functional type 1 ryanodine receptors in mouse dendritic cells', *FEBS Letters*, 512(1–3). doi: 10.1016/S0014-5793(01)03321-X.

O'Donovan, N., Fischer, A., Abdo, E. M., Simon, F., Peter, H. J., Gerber, H., Buergi, U. and Marti, U. (2002) 'Differential expression of IgG Fc binding protein (FcgammaBP) in human normal thyroid tissue, thyroid adenomas and thyroid carcinomas', *The Journal of endocrinology*. J Endocrinol, 174(3), pp. 517–524. doi: 10.1677/JOE.0.1740517.

Ockeloen, C. W., Gilhuis, H. J., Pfundt, R., Kamsteeg, E. J., Agrawal, P. B., Beggs, A. H., Dara Hama-Amin, A., Diekstra, A., Knoers, N. V. A. M., Lammens, M. and van Alfen, N. (2012) 'Congenital myopathy caused by a novel missense mutation in the CFL2 gene', *Neuromuscular Disorders*. Elsevier, 22(7), pp. 632–639. doi: 10.1016/j.nmd.2012.03.008.

Oehler, M. K. and Rees, M. C. P. (2003) 'Menorrhagia: An update', *Acta Obstetricia et Gynecologica Scandinavica*. doi: 10.1034/j.1600-0412.2003.00097.x.

Ogawa, S. K., Shin, M. C., Hirashima, M., Akaike, N. and Ito, Y. (2013) 'Effects of selenoprotein P on the contraction and relaxation of the airway smooth muscle.', *General Physiology and Biophysics*, 32(1), pp. 47–54. doi: 10.4149/gpb_2013012.

Ohta, T., Kawai, K., Ito, S. and Nakazato, Y. (1995) 'Ca2+ entry activated by emptying of intracellular Ca2+ stores in ileal smooth muscle of the rat', *British Journal of Pharmacology*. John Wiley & Sons, Ltd, 114(6), pp. 1165–1170. doi: 10.1111/j.1476-5381.1995.tb13329.x.

Ong, H. L., Brereton, H. M., Harland, M. L. and Barritt, G. J. (2003) 'Evidence for the expression of transient receptor potential proteins in guinea pig airway smooth muscle cells', *Respirology*. Respirology, 8(1), pp. 23–32. doi: 10.1046/j.1440-1843.2003.00424.x.

Orchard, S., Ammari, M., Aranda, B., Breuza, L., Briganti, L., Broackes-Carter, F., Campbell, N. H., Chavali, G., Chen, C., Del-Toro, N., *et al.* (2014) 'The MIntAct project - IntAct as a common curation platform for 11 molecular interaction databases', *Nucleic Acids Research*, 42(D1). doi: 10.1093/nar/gkt1115.

Orkin, S. H., Fisher, D. E., Ginsburg, D., Look, A. T., Lux, S. E. and Nathan, D. G. (2015) *Nathan and Oski's hematology and oncology of infancy and childhood, Inherited Bone Marrow Failure Syndromes Associated with Isolated Cytopenias*. 7th edn. Elsevier/Saunders. Available at: https://www.clinicalkey.com/#!/browse/book/3-s2.0-C20120011015 (Accessed: 15 March 2023).

Osol, G. and Cipolla, M. (1993) 'Interaction of myogenic and adrenergic mechanisms in isolated, pressurized uterine radial arteries from latepregnant and nonpregnant rats', *American Journal of Obstetrics and Gynecology*, 168(2). doi: 10.1016/0002-9378(93)90519-O.

Otsu, K., Khanna, V. K., Archibald, A. L. and MacLennan, D. H. (1991) 'Cosegregation of porcine malignant hyperthermia and a probable causal mutation in the skeletal muscle ryanodine receptor gene in backcross families', *Genomics*. doi: 10.1016/0888-7543(91)90083-Q.

Oyelese, Y. and Ananth, C. V. (2010) 'Postpartum hemorrhage: epidemiology, risk factors, and causes', *Clinical obstetrics and gynecology*. Clin Obstet Gynecol, 53(1), pp. 147–156. doi: 10.1097/GRF.0B013E3181CC406D.

Pacheco, L. D., Costantine, M. M. and Hankins, G. D. V. (2013) 'Physiologic Changes During Pregnancy', in *Clinical Pharmacology During Pregnancy*. doi: 10.1016/B978-0-12-386007-1.00002-7.

Palaia, I., Bellati, F., Calcagno, M., Musella, A., Perniola, G. and Panici, P. B. (2011) 'Invasive vulvar carcinoma and the question of the surgical margin', *International journal of gynaecology and obstetrics: the official organ of the International Federation of Gynaecology and Obstetrics*, 114(2), pp. 120–123. doi: 10.1016/J.IJGO.2011.02.012.

Palmer, S. K., Zamudio, S., Coffin, C., Parker, S., Stamm, E. and Moore, L. G. (1992) 'Quantitative estimation of human uterine artery blood flow and pelvic blood flow redistribution in pregnancy', *Obstetrics and Gynecology*, 80(6), pp. 1000–1006.

Pardi, G., Marconi, A. M. and Cetin, I. (2002) 'Placental-fetal Interrelationship in IUGR Fetuses—A Review', *Placenta*. W.B. Saunders, 23(SUPPL. 1), pp. S136–S141. doi: 10.1053/PLAC.2002.0802.

Paria, B. C., Zhao, X., Das, S. K., Dey, S. K. and Yoshinaga, K. (1999) 'Zonula Occludens-1 and E-cadherin Are Coordinately Expressed in the Mouse Uterus with the Initiation of Implantation and Decidualization', *Developmental Biology*. Academic Press, 208(2), pp. 488–501. doi: 10.1006/DBIO.1999.9206.

Parkington, H. C., Tonta, M. A., Brennecke, S. P. and Coleman, H. A. (1999) 'Contractile activity, membrane potential, and cytoplasmic calcium in human uterine smooth muscle in the third trimester of pregnancy and during labor', *American Journal of Obstetrics and Gynecology*. Mosby Inc., 181(6), pp. 1445–1451. doi: 10.1016/S0002-9378(99)70390-X.

Parkington, H. C., Tonta, M. A., Davies, N. K., Brennecke, S. P. and Coleman, H. A. (1999) 'Hyperpolarization and slowing of the rate of contraction in human uterus in pregnancy by prostaglandins E2 and F(2α): Involvement of the Na+ pump', *Journal of Physiology*. doi: 10.1111/j.1469-7793.1999.229af.x.

Parry, E., Shields, R. and Turnbull, A. C. (1970) 'Transit time in the small intestine in pregnancy', *BJOG: An International Journal of Obstetrics & Gynaecology*, 77(10). doi: 10.1111/j.1471-0528.1970.tb03423.x.

Patel, R. M. (2014) 'Functional and molecular characterisation of the uterus and cervix in a mouse model of reproductive ageing'. King's College London. Available at: https://ethos.bl.uk/OrderDetails.do?uin=uk.bl.ethos.676931 (Accessed: 27 November 2019).

Patel, R., Moffatt, J. D., Mourmoura, E., Demaison, L., Seed, P. T., Poston, L. and Tribe, R. M. (2017) 'Effect of reproductive ageing on pregnant mouse uterus and cervix', *The Journal of Physiology*. John Wiley & Sons, Ltd (10.1111), 595(6), pp. 2065–2084. doi: 10.1113/JP273350.

Perez-Garcia, V., Fineberg, E., Wilson, R., Murray, A., Mazzeo, C. I., Tudor, C., Sienerth, A.,

White, J. K., Tuck, E., Ryder, E. J., *et al.* (2018) 'Placentation defects are highly prevalent in embryonic lethal mouse mutants', *Nature 2018 555:7697*. Nature Publishing Group, 555(7697), pp. 463–468. doi: 10.1038/nature26002.

Pérez, G. J., Bonev, A. D., Patlak, J. B. and Nelson, M. T. (1999) 'Functional coupling of ryanodine receptors to KCa channels in smooth muscle cells from rat cerebral arteries.', *The Journal of general physiology*, 113(2), pp. 229–38. Available at: http://www.ncbi.nlm.nih.gov/pubmed/9925821 (Accessed: 5 February 2019).

Perlman, N. C. and Carusi, D. A. (2019) 'Retained placenta after vaginal delivery: risk factors and management', *International Journal of Women's Health*. Dove Press, 11, p. 527. doi: 10.2147/IJWH.S218933.

Petkov, G. V. and Boev, K. K. (1996) 'Cyclopiazonic acid-induced changes in contractile activity of smooth muscle strips isolated from cat and guinea-pig stomach', *European Journal of Pharmacology*. Elsevier, 318(1), pp. 109–115. doi: 10.1016/S0014-2999(96)00764-9.

Petry, C. J., Ong, K. K. and Dunger, D. B. (2007) 'Does the fetal genotype affect maternal physiology during pregnancy?', *Trends in Molecular Medicine*. Elsevier Current Trends, 13(10), pp. 414–421. doi: 10.1016/J.MOLMED.2007.07.007.

Petry, C. J., Sanz Marcos, N., Pimentel, G., Hayes, M. G., Nodzenski, M., Scholtens, D. M., Hughes, I. A., Acerini, C. L., Ong, K. K., Lowe, W. L. and Dunger, D. B. (2016) 'Associations between Fetal Imprinted Genes and Maternal Blood Pressure in Pregnancy', *Hypertension*. Lippincott Williams and Wilkins, 68(6), pp. 1459–1466. doi: 10.1161/HYPERTENSIONAHA.116.08261.

Philipp, C. S., Dilley, A., Miller, C. H., Evatt, B., Baranwal, A., Schwartz, R., Bachmann, G. and Saidi, P. (2003) 'Platelet functional defects in women with unexplained menorrhagia', *Journal of thrombosis and haemostasis : JTH*. J Thromb Haemost, 1(3), pp. 477–484. doi: 10.1046/J.1538-7836.2003.00061.X.

Philipp, C. S., Faiz, A., Bowling, N., Dilley, A., Michaels, L. A., Ayers, G., Miller, C. H., Bachmann, G., Evatt, B. and Saidi, P. (2005) 'Age and the prevalence of bleeding disorders in women with menorrhagia', *Obstetrics and Gynecology*, 105(1), pp. 61–66. Available at: https://journals.lww.com/greenjournal/Fulltext/2005/01000/Age_and_the_Prevalence_of_Ble eding_Disorders_in.12.aspx (Accessed: 23 February 2023).

Philipp, C. S., Faiz, A., Dowling, N. F., Beckman, M., Owens, S., Ayers, C. and Bachmann, G. (2008) 'Development of a screening tool for identifying women with menorrhagia for hemostatic evaluation', *American Journal of Obstetrics and Gynecology*. Mosby, 198(2), pp. 163.e1-163.e8. doi: 10.1016/J.AJOG.2007.08.070.

Philipp, C. S., Faiz, A., Heit, J. A., Kouides, P. A., Lukes, A., Stein, S. F., Byams, V., Miller, C. H. and Kulkarni, R. (2011) 'Evaluation of a screening tool for bleeding disorders in a US multisite cohort of women with menorrhagia', *American journal of obstetrics and gynecology*. NIH Public Access, 204(3), p. 209.e1. doi: 10.1016/J.AJOG.2010.10.897.

Phipps, K., Barker, D. J. P., Hales, C. N., Fall, C. H. D., Osmond, C. and Clark, P. M. S. (1993) 'Fetal growth and impaired glucose tolerance in men and women', *Diabetologia 1993 36:3*.

Springer, 36(3), pp. 225–228. doi: 10.1007/BF00399954.

Phupong, V., Dejthevaporn, T., Tanawattanacharoen, S., Manotaya, S., Tannirandorn, Y. and Charoenvidhya, D. (2003) 'Predicting the risk of preeclampsia and small for gestational age infants by uterine artery Doppler in low-risk women', *Archives of Gynecology and Obstetrics*, 268(3), pp. 158–161. doi: 10.1007/S00404-002-0361-0.

Plüger, S., Faulhaber, J., Fürstenau, M., Löhn, M., Waldschütz, R., Gollasch, M., Haller, H., Luft, F. C., Ehmke, H. and Pongs, O. (2000) 'Mice with disrupted BK channel beta1 subunit gene feature abnormal Ca(2+) spark/STOC coupling and elevated blood pressure.', *Circulation research*, 87(11). doi: 10.1161/01.res.87.11.e53.

Prefumo, F., Sebire, N. J. and Thilaganathan, B. (2004) 'Decreased endovascular trophoblast invasion in first trimester pregnancies with high-resistance uterine artery Doppler indices', *Human Reproduction*. Oxford University Press, 19(1), pp. 206–209. doi: 10.1093/humrep/deh037.

Prendiville W, E. D. (1989) 'Care during the third stage of labour', in Chambers I, E. M. K. M. (ed.) *Effective Care in Pregnancy and Childbirth*. Oxford: Oxford University Press, pp. 1145–1170. Available at: https://www.jameslindlibrary.org/chalmers-i-enkin-m-keirse-mjnc-1989/ (Accessed: 14 March 2023).

Prinz, G. and Diener, M. (2008) 'Characterization of ryanodine receptors in rat colonic epithelium', *Acta Physiologica*, 193(2). doi: 10.1111/j.1748-1716.2007.01802.x.

Priori, S. G., Napolitano, C., Memmi, M., Colombi, B., Drago, F., Gasparini, M., DeSimone, L., Coltorti, F., Bloise, R., Keegan, R., Cruz Filho, F. E. S., Vignati, G., Benatar, A. and DeLogu, A. (2002) 'Clinical and molecular characterization of patients with catecholaminergic polymorphic ventricular tachycardia', *Circulation*, 106(1), pp. 69–74. doi: 10.1161/01.CIR.0000020013.73106.D8.

Pritschow, B. W., Lange, T., Kasch, J., Kunert-Keil, C., Liedtke, W. and Brinkmeier, H. (2011) 'Functional TRPV4 channels are expressed in mouse skeletal muscle and can modulate resting Ca2+ influx and muscle fatigue', *Pflugers Archiv European Journal of Physiology*, 461(1), pp. 115–122. doi: 10.1007/s00424-010-0883-4.

Quane, K. A., Keating, K. E., Healy, J. ., Manning, B. M., Krivosic-Horber, R., Krivosic, I., Monnier, N., Lunardi, J. and McCarthy, T. V. (1994) 'Mutation screening of the RYR1 gene in malignant hyperthermia: detection of a novel Tyr to Ser mutation in a pedigree with associated central cores', *Genomics*. Academic Press, 23(1), pp. 236–239. doi: 10.1006/geno.1994.1483.

Radan, A. P., Baud, D., Favre, G., Papadia, A., Surbek, D., Baumann, M. and Raio, L. (2022) 'Low placental weight and altered metabolic scaling after severe acute respiratory syndrome coronavirus type 2 infection during pregnancy: a prospective multicentric study', *Clinical Microbiology and Infection*, 28(5). doi: 10.1016/j.cmi.2022.02.003.

Rai, A. and Cross, J. C. (2014) 'Development of the hemochorial maternal vascular spaces in the placenta through endothelial and vasculogenic mimicry', *Developmental Biology*. Academic Press, 387(2), pp. 131–141. doi: 10.1016/J.YDBIO.2014.01.015.

Ramathal, C. Y., Bagchi, I. C., Taylor, R. N. and Bagchi, M. K. (2010) 'ENDOMETRIAL DECIDUALIZATION: OF MICE AND MEN', *Seminars in reproductive medicine*. NIH Public Access, 28(1), p. 17. doi: 10.1055/S-0029-1242989.

Ramírez-González, J. A., Vaamonde-Lemos, R., Cunha-Filho, J. S., Varghese, A. C. and Swanson, R. J. (2016) 'Overview of the female reproductive system', in *Exercise and Human Reproduction: Induced Fertility Disorders and Possible Therapies*. doi: 10.1007/978-1-4939-3402-7_2.

Rampazzo, A., Nava, A., Erne, P., Eberhard, M., Vian, E., Slomp, P., Tiso, N., Thiene, G. and Danieli, G. A. (1995) 'A new locus for arrhythmogenic right ventricular cardiomyopathy (ARVD2) maps to chromosome 1q42-q43.', *Human molecular genetics*, 4(11), pp. 2151–4. doi: 10.1093/hmg/4.11.2151.

Rasmussen, P. E. and Nielsen, F. R. (1988) 'Hydronephrosis during pregnancy: a literature survey', *European Journal of Obstetrics and Gynecology and Reproductive Biology*, 27(3). doi: 10.1016/0028-2243(88)90130-X.

Rattray, J., Ed RGN, C., Jones, M. C., Psychol, C., Dip Ed, R., Nbs, D. and E S M C, J. N. (2007) 'Essential elements of questionnaire design and development', *Journal of Clinical Nursing*. John Wiley & Sons, Ltd, 16(2), pp. 234–243. doi: 10.1111/J.1365-2702.2006.01573.X.

Ravenscroft, G., Wilmshurst, J. M., Pillay, K., Sivadorai, P., Wallefeld, W., Nowak, K. J. and Laing, N. G. (2011) 'A novel ACTA1 mutation resulting in a severe congenital myopathy with nemaline bodies, intranuclear rods and type I fibre predominance', *Neuromuscular Disorders*. Elsevier, 21(1), pp. 31–36. doi: 10.1016/J.NMD.2010.08.005.

Rebbeck, R. T., Karunasekara, Y., Board, P. G., Beard, N. A., Casarotto, M. G. and Dulhunty, A. F. (2014) 'Skeletal muscle excitation-contraction coupling: Who are the dancing partners?', *International Journal of Biochemistry and Cell Biology*. doi: 10.1016/j.biocel.2013.12.001.

Reed, B. G. and Carr, B. R. (2018) 'The Normal Menstrual Cycle and the Control of Ovulation', *Endotext*. MDText.com, Inc. Available at: https://www.ncbi.nlm.nih.gov/books/NBK279054/ (Accessed: 7 March 2023).

Rees, M. (1987) 'Menorrhagia', *British Medical Journal (Clinical research ed.)*, 294(6574). doi: 10.1136/bmj.294.6574.759.

Rendi, M. H., Muehlenbachs, A., Garcia, R. L. and Boyd, K. L. (2012) *Female Reproductive System*. First Edit, *Comparative Anatomy and Histology*. First Edit. Elsevier Inc. doi: 10.1016/B978-0-12-381361-9.00017-2.

Rennie, M. Y., Whiteley, K. J., Adamson, S. L. and Sled, J. G. (2016) 'Quantification of gestational changes in the uteroplacental vascular tree reveals vessel specific hemodynamic roles during pregnancy in mice', *Biology of Reproduction*. Society for the Study of Reproduction, 95(2), pp. 43–44. doi: 10.1095/biolreprod.116.140681.

Rfos, E. and Pizarro, G. (1991) *Voltage Sensor of Excitation-Contraction Coupling in Skeletal Muscle*, *PHYSIOLOGICAL REVIEWS*.

Riazi, S., Bersselaar, L. R. va. den, Islander, G., Heytens, L., Snoeck, M. M. J., Bjorksten, A., Gillies, R., Dranitsaris, G., Hellblom, A., Treves, S., Kunst, G., Voermans, N. C. and Jungbluth, H. (2022) 'Pre-operative exercise and pyrexia as modifying factors in malignant hyperthermia (MH)', *Neuromuscular Disorders*. Elsevier Ltd, 32(8), pp. 628–634. doi: 10.1016/j.nmd.2022.06.003.

Riley, P., Anson-Cartwright, L. and Cross, J. C. (1998) 'The Hand1 bHLH transcription factor is essential for placentation and cardiac morphogenesis', *Nature Genetics*, 18(3). doi: 10.1038/ng0398-271.

Risnes, K. R., Romundstad, P. R., Nilsen, T. I. L., Eskild, A. and Vatten, L. J. (2009) 'Placental weight relative to birth weight and long-term cardiovascular mortality: findings from a cohort of 31,307 men and women', *American journal of epidemiology*, 170(5), pp. 622–631. doi: 10.1093/AJE/KWP182.

RNA Sequencing | RNA-Seq methods & workflows (no date). Available at: https://emea.illumina.com/techniques/sequencing/rna-sequencing.html (Accessed: 1 March 2023).

Robinson, J. T., Thorvaldsdóttir, H., Turner, D. and Mesirov, J. P. (2020) 'igv.js: an embeddable JavaScript implementation of the Integrative Genomics Viewer (IGV)', *bioRxiv*.

Robinson, J. T., Thorvaldsdóttir, H., Wenger, A. M., Zehir, A. and Mesirov, J. P. (2017) 'Variant review with the integrative genomics viewer', *Cancer Research*. doi: 10.1158/0008-5472.CAN-17-0337.

Robinson, J. T., Thorvaldsdóttir, H., Winckler, W., Guttman, M., Lander, E. S., Getz, G. and Mesirov, J. P. (2011) 'Integrative genomics viewer', *Nature Biotechnology*. doi: 10.1038/nbt.1754.

Robinson, R., Carpenter, D., Shaw, M. A., Halsall, J. and Hopkins, P. (2006) 'Mutations in RYR1 in malignant hyperthermia and central core disease', *Human mutation*. Hum Mutat, 27(10), pp. 977–989. doi: 10.1002/HUMU.20356.

Robson, A., Harris, L. K., Innes, B. A., Lash, G. E., Aljunaidy, M. M., Aplin, J. D., Baker, P. N., Robson, S. C. and Bulmer, J. N. (2012) 'Uterine natural killer cells initiate spiral artery remodeling in human pregnancy', *The FASEB Journal*. John Wiley & Sons, Ltd, 26(12), pp. 4876–4885. doi: 10.1096/FJ.12-210310.

Rodchenkov, I., Babur, O., Luna, A., Aksoy, B. A., Wong, J. V., Fong, D., Franz, M., Siper, M. C., Cheung, M., Wrana, M., *et al.* (2020) 'Pathway Commons 2019 Update: integration, analysis and exploration of pathway data', *Nucleic Acids Research*. Oxford Academic, 48(D1), pp. D489–D497. doi: 10.1093/NAR/GKZ946.

Rode, B., Bailey, M. A., Marthan, R., Beech, D. J. and Guibert, C. (2018) 'ORAI channels as potential therapeutic targets in pulmonary hypertension', *Physiology*. doi: 10.1152/PHYSIOL.00016.2018.

Rodeghiero, F., Castaman, G. and Dini, E. (1987) 'Epidemiological investigations of the prevalence of von Willebrand's disease', *Blood*, 69(2). doi: 10.1182/blood.v69.2.454.454.

Rodeghiero, F., Castaman, G., Tosetto, A., Batlle, J., Baudo, F., Cappelletti, A., Casana, P., De Bosch, N., Eikenboom, J. C. J., Federici, A. B., Lethagen, S., Linari, S. and Srivastava, A. (2005) 'The discriminant power of bleeding history for the diagnosis of type 1 von Willebrand disease: an international, multicenter study', *Journal of Thrombosis and Haemostasis*, 3(12), pp. 2619–2626. doi: 10.1111/J.1538-7836.2005.01663.X.

Romero, N. B., Monnier, N., Viollet, L., Cortey, A., Chevallay, M., Leroy, J. P., Lunardi, J. and Fardeau, M. (2003) 'Dominant and recessive central core disease associated with RYR1 mutations and fetal akinesia', *Brain*. doi: 10.1093/brain/awg244.

Rosen, E. M., van 't Erve, T. J., Boss, J., Sathyanarayana, S., Barrett, E. S., Nguyen, R. H. N., Bush, N. R., Milne, G. L., McElrath, T. F., Swan, S. H. and Ferguson, K. K. (2019) 'Urinary oxidative stress biomarkers and accelerated time to spontaneous delivery', *Free radical biology & medicine*. NIH Public Access, 130, p. 419. doi: 10.1016/J.FREERADBIOMED.2018.11.011.

Rosenberg, H., Davis, M., James, D., Pollock, N. and Stowell, K. (2007) 'Malignant hyperthermia', *Orphanet Journal of Rare Diseases*, 2(1). doi: 10.1186/1750-1172-2-21.

Rosenfeld, C. R., Cornfield, D. N. and Roy, T. (2001) 'Ca2+-activated K+ channels modulate basal and E2β-induced rises in uterine blood flow in ovine pregnancy', *American Journal of Physiology - Heart and Circulatory Physiology*, 281(1 50-1). doi: 10.1152/ajpheart.2001.281.1.h422.

Rosenfeld, C. R., White, R. E., Roy, T. and Cox, B. E. (2000) 'Calcium-activated potassium channels and nitric oxide coregulate estrogen-induced vasodilation', *American journal of physiology. Heart and circulatory physiology*. Am J Physiol Heart Circ Physiol, 279(1). doi: 10.1152/AJPHEART.2000.279.1.H319.

Rosero, E. B., Adesanya, A. O., Timaran, C. H. and Joshi, G. P. (2009) 'Trends and outcomes of malignant hyperthermia in the United States, 2000 to 2005', *Anesthesiology*. Anesthesiology, 110(1), pp. 89–94. doi: 10.1097/ALN.0B013E318190BB08.

Ross, J. W., Ashworth, M. D., White, F. J., Johnson, G. A., Ayoubi, P. J., DeSilva, U., Whitworth, K. M., Prather, R. S. and Geisert, R. D. (2007) 'Premature estrogen exposure alters endometrial gene expression to disrupt pregnancy in the pig', *Endocrinology*, 148(10), pp. 4761–4773. doi: 10.1210/EN.2007-0599.

Rossant, J. and Cross, J. C. (2001) *Placental development: Lessons from mouse mutants*, *Nature Reviews Genetics*. Nature Publishing Group. doi: 10.1038/35080570.

Royal College of Obstetricians & Gynaecologists (RCOG) (2011) *Antepartum Haemorrhage (Green-top Guideline No. 63)*. Available at: https://www.rcog.org.uk/guidance/browse-all-guidance/green-top-guidelines/antepartum-haemorrhage-green-top-guideline-no-63/ (Accessed: 13 March 2023).

Rubler, S., Damani, P. M. and Pinto, E. R. (1977) 'Cardiac size and performance during pregnancy estimated with echocardiography', *The American Journal of Cardiology*, 40(4). doi: 10.1016/0002-9149(77)90068-6.

Rugh, R. (1968) *The mouse. Its reproduction and development.*, *The mouse. Its reproduction and development.* Minneapolis, Minn.: Burgess Publishing Co.

Sabouri, M., Momeni, M., Khorvash, F., Rezvani, M. and Tabesh, H. (2017) 'The effect of a single dose dantrolene in patients with vasospasm following aneurysmal subarachnoid hemorrhage', *Advanced Biomedical Research*. Wolters Kluwer -- Medknow Publications, 6, p. 83. doi: 10.4103/2277-9175.210660.

Sabourin, J., Lamiche, C., Vandebrouck, A., Magaud, C., Rivet, J., Cognard, C., Bourmeyster, N. and Constantin, B. (2009) 'Regulation of TRPC1 and TRPC4 cation channels requires an alpha1-syntrophin-dependent complex in skeletal mouse myotubes', *The Journal of Biological Chemistry*, 284(52), pp. 36248–36261. doi: 10.1074/JBC.M109.012872.

Sadler, J. E. (2003) 'Von Willebrand disease type 1: a diagnosis in search of a disease', *Blood*. Blood, 101(6), pp. 2089–2093. doi: 10.1182/BLOOD-2002-09-2892.

Sadler, J. E., Mannucci, P. M., Berntorp, E., Bochkov, N., Boulyjenkov, V., Ginsburg, D., Meyer, D., Peake, I., Rodeghiero, F. and Srivastava, A. (2000) 'Impact, diagnosis and treatment of von Willebrand disease', *Thrombosis and Haemostasis*. Schattauer GmbH, 84(2), pp. 160–174. doi: 10.1055/S-0037-1613992/ID/JR1613992-11.

Saito, M., Nelson, C., Salkoff, L. and Lingle, C. J. (1997) 'A cysteine-rich domain defined by a novel exon in a slo variant in rat adrenal chromaffin cells and PC12 cells', *The Journal of Biological Chemistry*, 272(18), pp. 11710–11717. doi: 10.1074/JBC.272.18.11710.

Saito, Y., Komaki, H., Hattori, A., Takeuchi, F., Sasaki, M., Kawabata, K., Mitsuhashi, S., Tominaga, K., Hayashi, Y. K., Nowak, K. J., Laing, N. G., Nonaka, I. and Nishino, I. (2011) 'Extramuscular manifestations in children with severe congenital myopathy due to ACTA1 gene mutations', *Neuromuscular Disorders*. Elsevier, 21(7), pp. 489–493. doi: 10.1016/J.NMD.2011.03.004.

Salas, M., John, R., Saxena, A., Barton, S., Frank, D., Fitzpatrick, G., Higgins, M. J. and Tycko, B. (2004) 'Placental growth retardation due to loss of imprinting of Phlda2', *Mechanisms of Development*, 121(10). doi: 10.1016/j.mod.2004.05.017.

Salavati, N., Gordijn, S. J., Sovio, U., Zill-E-Huma, R., Gebril, A., Charnock-Jones, D. S., Scherjon, S. A. and Smith, G. C. S. (2018) 'Birth weight to placenta weight ratio and its relationship to ultrasonic measurements, maternal and neonatal morbidity: A prospective cohort study of nulliparous women', *Placenta*, 63. doi: 10.1016/j.placenta.2017.11.008.

Salomone, S., Soydan, G., Moskowitz, M. A. and Sims, J. R. (2009) 'Inhibition of cerebral vasoconstriction by dantrolene and nimodipine', *Neurocritical Care*. Springer, 10(1), pp. 93–102. doi: 10.1007/s12028-008-9153-0.

Salviati, G., Pierobon-Bormioli, S., Betto, R., Damiani, E., Angelini, C., Ringel, S. P., Salvatori, S. and Margreth, A. (1985) 'Tubular aggregates: Sarcoplasmic reticulum origin, calcium storage ability, and functional implications', *Muscle & Nerve*. John Wiley & Sons, Ltd, 8(4), pp. 299–306. doi: 10.1002/mus.880080406.

Samani, R. O., Hashiani, A. A., Razavi, M., Vesali, S., Rezaeinejad, M., Maroufizadeh, S. and

Sepidarkish, M. (2018) 'The prevalence of menstrual disorders in Iran: A systematic review and meta-analysis', *International Journal of Reproductive Biomedicine*. Shahid Sadoughi University of Medical Sciences and Health Services, 16(11), p. 665. Available at: /pmc/articles/PMC6350848/ (Accessed: 17 March 2023).

Sambuughin, N., McWilliams, S., De Bantel, A., Sivakumar, K. and Nelson, T. E. (2001) 'Single-amino-acid deletion in the RYR1 gene, associated with malignant hyperthermia susceptibility and unusual contraction phenotype', *American Journal of Human Genetics*. doi: 10.1086/321270.

Sanborn, B. M. (2016) 'Relationship of Ion Channel Activity to Control of Myometrial Calcium', *Reproductive Sciences*. SAGE PublicationsSage CA: Thousand Oaks, CA, 7(1), pp. 4–11. doi: 10.1177/107155760000700103.

Sanders, K. M. (1996) 'A case for interstitial cells of Cajal as pacemakers and mediators of neurotransmission in the gastrointestinal tract', *Gastroenterology*, 111(2). doi: 10.1053/gast.1996.v111.pm8690216.

Santos, I. S., Minten, G. C., Valle, N. C. J., Tuerlinckx, G. C., Silva, A. B., Pereira, G. A. R. and Carriconde, J. F. (2011) 'Menstrual bleeding patterns: A community-based cross-sectional study among women aged 18-45 years in Southern Brazil', *BMC women's health*. BMC Womens Health, 11(1). doi: 10.1186/1472-6874-11-26.

Sarkar, A. A., Nuwayhid, S. J., Maynard, T., Ghandchi, F., Hill, J. T., Lamantia, A. S. and Zohn, I. E. (2014) 'Hectd1 is required for development of the junctional zone of the placenta', *Developmental Biology*. Dev Biol, 392(2), pp. 368–380. Available at: https://pubmed.ncbi.nlm.nih.gov/24855001/ (Accessed: 18 February 2023).

Sato, Y., Sakurai, K., Tanabe, H., Kato, T., Nakanishi, Y., Ohno, H. and Mori, C. (2019) 'Maternal gut microbiota is associated with newborn anthropometrics in a sex-specific manner', *Journal of Developmental Origins of Health and Disease*. Cambridge University Press, 10(6), pp. 659–666. doi: 10.1017/S2040174419000138.

Sauer, M. V. (2015) 'Reproduction at an advanced maternal age and maternal health', *Fertility and Sterility*. doi: 10.1016/j.fertnstert.2015.03.004.

Savineau, J. P. and Mironneau, J. (1990) 'Caffeine acting on pregnant rat myometrium: analysis of its relaxant action and its failure to release Ca2+ from intracellular stores.', *British Journal of Pharmacology*. Wiley-Blackwell, 99(2), p. 261. doi: 10.1111/J.1476-5381.1990.TB14691.X.

Sayers, E. W., Bolton, E. E., Brister, J. R., Canese, K., Chan, J., Comeau, D. C., Connor, R., Funk, K., Kelly, C., Kim, S., *et al.* (2022) 'Database resources of the national center for biotechnology information', *Nucleic Acids Research*, 50(D1). doi: 10.1093/nar/gkab1112.

Schaletzky, J., Dove, S. K., Short, B., Lorenzo, O., Clague, M. J. and Barr, F. A. (2003) 'Phosphatidylinositol-5-phosphate activation and conserved substrate specificity of the myotubularin Phosphatidylinositol 3-phosphatases', *Current Biology*, 13(6), pp. 504–509. doi: 10.1016/S0960-9822(03)00132-5.

Schartner, V., Romero, N. B., Donkervoort, S., Treves, S., Munot, P., Pierson, T. M., Dabaj, I., Malfatti, E., Zaharieva, I. T., Zorzato, F., *et al.* (2017) 'Dihydropyridine receptor (DHPR, CACNA1S) congenital myopathy', *Acta Neuropathologica*, 133(4). doi: 10.1007/s00401-016-1656-8.

Schmalenberger, K. M., Tauseef, H. A., Barone, J. C., Owens, S. A., Lieberman, L., Jarczok, M. N., Girdler, S. S., Kiesner, J., Ditzen, B. and Eisenlohr-Moul, T. A. (2021) 'How to study the menstrual cycle: Practical tools and recommendations', *Psychoneuroendocrinology*. NIH Public Access, 123, p. 104895. doi: 10.1016/J.PSYNEUEN.2020.104895.

Schmidt, K., Dubrovska, G., Nielsen, G., Fesüs, G., Uhrenholt, T. R., Hansen, P. B., Gudermann, T., Dietrich, A., Gollasch, M., De Wit, C. and Köhler, R. (2010) 'Amplification of EDHF-type vasodilatations in TRPC1-deficient mice', *British Journal of Pharmacology*. Br J Pharmacol, 161(8), pp. 1722–1733. doi: 10.1111/j.1476-5381.2010.00985.x.

Schneider, M. F. (1994) 'Control of Calcium Release in Functioning Skeletal Muscle Fibers', *Annual Review of Physiology*, 56(1), pp. 463–484. doi: 10.1146/annurev.ph.56.030194.002335.

Schoen, C. and Rosen, T. (2009) 'Maternal and perinatal risks for women over 44-A review', *Maturitas*. doi: 10.1016/j.maturitas.2009.08.012.

Schredelseker, J., Dayal, A., Schwerte, T., Franzini-Armstrong, C. and Grabner, M. (2009) 'Proper restoration of excitation-contraction coupling in the dihydropyridine receptor β 1-null zebrafish relaxed is an exclusive function of the β 1a subunit', *Journal of Biological Chemistry*, 284(2). doi: 10.1074/jbc.M807767200.

Sei, Y., Gallagher, K. L. and Basile, A. S. (1999) 'Skeletal muscle type ryanodine receptor is involved in calcium signaling in human B lymphocytes', *Journal of Biological Chemistry*, 274(9). doi: 10.1074/jbc.274.9.5995.

du Sert, N. P., Ahluwalia, A., Alam, S., Avey, M. T., Baker, M., Browne, W. J., Clark, A., Cuthill, I. C., Dirnagl, U., Emerson, M., *et al.* (2020) 'Reporting animal research: Explanation and elaboration for the arrive guidelines 2.0', *PLoS Biology*. doi: 10.1371/journal.pbio.3000411.

du Sert, N. P., Hurst, V., Ahluwalia, A., Alam, S., Avey, M. T., Baker, M., Browne, W. J., Clark, A., Cuthill, I. C., Dirnagl, U., *et al.* (2020) 'The arrive guidelines 2.0: Updated guidelines for reporting animal research', *PLoS Biology*, 18(7). doi: 10.1371/journal.pbio.3000410.

Shafiei, S. and Dufort, D. (2021) 'Maternal Cripto is critical for proper development of the mouse placenta and the placental vasculature', *Placenta*. W.B. Saunders, 107, pp. 13–23. doi: 10.1016/J.PLACENTA.2021.02.016.

Shankar, M., Lee, C. A., Sabin, C. A., Economides, D. L. and Kadir, R. A. (2004) 'Von Willebrand disease in women with menorrhagia: A systematic review', *BJOG: An International Journal of Obstetrics and Gynaecology*. doi: 10.1111/j.1471-0528.2004.00176.x.

Shapley, M., Jordan, K. and Croft, P. R. (2004) 'An epidemiological survey of symptoms of menstrual loss in the community', *The British Journal of General Practice*. Royal College of

General Practitioners, 54(502), p. 359. Available at: /pmc/articles/PMC1266170/ (Accessed: 8 March 2023).

Sharathkumar, A. A. and Shapiro, A. (2008) *Platelet function disorders.*

Shaw, R. W., Brickley, M. R., Evans, L. and Edwards, M. J. (1998) 'Perceptions of women on the impact of menorrhagia on their health using multi-attribute utility assessment', *BJOG: An International Journal of Obstetrics & Gynaecology.* John Wiley & Sons, Ltd, 105(11), pp. 1155–1159. doi: 10.1111/J.1471-0528.1998.TB09968.X.

Shi, J., Miralles, F., Birnbaumer, L., Large, W. A. and Albert, A. P. (2017) 'Store-operated interactions between plasmalemmal STIM1 and TRPC1 proteins stimulate PLCβ1 to induce TRPC1 channel activation in vascular smooth muscle cells', *Journal of Physiology.* Blackwell Publishing Ltd, 595(4), pp. 1039–1058. doi: 10.1113/JP273302.

Shime, J., Gare, D., Andrews, J. and Britt, B. (1988) 'Dantrolene in pregnancy: Lack of adverse effects on the fetus and newborn infant', *American Journal of Obstetrics and Gynecology.* Elsevier, 159(4), pp. 831–834. doi: 10.1016/S0002-9378(88)80147-9.

Shin, Y. K., Kim, Y. D., Collea, J. V. and Belcher, M. D. (1995) 'Effect of dantrolene sodium on contractility of isolated human uterine muscle', *International Journal of Obstetric Anesthesia*, 4(4), pp. 197–200. doi: 10.1016/0959-289X(95)82910-3.

Shivhare, S. B., Bulmer, J. N., Innes, B. A., Hapangama, D. K. and Lash, G. E. (2014) 'Altered vascular smooth muscle cell differentiation in the endometrial vasculature in menorrhagia', *Human Reproduction.* Oxford Academic, 29(9), pp. 1884–1894. doi: 10.1093/HUMREP/DEU164.

Shmigol, A. V., Eisner, D. A. and Wray, S. (1998) 'Properties of voltage-activated [Ca 2+](i) transients in single smooth muscle cells isolated from pregnant rat uterus', *Journal of Physiology.* doi: 10.1111/j.1469-7793.1998.803bg.x.

Shmygol, A., Gullam, J., Blanks, A. and Thornton, S. (2006) 'Multiple mechanisms involved in oxytocin-induced modulation of myometrial contractility', *Acta Pharmacologica Sinica.* doi: 10.1111/j.1745-7254.2006.00393.x.

Sidonio, R. F., Zia, A. and Fallaize, D. (2020) 'Potential Undiagnosed VWD Or Other Mucocutaneous Bleeding Disorder Cases Estimated From Private Medical Insurance Claims', *Journal of Blood Medicine.* Dove Press, 11, p. 1. doi: 10.2147/JBM.S224683.

Silver, R. M., Landon, M. B., Rouse, D. J., Leveno, K. J., Spong, C. Y., Thom, E. A., Moawad, A. H., Caritis, S. N., Harper, M., Wapner, R. J., *et al.* (2006) 'Maternal morbidity associated with multiple repeat cesarean deliveries', *Obstetrics and Gynecology*, 107(6), pp. 1226–1232. doi: 10.1097/01.AOG.0000219750.79480.84.

Simmons, D. G. and Cross, J. C. (2005) 'Determinants of trophoblast lineage and cell subtype specification in the mouse placenta', *Developmental Biology.* doi: 10.1016/j.ydbio.2005.05.010.

Simmons, D. G., Fortier, A. L. and Cross, J. C. (2007) 'Diverse subtypes and developmental

origins of trophoblast giant cells in the mouse placenta', *Developmental Biology*, 304(2). doi: 10.1016/j.ydbio.2007.01.009.

Simmons, D. G., Rawn, S., Davies, A., Hughes, M. and Cross, J. C. (2008) 'Spatial and temporal expression of the 23 murine Prolactin/Placental Lactogen-related genes is not associated with their position in the locus', *BMC Genomics*, 9. doi: 10.1186/1471-2164-9-352.

Singh, S., Bermudez-Contreras, E., Nazari, M., Sutherland, R. J. and Mohajerani, M. H. (2019) 'Low-cost solution for rodent home-cage behaviour monitoring', *PLOS ONE*. Public Library of Science, 14(8), p. e0220751. doi: 10.1371/JOURNAL.PONE.0220751.

Singh, V., Ram, M., Kandasamy, K., Thangamalai, R., Choudhary, S., Dash, J. R., Kumar, D., Parida, S., Singh, T. U. and Mishra, S. K. (2015) 'Molecular and functional characterization of TRPV4 channels in pregnant and nonpregnant mouse uterus', *Life Sciences*. Elsevier Inc., 122, pp. 51–58. doi: 10.1016/j.lfs.2014.12.010.

Siu, K. F., Cheung, H. C. and Wong, J. (1986) 'Shrinkage of the esophagus after resection for carcinoma', *Annals of Surgery*, 203(2), pp. 173–176. doi: 10.1097/00000658-198602000-00011.

Skarnes, R. C. and Harper, M. J. K. (1972) 'Relationship between endotoxin-induced abortion and the synthesis of prostaglandin F', *Prostaglandins*, 1(3), pp. 191–203. doi: 10.1016/0090-6980(72)90004-4.

Slater, D. M., Dennes, W. J. B., Campa, J. S., Poston, L. and Bennett, P. R. (1999) 'Expression of cyclo-oxygenase types-1 and -2 in human myometrium throughout pregnancy', *Molecular Human Reproduction*, 5(9), pp. 880–884. doi: 10.1093/molehr/5.9.880.

Smiesko, V. and Johnson, P. (1993) 'The arterial lumen is controlled by flow-related shear stress', *Physiology*, 8(1). doi: 10.1152/physiologyonline.1993.8.1.34.

Smith, G. C. S., Cordeaux, Y., White, I. R., Pasupathy, D., Missfelder-Lobos, H., Pell, J. P., Charnock-Jones, D. S. and Fleming, M. (2008) 'The effect of delaying childbirth on primary cesarean section rates', *PLoS Medicine*, 5(7). doi: 10.1371/journal.pmed.0050144.

Smith, R. (2007) 'Parturition', *New England Journal of Medicine*. Massachusetts Medical Society, 356(3), pp. 271–283. doi: 10.1056/NEJMRA061360.

Smith, R., Van Helden, D., Hirst, J., Zakar, T., Read, M., Chan, E. C., Palliser, H., Grammatopoulos, D., Nicholson, R. and Parkington, H. C. (2007) 'Pathological interactions with the timing of birth and uterine activation', *Australian and New Zealand Journal of Obstetrics and Gynaecology*. doi: 10.1111/j.1479-828X.2007.00775.x.

Snel, B., Lehmann, G., Bork, P. and Huynen, M. A. (2000) 'STRING: A web-server to retrieve and display the repeatedly occurring neighbourhood of a gene', *Nucleic Acids Research*, 28(18), pp. 3442–3444. doi: 10.1093/nar/28.18.3442.

Snoeck, M., van Engelen, B. G. M., Küsters, B., Lammens, M., Meijer, R., Molenaar, J. P. F., Raaphorst, J., Verschuuren-Bemelmans, C. C., Straathof, C. S. M., Sie, L. T. L., *et al.* (2015) 'RYR1-related myopathies: A wide spectrum of phenotypes throughout life', *European*

Journal of Neurology. Blackwell Publishing Ltd, 22(7), pp. 1094–1112. doi: 10.1111/ene.12713.

Soares, M. J. (2004) 'The prolactin and growth hormone families: Pregnancy-specific hormones/cytokines at the maternal-fetal interface', *Reproductive Biology and Endocrinology*. BioMed Central, 2(1), pp. 1–15. doi: 10.1186/1477-7827-2-51/TABLES/4.

Sobinoff, A. P., Beckett, E. L., Jarnicki, A. G., Sutherland, J. M., McCluskey, A., Hansbro, P. M. and McLaughlin, E. A. (2013) 'Scrambled and fried: Cigarette smoke exposure causes antral follicle destruction and oocyte dysfunction through oxidative stress', *Toxicology and Applied Pharmacology*, 271(2). doi: 10.1016/j.taap.2013.05.009.

Sokanovic, S. J., Constantin, S., Lamarca Dams, A., Mochimaru, Y., Smiljanic, K., Bjelobaba, I., Prévide, R. M. and Stojilkovic, S. S. (2023) 'Common and female-specific roles of protein tyrosine phosphatase receptors N and N2 in mice reproduction', *Scientific Reports 2023 13:1*. Nature Publishing Group, 13(1), pp. 1–16. doi: 10.1038/s41598-023-27497-4.

Somlyo, A. P. and Somlyo, A. V. (2003) 'Ca2+ sensitivity of smooth muscle and nonmuscle myosin II: Modulated by G proteins, kinases, and myosin phosphatase', *Physiological Reviews*. American Physiological Society, 83(4), pp. 1325–1358. doi: 10.1152/PHYSREV.00023.2003/ASSET/IMAGES/LARGE/9J0430273006.JPEG.

Song, M., Zhu, N., Olcese, R., Barila, B., Toro, L. and Stefani, E. (1999) 'Hormonal control of protein expression and mRNA levels of the MaxiK channel α subunit in myometrium', *FEBS Letters*, 460(3), pp. 427–432. doi: 10.1016/S0014-5793(99)01394-0.

Song, R., Hu, X. Q., Romero, M., Holguin, M. A., Kagabo, W., Xiao, D., Wilson, S. M. and Zhang, L. (2021) 'Ryanodine receptor subtypes regulate Ca2+sparks/spontaneous transient outward currents and myogenic tone of uterine arteries in pregnancy', *Cardiovascular Research*, 117(3), pp. 792–804. doi: 10.1093/cvr/cvaa089.

Soysal, C. and Işıkalan, M. M. (2020) 'The value of measuring cervical length between 24 and 28 weeks of gestation for predicting the risk of late and post-term pregnancy', *https://doi.org/10.1080/14767058.2020.1860934*. Taylor & Francis, 34(20), pp. 3402–3407. doi: 10.1080/14767058.2020.1860934.

Spiers, A. and Padmanabhan, N. (2005) 'A guide to wire myography', in *Hypertension*. doi: 10.1385/1-59259-850-1:091.

Spong, C. Y. (2013) 'Defining "term" pregnancy: recommendations from the defining "term" pregnancy workgroup', *JAMA*. American Medical Association, 309(23), pp. 2445–2446. doi: 10.1001/JAMA.2013.6235.

Sprague, B. J., Phernetton, T. M., Magness, R. R. and Chesler, N. C. (2009) 'The effects of the ovarian cycle and pregnancy on uterine vascular impedance and uterine artery mechanics', *European Journal of Obstetrics and Gynecology and Reproductive Biology*. Elsevier Ireland Ltd, 144(SUPPL 1), p. S170. doi: 10.1016/j.ejogrb.2009.02.041.

Sriprasert, I., Pakrashi, T., Kimble, T. and Archer, D. F. (2017) 'Heavy menstrual bleeding diagnosis and medical management', *Contraception and Reproductive Medicine*, 2(1). doi:

10.1186/s40834-017-0047-4.

Stanley, J. L., Ashton, N., Taggart, M. J., Davidge, S. T. and Baker, P. N. (2009) 'Uterine artery function in a mouse model of pregnancy complicated by diabetes', *Vascular Pharmacology*, 50(1–2). doi: 10.1016/j.vph.2008.08.002.

Stoll, B. J., Hansen, N. I., Bell, E. F., Shankaran, S., Laptook, A. R., Walsh, M. C., Hale, E. C., Newman, N. S., Schibler, K., Carlo, W. A., *et al.* (2010) 'Neonatal outcomes of extremely preterm infants from the NICHD Neonatal Research Network', *Pediatrics*. American Academy of Pediatrics, 126(3), pp. 443–456. doi: 10.1542/peds.2009-2959.

Stormorken, H., Sjaastad, O., Langslet, A., Sulg, I., Egge, K. and Diderichsen, J. (2008) 'A new syndrome: thrombocytopathia, muscle fatigue, asplenia, miosis, migraine, dyslexia and ichthyosis', *Clinical Genetics*. John Wiley & Sons, Ltd, 28(5), pp. 367–374. doi: 10.1111/j.1399-0004.1985.tb02209.x.

Stranik, J., Kacerovsky, M., Soucek, O., Kolackova, M., Musilova, I., Pliskova, L., Bolehovska, R., Bostik, P., Matulova, J., Jacobsson, B. and Andrys, C. (2021) 'IgGFc-binding protein in pregnancies complicated by spontaneous preterm delivery: a retrospective cohort study', *Scientific Reports*. Nature Publishing Group, 11(1), p. 6107. doi: 10.1038/S41598-021-85473-2.

Streff, H., Bi, W., Miyake, C. Y., Colón, A. G., Adesina, A. M. and Lalani, S. R. (2019) 'Amish nemaline myopathy and dilated cardiomyopathy caused by a homozygous contiguous gene deletion of TNNT1 and TNNI3 in a Mennonite child', *European journal of medical genetics*. NIH Public Access, 62(11), p. 103567. doi: 10.1016/J.EJMG.2018.11.001.

Sugimoto, Y., Yamasaki, A., Segi, E., Tsuboi, K., Aze, Y., Nishimura, T., Oida, H., Yoshida, N., Tanaka, T., Katsuyama, M., *et al.* (1997) 'Failure of parturition in mice lacking the prostaglandin F receptor', *Science (New York, N.Y.)*. Science, 277(5326), pp. 681–683. doi: 10.1126/SCIENCE.277.5326.681.

Sullivan, J. M., Zimanyi, C. M., Aisenberg, W., Bears, B., Chen, D. H., Day, J. W., Bird, T. D., Siskind, C. E., Gaudet, R. and Sumner, C. J. (2015) 'Novel mutations highlight the key role of the ankyrin repeat domain in TRPV4-mediated neuropathy', *Neurology: Genetics*. Lippincott Williams and Wilkins, 1(4). doi: 10.1212/NXG.0000000000000029.

Sundheimer, L. W. and Pisarska, M. D. (2017) 'Abnormal placentation associated with infertility as a marker of overall health', *Seminars in reproductive medicine*. NIH Public Access, 35(3), p. 205. doi: 10.1055/S-0037-1603570.

Sutko, J. L. and Airey, J. A. (1996) 'Ryanodine receptor Ca2+ release channels: Does diversity in form equal diversity in function?', *Physiological Reviews*. doi: 10.1152/physrev.1996.76.4.1027.

Sutovska, M., Kocmalova, M., Sadlonova, V., Dokus, K., Adamkov, M., Luptak, J. and Franova, S. (2015) 'Orai1 protein expression and the role of calcium release-activated calcium channels in the contraction of human term-pregnant and non-pregnant myometrium', *Journal of Obstetrics and Gynaecology Research*, 41(5), pp. 704–711. doi: 10.1111/jog.12626.

Szklarczyk, D., Gable, A. L., Nastou, K. C., Lyon, D., Kirsch, R., Pyysalo, S., Doncheva, N. T., Legeay, M., Fang, T., Bork, P., Jensen, L. J. and von Mering, C. (2021) 'The STRING database in 2021: Customizable protein-protein networks, and functional characterization of user-uploaded gene/measurement sets', *Nucleic Acids Research*, 49(D1), pp. D605–D612. doi: 10.1093/nar/gkaa1074.

Taggart, M. J. and Wray, S. (1998) 'Contribution of sarcoplasmic reticular calcium to smooth muscle contractile activation: gestational dependence in isolated rat uterus', *The Journal of Physiology*. John Wiley & Sons, Ltd (10.1111), 511(1), pp. 133–144. doi: 10.1111/j.1469-7793.1998.133bi.x.

Takahashi, K., Nakayama, K. I. and Nakayama, K. (2000) 'Mice Lacking a CDK Inhibitor, p57Kip2, Exhibit Skeletal Abnormalities and Growth Retardation', *The Journal of Biochemistry*. Oxford Academic, 127(1), pp. 73–83. doi: 10.1093/OXFORDJOURNALS.JBCHEM.A022586.

Takeshima, H., Ikemoto, T., Nishi, M., Nishiyama, N., Shimuta, M., Sugitani, Y., Kuno, J., Saito, I., Saito, H., Endo, M., Iino, M. and Noda, T. (1996) 'Generation and characterization of mutant mice lacking ryanodine receptor type 3', *Journal of Biological Chemistry*, 271(33). doi: 10.1074/jbc.271.33.19649.

Takeshima, H., Lino, M., Takekura, H., Nishi, M., Kuno, J., Minowa, O., Takano, H. and Noda, T. (1994) 'Excitation-contraction uncoupling and muscular degeneration in mice lacking functional skeletal muscle ryanodine-receptor gene', *Nature*. Nature Publishing Group, 369(6481), pp. 556–559. doi: 10.1038/369556a0.

Takeshima, H., Nishimura, S., Matsumoto, T., Ishida, H., Kangawa, K., Minamino, N., Matsuo, H., Ueda, M., Hanaoka, M., Hirose, T. and Numa, S. (1989) 'Primary structure and expression from complementary DNA of skeletal muscle ryanodine receptor', *Nature*, 339(6224). doi: 10.1038/339439a0.

Tamada, H., McMaster, M. T., Flanders, K. C., Andrews, G. K. and Dey, S. K. (1990) 'Cell type-specific expression of transforming growth factor-β1 in the mouse uterus during the periimolantation period', *Molecular Endocrinology*, 4(7), pp. 965–972. doi: 10.1210/mend-4-7-965.

Tarrade, A., Panchenko, P., Junien, C. and Gabory, A. (2015) 'Placental contribution to nutritional programming of health and diseases: epigenetics and sexual dimorphism', *Journal of Experimental Biology*. The Company of Biologists, 218(1), pp. 50–58. doi: 10.1242/JEB.110320.

Taylor, G. S., Maehama, T. and Dixon, J. E. (2000) 'Myotubularin, a protein tyrosine phosphatase mutated in myotubular myopathy, dephosphorylates the lipid second messenger, phosphatidylinositol 3-phosphate', *Proceedings of the National Academy of Sciences of the United States of America*, 97(16), pp. 8910–8915. doi: 10.1073/pnas.160255697.

Tekola-Ayele, F., Workalemahu, T., Gorfu, G., Shrestha, D., Tycko, B., Wapner, R., Zhang, C. and Louis, G. M. B. (2019) 'Sex differences in the associations of placental epigenetic aging with fetal growth', *Aging (Albany NY)*. Impact Journals, LLC, 11(15), p. 5412. doi: 10.18632/AGING.102124.

The Animals (Scientific Procedures) Act 1986 Amendment Regulations 2012 (2012). Available at: http://www.legislation.gov.uk/uksi/2012/3039/pdfs/uksi_20123039_en.pdf.

The Royal College of Obstetricians and Gynaecologists, R. (2014) *Heavy Menstrual Bleeding Audit Final Report – HQIP*. London. Available at: https://www.hqip.org.uk/resource/heavy-menstrual-bleeding-audit-reports-from-2011-to-2014/#.ZAjmwHbP2Uk (Accessed: 8 March 2023).

Thermo Fisher Scientific (no date) *T042-TECHNICAL BULLETIN NanoDrop Spectrophotometers*. Wilmington, Delaware USA. doi: 302-479-7707.

Thiyagarajan, D. K., Basit, H. and Jeanmonod, R. (2022) 'Physiology, Menstrual Cycle', *StatPearls*. StatPearls Publishing. Available at: https://www.ncbi.nlm.nih.gov/books/NBK500020/ (Accessed: 8 March 2023).

Thomas, P. D., Ebert, D., Muruganujan, A., Mushayahama, T., Albou, L. P. and Mi, H. (2022) 'PANTHER: Making genome-scale phylogenetics accessible to all', *Protein Science*. John Wiley and Sons Inc, 31(1), pp. 8–22. doi: 10.1002/PRO.4218.

Thompson, J., Koumari, R., Wagner, K., Barnert, S., Schleussner, C., Schrewe, H., Zimmermann, W., Müller, G., Schempp, W., Zaninetta, D., Ammaturo, D. and Hardman, N. (1990) 'The human pregnancy-specific glycoprotein genes are tightly linked on the long arm of chromosome 19 and are coordinately expressed', *Biochemical and Biophysical Research Communications*, 167(2), pp. 848–859. doi: 10.1016/0006-291X(90)92103-7.

Thorvaldsdóttir, H., Robinson, J. T. and Mesirov, J. P. (2013) 'Integrative Genomics Viewer (IGV): High-performance genomics data visualization and exploration', *Briefings in Bioinformatics*, 14(2). doi: 10.1093/bib/bbs017.

Tilly, J. L. and Sinclair, D. A. (2013) 'Germline energetics, aging, and female infertility', *Cell Metabolism*. doi: 10.1016/j.cmet.2013.05.007.

Ting, S. O. and Burke, C. (2019) 'Ultrasound assessment of uterine morphology in menorrhagia: case control study', *https://doi.org/10.1080/01443615.2019.1622084*. Taylor & Francis, 40(2), pp. 260–263. doi: 10.1080/01443615.2019.1622084.

Tiso, N., Dietrich, S., Nava, A., Bagattin, A., Devaney, J., Stanchi, F., Larderet, G., Brahmbhatt, B., Brown, K., Bauce, B., *et al.* (2001) 'Identification of mutations in the cardiac ryanodine receptor gene in families affected with arrhythmogenic right ventricular cardiomyopathy type 2 (ARVD2)', *Human Molecular Genetics*. Oxford University Press (OUP), 10(3), pp. 189–194. doi: 10.1093/hmg/10.3.189.

Tobacman, L. S. (1996) 'Thin Filament-Mediated Regulation of Cardiac Contraction', *Annual Review of Physiology*. Annual Reviews Inc., 58(1), pp. 447–481. doi: 10.1146/annurev.ph.58.030196.002311.

Togashi, K. (2007) 'Uterine contractility evaluated on cine magnetic resonance imaging', *Annals of the New York Academy of Sciences*, 1101(1), pp. 62–71. doi: 10.1196/annals.1389.030.

Tomarken, A. J. and Serlin, R. C. (1986) 'Comparison of anova Alternatives Under Variance Heterogeneity and Specific Noncentrality Structures', *Psychological Bulletin*, 99(1). doi: 10.1037/0033-2909.99.1.90.

Tong, J., McCarthy, T. V. and MacLennan, D. H. (1999) 'Measurement of resting cytosolic Ca2+ concentrations and Ca2+ store size in HEK-293 cells transfected with malignant hyperthermia or central core disease mutant Ca2+ release channels', *Journal of Biological Chemistry*, 274(2). doi: 10.1074/jbc.274.2.693.

Tong, W. and Giussani, D. A. (2019) 'Preeclampsia link to gestational hypoxia', in *Journal of Developmental Origins of Health and Disease*. doi: 10.1017/S204017441900014X.

Tosetto, A., Rodeghiero, F., Castaman, G., Goodeve, A., Federici, A. B., Batlle, J., Meyer, D., Fressinaud, E., Mazurier, C., Goudemand, J., *et al.* (2006) 'A quantitative analysis of bleeding symptoms in type 1 von Willebrand disease: Results from a multicenter European study (MCMDM-1 VWD)', *Journal of Thrombosis and Haemostasis*, 4(4), pp. 766–773. doi: 10.1111/j.1538-7836.2006.01847.x.

Traglia, M., Croen, L. A., Jones, K. L., Heuer, L. S., Yolken, R., Kharrazi, M., DeLorenze, G. N., Ashwood, P., Van de Water, J. and Weiss, L. A. (2018) 'Cross-genetic determination of maternal and neonatal immune mediators during pregnancy', *Genome Medicine*. BioMed Central Ltd., 10(1), pp. 1–17. doi: 10.1186/S13073-018-0576-8/FIGURES/5.

Traglia, M., Croen, L. A., Lyall, K., Windham, G. C., Kharrazi, M., DeLorenze, G. N., Torres, A. R. and Weiss, L. A. (2017) 'Independent maternal and fetal genetic effects on midgestational circulating levels of environmental pollutants', *G3: Genes, Genomes, Genetics*. Genetics Society of America, 7(4), pp. 1287–1299. doi: 10.1534/G3.117.039784/-/DC1.

Treloar, A. E., Boynton, R. E., Behn, B. G. and Brown, B. W. (1970) 'Variation of the human menstrual cycle through reproductive life', *International Journal of Fertility*, 12(1), pp. 77–126. doi: 10.1097/00006254-196801000-00019.

Treves, S., Jungbluth, H., Muntoni, F. and Zorzato, F. (2008) 'Congenital muscle disorders with cores: the ryanodine receptor calcium channel paradigm', *Current Opinion in Pharmacology*, pp. 319–326. doi: 10.1016/j.coph.2008.01.005.

Tribe, R. M. (2001) 'Regulation of human myometrial contractility during pregnancy and labour: Are calcium homeostatic pathways important?', *Experimental Physiology*, 86(2), pp. 247–254. doi: 10.1113/eph8602180.

Tribe, R. M., Moriarty, P. and Poston, L. (2000) 'Calcium Homeostatic Pathways Change with Gestation in Human Myometrium1', *Biology of Reproduction*. Narnia, 63(3), pp. 748–755. doi: 10.1095/biolreprod63.3.748.

Tribe, R. M. and Taggart, M. (2007) 'Cellular ionic mechanisms controlling uterine smooth muscle contraction: effects of gestational state', in *New Frontiers in Smooth Muscle Biology and Physiology*. Transworld Research Network, pp. 523–549.

Tricarico, D., Petruzzi, R. and Conte Camerino, D. (1997) 'Changes of the biophysical properties of calcium-activated potassium channels of rat skeletal muscle fibres during aging',

Pflugers Archive European Journal of Physiology, 434(6), pp. 822–829. doi: 10.1007/s004240050471.

Tsujita, K., Itoh, T., Ijuin, T., Yamamoto, A., Shisheva, A., Laporte, J. and Takenawa, T. (2004) 'Myotubularin regulates the function of the late endosome through the GRAM domain-phosphatidylinositol 3,5-bisphosphate interaction', *Journal of Biological Chemistry*. J Biol Chem, 279(14), pp. 13817–13824. doi: 10.1074/jbc.M312294200.

Tubular aggregate myopathy - Genetics Home Reference - NIH (no date). Available at: https://ghr.nlm.nih.gov/condition/tubular-aggregate-myopathy# (Accessed: 21 September 2020).

Tunçalp, Ö., Souza, J. P. and Gülmezoglu, M. (2013) 'New WHO recommendations on prevention and treatment of postpartum hemorrhage', *International Journal of Gynecology and Obstetrics*, 123(3). doi: 10.1016/j.ijgo.2013.06.024.

Uemura, Y., Liu, T. Y., Narita, Y., Suzuki, M., Ohshima, S., Mizukami, S., Ichihara, Y., Kikuchi, H. and Matsushita, S. (2007) 'Identification of functional type 1 ryanodine receptors in human dendritic cells', *Biochemical and Biophysical Research Communications*, 362(2). doi: 10.1016/j.bbrc.2007.08.024.

Uprichard, J. and Perry, D. J. (2002) 'Factor X deficiency', *Blood Reviews*. Churchill Livingstone, 16(2), pp. 97–110. doi: 10.1054/blre.2002.0191.

Urner, F., Zimmermann, R. and Krafft, A. (2014) 'Manual removal of the placenta after vaginal delivery: An unsolved problem in obstetrics', *Journal of Pregnancy*. Hindawi Limited, 2014. doi: 10.1155/2014/274651.

Vandebrouck, C., Martin, D., Schoor, M. C. Van, Debaix, H. and Gailly, P. (2002) 'Involvement of TRPC in the abnormal calcium influx observed in dystrophic (mdx) mouse skeletal muscle fibers', *Journal of Cell Biology*, 158(6), pp. 1089–1096. doi: 10.1083/jcb.200203091.

Vandesompele, J., De Preter, K., Pattyn, F., Poppe, B., Van Roy, N., De Paepe, A. and Speleman, F. (2002) 'Accurate normalization of real-time quantitative RT-PCR data by geometric averaging of multiple internal control genes', *Genome Biology*. BioMed Central, 3(7). Available at: https://genomebiology.biomedcentral.com/articles/10.1186/gb-2002-3-7-research0034 (Accessed: 7 April 2020).

Vandraas, K. F., Vikanes, A. V., Støer, N. C., Vangen, S., Magnus, P. and Grjibovski, A. M. (2013) 'Is hyperemesis gravidarum associated with placental weight and the placental weight-to-birth weight ratio? A population-based Norwegian cohort study', *Placenta*, 34(11). doi: 10.1016/j.placenta.2013.08.001.

Vannuccini, S., Jain, V., Critchley, H. and Petraglia, F. (2022) 'From menarche to menopause, heavy menstrual bleeding is the underrated compass in reproductive health', *Fertility and sterility*. Fertil Steril, 118(4), pp. 625–636. doi: 10.1016/J.FERTNSTERT.2022.07.021.

Veerareddy, S., Cooke, C. L. M., Baker, P. N. and Davidge, S. T. (2002) 'Vascular adaptations to pregnancy in mice: Effects on myogenic tone', *American Journal of Physiology - Heart and*

Circulatory Physiology, 283(6 52-6). doi: 10.1152/ajpheart.00593.2002.

Vernochet, C., Caucheteux, S. M. and Kanellopoulos-Langevin, C. (2007) 'Bi-directional cell trafficking between mother and fetus in mouse placenta', *Placenta*, 28(7). doi: 10.1016/j.placenta.2006.10.006.

Versteeg, H. H., Heemskerk, J. W. M., Levi, M. and Reitsma, P. H. (2013) 'New Fundamentals in hemostasis', *Physiological Reviews*. doi: 10.1152/physrev.00016.2011.

Vukcevic, M., Spagnoli, G. C., Iezzi, G., Zorzato, F. and Treves, S. (2008) 'Ryanodine receptor activation by cav1.2 is involved in dendritic cell major histocompatibility complex class ii surface expression', *The Journal of Biological Chemistry*. American Society for Biochemistry and Molecular Biology, 283(50), p. 34913. doi: 10.1074/JBC.M804472200.

Vukcevic, M., Zorzato, F., Keck, S., Tsakiris, D. A., Keiser, J., Maizels, R. M. and Treves, S. (2013) 'Gain of function in the immune system caused by a ryanodine receptor 1 mutation', *Journal of Cell Science*. Company of Biologists, 126(Pt 15), pp. 3485–92. doi: 10.1242/jcs.130310.

Wakle-Prabagaran, M., Lorca, R. A., Ma, X., Stamnes, S. J., Amazu, C., Hsiao, J. J., Karch, C. M., Hyrc, K. L., Wright, M. E. and England, S. K. (2016) 'BKCa channel regulates calcium oscillations induced by alpha-2-macroglobulin in human myometrial smooth muscle cells', *Proceedings of the National Academy of Sciences of the United States of America*. National Academy of Sciences, 113(16), pp. E2335–E2344. doi: 10.1073/pnas.1516863113.

Walter, M. C., Rossius, M., Zitzelsberger, M., Vorgerd, M., Müller-Felber, W., Ertl-Wagner, B., Zhang, Y., Brinkmeier, H., Senderek, J. and Schoser, B. (2015) '50 years to diagnosis: Autosomal dominant tubular aggregate myopathy caused by a novel STIM1 mutation', *Neuromuscular Disorders*. Elsevier Ltd, 25(7), pp. 577–584. doi: 10.1016/j.nmd.2015.04.005.

Wang, F. han, Peng, X., Chen, Y., Wang, Y., Yang, M. and Guo, M. yao (2019) 'Se regulates the contractile ability of uterine smooth muscle via selenoprotein N, selenoprotein T, and selenoprotein W in mice', *Biological Trace Element Research*. Humana Press Inc., 192(2), pp. 196–205. doi: 10.1007/s12011-019-1647-4.

Wang, J. P. and Chen, C. C. (1998) 'Magnolol induces cytosolic-free Ca2+ elevation in rat neutrophils primarily via inositol trisphosphate signalling pathway', *European Journal of Pharmacology*, 352(2–3). doi: 10.1016/S0014-2999(98)00363-X.

Wang, T., Liao, L., Tang, X., Li, B. and Huang, S. (2021) 'Effects of different vasopressors on the contraction of the superior mesenteric artery and uterine artery in rats during late pregnancy', *BMC Anesthesiology*. BioMed Central Ltd, 21(1), pp. 1–7. doi: 10.1186/S12871-021-01395-6/TABLES/2.

Wang, X., Huang, Q. Q., Breckenridge, M. T., Chen, A., Crawford, T. O., Holmes Morton, D. and Jin, J. P. (2005) 'Cellular fate of truncated slow skeletal muscle troponin T produced by Glu180 nonsense mutation in amish nemaline myopathy', *Journal of Biological Chemistry*. American Society for Biochemistry and Molecular Biology, 280(14), pp. 13241–13249. doi: 10.1074/jbc.M413696200.

Wang, Y. X., Arvizu, M., Rich-Edwards, J. W., Stuart, J. J., Manson, J. A. E., Missmer, S. A., Pan, A. and Chavarro, J. E. (2020) 'Menstrual cycle regularity and length across the reproductive lifespan and risk of premature mortality: prospective cohort study', *BMJ (Clinical research ed.)*. BMJ, 371, p. m3464. doi: 10.1136/BMJ.M3464.

Wang, Y., Yang, D., Zhu, R., Dai, F., Yuan, M., Zhang, L., Zheng, Y., Liu, S., Yang, X. and Cheng, Y. (2022) 'YY1/ITGA3 pathway may affect trophoblastic cells migration and invasion ability', *Journal of Reproductive Immunology*. Elsevier, 153, p. 103666. doi: 10.1016/J.JRI.2022.103666.

Wangler, M. F., Chang, A. S., Moley, K. H., Feinberg, A. P. and DeBaun, M. R. (2005) 'Factors associated with preterm delivery in mothers of children with Beckwith–Wiedemann syndrome: A case cohort study from the BWS registry', *American Journal of Medical Genetics Part A*. John Wiley & Sons, Ltd, 134A(2), pp. 187–191. doi: 10.1002/AJMG.A.30595.

Wappler, F. (2010) 'Anesthesia for patients with a history of malignant hyperthermia', *Current Opinion in Anaesthesiology*, pp. 417–422. doi: 10.1097/ACO.0b013e328337ffe0.

Wassel, K., Kuhn, G., Gassmann, M. and Vogel, J. (2005) 'Permanently increased conductance of the murine uterine arcade after the first pregnancy', *European Journal of Morphology*, 42(4–5), pp. 225–232. doi: 10.1080/09243860600746916.

Watanabe, H., Murakami, M., Ohba, T., Takahashi, Y. and Ito, H. (2008) 'TRP channel and cardiovascular disease', *Pharmacology and Therapeutics*. Pharmacol Ther, pp. 337–351. doi: 10.1016/j.pharmthera.2008.03.008.

Watanabe, M., Kida, M., Yamada, Y. and Saigenji, K. (2004) 'Measuring tumor volume with three-dimensional endoscopic ultrasonography: an experimental and clinical study (including video)', *Endoscopy*, 36(11), pp. 976–981. doi: 10.1055/S-2004-825866.

Watson, E. D. and Cross, J. C. (2005) *Development of structures and transport functions in the mouse placenta*, *Physiology*. American Physiological Society. Available at: https://journals.physiology.org/doi/10.1152/physiol.00001.2005 (Accessed: 19 February 2023).

Wedel, T., Van Eys, G. J. J. M., Waltregny, D., Glénisson, W., Castronovo, V. and Vanderwinden, J. M. (2006) 'Novel smooth muscle markers reveal abnormalities of the intestinal musculature in severe colorectal motility disorders', *Neurogastroenterology and Motility*, 18(7). doi: 10.1111/j.1365-2982.2006.00781.x.

Weiss, R. G., O'Connell, K. M. S., Flucher, B. E., Allen, P. D., Grabner, M. and Dirksen, R. T. (2004) 'Functional analysis of the R1086H malignant hyperthermia mutation in the DHPR reveals an unexpected influence of the III-IV loop on skeletal muscle EC coupling', *American Journal of Physiology - Cell Physiology*, 287(4 56-4). doi: 10.1152/ajpcell.00173.2004.

Wenceslau, C. F., McCarthy, C. G., Earley, S., England, S. K., Filosa, J. A., Goulopoulou, S., Gutterman, D. D., Isakson, B. E., Kanagy, N. L., Martinez-Lemus, L. A., *et al.* (2021) 'Guidelines for the measurement of vascular function and structure in isolated arteries and veins', *American Journal of Physiology - Heart and Circulatory Physiology*, 321(1). doi: 10.1152/AJPHEART.01021.2020.

WHO recommendations for the prevention and treatment of postpartum haemorrhage (no date). Available at: www.who.int/maternal_child_adolescent (Accessed: 13 March 2023).

Women with Bleeding Disorders (no date) *The Haemophilia Society*. Available at: https://haemophilia.org.uk/bleeding-disorders/women-with-bleeding-disorders/ (Accessed: 19 March 2023).

Wong, J. V., Franz, M., Siper, M. C., Fong, D., Durupinar, F., Dallago, C., Luna, A., Giorgi, J., Rodchenkov, I., Babur, Ö., *et al.* (2021) 'Author-sourced capture of pathway knowledge in computable form using Biofactoid', *eLife*. eLife Sciences Publications Ltd, 10. doi: 10.7554/ELIFE.68292.

Wooding, F. B. P. and Flint, A. P. F. (1994) 'Placentation', *Marshall's Physiology of Reproduction*. Dordrecht: Springer, Dordrecht, pp. 233–460. doi: 10.1007/978-94-011-1286-4_4.

Woods, L., Perez-Garcia, V. and Hemberger, M. (2018) 'Regulation of placental development and its impact on fetal growth—new insights from mouse models', *Frontiers in Endocrinology*. Frontiers Media S.A., 9, p. 570. doi: 10.3389/FENDO.2018.00570/BIBTEX.

Word, R. A., Stull, J. T., Casey, M. L. and Kamm, K. E. (1993) 'Contractile elements and myosin light chain phosphorylation in myometrial tissue from nonpregnant and pregnant women', *Journal of Clinical Investigation*. doi: 10.1172/JCI116564.

World Health Organisation (WHO) (2023) *WHO postpartum haemorrhage (PPH) summit*. Dubai, United Arab Emirates. Available at: https://www.who.int/publications/m/item/who-postpartum-haemorrhage-(pph)-summit (Accessed: 13 March 2023).

Wray, S. (2007) 'Insights into the uterus', *Experimental Physiology*, 92(4), pp. 621–631. doi: 10.1113/expphysiol.2007.038125.

Wray, S. (2015) 'Insights from physiology into myometrial function and dysfunction', *Experimental Physiology*, 100(12), pp. 1468–1476. doi: 10.1113/EP085131.

Wray, S., Burdyga, T. and Noble, K. (2005) 'Calcium signalling in smooth muscle', *Cell Calcium*. Churchill Livingstone, 38(3–4), pp. 397–407. doi: 10.1016/J.CECA.2005.06.018.

Wray, S., Jones, K., Kupittayanant, S., Li, Y., Matthew, A., Monir-Bishty, E., Noble, K., Pierce, S. J., Quenby, S. and Shmygol, A. V. (2003) 'Calcium signaling and uterine contractility', *Journal of the Society for Gynecologic Investigation*, pp. 252–264. doi: 10.1016/S1071-5576(03)00089-3.

Wu, G. and Haw, R. (2017) 'Functional interaction network construction and analysis for disease discovery', in *Methods in Molecular Biology*. doi: 10.1007/978-1-4939-6783-4_11.

Wu, J. A., Johnson, B. L., Chen, Y., Ha, C. T. and Dveksler, G. S. (2008) 'Murine pregnancy-specific glycoprotein 23 induces the proangiogenic factors transforming-growth factor beta 1 and vascular endothelial growth factor A in cell types involved in vascular remodeling in pregnancy', *Biology of Reproduction*, 79(6). doi: 10.1095/biolreprod.108.070268.

Wynne, F., Ball, M., McLellan, A. S., Dockery, P., Zimmermann, W. and Moore, T. (2006) 'Mouse pregnancy-specific glycoproteins: tissue-specific expression and evidence of association with maternal vasculature', *Reproduction*. Society for Reproduction and Fertility, 131(4), pp. 721–732. doi: 10.1530/rep.1.00869.

Yamazawa, T., Kobayashi, T., Kurebayashi, N., Konishi, M., Noguchi, S., Inoue, T., Inoue, Y. U., Nishino, I., Mori, S., Iinuma, H., *et al.* (2021) 'A novel RyR1-selective inhibitor prevents and rescues sudden death in mouse models of malignant hyperthermia and heat stroke', *Nature Communications*, 12(1). doi: 10.1038/s41467-021-24644-1.

Yang, C., Li, Y., Pan, H. Y., Li, M. Y., Pan, J. M., Chen, S. T., Zhang, H. Y., Yang, Z. S., Dou, H. T. and Yang, Z. M. (2021) 'Female reproductive abnormalities in mouse adolescent pregnancy', *Reproduction (Cambridge, England)*. Reproduction, 162(5), pp. 353–365. doi: 10.1530/REP-21-0240.

Yang Chou, J. and Zilberstein, M. (1990) 'Expression of the pregnancy-specific β1-glycoprotein gene in cultured human trophoblasts', *Endocrinology*, 127(5). doi: 10.1210/endo-127-5-2127.

Yang, X. R., Lin, A. H. Y., Hughes, J. M., Flavahan, N. A., Cao, Y. N., Liedtke, W. and Sham, J. S. K. (2012) 'Upregulation of osmo-mechanosensitive TRPV4 channel facilitates chronic hypoxia-induced myogenic tone and pulmonary hypertension', *American Journal of Physiology - Lung Cellular and Molecular Physiology*, 302(6). doi: 10.1152/ajplung.00005.2011.

Yang, Y., Sohma, Y., Nourian, Z., Ella, S. R., Li, M., Stupica, A., Korthuis, R. J., Davis, M. J., Braun, A. P. and Hill, M. A. (2013) 'Mechanisms underlying regional differences in the Ca2+ sensitivity of BK(Ca) current in arteriolar smooth muscle', *The Journal of physiology*. J Physiol, 591(5), pp. 1277–1293. doi: 10.1113/JPHYSIOL.2012.241562.

Yang, Y., Vassilakos, G., Hammers, D. W., Yang, Z., Barton, E. R. and Sweeney, H. L. (2019) 'Smooth muscle atrophy and colon pathology in SMN deficient mice', *American Journal of Translational Research*. e-Century Publishing Corporation, 11(3), p. 1789. Available at: /pmc/articles/PMC6456546/ (Accessed: 23 February 2023).

Yin, X.-M., Lin, J.-H., Cao, L., Zhang, T.-M., Zeng, S., Zhang, K.-L., Tian, W.-T., Hu, Z.-M., Li, N., Wang, J.-L., *et al.* (2017) 'Familial paroxysmal kinesigenic dyskinesia is associated with mutations in the KCNA1 gene', *Human Molecular Genetics*, 27(4), pp. 625–637. doi: 10.1093/hmg/ddx430.

Ying, L., Becard, M., Lyell, D., Han, X., Shortliffe, L., Husted, C. I., Alvira, C. M. and Cornfield, D. N. (2015) 'The transient receptor potential vanilloid 4 channel modulates uterine tone during pregnancy', *Science Translational Medicine*. American Association for the Advancement of Science, 7(319), pp. 319ra204-319ra204. doi: 10.1126/SCITRANSLMED.AAD0376.

Yomogita, H., Ito, H., Hashimoto, K., Kudo, A., Fukushima, T., Endo, T., Hirate, Y., Akimoto, Y., Komada, M., Kanai, Y., Miyasaka, N. and Kanai-azuma, M. (2023) 'A possible function of Nik-related kinase in the labyrinth layer of delayed delivery mouse placentas', *The Journal of Reproduction and Development*, 69(1). doi: 10.1262/JRD.2022-120.

Yue, F., Cheng, Y., Breschi, A., Vierstra, J., Wu, W., Ryba, T., Sandstrom, R., Ma, Z., Davis, C., Pope, B. D., *et al.* (2014) 'A comparative encyclopedia of DNA elements in the mouse genome', *Nature*, 515(7527), pp. 355–364. doi: 10.1038/nature13992.

Zalk, R. and Marks, A. R. (2017) 'Ca2+ Release Channels Join the "Resolution Revolution"', *Trends in Biochemical Sciences*. Elsevier Current Trends, 42(7), pp. 543–555. doi: 10.1016/J.TIBS.2017.04.005.

Zanou, N., Shapovalov, G., Louis, M., Tajeddine, N., Gallo, C., Van Schoor, M., Anguish, I., Cao, M. L., Schakman, O., Dietrich, A., *et al.* (2010) 'Role of TRPC1 channel in skeletal muscle function', *American Journal of Physiology - Cell Physiology*, 298(1). doi: 10.1152/ajpcell.00241.2009.

Zavaritskaya, O., Dudem, S., Ma, D., Rabab, K. E., Albrecht, S., Tsvetkov, D., Kassmann, M., Thornbury, K., Mladenov, M., Kammermeier, C., *et al.* (2020) 'Vasodilation of rat skeletal muscle arteries by the novel BK channel opener GoSlo is mediated by the simultaneous activation of BK and Kv7 channels', *British Journal of Pharmacology*. John Wiley and Sons Inc., 177(5), pp. 1164–1186. doi: 10.1111/bph.14910.

Zhang, K., Xu, J., Ding, Y., Shen, C., Lin, M., Dai, X., Zhou, H., Huang, X., Xue, B. and Zheng, B. (2021) 'BMI1 promotes spermatogonia proliferation through epigenetic repression of Ptprm', *Biochemical and Biophysical Research Communications*. Academic Press, 583, pp. 169–177. doi: 10.1016/J.BBRC.2021.10.074.

Zhang, P., Luo, Y., Chasan, B., González-Perrett, S., Montalbetti, N., Timpanaro, G. A., del Rocío Cantero, M., Ramos, A. J., Goldmann, W. H., Zhou, J. and Cantiello, H. F. (2009) 'The multimeric structure of polycystin-2 (TRPP2): Structural - Functional correlates of homo- and hetero-multimers with TRPC1', *Human Molecular Genetics*. Oxford Academic, 18(7), pp. 1238–1251. doi: 10.1093/hmg/ddp024.

Zhang, W. S., Fei, K. L., Wu, M. T., Wu, X. H. and Liang, Q. H. (2012) 'Neuromedin B and its receptor influence the activity of myometrial primary cells in vitro through regulation of Il6 expression via the Rela/p65 pathway in mice', *Biology of Reproduction*, 86(5). doi: 10.1095/biolreprod.111.095984.

Zhang, W. S., Liang, Q. H., Xie, Q. S., Wu, Z. Di and Wu, X. H. (2007) '[Scanning of drug targets related to uterus contraction from the uterine smooth muscles by cDNA microarray]', *Zhong nan da xue xue bao. Yi xue ban = Journal of Central South University. Medical sciences*. Zhong Nan Da Xue Xue Bao Yi Xue Ban, 32(4), pp. 579–583. Available at: https://pubmed.ncbi.nlm.nih.gov/17767045/ (Accessed: 24 January 2023).

Zhang, W. S., Xie, Q. S., Wu, X. H. and Liang, Q. H. (2011) 'Neuromedin B and its receptor induce labor onset and are associated with the RELA (NFKB P65)/IL6 pathway in pregnant mice', *Biology of reproduction*. Biol Reprod, 84(1), pp. 113–117. doi: 10.1095/BIOLREPROD.110.085746.

Zhang, Y., Soelter, B. and Brinkmeier, H. (2015) 'Functional Expression of TRPC6 and TRPV4 Channels in Mouse Skeletal Muscle Fibers', *Biophysical Journal*. Elsevier BV, 108(2), p. 282a. doi: 10.1016/J.BPJ.2014.11.1539.

Zhao, F., Li, P., Chen, S. R. W., Louis, C. F. and Fruen, B. R. (2001a) 'Dantrolene inhibition of ryanodine receptor Ca2+ release channels. Molecular mechanism and isoform selectivity', *Journal of Biological Chemistry*. American Society for Biochemistry and Molecular Biology, 276(17), pp. 13810–6. doi: 10.1074/jbc.M006104200.

Zhao, F., Li, P., Chen, S. R. W., Louis, C. F. and Fruen, B. R. (2001b) 'Dantrolene Inhibition of Ryanodine Receptor Ca2+Release Channels: MOLECULAR MECHANISM AND ISOFORM SELECTIVITY', *Journal of Biological Chemistry*. Elsevier, 276(17), pp. 13810–13816. doi: 10.1074/JBC.M006104200.

Zhao, G., Zhao, Y., Pan, B., Liu, J., Huang, X., Zhang, X., Cao, C., Hou, N., Wu, C., Zhao, K. S. and Cheng, H. (2007) 'Hypersensitivity of BKCa to Ca2+ sparks underlies hyporeactivity of arterial smooth muscle in shock', *Circulation Research*, 101(5). doi: 10.1161/CIRCRESAHA.107.157271.

Zhao, M., Yang, Y., Guo, Z., Shao, C., Sun, H., Zhang, Y., Sun, Y., Liu, Y., Song, Y., Zhang, L., *et al.* (2018) 'A comparative proteomics analysis of five body fluids: plasma, urine, cerebrospinal fluid, amniotic fluid, and saliva', *Proteomics - Clinical Applications*, 12(6). doi: 10.1002/prca.201800008.

Zhao, R., Du, L., Huang, Y., Wu, Y. and Gunst, S. J. (2008) 'Actin depolymerization factor/cofilin activation regulates actin polymerization and tension development in canine tracheal smooth muscle', *Journal of Biological Chemistry*, 283(52), pp. 36522–36531. doi: 10.1074/jbc.M805294200.

Zhao, X., Ma, R., Zhang, X., Cheng, R., Jiang, N., Guo, M., Rong, B., Liu, Y., Chen, M., Feng, W. and Xia, T. (2021) 'Reduced growth capacity of preimplantation mouse embryos in chronic unpredictable stress model', *Molecular Reproduction and Development*, 88(1), pp. 80–95. doi: 10.1002/mrd.23439.

Zhao, Y., Pasanen, M. and Rysä, J. (2023) 'Placental ion channels: potential target of chemical exposure', *Biology of Reproduction*. Oxford Academic, 108(1), pp. 41–51. doi: 10.1093/BIOLRE/IOAC186.

Zheng, L., Lindsay, A., McSweeney, K., Aplin, J., Forbes, K., Smith, S., Tunwell, R. and Mackrill, J. J. (2022) 'Ryanodine receptor calcium release channels in trophoblasts and their role in cell migration', *Biochimica et Biophysica Acta (BBA) - Molecular Cell Research*. Elsevier, 1869(1), p. 119139. doi: 10.1016/J.BBAMCR.2021.119139.

Zhou, J., Li, C., Gu, G., Wang, Q. and Guo, M. (2018) 'Selenoprotein N was required for the regulation of selenium on the uterine smooth muscle contraction in mice', *Biological Trace Element Research*. Humana Press Inc., 183(1), pp. 138–146. doi: 10.1007/s12011-017-1130-z.

Zhou, J., Xiao, D., Hu, Y., Wang, Z., Paradis, A., Mata-Greenwood, E. and Zhang, L. (2013) 'Gestational hypoxia induces preeclampsia-like symptoms via heightened endothelin-1 signaling in pregnant rats', *Hypertension*, 62(3). doi: 10.1161/HYPERTENSIONAHA.113.01449.

Zhou, X. B., Wang, G. X., Ruth, P., Hüneke, B. and Korth, M. (2000) 'BK(Ca) channel

activation by membrane-associated cGMP kinase may contribute to uterine quiescence in pregnancy', *American Journal of Physiology - Cell Physiology*. American Physiological Society, 279(6 48-6). doi: 10.1152/ajpcell.2000.279.6.c1751.

Zhu, T., Chen, J., Zhao, Y., Zhang, J., Peng, Q., Huang, J., Luo, J. and Zhang, W. (2019) 'Neuromedin B mediates IL-6 and COX-2 expression through NF-κB/P65 and AP-1/C-JUN activation in human primary myometrial cells', *Bioscience Reports*. Portland Press Ltd, 39(10). doi: 10.1042/BSR20192139.

Zia, A., Jain, S., Kouides, P., Zhang, S., Gao, A., Salas, N., Lau, M., Wilson, E., DeSimone, N. and Sarode, R. (2020) 'Bleeding disorders in adolescents with heavy menstrual bleeding in a multicenter prospective US cohort', *Haematologica*, 105(7). doi: 10.3324/haematol.2019.225656.

Zwart, J. J., Richters, J. M., Ory, F., de Vries, J. I., Bloemenkamp, K. W. and van Roosmalen, J. (2009) 'Severe maternal morbidity during pregnancy, delivery, and puerperium in the netherlands: A nationwide population-based study of 371,000 pregnancies', *Obstetric Anesthesia Digest*, 29(1). doi: 10.1097/01.aoa.0000344677.99496.9a.

11 Appendices

List of appendices

1. Permissions table

2. RNA-seq DESeq analysis by Dr Flavia Flaviani and Dr Prasanth Sivakumar

3. Macros for the analysis of immunofluorescent-stained images

4. Sample MCMDM-1VWD form

5. MCMDM-1WD scoring key

6. Information sheet for healthy participants

7. Information sheet for RYR1 participants

8. Correspondence for ethical approval for questionnaire study

9. Sample bleeding questionnaire

11.1 Appendix 1

Page No.	Type of work:	Name of work	Source of work	Copyright holder and contact	permission requested on	I have permission yes /no	Permission note
32	Figure	Figure 2. Proteins involved in skeletal muscle excitation contraction coupling	Congenital myopathies: disorders of excitation–contraction coupling and muscle contraction. Heinz Jungbluth et al. 2018. Nature Reviews Neurology. 14(3). Pages 151- 167. doi:10.1038/nrneurol.2017.191	Springer Nature	17/05/2023	Yes	Licences obtained for reuse in an electronic dissertation/thesis License Number: 5551561158890 License date: May 17, 2023
47	figure	Figure 3. Coronal *ex vivo* sections of the non-pregnant (A) human and (B) mouse reproductive anatomy	Mara H. Rendi, Atis Muehlenbachs, Rochelle L. Garcia, Kelli L. Boyd, 17 - Female Reproductive System, Editor(s): Piper M. Treuting, Suzanne M. Dintzis, Comparative Anatomy and Histology, Academic Press, 2012, Pages 253-284, ISBN 9780123813619, https://doi.org/10.1016/B978-0-12-381361-9.00017-2.	Elsevier	17/05/2023	Yes	Licences obtained for reuse in an electronic dissertation/thesis License Number: 5551581274858 License date: May 17, 2023
47	figure	Figure 3. Coronal *ex vivo* sections of the non-pregnant (A) human and (B) mouse reproductive anatomy	Ramírez-González, J., Vaamonde-Lemos, R., Cunha-Filho, J., Varghese, A., Swanson, R. (2016). Overview of the Female Reproductive System. In: Vaamonde, D., du Plessis, S., Agarwal, A. (eds) Exercise and Human Reproduction. Springer, New York, NY. https://doi.org/10.1007/978-1-4939-3402-7_2	Springer Nature	17/05/2023	Yes	Licences obtained for reuse in an electronic dissertation/thesis License Number: 5551591320240 License date: May 17, 2023

| 49 | figure | Figure 4. Human menstrual cycle with characteristic fluctuations of the ovarian hormones estradiol (E2) and progesterone (P4) in the follicular and luteal phases, from (Schmalenberger et al., 2021). | Katja M. Schmalenberger,Hafsah A. Tauseef,Jordan C. Barone,Sarah A. Owens,Lynne Lieberman,Marc N. Jarczok,Susan S. Girdler,Jeff Kiesner,Beate Ditzen,Tory A. Eisenlohr-Moul. How to study the menstrual cycle: Practical tools and recommendations. January 2021. Psychoneuroendocrinology | Elsevier | 25/05/2023 | Yes | Licences obtained for reuse in an electronic dissertation/thesis License Number: 5556120273154 License date: May 25, 2023 |
| 113 | figure | Figure 11. Collection of vaginal fluid secretion in non-pregnant mice. | Caligioni CS. Assessing reproductive status/stages in mice. Curr Protoc Neurosci. 2009 Jul;Appendix 4:Appendix 4I. doi: 10.1002/0471142301.nsa04is48. PMID: 19575469; PMCID: PMC2755182. | John Wiley & Sons, Inc. | 03/07/2023 | Yes | Licences obtained for reuse in an electronic dissertation/thesis Licences order ID: 1371842-1 License date: July 03, 2023 . |

11.2 Appendix 2

RNA-sequencing project proposal and data analysis by Dr Flavia Flaviani and Dr Prasanth Sivakumar

The data for this project is stored on CREATE, access via path:

/scratch/prj/rnaseq_mouse_myometrium.

General summary of project: The project aims to determine the impact of the skeletal RYR1 Y522S mutation on gene expression variability in mouse myometrial tissue using RNA sequencing. A selection of patients with RYR1 mutations have reported mild abnormal bleeding events e.g. Postpartum haemorrhage, menorrhagia, post operative bleeding. Therefore, we hypothesise that skeletal RYR1 may also play a role in smooth muscle function, specifically myometrial and uterine vascular smooth muscle in pregnancy. We are using a malignant hyperthermia susceptible mouse model RYR1 (Y522S /+) to study differential gene expression as a result of Y522S supposedly creating a gain-of-function. This work will complement current ex vivo experiments on myometrial and uterine artery tissue contractility.

Type of data Total RNA from myometrial tissue. Animal model: C57/B6 mouse background with RYR1 Y522S substation – see Chelu et al 2006

Number of samples: 13 samples sequenced in total. No technical replicates but there are biological replicates (1) WT (n=7) (2) Heterozygous RYR1 Y522S/+ (n=6). There are 2 files per samples, one R and one F.

Sequencing method *Library prep protocol*: NEBNext Ultra II Directional RNA library Prep kit for Illumina

rRNA reduction protocol: NEBNext Poly(A) mRNA Magnetic Isolation Module

Sequencer: NovaSeq

Analyses performed by Prasanth: Alignment of the data performed in Rosalind with STAR v2.7.8 using reference GRCm39

Index for the reference (GRCm39) was generated with FASTA: Mus_musculus.GRCm39.dna.primary_assembly.fa, and GTF: Mus_musculus.GRCm39.104.gtf, both from Ensembl

Counts matrix was generated using featureCounts from subread v2.0.1 using the same GTF as above.

Parameters used for the alignment: xxx

Check the environment and load the libraries:

Assuming this is a clean R installation without packages installed: This first will be run only once. eval=FALSE allow you to ignore this chunk

```
# install packages:

# install.packages('knitr') # This will need to be done only once  :comment out this line after run
```

```r
if (!requireNamespace("BiocManager", quietly=TRUE)) # This will need to be done only once  : comment out this line after run

   install.packages("BiocManager") # This will need to be done only once  : comment out this line after run


BiocManager::install("BiocStyle")  # This will need to be done only once  : comment out this line after run
```

Check if we need these other packages: library("ggbeeswarm") library(affy) #bio library("gplots")

Note: make sure the output is all TRUE. If you have FALSE it means some packages are not installed / loaded

```r
# Load packages into session, and print package version
sapply(c(.cran_packages, .bioc_packages), require, character.only=TRUE)
## Loading required package: ggplot2
## Loading required package: RColorBrewer
## Loading required package: dplyr
##
## Attaching package: 'dplyr'
## The following objects are masked from 'package:stats':
##
##     filter, lag
## The following objects are masked from 'package:base':
##
##     intersect, setdiff, setequal, union
## Loading required package: tibble
## Loading required package: pheatmap
## Loading required package: tidyverse
## ── Attaching packages ─────────────────────────────────────── tidyverse 1.3.1 ──
## ✓ tidyr   1.1.3     ✓ stringr 1.4.0
## ✓ readr   2.0.1     ✓ forcats 0.5.1
## ✓ purrr   0.3.4
## ── Conflicts ─────────────────────────────────────── tidyverse_conflicts() ──
## x dplyr::filter() masks stats::filter()
## x dplyr::lag()    masks stats::lag()
```

```
## Loading required package: limma
## Loading required package: gplots
##
## Attaching package: 'gplots'
## The following object is masked from 'package:stats':
##
##     lowess
## Loading required package: tximport
## Loading required package: GenomicFeatures
## Loading required package: BiocGenerics
## Loading required package: parallel
##
## Attaching package: 'BiocGenerics'
## The following objects are masked from 'package:parallel':
##
##     clusterApply, clusterApplyLB, clusterCall, clusterEvalQ,
##     clusterExport, clusterMap, parApply, parCapply, parLapply,
##     parLapplyLB, parRapply, parSapply, parSapplyLB
## The following object is masked from 'package:limma':
##
##     plotMA
## The following objects are masked from 'package:dplyr':
##
##     combine, intersect, setdiff, union
## The following objects are masked from 'package:stats':
##
##     IQR, mad, sd, var, xtabs
## The following objects are masked from 'package:base':
##
##     anyDuplicated, append, as.data.frame, basename, cbind, colnames,
##     dirname, do.call, duplicated, eval, evalq, Filter, Find, get, grep,
##     grepl, intersect, is.unsorted, lapply, Map, mapply, match, mget,
##     order, paste, pmax, pmax.int, pmin, pmin.int, Position, rank,
##     rbind, Reduce, rownames, sapply, setdiff, sort, table, tapply,
```

```
##     union, unique, unsplit, which, which.max, which.min
## Loading required package: S4Vectors
## Loading required package: stats4
##
## Attaching package: 'S4Vectors'
## The following object is masked from 'package:gplots':
##
##     space
## The following object is masked from 'package:tidyr':
##
##     expand
## The following objects are masked from 'package:dplyr':
##
##     first, rename
## The following object is masked from 'package:base':
##
##     expand.grid
## Loading required package: IRanges
##
## Attaching package: 'IRanges'
## The following object is masked from 'package:purrr':
##
##     reduce
## The following objects are masked from 'package:dplyr':
##
##     collapse, desc, slice
## Loading required package: GenomeInfoDb
## Loading required package: GenomicRanges
## Loading required package: AnnotationDbi
## Loading required package: Biobase
## Welcome to Bioconductor
##
##     Vignettes contain introductory material; view with
##     'browseVignettes()'. To cite Bioconductor, see
```

```
##     'citation("Biobase")', and for packages 'citation("pkgname")'.
##
## Attaching package: 'AnnotationDbi'
## The following object is masked from 'package:dplyr':
##
##     select
## Loading required package: DESeq2
## Loading required package: SummarizedExperiment
## Loading required package: DelayedArray
## Loading required package: matrixStats
##
## Attaching package: 'matrixStats'
## The following objects are masked from 'package:Biobase':
##
##     anyMissing, rowMedians
## The following object is masked from 'package:dplyr':
##
##     count
## Loading required package: BiocParallel
##
## Attaching package: 'DelayedArray'
## The following objects are masked from 'package:matrixStats':
##
##     colMaxs, colMins, colRanges, rowMaxs, rowMins, rowRanges
## The following object is masked from 'package:purrr':
##
##     simplify
## The following objects are masked from 'package:base':
##
##     aperm, apply, rowsum
## Loading required package: affy
## Loading required package: genefilter
##
## Attaching package: 'genefilter'
```

The following objects are masked from 'package:matrixStats':

##

rowSds, rowVars

The following object is masked from 'package:readr':

##

spec

ggplot2   RColorBrewer   dplyr   tibble   pheatmap

TRUE   TRUE   TRUE   TRUE   TRUE

tidyverse   limma   gplots   tximport GenomicFeatures

TRUE   TRUE   TRUE   TRUE   TRUE

readr   DESeq2   affy   genefilter

TRUE   TRUE   TRUE   TRUE

```r
# function to run some plots : https://stackoverflow.com/questions/15720545/use-stat-summary-to-annotate-plot-with-number-of-observations
n_fun <- function(x){
  return(data.frame(y=-2, label=paste0("n=",length(x))))
}


sessionInfo()
```

R version 3.6.3 (2020-02-29)

Platform: x86_64-pc-linux-gnu (64-bit)

Running under: Ubuntu 18.04.5 LTS

##

Matrix products: default

BLAS: /usr/lib/x86_64-linux-gnu/atlas/libblas.so.3.10.3

LAPACK: /usr/lib/x86_64-linux-gnu/atlas/liblapack.so.3.10.3

##

locale:

[1] LC_CTYPE=en_GB.UTF-8   LC_NUMERIC=C

[3] LC_TIME=en_GB.UTF-8   LC_COLLATE=en_GB.UTF-8

[5] LC_MONETARY=en_GB.UTF-8   LC_MESSAGES=en_GB.UTF-8

[7] LC_PAPER=en_GB.UTF-8   LC_NAME=C

[9] LC_ADDRESS=C   LC_TELEPHONE=C

[11] LC_MEASUREMENT=en_GB.UTF-8 LC_IDENTIFICATION=C

##

```
## attached base packages:
## [1] stats4   parallel stats     graphics grDevices utils     datasets
## [8] methods   base
##
## other attached packages:
##  [1] genefilter_1.68.0        affy_1.64.0
##  [3] DESeq2_1.26.0            SummarizedExperiment_1.16.1
##  [5] DelayedArray_0.12.3      BiocParallel_1.20.1
##  [7] matrixStats_0.60.1       GenomicFeatures_1.38.2
##  [9] AnnotationDbi_1.48.0     Biobase_2.46.0
## [11] GenomicRanges_1.38.0     GenomeInfoDb_1.22.1
## [13] IRanges_2.20.2           S4Vectors_0.24.4
## [15] BiocGenerics_0.32.0      tximport_1.14.2
## [17] gplots_3.1.1             limma_3.42.2
## [19] forcats_0.5.1            stringr_1.4.0
## [21] purrr_0.3.4              readr_2.0.1
## [23] tidyr_1.1.3              tidyverse_1.3.1
## [25] pheatmap_1.0.12          tibble_3.1.4
## [27] dplyr_1.0.7              RColorBrewer_1.1-2
## [29] ggplot2_3.3.5            BiocStyle_2.14.4
## [31] knitr_1.33
##
## loaded via a namespace (and not attached):
##  [1] readxl_1.3.1          backports_1.2.1     Hmisc_4.5-0
##  [4] BiocFileCache_1.10.2  splines_3.6.3       digest_0.6.27
##  [7] htmltools_0.5.2       fansi_0.5.0         magrittr_2.0.1
## [10] checkmate_2.0.0       memoise_2.0.0       cluster_2.1.2
## [13] tzdb_0.1.2            Biostrings_2.54.0   annotate_1.64.0
## [16] modelr_0.1.8          askpass_1.1         prettyunits_1.1.1
## [19] jpeg_0.1-9            colorspace_2.0-2    blob_1.2.2
## [22] rvest_1.0.1           rappdirs_0.3.3      haven_2.4.3
## [25] xfun_0.25             crayon_1.4.1        RCurl_1.98-1.4
## [28] jsonlite_1.7.2        survival_3.2-13     glue_1.4.2
## [31] gtable_0.3.0          zlibbioc_1.32.0     XVector_0.26.0
```

```
## [34] scales_1.1.1          DBI_1.1.1           Rcpp_1.0.7
## [37] xtable_1.8-4          progress_1.2.2      htmlTable_2.2.1
## [40] foreign_0.8-76        bit_4.0.4           preprocessCore_1.48.0
## [43] Formula_1.2-4         htmlwidgets_1.5.3   httr_1.4.2
## [46] ellipsis_0.3.2        pkgconfig_2.0.3     XML_3.99-0.3
## [49] nnet_7.3-16           sass_0.4.0          dbplyr_2.1.1
## [52] locfit_1.5-9.4        utf8_1.2.2          tidyselect_1.1.1
## [55] rlang_0.4.11          munsell_0.5.0       cellranger_1.1.0
## [58] tools_3.6.3           cachem_1.0.6        cli_3.0.1
## [61] generics_0.1.0        RSQLite_2.2.8       broom_0.7.9
## [64] evaluate_0.14         fastmap_1.1.0       yaml_2.2.1
## [67] bit64_4.0.5           fs_1.5.0            caTools_1.18.2
## [70] xml2_1.3.2            biomaRt_2.42.1      compiler_3.6.3
## [73] rstudioapi_0.13       curl_4.3.2          png_0.1-7
## [76] affyio_1.56.0         reprex_2.0.1        geneplotter_1.64.0
## [79] bslib_0.3.0           stringi_1.7.4       lattice_0.20-44
## [82] Matrix_1.3-4          vctrs_0.3.8         pillar_1.6.2
## [85] lifecycle_1.0.0       BiocManager_1.30.16 jquerylib_0.1.4
## [88] data.table_1.14.0     bitops_1.0-7        rtracklayer_1.46.0
## [91] R6_2.5.1              latticeExtra_0.6-29 KernSmooth_2.23-20
## [94] gridExtra_2.3         gtools_3.9.2        assertthat_0.2.1
## [97] openssl_1.4.5         withr_2.4.2         GenomicAlignments_1.22.1
## [100] Rsamtools_2.2.3      GenomeInfoDbData_1.2.2 hms_1.1.0
## [103] grid_3.6.3           rpart_4.1-15        rmarkdown_2.10
## [106] lubridate_1.7.10     base64enc_0.1-3
```

To start we want to make sure we are in the correct working directory- if not set it up, this has to be the directory / folder where you have your data (e.g. the count matrix). Note that the output, unless otherwise specified will be saved in this directory:

```
getwd()
```

```
## [1] "/home/flavia/Documents/Arti"
```

```
setwd(dir="~/Documents/Arti/") # change inside the double quotes
```

Input the count data file:

```
countmatrix <- read.table("arti_ryr1_counts_matrix.txt", header=TRUE, sep="\t", row.names=1)
head(countmatrix)
```

```
##                sample_name_1 sample_name_2 sample_name_3 sample_name_4
## ENSMUSG00000102628          0             0             0             0
## ENSMUSG00000100595          0             0             0             0
## ENSMUSG00000097426          0             0             0             0
## ENSMUSG00000104478          0             0             0             0
## ENSMUSG00000104385          0             0             0             0
## ENSMUSG00000086053          0             0             0             0
##                sample_name_5 sample_name_6 sample_name_7 sample_name_8
## ENSMUSG00000102628          0             0             0             0
## ENSMUSG00000100595          0             0             0             0
## ENSMUSG00000097426          1             0             0             0
## ENSMUSG00000104478          0             0             0             0
## ENSMUSG00000104385          0             0             0             0
## ENSMUSG00000086053          0             0             0             0
##                sample_name_9 sample_name_10 sample_name_11 sample_name_12
## ENSMUSG00000102628          0              0              0              0
## ENSMUSG00000100595          0              0              0              0
## ENSMUSG00000097426          0              0              0              0
## ENSMUSG00000104478          0              0              0              0
## ENSMUSG00000104385          0              0              0              0
## ENSMUSG00000086053          0              0              0              0
##                sample_name_13
## ENSMUSG00000102628          0
## ENSMUSG00000100595          0
## ENSMUSG00000097426          0
## ENSMUSG00000104478          0
## ENSMUSG00000104385          0
## ENSMUSG00000086053          0

#rownames(countmatrix) <- countmatrix$Geneid

class(countmatrix) # if not a matrix transform to a matrix
## [1] "data.frame"

countmatrix <- as.matrix(countmatrix)

class(countmatrix)
```

```
## [1] "matrix"
```

```
head(countmatrix)
```

```
##                     sample_name_1 sample_name_2 sample_name_3 sample_name_4
## ENSMUSG00000102628              0             0             0             0
## ENSMUSG00000100595              0             0             0             0
## ENSMUSG00000097426              0             0             0             0
## ENSMUSG00000104478              0             0             0             0
## ENSMUSG00000104385              0             0             0             0
## ENSMUSG00000086053              0             0             0             0
##                     sample_name_5 sample_name_6 sample_name_7 sample_name_8
## ENSMUSG00000102628              0             0             0             0
## ENSMUSG00000100595              0             0             0             0
## ENSMUSG00000097426              1             0             0             0
## ENSMUSG00000104478              0             0             0             0
## ENSMUSG00000104385              0             0             0             0
## ENSMUSG00000086053              0             0             0             0
##                     sample_name_9 sample_name_10 sample_name_11 sample_name_12
## ENSMUSG00000102628              0              0              0              0
## ENSMUSG00000100595              0              0              0              0
## ENSMUSG00000097426              0              0              0              0
## ENSMUSG00000104478              0              0              0              0
## ENSMUSG00000104385              0              0              0              0
## ENSMUSG00000086053              0              0              0              0
##                     sample_name_13
## ENSMUSG00000102628               0
## ENSMUSG00000100595               0
## ENSMUSG00000097426               0
## ENSMUSG00000104478               0
## ENSMUSG00000104385               0
## ENSMUSG00000086053               0
```

Next you want to read the metadata file in. This file contain the information for each sample. For every sample you will need to have for every column name in the count matrix information for example

	Sample
Sample_name_01	
Sample_name_02	
…	

You can create this in excel and save it as csv

Here I am uploading a sample from

```
sampleInfo <- read.csv('Arti_metadata.csv' , header=T)
head(sampleInfo)
##    Sample_name sample_ID sample_type   Group Concentrations_ng_ml
## 1 sample_name_1     401  Myometrium G2_HT_P              1433
## 2 sample_name_2     402  Myometrium G2_HT_P              3357
## 3 sample_name_3     398  Myometrium G2_HT_P              3086
## 4 sample_name_4     393  Myometrium G2_HT_P              3033
## 5 sample_name_5     420  Myometrium G2_HT_P              1970
## 6 sample_name_6     414  Myometrium G2_HT_P              2037
dim(sampleInfo)
## [1] 13  5
rownames(sampleInfo) <-sampleInfo$Sample_name
```

Few checks before running DESeq2:

Before running DESeq2 it is always best to look at the data. This can be done easily with some basic plots.

Barplot of the library size: This plot will show us how many reads we have for every sample Here we can see that samples 8 and 9 have lower counts . 13 is much higher

```
librarySizes <- colSums(countmatrix)
barplot(librarySizes,
    names=names(librarySizes),
    las=2,
```

```
    main="Barplot of library sizes")
abline(h=20e6, lty=2)
```

Barplot of library sizes
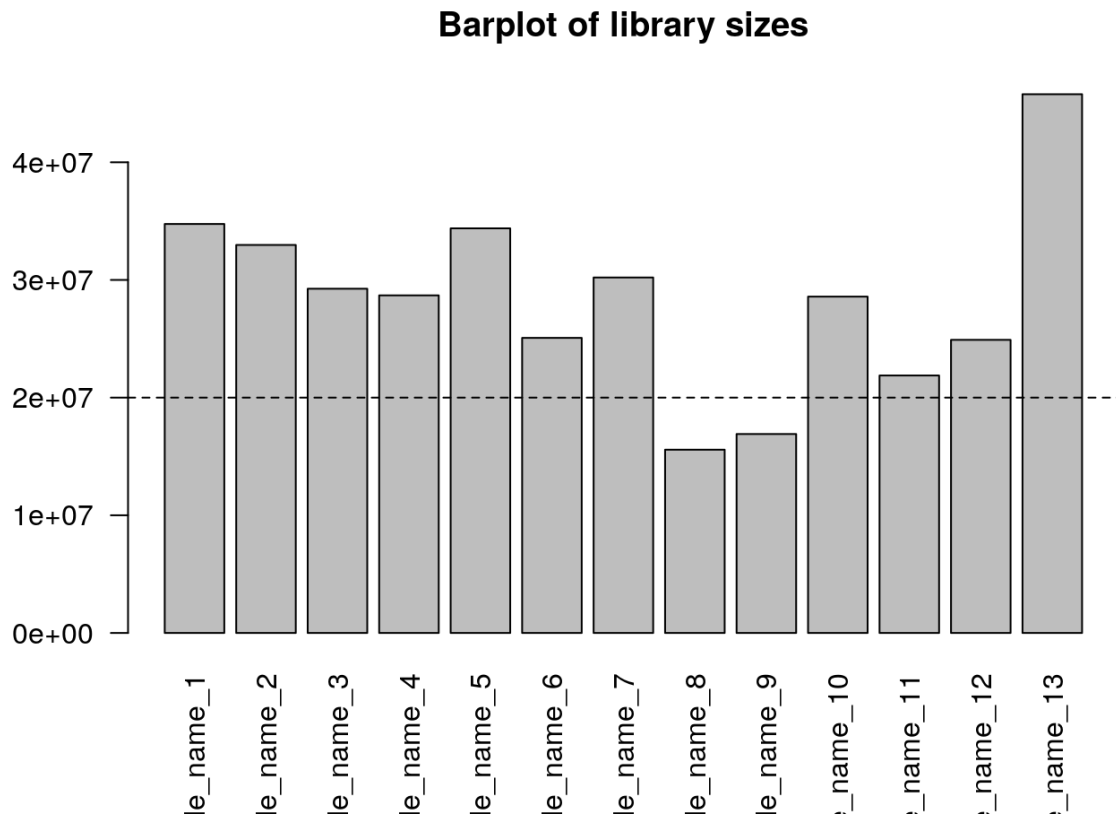
Now we can look at the count distribution as boxplot:

For your data you can change the vector statusCol base on your metadata of interest. For example if you have Reactions yes/no or different type of drugs etc…

```
# Get log2 counts
logcounts <- log2(countmatrix + 1)


# unique(sampleInfo$Group) #  G2_HT_P G3_WT_P


# make a colour vector
statusCol <- match(sampleInfo$Group, c("G2_HT_P", "G3_WT_P")) + 1


# Check distributions of samples using boxplots
boxplot(logcounts,
    xlab="",
    ylab="Log2(Counts)",
    las=2,
```

```
        col=statusCol)
```

abline(h=median(as.matrix(logcounts)), col="blue") *# Let's add a blue horizontal line that correspond s to the median*
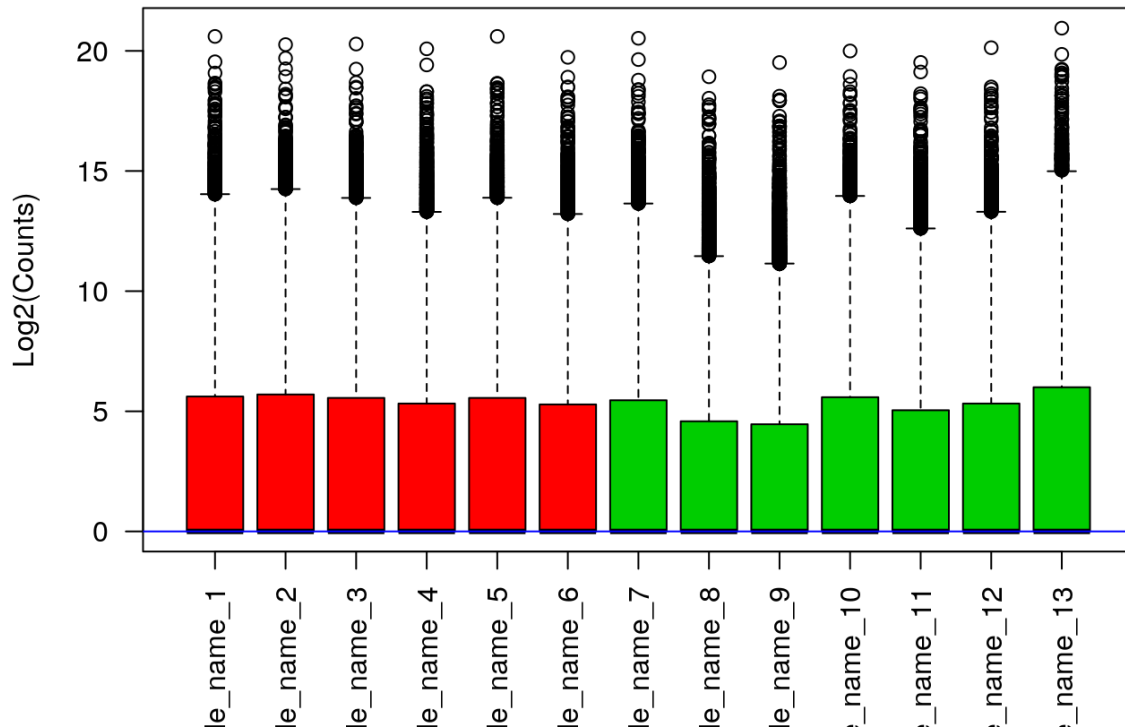
Here we can see that we have counts=to zero. If this is the case for your matrix we need to delete this.

@Prasanth: will you suggest keeping >1 or >5? **Suggestion from Prasanth:** set it at the size of the smallest variable of interest group -1. So in your case Arti it will be 6-1=5 with the reasoning being that at least sample in any group will have a 0 count so very unlikely to be of interest.

keep <- rowSums(countmatrix) > 5 *# might try with one*

countmatrix.reduce <- countmatrix[keep,]

dim(countmatrix) *# from 55416*

[1] 55416   13

dim(countmatrix.reduce) *# to 25812*

[1] 25812   13

Now let's re-run the plot:

 # Get log2 counts

logcounts.reduce <- log2(countmatrix.reduce + 1)

Next we are ready to run DESeq2

Arti here is where base on your metadata you create your design. For example if you have treatment and days or treatment and outcome

```
                                    design=~Group)
```

Let's run the Differential expression analysis with DESeq2

ddsObj.raw

class: DESeqDataSet

dim: 25812 13

metadata(1): version

assays(1): counts

rownames(25812): ENSMUSG00000102135 ENSMUSG00000100764 ...

ENSMUSG00000095041 ENSMUSG00000095742

rowData names(0):

colnames(13): sample_name_1 sample_name_2 ... sample_name_12

sample_name_13

colData names(5): Sample_name sample_ID sample_type Group

Concentrations_ng_ml

colData(ddsObj.raw) *# as we have set up the rownames as sampleID we can see it here*

DataFrame with 13 rows and 5 columns

Sample_name sample_ID sample_type   Group

<factor> <integer>   <factor> <factor>

sample_name_1   sample_name_1   401 Myometrium G2_HT_P

sample_name_2   sample_name_2   402 Myometrium G2_HT_P

sample_name_3   sample_name_3   398 Myometrium G2_HT_P

sample_name_4   sample_name_4   393 Myometrium G2_HT_P

sample_name_5   sample_name_5   420 Myometrium G2_HT_P

...   .

sample_name_9   sample_name_9   410 Myometrium G3_WT_P

sample_name_10 sample_name_10   421 Myometrium G3_WT_P

sample_name_11 sample_name_11   416 Myometrium G3_WT_P

sample_name_12 sample_name_12   417 Myometrium G3_WT_P

sample_name_13 sample_name_13   412 Myometrium G3_WT_P

Concentrations_ng_ml

<integer>

sample_name_1   1433

```
## sample_name_2          3357
## sample_name_3          3086
## sample_name_4          3033
## sample_name_5          1970
## ...                     ...
## sample_name_9          2675
## sample_name_10          2920
## sample_name_11          2019
## sample_name_12          1976
## sample_name_13          2484
```

head(assay(ddsObj.raw))

```
##                sample_name_1 sample_name_2 sample_name_3 sample_name_4
## ENSMUSG00000102135           23            26            17            58
## ENSMUSG00000100764            9             4             3             6
## ENSMUSG00000100635            4             3             2             1
## ENSMUSG00000100480            7             7             9             8
## ENSMUSG00000114212            3            12             3             4
## ENSMUSG00000114943            0             2             0             1
##                sample_name_5 sample_name_6 sample_name_7 sample_name_8
## ENSMUSG00000102135           17            36            19            10
## ENSMUSG00000100764            8             0             3             4
## ENSMUSG00000100635            1             1             0             1
## ENSMUSG00000100480            5             3             6             0
## ENSMUSG00000114212            0             0             0             3
## ENSMUSG00000114943            0             0             1             1
##                sample_name_9 sample_name_10 sample_name_11 sample_name_12
## ENSMUSG00000102135            7            13            25            35
## ENSMUSG00000100764            2             8             4             5
## ENSMUSG00000100635            1             4             0             2
## ENSMUSG00000100480            1             6             8             2
## ENSMUSG00000114212            0             3             0             6
## ENSMUSG00000114943            1             1             2             0
##                sample_name_13
## ENSMUSG00000102135           45
```

```
## ENSMUSG00000100764          5

## ENSMUSG00000100635          0

## ENSMUSG00000100480          3

## ENSMUSG00000114212          0

## ENSMUSG00000114943          0
```

```
ddsObj <- estimateSizeFactors(ddsObj.raw)

colData(ddsObj.raw)
```

```
## DataFrame with 13 rows and 5 columns

##                Sample_name sample_ID sample_type    Group

##                   <factor> <integer>    <factor> <factor>

## sample_name_1   sample_name_1     401 Myometrium  G2_HT_P

## sample_name_2   sample_name_2     402 Myometrium  G2_HT_P

## sample_name_3   sample_name_3     398 Myometrium  G2_HT_P

## sample_name_4   sample_name_4     393 Myometrium  G2_HT_P

## sample_name_5   sample_name_5     420 Myometrium  G2_HT_P

## ...                   ...       ...         ...      ...

## sample_name_9   sample_name_9     410 Myometrium  G3_WT_P

## sample_name_10 sample_name_10     421 Myometrium  G3_WT_P

## sample_name_11 sample_name_11     416 Myometrium  G3_WT_P

## sample_name_12 sample_name_12     417 Myometrium  G3_WT_P

## sample_name_13 sample_name_13     412 Myometrium  G3_WT_P

##                Concentrations_ng_ml

##                           <integer>

## sample_name_1                  1433

## sample_name_2                  3357

## sample_name_3                  3086

## sample_name_4                  3033

## sample_name_5                  1970

## ...                             ...

## sample_name_9                  2675

## sample_name_10                 2920

## sample_name_11                 2019

## sample_name_12                 1976

## sample_name_13                 2484
```

Now you can see here that in the assay the row names are the transcripts. Still trying to find a solution there to put gene/transcript names

To view the summary per sample:

```
head(summary(assay(ddsObj.raw)))
## sample_name_1    sample_name_2    sample_name_3    sample_name_4
## Min.  :    0.0  Min.  :    0.0  Min.  :     0  Min.  :    0.0
## 1st Qu.:   5.0  1st Qu.:   5.0  1st Qu.:    4  1st Qu.:   4.0
## Median :   76.0  Median :   81.0  Median :    73  Median :   62.5
## Mean  : 1346.4  Mean  : 1277.3  Mean  :  1133  Mean  : 1111.4
## 3rd Qu.:  728.2  3rd Qu.:  726.2  3rd Qu.:   691  3rd Qu.:  583.0
## Max.  :1590259.0  Max.  :1255222.0  Max.  :1276735  Max.  :1112167.0
## sample_name_5    sample_name_6    sample_name_7    sample_name_8
## Min.  :    0.0  Min.  :    0.0  Min.  :    0.0  Min.  :    0.0
## 1st Qu.:   4.0  1st Qu.:   4.0  1st Qu.:   4.0  1st Qu.:   2.0
## Median :   75.0  Median :   61.0  Median :   68.0  Median :   37.5
## Mean  : 1332.0  Mean  : 971.4  Mean  : 1170.3  Mean  : 603.4
## 3rd Qu.:  756.2  3rd Qu.:  543.2  3rd Qu.:  661.2  3rd Qu.:  344.0
## Max.  :1590915.0  Max.  :870668.0  Max.  :1506780.0  Max.  :496801.0
## sample_name_9  sample_name_10  sample_name_11   sample_name_12
## Min.  :    0  Min.  :    0  Min.  :    0.0  Min.  :    0.0
## 1st Qu.:   2  1st Qu.:   4  1st Qu.:   3.0  1st Qu.:   4.0
## Median :  33  Median :  75  Median :   51.0  Median :   61.0
## Mean  : 655  Mean  : 1107  Mean  : 847.6  Mean  : 964.9
## 3rd Qu.:  336  3rd Qu.:  703  3rd Qu.:  474.0  3rd Qu.:  547.2
## Max.  :748949  Max.  :1045238  Max.  :751158.0  Max.  :1148170.0
## sample_name_13
## Min.  :    0
## 1st Qu.:   6
## Median :  99
## Mean  : 1774
## 3rd Qu.:  934
## Max.  :2017651
```

```
head(summary(assay(ddsObj)))
## sample_name_1    sample_name_2    sample_name_3    sample_name_4
```

```
## Min.   :    0.0 Min.   :    0.0 Min.   :    0 Min.   :    0.0
## 1st Qu.:    5.0 1st Qu.:    5.0 1st Qu.:    4 1st Qu.:    4.0
## Median :   76.0 Median :   81.0 Median :   73 Median :   62.5
## Mean   : 1346.4 Mean   : 1277.3 Mean   : 1133 Mean   : 1111.4
## 3rd Qu.:  728.2 3rd Qu.:  726.2 3rd Qu.:  691 3rd Qu.:  583.0
## Max.   :1590259.0 Max.   :1255222.0 Max.   :1276735 Max.   :1112167.0
## sample_name_5   sample_name_6   sample_name_7   sample_name_8
## Min.   :    0.0 Min.   :    0.0 Min.   :    0.0 Min.   :    0.0
## 1st Qu.:    4.0 1st Qu.:    4.0 1st Qu.:    4.0 1st Qu.:    2.0
## Median :   75.0 Median :   61.0 Median :   68.0 Median :   37.5
## Mean   : 1332.0 Mean   :  971.4 Mean   : 1170.3 Mean   :  603.4
## 3rd Qu.:  756.2 3rd Qu.:  543.2 3rd Qu.:  661.2 3rd Qu.:  344.0
## Max.   :1590915.0 Max.   :870668.0 Max.   :1506780.0 Max.   :496801.0
## sample_name_9   sample_name_10  sample_name_11  sample_name_12
## Min.   :    0 Min.   :    0 Min.   :    0.0 Min.   :    0.0
## 1st Qu.:    2 1st Qu.:    4 1st Qu.:    3.0 1st Qu.:    4.0
## Median :   33 Median :   75 Median :   51.0 Median :   61.0
## Mean   :  655 Mean   : 1107 Mean   :  847.6 Mean   :  964.9
## 3rd Qu.:  336 3rd Qu.:  703 3rd Qu.:  474.0 3rd Qu.:  547.2
## Max.   :748949 Max.   :1045238 Max.   :751158.0 Max.   :1148170.0
## sample_name_13
## Min.   :    0
## 1st Qu.:    6
## Median :   99
## Mean   : 1774
## 3rd Qu.:  934
## Max.   :2017651
```

Let's have a look at the number of reads per each sample:

```
barplot(colSums(assay(ddsObj.raw))/1000000,
    main="Total number of reads per sample (million)",
    col=ddsObj.raw$Status,
    #    names.arg="",
    las=1, horiz=TRUE,
    ylab="", cex.names=0.5,
```

```
    xlab="Million counts")
```

Total number of reads per sample (million)
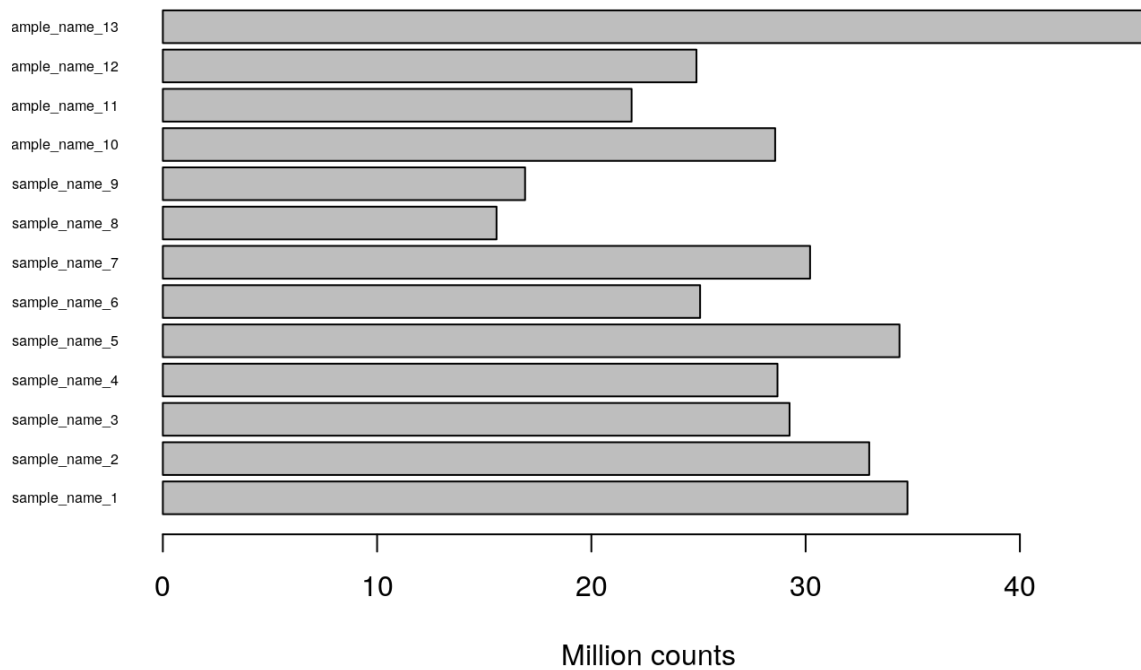
Let's have a look at the number of reads per each sample:

```
barplot(colSums(assay(ddsObj))/1000000,
    main="Total number of reads per sample (million)",
    col=ddsObj$Group,
#       names.arg="",
    las=1,  horiz=TRUE,
    ylab="", cex.names=0.5,
    xlab="Million counts")
```

Total number of reads per sample (million)
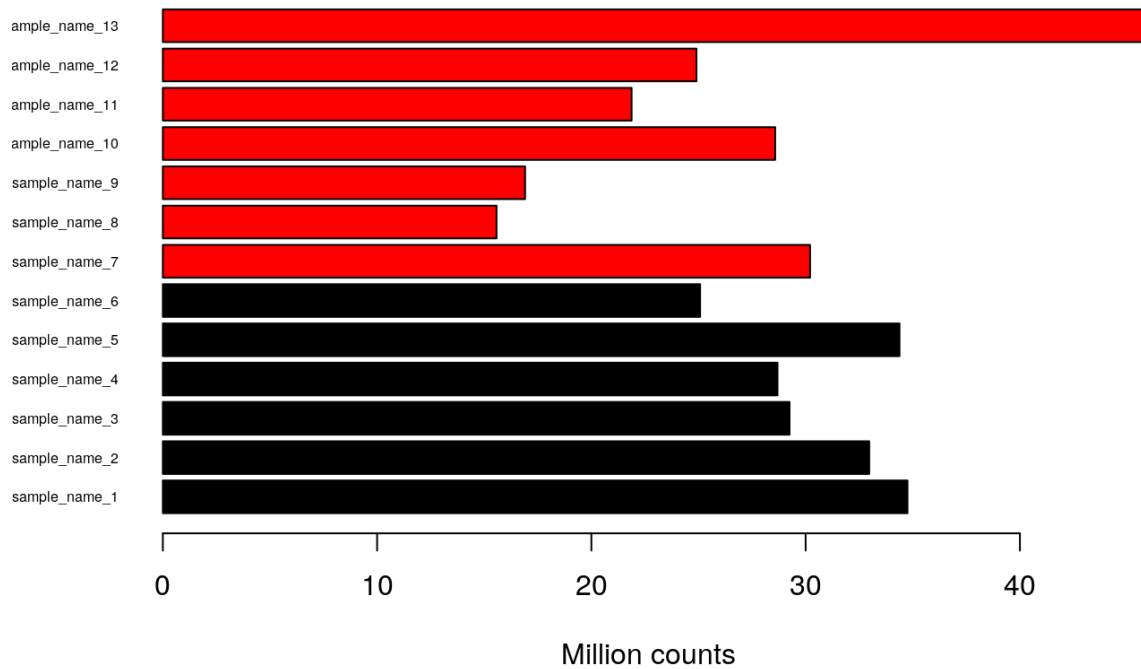
Plot by eliminating undetected genes:

```
prop.null <- apply(assay(ddsObj), 2, function(x) 100*mean(x==0))

print(head(prop.null))

## sample_name_1 sample_name_2 sample_name_3 sample_name_4 sample_name_5

##     7.577871     7.264063     8.186115    10.378894     8.941578

## sample_name_6

##    10.588099

barplot(prop.null, main="Percentage of null counts per sample",

    horiz=TRUE, cex.names=0.5, las=1,

    col=ddsObj$Group, ylab='', xlab='% of null counts')
```

Percentage of null counts per sample
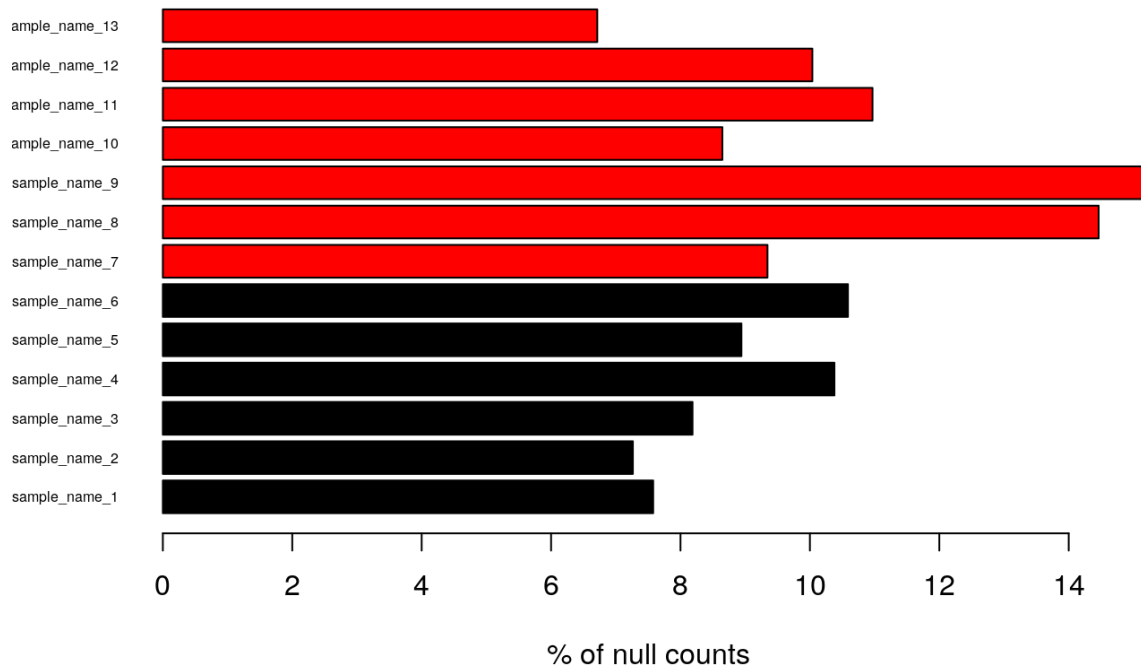
More exploration on the count data:

```
logcounts <- log2(countmatrix.reduce + 1)


limma::plotMA(logcounts)
abline(h=0, col="red")
```
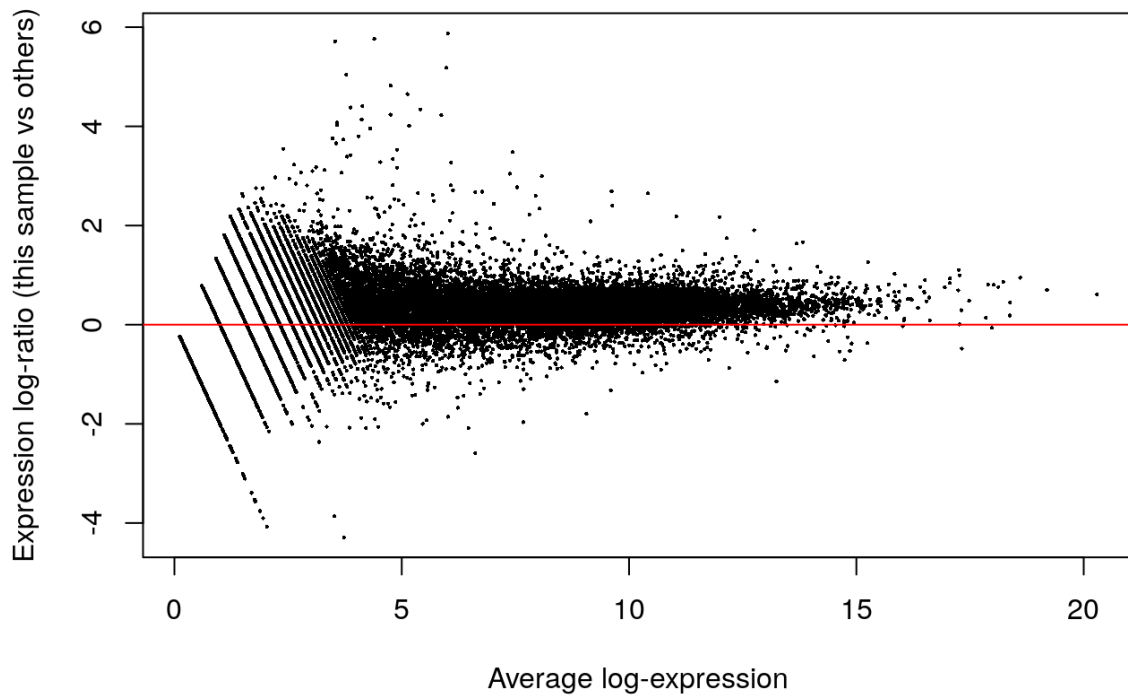
sample_name_1

Normalizing the counts:

```
normalizedCounts <- counts(ddsObj, normalized=TRUE)

logNormalizedCounts <- log2(normalizedCounts + 1)


limma::plotMA(logNormalizedCounts)

abline(h=0, col="red")
```

sample_name_1
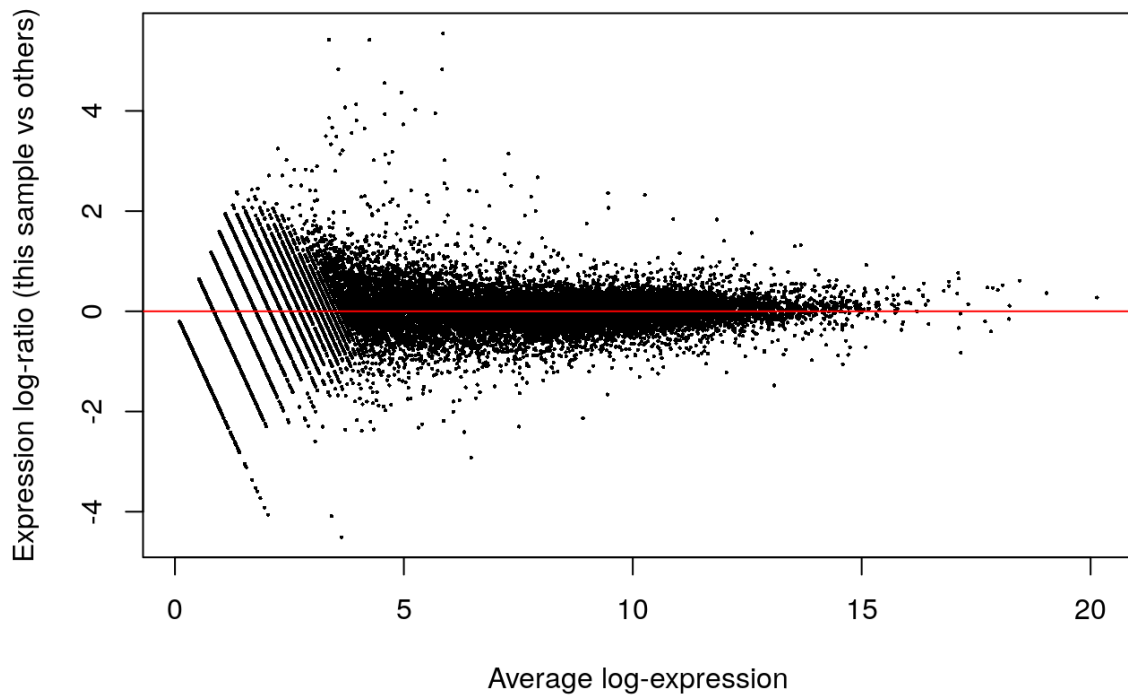
Now run some plots to check: Plot 1: raw counts. the scale is determined by the gene with the highest count, which is apparently an outlier

```
hist(as.matrix(assay(ddsObj)), col="blue", border="white", breaks=100)
```

Histogram of as.matrix(assay(ddsObj))
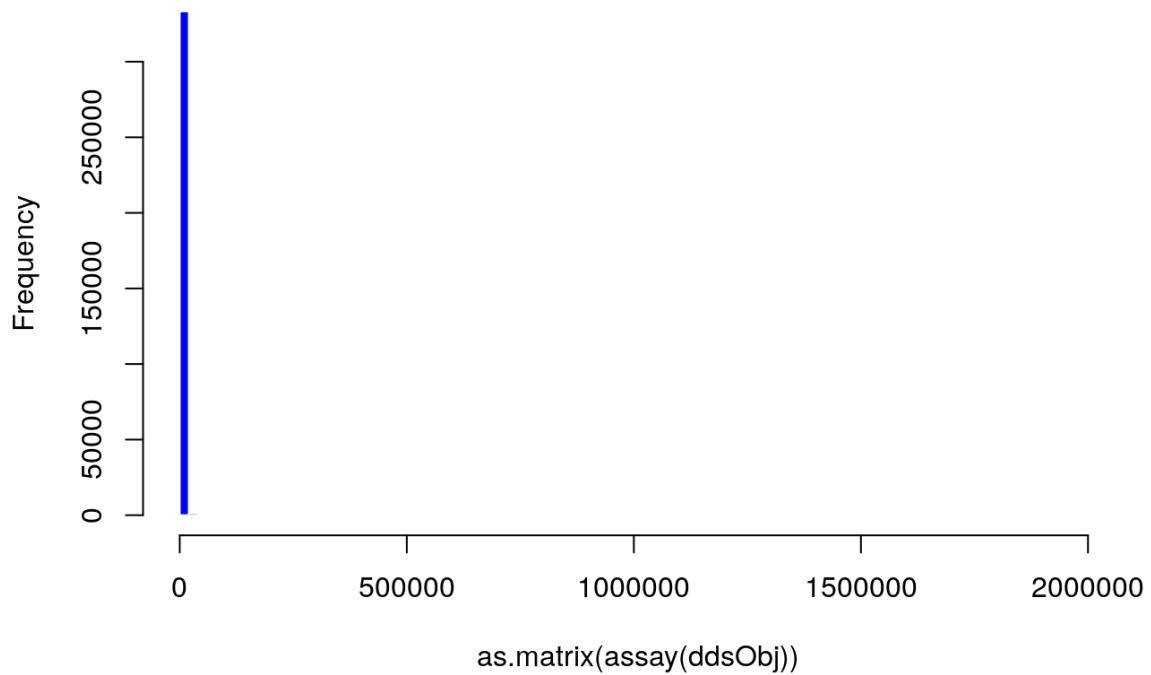
Plot 2: raw counts, with X axis truncated to 2000 in order to display a representative range despite outliers

```
hist(as.matrix(assay(ddsObj)), col="blue", border="white",
    breaks=20000, xlim=c(0,2000), main="Counts per gene",
    xlab="Counts (truncated axis)", ylab="Number of genes",
    las=1, cex.axis=0.7)
```

Counts per gene
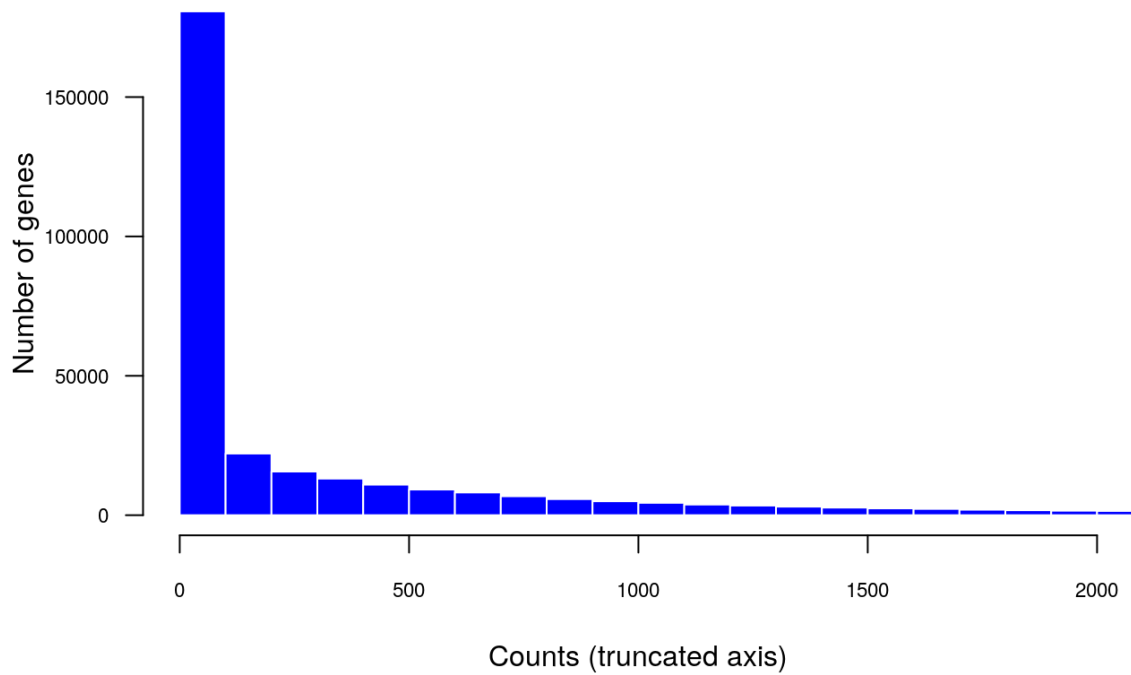
Plot3: log2-transformed counts (bottom) per gene, with a pseudocount of 1 to avoid minus infinitevalues resulting from zero counts and add offset of 1 to avoid problems with log(0)

```r
hist(as.matrix(log2(assay(ddsObj) + 1)), breaks=100, col="blue", border="white",
    main="Log2-transformed counts per gene", xlab="log2(counts+1)", ylab="Number of genes",
    las=1, cex.axis=0.7)
```

Log2-transformed counts per gene
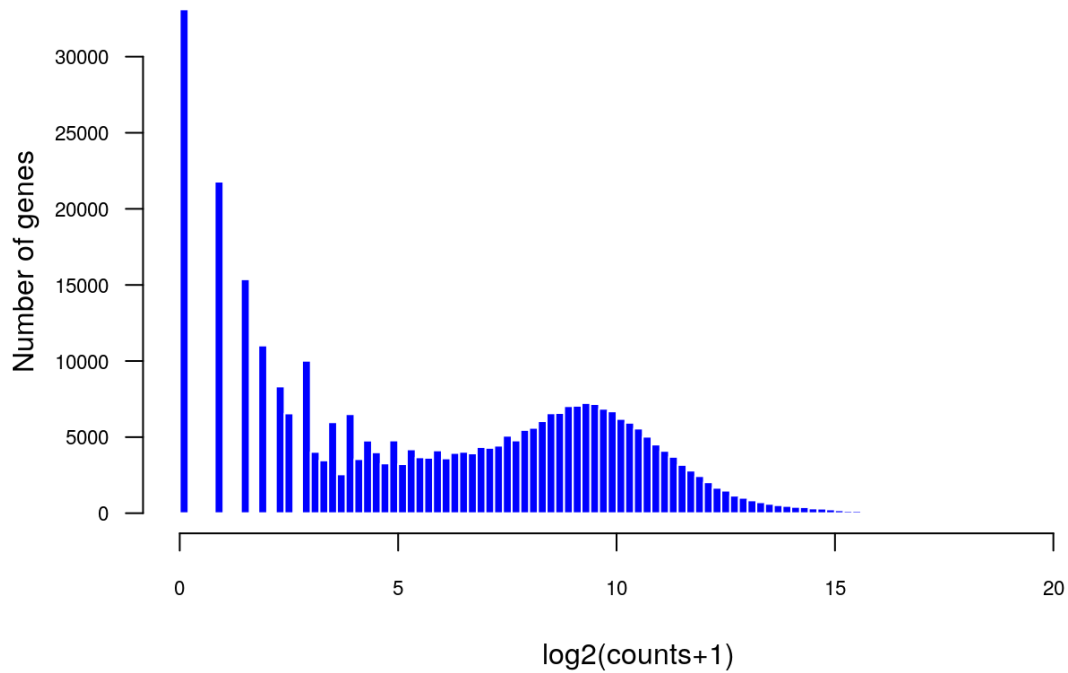
Boxplots of gene count distributions per sample:

```
boxplot(log2(assay(ddsObj) + 1),

    col =ddsObj$Group,

    pch=".",

    horizontal=TRUE, cex.axis=0.5,

    las=1, ylab="", xlab="log2(Counts +1)", main="Box plots of non-normalized log2(counts) per sa
mple")
```

Box plots of non-normalized log2(counts) per sample
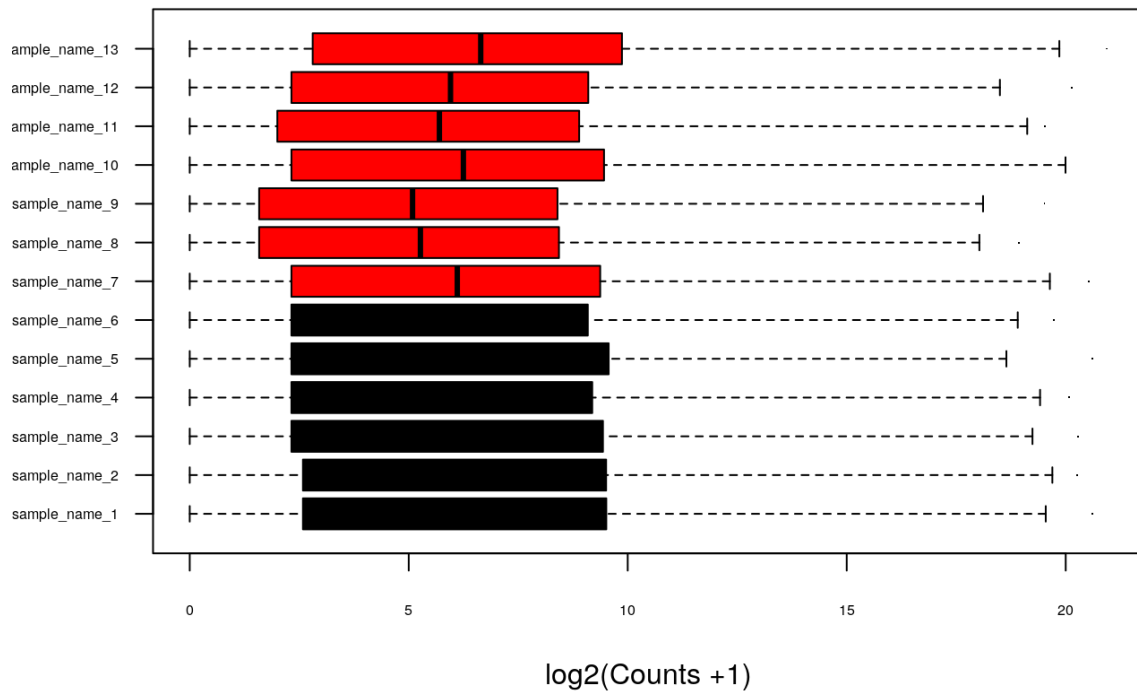
log2(Counts +1)

Density plot:

```
plot.new()

plotDensity(log2(assay(ddsObj) + 1), lty=1, col=ddsObj$Group, lwd=2)

#grid()

legend("topright", legend=unique(ddsObj$Group), col=unique(ddsObj$Group), lwd=2)
```
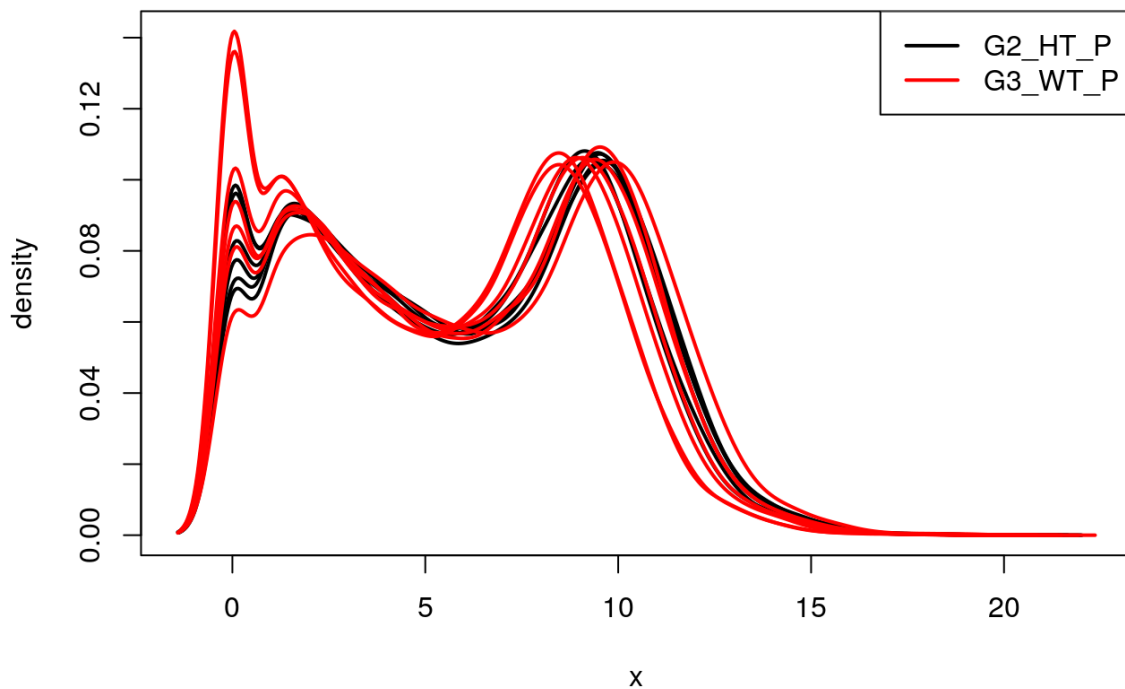
Scatter plot of log2-counts for a random selection of samples. For all samples as you have 6 – you can change nb.pairs as you have few samples in the secodn set

```
nb.pairs <- 13 # change here to use more samples



plotFun <- function(x,y){
  dns <- densCols(x,y);
  points(x,y, col=dns, pch=".", panel.first=grid());
  abline(a=0, b=1, col="brown")
}


set.seed(123) # forces the random number generator to produce fixed results. Should generally not be used, except for the sake of demonstration with a particular selection.
pairs(log2(assay(ddsObj)[,sample(ncol(assay(ddsObj)), nb.pairs)] + 1),
    panel=plotFun, lower.panel=NULL)
```
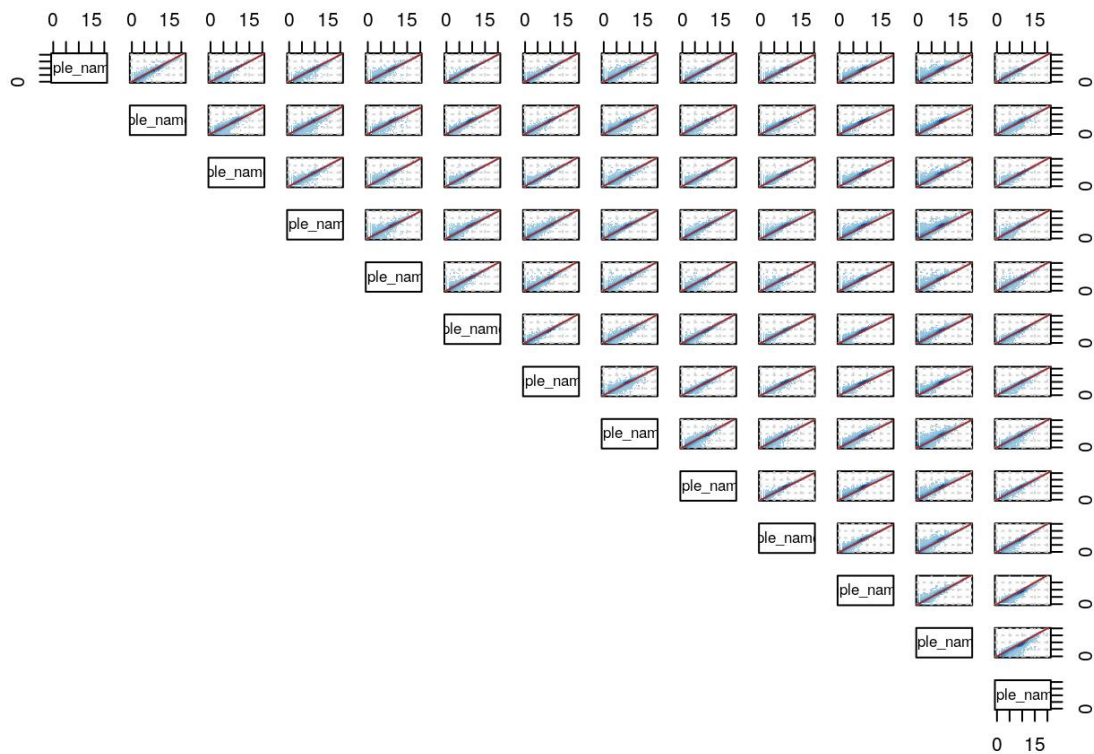
We are now going to explore the dataset before running DEG- differentiaally expressed gene - analyses Here you can see the the rdl is corrected by *using 'avgTxLength' from assays(dds), correcting for library size*

```
rld <- rlog(ddsObj, blind=TRUE)
```

We can look at the differences. First these are the counts from our dataset (integer)

```
head(assay(ddsObj))
## sample_name_1 sample_name_2 sample_name_3 sample_name_4
## ENSMUSG00000102135     23       26       17       58
## ENSMUSG00000100764      9        4        3        6
## ENSMUSG00000100635      4        3        2        1
## ENSMUSG00000100480      7        7        9        8
## ENSMUSG00000114212      3       12        3        4
## ENSMUSG00000114943      0        2        0        1
## sample_name_5 sample_name_6 sample_name_7 sample_name_8
## ENSMUSG00000102135     17       36       19       10
## ENSMUSG00000100764      8        0        3        4
## ENSMUSG00000100635      1        1        0        1
## ENSMUSG00000100480      5        3        6        0
```

475

```
## ENSMUSG00000114212          0          0          0          3
## ENSMUSG00000114943          0          0          1          1
##               sample_name_9 sample_name_10 sample_name_11 sample_name_12
## ENSMUSG00000102135          7         13         25         35
## ENSMUSG00000100764          2          8          4          5
## ENSMUSG00000100635          1          4          0          2
## ENSMUSG00000100480          1          6          8          2
## ENSMUSG00000114212          0          3          0          6
## ENSMUSG00000114943          1          1          2          0
##               sample_name_13
## ENSMUSG00000102135         45
## ENSMUSG00000100764          5
## ENSMUSG00000100635          0
## ENSMUSG00000100480          3
## ENSMUSG00000114212          0
## ENSMUSG00000114943          0
```

And these are the corrected by avgTxLength (floats)

```
head(assay(rld))
##               sample_name_1 sample_name_2 sample_name_3 sample_name_4
## ENSMUSG00000102135    4.4195105    4.4902176    4.3267738    5.1266272
## ENSMUSG00000100764    2.2472974    2.1049069    2.0787933    2.2104458
## ENSMUSG00000100635    0.6141201    0.5849572    0.5554375    0.5277440
## ENSMUSG00000100480    2.2430868    2.2480791    2.3170163    2.3289106
## ENSMUSG00000114212    1.2526065    1.5229050    1.2608131    1.3193509
## ENSMUSG00000114943   -0.4894386   -0.4148454   -0.4887218   -0.4423788
##               sample_name_5 sample_name_6 sample_name_7 sample_name_8
## ENSMUSG00000102135    4.2809982    4.8195135    4.3926549    4.4075073
## ENSMUSG00000100764    2.2138820    1.9806404    2.0842380    2.2203371
## ENSMUSG00000100635    0.5152665    0.5292249    0.4834940    0.5527140
## ENSMUSG00000100480    2.1798063    2.1577313    2.2366540    2.0598643
## ENSMUSG00000114212    1.1455613    1.1547264    1.1497931    1.3405729
## ENSMUSG00000114943   -0.4896863   -0.4866936   -0.4476436   -0.4232834
##               sample_name_9 sample_name_10 sample_name_11 sample_name_12
## ENSMUSG00000102135    4.2890382    4.2287865    4.6822966    4.7998365
```

## ENSMUSG00000100764	2.1175267	2.2366030	2.1658780	2.1802584
## ENSMUSG00000100635	0.5525435	0.6228573	0.4888152	0.5702308
## ENSMUSG00000100480	2.1164754	2.2281500	2.3703028	2.1176574
## ENSMUSG00000114212	1.1698211	1.2606771	1.1591294	1.3984454
## ENSMUSG00000114943	-0.4233724	-0.4493835	-0.3873893	-0.4867272

```
##               sample_name_13
## ENSMUSG00000102135   4.6316915
## ENSMUSG00000100764   2.0941445
## ENSMUSG00000100635   0.4778565
## ENSMUSG00000100480   2.0932246
## ENSMUSG00000114212   1.1397616
## ENSMUSG00000114943  -0.4915740
```

We can plot it to see a bit better. Explore effect of transformation: you can repeat for the rest by changing the numbers inside []

```
par( mfrow=c( 1, 2 ) )

ddsObj.ef <- estimateSizeFactors(ddsObj)

#first plot using the log2 function - here we need to log2 method, we need estimate size factors to account for sequencing depth (this is done automatically for the rlog method)
plot( log2( 1 + counts(ddsObj.ef, normalized=TRUE)[ , 1:2] ),
    col=rgb(0,0,0,.2), pch=16, cex=0.3 )

#second plot: the rlog-transformed values
plot( assay(rld)[ , 1:2],
    col=rgb(0,0,0,.2), pch=16, cex=0.3 )
```
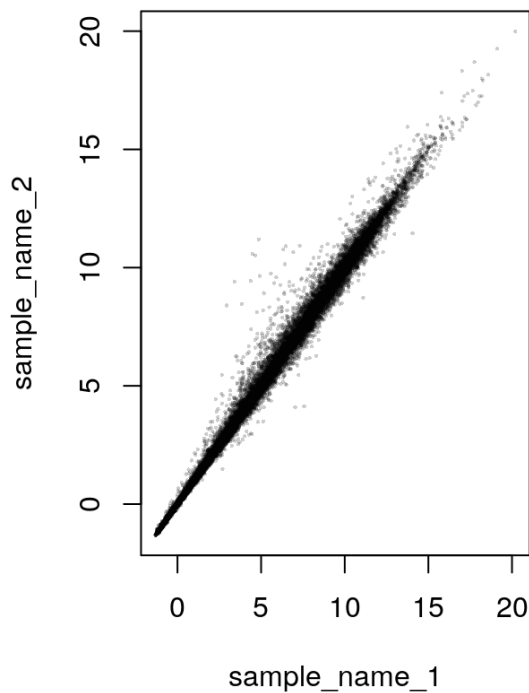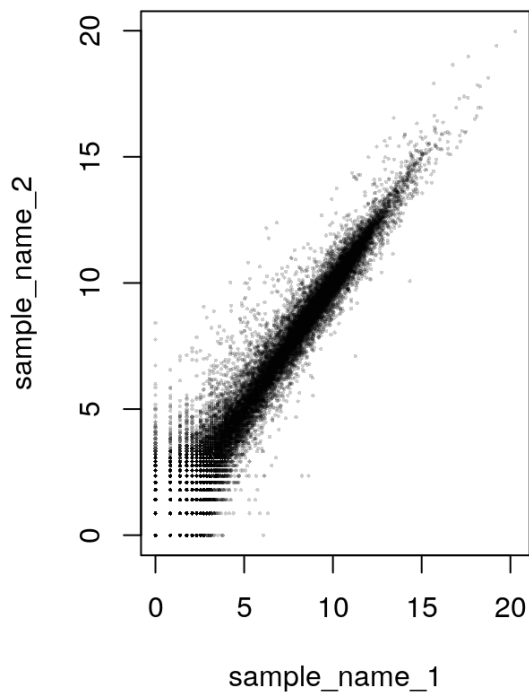
```
#reset par :
par( mfrow=c( 1, 1) )
#dev.off( )
```

Again before moving forward more exploratory we want to assess overall similarity between samples. For example which samples are similar to each other, which are different? Does this fit to the expectation from the experiment's design?

```
sampleDists <- dist(t(assay(rld)))
#sampleDists
sampleDistMatrix <- as.matrix(sampleDists)
```

Plot the heatmap for the distance matrix (again remember we are looking at the distance between samples here):

```
colors <- colorRampPalette(rev(brewer.pal(9, "Blues")) )(255)
hc <- hclust(sampleDists)
heatmap.2(sampleDistMatrix, Rowv=as.dendrogram(hc),
        symm=TRUE, trace="none", col=colors,
        margins=c(2,10), labCol=FALSE )
```
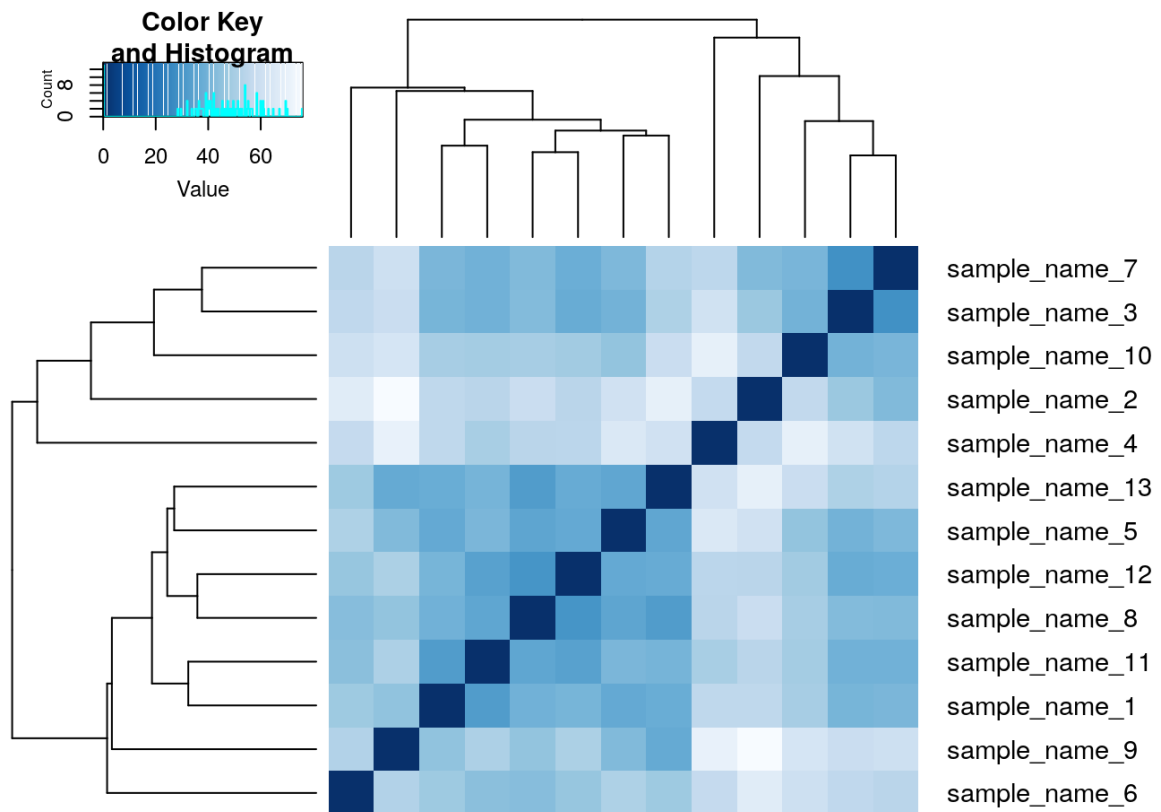
Next we can look at the PCA, based on different sample information

```
plotPCA(rld, intgroup ="Group")
```
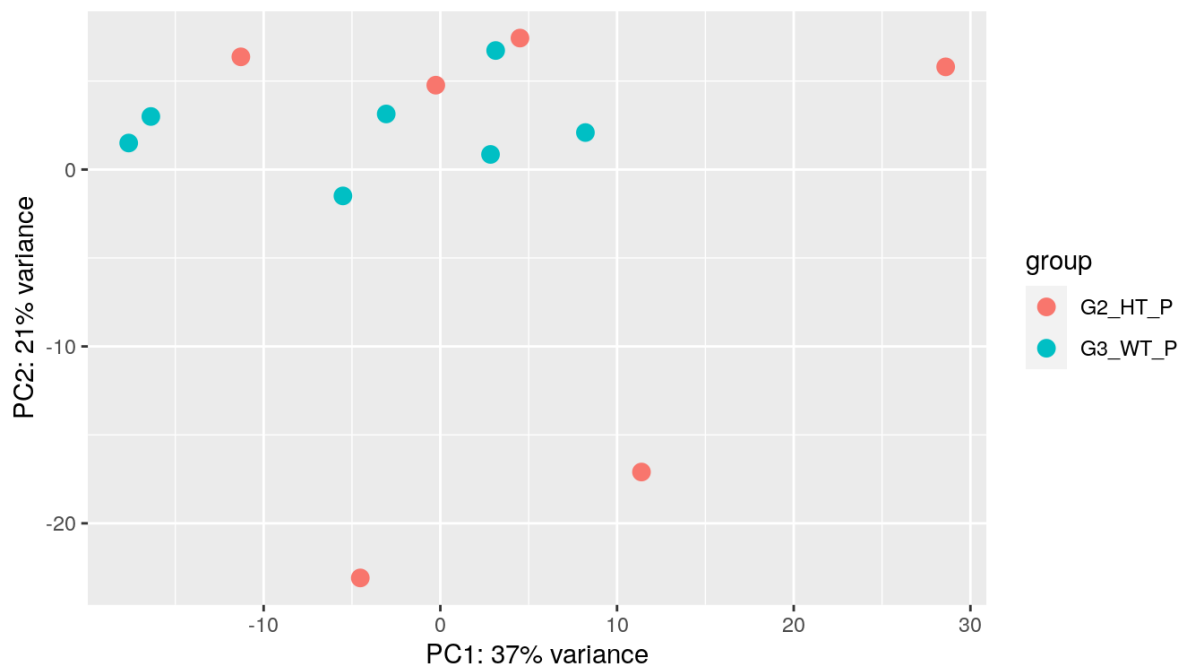
To save the data from the PCA and so you can use it to run other type of plots:

```
data <- plotPCA(rld, intgroup=c("Group"), returnData=TRUE) # if you have more factors: intgroup=c
( "Treatment", "Passage")

head(data)

##                PC1       PC2   group   Group        name
## sample_name_1 -0.2565147   4.768483 G2_HT_P G2_HT_P sample_name_1
## sample_name_2 28.6005149   5.804103 G2_HT_P G2_HT_P sample_name_2
## sample_name_3  4.5074245   7.430339 G2_HT_P G2_HT_P sample_name_3
## sample_name_4 11.3842876 -17.100164 G2_HT_P G2_HT_P sample_name_4
## sample_name_5 -11.2903727   6.369373 G2_HT_P G2_HT_P sample_name_5
## sample_name_6 -4.5304342 -23.087795 G2_HT_P G2_HT_P sample_name_6

#rownames(data) <- sub(".bam", "", rownames(data))

#head(data)

percentVar <- round(100 * attr(data, "percentVar"))

qplot(PC1, PC2, color=Group,  data=data) + #shape=Batch,

  xlab(paste0("PC1: ",percentVar[1],"% variance")) +

  ylab(paste0("PC2: ",percentVar[2],"% variance"))  +

  geom_text(label= rownames(data) , size=2.5, color="black")
```
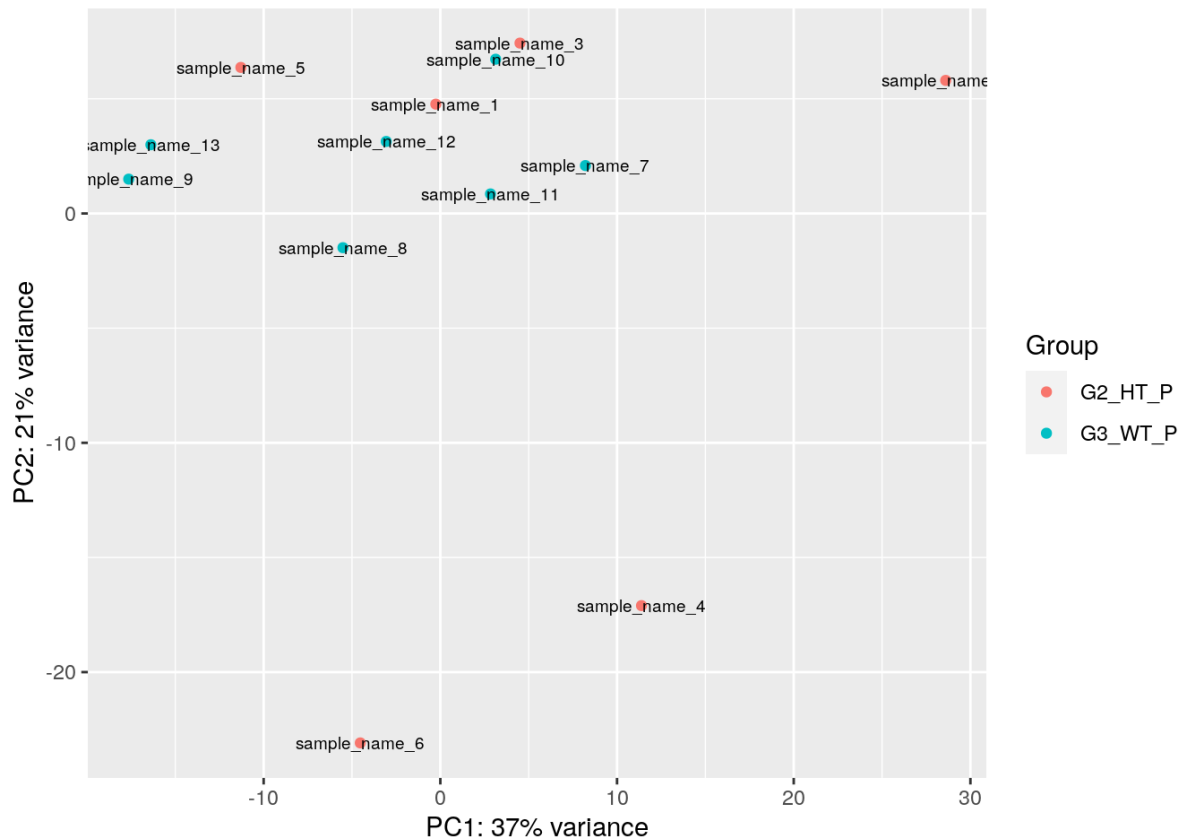
Repeat plot above if you have other variables to explore

IMPORTANT DESeq2 doesn't actually use normalized counts, rather it uses the raw counts and models the normalization inside the Generalized Linear Model (GLM). These normalized counts will be useful for downstream visualization of results, but cannot be used as input to DESeq2 or any other tools that perform differential expression analysis that use the negative binomial model.

To prepare the normalise counts in case you want to run some plots run the following:

```
ddsObj.norm <- estimateSizeFactors(ddsObj)

sizeFactors(ddsObj.norm)

## sample_name_1 sample_name_2 sample_name_3 sample_name_4 sample_name_5
##     1.2503732     1.2186079     1.1540061     0.9629107     1.2864324
## sample_name_6 sample_name_7 sample_name_8 sample_name_9 sample_name_10
##     0.9324751     1.1029308     0.5831688     0.5850459     1.1555149
## sample_name_11 sample_name_12 sample_name_13
##     0.8091009     0.9356377     1.6213211

normalized_counts <- counts(ddsObj.norm, normalized=TRUE)

head(normalized_counts)

##                 sample_name_1 sample_name_2 sample_name_3 sample_name_4
## ENSMUSG00000102135     18.394508     21.335820     14.731291     60.234040
## ENSMUSG00000100764      7.197851      3.282434      2.599640      6.231108
```

```
## ENSMUSG00000100635    3.199045    2.461825    1.733093    1.038518
## ENSMUSG00000100480    5.598328    5.744259    7.798919    8.308143
## ENSMUSG00000114212    2.399284    9.847302    2.599640    4.154072
## ENSMUSG00000114943    0.000000    1.641217    0.000000    1.038518
##              sample_name_5 sample_name_6 sample_name_7 sample_name_8
## ENSMUSG00000102135   13.2148417   38.606929   17.2268284   17.147693
## ENSMUSG00000100764    6.2187490    0.000000    2.7200255    6.859077
## ENSMUSG00000100635    0.7773436    1.072415    0.0000000    1.714769
## ENSMUSG00000100480    3.8867181    3.217244    5.4400511    0.000000
## ENSMUSG00000114212    0.0000000    0.000000    0.0000000    5.144308
## ENSMUSG00000114943    0.0000000    0.000000    0.9066752    1.714769
##              sample_name_9 sample_name_10 sample_name_11 sample_name_12
## ENSMUSG00000102135   11.964873   11.2503962   30.898493   37.407642
## ENSMUSG00000100764    3.418535    6.9233208    4.943759    5.343949
## ENSMUSG00000100635    1.709268    3.4616604    0.000000    2.137580
## ENSMUSG00000100480    1.709268    5.1924906    9.887518    2.137580
## ENSMUSG00000114212    0.000000    2.5962453    0.000000    6.412739
## ENSMUSG00000114943    1.709268    0.8654151    2.471879    0.000000
##              sample_name_13
## ENSMUSG00000102135   27.755144
## ENSMUSG00000100764    3.083905
## ENSMUSG00000100635    0.000000
## ENSMUSG00000100480    1.850343
## ENSMUSG00000114212    0.000000
## ENSMUSG00000114943    0.000000
```

#To save the file:

write.csv(normalized_counts, file="normalized_counts_Arti.csv", row.names=TRUE)

Differential Gene expression analyses:

Pay attention at the output here as it will tell you what it is using for correcting the library size. Currently it's using the avgTxLength . If you want to change it look at the options from the DESeq manual. From the DESeq run this is the output:

using pre-existing size factors estimating dispersions gene-wise dispersion estimates mean-dispersion relationship final dispersion estimates fitting model and testing – replacing outliers and refitting for 242 genes – DESeq argument 'minReplicatesForReplace'=7 – original counts are preserved in counts(dds) estimating dispersions fitting model and testing

```
dds2 <- ddsObj #this is the object where we have removed the zeros - set paramether 1-3 or 5

dds2 <- DESeq(dds2)

## using pre-existing size factors

## estimating dispersions

## gene-wise dispersion estimates

## mean-dispersion relationship

## final dispersion estimates

## fitting model and testing

## -- replacing outliers and refitting for 242 genes

## -- DESeq argument 'minReplicatesForReplace'=7

## -- original counts are preserved in counts(dds)

## estimating dispersions

## fitting model and testing

is(dds2) # it will tell you what is in the object

## [1] "DESeqDataSet"           "RangedSummarizedExperiment"

## [3] "SummarizedExperiment"       "Vector"

## [5] "Annotated"              "vector_OR_Vector"

slotNames(dds2) # The list of slot names

## [1] "design"           "dispersionFunction" "rowRanges"

## [4] "colData"          "assays"           "NAMES"

## [7] "elementMetadata"    "metadata"

# normalizationFactors(dds2)

resultsNames(dds2) #Group_G3_WT_P_vs_G2_HT_P

## [1] "Intercept"              "Group_G3_WT_P_vs_G2_HT_P"

plotDispEsts(dds2)
```
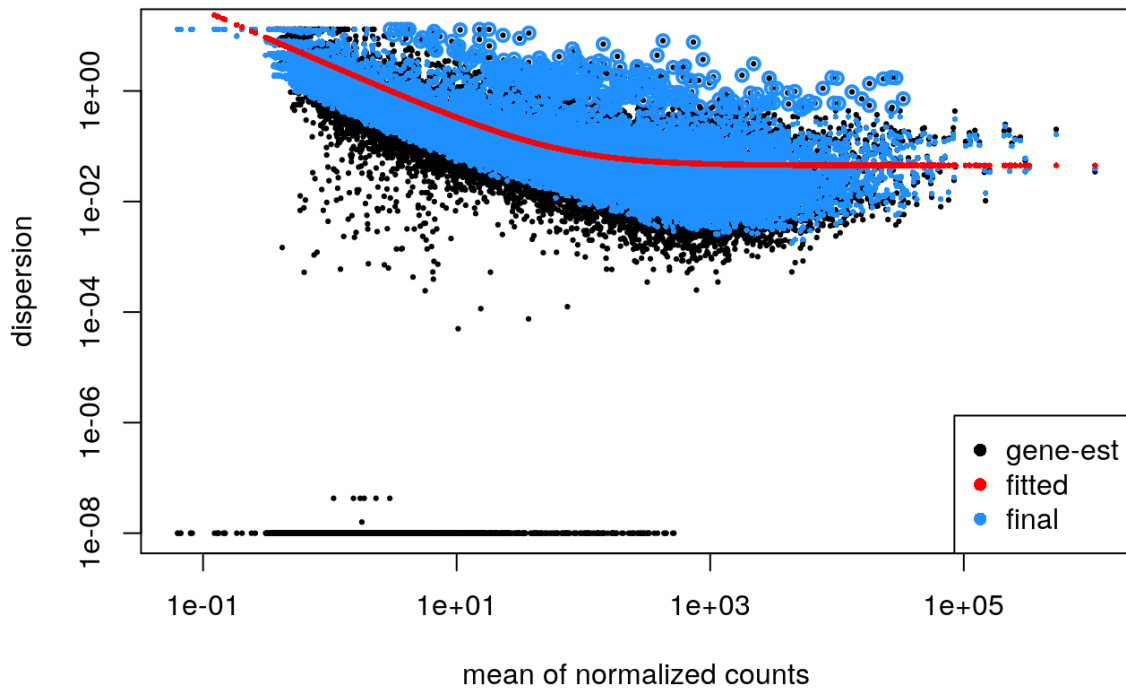
We can pull out the contrast to upload later on IPA These will be for example treatment vs control druga vs drugb druga vs drugc drugb vs drugc (etc)

To save the files you can set for top 5000 genes by selecting adjusted pvalues smaller than 0.05 (This is the significance cutoff used for optimizing the independent filtering (by default it is set to 0.1))

Important Note: The order of the names determines the direction of fold change that is reported. Also : option for p.adjust : p.adjust.methods : "holm", "hochberg", "hommel", "bonferroni", "BH", "BY", "fdr", "none"

The lfc.cutoff is set to 0.58; remember that we are working with log2 fold changes so this translates to an actual fold change of 1.5 which is pretty reasonable.

```
# To pull the full results
res <- results(dds2, alpha=0.05)
res
## log2 fold change (MLE): Group G3 WT P vs G2 HT P
## Wald test p-value: Group G3 WT P vs G2 HT P
## DataFrame with 25812 rows and 6 columns
##                      baseMean    log2FoldChange          lfcSE
##                     <numeric>         <numeric>      <numeric>
## ENSMUSG00000102135  24.6283460914837  -0.31558208918719 0.416170107424959
## ENSMUSG00000100764  4.52479631608259   0.11076510553664 0.541286267245177
```

```
## ENSMUSG00000100635  1.48503971480639 -0.489864386635388 0.942183973228078
## ENSMUSG00000100480  4.67468165948132 -0.580912451816887 0.550039562729969
## ENSMUSG00000114212   2.5502760301535 -0.682460104167013   1.2693939548233
## ...                  ...               ...              ...
## ENSMUSG00000079190 0.785271745409263  -1.87813949086817  1.26383042183822
## ENSMUSG00000062783  1.75635484363603 -0.281831088166237 0.810707798768583
## ENSMUSG00000079808   5.2164702134824 -0.198926728649688 0.504859651221177
## ENSMUSG00000095041   3072.0729638917 -0.101772633588557 0.195799460503383
## ENSMUSG00000095742  1624.41997162315  0.127470201038285 0.192724329134084
##                        stat          pvalue         padj
##                     <numeric>      <numeric>      <numeric>
## ENSMUSG00000102135 -0.758300712994129 0.448270980552261 0.994582265819313
## ENSMUSG00000100764  0.204633134515619 0.837858765572348 0.994582265819313
## ENSMUSG00000100635 -0.519924346576425 0.603116305434437 0.994582265819313
## ENSMUSG00000100480   -1.0561284881649 0.290909516630888 0.994582265819313
## ENSMUSG00000114212 -0.537626716728779 0.590834781706764 0.994582265819313
## ...                     ...               ...              ...
## ENSMUSG00000079190 -1.48606922132516 0.137260812447872 0.994582265819313
## ENSMUSG00000062783 -0.347635841907925 0.728113685261111 0.994582265819313
## ENSMUSG00000079808 -0.394023820617304 0.693563452631695 0.994582265819313
## ENSMUSG00000095041 -0.519779948968745 0.603216956141593 0.994582265819313
## ENSMUSG00000095742  0.661412088504924 0.508348075602878 0.994582265819313
```

Now check the distribution of p-values in the results

From Prasanth: If there are few or no DEGs then each bin may have broadly equal frequency. If the histogram comes back with the highest frequency bins clearly away from p=0.05 then again this may suggest a model issue.

```
hist(res$pvalue)
```

Histogram of res$pvalue
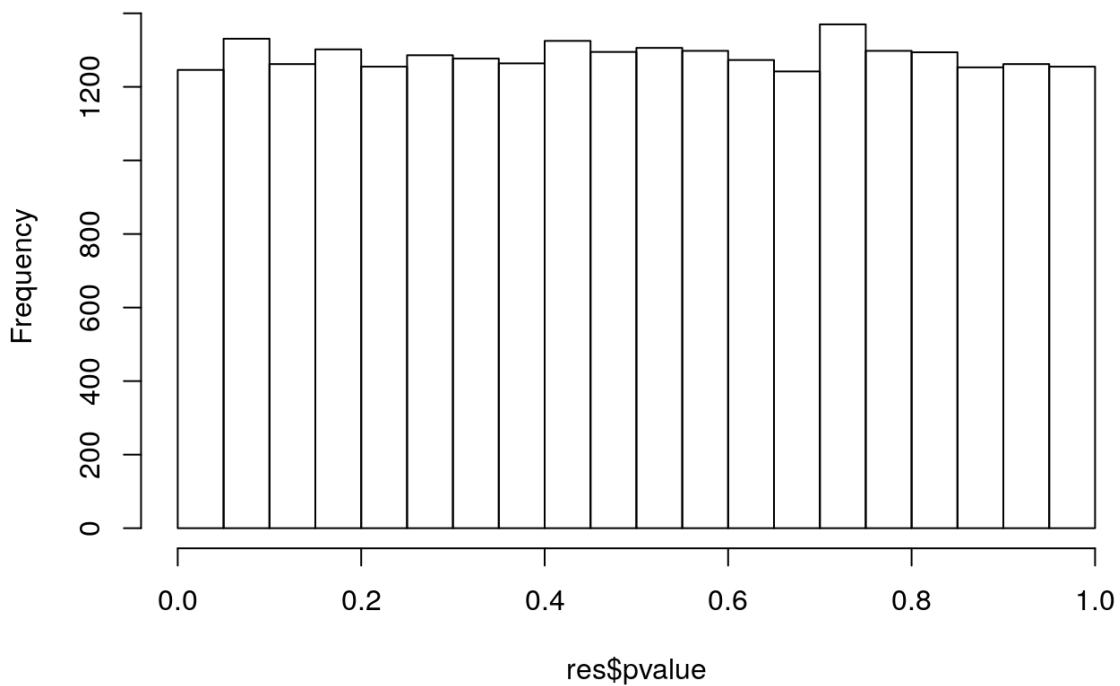

```
#For a specific contrast:
resPvV_status <- results(dds2,
        name="Group_G3_WT_P_vs_G2_HT_P",
        alpha=0.05)
resPvV_status
```

log2 fold change (MLE): Group G3 WT P vs G2 HT P

Wald test p-value: Group G3 WT P vs G2 HT P

DataFrame with 25812 rows and 6 columns

##	baseMean	log2FoldChange	lfcSE
##	\<numeric\>	\<numeric\>	\<numeric\>
## ENSMUSG00000102135	24.6283460914837	-0.31558208918719	0.416170107424959
## ENSMUSG00000100764	4.52479631608259	0.11076510553664	0.541286267245177
## ENSMUSG00000100635	1.48503971480639	-0.489864386635388	0.942183973228078
## ENSMUSG00000100480	4.67468165948132	-0.580912451816887	0.550039562729969
## ENSMUSG00000114212	2.5502760301535	-0.682460104167013	1.2693939548233
## ...	...	...	...
## ENSMUSG00000079190	0.785271745409263	-1.87813949086817	1.26383042183822
## ENSMUSG00000062783	1.75635484363603	-0.281831088166237	0.810707798768583

```
## ENSMUSG00000079808   5.2164702134824 -0.198926728649688 0.504859651221177
## ENSMUSG00000095041   3072.0729638917 -0.101772633588557 0.195799460503383
## ENSMUSG00000095742   1624.41997162315  0.127470201038285 0.192724329134084
##                         stat          pvalue          padj
##                     <numeric>       <numeric>      <numeric>
## ENSMUSG00000102135 -0.758300712994129 0.448270980552261 0.994582265819313
## ENSMUSG00000100764  0.204633134515619 0.837858765572348 0.994582265819313
## ENSMUSG00000100635 -0.519924346576425 0.603116305434437 0.994582265819313
## ENSMUSG00000100480  -1.0561284881649 0.290909516630888 0.994582265819313
## ENSMUSG00000114212 -0.537626716728779 0.590834781706764 0.994582265819313
## ...                       ...             ...            ...
## ENSMUSG00000079190 -1.48606922132516 0.137260812447872 0.994582265819313
## ENSMUSG00000062783 -0.347635841907925 0.728113685261111 0.994582265819313
## ENSMUSG00000079808 -0.394023820617304 0.693563452631695 0.994582265819313
## ENSMUSG00000095041 -0.519779948968745 0.603216956141593 0.994582265819313
## ENSMUSG00000095742  0.661412088504924 0.508348075602878 0.994582265819313
```

How many of the differentially expressed genes are there at FDR < 0.05

```
sum(resPvV_status$padj < 0.05, na.rm=TRUE) #2
## [1] 2
```

Write this to file so we can use it to upload to IPA:

```
write.csv(resPvV_status, 'resPvV_status_deg_allvalues_arti.csv')
```

If you want to extract only if P.adjusted < 0.05 then:

```
resPvV_status_reduced  <- resPvV_status%>%
  data.frame() %>%
  rownames_to_column(var="gene") %>%
  filter(padj< 0.05 )


#compare the two objects


dim(resPvV_status) # 25812
## [1] 25812    6
dim(resPvV_status_reduced) #2
```

[1] 2 7

Volcano plot for comparison virgin vs lactate:

Note : you can change the axis later to save figure # here adjustin the yaxis

```
cols <- densCols(resPvV_status$log2FoldChange, -log10(resPvV_status$pvalue))

plot(resPvV_status$log2FoldChange, -log10(resPvV_status$padj), col=cols, panel.first=grid(),

    main="Volcano plot virgin vs lzctate", xlab="Effect size: log2(fold-change)", ylab="-log10(adjusted p-value)",

    pch=20, cex=0.6, xlim=c(10, -10), ylim=c(0,15))

abline(v=0)

abline(v=c(-1,1), col="brown")

abline(h=-log10(0.05), col="brown")
```

Volcano plot virgin vs lzctate
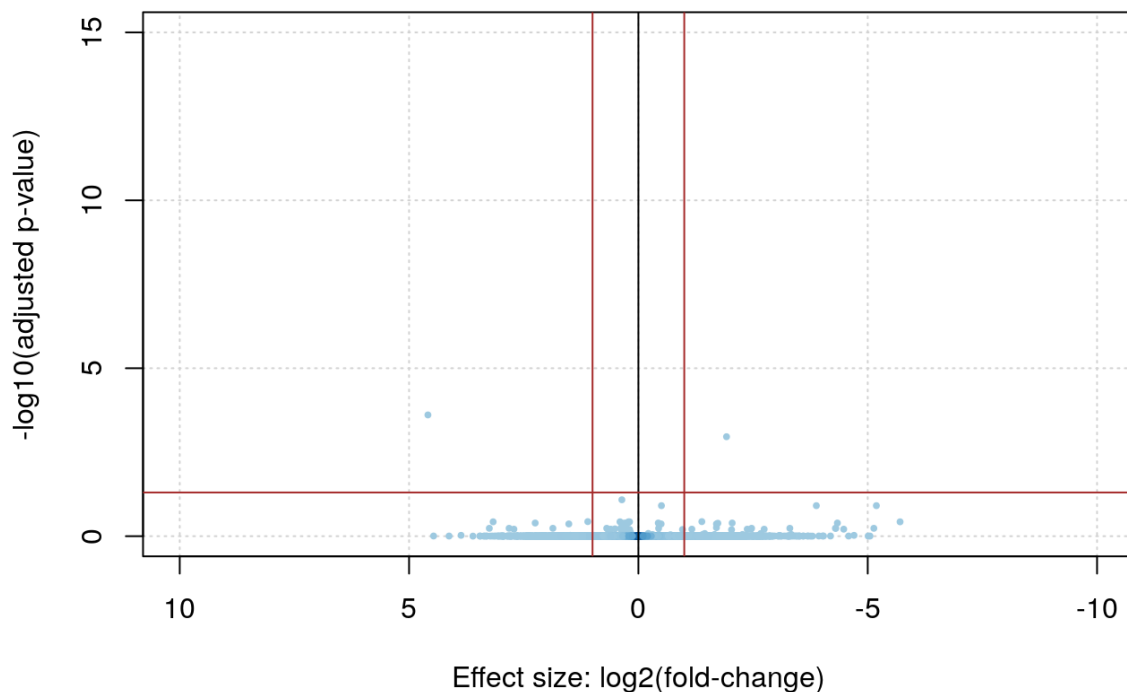
Extract the toip genes:

```
#top 100
topGenesPvV <- as.data.frame(resPvV_status) %>%

    rownames_to_column("GeneID") %>%

    arrange(padj) %>%

    head(100)
```

topGenesPvV

```
##          GeneID     baseMean log2FoldChange     lfcSE     stat
## 1   ENSMUSG00000096638 1.606135e+01     4.5889501 0.79966831  5.738567
## 2   ENSMUSG00000047730 3.716552e+03    -1.9212780 0.35870699 -5.356121
## 3   ENSMUSG00000033278 3.759892e+02     0.3602137 0.08139435  4.425537
## 4   ENSMUSG00000066760 1.087426e+02    -5.1885285 1.23435023 -4.203449
## 5   ENSMUSG00000025723 2.320276e+02    -0.5026479 0.12016981 -4.182813
## 6   ENSMUSG00000033765 2.072713e+01    -3.8795434 0.91538964 -4.238133
## 7   ENSMUSG00000113651 2.613730e+01     1.1034870 0.28608262  3.857232
## 8   ENSMUSG00000034634 1.874506e+02    -1.3833209 0.35810174 -3.862927
## 9   ENSMUSG00000014498 5.715808e+02     0.4012978 0.10490733  3.825260
## 10  ENSMUSG00000025332 2.174663e+03     0.1928568 0.05094307  3.785732
## 11  ENSMUSG00000042520 2.482991e+03     0.2167295 0.05783623  3.747296
## 12  ENSMUSG00000076514 5.045888e+01     3.1669402 0.84820837  3.733682
## 13  ENSMUSG00000070796 1.326174e+02    -5.7050063 1.52345899 -3.744772
## 14  ENSMUSG00000076522 6.232464e+01     2.2503011 0.61172619  3.678608
## 15  ENSMUSG00000055679 9.909447e+00    -4.3386044 1.19994930 -3.615656
## 16  ENSMUSG00000042700 2.141812e+03     0.2835914 0.07838807  3.617788
## 17  ENSMUSG00000022390 1.496407e+03     0.2285162 0.06244764  3.659325
## 18  ENSMUSG00000022604 1.163456e+02    -0.4333423 0.11827775 -3.663768
## 19  ENSMUSG00000045027 2.731805e+01    -2.0444203 0.56360402 -3.627405
## 20  ENSMUSG00000025857 4.337599e+02     0.3343401 0.09290706  3.598651
## 21  ENSMUSG00000021194 9.498266e+00    -1.7323011 0.48316215 -3.585341
## 22  ENSMUSG00000027368 1.885328e+02    -0.4954535 0.14045862 -3.527398
## 23  ENSMUSG00002075231 9.974320e+00     1.5170801 0.42914636  3.535111
## 24  ENSMUSG00000038371 7.971266e+02     0.3599161 0.10192068  3.531335
## 25  ENSMUSG00000047428 3.166235e+01    -1.7021382 0.48071775 -3.540827
## 26  ENSMUSG00000070462 3.362410e+03     0.2848233 0.08172784  3.485022
## 27  ENSMUSG00000095105 5.286996e+00    -1.7014125 0.49480261 -3.438568
## 28  ENSMUSG00000033544 5.123158e+00     2.8187456 0.83823678  3.362708
## 29  ENSMUSG00000029371 3.891319e+01    -2.4678010 0.73880250 -3.340272
## 30  ENSMUSG00000034687 5.229693e+01     0.6909381 0.20707229  3.336700
## 31  ENSMUSG00000076518 4.671483e+00     3.2500143 0.97716426  3.325965
## 32  ENSMUSG00000068536 7.369468e+00    -4.3029902 1.29405996 -3.325186
```

```
## 33  ENSMUSG00000029700 1.182250e+01  -5.1334390 1.53451593 -3.345315
## 34  ENSMUSG00000040466 9.844452e+02  -0.4406518 0.13045662 -3.377765
## 35  ENSMUSG00000109205 1.813230e+00  -4.2962281 1.27358776 -3.373327
## 36  ENSMUSG00000031617 2.959462e+02   0.3873499 0.11514782  3.363936
## 37  ENSMUSG00000025278 5.974315e+03   0.3626438 0.10774594  3.365730
## 38  ENSMUSG00000032291 1.412469e+01  -3.3018506 0.97488181 -3.386924
## 39  ENSMUSG00000105547 4.721350e+01   1.8643484 0.55247059  3.374566
## 40  ENSMUSG00000079487 5.659801e+02   0.5104672 0.15434820  3.307245
## 41  ENSMUSG00000032724 9.899529e+01   0.6027349 0.18434370  3.269626
## 42  ENSMUSG00000031386 1.158656e+03   0.3173332 0.09781607  3.244183
## 43  ENSMUSG00000041977 9.873383e+02   0.2473358 0.07623473  3.244397
## 44  ENSMUSG00000027870 1.748783e+01  -4.4762822 1.37367307 -3.258623
## 45  ENSMUSG00000056054 3.951578e+01  -2.4528423 0.75370591 -3.254376
## 46  ENSMUSG00000028435 3.517046e+01  -2.3729592 0.72756291 -3.261518
## 47  ENSMUSG00000094902 4.097581e+00   2.7142665 0.83653183  3.244666
## 48  ENSMUSG00000030413 1.689230e+03  -1.1653185 0.35866784 -3.249019
## 49  ENSMUSG00000071176 8.326389e+02   0.3735050 0.11359770  3.287963
## 50  ENSMUSG00000062257 4.992502e+01  -2.7419885 0.84687687 -3.237765
## 51  ENSMUSG00000046814 2.113487e+01  -0.9615155 0.29873363 -3.218638
## 52  ENSMUSG00000000131 1.375927e+03   0.1917181 0.05947644  3.223429
## 53  ENSMUSG00000021990 5.451996e+02   0.2520760 0.07841217  3.214756
## 54  ENSMUSG00000064443 6.259597e+00  -2.0310483 0.63371968 -3.204963
## 55  ENSMUSG00000094526 5.103505e+01   0.6366596 0.20012506  3.181309
## 56  ENSMUSG00000036057 2.106217e+03   0.1705438 0.05429323  3.141161
## 57  ENSMUSG00000038473 2.956291e+01   0.6605102 0.21234136  3.110606
## 58  ENSMUSG00000037740 1.090118e+03  -0.2152624 0.06917750 -3.111740
## 59  ENSMUSG00000028433 1.621416e+03   0.2474633 0.08020781  3.085277
## 60  ENSMUSG00000031762 1.229141e+04  -1.4460796 0.46822408 -3.088435
## 61  ENSMUSG00000091694 6.432049e+00  -2.6677461 0.86063182 -3.099753
## 62  ENSMUSG00000023972 1.410308e+03   0.3698616 0.11992743  3.084045
## 63  ENSMUSG00000024913 1.449943e+03   0.3695188 0.11954543  3.091032
## 64  ENSMUSG00000046337 6.874915e+01  -1.4008051 0.46111438 -3.037869
## 65  ENSMUSG00000039395 1.839831e+01  -1.6601715 0.54531303 -3.044438
## 66  ENSMUSG00000074445 7.718125e+00  -2.2697331 0.74645380 -3.040688
```

```
## 67  ENSMUSG00000119232 2.412843e+00    -3.3325730 1.09722973 -3.037261
## 68  ENSMUSG00000011632 2.373208e+03    -0.4441725 0.14570811 -3.048372
## 69  ENSMUSG00000024608 3.507244e+04    -0.3059170 0.10023579 -3.051974
## 70  ENSMUSG00000053985 6.793986e+01    -0.6997946 0.23115742 -3.027351
## 71  ENSMUSG00000035621 1.785042e+03     0.2565455 0.08485481  3.023346
## 72  ENSMUSG00000026837 1.751865e+04     0.4069848 0.13480924  3.018968
## 73  ENSMUSG00000074578 9.035542e+02    -0.3480066 0.11733243 -2.965988
## 74  ENSMUSG00000028795 5.264564e+02    -0.2681557 0.09007148 -2.977143
## 75  ENSMUSG00000028868 2.438784e+03     0.1734782 0.05778289  3.002241
## 76  ENSMUSG00000096490 1.012869e+02     1.4857308 0.49789046  2.984051
## 77  ENSMUSG00000046541 1.324016e+02     0.4036876 0.13525932  2.984545
## 78  ENSMUSG00000113262 1.010141e+01    -0.9820359 0.32859788 -2.988564
## 79  ENSMUSG00000031486 3.681267e+03     0.5501198 0.18565301  2.963161
## 80  ENSMUSG00000053310 2.103620e+02    -1.1977711 0.40166182 -2.982039
## 81  ENSMUSG00000034575 4.525024e+02     0.2727202 0.09204026  2.963053
## 82  ENSMUSG00000021337 5.841025e+00    -4.7011497 1.58412507 -2.967663
## 83  ENSMUSG00000076655 1.811196e+01     3.8662859 1.29376837  2.988391
## 84  ENSMUSG00000087066 5.826276e+00    -3.0803752 1.04144032 -2.957803
## 85  ENSMUSG00000113258 2.226966e+01     0.9120104 0.30922165  2.949374
## 86  ENSMUSG00000049489 3.196870e+02    -0.2055488 0.06978497 -2.945460
## 87  ENSMUSG00000020900 1.354353e+03     0.3481581 0.11841904  2.940052
## 88  ENSMUSG00000104045 3.303964e+00     2.3274807 0.79496868  2.927764
## 89  ENSMUSG00000099481 1.066921e+02    -0.3286453 0.11218368 -2.929529
## 90  ENSMUSG00000020081 1.455525e+00    -3.0687385 1.04849864 -2.926793
## 91  ENSMUSG00000050578 1.478208e+01    -2.1909247 0.74896855 -2.925256
## 92  ENSMUSG00000033352 1.011471e+03     0.2549393 0.08727375  2.921145
## 93  ENSMUSG00000026043 1.597831e+05     0.3456991 0.14815638  2.333339
## 94  ENSMUSG00000026042 1.926613e+04     0.2662421 0.10206565  2.608538
## 95  ENSMUSG00000025986 2.175589e+02     0.3615218 0.15719694  2.299802
## 96  ENSMUSG00000101784 4.030942e+00     1.3818543 0.61311618  2.253821
## 97  ENSMUSG00000026511 1.432113e+03    -0.2770516 0.10128655 -2.735325
## 98  ENSMUSG00000104378 2.645432e+00    -1.7333450 0.74082263 -2.339757
## 99  ENSMUSG00000046404 1.316528e+02    -0.3414563 0.12677887 -2.693322
## 100 ENSMUSG00000100131 4.709393e+02     1.0905076 0.44254637  2.464166
```

```
##        pvalue        padj
## 1   9.548108e-09 0.0002452527
## 2   8.502761e-08 0.0010920096
## 3   9.620280e-06 0.0823688381
## 4   2.628782e-05 0.1232601996
## 5   2.879238e-05 0.1232601996
## 6   2.253858e-05 0.1232601996
## 7   1.146784e-04 0.3682037196
## 8   1.120365e-04 0.3682037196
## 9   1.306344e-04 0.3728304871
## 10  1.532565e-04 0.3728437396
## 11  1.787509e-04 0.3728437396
## 12  1.887008e-04 0.3728437396
## 13  1.805578e-04 0.3728437396
## 14  2.345099e-04 0.4050108032
## 15  2.995875e-04 0.4050108032
## 16  2.971319e-04 0.4050108032
## 17  2.528803e-04 0.4050108032
## 18  2.485319e-04 0.4050108032
## 19  2.862836e-04 0.4050108032
## 20  3.198718e-04 0.4108114140
## 21  3.366380e-04 0.4117564097
## 22  4.196649e-04 0.4311804774
## 23  4.076036e-04 0.4311804774
## 24  4.134677e-04 0.4311804774
## 25  3.988757e-04 0.4311804774
## 26  4.920973e-04 0.4861543166
## 27  5.847993e-04 0.5563390868
## 28  7.718195e-04 0.5819494513
## 29  8.369650e-04 0.5819494513
## 30  8.477936e-04 0.5819494513
## 31  8.811295e-04 0.5819494513
## 32  8.835953e-04 0.5819494513
## 33  8.218920e-04 0.5819494513
```

```
## 34  7.307752e-04 0.5819494513
## 35  7.426568e-04 0.5819494513
## 36  7.683927e-04 0.5819494513
## 37  7.634128e-04 0.5819494513
## 38  7.068095e-04 0.5819494513
## 39  7.393223e-04 0.5819494513
## 40  9.421859e-04 0.6050246793
## 41  1.076899e-03 0.6174499459
## 42  1.177881e-03 0.6174499459
## 43  1.176994e-03 0.6174499459
## 44  1.119545e-03 0.6174499459
## 45  1.136418e-03 0.6174499459
## 46  1.108176e-03 0.6174499459
## 47  1.175884e-03 0.6174499459
## 48  1.158039e-03 0.6174499459
## 49  1.009151e-03 0.6174499459
## 50  1.204699e-03 0.6188779983
## 51  1.288009e-03 0.6327251089
## 52  1.266656e-03 0.6327251089
## 53  1.305553e-03 0.6327251089
## 54  1.350797e-03 0.6425290080
## 55  1.466113e-03 0.6847013526
## 56  1.682798e-03 0.7718632817
## 57  1.867041e-03 0.8268416085
## 58  1.859884e-03 0.8268416085
## 59  2.033628e-03 0.8325808630
## 60  2.012137e-03 0.8325808630
## 61  1.936820e-03 0.8325808630
## 62  2.042069e-03 0.8325808630
## 63  1.994620e-03 0.8325808630
## 64  2.382575e-03 0.8887306942
## 65  2.331158e-03 0.8887306942
## 66  2.360383e-03 0.8887306942
## 67  2.387387e-03 0.8887306942
```

```
## 68  2.300850e-03 0.8887306942

## 69  2.273419e-03 0.8887306942

## 70  2.467074e-03 0.9044226897

## 71  2.499961e-03 0.9044226897

## 72  2.536373e-03 0.9048510589

## 73  3.017120e-03 0.9426565139

## 74  2.909484e-03 0.9426565139

## 75  2.679995e-03 0.9426565139

## 76  2.844589e-03 0.9426565139

## 77  2.840002e-03 0.9426565139

## 78  2.802914e-03 0.9426565139

## 79  3.044971e-03 0.9426565139

## 80  2.863358e-03 0.9426565139

## 81  3.046036e-03 0.9426565139

## 82  3.000729e-03 0.9426565139

## 83  2.804504e-03 0.9426565139

## 84  3.098402e-03 0.9474470787

## 85  3.184181e-03 0.9622219681

## 86  3.224751e-03 0.9631507738

## 87  3.281574e-03 0.9688565749

## 88  3.414090e-03 0.9714754919

## 89  3.394761e-03 0.9714754919

## 90  3.424768e-03 0.9714754919

## 91  3.441730e-03 0.9714754919

## 92  3.487476e-03 0.9736882273

## 93  1.963034e-02 0.9866046846

## 94  9.092986e-03 0.9866046846

## 95  2.145945e-02 0.9866046846

## 96  2.420742e-02 0.9866046846

## 97  6.231874e-03 0.9866046846

## 98  1.929629e-02 0.9866046846

## 99  7.074400e-03 0.9866046846

## 100 1.373326e-02 0.9866046846
```

Here it ends this part of analyses for the creation of the differentially express genes table.

11.3 Appendix 3

Macros used for the analysis of immunofluorescent-stained placental images

Language IJ1 Macro

DAPI

1. setAutoThreshold("Default dark no-reset");
2. //run("Threshold...");
3. setThreshold(3405, 65535);
4. run("Create Selection");
5. run("Analyze Particles...", "size=0.00-1000.00 display clear in_situ");

Ki67

1. setAutoThreshold("Default dark no-reset");
2. //run("Threshold...");
3. setThreshold(9766, 65535);
4. run("Analyze Particles...", "size=20-1000 display clear in_situ");

11.4 Appendix 4

Sample of original MCMDM-1VWD form

CONDENSED MCMDM-1 BLEEDING QUESTIONNAIRE:

Patient Information

Name _____

Address _____

_____

Phone Number _____   **Email** _____

Gender   **Male** ☐   **Female** ☐

Age _____   **Date of Birth** _____ (DD/MO/YYYY)

Ethnic Background _____

Presenting complaint of bleeding or bruising today	Yes ☐	No ☐
Personal history of bleeding or bruising	Yes ☐	No ☐
Ever been diagnosed with a bleeding disorder? Diagnosis: _____	Yes ☐	No ☐
Family history of bleeding (at least one family member)	Yes ☐	No ☐

If yes, what was the diagnosis? _____
Pedigree:

Are you currently taking Oral Contraceptive Pills?	Yes ☐	No ☐

If yes, brand name _____

Are you pregnant? _____   **Gestation time** _____

Specify any herbals and/or medications that you have taken in the past 30 days:

Name	Dose	Route	Frequency	Duration
_____	_____	_____	_____	_____
_____	_____	_____	_____	_____
_____	_____	_____	_____	_____
_____	_____	_____	_____	_____

MCMDM-1WD scoring key

Scoring Key

Symptom	Score -1	0	1	2	3	4
Epistaxis	--	No or trivial (less than 5)	> 5 or more than 10'	Consultation only	Packing or cauterization or antifibrinolytic	Blood transfusion or replacement therapy or desmopressin
Cutaneous	--	No or trivial (< 1cm)	> 1 cm and no trauma	Consultation only	--	--
Bleeding from minor wounds	--	No or trivial (less than 5)	> 5 or more than 5'	Consultation only	Surgical hemostasis	Blood transfusion or replacement therapy or desmopressin
Oral cavity	--	No	Referred at least one	Consultation only	Surgical hemostasis or antifibrinolytic	Blood transfusion or replacement therapy or desmopressin
Gastrointestinal bleeding	--	No	Associated with ulcer, portal hypertension, hemorrhoids, angiodysplasia	Spontaneous	Surgical hemostasis, blood transfusion, replacement therapy, desmopressin, antifibrinolytic	--
Tooth extraction	No bleeding in at least 2 extractions	None done or no bleeding in 1 extraction	Reported, no consultation	Consultation only	Resuturing or packing	Blood transfusion or replacement therapy or desmopressin
Surgery	No bleeding in at least 2 surgeries	None done or no bleeding in 1 surgery	Reported, no consultation	Consultation only	Surgical hemostasis or antifibrinolytic	Blood transfusion or replacement therapy or desmopressin
Menorrhagia	--	No	Consultation only	Antifibrinolytics, pill use	Dilation & curettage, iron therapy, ablation	Blood transfusion or replacement therapy or desmopressin or hysterectomy
Postpartum hemorrhage	No bleeding in at least 2 deliveries	None done or no bleeding in 1 surgery	Consultation only	Dilation & curettage, iron therapy, antifibrinolytics	Blood transfusion or replacement therapy or desmopressin	Hysterectomy
Muscle hematomas	--	Never	Post trauma, no therapy	Spontaneous, no therapy	Spontaneous or traumatic, requiring desmopressin or replacement therapy	Spontaneous or traumatic, requiring surgical intervention or blood transfusion
Hemarthrosis	--	Never	Post trauma, no therapy	Spontaneous, no therapy	Spontaneous or traumatic, requiring desmopressin or replacement therapy	Spontaneous or traumatic, requiring surgical intervention or blood transfusion
Central nervous system bleeding	--	Never	--	--	Subdural, any intervention	Intracerebral, any intervention

11.6 Appendix 6

Information sheet for healthy participants

INFORMATION SHEET FOR PARTICIPANTS

Ethical Clearance Reference Number: LRS-20/21-22085

YOU WILL BE GIVEN A COPY OF THIS INFORMATION SHEET

Title of project

Abnormal bleeding and pregnancy related complications in women with skeletal type 1 ryanodine receptor (RYR1) mutations

Invitation Paragraph

I would like to invite you to participate in this research project which forms part of an intercalated Bachelor of Science and a PhD project for studies in Women and Children s Health and King s College London. Before you decide whether you want to take part, it is important for you to understand why the research is being done and what your participation will involve. Please take time to read the following information carefully and discuss it with others if you wish. Ask me if there is anything that is not clear or if you would like more information.

What is the purpose of the project?

The purpose of the project is to develop an online questionnaire to assess whether women with RYR1 mutations experience bleeding abnormalities and abnormalities during pregnancy and in childbirth.

Why have I been invited to take part?

You are being invited to participate in this project because you are a healthy female volunteer taking part in the pilot phase of this study to assess the functionality of the questionnaire.

What will happen if I take part?

If you choose to take part in the project you will be asked to take the questionnaire yourself and let us know if any areas are hard to understand or poorly formatted. An example question is:

When on your period, do you ever have to change pads or tampons every hour or two, or empty your menstrual cup more often than it recommends to prevent leakage?

A) Never
B) Rarely, or some periods
C) Often, or most periods

You will also be asked to let us know if you have experienced any episodes of abnormal bleeding that we have not included when writing the questionnaire. Participation will take place between the 15/03/2021 and the 15/03/2022. It will only require one session of answering the questionnaire and this will require an internet connection. The questionnaire will take approximately 15 minutes. The data collected will be completely anonymous, if you are worried that something you are inputting to the questionnaire might be identifiable then this is also important feedback for us. Your experience using the questionnaire will allow us to make modifications to improve format and content, it will then be distributed to women living with RYR1 mutations. Results will then advise possible management of these patients in relation to bleeding, pregnancy and childbirth.

Do I have to take part?

Participation is completely voluntary. You should only take part if you want to and choosing not to take part will not disadvantage you in anyway. Once you have read the information sheet, please contact us if you have any questions that will help you make a decision about taking part. If you do decide to take part, we will ask you to sign a consent form and you will be given a copy of this consent form to keep.

What are the possible risks of taking part?

As part of participation, you will be asked to provide information about previous bleeding episodes, menstruation, and, if applicable, your experiences with pregnancy and childbirth.

Some of the questions may involve recollecting unpleasant memories and experiences as the questionnaire asks about miscarriage, infertility and post-partum haemorrhage (heavy bleeding after giving birth). You are under no obligation to answer all of these questions if they are too personal.

Your results will be anonymised therefore we cannot contact you regarding your answers to the questionnaire. If your answers cause you to believe you may have a condition that leads to

abnormal bleeding, problems in pregnancy or childbirth please go through normal NHS channels as we cannot advise you regarding this. You are able to withdraw at any point until you have completed the questionnaire due to your response being anonymised.

What are the possible benefits of taking part?

There are no possible benefits to yourself to taking part, it will purely advise the improvement of the questionnaire and future management of individuals with RYR1 mutations.

Data handling and confidentiality

- Your data will be processed in accordance with the General Data Protection Regulation 2016 (GDPR) and will be used for a thesis, journals and conferences.
- The questionnaire will be completed via **Microsoft Forms** and will be completely anonymised with no record of your identity or email.
- Data will be stored on KCL OneDrive and password protected on an external hard drive.
- The questions are not intended to elicit information that can be used to identify participants. To safeguard your rights, we will use the minimum personally-identifiable information possible. If you are concerned your answer to a question may lead to you being identified, you do not have to answer, and this is important information for us to know in order to improve the questionnaire.
- The data generated from this project/ questionnaire will be stored in line with the King s College London data retention schedule. Specifically, the data will be kept for no longer than 7 years post the completion of the final thesis.
- Data will only be shared within the research team and not outside of the EU.

Data Protection Statement

Your data will be processed in accordance with the General Data Protection Regulation 2016 (GDPR). If you would like more information about how your data will be processed in accordance with GDPR please visit the link below:

https://www.kcl.ac.uk/research/support/research-ethics/kings-college-london-statement-on-use-of-personal-data-in-research

We have also attached a PDF of this ethics statement to the advertising email.

What if I change my mind about taking part?

Your rights to access, change or move your information are limited, as we need to manage your information in specific ways to ensure anonymity and that our results are reliable and accurate. You are able to withdraw your data from the project up until you have completed the

questionnaire after which withdrawal of your data will no longer be possible. This is because we will not be able to identify which set of responses are yours as they will be anonymous.

How is the project being funded?

This project is being funded by King s Health Partners Institute for Women and Children s Health

https://www.kingshealthpartners.org/institutes/women-and-childrens-health

What will happen to the results of the project?

The anonymised results of the project will be summarised in a Women s Health iBSc project and Women and Children s Health PhD thesis. Results may be disseminated in a research journal and conferences

Who should I contact for further information?

If you have any questions or require more information about this project, please contact me using the following contact details:

Arti.mistry@kcl.ac.uk

What if I have further questions, or if something goes wrong?

If this project has harmed you in any way, or if you wish to make a complaint about the conduct of the project you can contact King's College London using the details below for further advice and information:

Academic supervisor: Rachel.tribe@kcl.ac.uk

The Chair: rec@kcl.ac.uk

Departmental postal address:

Department of Women and Children's Health
School of Life Course Science
King s College London
10th Floor
North Wing
St Thomas Hospital

Westminster Bridge Road
London SE1 7EH

Thank you for reading this information sheet and for considering taking part in this research.

Information sheet for RYR1 participants

INFORMATION SHEET FOR PARTICIPANTS

Ethical Clearance Reference Number: LRM-21/22-22085

YOU WILL BE GIVEN A COPY OF THIS INFORMATION SHEET

<u>**Title of project**</u>

<u>**Abnormal bleeding and pregnancy related complications in women with skeletal type 1 ryanodine receptor (RYR1) mutations**</u>

<u>**Invitation**</u>

I would like to invite you to participate in this research project which forms part of a PhD project for studies in Women and Children's Health at King's College London. Before you decide whether you want to take part, it is important for you to understand why the research is being done and what your participation will involve. Please take time to read the following information carefully and discuss it with others if you wish. Ask me if there is anything that is not clear or if you would like more information.

<u>**What is the purpose of the project?**</u>

The purpose of the project is to assess whether women with RYR1 mutations experience bleeding abnormalities and abnormalities during pregnancy and in childbirth.

<u>**Why have I been invited to take part?**</u>

You are being invited to participate in this project because:

1) You have been in contact with a support organisation for RYR1 and related neuromuscular disorders including malignant hyperthermia susceptibility.

   Or

2) You are the relative of someone with a RYR1 mutation and you do not have a mutation in the RYR1 gene nor any related symptoms.

What will happen if I take part?

If you choose to take part in the project you will be asked to take the questionnaire. As part of participation, you will be asked to provide information about previous bleeding episodes, menstruation, and, if applicable, your experiences with pregnancy and childbirth.

An example question is:

When on your period, do you ever have to change pads or tampons every hour or two, or empty your menstrual cup more often than it recommends to prevent leakage?

A) Never
B) Rarely, or some periods
C) Often, or most periods

You will also be asked to let us know if you have experienced any episodes of abnormal bleeding that we have missed when writing the questionnaire. Participation will take place between the 15/10/2021 and the 15/10/2022. It will only require one session of answering the questionnaire and this will require an internet connection. The questionnaire will take approximately 15 minutes. The data collected will be completely anonymous. The results of this study will then advise possible management of individuals with RYR1 mutations in relation to bleeding, pregnancy and childbirth.

Do I have to take part?

Participation is completely voluntary. You should only take part if you want to and choosing not to take part will not disadvantage you in anyway. Once you have read the information sheet, please contact us if you have any questions that will help you make a decision about taking part. Your submission of the questionnaire will be considered consent to take part.

Some of the questions may involve recollecting unpleasant memories and experiences as the questionnaire asks about miscarriage, stillbirth, infertility, and post-partum haemorrhage (heavy bleeding after giving birth). You are under no obligation to answer all of these questions if they are too personal.

What are the possible risks of taking part?

Your results will be anonymised therefore we cannot contact you regarding your answers to the questionnaire. If your answers cause you to believe you may have a condition that leads to abnormal bleeding, problems in pregnancy or childbirth please go through normal medical professional channels as we cannot advise you regarding this. You are able to withdraw at any point until you have completed the questionnaire due to your response being anonymised.

What are the possible benefits of taking part?

There are no possible benefits to yourself to taking part, it will purely advise the improvement of the questionnaire and future management of individuals with RYR1 mutations.

Data handling and confidentiality

- Your data will be processed in accordance with the General Data Protection Regulation 2016 (GDPR) and will be used for a thesis, journals and conferences.
- The questionnaire will be completed via **Microsoft Forms** and will be completely anonymised with no record of your identity or email.
- Data will be stored on KCL OneDrive and password protected on an external hard-drive.
- The questions are not intended to elicit information that can be used to identify participants. If you are concerned your answer to a question may lead to you being identified, you do not have to answer.
- The data generated from this project/ questionnaire will be stored in line with the King's College London data retention schedule. Specifically, the data will be kept for no longer than 7 years post the completion of the final thesis.
- Data will only be shared within the research team and not outside of the EU.

Data Protection Statement

Your data will be processed in accordance with the General Data Protection Regulation 2016 (GDPR). If you would like more information about how your data will be processed in accordance with GDPR please visit the link below:

https://www.kcl.ac.uk/research/support/research-ethics/kings-college-london-statement-on-use-of-personal-data-in-research

We have also attached a PDF of this ethics statement to the advertising email.

What if I change my mind about taking part?

Your rights to access, change or move your information are limited, as we need to manage your information in specific ways to ensure anonymity and that our results are reliable and accurate. You are able to withdraw your data from the project up until you have completed the questionnaire after which withdrawal of your data will no longer be possible. This is because we will not be able to identify which set of responses are yours as they will be anonymous.

How is the project being funded?

This project is being funded by King's Health Partners Institute for Women and Children's Health
https://www.kingshealthpartners.org/institutes/women-and-childrens-health

What will happen to the results of the project?

The anonymised results of the project will be summarised in a Women and Children's Health PhD thesis. Results may be disseminated in a research journal and conferences

Who should I contact for further information?

If you have any questions or require more information about this project, please contact me using the following contact details:

Arti.mistry@kcl.ac.uk

What if I have further questions, or if something goes wrong?

If this project has harmed you in any way, or if you wish to make a complaint about the conduct of the project you can contact King's College London using the details below for further advice and information:

Academic supervisor: Rachel.tribe@kcl.ac.uk

The Chair: rec@kcl.ac.uk

Departmental postal address:

Department of Women and Children's Health
School of Life Course Science
King's College London
10th Floor
North Wing
St Thomas' Hospital
Westminster Bridge Road
London SE1 7EH

Thank you for reading this information sheet and for considering taking part in this research.

11.8 Appendix 8

Correspondence for ethical approval for questionnaire study

Research Ethics
Office

Franklin Wilkins Building
5.9 Waterloo Bridge Wing
Waterloo Road
London SE1 9NH
Telephone 020 7848 4020/4070/4077
rec@kcl.ac.uk

King's College LONDON

Arti Mistry

20/04/2021

Dear Arti,

LRS-20/21-22065: Abnormal bleeding and pregnancy related complications in women with skeletal RYR1 mutations

Thank you for submitting your application for the above project. I am pleased to inform you that full approval has been granted by the BDM Research Ethics Panel

Important coronavirus update: In light of the COVID-19 pandemic, the College Research Ethics Committee has temporarily suspended all primary data collection involving face to face participant interactions until further notice. **Ethical clearance for this project is granted. However, the clearance outlined in the attached letter is contingent on your adherence to the latest College measures when conducting your research.** Please do not commence data collection until you have carefully reviewed the update and made any necessary project changes:

https://internal.kcl.ac.uk/innovation/research/ethics/applications/COVID-19-Update-for-Researchers

Ethical approval has been granted for a period of **three years** from 20 April 2021. You will not be sent a reminder when your approval has lapsed and if you require an extension you should complete a modification request, details of which can be found here:

https://internal.kcl.ac.uk/innovation/research/ethics/applications/modifications.aspx

Please ensure that you follow the guidelines for good research practice as laid out in UKRIO's Code of Practice for research: http://ukrio.org/publications/code-of-practice-for-research/

Any unforeseen ethical problems arising during the course of the project should be reported to the panel Chair, via the Research Ethics Office.

Please note that we may, for the purposes of audit, contact you to ascertain the status of your research.

We wish you every success with your research.

Yours sincerely,

Mr James Patterson

Senior Research Ethics Officer

For and on behalf of:

BDM Research Ethics Panel

Franklin Wilkins Building
5.9 Waterloo Bridge Wing
Waterloo Road
London SE1 9NH
Telephone 020 7848 4020/4070/4077
rec@kcl.ac.uk

KING'S College LONDON

26/10/2021

Dear Arti,

Reference Number: LRM-21/22-22065

Study Title: Abnormal bleeding and pregnancy related complications in women with skeletal RYR1 mutations

Modification Review Outcome: Full Approval

Thank you for submitting a modification request for the above study. This is a letter to confirm that your request has now been granted Full Approval.

Important COVID-19 update: Please consult the latest College guidance (linked below) and ensure you have completed the risk assessment procedure prior to any data collection involving face-to-face participant interactions.

https://internal.kcl.ac.uk/innovation/research/ethics/applications/COVID-19-Update-for-Researchers

If you have any questions regarding your application please contact the Research Ethics Office at rec@kcl.ac.uk.

Kind regards,

Mr James Patterson

Research Ethics Facilitator

on behalf of

BDM Research Ethics Panel

KING'S
College
LONDON

Arti Mistry

15 April 2021

Dear Arti,

Reference Number: LRS-20/21-22085

Study Title: Abnormal bleeding and pregnancy related complications in women with skeletal RYR1 mutations

Review Outcome: Further amendments/clarifications required <u>before</u> approval can be granted.

Thank you for submitting the above application for ethical approval. Your application has been reviewed and has been approved pending amendments. You are now required to address a number of issues before full approval is granted. These are specified in the feedback table below. Please respond to each point raised by the reviewer and amend your application form, and appendices, accordingly. **Please note that research involving human participants must not commence until your amended application has been reviewed and Full Approval has been granted.**

In order to amend the application, you will simply need to log on onto REMAS and modify the existing application. Once again, your academic supervisor will be required to provide verification.

The submission of your amended application must be accompanied by a cover letter outlining the changes you have made in response to each of the Committee's requests. For ease of completion we recommend that you cut and paste the feedback table from your outcome letter into your cover letter and respond to each point individually. The cover letter should be attached as a Supporting Document in section I9 of your application. Failure to attach a cover letter to your resubmitted application will result in your application being marked as 'Invalid' and returned to you by the Research Ethics Office prior to review.

Please note, once submitted amendments will be reviewed within 15 working days.

If for some reason you choose not to proceed with this research ethics application, please inform the Research Ethics Office.

Yours sincerely,

Mr James Patterson

Senior Research Ethics Officer

For and on behalf of

BDM Research Ethics Panel

Cc: Professor Rachel Tribe, Professor Heinz Jungbluth

Major Issues (will require substantial consideration by the applicant before approval can be granted)

Minor Issues related to application (the reviewer should identify the relevant section number before each comment)

1. Section B9: Specify the online platform that will be used to host the questionnaire.

2. Section C4: Provide more information about the platforms that will be used to advertise for participants for the second phase of the study.

3. Section C6: The Panel is of the view that you are using a gatekeeper. Therefore, you should change your answer accordingly and provide more information about the RYR1 support groups.

4. Section H6: Please ensure that your correspondence with the gatekeeper can be made available to the Research Ethics Office upon request.

511

Research Governance & Data Protection Issues

Minor Issues related to recruitment documents

5. Information Sheet:

i. Include a departmental postal address within the contact details provided for your and your academic supervisor.

ii. As this is a student project, the paragraph beginning with 'If this study has harmed you in any way...' should only appear before the College contact details for your academic supervisor. It should be clear that you are to be contacted by those with queries about the study.

Advice and Comments (do not have to be adhered to, but may help to improve the research)

512

Sample bleeding questionnaire form

Abnormal bleeding and pregnancy related complications in women with skeletal *RYR1* mutation ⸙

Ethical Clearance Reference Number: **LRM-21/22-22085**

Phase II

Please select submit when you have completed the questionnaire or your response will not be recorded.

* Required

Personal details

1. Do you consider English to be your native language? *

○ Yes

○ No

○ I am bilingual

○ Prefer not to say

2. What is your country of residence? *

If you prefer not to say, please type 'prefer not to say'

[   ]

3. Age *

[   ]

4. Ethnicity * White

○ Black

○ Asian

○ Arab

○ Mixed/ multiple ethnic groups

○ Other

○ 5.　　　White - please specify *

Examples of 'other' include 'American', 'German', 'Hispanic'

○ English/ Welsh/ Scottish/ Northern Irish/ British

○ Irish

○ Gypsy or Irish Traveller

○ Other

6. Black, please specify *

○ African

○ Caribbean

○ Other

7. Asian, please specify *

○ Indian

○ Pakistani

○ Bangladeshi

○ Chinese

○ Other

8. Mixed/ multiple ethnic groups *

○ White and Black Caribbean

○ White and Black African

○ White and Asian

○ Other

Medical history

9. Have you ever been diagnosed with an inherited bleeding disorder? *

   ○ Yes - Haemophilia A

   ○ Yes - Haemophilia B

   ○ Yes - Von Willebrand's disease

   ○ No

   ○ Don't know

   ○ Other

10. Have you ever been diagnosed with any of the below conditions? *

   ☐ Type 1 diabetes

   ☐ Antiphospholipid syndrome

   ☐ Polycystic ovarian syndrome (PCOS)

   ☐ Hypothyroidism

   ☐ Hyperthyroidism

   ☐ Abnormally-shaped womb

   ☐ Cervical weakness

   ☐ No

11. Have you ever been diagnosed with an *RYR1* mutation? *

   ○ Yes

   ○ No

   ○ Don't know

12. Please specify mutation if known

13. Is the mutation that causes your disorder autosomal dominant or autosomal recessive?*

   We all have two copies of each gene, each inherited from a different parent. Autosomal dominant means you have a single faulty copy of the RYR1 gene (with the fault inherited from a similarly affected parent, or, less frequently, having occurred anew in yourself) causing your symptoms, autosomal recessive means you have two faulty copies of the RYR1 gene (typically inherited from both unaffected parents) causing your symptoms.

515

○ Autosomal Dominant

○ Autosomal Recessive

○ Don't know

○ Other

14. Are you a relative of someone with an RYR1 mutation? *

○ Yes

○ No

○ Don't know

15. Have you been diagnosed with any of the below conditions? *

☐ Central Core Disease (CCD)

☐ Multi-minicore Disease (MmD)

☐ Centronuclear Myopathy (CNM)

☐ Congenital Fibre Type Disproportion (CFTD)

☐ Congenital myopathy (without specific muscle biopsy findings)

☐ Malignant hyperthermia (MH)

☐ King-Denborough syndrome (KDS)

☐ (Exertional) rhabdomyolysis

☐ (Exertional) heat illness (sometimes also called heatstroke)

☐ Periodic paralyses

☐ None of the above

☐ Other

16. Have you ever been treated with dantrolene? *

○ Yes

○ No

○ Don't know

17. Have you ever had severe migraines requiring medical attention or medication? * Yes

○ No

○ Don't know

○ 18.   Please describe what treatment you received: *

☐ Consultation with a general practitioner only

☐ Attending a specialist migraine clinic

☐ Painkillers such as ibuprofen, paracetamol or aspirin

☐ Stronger medications such as triptans

☐ Anti sickness medicine (known as anti emetics)

☐ Acupuncture

☐ Transcranial magnetic stimulation - this involves holding a small electrical device to your head that delivers magnetic pulses through your skin

☐ Other

19. Have you ever been treated for anaemia? *

○ Yes

○ No

○ Don't know

20. Have you been diagnosed with a high or low blood pressure? *

○ No

○ Yes - high blood pressure (hypertension)

○ Yes - low blood pressure (hypotension)

○ Don't know

21. Are you receiving any treatment or medication for your blood pressure? *

If so please describe

☐ I am not receiving any treatment

☐ Lifestyle changes such as changing diet, quitting smoking, drinking less alcohol, increasing exercise, losing weight

☐ ACE inhibitor (e.g. ramipril, enalapril, lisinopril, perindopril)

☐ Angiotensin-2 receptor blocker ARB (e.g. candesartan, irbesartan, losartan, valsartan or olmesartan)

☐ Calcium channel blocker (e.g. amlodipine, felodipine or nifedipine)

☐ Diuretic also known as a water pill (e.g. indapamide and bendroflumethiazide)

☐ Beta blocker (e.g. atenolol and bisoprolol)

Other

22. Are you receiving any treatment or medication for your blood pressure? *

If so please describe

○ Wearing support stockings

○ Lifestyle changes such as changes to diet and drinking habits

○ Other

23. Have you ever been diagnosed with bowel or bladder problems? *

If yes please describe

☐ No

☐ Constipation (difficulty passing stool)

☐ Diarrhoea (runny or frequent bowel movements)

☐ Bowel inflammation

☐ Vesicourethral reflux (movement of urine from the bladder into the kidneys)

☐ Urinary incontinence

☐ Other

24. Do you have any other medical conditions you would like to disclose?

[text box]

Family history

25. Has anyone in your family been diagnosed with an inherited bleeding disorder? *

  ○ Yes - Haemophilia A

  ○ Yes - Haemophilia B

  ○ Yes - Von Willebrand's disease

  ○ No

  ○ Don't know

  ○ Other

26. If you have any children, have any of them been diagnosed with an RYR1 mutation? *

  ○ I do not have children

  ○ Yes, I have a child who has been diagnosed with an RYR1 mutation

  ○ I have children but none have been diagnosed with an RYR1 mutation

  ○ Don't know

27. Please specify which child (e.g. first child) and mutation if known

Nosebleeds

28. Have you ever had a nosebleed that needed medical treatment OR lasted for longer than 5 minutes? *
(Especially if you had it as a teenager or adult)

○ Yes

○ No or only short nosebleeds

Please describe your general experience of nosebleed

29. How many nosebleeds do you have a year? *

○ Less than 1

○ 1 to 5

○ 6 to 12

○ More than 12

30. How long does your nosebleed usually last? *

○ 1 minute or less

○ 1 to 10 minutes

○ More than 10 minutes

31. Have you noticed if the nosebleeds happen more at a certain time of year (e.g. spring/ winter)? *

○ Yes

○ No

Please describe your worst nosebleed

32. How old were you when you had your worst bleed? *

○ Less than 14 years

○ 14 to 45 years

○ More than 45 years

33. Was the bleeding unexpected? *

e.g. With nothing like a knock to the nose causing it.

      ○ Yes

      ○ No

34. How long did the bleeding last *

      ○ 1 minute or less

      ○ 1 to 10 minutes

      ○ More than 10 minutes

35. Did it involve both nostrils? *

      ○ Yes

      ○ No

36. Did it occur after you had taken a medicine? *

    e.g. Aspirin

      ○ Yes

      ○ No

37. How was the bleeding stopped? *

○ It stopped by itself

○ After short compression (e.g. squeezing your nose with a tissue for a few minutes)

○ It only stopped after compressing for longer than 15 minutes

○ A doctor or nurse looking at and talking about your nosebleed only

○ A chemical or electrical device put up the nose to stop the bleeding with small burns (Cauterization)

○ Special sponges or padding in your nose to stop the bleeding with pressure (Packing)

○ Blood transfusion

Other

Symptoms on skin

Any unexplained bruise and/ or swelling larger than 3 centimetres or surprisingly large after a small injury. This can also look like groups of small purple, red or brown spots (petechiae)

38. Have you ever experienced skin symptoms as described above? *

○ Yes

○ No or only minor

39. How many times do you have this type of bruising a year? *

[   ]

40. What is the type of bruising? *

○ Small purple, red, or brown spots on the skin (petechiae)

○ Bruises

○ Large bruises with lots of swelling (haematomas)

Describing your worst ever bruising

41. What was the type of bruising? *

○ Small purple, red, or brown spots on the skin (petechiae) Bruises

○ Large bruises with lots of swelling (haematomas)

42. Where was the location? (if any) *

○ Feet, legs, hands, arms or face (exposed sites)

○ Body (unexposed sites)

○ Don't know

43. Did you have a fall or any injury before this bruising? *

○ Yes

○ Only a small or no injury

44. Did you seek medical treatment? Please describe *

○ No

○ Yes - consultation only

○ Other

Small cuts: Any bleeding for longer than 5 minutes caused by small cuts to your skin

e.g. a graze or by knife, scissors, or paper

45. Have you had bleeding for longer than 5 minutes caused by small cuts to your skin? *

○ Yes

○ No or only minor (not unexpected for the injury)

Describing your average bleeding episode

46. How many times a year do you have this bleeding? *

○ Every time my skin is cut,

○ Most times when my skin is cut,

○ Sometimes when my skin is cut,

○ Rare occasions when my skin is cut

47. How long does the bleeding last (in minutes)? *

○ 1 minute or less

○ 1 to 10 minutes

○ More than 10 minutes

Describing your worst bleed from a small cut

48. How long did the bleeding last? (in minutes) *

○ 1 minute or less

○ 1 to 10 minutes

○ More than 10 minutes

49. Did you need any medical treatment to stop the bleeding? *

○ Surgery to stop the bleeding, this might be stitches, staples or glue (surgical haemostasis)

○ Blood transfusion

○ Other

Bleeding from your mouth

Any heavy bleeding in your mouth that was not expected and lasts for longer than a minute. This could also be seen as swelling to your tongue or lips

50. Have you ever experienced this type of bleeding? *

○ Yes

○ No or only small amounts of blood not lasting a minute

Describing the worst bleeding you've had

51. What was the type of bleeding? *

○ Bleeding when a new tooth is coming through the gum (e.g. wisdom teeth coming in)

○ Gums bleeding, with no cause

○ Gums bleeding, after brushing

○ Bleeding after bites to lip & tongue

52. Did you seek medical advice? *

If yes please describe the treatment you received

○ No

○ Consultation only

○ Stitches or fabric pads to stop the bleeding (surgical haemostasis)

○ Blood transfusion

Gastrointestinal bleeding: Any bleeding from your stomach or intestines

This might be blood seen in your stool or in your sick

53. Have you ever experienced this type of bleeding? *

   ○ Yes

   ○ No or only minor

54. How many times have you had this bleeding? *

   [   ]

55. What form does this bleeding take? *

   ○ Blood in your vomit (sick), this could be bright or dark

   ○ Dark black bloody stool (faeces)

   ○ Fresh bright red blood in your stool (faeces)

56. Do you have a condition that causes the bleeding? *

   If yes please describe

   ○ No

   ○ Stomach or intestinal ulcer

   ○ Portal hypertension – high blood pressure in the portal vein

   ○ Angiodysplasia – problems with the blood vessels in the mouth, oesophagus, intestines, stomach or anus

Describing the worst time you've ever had this bleeding

57. What form does this bleeding take? *

- ◯ Blood in your vomit (sick), this could be bright or dark

- ◯ Dark black bloody stool (faeces)

- ◯ Fresh bright red blood in your stool (faeces)

58. Did you seek medical advice? *

If yes please describe the treatment you received

- ◯ No

- ◯ Consultation only

- ◯ Blood transfusion

- ◯ Surgery

Tooth removal

59. How many teeth have you had removed? *

   ○ 0

   ○ 1

   ○ 2

   ○ 3

   ○ 4

   ○ 5

   ○ 6 +

60. How many times have you had heavy bleeding after tooth removal? *

   This might have been any heavy bleeding after leaving the dentist's office or bleeding for a long time at the dentist's office causing the treatment to take longer

   ○ 0

   ○ 1

   ○ 2

   ○ 3

   ○ 4

   ○ 5

   ○ 6+

Describing the worst bleeding you have had after a tooth removal

61. How old were you when you had this tooth removed? *

   [   ]

   The value must be a number

62. What was the type of tooth you had taken out? *

   ○ Baby or milk tooth

   ○ Adult tooth

   ○ Molar tooth

63. Were any actions taken to control the bleeding? *

Select all that apply

☐ No

☐ Stitches to stop the bleeding

☐ Packing with cotton pads or fabric to stop the bleeding

☐ Blood transfusion

Surgery

64. How many operations have you had? *

○ 0

○ 1

○ 2

○ 3

○ 4

○ 5

○ 6 +

65. Have you ever had an operation where they've put you to sleep? *

○ Yes

○ No or don't know

66. Did you have any bad reactions to the anaesthetic? *

○ Yes

○ No

○ Don't know

67. Please describe what happened *

Select all that apply

☐ Feeling or being very sick

☐ Allergic reaction

☐ Malignant hyperthermia

☐ Very high temperature

☐ Excessive sweating

☐ Rapid shallow breaths and problems with low oxygen/high carbon dioxide

☐ Severe muscle rigidity or spasms

☐ Rapid or abnormal heart rate

☐ Other

68. Have you had any surgeries that were followed by heavy bleeding? *

Any heavy bleeding during or after the operation that meant you needed more treatment or had to spend more time in hospital

○ 0

○ 1

○ 2

○ 3

○ 4

○ 5

○ 6+

Describing your worst bleeding after an operation

69. How old were you when you had the operation? *

[   ]

The value must be a number

70. Did you receive any dantrolene before the surgery? *

○ Yes

○ No

○ Don't know

71. Where did you have the surgery? *

○ Head

○ Neck

○ Chest area

○ Arm or hand

○ Leg or foot

○ Womb, uterus, vagina or ovaries

○ Other

72. What was the name of the surgery you had bleeding after? *

73. What treatment did you have to stop the bleeding? *

Select all that apply

☐ None

☐ More stitches or surgery

☐ Blood transfusion

☐ Dantrolene - after surgery

☐ Other

74. Was the operation meant to be only a day case? *

e.g. you go home the same day you have the operation

○ Yes

○ No

○ Don't know

531

75. How long were you in hospital after the operation? *

Please enter the number of days e.g. 1 for 1 day spent in the
hospital

Biological sex

76. What is your biological sex? *

We are asking this because the following questions ask about experiences of periods, contraception and pregnancy.

○ Male

○ Female

○ I am intersex and I have/ have had periods

○ I am intersex and I have never had periods

Periods and menstrual cycle

77. Do you currently have periods? *

○ Yes

○ No - please answer the questions as well as you can

78. Have you been through menopause? *

○ No

○ Don't know

○ Currently experiencing menopausal symptoms

○ Yes - please answer the following questions to the best of your memory

79. How long is/ was your usual menstrual cycle? (The time from the start of one period to the start of your next period) *

○ Less than 21 days

○ 21 to 26 days

○ 27 to 32 days

○ 33 to 38

○ More than 38 days

○ My cycle is rarely the same length

○ Don't know

80. How many days does/ did your period usually last, from the time bleeding began until it completely stopped? *

○ Less than 3 days

○ 3 days to 5 days

○ 6 days to 8 days

○ More than 8 days

○ Don't know

81. During your period how often do/ did you: *

	Never	Rarely, or some periods	Often, or most periods	Don't know
Change your routine? (This could be taking time off work, stopping exercise, or could be not going out with your friends)	○	○	○	○
Avoid travelling or even stay home?	○	○	○	○
Change pad or tampon every 2 hours, or more frequently, or empty menstrual cup more often than recommended to avoid leakage?	○	○	○	○
Change sanitary protection or empty menstrual cup during the night to avoid leaks?	○	○	○	○
Use 2 types of protection at the same time to avoid leaks? (e.g. pad and tampon)	○	○	○	○
Pass clots larger than a 10p coin?	○	○	○	○
Have any other bleeding between periods?	○	○	○	○
Experience period cramps?	○	○	○	○

82. On a scale of 0 to 10 how painful are/ were your period cramps? *

0	1	2	3	4	5	6	7	8	9	1

Not at all painful   The most painful

83. Have you been diagnosed with any of the below conditions? *

☐ No

☐ Uterine polyps

☐ Endometriosis

☐ Adenomyosis

☐ Pelvic inflammatory disease (PID)

84. Have you ever had treatment for heavy periods? * No

○ Sought medical advice but received no treatment

○ Pill or other hormonal contraception use

○ Dilatation and curettage

○ Hysterectomy

○ Blood transfusion

○ Taking iron tablets

○ Tranexamic acid

○ Other

Contraception and period

86. Are you currently on any long term contraception? *

    ○ Yes

    ○ No

87. Please specify *

    ○ Combined oral contraceptive pill e.g. microgynon, rigevidon, gedarel

    ○ Progesterone only contraceptive pill e.g. cerazette, norgeston, micronor

    ○ Contraceptive pill, unsure what type

    ○ Contraceptive implant

    ○ Intrauterine system IUS (Mirena coil releases progesterone)

    ○ Intrauterine device IUD (Copper coil)

    ○ Vaginal ring

    ○ Contraceptive patch

    ○ Contraceptive injection

    ○ Other

88. Since you started using the contraception did you notice any changes to your period cramps? *

    ○ Yes, they became more painful

    ○ Yes, they became less painful

    ○ No change

    ○ Don't know

89. Since you started using contraception has the amount you bleed changed? *

    ○ Yes, I had more bleeding

    ○ Yes, I had less bleeding

    ○ No change

    ○ Don't know

Obstetric section

90. Is it alright if we ask you some questions about becoming pregnant? *

    ○ Yes

    ○ No

91. Have you ever tried to become pregnant? *

    ○ Yes

    ○ No

    ○ Prefer not to say

92. Have you ever been pregnant? *

    ○ Yes

    ○ No

    ○ Prefer not to say

93. How many times have you been pregnant?

    _____

94. Did you receive any help from doctors to become pregnant? *

    If so what help or treatment did you receive?

    ☐ I have never received any help from doctors to become pregnant

    ☐ Consultation only

    ☐ Intrauterine insemination (IUI)

    ☐ In vitro fertilisation (IVF)

    ☐ Intracytoplasmic sperm injection (ICSI)

    ☐ Donor egg

    ☐ Donor sperm

    ☐ Donor embryo

    ☐ Other

95. Is it alright if we ask you some questions about the miscarriage or the loss of a baby in the first 13 weeks? *

○ Yes

○ No

96. Have you ever lost a pregnancy or baby before 13 weeks? *

This might have been called a miscarriage

○ Yes - once

○ Yes - more than once

○ No

○ Don't know

○ Prefer not to say

97. How many miscarriages before 13 weeks have you had?

[   ]

98. Have you ever had 3 or more consecutive miscarriages? *

This is the loss of 3 or more pregnancies in a row

○ Yes

○ No

○ Don't know

○ Prefer not to say

99. Have you ever had a bleeding problem after the loss of a pregnancy or baby in the first 13 weeks? *

This might have been bleeding which lasted longer than 3 weeks after the miscarriage or caused you to change sanitary pads more than once an hour

○ Yes

○ No

○ Don't know

○ Prefer not to say

100. Did you have any treatment for this bleeding? *

☐ ╷ had no treatment

☐ Don't know

☐ Prefer not to say

☐ Sought medical advice but received no treatment

☐ Dilatation and curettage (D&C)

☐ Removal of the uterus - Hysterectomy

☐ Blood transfusion

☐ Taking iron tablets

☐ Injected medications (e.g. oxytocin, tranexamic acid)

☐ Other

101. Is it alright if we ask you some questions about the loss of a pregnancy or baby between 14 weeks and 24 weeks and stillbirth? *

○ Yes

○ No

102. Have you ever lost a pregnancy or baby between 14 weeks and 24 weeks or had a child die soon after birth? *

This might have been due to them being born too early or because they had a condition that was too severe for them to survive

○ Yes, once

○ Yes, more than once

○ No

○ Prefer not to say

103. Is it alright if we ask you some more questions about this delivery? *

○ Yes

○ No

104. How many weeks was this pregnancy?

The value must be a number

105. Did you have a problem with unusually heavy bleeding following this delivery? *

This might have been called postpartum haemorrhage

○ Yes

○ No

○ Don't know

○ Prefer not to say

106. Is it alright if we ask you some more questions about these deliveries? *

○ Yes

○ No

107. How many weeks were these pregnancies?

Please only fill in the relevant rows (e.g. if you have only lost one child soon after birth then only fill in the first row)

	15 weeks or less	16 to 19 weeks	20 to 23 weeks	24 weeks or more	Don't know	Prefer not to say
First	○	○	○	○	○	○
Second	○	○	○	○	○	○
Third	○	○	○	○	○	○
Fourth	○	○	○	○	○	○
Fifth	○	○	○	○	○	○

108. Have you ever had a problem with unusually heavy bleeding following any of these deliveries? *

This might have been called postpartum haemorrhage

○ Yes

○ No

○ Don't know

○ Prefer not to say

109. Did you receive any additional treatment for bleeding? If so please describe *

please select all that apply

540

☐ No

☐ Don't know

☐ Prefer not to say

☐ Consultation only

☐ Dilatation and curettage (D&C)

☐ Removal of the uterus - Hysterectomy

☐ Blood transfusion

☐ Taking iron tablets

☐ Dantrolene

☐ Injected medications (e.g. oxytocin, tranexamic acid)

☐ Other

110. Have you had any other pregnancies that resulted in a live birth? *

○ Yes

○ No

○ Prefer not to say

111. Have you had any children? *

○ Yes

○ No

○ Prefer not to say

112. Is it alright if we ask you some more questions about this child/ these children? *

○ Yes

○ No

113. What was the birthweight of each child?

Please only answer for the relevant rows i.e. if you have only had 2 children leave rows 3 and 4 blank

	4lb 15oz (2.23kg) or less	5lb to 7lb (2.26 - 3.18kg)	7lb 1oz to 10lb (3.20 - 4.54kg)	10lb 1oz (4.56 kg) or more	Don't know	Prefer not to say
First child	○	○	○	○	○	○
Second child	○	○	○	○	○	○
Third child	○	○	○	○	○	○
Fourth child	○	○	○	○	○	○
Fifth child	○	○	○	○	○	○

114. What sort of delivery did you have for each child?

	Vaginal delivery with no instruments	Vaginal delivery with forceps or ventouse (suction cup attached to baby head)	Planned caesarean	Emergency caesarean	Prefer not to say
First child	○	○	○	○	○
Second child	○	○	○	○	○
Third child	○	○	○	○	○
Fourth child	○	○	○	○	○
Fifth child	○	○	○	○	○

115. For each child how many weeks pregnant were you when you gave birth? i.e. what was the length of your pregnancy

	29 weeks or less	30 to 33 weeks	34 to 37 weeks	38 to 41 weeks	42 weeks or more	Don't know	Prefer not to say
First child	○	○	○	○	○	○	○
Second child	○	○	○	○	○	○	○
Third child	○	○	○	○	○	○	○
Fourth child	○	○	○	○	○	○	○
Fifth child	○	○	○	○	○	○	○

116. How long was your labour for each child?

This is the time from being diagnosed in labour by a midwife until the time you delivered your baby

	Shorter than 5 hours	5 to 10 hours	11 to 16 hours	17 to 21 hours	More than 21 hours	Don't know	Prefer not to say
First child	○	○	○	○	○	○	○
Second child	○	○	○	○	○	○	○
Third child	○	○	○	○	○	○	○
Fourth child	○	○	○	○	○	○	○
Fifth child	○	○	○	○	○	○	○

117. Have you ever been diagnosed with unusually heavy bleeding after the delivery of any of your children? *

This might have been called postpartum haemorrhage

○ Yes

○ No

○ Don't know

118. Which births did you have a bleeding problem after?

This might have been called postpartum haemorrhage

	Normal bleeding	Unusually heavy bleeding after the birth	Prefer not to say
First child	○	○	○
Second child	○	○	○
Third child	○	○	○
Fourth child	○	○	○
Fifth child	○	○	○

119. If you were diagnosed with postpartum haemorrhage what sort was this? *

☐ Primary (heavy bleeding in the first 24 hours following delivery)

☐ Secondary (heavy bleeding between 24 hours and up to 2 weeks following delivery)

☐ I don't know

☐ I was not diagnosed with postpartum haemorrhage

120. Do you know how much blood did you lost each time you have had this heavy bleeding? We understand you may not.

You might have been told in ml, pints or as a % of your total blood volume

121. Did you receive any additional treatment for bleeding? *

If so please select all that apply

☐ I didn't receive any additional treatment

☐ Don't know

☐ Prefer not to say

☐ Consultation only

☐ Dilatation and curettage (D&C)

☐ Removal of the uterus - Hysterectomy

☐ Blood transfusion

☐ Taking iron tablets

☐ Dantrolene

☐ Injections of medications - this might have been oxytocin, tranexamic acid

☐ Other

122. Did you have any of these complications during pregnancy or birth? (part 1/2)

If none please move to the next question

	Pregnancy induced hypertension (high blood pressure)	Preeclampsia	Growth restriction	Gestational diabetes	Overdistended uterus (too much water around the baby in the uterus)
First birth	○	○	○	○	○
Second birth	○	○	○	○	○
Third birth	○	○	○	○	○
Fourth birth	○	○	○	○	○
Fifth birth	○	○	○	○	○

123. Did you have any of these complications during pregnancy or birth? (part 2/2)

If none please move to the next question

	Placental praevia (placenta near or covering the opening of the cervix blocking the baby's passage through out of the vagina)	Placental abruption (early separation of the placenta from the uterus)	Retained placenta (when you don't pass all the placenta during the birth)	Antenatal bleeding (vaginal bleeding during the pregnancy)
First birth	○	○	○	○
Second birth	○	○	○	○
Third birth	○	○	○	○
Fourth birth	○	○	○	○
Fifth birth	○	○	○	○

Final section: Other bleeding episodes

124. Have you experienced any other bleeding that hasn't been covered by the survey? *

○ Yes

○ No or only minor

Section describing your average bleed of this type

125. Please describe the type of bleeding

[   ]

126. How often do you have this bleeding a year?

[   ]

The value must be a number

<div align="center">Describing the worst time you had this type of bleeding</div>

127. How long did the bleeding last?

Please enter the number of hours

[   ]

The value must be a number

128. Did you have any treatment for this bleeding? *

If yes please describe

○ No

○ Blood transfusion

○ An injection of something to stop the bleeding e.g. desmopressin

○ Replacement therapy

○ Taking iron tablets

○ Other

129. Have you previously answered this questionnaire? *

○ Yes

○ Yes but it was incomplete

○ No

130. How did you find out about this questionnaire? *

Please state the organisation from which you received this questionnaire

[   ]